

NASA Conference Publication 2129

NASA-CP-2129 19800020595

Proceedings of the Eleventh Annual Precise Time and Time Interval (PTTI) Applications and Planning Meeting

FOR REFERENCE

NOT TO BE TAKEN FROM THIS ROOM

A meeting held at the
Goddard Space Flight Center
Greenbelt, Maryland
November 27-29, 1979



NASA Conference Publication 2129

**Proceedings of the Eleventh Annual
Precise Time and Time Interval (PTTI)
Applications and Planning Meeting**

**A meeting held at the
Goddard Space Flight Center
Greenbelt, Maryland
November 27-29, 1979**

**Sponsored by
Naval Electronic Systems Command
NASA Goddard Space Flight Center
Naval Research Laboratory
Naval Observatory
Defense Communications Agency**

NASA

**National Aeronautics and
Space Administration**

**Scientific and Technical
Information Office**

EXECUTIVE COMMITTEE

Ralph T. Allen
Naval Electronic Systems Command

Charles A. Bartholomew
Naval Research Laboratory

Laura C. Charron
Naval Observatory

Andrew R. Chi
NASA Goddard Space Flight Center

Andrew C. Johnson
Naval Observatory

James A. Murray, Jr.
Naval Research Laboratory

Dr. Harris A. Stover
Defense Communications Agency

Schuyler C. Wardrip
NASA Goddard Space Flight Center

GENERAL CHAIRMAN

ROGER EASTON
Naval Research Laboratory

PTTI 1979

TECHNICAL PROGRAM COMMITTEE

DR. ARTHUR O. McCOUBREY—CHAIRMAN
National Bureau of Standards

RALPH T. ALLEN
Naval Electronic Systems Command

DR. HELMUT HELLWIG
Frequency and Time Systems, Inc.

ANDREW R. CHI
NASA Goddard Space Flight Center

DR. SAMUEL R. STEIN
National Bureau of Standards

DR. CECIL COSTAIN
National Research Council of Canada

JAMES WILSON
Airborne Navigation, Inc.

EDITORIAL COMMITTEE

L. J. RUEGER — CHAIRMAN
Johns Hopkins University
Applied Physics Laboratory

DR. ROGER E. BEEHLER
National Bureau of Standards

DR. HARRIS A. STOVER
Defense Communications Agency

DR. ERIC BLOMBERG
Smithsonian Astrophysical Observatory

SCHUYLER C. WARDRIP
NASA Goddard Space Flight Center

DR. R. GLENN HALL
Naval Observatory

MILES M. ZICH
Naval Electronic Systems Command

JAY OAKS
Naval Research Laboratory

CHARLOTT M. HARRIGAN — SECRETARY
Applied Physics Laboratory

SESSION CHAIRMEN

SESSION I

DR. Gernot M. R. Winkler
Naval Observatory

SESSION II

Dr. Samuel R. Stein
National Bureau of Standards

SESSION III

Prof. S. Leschiutta
Istituto Elettrotecnico Nazionale

SESSION IV

Charles A. Bartholomew
Naval Research Laboratory

SESSION V

Dr. Donald L. Hammond
Hewlett Packard

SESSION VI

Andrew R. Chi
NASA Goddard Space Flight Center

ARRANGEMENTS

Shirley E. Darby, GSFC
Donald C. Kaufmann, GSFC
Paul J. Kushmeider, GSFC
William O'Leary, GSFC
Dr. Victor S. Reinhardt, GSFC
Schuyler C. Wardrip, GSFC

FINANCE COMMITTEE

Laura C. Charron, USNO
Schuyler C. Wardrip, GSFC

PUBLICATIONS

George W. Freas, Jr., GSFC
Schuyler C. Wardrip, GSFC
Patricia M. Sturiale, SASC

PRINTING

Charles V. Hardesty, GSFC
Donald E. Ellis, GSFC

RECEPTIONISTS

Kathy McDonald, NRL
Marie Nader, GSFC
Dorothy Outlaw, USNO
Stella Scates, NRL
Emma Thomas, GSFC

BANQUET SPEAKER

Prof. Norman F. Ramsey
Subject: Inner Space

CALL TO SESSION

Dr. Arthur McCoubrey
National Bureau of Standards

WELCOME ADDRESS

Robert E. Smylie
Acting Director, Goddard Space Flight Center

OPENING COMMENTS

Rear Adm. Henry D. Arnold
Vice Commander, Naval Electronic Systems Command

Capt. Raymond A. Vohden
Superintendent, U.S. Naval Observatory

CONTENTS

	<u>Page</u>
CALL TO SESSION	1
<i>Dr. Arthur McCoubrey</i>	
WELCOME ADDRESS	3
<i>Dr. Robert Smylie</i>	
OPENING COMMENTS	5
<i>Rear Admiral Henry D. Arnold</i>	
OPENING COMMENTS	7
<i>Captain Raymond A. Vohden</i>	

SESSION I PTTI REQUIREMENTS, APPLICATIONS AND PLANS

The Joint Tactical Information Distribution System – Description of Systems Operation and Timing Requirements.	11
<i>J. Sonsini</i>	
Suggested Attributes For Timing in a Digital DCS.	15
<i>Harris A. Stover</i>	
Impact of Improved Clocks and Oscillators on Communications and Navigation Systems	31
<i>Samuel R. Stein</i>	
The Frequency and Time Program at The Jet Propulsion Laboratory	41
<i>R. L. Sydnor</i>	
Satellite Time Transfer via TDRSS and Applications.	45
<i>Andrew R. Chi</i>	
Timing and Frequency Considerations in the Worldwide Testing of a Spread Spectrum Communication System.	65
<i>D. G. Woodring, S. A. Nichols, and Roger Swanson</i>	

CONTENTS (continued)

Page

SESSION II OUTLOOK ON NEW TECHNOLOGIES

Limitations on Long-Term Stability and Accuracy in Atomic Clocks	81
<i>D. J. Wineland</i>	
The Performance of Primary Cs Beam Clocks Using Quadrupole and Hexapole Deflection Systems. Consequences for Time Keeping.	113
<i>Gerhard Becker</i>	
The Lasso Experiment.	145
<i>Bernard Serène and Pierre Albertinoli</i>	
Some Implications of Reciprocity for Two-Way Clock Synchronization.	171
<i>James L. Jespersen</i>	
Evolution of The International Atomic Time TAI Computation.	185
<i>Michel Granveaud</i>	
Hydrogen Maser Implementation in the Deep Space Network at the Jet Propulsion Laboratory.	197
<i>Paul F. Kuhnle</i>	

SESSION III DISSEMINATION SYSTEMS I

Time Dissemination – An Update.	213
<i>Kenneth Putkovich</i>	
Time Transfer with the NAVSTAR Global Position System	235
<i>Ben Roth, William Klepczynski, and R. Glenn Hall</i>	
Precise Time and Time Interval (PTTI) Measurements from the Navigation Technology Satellites and the GPS NAVSTAR-4 Satellite	255
<i>J. A. Buisson, T. B. McCaskill, O. J. Oaks, M. M. Jeffries, and S. B. Stebbins</i>	
Time Recovery Measurements Using Operational GOES and TRANSIT Satellites	283
<i>R. E. Beehler, D. D. Davis, J. V. Cateora, A. J. Clements, J. A. Barnes, and E. Méndez-Quñones</i>	

CONTENTS (continued)

Page

SESSION IV DISSEMINATION SYSTEMS II

T&F Comparisons via Broadcasting Satellite and Navigation Technology Satellite	315
<i>Y. Saburi, Y. Yasuda, S. Kobayashi, and T. Sato</i>	
One Way Time Transfer via METEOSAT Capable of 30 ns Accuracy	329
<i>Klemens Nottarp, Wolfgang Schlüter and Udo Hübner</i>	
Time Dissemination in The Hydro Quebec Network	343
<i>G. Missout, W. LeFrancois, and Louis LaRoche</i>	
Time Coded Distribution via Broadcasting Stations.	351
<i>S. Leschiutta, V. Pettiti, and E. Detoma</i>	
Voice Announcements of Time: A New Approach.	363
<i>J. Jespersen, G. Kamas, and M. Weiss</i>	

SESSION V RECENT ADVANCES

A Study of Time Dissemination via Satellite in India	387
<i>B. S. Mathur, P. Banerjee, P. C. Sood, Mithlesh Saxena, Nand Kumar, A. K. Suri, C. L. Jain, and K. Kumar</i>	
Advances in the Stability of High Precision Crystal Resonators.	403
<i>Arthur Ballato and John R. Vig</i>	
Galileo Quartz Clock	441
<i>M. Bloch, M. Meirs, M. Rosenfeld, and P. Garriga</i>	
Initial Results on 5 MHz Quartz Oscillators Equipped with BVA Resonators	457
<i>Raymond J. Besson and Donald A. Emmons</i>	
Time Transfer via Satellite-Link Radio Interferometry	471
<i>S. H. Knowles, W. B. Waltman, J. L. Yen, W. H. Cannon, W. Petrachenko, N. W. Broten, C. Costain, D. H. Fort, J. A. Galt, J. A. Popelar, and G. W. Swenson</i>	

CONTENTS (continued)

Page

SESSION VI
SYNCHRONIZATION SYSTEMS

Comparison of Different Time Synchronization Techniques	485
<i>R. Kaarls and G. deJong</i>	
Two-Way Time Transfer via Geostationary Satellites NRC/NBS, NRC/USNO and NBS/USNO via Hermes and NRC/LPTF (France) via Symphonie	499
<i>C. C. Costain, J.-S. Boulanger, H. Daams, D. W. Hanson, R. E. Beehler, A. J. Clements, D. D. Davis, W. J. Klepczynski, L. Veenstra, J. Kaiser, B. Guinot, J. Azoubib, P. Parcelier, G. Freon, and M. Brunet</i>	
The SIRIO-1 Timing Experiment	521
<i>E. Detoma and S. Leschiutta</i>	
Demonstration of Remote Clock Monitoring by VLBI, with Three Baseline Closure	557
<i>C. M. Cheetham, W. J. Hurd, J. W. Layland, G. A. Madrid, and T. P. Yunck</i>	
Traveling Clock Verification of VLBI Clock Synchronization	577
<i>L. E. Young</i>	
Early Results from a Prototype VLBI Clock Monitoring System	585
<i>T. P. Yunck and G. A. Madrid</i>	
Source Structure Errors in the Synchronization of Clocks by Radio Interferometry	599
<i>J. B. Thomas</i>	
The Lasso Program — An Overview	617
<i>Professor S. Leschiutta</i>	
Prospects for Advances in Microwave Atomic Frequency Standards	619
<i>F. L. Walls</i>	
Clock Performance, Reliability and Cost Interrelationships	643
<i>Martin W. Levine</i>	
The Frequency and Time Standard and Activities at The Beijing Institute of Radio Metrology and Measurements	657
<i>H. T. Wang</i>	
Recent Progress of the Research Works on Frequency and Time at the NIM	685
<i>Huang Bingying</i>	
11th Annual PTTI Registration	689

CALL TO SESSION

Dr. Arthur McCoubrey
National Bureau of Standards

DR. MCCOUBREY: I am Art McCoubrey. I am the Chairman of the Technical Program Committee of PTTI, this year. It is my duty to call to session this meeting of PTTI. So it is my pleasure to call to order this meeting of the 11th Annual PTTI. And having done that, I am going to introduce to you the General Chairman of PTTI. He is head of the Space Applications Branch of NRL, Roger Easton.

DR. EASTON: Thank you Arthur. Now for welcoming remarks, we will hear from the Acting Director of the Goddard Space Flight Center, Mr. Robert Smylie.

WELCOME ADDRESS

Mr. Robert Smylie
Acting Director of the
Goddard Space Flight Center

On behalf of the Goddard Space Flight Center, I would like to welcome all of the delegates here and the people coming to this conference to the Center. I understand that this is the 11th such conference that has been held on this subject, although the name has changed a little bit over the years for various reasons. It is a very important activity to the Goddard Space Flight Center because of the work that we are engaged in and the need for increased capability in the area of precise time and time interval. I was glad to see that the speaker called it "PTTI" because it is really a mouthful to say that whole acronym out all at once.

One of the things that happens when you come here and invite me to speak is that you get a few words about the Goddard Space Flight Center because it has been my view that people coming from around the world and around the country get stuck in an auditorium or a conference room somewhere for several days and go away and say that they have been to the Goddard Space Flight Center but they really don't know anything about the place except what they saw as they walked across the campus and into the auditorium. So I would like to spend just a couple of minutes telling you what Goddard is and what we do and why it is that the kinds of things you consider here over the next three days are important to us. And I think that if you can find the time and want to get around the Center and see some of the things going on here that there may be ways that we could arrange to do that.

OPENING COMMENTS

Rear Admiral Henry D. Arnold
Vice Commander
Naval Electronic Systems Command

INTRODUCTION BY DR. EASTON

Admiral Arnold is a native of Tulsa, Oklahoma. He graduated from the Naval Academy in June, 1950, which put him just beyond where he would not have been in the academy when President Carter was there. He has served in numerous Naval assignments. He is a Naval aviator. He saw service in Korea. He was Commander of Air Wing 11, Executive Assistant to the Assistant Secretary of the Navy for R&D, Commanding Officer of the Naval Air Station at Whidbey Island, Commander, 13th Naval District, and Director, Tactical Air Surface and Electronic Warfare Development. He was Commander, Medium Attack Tactical Electronic Warfare Wing.

His decorations include the Silver Star, the Legion of Merit, Distinguished Flying Cross, Bronze Star, Air Medals, Presidential Unit Citation, Navy Unit Commendation, and the Navy Commendation Medal.

It is a great pleasure to introduce Rear Admiral Duff Arnold.

ADMIRAL ARNOLD:

Well I don't know about that introduction where being in the class of '50 relative to Jimmy Carter stands in my repertoire there, but I would like to welcome you to this PTTI Conference and let you know that we in NAVELEX are very happy to be co-sponsors of this kind of a gathering. Certainly my recent experience goes a long way in heartily endorsing the theme of this conference. That is, let's think about the user when we start putting these devices together. I know in this very exotic age of electronic capability, digital computations and measurements devices that we are able to very precisely come up with what is going on and keep track of things. Based upon my experience as an A-4 driver, I used to believe that you knew what time it was and you knew where you were and everything was in order - you were going to be able to get to the target in good shape. If either one of those things were getting out of synch though, the probability of hitting your CEP was very poor. We have come a long way since the old seat of the pants flying by map in those days, but this morning, I toured most of this part of Maryland trying to find the Goddard Space Lab based upon the map that I had. I

I am still not a very good navigator, I guess. I did know what time it was though and I arranged to be here on time. That was a positive result.

I would like to re-echo though that the user is the important person on the military side. We have got to think about the user when we put black boxes together. When they get out in the fleet and have to go through the rigors of the operational environment, they must stand up, be maintainable and be available when time and time interval are needed.

You may recall Gordon Smith being here last year kicking this thing off and I would like to bring you the latest chapter in the saga of Mr. Clock, who you all know and remember was the cesium clock that we had to get first-class transportation for on the airlines because that was the only place that adequate power was available for this long, around the world junket he was making to calibrate our VERDIN System.

Well, the latest is, that one year later Mr. Clock has had a very healthy trip. He has made it all the way around, drinking electrons all the way while his partner has been having martinis for two.

Again, I hope you have a very fruitful meeting. I noticed some very interesting subjects on the agenda. I am sorry that I can't spend the time out here to be with you for the entire meeting, but again let me say that NAVELEX is happy to be able to sponsor this kind of a get-together. It is at this kind of a get-together where coordination and cooperation can occur that we discover a multiplying effect which is far-reaching and will enhance our posture as time goes on.

Thank you very much. Have a very good meeting.

OPENING COMMENTS

Captain Raymond A. Vohden

Superintendent, U. S. Naval Observatory

CAPT VOHDEN: Mr. Chairman, Ladies and Gentlemen: Although time is fabricated at the U. S. Naval Observatory, I have not yet been provided with enough of it in my first two months as Superintendent. As a result, I stand here before you knowing very little about the subject you are about to discuss. But one thing I have learned already: Dr. Winkler has told me that because our time is precise time, there are precisely 5,529,600 precise seconds in 64 days, and he just cannot provide any more for me. If it had been January now, he would have given me one extra second on December 31-- the leap second. Now 5 1/2 million seconds seem a lot to any layman like me. Imagine my consternation when I found that Dr. Winkler counts time in nanoseconds, and that I have already used up 5 1/2 times 10^{15} or 5 1/2 kilo-tera-nanoseconds. A frightening thought!

A famous astronomer, Ejnar Hertzsprung, once said: "We don't know what data astronomers want in the next twenty years, but we are sure that they want it with much greater accuracy." While this quote addressed astronomers' needs, it could equally well refer to the DoD. Requirements for precise time in some current applications or in systems now in the definition stage quote precision of 5 to 10 nanoseconds. The best portable clock trips occasionally reach that precision, but the platform clock that was synchronized with the Naval Observatory Master Clock this way will not retain its synchronization very long. Consequently, as DoD manager of PTTI, the Observatory is continuously looking for means to improve time transfer and make the U. S. Master Clock more accurate and conveniently available. The GPS time will be directly traceable to the Naval Observatory, so that in another five years we might expect 10 nanosecond precision anywhere around the globe-- provided timing capability is available in the GPS receivers or special time receivers, such as the one now undergoing acceptance testing by the Naval Observatory.

But with the famous astronomer, "we are sure that DoD-- and others-- will want time with much greater accuracy" in the future. Perhaps we don't know why they might want it, but time transfer capability of 1 nanosecond or better is a requirement we can be almost sure will be with us in the late eighties or early nineties-- and perhaps earlier. This is a challenge for the Naval Observatory. On the one hand, there is no platform requirement now, while on the other hand it will take many years to develop such a capability. Moreover, as we have found all too often, the user simply assumes that the Naval Observatory can provide whatever accuracy is needed. And although I came to the observatory with an exalted view of the capabilities of the staff, I have come to realize that Dr. Winkler is actually a

human being just like you and me, who needs lead-time in order to be there when he is needed.

It is for these reasons that the U. S. Naval Observatory is attempting to obtain funding for experiments in Laser time transfer via satellite (the highest precision technology in existence and in principle), for very-long-baseline interferometry, and for highest precision time-keeping in general.

Upgrading of the master clock is in progress. We hope in five years to be able to guarantee 1 nanosecond real-time precision, a first step toward the sub-nanosecond master clock we expect will be required in the nineties.

But enough about plans. The Annual PTTI Applications and Planning Meeting, has, I understand, become an important forum for the PTTI community to look at the state of the art, to elaborate needs, and to look into the future. I have noted many papers on time transfer in this meeting starting today. Navigation is rapidly becoming again a time-ordered discipline, requiring a world-wide synchronized time distribution system.

In wishing you a successful meeting, may I express confidence that out of meetings such as this one may grow a collaboration which avoids, after initial experimentation, the danger of a multitude of competing systems, to the detriment both of the user and the taxpayer.

May the next 58 tera-nanoseconds (= 16 hours of talks) be a success!

Thank you.

SESSION I

PTTI REQUIREMENTS, APPLICATIONS AND PLANS

Dr. Gernot M. R. Winkler, Chairman
Naval Observatory

**THE JOINT TACTICAL INFORMATION DISTRIBUTION
SYSTEM – DESCRIPTION OF SYSTEMS OPERATION
AND TIMING REQUIREMENTS**

**J. Sonsini
Electronics Systems Division
Hanscom Air Force Base, Massachusetts**

(PAPER NOT AVAILABLE FOR PUBLICATION)

QUESTIONS AND ANSWERS

QUESTION:

How do you protect from inputs from two different master terminals?

MR. SONSINI:

There is only one master terminal per network. We use one master terminal and if that one goes out then the next higher order of hierarchy would take over the master function. If more than one took over then the first time that the second terminal that took over heard the first one transmitting, he would immediately go back to a non-master mode. So within line of sight there would only be one master terminal.

DR. STOVER:

What if you would move from one network to another? For example, what if one aircraft would move from one network to the next network and if the two networks weren't alike that could create a problem. You didn't mention anything about trying to tie your network to Observatory time.

MR. SONSINI:

Currently, that would be a problem. Two non-interlinked networks would not be synchronized and a plane flying from one network to the other would have to resynchronize in the second network. That is why I mentioned both tying JTIDS in with the GPS or the continuous clock for all terminals which would maintain prime synchronization as an absolute time quality.

DR. WINKLER:

You mentioned frequency hopping in that frequency range, in UHF. Is that done phase coherently or is coherence lost?

MR. SONSINI:

I think you lost me.

DR. WINKLER:

Well, when you hop frequency, you can do it in two ways. You can modulate your carrier frequency generator, and if you do that, then phase coherence will be maintained. Or, you can switch between different oscillators and then they may not necessarily be phase coherent.

MR. SONSINI:

It is a single oscillator, a large termination of local oscillators and mixers and the same local oscillators are used for all frequencies.

SUGGESTED ATTRIBUTES FOR TIMING IN A DIGITAL DCS

Harris A. Stover
Defense Communications Engineering Center
1860 Wiehle Avenue
Reston, Virginia 22090
Telephone: (703) 437-2316

ABSTRACT

Sometime in the future, the Defense Communications System (DCS) will predominately employ digital techniques. To be effective, such a system, which employs time division multiplexing of digital signals, must include a system timing capability. This follows because the time relationship of each particular pulse to the other pulses in the same sequential stream is fundamental to interpreting the information contained in each pulse. This time relationship determines the assignment of a particular bit to a particular use and a particular meaning. The loss of proper timing can cause all received information to be meaningless--a totally unacceptable condition. Thus, timing is a function of major importance in a digital military communications system (particularly if encrypted). Fortunately, correct timing is not difficult to achieve in a simple point-to-point digital communications system, and many approaches can provide at least a minimal timing capability in even the most complex digital communications systems. However, some of these approaches are unacceptable for the DCS, and the remaining ones have various degrees of acceptability.

To determine the value and effectiveness of the different approaches in satisfying the needs of the DCS, a set of desired attributes is needed against which they can be evaluated. This paper presents a set of suggested attributes for a timing capability for the DCS which must be capable of supporting full-scale warfare in addition to peacetime needs. Reasons for each attribute are given.

INTRODUCTION

Although this paper which is devoted to needed characteristics for a particular application of timing technology might seem a little out of place among the many technical papers presented here, this is a "Planning and Applications" meeting, and this paper is intended to call attention to some important applications considerations for

timing* capability needed by a digital Defense Communications System (DCS). Requisites of a specific application are often equally as important as technical items and sometimes more so. For good planning, both technical factors and their specific application must be considered in determining a course of action. In previous annual meetings, technical possibilities for synchronizing a digital DCS have been discussed, so that it should be understood that providing the attributes suggested in this paper for timing in a digital DCS [1,2,3,4] is technically and economically practical. However, the requisites of the specific application probably have not been adequately considered in those previous papers. In particular, they did not demonstrate an adequate appreciation for the differences between the needs of peacetime civilian digital communications networks and worldwide military networks, such as the DCS, which are needed for support of any full-scale war. The suggested attributes presented here for timing in a digital DCS are offered for consideration as fundamental needs for such a system. It is believed that as new equipments are developed and procured, with proper planning these attributes can be provided quite economically and numerous problems avoided.

BACKGROUND

It is generally accepted that for the types of communications provided by the DCS, the advantages of digital systems over analog systems are almost overwhelming [5]. Therefore, it is expected that sometime in the future, the DCS will predominately employ digital techniques. Such a digital communications system requires a timing (synchronization) function in order to be effective. The time relationship of each particular pulse to other pulses in the same sequential stream is fundamental to interpreting the information contained in the pulses. If time division multiplexing is used, this time relationship determines to whom the information belongs and also what it means; i.e., particular time slots are assigned for particular purposes.

* Note: The word timing is used here in the general sense which includes synchronizing as a special case. It implies a wide variety of related meanings including: (a) scheduling; (b) making coincident in time or causing to occur in unison; (c) setting the tempo or regulating the speed; (d) ascertaining the length of time or period during which an action, process, condition or the like continues; (e) causing an action to occur at a desired instant relative to some other action or event; (f) producing a desired relative motion between objects; (g) causing to occur after a particular time delay; or (h) determining the moment of an event.

In analog communications systems, noise or small errors in either signal amplitude or frequency can cause undesirable but usually acceptable signal degradation, and the same can be said for isolated errors in a digital communications system. However, the loss of proper timing in a digital system can be catastrophic, causing all received information to be meaningless -- a totally unacceptable situation. This characteristic makes the timing/synchronization function one of the most important functions in a digital communications system. Fortunately, correct timing is not difficult to achieve in a simple point-to-point communications system, and there are many different approaches that can provide at least a minimal timing capability for even the most complex digital communications systems [1,2]. However, some of these approaches are unacceptable for application in the DCS and those remaining have various degrees of desirability. A set of desired attributes is needed against which the different approaches to timing can be evaluated. This paper offers a suggested set of such attributes and explains their importance to the DCS.

One of the most fundamental changes that is going on in the DoD community is the change in perception of the DCS from that of a peacetime system to a communications system capable of supporting full-scale war [5]. In developing desired attributes for the timing/synchronization of a digital DCS, it is assumed that the DCS will not only transition from analog to digital, but also to a network capable of supporting full-scale war. The major difference between a communications system designed for peacetime and one designed for wartime is the need for survivability of sufficient communications capability to make our military forces effective. Survival of the timing function in a digital communications network is essential to survival of the communications function. It can also be highly desirable to have an acceptable timing capability available even when the communications function is not available. One reason is that the timing function can be useful for establishing or reestablishing the communications function. For example, the length of time required to acquire synchronization of a spread spectrum signal that is being jammed, depends on the size of the search window. An acquisition search window of a few milliseconds might require a thousand times longer to acquire synchronization than a window of only a few microseconds. This capability (accuracy of a few microseconds) is already used in the DSCS to permit the acquisition of spread spectrum signals within a reasonable period of time in a jamming environment.

In the past, problems have occurred in the timing relationship between different digital communications networks that were not originally engineered to communicate with one another. In some cases, these problems were overcome by the addition of variable storage

buffers and adequate clocks to control them, while in other cases modification of equipments might also be required. Even after these corrective measures, it might sometimes be necessary to interrupt traffic to reset the variable storage buffers. It is not always possible, at the time of equipment development, to predict just what system interfaces will be required during the lifetime of an equipment. Therefore, design of the equipment to meet a minimum timing compatibility standard is highly desirable for avoiding future problems. Such a timing compatibility standard should be developed to follow a well-developed DCS timing plan. This DCS timing plan should satisfy a set of desired DCS timing system attributes such as those presented and discussed in this paper.

DESIRED TIMING SYSTEM ATTRIBUTES

In this section, a set of suggested timing system attributes for a digital DCS are presented, following which the importance of each attribute is discussed. Parts of the discussion of some of the attributes presented early on will also apply to attributes that follow. This is particularly true of the discussion of the first attribute.

Time and frequency reference information utilized in applicable Federal Government telecommunications facilities and systems shall be referenced to (known in terms of) the existing standards of time and frequency maintained by the U.S. Naval Observatory, UTC (USNO), or the National Bureau of Standards, UTC (NBS).

Discussion: This is a direct quote from FED-STD-1002, and it is DoD policy to comply with Federal Standards. However, different people have chosen to interpret this standard in different ways. The following discussion will illustrate the need for using a standard timing reference and should help to bring out a desirable interpretation of the first attribute as applied to a digital DCS.

Can you imagine trying to make connection at a busy airport, such as Chicago's O'Hare, if each airline used only its own clocks, and clock time for each airline was different from that of the other airlines? At the least, it would cause considerable unnecessary inconvenience. A century ago, that was the situation that existed in some large railroad stations. You could set your pocket watch to any one of a number of clocks on the station wall, each indicating the official time for its associated railroad line. Problems with this are obvious, but the railroads were heavily criticized when they adopted a standard railroad time in 1883. Standard time slowly gained popularity, and in 1918 congress passed the Standard Time Act. The advantage of standard time for planning interconnecting flights when

using modern air travel is quite obvious. Crossing time zones can cause problems to travelers in keeping track of which time zone applies to their present location. These time zone problems are sometimes alleviated for both travelers and long distance electromagnetic communications by using a worldwide time standard such as coordinated universal time (UTC).

The problems of scheduling the transfer of bits of information from one transmission link to another, where each bit must be made to coincide with its assigned time slot, are somewhat similar to those of transferring passengers from one airline to another. Each is made simpler by well planned and well maintained traffic schedules. However, a major node of the digital communications network will typically handle many millions of bits each second, and the bits travel between nodes at speeds up to 186,000 miles per second (3×10^8 m/s). As with the passenger trains, although it is not necessary that all clocks read the same (bits can be stored in buffers just as passengers can be stored in depots), it is obviously highly desirable; and whereas tolerances of a few minutes were acceptable for the railroads, tolerances of a few microseconds are desirable for a high capacity digital communications network. Corrective action for an information bit that misses its assigned time slot might be even more difficult than corrective action for a passenger who misses an assigned aircraft flight. Unlike the airline passenger, a single communications bit that misses its time slot assignment is likely to cause those that follow to miss theirs also.

Whenever a new communications system is planned, the system planners seem to quickly arrive at the conclusion that it is only important to provide synchronism within their own system -- that they don't have to worry about other systems that are being planned. Doesn't that sound like those old railroads where each had its own time? Like the railroads, each can be made to work, but also like the railroads, taken together they present problems that can easily be avoided by using a standard time system.

In the past, this country's largest telephone company has provided for its own digital synchronization needs as it saw those needs, and interfacing companies had to accept timing from that company. Although that policy has not changed, present planning is to eventually reference that company's atomic clocks to the National Bureau of Standards. What is wrong with an approach where one telephone company provides a timing reference for all of the others? First, there are two U.S. Government organizations charged with keeping standards of time and frequency - the National Bureau of Standards and the Naval Observatory. Master clock time at each of these organizations is in close agreement with Coordinated Universal

Time as determined by the Bureau International de l'Heure, to which both of these U.S. Government organizations contribute timing information. Second, although smaller U.S. telephone companies might be willing to accept their timing reference from the largest U.S. telephone company, the likelihood of this occurring internationally is much smaller -- an international time standard should be used. Third, as now being implemented by the telephone company, their synchronization system permits time delays to accumulate as the timing information is passed through the system, and in some cases individual local clock errors also can accumulate through long tandem connections. This means that clocks in different parts of the network have somewhat different time (or phase), although clocks at adjacent nodes are within acceptable (bufferable) tolerances. Although this is quite satisfactory for civilian digital communications, it is quite likely that it could not be tolerated by some future military systems. The functional division between digital communications and computation by digital computer is becoming less distinct, as well as that between communications and navigation or position location. For these relationships to be mutually beneficial, all should be based on common time standards. From a wide variety of viewpoints, the digital networks of the DCS should fully comply with a restrictive interpretation of FED-STD-1002.

Timing tolerances (clock errors) at major nodes of digital DCS networks should be specified in time or continuous phase (not modulo 360 degrees) rather than frequency.

Discussion: Relating this to the previous example of making connections between flights at busy airports, it is not enough to have the clocks for all airlines running at the same rate, but they should also indicate nearly the same time. In digital communications, the timing/synchronization system is used for assigning individual communications pulses to specific time slots. For this to be effective, tolerances should be established on the location (in time or phase) of the time slot and also on the arrival time (or phase) of the assigned pulse. Received bits should be retimed by temporarily storing them in variable storage buffers from which they are removed at the proper time as determined by the local clock. If the local clock pulse is not at exactly the right time, it will be either early or late by a certain phase angle at the pulse repetition rate; or, alternatively, early or late by a certain amount of time (in microseconds). A timing tolerance stated in microseconds is normalized, which makes it convenient to apply to any of a large number of data rates likely to be encountered throughout the communications system. The size of the variable storage buffer determines the ability to accommodate early or late arrival of pulses relative to the local clock. The phase (or time) tolerances of the local clocks and the bit rate of the communications stream along with expected variations

in signal path delays determine the necessary size of the buffers.

There is no simple way that these timing errors (the ones of basic significance to the digital communications timing system) can be stated as frequency errors (Hertz) or fractional frequency errors. However, because of the relationship between phase angle and frequency (frequency is the time derivative of phase angle), the phase angle error at any time can be determined from an initial phase angle error plus the time integral of the frequency error from the time of the initial phase error to the time of the measurement of interest. In order for the phase angle (or time) error to be bounded, the average frequency error must be zero. Any nonzero average frequency error will eventually result in an unacceptable phase error; i.e., it will eventually require interruption of the communications traffic to reset the variable storage buffers to prevent them from either emptying or overflowing. If the allowable phase (or time) tolerance has been specified, average frequency errors that will permit that tolerance to be maintained for a specific time can be determined. In general, relatively high errors can be accepted in the pulse rate for a short period of time. As an example, assume that the pulse frequency in a system which initially has no phase error, is 1 percent low over a period of five pulses, and then is 1 percent high for the following five pulses. After the first five pulses, there will be a phase (or time) error equal to 5 percent of the pulse period -- a normally acceptable value -- and after the second five pulses (a total of ten pulses) the error will be zero again. Now as a further example, assume that the frequency had been high for five billion pulses instead of only five pulses and then low for another five billion pulses. Then, if the maximum phase (or time) error were not to exceed 5 percent of the pulse period, the frequency error could only be one billionth of 1 percent. In both examples, the phase (or time) error is the item of predominant interest, and the frequency error is of interest only because of its relationship to the phase (or time) error.

The timing/synchronization function in the DCS should not be solely dependent on the continued operation of any particular network node, transmission link, or facility external to the network.

Discussion: Since nodes of the DCS and the transmission links interconnecting them are subject to enemy destruction or electromagnetic jamming attack, it is obviously desirable to construct the timing system to minimize the impact that the loss of any link or node, or any combination of links and nodes, would have on the timing function for the surviving portions of the network. No specific nodes or links in the network should have such individual importance to the network timing function that a successful enemy attack on them would seriously degrade the network timing. No specific parts of the timing system

either within or external to the communications network should appear to be particularly attractive targets to an enemy. This implies that control of the timing system should be distributed rather than centralized.

Following the loss of any node or transmission link of significance to the timing function, either through failure or enemy action, the timing system for the DCS should automatically reorganize itself.

Discussion: For any communications network timing approach, there is either some optimum hierarchy of the links and nodes, or some optimum set of parameters for providing a stable system, or both. When links or nodes of the network are lost, adjustments to the networks (which might include partitioning or reconfiguration) should be made to assure that degradation of the timing function is acceptably minimized. In civilian peacetime systems, where the need for such adjustments only results from occasional equipment failures or rare acts of nature, it is acceptable to manually make the necessary adjustments, and necessary repairs to the failed equipment could be expected to be made promptly. However, in a wartime situation, extensive damage to the military communications system due to enemy action might simultaneously occur in many widely separated areas. The maintenance and repair function might be intentionally or unintentionally impeded by enemy action. Access to areas where repairs are needed might be severely restricted, and required skilled personnel might not be available when needed. Therefore, the timing/synchronization system for a military communications system should be highly automated. In particular, the reorganization of the timing system following the loss of any link or node of the communications system should be totally automatic; and by attribute number 3, it should also be distributed rather than centralized.

So long as any communication link to a node survives, it should be capable of supporting the timing function.

Discussion: Unlike a civilian communications system where failures in the timing system can be expected to be random and infrequent, sudden massive destruction of many parts of the wartime military communications system can be expected over a short period of time. Whereas a couple of backup paths would be quite adequate to assure timing at a particular node in the peacetime civilian system, it might not be unusual to lose all but one communications link to a major node (or even several nodes) in a wartime military system. Since it is not possible to assure which link might remain intact following such an attack, every link must be capable of supporting the timing function.

A node temporarily disconnected from the network should have the

timing capability to rapidly reenter the network -- including capability for rapid synchronization of spread spectrum signals in a jamming environment.

Discussion: Under jamming conditions, the length of time required to test a given timing relationship to determine whether or not it is in synchronization is greatly increased. If 1 second of sampling time is required to make a decision between being in synchronization or out of synchronization for each 10 nanoseconds change in timing, an uncertainty window of 10 microseconds could require a total of 1000 seconds to search. If correct synchronization were not found the first time through, the window would have to be searched again. Obviously, the amount of search time required depends upon the design of the system and the environment in which it must function, but it is desirable to maintain a small search window for acquiring or reacquiring synchronization in a military communications system which is subject to enemy jamming. In addition to speeding up the synchronization process for spread spectrum equipment, good system timing can also be used to speed the synchronization of multiplexing and cryptographic equipment. This reduces the amount of time the equipment is out of synchronization following signal outages, thereby minimizing the loss of communications traffic.

To the extent practicable, disturbances in the clocks at individual nodes of the network should be prevented from propagating to other nodes of the network.

Discussion: Errors in local clocks as a result of disturbances at remote clocks propagating to the local clocks use up a portion of the available phase tolerance at the local node and make it more susceptible to loss of synchronization from other causes. This includes an overall reduction in the stability of the timing system making it less capable of accommodating signal fades and other transmission disturbances. This attribute is particularly important if the disturbances occurs just prior to the time a node enters a backup free-running mode of operation where an induced frequency error will be integrated over a long period of time producing a very large phase error. This attribute provides increased resistance to enemy attack and perturbations.

A normally operating timing system should not require interruption of traffic solely for resetting variable storage buffers to accommodate errors in uncoordinated system clocks.

Discussion: Planners of several civilian digital communications systems in North America considered the use of accurate free-running clocks with provision for occasional interruption of traffic to reset

variable storage buffers [6]. All of these system planners rejected this approach because they felt that it would be unacceptable to their customers. It is even less desirable in a military system where there are additional functions, such as encryption and spread spectrum transmission, which require synchronization. The worldwide nature of a military network prevents use of a low traffic night time period for such interruptions because the sun never sets on such a worldwide network.

Capabiliy to reset variable storage buffers with minimum interruption of traffic should be provided in order to permit continued communications by operating in a free-running mode whenever means for clock coordination is not available.

Discussion: This is a last ditch backup mode of operation to permit continued communications (although degraded because of required interruptions) if all means of clock coordination should be lost while at least one communications link is otherwise intact. In a well designed system, it should be a very rare occasion when this mode of operation would be required, but it would be shortsighted not to provide this capability. The timing system should not be permitted to be the sole reason for communications not being available. This attribute could be very important for the very rare occasions when it is needed, because this could be a period of time when continued communications is of utmost importance.

Systematic self-monitoring of the timing function should be provided.

The timing function in a digital DCS is expected to be very reliable. Under normal operating conditions, undisturbed by hostilities, failures will occur very rarely. Under these conditions, it will be very difficult to maintain well trained, experienced personnel for servicing failures to the timing system. Because of this, it is important that the timing system provide automatic self-monitoring and fault diagnosis. It is desirable that such monitoring include the monitoring of the actual timing function in addition to normal power-supply voltage measurements and signal level measurements. Many types of failures that can affect the operation of a timing system can only be detected by monitoring the actual timing function. It is also important to detect pending timing failures long before any interruptions to communications traffic occur. Trend information and automatic statistical evaluation of systematic self-monitoring of the timing function can be used to automatically provide early detection of problems and self-diagnosis of their causes. This information can then be used to automatically indicate the needed corrective action.

Options with potential importance for satisfying future timing

requirements should not be precluded without good reason.

It is a common occurrence that inadequate planning for future needs finally results in a situation requiring either (1) a very large expenditure of funds or (2) forgoing the service. When it arises, this situation always seems to be unexpected because it was not included in the original planning. Sometimes the capability could have been provided at no extra cost at the time of original equipment development, and nearly always at a small fraction of the cost for retrofit after the equipment is fielded. It is difficult to predict at the time of equipment development all of its applications during its lifetime. Therefore, it is very desirable to leave open all options that might make it possible to satisfy those unpredicted applications as they arise, unless this results in some significant penalty, e.g., significant additional costs.

SUMMARY

A set of desirable attributes for timing in the digital DCS has been suggested. The suggested attributes provide for keeping the major nodes of the DCS within acceptable phase tolerances of one another by coordinating all of their phases with the standard provided by the U.S. Naval Observatory (UTC (USNO)) or the National Bureau of Standards (UTC (NBS)) whenever either is available. If UTC is not available, a particular clock within the network is automatically selected as a reference for the rest of the network. Survivability of the network is further enhanced by: (1) assuring that it is not dependent on any one point of centralized or concentrated vulnerability to enemy action, (2) providing adequate automation to accomplish most corrective actions (other than equipment repair or replacement) without manual intervention, (3) assuring that timing coordination is available at any node so long as there remains one functioning communications link to that node, and (4) providing a backup mode for degraded operation of any node that finds its ability to coordinate its clock has been lost for any reason. Any improvement in stability and accuracy through improved clock disciplining procedures will further enhance a system's capability to provide all of these attributes under all conditions likely to occur in a full-scale war.

References:

(1) Harris A. Stover, "Overview of Timing/ Synchronization for Digital Communications Systems," Proceedings of the Tenth Annual Precise Time and Time Interval (PTTI) Applications and Planning Meeting, Goddard Space Flight Center, November 1978, pp 393-403.

(2) D. B. Bradley, J. B. Cain III, and M. W. Williard, "An Evaluation of Optional Timing/Synchronization Features to Support Selection of an Optimum Design for the DCS Digital Communications Network," Proceedings of the Tenth Annual Precise Time and Time Interval (PTTI) Applications and Planning Meeting, Goddard Space Flight Center, November 1978, pp 437-461.

(3) D. B. Kinsey, "Effect of Various Features on the Life Cycle Cost of the Timing/Synchronization Subsystem of the DCS Digital Communications Network," Proceedings of the Tenth Annual Precise Time and Time Interval (PTTI) Applications and Planning Meeting, Goddard Space Flight Center, November 1978, pp 463-489.

(4) Harris A. Stover, "Improved Time Reference Distribution for a Synchronous Digital Communications Network," Proceedings of the Eighth Annual Precise Time and Time Interval (PTTI) Applications and Planning Meeting, U.S. Naval Research Center, November 1976, pp 147-166.

(5) VADM Samuel L. Gravely, Jr., "DCS at the Crossroads," Signal, May/June 1979, pp 53-58.

(6) Ronald L. Mitchell, "Survey of Timing/Synchronization of Operating Wideband Digital Communications Networks," Proceedings of the Tenth Annual Precise Time and Time Interval (PTTI) Applications and Planning Meeting, Goddard Space Flight Center, November 1978, pp 405-435.

QUESTIONS AND ANSWERS

MR. CHI:

I would like to make a comment. Particularly I like your example of the illustration of comparison between people and bits, that is in terms of the requirements between the railroad for the timing and digital communications. I think it was very well illustrated. We talk about the requirements for time, but the fact that you have illustrated it and gave us a very simple example in such a way that most people can understand what it is. Thank you.

DR. STOVER:

The railroads had a hard time, you know, getting standard time across. We are having that same kind of a problem.

DR. WINKLER:

Maybe I should say a few things, particularly about your items 7 and 11, which struck me as very important and very general. Seven has been, if I remember correctly, that means should be provided to prevent the disturbances of a single clock to propagate throughout the system. Now that is something which is, of course, important, not only for your particular application, it is essential to all timekeeping. And what does one do in order to prevent that?

And now, it appears to me that the approach which is usually taken is to just straight average and this is something which has been criticized by several people, the last one, which impressed me most, was an article which I read two years ago in "Die Klein-Hallbacher Berichte", the German URSI reports about the falacies of using the mean as the best estimator in cases of disturbances which are not at all Gaussian and may not be right in time correlation. And in that article, the great advantage of using the median was discussed, that in fact the median, the central point of all incoming time reports which a model point would get from its surrounding points would be a completely insensitive estimator to any individual disturbance. A clock could go any arbitrary amount off and by taking the median instead of the mean, you are safe. It would not be affected at all and I wanted to point that out, that in filtering, in selecting routines to reject such outliers, the assumption of the normal distribution is an incorrect one because as we deal with digital systems, digital systems are usually outrageously wrong and not Gaussian distributed.

And 11, the importance of satisfying future requirements. That strikes me as something of even greater generality.

DR. STOVER:

It is even harder to get examples of.

DR. WINKLER:

That we so often find the role of management defined as -- These people must think that management must have something to do with monocles to restrict people's choices in the future, while in fact good management ought to enlarge the choices which the future generations have. And I think excellent technical management would be one which keeps wide open all these future choices instead of restricting them in too short-sighted a view. And that, again, is an overriding generality.

QUESTION:

I too have had access to some of the German publications and especially when you are talking about different types of weapons which may be releasing electromagnetic radiation which could affect large numbers of clocks in an area, but the aspect of going to the median also bothers me because there may not be a discrete median. There is a range for which there is a set of values can be the median, so how do you try to solve this problem of large-scale, propagation disturbances with large numbers of clocks being simultaneously disturbed with the ionosphere being disturbed and which all would masquerade and it is the same. I think that is a very major problem in tying everything together.

DR. STOVER:

Well, one of the things that I had in mind at the time that I wrote that was one of the systems that has been very highly discussed in the communications literature for timing for digital communications systems is the so-called "mutual system", in which all the clocks in the whole communications network effect each other, so that the whole system can float around, so to speak, with bulges here and bulges there as far as the error is concerned and everything effects each other. And one flaw in one clock will effect all the other clocks. That was the thing I was really trying to rule out when I wrote that statement. And my preference is to tie everything to UTC, as was stated in the very first one which is a Federal Standard. But as you read that Federal

Standard, different people can interpret it differently, when it says it is traceable to the Naval Observatory, some people will say that it has some frequency that is traceable to the Naval Observatory, while I would like to say time or phase which is stated in one of the later ones. And some people will say that the accuracy with which that frequency needs to be traced to the Observatory is not really very great. Now I disagree with both of those statements as you can tell, and think that we should accurately, in phase, in time, clock the DCS, because it is a war-time system.

DR. WINKLER:

I agree very much and I think that agrees with general principles which have been mentioned recently by Professor Becker. Is he here? Would he like to say something about that?

DR. BECKER:

I will address it in my paper later.

DR. KAHAN:

Have these attributes that you have listed been accepted and implemented within the DCS system?

DR. STOVER:

No. This is the first time that they have been presented as a group, as a desirable. We have to get them accepted. You know how the military works. When you tell somebody you have a requirement, they want to know which directive from the Joint Chiefs state it as being a requirement. So you have to beat on these things a long time before they can be stated as being requirements. So that is why we are calling them "desirable attributes".

QUESTION:

You mentioned item 7 here as non-propagation of errors. Do either one of you have any suggestions as how one might implement the desirable attributes?

DR. STOVER:

Well, the thing I had in mind, of course, was the types of things that I have presented at previous meetings here. I am biased there, of course, and so if you would read the proceedings from the year before last you would get an excellent idea of what I would consider an outline of how to do that.

IMPACT OF IMPROVED CLOCKS AND OSCILLATORS ON
COMMUNICATIONS AND NAVIGATION SYSTEMS
(Special Report)

Samuel R. Stein
Frequency and Time Standards Group
National Bureau of Standards
Boulder, CO 80303
(303) 499-1000, ext. 3277

In September of this year, the National Bureau of Standards held a Workshop in the Washington D.C. area which addressed the role of clocks and oscillators in large scale systems, particularly communications and navigation. The ultimate purpose of this Workshop was to do two things: first, to provide research and development people in government, at universities and in companies with adequate information to appropriately direct their research activities towards the real needs for clock and oscillator improvements; second, to determine whether or not there are any ways in which existing oscillators and clocks could serve systems better than they are doing now. The Workshop took place over a period of three-days, with several technical papers and two panel sessions which were instrumental in determining the state of opinion in this field. Many government agencies and private companies were represented. I am not going to repeat the technical details. Instead, I would like to present a distillation of the ideas and concepts; some of the ideas are my own, but many came from other participants.

There are two generic alternatives to obtaining timing information in a distributed system - the use of independent clocks or the use of coordination. This paper will not address this choice at all, but will concentrate on systems which use clocks. For military systems in particular and in many cases for civilian systems, there are reasons to choose solutions based on precise clocks or oscillators. Low error rate in digital communications, anti-jam characteristics and fast signal acquisition all require very precise timing information. Survivability and independence depend upon a a priori knowledge that comes from having precision clocks in the system and that is not available to unauthorized persons. Independent operation of system elements protects the system from human error and various disasters. Finally, there is often fallout resulting from the inclusion of clocks and oscillators in a system. For example, having a very precise oscillator on a satellite permits improved determination of the orbit of that satellite. This technique is being applied today in the GPS system and may be applied in the future to many satellite systems if the satellites carry low cost but high precision clocks.

Contribution of the National Bureau of Standards.
Not subject to copyright.

In a paper presented at the last PTTI conference, two basic mechanisms were suggested for achieving improved systems; better clocks and system redesign could lead to improved performance or different operational procedures and system redesign could lead to relaxed clock dependence. The conclusion which I reached as a result of the Workshop is that the real deficiency from which we suffer today is a lack of effective and efficient utilization of existing resources. Engineers today, particularly systems engineers, will often go a long long way to avoid using clocks in their systems. The JTIDS system is probably a good example of that. The operator needs to enter his time with approximately 6 second precision. Doing better does not save any time in acquiring utilization of the system. Typical requirements to satisfy the position location, identification and the information distribution aspects of the system can be accomplished with oscillator precisions in the 10^{-4} to the 10^{-7} range, orders of magnitude below what is available today. I am going to discuss why this situation occurs and then how to optimize the use of available devices to achieve the required performance and reliability and how the specification of oscillators affects our ability to accomplish this at minimum cost. We will consider the traps of applying false economic considerations and the problem of functional duplication where many subsystems provide the same attributes and none provide the reliability and the redundancy that is necessary. There was a near unanimous agreement that more development is needed on two fundamentally different varieties of clocks. We will review the state of the industry and its capability of providing these requirements.

There is a large gap between what is being produced and the state-of-the-art, i.e., what has been achieved in the laboratory under ideal conditions. One of the things that we'd like to be able to do, of course, is to purchase large numbers of these best units. The idea may be a little bit controversial but I believe there really is no large problem with regard to the ultimate performance capability, i.e., the noise floor of our existing technology; combinations of hydrogen, rubidium, and cesium standards have been demonstrated to provide pretty much all that most people need at the present time. However, there are significant areas of deficiency relating to operating standards in the field. The turn-on time, the environmental sensitivity and the radiation resistance of our current standards simply do not satisfy systems designers. Many systems, SEEK-TALK and JTIDS for example, would like to have oscillators with any where from a part in 10^9 to a part in 10^{11} precision and accuracy that turn on in 30 seconds. Operationally, they are using oscillators that turn on in 40 minutes at the part in 10^8 level. Commercial manufacturers have published results of oscillators that accomplish parts in 10^{10} repeatability in five minutes. So there is a large discrepancy. System functions are also pushed onto the

clock with unenviable results. Manufacturers are asked to provide output at frequencies such as 5,10,10.23,5.115,9.116 and 4.016 MHz. They are also asked to provide high degrees of setability and tunability which are essentially system functions.

The first area that I would like to talk about is probably the most important one, reliability. It is something that we pay lip service to, something we worry about after the fact. One of the major concerns expressed in the Workshop was what can we do today to plan for reliability in our future developments? The performance which we need exists; the reliability that we want is only going to come from more experience with the very standards that we currently have. We make the mistake of constantly trying to push the state-of-the-art and push the performance of our standards with the same devices that are supposed to produce high reliability and a long lifetime. The only way we are going to find the problems in clocks and oscillators and solve them is to produce hundreds of these devices, and get them out into field operation so that the design flaws which are built-in can become known. Otherwise there will be a wide variety of circuits and features in supposedly high reliability devices that have only been produced two or three times. The strategy which I recommend is that we invest our money in buying large numbers of identical clocks. This will help generate a guaranteed market for the companies that produce the clocks and will encourage the needed engineering and development investment in the clocks. This approach would be costly, but not as costly as the failure of important systems. Another consideration that we should take into account is that the various attributes which we assign to a clock are not independent. For example, if we want super performance from a device then we are going to have to pay for that performance in a variety of areas, in reliability and cost for example.

The use of custom made devices is another significant problem area. We tend to set goals for our system clocks which are either the best results we know of or, worse, something a little bit better. We ask the small R&D company to develop a few units with that performance but also having custom features that match our system requirements - our frequency, size, configuration, power, weight, and warmup time. But custom units in general perform worse than standard off-the-shelf-units. Not only that, the process of producing a customized product ties up the technical capability of the small company which is then not available to do the advanced development needed to get better performance. This scenario is probably true even in the case of the most trivial changes because the risks of making these changes are high.

We do a further disservice by not paying enough attention to the whole problem of specification. The process of specification is unique to each system application and cannot be done in a genera-

lized fashion. We should always use the ultimate criterion; if the system is to provide timing, then the specification should be in terms of the maximum time deviation permitted for the duration of the mission or experiment. Systematics are particularly important to specify correctly. Several kinds of modeling can be done, but most often, modeling is unsuccessful in removing systematics. The principle reason is that the systematic effects of the clocks often have the same functional dependences as the systematics from other parts of the system. The GPS program is a good example of that. Quadratic systematics in the clock are inseparable from similar phenomena in the orbit.

Our specifications are often unreasonable. We sometimes specify a much better device than is needed because we know it is producible, but that runs up the cost and prevents the manufacturer from trading off that performance against some other important criterion. One has an obligation to specify the true system performance requirements rather than anticipate unforeseen eventualities. Once the specifications of a system are fixed, the performance of the system clock or oscillator is determined. A different system design might not require the same oscillator performance but once the requirements are set one is forced to pay for the unnecessarily difficult specifications. A related problem is the totally ingrained notion of many engineers that they know the value of the clock in their system a priori, based upon the final price of the system. I think this a priori "knowledge" of the value of the clock is grossly in error. For example, quartz oscillators look rather simple. They are small devices; the best of them cost only a few thousand dollars. Systems engineers sometimes don't comprehend that the state-of-the-art quartz oscillator is splitting a resonance line to a part per million. This is mostly a science, but partially an art. It is not a situation where additional engineering effort is going to produce a fundamental decrease in the cost. As another example, I'd like to talk briefly about possibilities for a very inexpensive GPS receiver. The performance achieved in the GPS system is interesting for commercial applications. The clear acquisition signal has more power than the P code and it may become available on both the L_1 and L_2 frequencies. People are talking about two-printed-circuit-board receivers that will sell for \$2,000 and cost less than \$1,000 dollars to produce. In this context, the value assigned to the clocks is \$150 and the performance requirement is a part in 10^{11} stability for hundreds of seconds. It is probably impossible to produce such a device with today's technology.

The development costs of custom clocks and oscillators are usually not recoverable by sales of a large number of units. In fact, the small, high technology companies that serve the custom product market run the risk of developing new devices which, if they have large profit potential, may attract other companies to

compete for the market. In addition, specifying state-of-the-art performance in a system diminishes the possibility that there will be significant economies due to large scale production. Super high performance is achieved by a process of measurement, testing and selection and these processes are labor intensive. In fact, they are essentially an impediment to ever producing large numbers of super high performance clocks. We need to recognize that research and development for new products will have to be paid for by the government or by the systems developer.

In order to improve productivity, it would be beneficial to separate the problem of making a device that works from the problem of making it in a cost effective manner. The engineers and scientists who have to produce new developments should not have the added burden of doing it inexpensively. I have seen this policy applied in the solar power conversion industry and it appears to be very successful. We ought to increase the utilization of standard components in a variety of systems. One aircraft could eventually carry operational JTIDS, SEEK-TALK and GPS receivers. Right now, because of the differing specifications those will all contain independent frequency standards. There is no reason why they could not all run from a single distribution unit. In fact, there is an advantage because of the redundancy resulting from using an ensemble of standards.

There was a consensus of opinion at the Workshop that there are three types of standards requiring more development. The first is a special purpose standard. Various systems stress different attributes which can be combined in a single device. The JTIDS system needs fast warmup. A part in 10^9 accuracy satisfies all functions of that system. The SEEK-TALK program is principally interested in achieving a part in 10^{10} accuracy with fast warmup. For GPS user equipment, stability is important in commercial applications which observe satellites sequentially. Spread spectrum communication systems need near zero bit error rates which requires in the vicinity of part of 10^{10} to parts in 10^{11} stability. The second type of standard needing further development is the very, very high stability oscillator. Parts in 10^4 and better performance have been achieved, but the devices are not field deployable and are not sufficiently reliable. This kind of performance is needed for times up to a week in order to increase calibration intervals, to speed up measurements, to allow the use of higher frequencies in our communications systems, and to make better use of station keeping satellites in TDMA systems.

What is the state of research and development that is supposed to produce these results? Crystals, cesium, rubidium and hydrogen are all old technologies. We are existing off the developments of the past, but there are many new ideas. In fact there is a plethora

of new ideas, only a few of which may be superior to the existing concepts. We must carefully analyze this situation, and put our research and development resources in the direction of devices that really have potential for replacing or adding to the existing concepts. Advanced development is in a worse state. Whereas, the civilian and the military funding agencies spend a fairly large amount of money on basic research, there is not much funding for advanced development. Private companies are tied up producing the customized devices required by systems engineers. Bell Telephone which was spending millions per year on crystal research is now out of the field, having satisfied their own needs for the foreseeable future. Organizations like the USAERADCOM are shrinking in size, no longer providing the advanced development that they were doing at the end of the second world war. This problem is exacerbated by the fact that the development of the standard up to the preproduction model is far more costly than the initial laboratory demonstration. Even if the new clocks and oscillators needed by our systems in the near future are developed we will not easily be able to manufacture them. The manufacturing capability that is needed is considerable. The utility type standards will be required in quantities greater than ten thousand units, and they can't be created overnight. It will probably take years and cost millions of dollars to establish that kind of production facility. We've even lost some of the facilities that we had. Our crystal capabilities have gone overseas for the most part; the entire commercial industry to Japan and 50% of the precision capability is gone. There is only one source of precision crystals in this country marketing resonators without oscillators and the quality of the quartz that is available has deteriorated markedly since 1970.

Finally, there is also a problem of system implementation. We all share this problem; we get caught up in developing new things. That's where most of the credit lies. We are so caught up in developing new things that good devices already developed are often not implemented. The new technologies never get to mature. On the other hand, technologies that are out in the field aren't replaced. Some are 40 years old and they are not only mature they are senile! It is necessary to separate the problems of research and production. We have to be satisfied with using devices that perform well, even if next year's device will perform better. We have to get those devices out into systems and we have to concentrate on the research and development that will produce new devices for the future. Systems engineers should worry about systems problems. It will continue to debilitate clock research efforts to continue considering things like output frequency, power level, tunability and other system attributes to be problems for the clock designer to solve.

QUESTIONS AND ANSWERS

DR. WINKLER:

Thank you very much, Sam, for your very thoughtful remarks. Maybe a little pessimistic, but it is certainly better to face the issues and I wonder whether we have any comments to that?

MR. VESSOT, Smithsonian Astrophysical Observatory

I think one thing that has been perhaps overlooked is that the technology that has led us to the successes we have made, have rarely come from an intention to develop a clock. If you look in the past, I suspect that the pendulum had nothing to do with the clock when its properties were first observed, and going a little more recently, the discovery of Cate's electricity had nothing to do with crystal oscillators. Ramsey, I am sure, didn't design his Ramsey Structure with the idea of making a clock. He was out to resolve some spectral lines. And the masers and lasers, I am sure, weren't motivated by clocks.

I guess what I am saying is that you can pour an awful lot of effort into directed research and get nowhere and I think what the country is lacking is the general outlook of undirected research in the hopes that technology can ensue that will benefit somewhere; but I really feel very uncomfortable about the attitude of, "Let's go and direct our fundamental research in a given direction". Applications nearly always arise from availability of technology, but requirements or needs don't always result in improved technology. And I think the main plea we might make is to hope that our support for fundamental research in the country will not be throttled back, and it is usually the first thing that is throttled back in a situation of a tight economy.

DR. STEIN:

I think you raised an extremely important point, Bob, and I didn't mean to imply that that wasn't true. I think it is very true. However, I was trying to elucidate some of the problems we have in accomplishing the transition from once you have identified a new technique, a new physical process, whatever it is, to then the implementation of a working clock, something like ion storage, cooled ions, lasers, are identified. They can be thought out very carefully. In many cases they are not thought out very carefully and we can identify, I think, where to best place development dollars.

DR. MCCOUBREY:

I agree with the remarks that Bob Vessot said, drawing attention to the declining support for the research that underlies these technologies that are important. I think there is another consideration also, which seems to me to apply in the case of the clocks, which have been important system components for many many years. I think that there has been less planning and less support for the design qualification and advanced development. I think you had your finger on it, Sam, when you pointed out the cost of advanced development to bring these things to a point of usefulness. It seems to me, for example, that in the case of other system components, for example, power plants and propulsion systems, or control systems, flight control systems, that there is a much greater amount of planning given to the refinement of the system and the qualification of the system beyond the development of the fundamental concepts in order to get components that are reliable. And I think one only has to look at the propulsion systems that are available and even the flight control systems now. Probably there are other components also.

DR WINKLER:

It is my impression that what is really at the root of what we are discussing here are two components. Number one, we have to ask ourselves well what are all these people doing now, which we would like to see working on the things which Sam Stein has mentioned, what are they doing? Well, they are gone? No. They are certainly still doing something and I think we may be overlooking the tremendous impact which we still have to see, which we still can, in fact, can expect coming from LSI technologies, from microcomputers, digital electronics, in other words. That impact has not yet come in the field of, certainly, of high precision frequency control. But it will; and it will change the scene radically, I think.

And number two, I think we are suffering, in fact, not from a syndrome of undermanagement or mismanagement but from overmanagement. It is a question of-- Well, I see a great deal of sympathy in the audience to what I say and I feel very strongly about it, that if we would devote all these energies which are being spent today in trying to split up things exactly into certain bins, 6.1, .2, .3, .4, .5, and to decide exactly what should be done and what should be done here. We are overdoing things. That is really what Bob Vessot has meant, that we cannot specify in such detail the future. It is impossible. We have to allow a certain degree of freedom, of liberty. If we do away with it, if we become completely enslaved to superplanning I think we will be in serious trouble in these advanced R&D concepts. There have

been many examples cited that none of the real great breakthroughs which have been made, would be possible today. They would all be declined as outrageous requests for funding. All of them. Einstein would never be permitted to work on such crazy things in the Patent Office. I think that management was very poor which allowed him to do that. And the story of penicillin and of many other discoveries, in fact, even the laser, if you go really to it, all of that was accomplished because at that time there still existed a certain degree of lack of definition. The bean counters didn't really know too well the details. Today they know everything and I think that is the real problem.

DR. STEIN:

May I defend myself?

DR. WINKLER:

No, but I was going to ask for more questions, and if we have no more question, then I think that we will adjourn.

There is one item which was brought up by Dr. Walls just in discussion which refers somewhat to the last paper by Dr. Stein and I feel that it is a very important point and that is he urges users of clocks or those who specify clocks, do not deviate from the standard operating frequency which should be 5 megahertz. The reason is that there is a considerable technology available and a considerable production experience and the point applied very much that if you specify something different, you also specify additional troubles and it is much better to specify low-noise frequency translators which are more within the state of the art in production capability using our new technologies as compared with odd frequency, output frequencies for frequency standards.

THE FREQUENCY AND TIME PROGRAM
AT THE JET PROPULSION LABORATORY

R. L. Sydnor
Jet Propulsion Laboratory
Pasadena, California

(PAPER NOT AVAILABLE FOR PUBLICATION)

QUESTIONS AND ANSWERS

DR. STEIN:

On your last slide you showed time synchronization requirements that varied in the 10 to the minus 14 to 10 to the minus 15 and I was wondering where the frequency stability requirement for 10 to the minus 15 comes from? For what applications?

DR. SYDNOR:

There are differences as we have seen in the past between requirements, desires, and needs. And this is probably the minimum that the frequency, the time synchronization people will accept. The three parts in 10 to the 16th is what they need to get the residuals down to a level where they are not bothering their solutions too greatly. At this point the major error source is the frequency standard as I understand it.

DR. STOVER:

What concerns me is whether you are putting one of these block diagrams at each station or is that the one at the Jet Propulsion Lab?

DR. SYDNOR:

This is at each station. At least at each of the major stations. Some of the minor stations have a somewhat reduced set of blocks in the block diagrams.

DR. STOVER:

You showed a present requirement of Observatory or Bureau of Standards time as being 50 microseconds and your next was just a few nanoseconds. There are three orders of magnitude difference there. Why is that?

DR. SYDNOR:

There is a difference there between the precision that we need to synchronize our various stations and the precision that we need to know absolute time, epoch. And if you look at the 10 nanoseconds, that is an internal problem. While on that same slide the need to know epoch time was like 100 nanoseconds in the same timeframe. And it is true that between now and five years from now there are three orders of magnitude difference, but right now we are working on that other one. And we have some results which you will hear later about how well we are doing.

QUESTION:

You mentioned going exclusively to the 36-bit NASA code. Is this something that is absolutely going to happen and if so, what would be the earliest possible time in years?

DR. SYDNOR:

Well it is not absolutely going to happen. This is something that we are considering at the moment. With this great number of codes, especially with the binary codes with the 50 lines going out all of the places, it is prone to a lot of failure. We would like to standardize our equipment so we don't have the spares and the maintenance problems, and simplify everything. We think it will happen. If it does happen, it will be 5 years downstream.

SATELLITE TIME TRANSFER VIA TDRSS AND APPLICATIONS

Andrew R. Chi
NASA Goddard Space Flight Center
Greenbelt, Maryland

ABSTRACT

In the early 1980's NASA will enter a new era of space program, i.e., space transportation through Space Shuttle. It will have a new large scale space communication system for satellite tracking and data transmission known as the Tracking and Data Relay Satellite System (TDRSS). With two geosynchronous relay satellites TDRSS can provide nearly worldwide coverage for communication between all near orbiting satellites and the satellite control center at Goddard Space Flight Center. Each future NASA satellite will carry a TDRSS transponder with which the satellite can communicate through a TDRS to the ground station at White Sands, New Mexico. It is using this system that the ground station master clock time signal can be transmitted to the near earth orbiting satellite in which a clock may be maintained independently to the accuracy required by the experimenters. This paper presents the satellite time transfer terminal design concept and the application of the time signal in autonomously operated spacecraft clock. Some pertinent TDRSS parameters and corrections for the propagation delay measurement as well as the time code used to transfer the time signal will be given.

INTRODUCTION

The use of satellites for time transfer began soon after the first artificial satellite was placed in orbit. This was because the concept as well as the instrumentation design was simple. It was done as an experiment to demonstrate the capability in precision over long range and the favorable geometrical configuration for the signal to propagate through the medium. In comparison with the terrestrial propagated signal, the signal transmitted from or transponded by a satellite is relatively independent of the propagation medium. The stated precisions by investigators in the last two decades using different carrier frequencies, techniques, and satellites shows orders of magnitude of improvement, ranging from microseconds to nanoseconds, over the conventional techniques. Although the capability of precision time transfer using a satellite has been amply demonstrated, the limitation of further improvement still lies on the ability to measure the signal path delay. At present, this limitation is about 30 centimeters or 1 nanosecond.

Fortunately, the technology for the time generation and dissemination has been ahead of or at least in pace with the requirements [1]. As independence for timekeeping becomes an essential requirement for on-board navigation and spacecraft autonomy [2] satellite time transfer becomes a technology that is needed for immediate application. In this paper, I shall describe a particular satellite system through which clock time can be transferred from the ground to the users in satellites in near earth orbit or on the ground. The satellite system is called the Tracking and Data Relay Satellite System (TDRSS) [3].

TDRSS

The TDRSS is a new large scale space communication system to be shared between government and commercial use. It is a new NASA tracking and data acquisition and communication system. It also provides additional capability for growing communication traffic in the private sector. The system consists of 4 geosynchronous relay satellites. The first two are for NASA, the third (the advanced Weststar) is for commercial use, and the fourth is a common spare. The system concept is shown in Figure 1. It is represented by the two NASA geosynchronous relay satellites, 130° apart in longitude, and a ground terminal located at White Sands, New Mexico. The system will be capable of tracking, transmitting data to, and receiving data from user spacecraft over at least 85 percent of the user orbit. The ground terminal at White Sands, New Mexico is shown in Figure 2.

The satellite design is shown in Figure 3. Each satellite generates 1700 watts of electrical power from its solar arrays and transmits and receives in 3 frequency bands (S, C, and K) from 6 antennas, 3 of which are steerable. The weight is 2132 kilograms (4700 pounds) and the size is 17 meters (57 feet) from tip to tip. The satellite will be launched by the Space Shuttle in 1981 and 1982 and will have a lifetime of 10 years.

The steerable S and Ku-Band, 4.9 meter antennas, are used to provide communication service for the single access (SA) users, and the S-band antenna array is used to provide communication service for the multiple access (MA) users. The steerable K-band, 2.0 meter antenna, is for the forward and return communication links between space (TDRS) and the ground terminal. The two TDRS can support up to 4 S-band or K-band single access users (SSA or KSA) and up to 20 MA users.

The advantage of such a space communication system [4] can be seen in the next two figures. Figure 4 shows the present NASA tracking and acquisition network. There are 14 ground stations located throughout the world. Figure 5 shows the post TDRSS NASA tracking data acquisition and communications network. It shows 8 ground stations

including the Bermuda station to provide only the launch support. There is a 50 percent reduction in the number of the ground stations which also serves the deep space probes and the highly elliptical orbit satellites.

SATELLITE TIME TRANSFER USING TDRSS

A user configuration of a satellite time transfer system using a TDRS is shown in Figure 6. A master clock is located at the White Sands ground terminal. The user may be mobile, fixed on the ground or in a satellite. The master clock is calibrated via a TDRS to a national time standard such as the National Bureau of Standards (NBS) or the U.S. Naval Observatory (USNO), since the NBS and USNO time scales can be related to each other and to the Bureau International de l'Heure. The user's modes may be MA, SSA, or KSA, and the carrier frequencies for each mode are shown in the table in Figure 6. The satellite coverage for the time users at 5° and 10° elevation viewing angles for TDRSS at 41° west and 171° west is shown in Figure 7.

CONCEPT OF OPERATION

The philosophy of operation is directed toward automation, that is the clock time will be transferred from the White Sands terminal via a TDRS to a user satellite by a command sent from the Project Operations Control Center (POCC) at Goddard, Greenbelt, MD. The propagation delay may be measured by a two-way time transfer technique or maybe calculated based on the position information of the ground terminal and the two predicted satellite positions, if the calculated delay accuracy meets the time accuracy requirement. The received time signal in the user satellite is measured relative to the on-board clock by a time interval unit. After correction for the signal propagation path delay, the clock error is transmitted via the TDRS to the ground for monitoring and verification. The satellite clock is free running up to a pre-set maximum clock error at which time, by on-board computer program action, a step time or a step frequency correction is made. Should the correction be deleted, a command signal is needed to override the automatic clock correction. After such a command, a new value of the maximum clock error must be re-set if the automatic clock correction feature is to be maintained.

A functional block diagram of the ground station time transfer terminal is shown in Figure 8. The time signal data is divided into two parts. One part contains the grouped parallel binary time code (PB5) [5] which is transmitted as data through telemetry. Only the time unit in the time code that is larger than the propagation path delay is of significance. Thus it is called the coarse time. The other part contains a time epoch sequenced pseudo random noise (PN) code [6] which is transmitted through the range channel or the forward

link. It has an ambiguity time of 85 milliseconds. It is to this time data that the propagation path delay corrections must be applied. The data processor is shown at the extreme right of Figure 8. The step time and step frequency corrections are used to maintain the ground station clock to that of a national time standard.

The functional block diagram of a satellite clock system [7] is shown in Figure 9. It is identical to the ground station terminal. The only exception is the Global Positioning System (GPS) receiver. This feature is designed for a user satellite either to use the GPS time signal or to compare the time signals of the GPS and TDRSS time transfer systems.

TDRSS PARAMETERS

For detailed TDRSS parameters, signal characteristics and service capabilities, the readers are referred to the TDRSS Users' Guide which is available on request [8]. Some pertinent TDRSS parameters to satellite time transfers are given in Figures 10 and 11.

TIME SIGNAL CORRECTIONS USING TWO WAY TIME TRANSFER VIA A SYNCHRONOUS SATELLITE

In a two-way time transfer using a geosynchronous satellite, the propagation path delay can be approximated as shown in the upper part of Figure 12. This two-way delay is 46 milliseconds (ms). For simplicity of operation, the PN code period is considered to be longer than the two-way path delay, i.e. 46 ms. Thus 85 ms ambiguity is used for the PN code.

In a satellite-to-satellite time transfer, the relative satellite motion of the two satellites must be considered. Based on past data, the doppler motion for all satellites falls in the range of 6 to 8 KM/S which is equivalent to about 20 to 27 μ s/s rate. If the correction for doppler motion is made for 1/4 of a second, the residual error is 5 to 7 μ s, as shown in the lower table of Figure 12. If the same correction time of 1/4 of a second is applied for satellite motion in a geosynchronous orbit, the residual error is only 17 to 34 ns.

The propagation delay corrections due to the composite atmospheric medium depends on the assumed atmospheric model, season, and geographical locations. Using the example worked out by David Levine [9] in 1970, as shown in Figure 13, the maximum error is 65 ns at 8 GHz and 70 ns at 2 GHz if the atmospheric correction is not made.

ONE WAY TIME TRANSFER OPTION

For most space science users in the 1980's, the timing requirements are in the range of 10 to 1000 microseconds. To meet these needs, one-way time transfer via a TDRS is an attractive option. This is particularly true if the user satellite can navigate on-board to achieve one kilometer position accuracy. This is based on the capability of TDRSS orbit and position data which can be provided in near real-time as shown in Figure 14. Obviously, this service can be provided to a larger number of users through the multiple access mode.

SUMMARY

TDRSS can be used after 1982 as an operational service to transfer precise time by two-way or one-way technique. Using the two-way technique to measure the propagation path delay, the precision of time transfer, without corrections, can be of the order of hundreds of nanoseconds and with correction to the order of nanoseconds. The precision of one-way time transfer technique is limited by the accuracy of the path delay calculations. This is generally in the order of microseconds.

Potential applications in addition to serving the satellite users are for time comparison among navigation system clocks and the national laboratory primary clocks and for cross-calibration of other equally precise time transfer systems.

As in any system design, the accomplishment is the accumulated results of many research and development programs. The author expresses his appreciation without giving the names of those who have contributed to the satellite time transfer technology.

REFERENCES

- [1] Cooper, Robert S., and Andrew R. Chi, "A Review of Satellite Time Transfer for Technology: Accomplishment and Future Applications," Radio Science, vol 14, No. 4, pp 605-619, July-August 1979.
- [2] Hearsh, D.P., "A Forecast of Space Technology 1980 - 2000," NASA Spec Publ SP 387, 1976.
Also, Ferris, A. G. and E. P. Green, "A Proposed Concept for Improved NASA Mission Data Management Operations," NASA/GSFC Doc. X533-76-81, May 1977.
- [3] Carrier, Louis M. and Warren S. Pope, "An Overview of the Space Shuttle Orbiter Communication and Tracking System," IEEE Trans. Comm. vol com-26, no. 11, pp 1494-1506, November 1978.

- [4] Schwartz, John and Eugene J. Feinberg, "STDN in the TDRSS and Shuttle Era," IEEE Trans. Com. vol com 26, No. 11, pp 1506-1513, November 1978.
- [5] Chi, Andrew R., "A Grouped Binary Time Code for Telemetry and Space Application," Session XIII Standards and Applications, International Telemetry Conference, November 19-21, 1979, San Diego, CA.
- [6] Sabto, JCA, "Coding and the Spaceborne Atomic Clock," NASA/GSFC Document X-521-71-81, February 1971.
- [7] Chi, Andrew R., "Application of Satellite Time Transfer in Autonomous Spacecraft Clocks," NASA Tech Memo 80572, October 1979.
Also presented in NBS workshop on "Impact of Improved Clocks and Oscillators on Communications and Navigation Systems," November 18-20, Gaithersburg, MD.
- [8] "Tracking and Data Relay Satellite System (TDRSS) Users' Guide", Revision 4, NASA/GSFC Report STDN 101.2, Doc. Sec., Code 863.2, Goddard Space Flight Center, Greenbelt, MD
- [9] LeVine, David M., "Propagation Delay in the Atmosphere," NASA/GSFC Document X-521-70-404, November 1970.

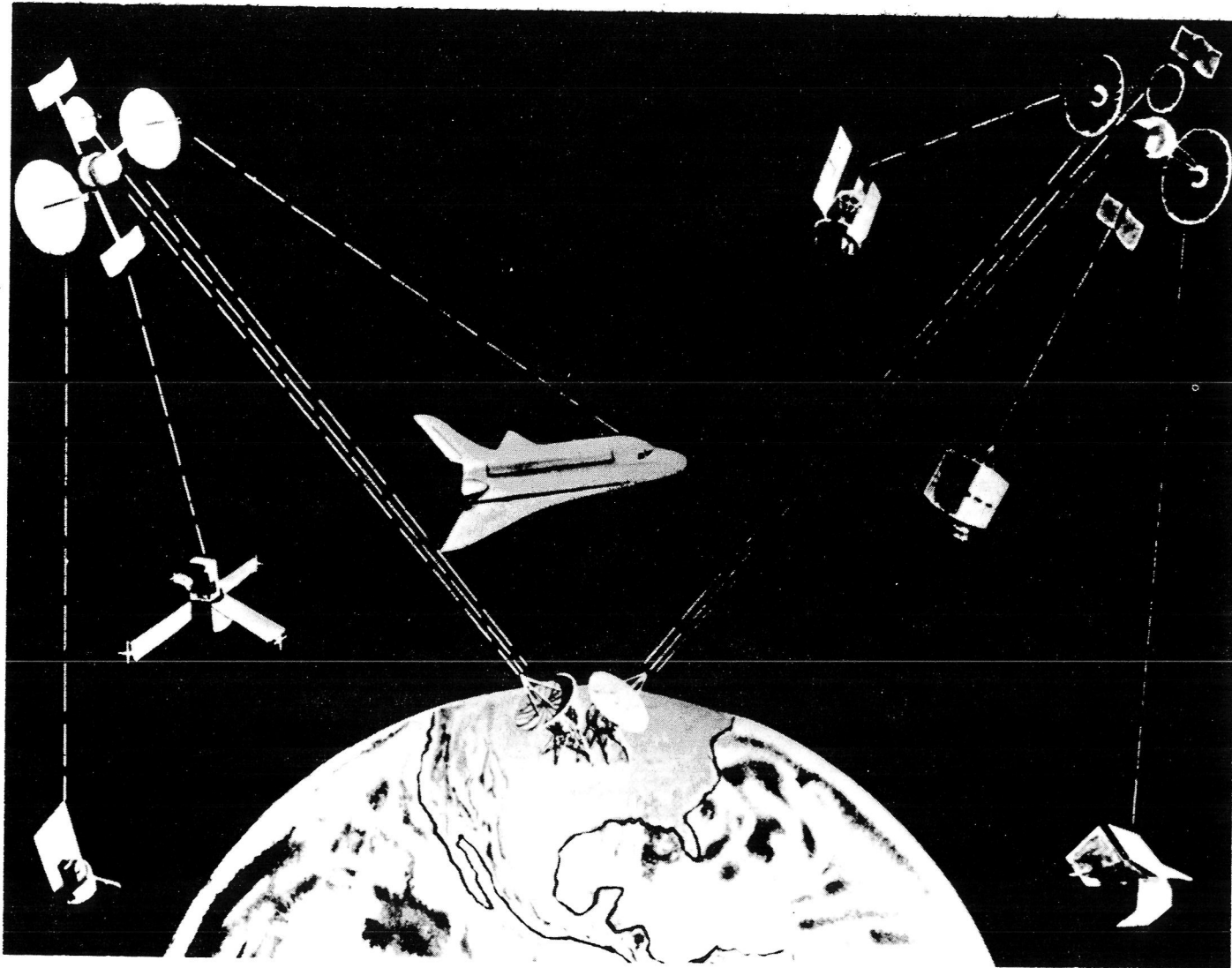


Figure 1. System Concept of the Tracking and Data Relay Satellites (TDRS)

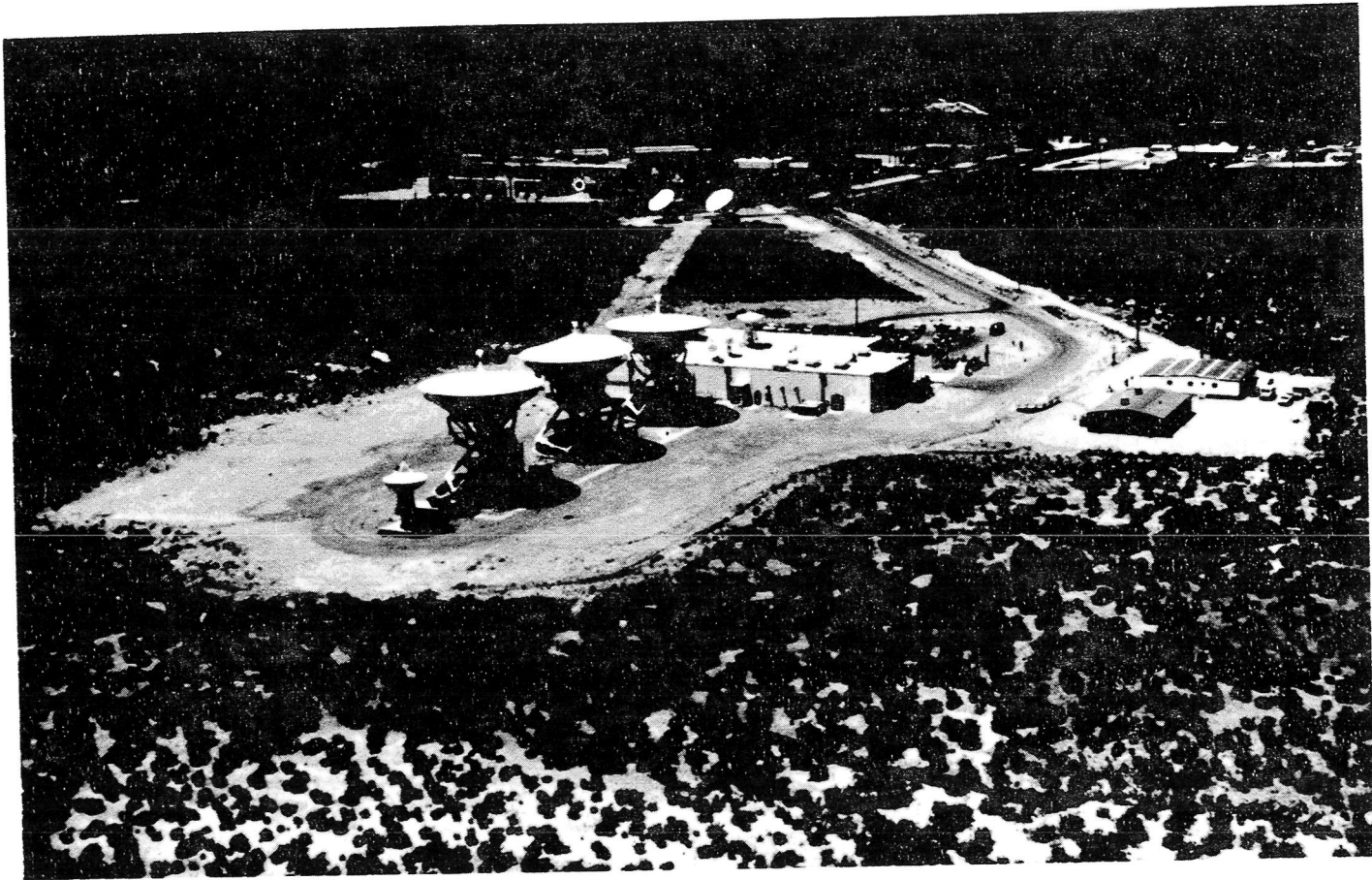


Figure 2. TDRSS Ground Station Communication Terminal, White Sands, New Mexico

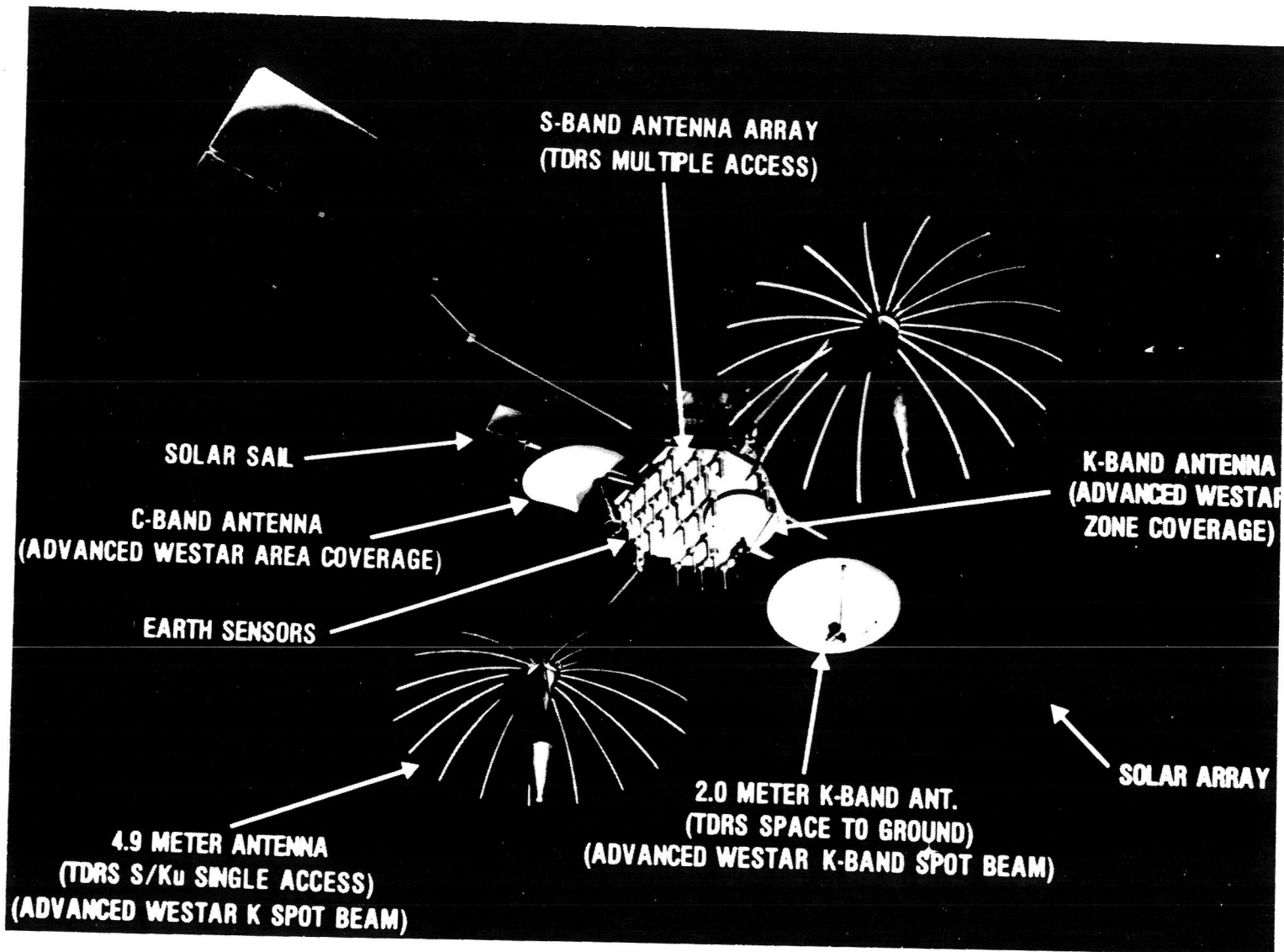


Figure 3. Antenna Design of the Tracking and Data Relay Satellite



Figure 4. Present NASA Tracking and Data Acquisition Network

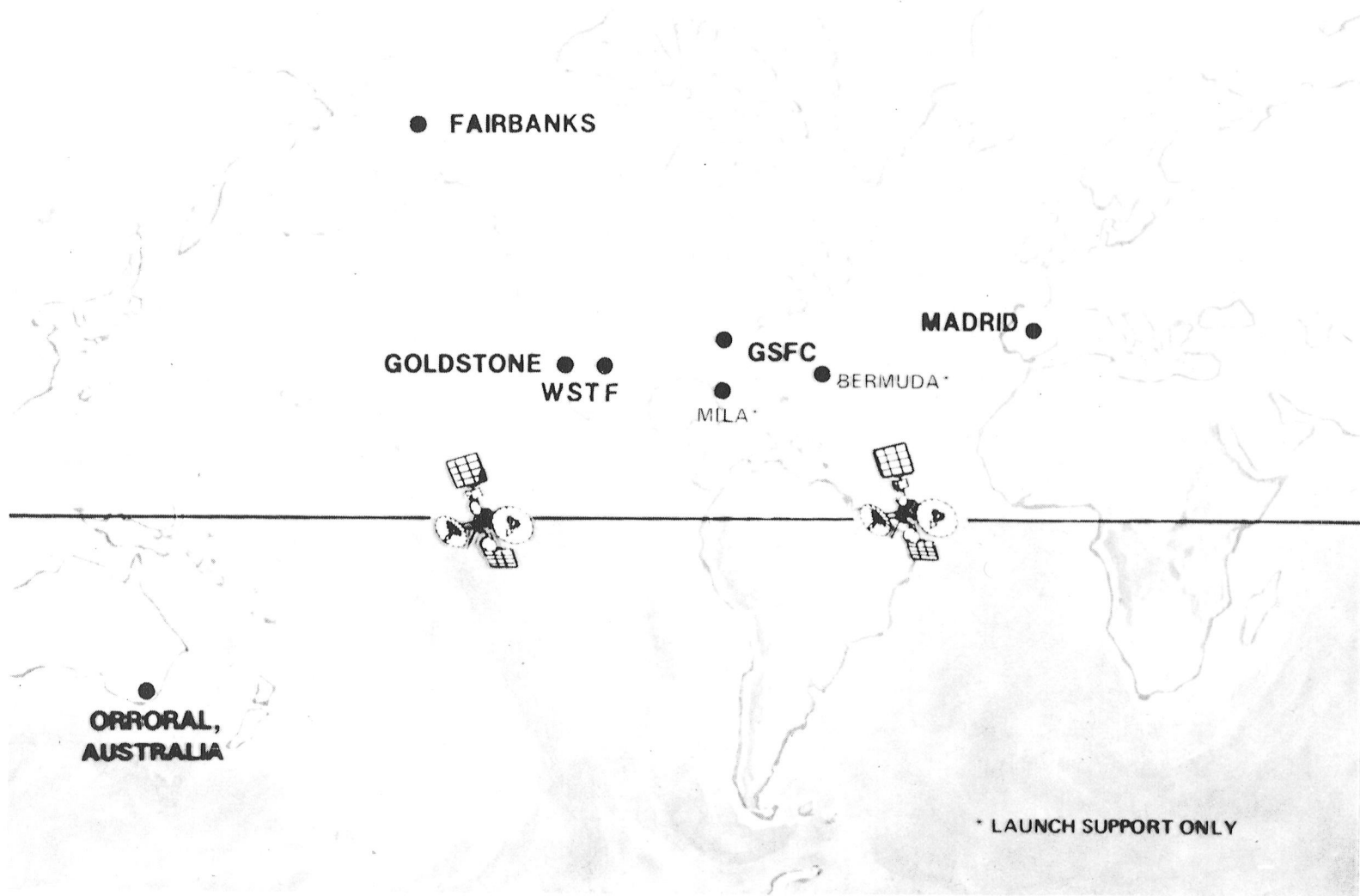
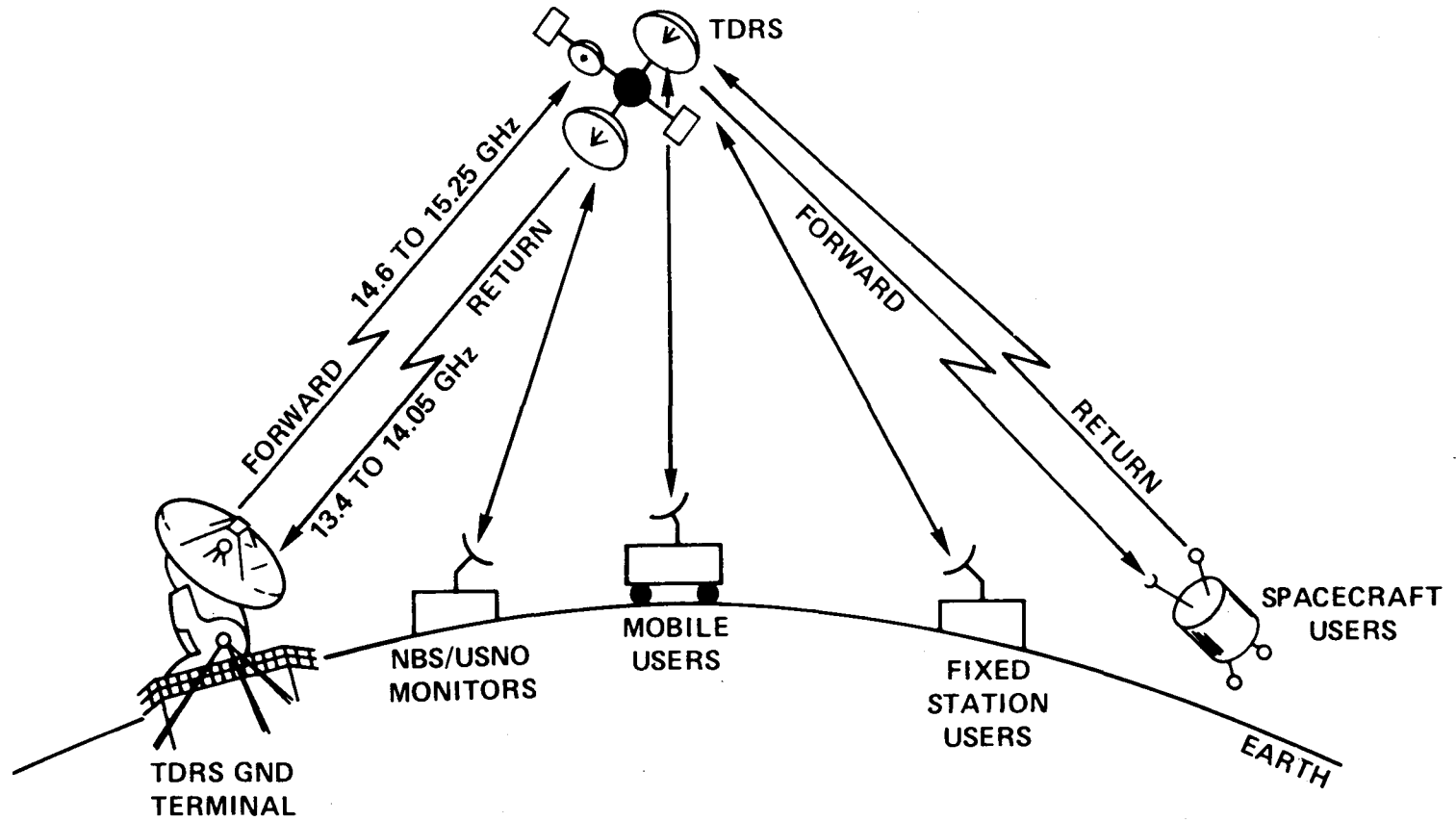


Figure 5. Post TDRSS NASA Tracking, Data Acquisition and Communication Network



USER	MODE	FORWARD LINK		RETURN LINK	
1	MA	2106.14	MHz	2287.5	MHz
2	SSA	2025-2120	MHz	2200-2300	MHz
3	KSA	13.775	GHz	15.0034	GHz

Figure 6. User Configuration of Satellite Time Transfer Using a TDRS

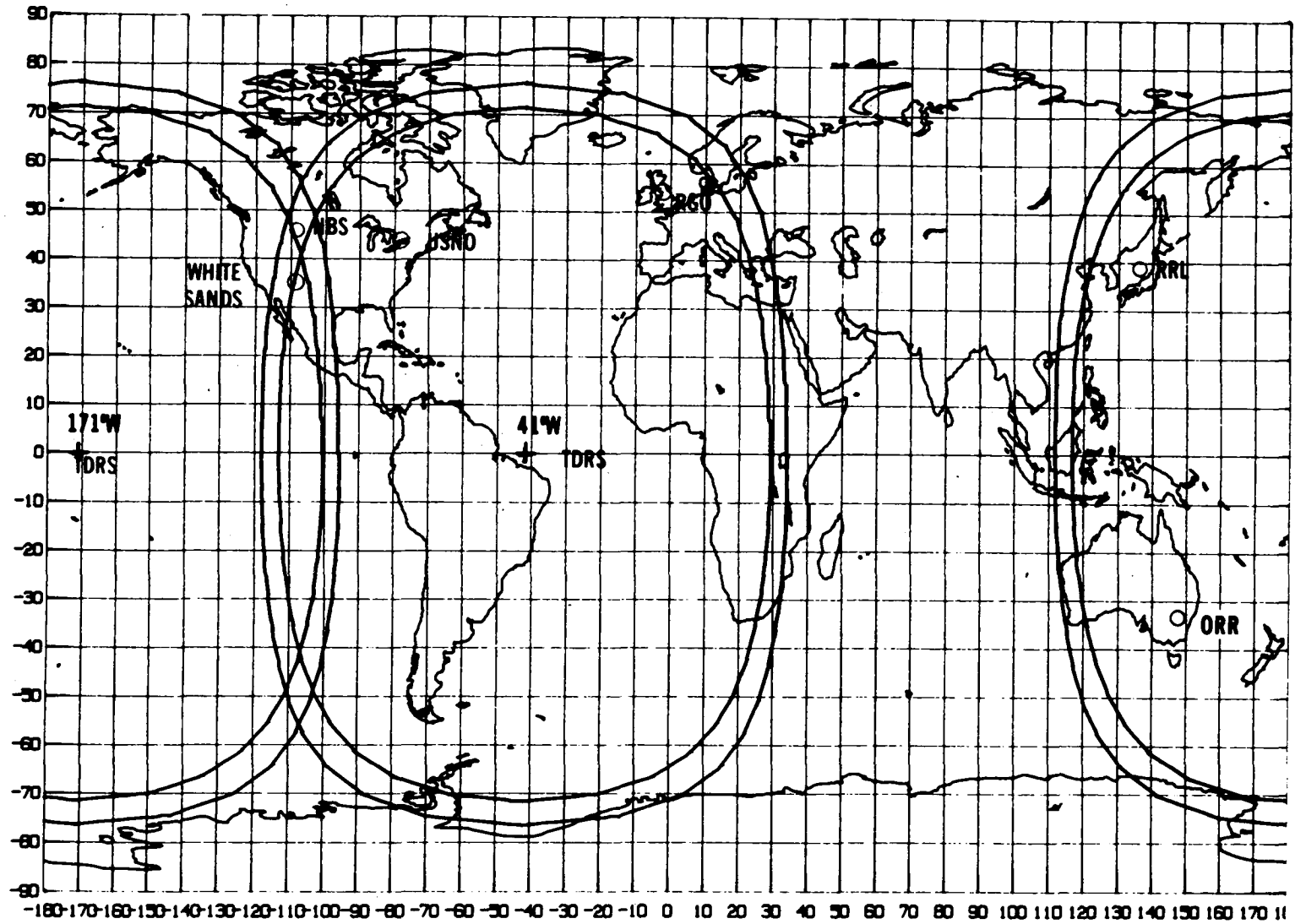


Figure 7. TDRSS Coverage for Time Users at 5° and 10° Elevation Viewing Angles

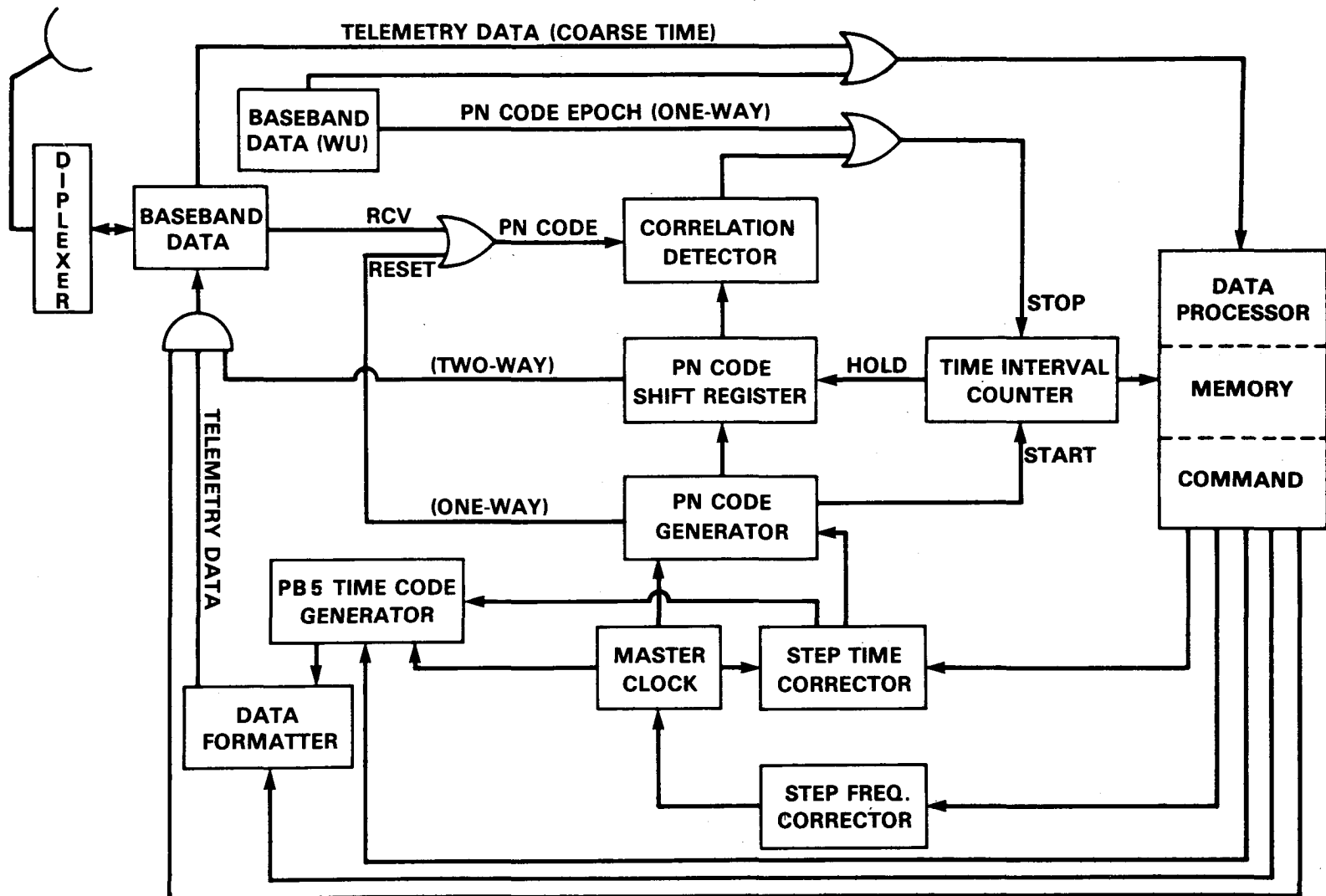


Figure 8. A Functional Block Diagram of the Ground Station Time Transfer Terminal

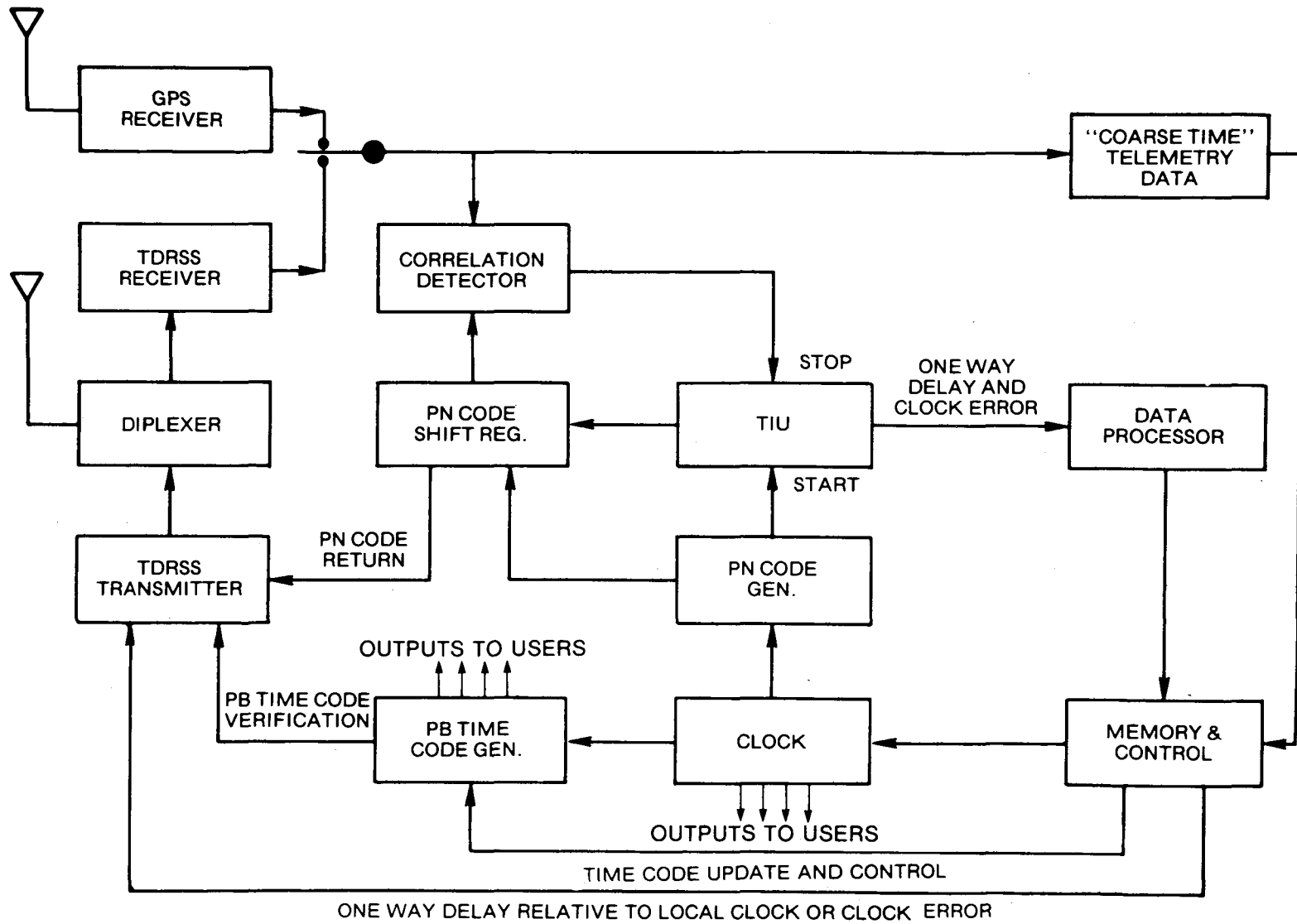


Figure 9. A Functional Block Diagram of Satellite Clock System

	MA	SSA	KSA
RF (MHz)			
FORWARD	2106.4	2025–2120	13775
RETURN	2287.5	2200–2300	15003
NO. OF RF LINKS			
FORWARD	2	4	4
RETURN	20	2	2
BANDWIDTH (MHz)			
BW (3db)	6	20	50
IF	NO	YES	YES
CHIP RATE			
FORWARD	$\frac{31F}{221 \times 96}$	$\frac{31F}{221 \times 96}$	$\frac{31F}{1469 \times 96}$
RETURN*	$\frac{31F_R}{240 \times 96}$	$\frac{31F_R}{240 \times 96}$	$\frac{31F_R}{1600 \times 96}$
DATA RATE	0.1–10kb/s	0.1–300kb/s	1kb/s–25Mb/s

* F_R IS THE DOPPLER COMPENSATED FREQUENCY RECEIVED BY THE USER.

Figure 10. Pertinent TDRSS Parameters

	COMMAND	RANGE
PN CODE LENGTH	$2^{10}-1$	$(2^{10}-1)2^8$
CHIP PERIOD (APPROX.)	332 ns	332 ns
RESOLUTION	3.3 ns	3.3 ns
AMBIGUITY PERIOD	333 μ s	85 ms
ACQUISITION TIME (sec)		
MA	20	10
SSA	20	10
KSA	4	2

Figure 11. Pertinent TDRSS Parameters

1. TIME AMBIGUITY CONSIDERATION

$$R_2 = \sqrt{R_1^2 + R_e^2} = \sqrt{(6.6175^2 + 1) R_e^2}$$

$$= 6.6926 R_e$$

$$t_2 = \frac{R_2}{C} = 142.385 \text{ ms}$$

$$t_1 = \frac{R_1 - R_e}{C} = 119.514 \text{ ms}$$

$$t_2 - t_1 = 22.871 \text{ ms} \quad 23 \text{ ms}$$

$$\text{TIME AMBIGUITY} = 2(t_2 - t_1) = 46 \text{ ms}$$

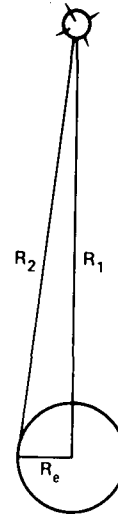
$$R_e = 6378.175 \text{ km}$$

$$C = 299792.5 \text{ km/s}$$

$$\cong 300 \text{ km/ms}$$

$$= 300 \text{ m}/\mu\text{s}$$

$$= 30 \text{ cm/ns}$$



2. PREDICTABLE OR MEASURABLE DOPPLER CORRECTIONS DUE TO SATELLITE MOTION

	RANGE OF DOPPLER	DOPPLER CORRECTIONS**		
		RATE	0.5 SEC.	1/4 SEC.
ALL SAT.	6-8 km/s	20-27 $\mu\text{s/s}$	10-14 μs	5-7 μs
SYN. SAT.*	20-40 m/s	67-133 ns/s	34-67 ns	17-34 ns

* MAXIMUM VALUES

** UNCERTAINTY IS MUCH LESS THAN THE KNOWN CORRECTION

Figure 12. Ambiguity Consideration and Propagation Delay Corrections

3. TOTAL COMPOSITE ATMOSPHERIC CORRECTIONS* PROPAGATION DELAYS

FREQUENCY (GHz)	Δt (ns)		
	ELECTION DENSITY		
	1×10^5	4×10^5	1.6×10^6
8	28	37	65
2	30	40	70

* BASED ON A TOTAL COMPOSITE ATMOSPHERE FROM THE SURFACE OF THE EARTH TO 5000 km ALTITUDE WITH A TYPICAL CONTRIBUTION FROM THE LOWER ATMOSPHERE MODELLED AFTER THAT ABOVE BARROW, ALASKA IN MAY. (SEE PROPAGATION DELAY IN THE ATMOSPHERE BY D.M. LeVINE GSFC DOCUMENT X-521-70-404, NOVEMBER 1970.)

Figure 13. Ambiguity Consideration and Propagation Delay Corrections

1. **TDRSS ORBIT AND POSITION DATA CAN BE PROVIDED TO ONE-WAY USERS, BASED ON:**

NO. OF GROUND STATIONS	7
POSITION ACCURACY OF GROUND STATIONS	200 m
RANGE ACCURACY	7 m
FREQ OF ORBIT DETERMINATION	ONCE PER DAY
ACCURACY OF ORBIT DETERMINATION	200 m
SATELLITE POSITION DATA OBTAINABLE	HOURS

2. **BASED ON PREDICTED POSITION OF TDRS, USER CAN USE ONE-WAY TIME TRANSFER OPTION IF HE KNOWS HIS POSITION TO REMOVE THE RANGE DELAY.**

Figure 14. One-Way Satellite Time Transfer Option and Accuracy

QUESTIONS AND ANSWERS

QUESTION:

The time codes which are used for the receivers, is this a standard code now or is it one you are proposing?

MR. CHI:

The time code is in the process of being reviewed by NASA and also by outside users. It is a power-binary time code, grouped-power-binary time code, which is under review and most likely will be in use for the spacecraft clock system. As I described before there is a truncated Julian date number with four digits and five digits for seconds of day and three digits for the milliseconds of seconds and so on. The total is 64 bits. That is an eight-bit, byte, R-entered code.

It is presented elsewhere so I did not want to repeat that code. If you are interested in it, I may have a copy of it and I would be happy to give it to you.

DR. KAHAN:

Can you compare this to transient rates on the GPS system? What is the difference in this case between the capabilities that this would provide and what one can get through their transient regular GPS receiver?

MR. CHI:

Obviously you can, provided of course you have the receiving terminal. For instance, I could suggest to have one of our terminals, which normally would be placed, for instance in Boulder, Colorado, that same type receiver can be placed into wherever time is wanted to be compared. For instance a monitoring station for our GPS if one wants to do that. You can receive the time from White Sands Station which will be synchronized to NBS.

Of course you can do it for all the monitoring stations that you wish. It is the same idea as for the primary time laboratories.

DR. WINKLER:

I think the comparison he asked for is the decision on that.

MR. CHI:

Oh, you use two-way propagation to measure the propagation delays. The method is to measure precisely the propagation delay time. Once you have the delay you can subtract the delay out. This could be to order the nanoseconds. It depends on the type of corrections one applies.

TIMING AND FREQUENCY CONSIDERATIONS
IN THE WORLDWIDE TESTING OF A
SPREAD SPECTRUM COMMUNICATION SYSTEM

D. G. Woodring, S. A. Nichols, Naval Research Laboratory, Washington, D.C. and Roger Swanson, Air Force Avionics Laboratory, Wright-Patterson Air Force Base, Dayton, Ohio

ABSTRACT

During 1978 and 1979, an Air Force C-135 test aircraft was flown to various locations in the North and South Atlantic and Pacific Oceans for satellite communications experiments by AFAL. A part of the equipment to be tested on the aircraft was the SEACOM spread spectrum modem developed for NRL by Raytheon.

Test results achieved in the program will be presented. The SEACOM modem operated at X band frequency from the aircraft via the DSCS II satellite to a ground station located at NRL. This modem incorporated the concepts of wide bandwidths, autonomous operation, high frequency multiplication factor and design-to-cost. For data to be phased successfully, it was necessary to maintain independent time and frequency accuracy over relatively long periods of time (up to two weeks) on the aircraft and at NRL.

To achieve this goal, two Efratom atomic frequency standards were used. One of these has been in service at NRL since 1973. One standard was used as a portable clock and the other was used as the modem frequency standard.

This paper will discuss the performance of these frequency standards as used in the spread spectrum modem, including the effects of high relative velocity, synchronization and the effects of the frequency standards on data performance. The aircraft environment, which includes extremes of temperature, as well as long periods of shutdown followed by rapid warmup requirements, will also be discussed. The limitations of maintained time in remote locations such as Thule, Greenland, Ascension Island, Lima, Peru, Hawaii and Dayton, Ohio will also be addressed.

INTRODUCTION

The Naval Research Laboratory and the Air Force Avionics Laboratory are engaged in various programs to improve long range military communications via satellite.

A joint test program was undertaken in 1978 to evaluate the performance of the SHF/EHF Advanced Communications (SEACOM) modem developed by Raytheon for NRL. This project was made part of an on-going comprehensive Air Force program for developing and testing advanced communications systems for airborne applications.

TEST PROGRAM DESCRIPTION

The SEACOM modem is a frequency hopped, spread spectrum system capable of data rates of either 75 or 2400 bps. The system provides half duplex operation at either SHF or EHF with an additional output at an IF frequency of 700 MHz. A detailed description of these equipments can be found in reference 1. The modem was integrated with an Air Force experimental dual band SATCOM terminal (AN/ASC-28) ² aboard a C-135. Figure 1 shows the test configuration. Two additional modems, at NRL's field site in Waldorf, Maryland, were integrated with either of the two amplifier/antenna configurations shown. The satellite used was ³ one of the Defense Satellite Communications Systems Phase II Satellites which was in synchronous orbit over the Atlantic Ocean.

One of the major objectives of this test program was to maintain and acquire time to an accuracy sufficient for two remote terminals to synchronize the spread spectrum waveform. The purpose of the joint test was to determine the performance of the SEACOM modem under various propagation and flight conditions.

A series of tests were run at NRL's Waldorf field site via the DSCS II satellite; first back to NRL to establish the baseline performance characteristics and then to the aircraft on the ground and in the air in a variety of high dynamic, multipath and elevation angle tests. These tests were conducted with a military aircraft operating out of various U. S. Air Force bases and foreign commercial airports. This paper will describe the techniques that were tried, their relative effectiveness and will also offer some suggestions for future testing.

MODEM TIMING CONSIDERATIONS

The signalling structure of the modem is shown in Figure 2. All timing and data is divided into 4 second frames. Once every 4 seconds during a transmission a 409 millisecond synchronization preamble consisting of a repeated 80 chip psuedo-random sequence is inserted into the data stream. This preamble is used by the receiving modem to adjust its own timing to that of the incoming signal prior to data demodulation.

The waveform requires that this timing be accurate to within 50 nanoseconds. This accuracy is achieved by adjusting the time of a locally generated replica of the preamble in 100 nanosecond steps until the signals match up or correlate. The number of steps employed is determined by the assumed maximum time error due to unknown range between the two terminals and drift between respective terminal clocks. For shipboard application, for which the SEACOM system was designed, this maximum error was specified as ± 1 millisecond. This requires a search of approximately 20,000 steps which are processed within the 1/2 second duration of the preamble. If the initial time error is greater than 1 msec. synchronization cannot be achieved by this process⁴. A description of how this initial clock accuracy of 1 msec. was accomplished is now explained.

The sources of time used for local operations were the Naval Observatory (via microwave link to Waldorf) and Loran C at Wright-Patterson Air Force Base. An experiment was also made with a GOES satellite receiver⁵ (unfortunately the receiver was not available during most of the testing). The GOES receiver had the capability of acquiring a satellite broadcast time signal within two minutes after turn on. If the range to the satellite is known, this unit will provide timing with 1 msec accuracy. In a test at Wright-Patterson, the timing of this signal varied between 220 μ sec and 260 μ sec with respect to Loran C over a two day period.

The aircraft in this test program is a C-135 shown in figure 3 operated by the 4950th Air Test Wing. Power is normally not applied to the aircraft except for specified periods (of 4 hours or less) of ground testing or during flights. Access to the aircraft was via either a cargo hatch or a crew entrance ladder as shown in figure 4. The crew entrance ladder is the normal mode of entry to the aircraft. This modem was designed for shipboard use where power outages would be infrequent and relatively brief. The battery in the integral frequency standard was used to keep power on the clock circuitry to provide a "hot" turn on. The modem on the test aircraft was turned off overnight and during stopovers. Since the on-board battery power was not designed for such long outages, portable clocks were generally used to reset the time.

PORTABLE CLOCK

For overseas operations, time was maintained with a portable clock which was carried off the aircraft during stopovers. Figure 5 shows a typical overseas operation which illustrates the environment that the portable clock must survive for a successful experiment. It should be noted that the post flight battery operation is critical in that the clock must be removed from the aircraft by the experimenter who must then find a primary power source in an unfamiliar environment before the batteries discharge. Typically on overseas flights there are many operational, legal and bureaucratic details to be looked after before the experimenter can find prime power. It was typically very difficult to locate

a local source of precise time within the restrictions of limited stopover time, complicated logistics due to usage of crew buses and difficulty in determining precise time availability in advance. These comments apply both to U. S. Air Force bases and to overseas cities that were visited.

One other source of time that was used when possible was a time signal from the Lincoln Laboratory LES 8 satellite which was in synchronous orbit over the Pacific Ocean.

OPERATIONAL RESULTS

Figure 6 shows the flight path of a two week trip in September 1978. The trip started at Wright-Patterson Air Force Base on 12 September and returned home on 26 September. An Efratom Rubidium frequency standard was carried as a portable clock and time was successfully maintained during this trip. Figure 7 shows the specifics of the trip and the highlights of the portable clock log. The clock was set at Wright-Patterson using Loran C just prior to takeoff. This trip was typical of several in the test program. Various legs of the flight provided low elevation angles, high elevation angles, high relative velocity and a high multipath environment. Successful synchronization was achieved in these environments. The trip log shows a check with NASA at Ascension Island which was typical of attempts to verify the operation of the portable clock at stopovers. It took half a day of negotiations to obtain a ride to the NASA site (on the other side of the island). Figure 8 shows the main building at the site, which housed an HP Cesium Standard that was estimated to be within 25 μ sec of UTC. Based upon known aging characteristics (figure 7) of the SEACOM portable clock, the SEACOM time was known to be within 10 μ sec of UTC. Figure 6 also indicates a power disruption at Rio caused by a blown fuse when the portable clock was inadvertently plugged in the wrong outlet. In Lima, Peru the aircraft was in range of the LES 8 satellite for the first time and a time check was possible which showed a time offset consistent with the drift rate measured on 7 September.

A number of clock synchronization techniques were attempted during the course of this program and they are listed in figure 9. The "Hot Turn-On" was the method of timekeeping intended by the manufacturer whereby the time was maintained by the battery in the integral frequency standard for short (less than 3 hours) power turn offs. A second technique was the use of a second clock with a compatible time code. Time could be transferred by connecting a cable between the two clocks. However, existing portable clocks usually do not have time code generators. These portable clocks can be used by manually entering the time via thumbwheel switches and synchronizing with a 1 PPS signal. If the accuracy of the portable clock was in doubt, a manual search could be made by offsetting the "range" control which can be varied in 500 Km/HR (2 msec) steps. This method could be very tedious and time consuming

since only one trial can be made during each 4 second frame. During the test program, a UHF satellite communications channel was available to relay test procedures and instructions. A "coarse" time calibration was occasionally used by having one operator "mark" his own time while the other noted his time. This technique was successful only when a precise 1 PPS signal was available. For local operation, it was occasionally possible to use a line-of-sight radio to a phone patch for the same technique. A feature designed into the modem, but never made operational, was for the transmitting modem to broadcast its own time code. The receive modem could then automatically acquire this time and reset its own clock.

RECOMMENDATIONS

A number of potential improvements to the SEACOM design could be implemented for operational military airborne satellite communications as shown in figure 10. The broadcast time of day could be a part of the network control that would broadcast a time code on a communications channel. This technique places the burden of synchronization on the transmitting source. The second approach provides the receiving operator with an optional mode that would permit a wide time search if synchronization were not achieved. This mode of operation is widely used in military communications networks and is generally referred to as a "net entry" mode, which is used by terminals which are entering the network for the first time or have had an extended outage. For example, a span of 1 second could be searched in 3 minutes with the existing equipment. A third technique would be to use a waveform that would be more tolerant of time offsets. Reduction of the PN rate would reduce the required synchronization time, allowing a larger initial time error to be accommodated in the short synchronization time. The last concept is more generalized and expanded in figure 11. This concept is primarily for test and evaluation efforts. The ideal portable clock would be capable of being carried in one hand across an aircraft parking area as well as up and down crew access ladders. It would be capable of operating on prime power anywhere in the world with automatic switching and tolerate the long delays between power down and access to prime power. It would interface with a serial or parallel time code "buss" (the specific type being determined by the system) and have the capability to measure the difference between an external 1 PPS signal and its own 1 PPS signal. Controls and indicators would be kept to an absolute minimum, particularly on the front panel. Reliability and price are also important considerations.

REFERENCES

1. S. A. Nichols, et. al., "Interim Test Report of the SEACOM Modem/Radio," NRL Memo Report 4138, 1979.
2. E. M. Perdue, et.al., "Dual Frequency SATCOM Low Level Terminal AN/ASC 28," AFAL-TR-78-201, Dec 1978.
3. D. E. Kendall, "Development of the Defense Satellite Communication System - Phase II," EASCON '78 Record, IEEE Electronics and Aerospace Convention Record, Sep 1978, p. 458.
4. S. A. Nichols and D. G. Woodring, "Applications of Atomic Frequency Standards to SATCOM Spread Spectrum," 32d Annual Symposium on Frequency Control Proceedings, Jun 1978, pp. 555-559.
5. D. W. Hanson, et.al, "Time from NBS by Satellite," Proceedings of the Ninth Annual Precise Time and Time Interval Planning Conference, Mar 1978, pp. 139-152.

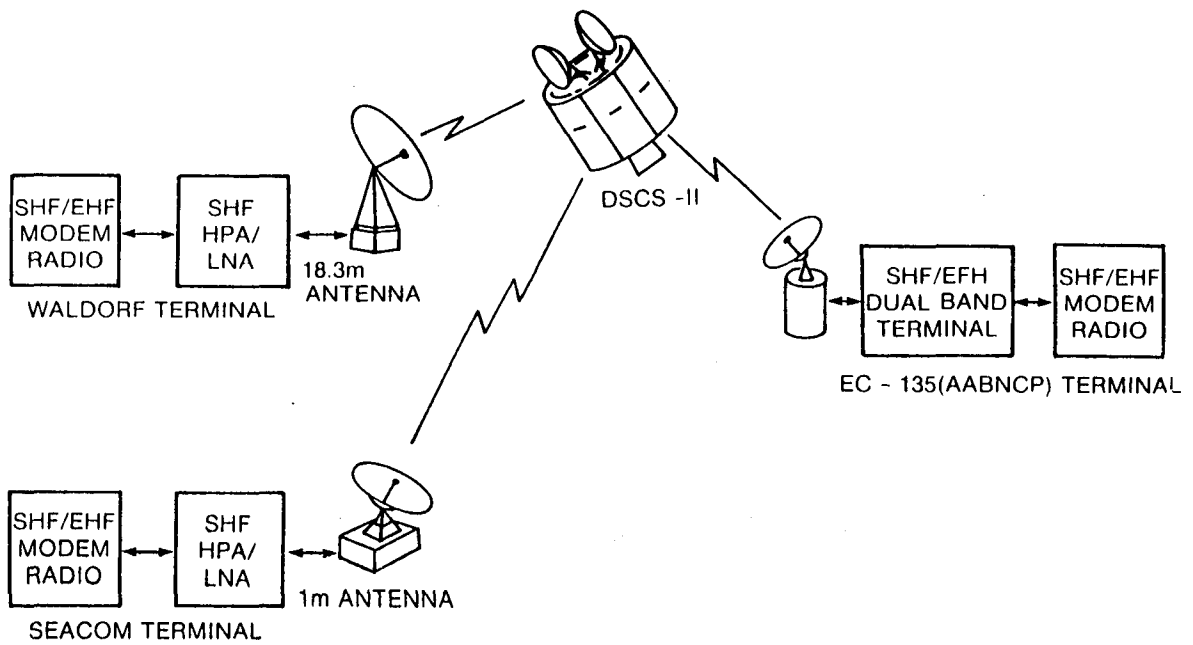


Figure 1. Test Configurations

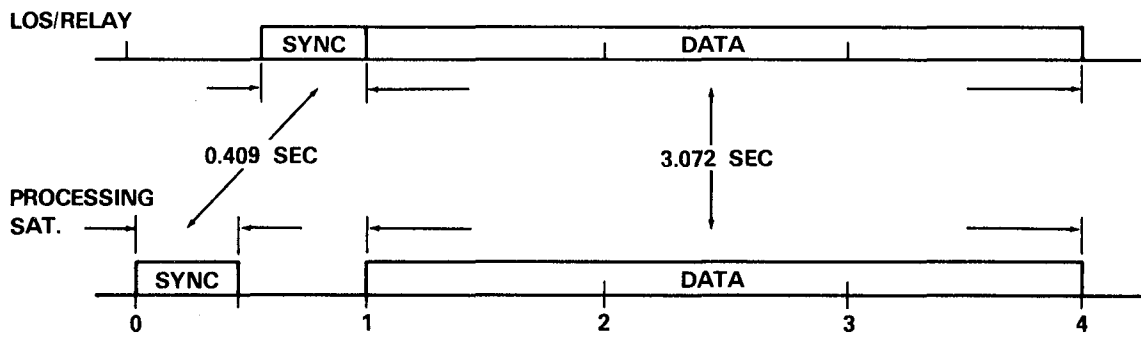


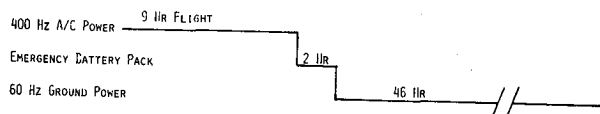
Figure 2. SEACOM Waveform: Time Slot Structure



Figure 3. C-135 Test Aircraft



Figure 4. Crew Entry Ladder for C-135



FLIGHT TIME - 9 HOURS
 LAND-TAXI - 20 MINUTES
 POST FLIGHT MAINT, DEBRIEF, WAIT FOR BUS - 1 HOUR 30 MINUTES
 (USUALLY NO POWER CART)
 BUS RIDE TO BASE OPERATIONS - 15 TO 20 MINUTES
 GETTING PERMISSION TO LEAVE STANDARD - 10 MINUTES
 GETTING ADAPTERS, PLUGGING IN - 5 MINUTES
 TOTAL GROUND TIME - 46 HOURS

Figure 5. Typical Overseas RON Operation for Rubidium Standard

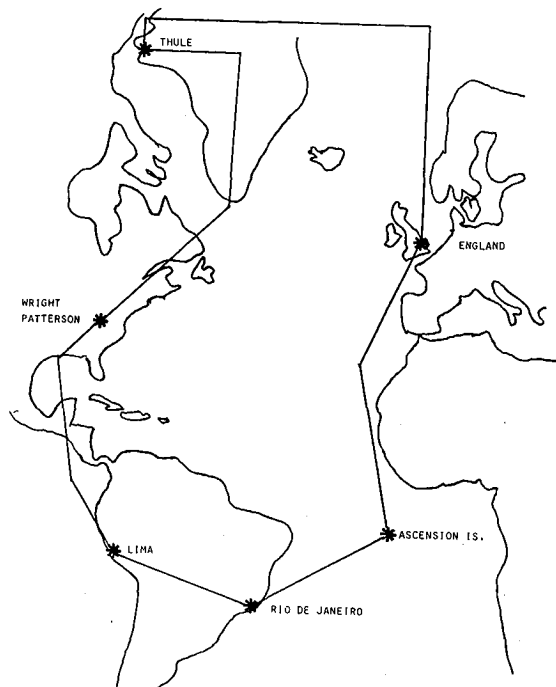


Figure 6. Overseas Test Flight Path

DATE	LOCATION	COMMENT
7 SEP	WRIGHT-PATTERSON AFB	$\frac{dF}{F} = -3.7 \times 10^{-11}$ (3.7 μ sec/DAY) SET DR
12 SEP	LEAVE WRIGHT-PATTERSON	
16 SEP	LEAVE ENGLAND	
18 SEP	ASCENSION ISLAND	CHECK WITH NASA
22 SEP	RIO DE JANEIRO, BRAZIL	POWER DISRUPTION
26 SEP	LIMA, PERU	-68 μ sec TO LES 3

Figure 7. Atlantic TDY Trip Log September 1978



Figure 8. NASA ST DN Station at Ascension Island

- HOT TURN ON
- HARDWIRE PATCH FROM CO-LOCATED CLOCK
- CARRY ON OF PORTABLE STANDARD FROM REMOTE CLOCK
- TIME SEARCH VIA RANGE INPUT THUMBWHEEL SWITCHES
- TIME COUNTDOWN VIA UHF SATCOM
- TIME COUNTDOWN VIA PHONE PATCH
- BROADCAST TIME-OF-DAY MODE (NOT OPERATIONAL)
- BROADCAST TIME-OF-DAY MODE
- SPECIAL INITIAL SYNCHRONIZATION MODE TO COVER GREATER TIME UNCERTAINTY ($\sim \pm \frac{1}{2}$ SECOND CAN BE SEARCHED IN 3 MIN)
- REDUCED PN RATE ON WAVEFORM TO REDUCE REQUIRED ACCURACY AND SHORTEN SYNCHRONIZATION TIME FOR A GIVEN TIME ERROR
- "IDEAL" PORTABLE CLOCK

Figure 10. Potential Improvements

Figure 9. Initial Synchronization Techniques (In Order of Increasing Difficulty/Reliability)

WEIGHT	< 30 LBS PER ITEM
PRIME POWER	110/230 V $\pm 20\%$ 50 - 400 Hz AUTOMATIC SELECTION
STANDBY POWER	4 HRS @ AMB. TEMP
OUTPUTS	1 PPS 5 MHz "BUSS" TIME CODE
INPUTS	1 PPS "BUSS" TIME CODE
DISPLAY	DAY, HR, MIN, SEC Δ (IPPS)
INDICATORS	ABSOLUTE MINIMUM
CONTROLS	ABSOLUTE MINIMUM (NONE ON OUTSIDE FRONT COVER)

Figure 11. The "Ideal" Portable Clock

QUESTIONS AND ANSWERS

DR. STEIN:

I think there are several programs which require just such a device as your ideal portable clock. And I believe such a device is being procured for the MECON program. Is there any cooperation between these different groups?

DR. NICHOLS:

I would say no. Raytheon is currently building a SHF satellite communications terminal for airborne uses and they are developing a portable clock for that. And I had an opportunity to go to the design review a couple of weeks ago and that portable clock was developed-- and I think that was why I put my ideal portable clock ideas up, because they developed it out of their own experience without going to the community at large and I think they are going to have problems with that clock. It has too many bells and whistles on it and they tried to make it do too many things and when they get it in the field it is just not going to work. That was my experience that the more things that could go wrong, when you get out there in these remote locations, the more that do go wrong.

MR. CHARLES GAMBEL, Air Force Metrology Center

And you said you made these tests in 1978?

DR. NICHOLS:

Yes.

MR. GAMBEL:

You said you didn't have any time in Thule, Greenland--

DR. NICHOLS:

Now, you have to remember that I am in an operational situation. I am in an airplane that is coming into a strange location and we go into the operations center, and, you know, time could be available next door, but the question is, do I know about it. And this is a problem too. Does the left hand know what the right hand is doing. You are going to say time was available in Thule.

MR. GAMBEL:

Yes. Time was available at Thule to 10 microseconds, and also was available in Hawaii. I just couldn't understand why it wasn't made available to you.

DR. NICHOLS:

Well, in Hawaii we went to PMEL and all the guy had was a WWVH receiver. It is probably another case of, maybe in another building someone had better time, but asking at the operations center, which is the people we dealt with as a transient aircraft, that was what we had to work with.

MR. GAMBEL:

Okay. Thank you.

DR. FRED WALLS, National Bureau of Standards

Let me again reiterate a plea for commonality in cooperation so that one ends up with standardized building blocks of a common frequency. And the reason for that is something that you have pointed out, several other people have pointed out, and that is survivability and reliability. If you produce a clock, a portable clock, a clock that goes in JTIDS, CTOC, or whatever, the experience has been until you make many of those things, perhaps as many as a hundred, the reliability is going to be low. And so if you have several of these, perhaps in different sets, that are all in the same frequency, they can act as reliability buffers for you, so if you have a failure in one you can use the frequency of one in another, and you get a great deal more experience so that you have many, many units deployed in the field and we can learn some of the design flaws and hardware flaws in these.

DR. NICHOLS:

I guess that fairly well summarizes what I was trying to do; the main point of my presentation.

MR. KAHAN:

Just to reiterate what Dr. Stein was mentioning, a clock, if you argue ideal conditions is being developed and further beginning with the cesium, especially for the EC-135 to go up the full ladder, up and down, that is the exact application it is being developed for.

DR. NICHOLS:

It would appear that Raytheon isn't aware of that--

MR. KAHAN:

No.

DR. NICHOLS:

--because that is not the approach they are taking.

MR. KAHAN:

I don't know about the Raytheon clock and I am not aware of that, but a cesium clock is being developed for the EC-135, portable, less than 30 pounds and all the attributes that you listed.

MR. BILL PICKSTON, Ford Aerospace Communication Corporation

I would like to know who is developing that clock?

MR. KAHAN:

It was reported on at the Atlantic City conference last summer by Frequency Electronics.

SESSION II

OUTLOOK ON NEW TECHNOLOGIES

**Dr. Samuel R. Stein, Chairman
National Bureau of Standards**

LIMITATIONS ON LONG-TERM STABILITY AND
ACCURACY IN ATOMIC CLOCKS*

D. J. Wineland
National Bureau of Standards
Boulder, Colorado

ABSTRACT

The limits to accuracy and long-term stability in present atomic clocks are examined. In order to achieve a significant increase in performance, it appears that the limitations must be attacked on a fundamental level. For instance, the problem of residual first-order and second-order Doppler shifts has for many years been approached by asking how we can better measure these shifts. A more fundamental approach might be to ask how we can significantly lower the velocity of the atoms.

An attempt will be made to put recent proposals for new frequency standards into perspective. The advantages and disadvantages of frequency standards based on such ideas as laser transitions, single atoms, and atom cooling are examined. In addition, the applicability of some of these new techniques to existing standards is discussed.

*Supported in part by the Air Force Office of Scientific Research.

INTRODUCTION

This paper attempts to answer the question: "What new ideas can lead to fundamental improvements in atomic frequency standards?" Since my answer can't be totally objective, what follows is vulnerable to criticism; nevertheless, it will be useful to examine some of these new ideas and speculate on what they might lead to.

This paper is not a survey of all new ideas for frequency standards; rather, some of these new ideas are used as examples to illustrate general areas in which fundamental problems might be attacked. Also, one will notice that the application of some of these ideas are impractical at the present time for a field usable standard, but most could be realized in a laboratory so that they may have more immediate application to a "primary" standard.

To make the problem somewhat more tractable, it will be assumed that the important question to ask is how to improve accuracy and that the improved long-term stability will naturally follow if the accuracy can be improved. I contend that this is generally true if not pushed too far; for example, if a way were found to drastically reduce wall shift, spin exchange shift, second-order Doppler shift, etc. in the H-maser then the fluctuations of these effects (which limit long-term stability) will also be reduced. We must also of course assume that we can improve the signal-to-noise so that the anticipated accuracy increase can be measured in a reasonable length of time.

In any case, the approach will be to ask not how we can better measure those effects in atomic clocks which limit their accuracy and long-term stability, but how we can get rid of them.

Later we will briefly ask what new ideas are likely to improve atomic clocks based on hydrogen, rubidium and cesium. More importantly, it will be interesting to look at other ideas for "atomic" clocks. First, however, it is useful to reexamine the ground rules—that is, what features do we really want in a frequency standard?

BASICS OF ATOMIC FREQUENCY STANDARDS

The requirements for making a good frequency standard are fairly simple^[1]:

- (1) it must be reproducible, and
- (2) it must be "reasonably usable," in the sense that it should have an output frequency easily used in measurements.

The first requirement implies that bulk devices (such as quartz crystal resonators, macroscopic rigid rotors, or superconducting cavity oscillators) are undesirable, because the frequency depends on parameters, such as size, that are difficult to control. This shortcoming does not, however, rule out the use of these devices as calibrated "flywheels" (i.e., free running, stable clocks).

Atomic (or molecular) resonances provide the necessary reproducibility; one derives a "standard" frequency ν_0 in terms of the energy difference between two states of the atom with energies E_1 and E_2 by the relation $h\nu_0 = E_2 - E_1$ where h is Planck's constant. To ensure reproducibility between different observations, the measured frequency is usually referred to the value that would be obtained in free space; consequently, various corrections are necessary to take account of environmental factors, such as magnetic fields. The problem then reduces to correcting for the

various perturbations to the measured frequency. Our task in this paper is to ask how we can significantly reduce (or adequately resolve) these perturbations.

Of course, perturbations at some level will always exist so we will also ask how we can reduce their influence. In many cases, the perturbations to the measured resonance frequency are proportional to Q^{-1} where $Q = \nu_0/\Delta\nu$, and $\Delta\nu$ is the width (in frequency units) of the energy difference measured at the half power points; therefore a high Q is desirable. Also, all measurements are limited in precision by various sources of noise. The fractional frequency stability $\sigma_y(\tau)$ relates to Q and signal-to-noise by

$$\sigma_y(\tau) \approx \left[Q \frac{S}{N}(\tau) \right]^{-1}$$

where $S/N(\tau)$ is the signal-to-noise ratio as a function of averaging time τ .

Satisfying the second requirement depends on technological limitations and may rule out some interesting frequency-standard possibilities. The output of the device (i.e., the operating frequency) must be convenient for general application. At the present time, this rules out for example, the use of certain transitions that can be observed at very high frequencies such as those in nuclei. Although the Q of these Mössbauer transitions can be as high as 10^{15} ,^[2] they are not generally usable because neither frequency nor wavelengths can be accurately measured in the gamma-ray region. In general, we can say that if we have a frequency standard which operates at a frequency ν_0 , we must be able to divide this frequency down (or multiply up a reference oscillator for comparison) in order to use the standard as a clock — that is, provide timing

signals. (We note however, that the use of the standard as a clock is not needed in some applications; for example, the gravitational red shift was first measured intercomparing the frequencies of two spatially separated samples using Mössbauer transitions.^[2])

We can summarize our criteria for a good general frequency standard as:

- (a) S/N large.
- (b) Q large.
- (c) Small perturbations to the frequency.
- (d) Must be able to measure frequency.

REALIZATION OF THE CRITERIA

We, of course, quickly learn that it is not easy to satisfy all these criteria simultaneously. Some of the reasons for this are fundamental, some are practical.

The resolution and Q is fundamentally limited by the Heisenberg uncertainty relation on time and energy:

$$\Delta E \Delta t \gtrsim \hbar/2.$$

Thus, for a single atom, if we have a time Δt to measure the energy-level difference $E_2 - E_1$, the measurement will be uncertain by at least an amount ΔE . Specifically, Δt may arise from the time of flight (transit time) of an atom through the apparatus, or from the lifetime of the atom in one or both of its energy states.

The uncertainty relation yields a fractional uncertainty in energy of $\Delta E/(E_2 - E_1) = Q^{-1}$. We can, of course, make ΔE small by making Δt large; this may be accomplished by slowing down the atoms as much as possible or by confining them. Unfortunately, the process of confinement causes perturbations such as the wall shift in the H-maser and buffer gas shifts as in the Rb frequency standard.

Also, there is often a trade-off between signal-to-noise and Q . Extremely high Q does not guarantee a good frequency standard because, if the signal-to-noise ratio is small, it may take an impractical length of time to realize the accuracy. Conversely, we can increase S/N at the expense of Q , as in gas cell standards, where S/N can be increased by increasing number, but we also increase perturbations due to atom-atom collisions.

An important category of perturbations which exists in all frequency standards to varying degrees is that of Doppler shifts. Doppler effects are related to the particular method of confinement. They represent perhaps the most important problem limiting the accuracy and resolution of existing or proposed frequency standards. In the usual way we can say that if an absorber of radiation moves relative to the source, the observed resonance frequency is shifted to the value

$$\omega_{\text{abs}} \cong \omega_0 + \vec{k} \cdot \vec{v} - \frac{1}{2} \omega_0 \left(\frac{v}{c} \right)^2 + \frac{\hbar \omega_0^2}{2Mc^2}$$

where the velocity \vec{v} and wave vector \vec{k} are measured relative to the source and M is the atomic mass. The first-order Doppler shift ($\vec{k} \cdot \vec{v}$), the "second-order" Doppler shift, $((v/c)^2)$ and the recoil shift (the last term) can be understood in terms of conservation of energy and momentum in the absorption process. The

so-called "second-order" Doppler shift is merely the relativistic time-dilation factor resulting from the movement of the atom relative to the apparatus. Its effect is small but important, particularly if we are talking about improving the state of the art. We can describe the first-order shift in terms of time dependence of a plane electromagnetic wave as seen by an atom. We have for the electric field

$$\vec{E}(x,t) = \vec{E}_0 \sin (\vec{k} \cdot \vec{x} - \omega t + \phi)$$

where \vec{x} is the atom position, \vec{k} is the field wave vector ($\vec{k} \cdot \vec{E}_0 = 0$), and ϕ is an arbitrary phase factor. If $\vec{x} = \vec{v}_x t$ then

$$\vec{E}(t) = \vec{E}_0 \sin [(\vec{k} \cdot \vec{v}_x - \omega)t + \phi]$$

and the particle sees a sinusoidally varying field of frequency $\omega' = \omega - \vec{k} \cdot \vec{v}_x$. If uncompensated, the result is the familiar Doppler broadening because, typically, the atoms in a sample have a Maxwellian velocity distribution leading to a distribution of ω' values. If one observes the full Doppler width, then the Q of the transition is limited to about 10^6 for room-temperature samples. If the particle is confined within dimensions $|\vec{x}| < k^{-1}$ (the so-called "Dicke regime")^[3] the resonance spectrum has a sharp central feature with natural width (Fig. 1).

This technique is of course used in the H-maser and Rb gas cell frequency standards and accounts for the negligible first-order Doppler effects. However, the price we have paid to avoid the first-order Doppler effect is the frequency shifts due to confinement (collision shifts).

To avoid the perturbing effects of confinement, a common approach is to use atomic beams. The most successful approach to avoid the first-order Doppler effect in this case is to make the atoms interact with the radiation in two, phase-coherent, spatially separated interaction regions. In each interaction region, the condition $\vec{k} \cdot \vec{v}_x \Delta t \lesssim 1$ is satisfied—where Wt is now the transit time through one of the interaction regions. However, the Q is now determined by the much longer transit time between interaction regions. This principle is the basis of Ramsey's separated oscillatory field technique^[4] which is used in all commercial and laboratory cesium clocks. Because it uses an atomic beam, the cesium device is free of the confining shifts, but suffers from residual first-order Doppler shifts due to the presence of running-wave components in the interaction cavities. This inability to obtain pure standing waves generally affects all of the "sub-Doppler" techniques where there is a net velocity associated with the atoms. Thus, we have a tradeoff between the confinement techniques, which "eliminate" first-order Doppler shifts but introduce perturbations due to the confinement, and the "free"-atom techniques, which have no confinement perturbation but introduce Doppler shifts. Moreover, all of the techniques, including those employing Dicke narrowing, suffer from the "second-order" Doppler shift because the atoms have a non-zero motion. Thus, if we hope to fundamentally improve the performance of frequency standards, we must address the question of Doppler shifts.

PRESENT LIMITS ON COMMON FREQUENCY STANDARDS

The limitations on accuracy and stability for present day frequency standards will be discussed more completely in another paper for this meeting by F. L. Walls. However, we briefly list the limitations and some possible cures.

Beam Devices (Cesium)

The dominant limitation appears to be due to cavity phase shift, which is a form of residual first-order Doppler effect. To first-order this effect can be measured by reversing the beam direction. It can be nulled ^[5] if measured periodically; however, exact beam retrace is required. This difficulty, along with the problem that the phase shift has a spatial dependence across the cross-section of the beam, ^[6] makes it difficult to deal with. The retrace problem and the problem of a spatially distributed phase shift are, in principle, eliminated if superconducting cavities are used. ^[7] These problems are substantially suppressed if an axially symmetric beam of small cross-section is used, ^[5] if a two-frequency interrogation method is used, ^[8] or if optical pumping state selection and detection is used. ^[8] Although the two-frequency method results in a degradation of Q by a factor of about 3, it has the advantage in possible commercial application in that beam reversal is not required to null the phase shift. ^[9] It would seem that more work needs to be invested to study these types of problems; a testament to this is the as yet unexplained frequency shift sometimes observed in cesium beam standards when the C field is reversed. ^[5,6,10,11]

Gas Cell Storage Devices (Hydrogen and Rubidium)

The fundamental limitations on accuracy appears to be due to our inability to measure the confinement shifts in the devices. For hydrogen, one might argue that the limit on long-term stability is due to cavity mistuning, but as this problem becomes solved by spin-exchange tuning ^[12] or cavity interrogating methods, ^[13] then the problem of the wall shift becomes more important. The varia-

ble volume^[14,15,16] or "large box"^[17] techniques are appealing, but have a problem in that the surfaces for both bulb configurations are not exactly the same.

The problems with the rubidium buffer gas standard are generically the same, although it suffers from incomplete spatial averaging.^[18] If coated cells are used to combat this problem,^[18] wall shifts become important. The problems associated with light shifts can be attacked using pulsing^[19] or perhaps diode laser sources.

NEW IDEAS FOR FUNDAMENTAL IMPROVEMENTS

This section attempts to highlight new ideas which may bring about fundamental improvements in atomic frequency standards. The selection of topics in this section is, of course, somewhat arbitrary, but hopefully is representative of those methods which may be applicable in the not-too-distant future. With some of these ideas it may be difficult to envisage a practical device, let alone a commercial device; however, if one has faith in the advancement of the general technology, they may in the future become quite practical.

A. Cold Atoms

The advantage of using "cold" or low velocity atoms has been realized for quite some time. Not only is the interaction time of atoms increased—thereby increasing Q in a fundamental way, but the problem of second-order and residual first-order Doppler shifts are attacked in a fundamental way. The possibility of using very slow atomic beams was investigated as early as 1953 by Zacharias in his "Fountain" experiment.^[20] In principle, only

the very slow atoms from an effusive source were selected by gravity. Unfortunately, the number of slow atoms available was too small to be useful. Since that time, various attempts have been made to produce slow atoms, but with very limited success. Some of the more recent experiments are mentioned here.

1. Cold Hydrogen: Very recently, hydrogen storage devices have been operated at cryogenic temperatures. [21,22,23,24] In the experiments of Crampton et.al., [21] the storage bulb was coated with solid H₂ at 4.2K and although their experiments showed a rather large phase shift per collision ($\cong - 0.3$ rad), this work may prove to be very useful in studies of the general problem. Moreover, a similar device might be used to generate a cold beam of polarized atomic hydrogen in other frequency standard schemes. In the work of Vessot et.al., [22] maser oscillation was achieved down to 25K and Q's of $\sim 2 \times 10^9$ were observed at 50K using a surface of tetrafluoromethane. Aside from the reduction in second-order Doppler shifts, low temperature H-storage devices have the following possible advantages:

- a. Thermal noise is substantially reduced. [23,25]
This affects the intrinsic maser stability and can also reduce the additive white phase noise, which is external to the maser.

- b. Spin exchange collision rates are reduced by about two orders of magnitude. [23,25] Hence, the maser could operate with higher line Q at increased flux. At higher flux, the power could be increased [25] or the maser operated with lower cavity Q, [23] thus reducing cavity pulling.

c. Mechanical rigidity should be more easily maintained at low temperatures^[23,25] resulting in more stable cavity pulling, etc.

Investigations will continue to search for wall coatings (perhaps frozen inert gases) which will give stable surfaces with small wall shift. Such investigations may hopefully give very good results in the future.

2. Laser Cooling: Aside from the interesting results obtained with hydrogen, there have been many attempts to make cryogenic beam sources for other atoms, but temperatures below about 50K have been difficult to achieve. In 1975, independent proposals were made to cool down a gas of neutral atoms^[26] or ions bound in an electromagnetic trap^[27] using radiation pressure. Since then, substantial cooling (<0.5K) has been achieved for bound ions^[28] and although only very limited atomic beam cooling has yet been obtained,^[29] the potential for substantial cooling exists.

For free atoms or weakly bound ions (motional vibration frequency \ll optical transition linewidth), the cooling process is explained^[30] by simply considering conservation of momentum and energy in a photon scattering event. If we average over the possible directions of reemission, we can find the average kinetic energy change per scattering event to be^[30]

$$\Delta K.E. (\text{atom}) = \hbar \vec{k} \cdot \vec{v} + 2R \quad (1)$$

where R is the "recoil" energy $R = (\hbar k)^2/2M$, \vec{k} is the photon

wave vector and \vec{v} is the atomic velocity before the scattering event. Since the scattering process is resonant, we can tune our light source (laser) below the atomic rest frequency, so that the atoms absorb only when they move toward the laser. Thus, we can make $\hbar\vec{k} \cdot \vec{v} < -2R$ and the atoms lose kinetic energy. Qualitatively, the atom's motion is retarded when it moves toward the laser because it receives a momentum kick in a direction opposite to \vec{v} for each scattering event.

This cooling process makes the possibility of stored ion frequency standards more attractive (see below), but a practical scheme for producing a slow atomic beam of adequate flux has not yet been demonstrated. Nevertheless, the possibility^[30] of very low temperatures ($< 10^{-3}$ to 10^{-4} K for strongly allowed transitions, less for weakly allowed transitions) makes this an attractive area of investigation.

B. Optical Traps

In the last few years, a fair number of papers have been written about the possibility of trapping neutral atoms in near-resonant light fields.^[31] More recently, the dipole forces necessary for optical trapping have been demonstrated by a group at Bell Labs.^[32] Such trapping is very attractive because atoms could be trapped in "cells" of a standing wave light field of dimensions $\lambda/2$. Hence, the potential confinement is extremely tight, i.e., the atoms would be well localized. The main disadvantage of this method for spectroscopy appears to be that in order to provide trapping, an optical transition must be driven at near saturation. Hence, any transition that might be interesting enough to provide a frequency standard would be broadened by the laser and also

subject to substantial light shifts. It would seem that the cure for this problem would be to turn off the "trapping" laser while the frequency standard transition is investigated. However, even if the theoretical limit^[30,31] on laser radiation pressure cooling could be obtained, the velocity is still rather high (for Na atoms $v_{\min} \approx 30$ cm/sec) and the atoms would diffuse away from the trapping region while the trapping fields are off.

Even if a way around these difficulties is not found, the optical traps might be incorporated with laser cooling to provide a cold beam source. For example, the optical trap might be in the form of a tube (focused Gaussian laser beam) in which the atom could be laser cooled and then allowed to escape from one end. As yet, a practical scheme for this has not been suggested.

C. Stored Ions

The possibility of obtaining very high resolution spectroscopy with ions stored in electromagnetic traps had been realized very early by Dehmelt and was developed in the early stages by him and his co-workers.^[33] Since that time, the radio-frequency (r.f.) trap has been developed to give rather encouraging numbers for an optically pumped ion standard. Noteworthy are the experiments of Major and Werth on mercury, which have been extended by others.^[34] This device uses optical pumping—double resonance (pumping from a lamp) to detect the ground state hyperfine resonance in $^{199}\text{Hg}^+$ (~ 40 GHz) and gives estimated stabilities near $\sigma_y(\tau) \approx 10^{-12} \tau^{-1/2}$. This success has prompted at least one commercial company to investigate the feasibility of such a standard.

The development of ion-storage frequency standards has been slowed somewhat because:

- (1) The number of ions that can be stored is very small (typically a maximum of about 10^6 for a trap with ~ 1 cm dimensions). This, coupled with the problem of the relatively low intensity of light from lamp sources for optical pumping and detection, has made resonance signals fairly weak.
- (2) The presence of significant second-order Doppler shifts in experiments with traps (particularly r.f. traps) has been recognized for some time. Although one has various ways of measuring the velocity distribution,^[35] this problem poses a serious limitation.

It may now be possible to overcome these limitations by using tunable lasers. By using a laser for optical pumping and detection, rather remarkable signals can be obtained. This is evidenced in two experiments^[28]:

- (1) In the NBS experiments on Mg^+ , the scattered photons from only about 500 Mg^+ ions stored in a Penning trap were observed with a signal to background of about 100. In this same experiment, the count rate was about 25,000/sec, while the net detection efficiency was only about 3×10^{-5} . This could be increased by 2 orders of magnitude in future designs.
- (2) More dramatically, in the experiments at Heidelberg, a single Ba^+ ion contained in a miniature r.f. trap was photographed with good contrast.

In both of these experiments, the ions were laser cooled to substantially less than 1 K, hence the second-order Doppler shift was greatly suppressed.

Other advantages occur if one uses a laser in an ion storage experiment:

- (1) Extremely weak optical pumping processes can be realized. This was demonstrated in the experiments at NBS where $^{25}\text{Mg}^+$ was pumped into the ($M_J = -\frac{1}{2}$, $M_I = -\frac{5}{2}$) ground state. Although many absorption-reemission cycles are required for this pumping to occur, this is acceptable since the ions remain in the trap essentially indefinitely, and laser intensities can nearly saturate the optical transition.

- (2) Transitions in double resonance experiments can be detected with nearly unit efficiency. In the experiments at NBS, the ions were caught in an optical trap (to be distinguished from spatial optical traps described earlier). That is, the ions were optically excited from a particular ground state level to a particular excited state level and (by selection rules) were forced to fall back into the original ground state level (this process can be repeated at very high rates). Thus, if we can arrange to drive a microwave transition (which will be, say, our frequency standard transition) that populates (or depopulates) the lower optical level, then we can produce (or exclude) many scattered optical photons for each ion that has made a microwave transition.^[36] This process allows one to compensate for the

loss in collection efficiency due, for example, to small solid angle or small quantum efficiency in the photon detector so that we can effectively detect atoms with unit efficiency (The ability to achieve many scattered photons for one microwave photon was realized in ref. 36, but the S/N was incorrectly over-estimated). For example, if we can trap 10^6 ions, then the signal-to-noise in the detection process can be about 10^3 , even though we may collect only about 1% of the total scattered photons.

It is useful to briefly compare the r.f. and Penning traps for possible frequency standard application. As is often pointed out, the r.f. trap has the potential advantage that magnetic fields are not required so that magnetic field induced frequency shifts do not pose a problem. However, this apparent difficulty can be overcome in the Penning trap by working at field extremum points.^[36,37] A disadvantage of the r.f. trap not shared by the Penning trap is the effect of r.f. heating. Although not totally understood, it has prevented cold temperatures from being achieved except for very small numbers of ions. A possible disadvantage of the Penning trap is that the ions are in an unstable equilibrium in the trap; whereas, for the r.f. trap, the orbits are stable. This problem appears to have been overcome in recent experiments however, and indefinite confinement in a Penning trap should be possible.^[38] At this point, it is unclear which type of trap will ultimately be better and more experiments are needed to decide this question. Perhaps a more important question to be addressed in the immediate future is how to get better optical sources for pumping and detection at the required frequencies. Simple schemes^[39] are difficult to come by, but this difficulty

can be partially overcome by finding narrow band sources farther in the u.v. (< 210nm).

Nevertheless, ion trap derived standards are extremely attractive because they satisfy the confinement problem without causing significant perturbations (essentially indefinite confinement appears possible—implying no first-order Doppler shifts and confinement shifts are estimated to be below 10^{-15}). In this regard, they may be unique and deserve more attention in the future.

D. Laser Standards

With high probability, the frequency and time standards of the future will be based on optical transitions in atoms or molecules. This conjecture relies mainly on the idea that in a given system, if the lifetime of the transition remains reasonably fixed due to relaxation, transit time, etc., then the Q of the transition scales with frequency. However, before laser standards are realized, some crucial obstacles must be overcome. These problems are addressed below (see also a detailed review of precision, stable lasers by J. Hall^[40]).

In contemplating laser standards, one first must realize that we are likely to be more susceptible to first-order Doppler shift since the wavelength of the radiation is so small; i.e., the Dicke criterion is harder to realize. However, the confinement criterion can be relaxed in important ways.

When we cannot meet the condition $|\vec{x}| \ll k^{-1}$, there is still the possibility of obtaining the same effect if we can satisfy the

more general condition $\vec{k} \cdot \vec{v}_x \Delta t \lesssim 1$, where Δt is the transit time of the atom through the apparatus. This is the general condition that must be met in a molecular beam apparatus. It allows for saturated absorption ("Lamb-dip") spectroscopy where atoms satisfying this condition are preferentially detected. Qualitatively, in this case, the detected atoms traverse the apparatus in a direction nearly normal to the traveling-wave propagation direction, and, therefore, the spatial phase change of the field experienced by the atoms is less than one radian.

The confinement problem has a rather unique solution, in the form of Doppler-free, two-photon spectroscopy. Here the atom interacts with counter-propagating plane waves of frequency $\nu_0/2$. The atom can resonantly absorb two photons simultaneously, one of frequency $1/2\nu_0(1 + \vec{v} \cdot \hat{k}/c)$ from one of the running waves and one with frequency $1/2\nu_0(1 - \vec{v} \cdot \hat{k}/c)$ from the counterrunning wave. The total energy from the two photons is $h\nu_0$, independent of the atomic velocity (to first order). Important applications exist in the optical region,^[41] but the technique may be limited in accuracy by dynamic Stark shifts resulting from the required intense light field.

Therefore, the problem of first-order Doppler shifts can be solved, but as is true in the case of microwave frequency standards, residual first-order Doppler shifts can occur.^[40] Moreover, the second-order Doppler shift remains unchanged.

As of now, rather impressive performance has been achieved with laser standards. For example,^[40] methane stabilized He-Ne lasers have been used to probe external methane resonances using saturation spectroscopy with $Q > 10^{11}$ and stabilities of 10^{-14} . However,

the velocity distribution of the interrogated molecules is difficult to evaluate and accuracy capabilities better than 10^{-13} will be difficult to achieve. In an experiment using a dye laser to observe saturated absorption resonances in an atomic Ca beam,^[42] line Q's greater than 10^{11} were observed; however, a primary limitation in accuracy in this experiment, as well as those on CH_4 , was the uncertainty in the second-order Doppler shift. Therefore, we note that possible laser standards must be attacked on a similar front as the microwave standards—that is, how can we reduce the Doppler shifts? Certainly some of the same cooling techniques as mentioned previously can be used; in addition, the use of ions stored in a trap will have the advantage of long confinement time with small perturbations.

Before such laser standards can be realized, we must solve two other basic problems:

- (1) Stable laser sources must be found. As in the microwave case, the local oscillators used in optical frequency standards must have the required short-term stability or the desired accuracy will not be realized in a reasonable length of time. At present, some gas-discharge lasers meet this requirement^[40]; however, these lasers are very limited in tuning and therefore only in rare instances have a frequency which coincides with a transition in a molecule or atom that might give a frequency standard. Dye, diode, and color center lasers give the desired tunability; however, this wide tunability and fluctuations in the dye medium, for example, make them far less stable. Nevertheless, superior stabilization schemes and perhaps new lasers will undoubtedly be found

and the problem of (local-oscillator) short-term stability will be solved.

- (2) If one desires to use a frequency standard as a time standard, one must in effect be able to count cycles of the oscillation. Phase-coherent measurements are at present very difficult to carry out at frequencies above about 100 GHz. However, by using harmonic mixing techniques in a boot strap fashion,^[43] laser frequencies have now been compared to the cesium hyperfine frequency. This has so far only been done in a non phase-coherent way in a frequency synthesis chain such as that of ref. 43 shown in Fig 2. Accuracies of intercomparison are near the 10^{-10} level. In order for an optical frequency standard to provide time, phase-coherence would have to be included at each step in this chain. This seems to be a fairly complicated (although achievable) proposition even if somewhat more simplified chains^[43] are realized. In dealing with this problem, one should of course recall that there are other uses of frequency standards than providing time. For example, some very interesting tests of gravitational effects can be examined^[40,44] using optical frequency standards, if all that is required is to intercompare two optical frequencies—a task which is trivial compared to providing time. However, the time problem is very important and a solution to the frequency synthesis problem should be sought. A conceptually simple but unproven scheme^[45] might be able to accomplish one-step frequency division from optical frequencies to microwave frequencies.

E. Single Atom (Ion) Frequency Standards

The idea of using a single atom is, of course, very appealing since, if suitably confined, it can be isolated from the perturbing influence of other atoms. Dehmelt was the first to suggest such an idea.^[46] He proposed to use an optical transition in Tl^+ ($^1S_0 \leftrightarrow ^3P_0$ transition @ 202 nm $Q \cong 10^{14}$) in an r.f. trap. The additional advantage of using a single ion confined to the center of an electromagnetic trap is that combined with laser cooling, it should be possible to closely satisfy the Dicke criterion in the optical region on an essentially unperturbed atom. Other possibilities exist, such as the B^+ ion, whose structure is shown in Fig. 3. This ion is also interesting because the fine structure transitions with $Q \gtrsim 10^{11}$ could provide a possible standard where the frequencies are fairly easily measured with state of the art precision. (This experiment could also of course be performed on a cloud of ions in a trap).

The primary drawback to using a single ion (or perhaps a single neutral atom in an optical trap) is that the S/N is rather poor. Therefore, single ion standards would seem to be more viable at very high frequencies where the Q can be quite high. Since the perturbations between many cold ions in an electromagnetic trap can be very small anyway, the use of a single ion may only be a philosophical advantage if one uses longer wavelengths. Of course, only the future will tell!

REFERENCES

- [1] H. Hellwig, K. M. Evenson, and D. J. Wineland, *Physics Today* 31, 23 (1978).
- [2] See for example: R. V. Pound, Proc. 2nd Freq. Stds. and Metrology Symposium, Copper Mountain, Colorado, July, 1976, p. 531.
- [3] R. H. Dicke, *Phys Rev.* 89, 472 (1953).
- [4] N. F. Ramsey, *Molecular Beams*, Clarendon, Oxford (1956).
- [5] G. Becker, *IEEE. Trans. Instr. Meas.* IM-27, 319 (1978). See also paper from this conference.
- [6] H. Hellwig, Proc. 5th Conf. on Atomic Masses and Fundamental Constants, ed. by J. Sanders and A. Wapstra, Plenum, 1976, p. 330. D. W. Allan, H. Hellwig, S. Jarvis, Jr, D. A. Howe and R. M. Garvey, Proc. 31st Ann. Symp. Frequency Control (U.S. Army Electronics Command, Fort Monmouth, N.J.) 1977, p. 555.
- [7] D. J. Wineland, *Metrologia* 13, 121 (1977).
- [8] R. M. Garvey, H. Hellwig, Stephen Jarvis, Jr., and D. J. Wineland, *IEEE.* IM-27, 349 (1978).
- [9] S. Jarvis, Jr., D. J. Wineland and H. Hellwig, *J. Appl. Phys.* 48, 5336 (1977).
- [10] A. G. Mungall, *Metrologia* 12, 151 (1976).
- [11] D.J. Wineland and H. Hellwig, *Metrologia* 13, 173 (1977).
- [12] S. B. Crampton, Thesis, Harvard Univ., 1964 (unpublished), C. Audoin, P. Lesage, J. Viennet and R. Barillet, Proc 32 Ann. Symp. Freq. Control (U.S. Electronics Command, Fort Monmouth, N.J.), 1978, p. 531.
- [13] F. L. Walls and H. Hellwig, Proc. 30th Ann. Symp. Freq. Control (U.S. Army Electronic Command, Fort Monmouth, N.J.) 473 (1976).
- [14] D. Brenner, *J. Appl. Phys.* 41, 2947 (1970).

- [15] P. E. Debely, Proc. 24th Ann. Symp. Freq. Control (U.S. Army Electronics Command, Fort Monmouth, N.J.) 1970, p. 259, P. Petit, M. Desaintfuscian, and C. Audoin, Proc. 31st Ann. Symp. Freq. Control (U.S. Army Electronics Command, Fort Monmouth, N.J.) 1977, p. 520.
- [16] J. Vanier and C. Audoin, Proc. 29th Ann. Symp. Freq. Control (U.S. Army Electronics Command, Fort Monmouth, N.J.) 1970, p. 371.
- [17] E. E. Uzgiris and N. F. Ramsey, Phys. Rev. A1, 429 (1970). V. Reinhardt, Proc. Freq. Standards and Metrology Seminar, Laval Univ., QUEBEC, Canada, Sept 1971, p. 158.
- [18] A. Risley, S. Jarvis Jr., and J. Vanier, Proc. 33rd Ann. Symp. Freq. Control (U.S. Army Electronic Command, Fort Monmouth, N.J.) 1979.
- [19] T. C. English, E. Jechart, and T. M. Kwon, Proc. 10th Ann. PTTI Appl and Planning Meeting, (Goddard Space Flight Center, Greenbelt, Md.) 1979, p. 147.
- [20] J. R. Zacharias, Phys. Rev. 94, 751 (1954).
- [21] S. B. Crampton, T. J. Greytak, D. Kleppner, W. D. Phillips, D. A. Smith, and A. Weinrib, Phys. Rev. Lett. 42, 1039 (1979).
- [22] W. N. Hardy, A. J. Berlinsky, and L. A. Whitehead, Phys. Rev. Lett. 42, 1042 (1979).
- [23] R. F. C. Vessot, E. M. Mattison, and E. L. Blomberg, Proc. 33rd Ann. Symp. Freq. Control (U. S. Army Electronics Command, Fort Monmouth, N.J.) 1979. R. F. C. Vessot, M. W. Levine, and E. M. Mattison, Proc. 9th Ann. PTTI Appl. and Planning Meeting, (Goddard Space Flight Center, Greenbelt, Md.) 1978, p. 549.
- [24] See also: M. E. Peters, Proc. 26th Ann. Symp. Freq. Control (U.S. Army Electronics Command, Fort Monmouth, N.J.) 1973.

- [25] S. B. Crampton, W. D. Phillips, and D. Kleppner, *Bull. Am. Phys. Soc.* 23, 86 (1978).
- [26] T. W. Hänsch and A. L. Schawlow, *Opt. Commun.* 13, 68 (1975).
- [27] D. J. Wineland and H. Dehmelt, *Bull. Am. Phys. Soc.* 20, 637 (1975).
- [28] D. J. Wineland, R. E. Drullinger, and F. L. Walls, *Phys. Rev. Lett.* 40, 1639 (1978). W. Neuhauser, M. Hohenstatt, P. Toschek, and H. Dehmelt, *Phys. Rev. Lett.* 41, 233 (1978). R. E. Drullinger, and D. J. Wineland, Laser Spectroscopy IV, ed. by H. Walther and K. W. Rothe, Springer-Verlag, Heidelberg, 1979, p. 66. W. Neuhauser, M. Hohenstatt, P. E. Toschek, H. G. Dehmelt, Laser Spectroscopy IV, ed. by H. Walther and K. W. Rothe, Springer-Verlag, Heidelberg, 1979, p. 73.
- [29] V. I. Balykin, V. S. Letokhov, and V. I. Mishin, *Letters to ZhETF* 29, 614 (1979).
- [30] D. J. Wineland and W. M. Itano, *Phys Rev.* A20, 1521 (1979).
- [31] See, for example, J. E. Bjorkholm, R. R. Freeman, A. Ashkin, and D. B. Pearson, *Phys. Rev. Lett.* 41, 1361 (1978), A. Ashkin, *Phys. Rev. Lett.* 40, 729 (1978), V. S. Letokhov, V. G. Minogin, and B. D. Pavlik, *Zh. Eksp. Teor. Fiz.* 72, 1328 (1977), *Sov. Phys. JETP* 45, 698 (1977), A. P. Kazantsev, *Usp. Fiz. Nauk.* 124, 113 (1978). *Sov. Phys. Usp.* 21, 58 (1978), A. Ashkin and J. P. Gordon, *Opt. Lett.* 4, 161 (1979).
- [32] J. E. Bjorkholm, R. R. Freeman, A. Ashkin, and D. B. Pearson, Laser Spectroscopy IV, ed. by H. Walther and K. W. Rothe, Springer-Verlag, Heidelberg, 1979, p. 49.
- [33] H. Dehmelt, in Advances in Atomic and Molecular Physics, ed. D. R. Bates and I. Esterman (Academic, New York, 1967 and 1969) Vols. 3 and 5.

- [34] F. G. Major and G. Werth, Phys. Rev. Lett. 30, 1155 (1973).
M. D. McGuire, R. Petsch, and G. Werth, Phys. Rev. A. 17,
1999 (1978). M. Jardino, F. Plumelle, M. Desaintfuscien,
and C. Audoin, Proc. Int. Cong. of Chronometry, Geneva,
Sept. 1979. G. Werth, Proc. Int. Cong. of Chronometry,
Geneva, Sept. 1979.
- [35] H. A. Schuessler, Appl. Phys. Lett. 18, 117 (1971). F. G.
Major and J. L. Duchene, J. de Physique 36, 953 (1975).
- [36] F. L. Walls, D. J. Wineland, and R. E. Drullinger, Proc.
32nd Ann. Symp. Freq. Control (U.S. Army Electronics Command,
Fort Monmouth, N.J.) 1978, p. 453.
- [37] F. Strumia, Proc. 32nd Ann. Symp. Freq. Control (U.S. Army
Electronics Command, Fort Monmouth, N.J.) 1978, p. 444.
- [38] D. J. Wineland, R. E. Drullinger, J. C. Bergquist, and W. M.
Itano, Bull. Am. Phys. Soc. 24, 1185 (1979).
- [39] W. M. Itano and D. J. Wineland, Bull. Am. Phys. Soc. 24,
1185 (1979).
- [40] J. L. Hall, Science 202, 147 (1978).
- [41] T. W. Hänsch, Physics Today, May 1977, p. 34.
- [42] J. C. Bergquist, R. L. Barger, and D. J. Glaze, Laser
Spectroscopy IV, ed. by H. Walther and K. W. Rothe,
Springer-Verlag, Heidelberg, 1979, p. 120. R. L. Barger,
T. C. English and J. B. West, Proc. 29th Ann. Symp. Freq.
Control (U.S. Army Electronics Command, Fort Monmouth, N.J.)
1975, p. 316.
- [43] D. A. Jennings, F. R. Peterson, and K. M. Evenson,
Laser Spectroscopy IV, ed. by H. Walther and K. W. Rothe,
Springer-Verlag, Heidelberg, 1979, p. 39.
- [44] A. Brillet and J. L. Hall, Laser Spectroscopy IV, ed. by H.
Walther and K. W. Rothe. Springer-Verlag, Heidelberg, 1979,
p. 12.

- [45] D. J. Wineland, J. Appl. Phys. 50, 2528 (1979). J. C. Bergquist and D. J. Wineland, Proc 33rd Ann. Symp. Freq. Control (U.S. Army Electronics Command, Fort Monmouth, N.J.) 1979.
- [46] H. G. Dehmelt, Bull. Am. Phys. Soc. 18, 1521 (1973) and 20, 60 (1975).

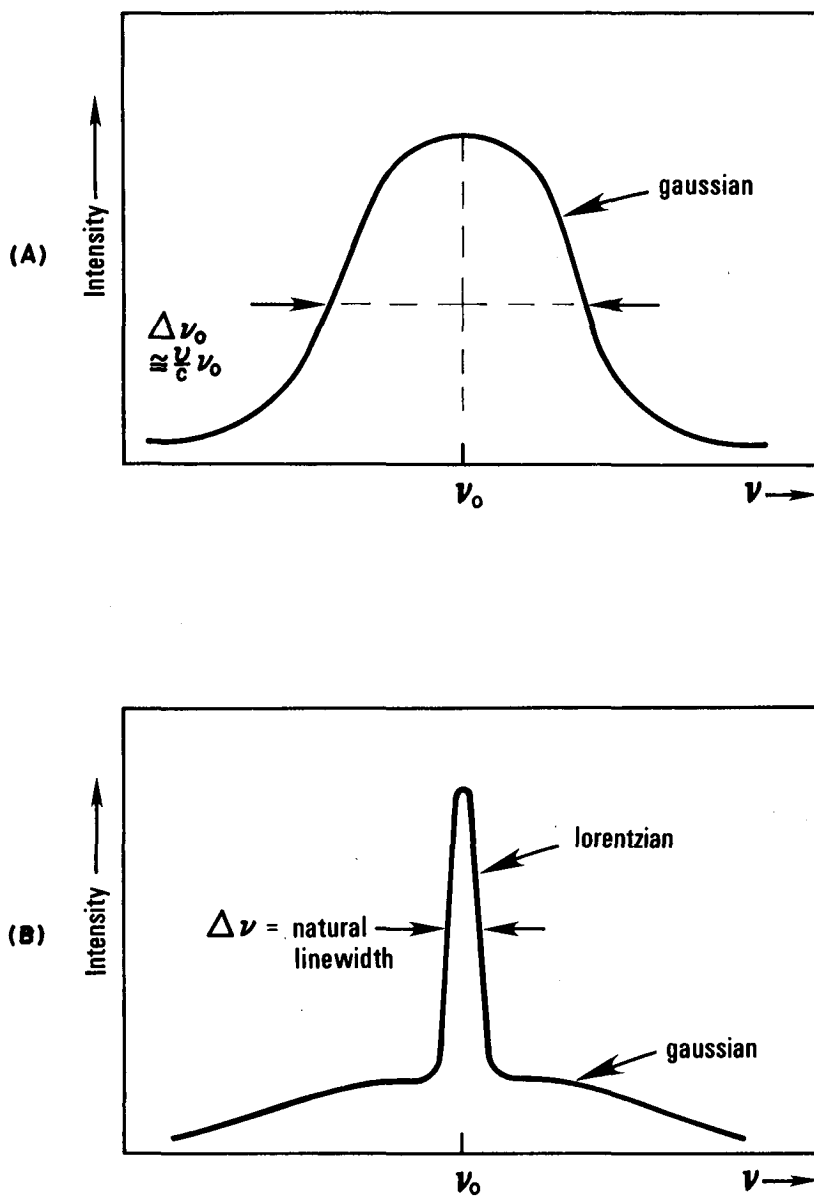


FIGURE 1. Part A shows the situation when the atoms are unbound and the resonance feature has the full Doppler width $\Delta \nu_D \approx (v/c)\nu_0$. When the atom is confined to dimensions less than the wavelength, the Doppler profile is suppressed and the central feature has the natural width $\Delta \nu$. This condition is most easily realized in the microwave region of the spectrum.

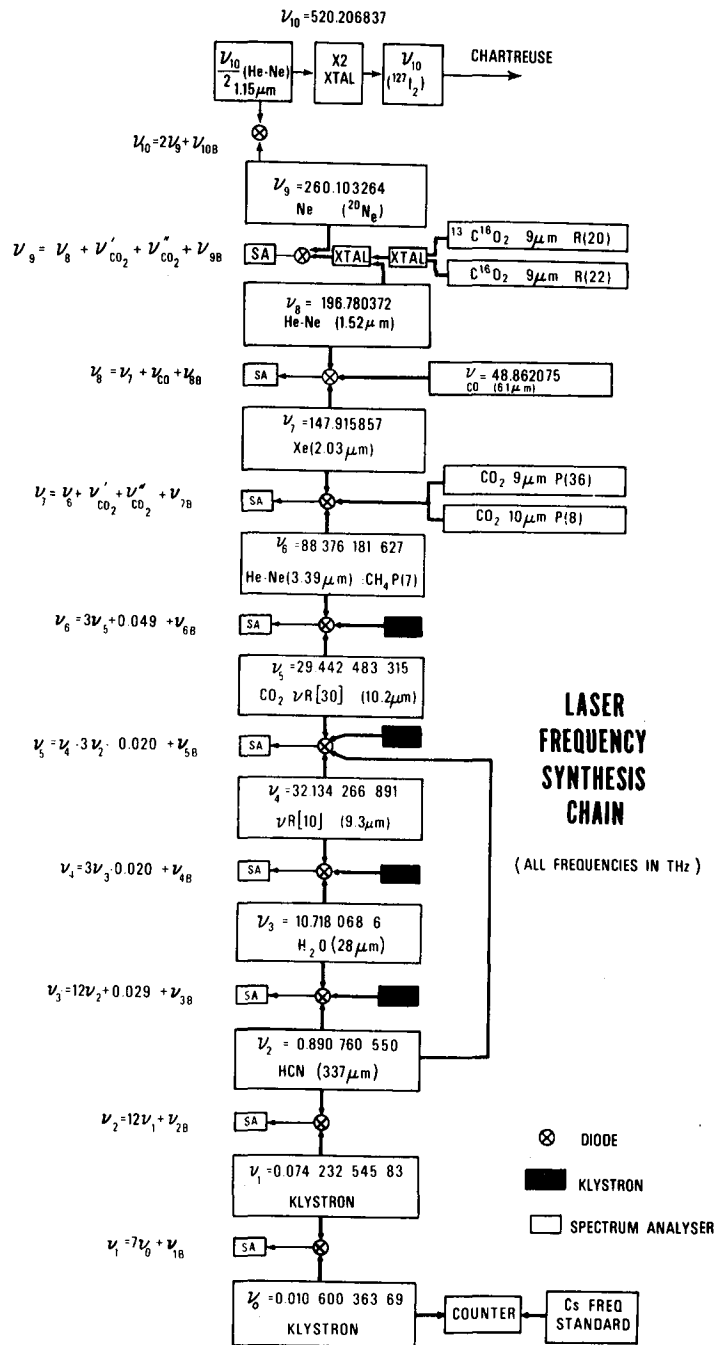


FIGURE 2. Synthesis "chain" used at NBS^[43] to measure visible laser frequency.

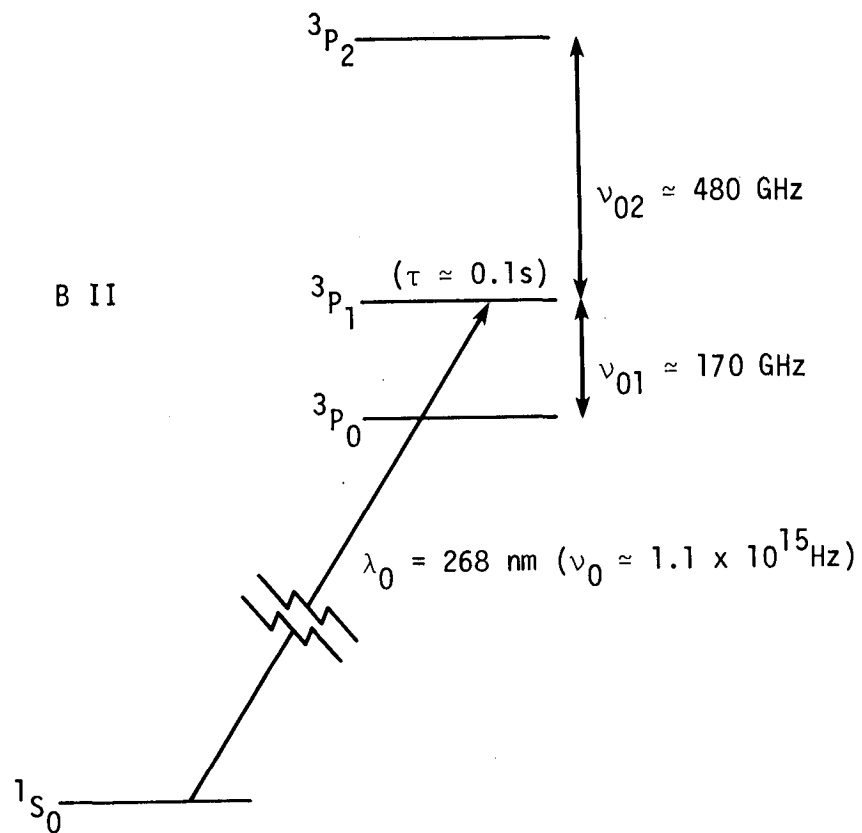


FIGURE 3. Energy level scheme of singly ionized Boron showing energy separations of interest.

QUESTIONS AND ANSWERS

DR. VESSOT:

Just a couple of comments. First, I think, I might remind you that the idea of running a cold clock came from Zacharias in 1958 and 1959, and I know because I was sweating bullets trying to get a cesium maser to work. And Zak had the idea, which I think is an excellent one. Remember that fountain experiment which did not work because of no slow atoms, he thought the idea might have been to buffer these gases to a slow velocity. So he took a beam of cesium and ran it into a cavity at 2 kelvins, where we had a buffer gas of helium. It didn't work. We looked for 10 to the minus 18 watts and didn't find any. But I think it was the germ of the idea of going to low temperatures.

The other thing is that, it is a minor point, but I thought I would bring it up, in that Blomberg, Madison, and I have gotten to 25 kelvins to make the maser oscillate and the importance of that is, it is not just a question of how close can you get, but I think we are getting close to another threshold and that is superconductivity. And if we can use superconducting effects for magnetic shields and perhaps improve a bit the Q of the cavity, which is really a very minor point, because you don't want any at those temperatures, but at least improve the power transfer, the RF power. There are some marvelously useful properties there that I think can be exciting.

QUESTION:

There was quite a bit of published work on a heat clock using magnesium that was done in Italy by a man named Luria, and three papers were published and then it suddenly disappeared. And I would like to know what happened? It seemed very promising.

DR WINELAND:

Okay. I think you are talking about the infrared, rather high microwave transitions in the finite structure of magnesium? Okay. I don't know the status of that work at present. I know, for example, that Strumia was working on it. Dr. Leschiutta may want to comment on that.

DR. LESCHIUTTA:

Yes, thank you. The problem is dissipation after they have made the magnesium beam, we ran into serious problems in order to obtain enough microwaves at the right frequency. We made a synthesis of

the frequency but with a power level not sufficient in order to detect the transition. This was the major problem.

And second, the work was stopped in the last year because, I must confess, the people who were working on that magnesium standard left. We hope to resume that work but at the moment the work is stopped. Thank you very much.

DR. WINELAND:

Let me also add that there is another group working on that, at least one other group, and that is -- I am afraid I don't know the leader, but at least the guy who is really doing the work, or at least part of the work is Bill Bloomberg at Lincoln Labs. And they, for example, are using Schotky diodes to mix and generate millimeter waves to interrogate, for example, just those transitions. I know they are thinking about magnesium. But I don't know the status of that work.

QUESTION:

But that is not a beam though.

DR. WINELAND:

At present it is not, but I know they are thinking about beams for the future. The idea is the same.

MR. HARRY PETERS:

I thought I would mention in relation to hydrogen, there was some work at Goddard Space Flight Center about five years ago with a hydrogen beam device where nice resonances in a real device were obtained with atoms which were at 10 degrees kelvin. These used a source similar to a hydrogen maser source but which was cooled with liquid nitrogen and low velocity atoms were selected from that. I think it still has possibilities.

DR. WINELAND:

Yes, Harry. I apologize. I am aware of that work. I tried to uniformly slight the various fields. I had trouble covering the different ideas but I am aware of that work and I apologize for not being able really to cover some of those other interesting things.

THE PERFORMANCE OF PRIMARY Cs BEAM CLOCKS USING
QUADRUPOLE AND HEXAPOLE DEFLECTION SYSTEMS.
CONSEQUENCES FOR TIME KEEPING

Gerhard Becker

Physikalisch-Technische Bundesanstalt
D-33 Braunschweig, Federal Republic of Germany

ABSTRACT

Since 1978 the time-and-frequency standard CS1 of the Physikalisch-Technische Bundesanstalt (PTB) has operated continuously as a "primary clock". Its uncertainty ($7 \cdot 10^{-15}$) is considerably smaller than that of the other existing primary standards. CS1 is equipped with a combination of quadrupole and hexapole magnets and uses a longitudinal C-field. Consequences of utilizing primary clocks of this quality for the generation of the International Atomic Time Scale TAI are discussed.

INTRODUCTION

In contrast to the other existing primary time and frequency standards the Cs standard CS1 of the Physikalisch-Technische Bundesanstalt (PTB) is equipped with a two-dimensional beam deflection system and a longitudinal C-field. Details of the construction and the performance can be found in /1, 2, 3, 4/. Uncertainty evaluations were published in 1969 /5/, 1974 /6/ and 1979 /7/. Measurements of the frequency of the International Atomic Time Scale TAI carried out since 1969 with CS1 have revealed for the first time a rather strong frequency deviation from nominal and a frequency drift of TAI of about $-1 \cdot 10^{-13}$ per year /8/.

In 1974 the uncertainty of CS1 was evaluated at $26 \cdot 10^{-15}$ using the beam reversal method and selecting slow atoms in the beam. Since it was thought at that time that unknown frequency shifting effects might exist, the uncertainty of CS1 was settled at $1.5 \cdot 10^{-13}$ (1σ). In the course of further experimental and theoretical investigations /3, 4, 9/ it was possible to gradually reduce the uncertainty. The 1979 evaluation /7/ resulted in an uncertainty of $7 \cdot 10^{-15}$ (1σ) and an instability of $4 \cdot 10^{-15}$, both values based on a measurement time of 80 d (Table 1).

CS1 is one of the three standards used for the "steering" of the TAI frequency. The other standards have been developed at the National Research Council (NRC), Canada, /10/ (the 1σ uncertainty of the standard CsV being $53 \cdot 10^{-15}$) and at the National Bureau of Standards (NBS), USA, /11/ (the 1σ uncertainty of the standard NBS-6 being $85 \cdot 10^{-15}$).

Since July 1978 CS1 has operated continuously as a "primary clock". The NRC standard has operated continuously since 1975 /12/. The NBS performs about one TAI frequency calibration with reference to NBS-6 per year.

The quality of CS1 is based on the following:

- a. principal advantages of the quadrupole/hexapole beam deflection and a longitudinal C-field
- b. specific technical design of CS1
- c. operating practice of CS1

Principal qualities of Cs beam standards with a quadrupole/hexapole deflection system

Holloway and Lacey proposed a flop-in Cs beam standard with hexapole magnets, a coaxial resonator and a ring detector /13/. The realization of a coaxial resonator with an interaction length of about 0.8 m failed at the PTB. Little chance was given for the usefulness of a flop-in ring detector in combination with an analyser hexapole magnet. In /14/ it is shown that a conical quadrupole analyser magnet in combination with a ring detector is preferable. Nevertheless, in view of the relatively large ring detector surface necessary the flop-out system with a point detector on the axis is preferred at the PTB. We have had no experience with a double dipole flop-in analyser magnet as proposed by Kartaschoff /15/.

Figure 1 shows the basic arrangement of the standard CS1. In the following, it is assumed that the functioning principle is known. The characteristic qualities of this arrangement will be discussed.

1. Beam deflection system

The dimensions of the quadrupole/hexapole deflection system used as the polarizer and analyser are given in /4/. It selects atoms with an average velocity of 92,7 m/s (in a relatively narrow velocity range of about 7%) from the atoms leaving the oven with a modified Maxwell-Boltzmann velocity distribution (Fig.2 and Fig.3). The temperature of the selected atoms is about 65 K. Due to the small velocity and velocity range, the first and second order Doppler shifts are small. In dipole system standards, velocity ranges of, e.g., 30 to 50% are used. Phase differences between the end resonators cannot be completely avoided. Changes of the HF radiation then produce changes of the frequency ("power

shift") which, of course, are smaller for small velocity ranges in the beam.

The conclusion that a device using only a small velocity range is disadvantageous because of "wasting" atoms is unjustified /4/. The aperture of the beam optics for quadrupole and hexapole magnets is much larger than that of a dipole system.

As shown in /3/ and /4/ the velocity range in the beam is larger for a hexapole polarizer than for a quadrupole polarizer assuming comparable dimensioning of the magnets. If, e.g., for simplicity of construction, only one magnet is used, either hexapole or quadrupole, in many cases, the quadrupole magnet will be advantageous. Its velocity range decreases with decreasing magnetic field.

A long interaction length necessitates a very precise deflection of the atoms in the polarizer. This means that the shape of the pole tips should be as close as possible to ideal.

In the interest of a high beam intensity in relation to the Cs consumption, the beam source diameter d has to be rather small. A single channel with $d = 0.1$ mm and a length of some tenths of mm is used in CS1. It is necessary to operate the oven at a rather high temperature (160 to 180°C) in order to achieve an adequate Cs beam. This means that the relative content of atoms with the desired velocity referred to the total flux is less favourable than in the case of dipole devices whose oven temperature is only of the order of 100°C. The directivity factor χ of the CS1 beam source is rather low under the conditions described. On the other hand, the large aperture angle of the polarizer system limits the admissible χ -factor to a value which in practical cases will be below 10.

2. Phase distribution in the end resonators

The CS1 uncertainty evaluation of 1974 /6/ already took into account the existence of a phase gradient (of about $1.6 \cdot 10^{-5}$ rad/mm) in the end resonators perpendicular to the beam direction. For the uncertainty estimation it was assumed that the beam paths for both beam directions might differ by a few tenths of mm. In the evaluation of 1979 /7/, the frequency uncertainty due to the phase distribution in the end resonators is the largest contribution to the total uncertainty.

Obviously, this most important uncertainty can be reduced by reducing the beam diameter and by proper alignment. CS1 uses a beam diameter of 3 mm. In dipole devices beam widths of about 10 mm and more are used. Hence, it can be expected that the problem of the phase distribution is less severe by a factor of about 3 for CS1.

In the dipole system, the actual phase difference between the end resonators is dependent rather strongly on the HF radiation power: increasing, e.g., the radiation favours faster atoms at different trajectories to contribute to the signal. This results in a specific power-dependent frequency shift due to the phase distribution. Not only is the velocity range in the quadrupole/hexapole system much smaller, but the velocity distribution across the beam has also a rotational symmetry cancelling the power-dependent phase difference between the end resonators to the first approximation. Taking this into account it is supposed that, altogether, the phase distribution problem is more severe by a factor of 3 in the dipole device than in the CS1 device.

3. Magnetic C-field

The magnetic shielding of CS1 consists of three concentric Mu metal cylinders with a wall thickness of 5 mm each. The longitudinal magnetic field H produced on the axis by a solenoid has been measured with a magnetometer. Neglecting the measured difference between $\overline{H^2}$ and H^2 produces an error of $1 \cdot 10^{-17}$ only.

As a primary clock, CS1 operates with $H \approx 4A/m$. Due to the following reasons, operation with such a low field is feasible without overlapping of the adjacent transitions: These resonances are relatively small due to the low beam velocity and, additionally, due to the long interaction length in the Rabi field; the atoms pass the waveguide in its longer diameter. Furthermore, the HF excitation amplitude for the atoms passing the waveguide is a sinusoidal and not a rectangular function as in the case of a design with a transverse C-field. If necessary, H could be reduced even further. It is not necessary to apply HF excitation below optimum radiation.

The shielding factor in the direction of the axis of a shielding cylinder is smaller than that perpendicular to the axis. This may be a basic disadvantage of devices with longitudinal C-field.

In order to avoid Majorana transitions between the different Zeeman levels, longitudinal "guiding fields" are used between the deflection magnets and the magnetic screening.

4. Detector

The surface necessary of a hot wire detector located at the focal point of the analyser may be as small as $0.1 \text{ mm}^2 / 4$. This allows a considerable reduction of the Cs background flux.

5. Signal-to-noise ratio

It may be of interest to compare the Cs beam flux on the detector, N_D , for a quadrupole/hexapole system (4P/6P) with that of a dipole system (2P). Using a formula for $N_D(4P/6P)$ derived in /4/ in the case of a standard such as CS1 and describing the dipole system by a rectilinear beam of velocity v and a velocity range $\Delta v(2P)$ results in:

$$\frac{N_D(4P/6P)}{N_D(2P)} \approx 8 \cdot \frac{r_0 - r_{CD}}{d} \cdot \frac{1}{k} \cdot \frac{v}{\Delta v(2P)} \frac{\mathcal{K}(4P/6P)}{\mathcal{K}(2P)}$$

for beams with the same cross section and with the same average velocity v . r_0 (1.5 mm) is the radius of the beam, r_{CD} (0.4 mm) is the radius of the central disc according to Fig.1. k (1,8) is a constant characterizing the deflection /4/, $\mathcal{K}(4P/6P)$ (about 2) is the directivity factor of the beam source and $\mathcal{K}(2P)$ is that of the dipole device. Values for CS1 are given in parentheses. With a multi-channel source $\mathcal{K}(2P) = 50$ may perhaps be achievable. Assuming $\Delta v(2P)/v \approx 1/3$ results in

$$\frac{N_D(4P/6P)}{N_D(2P)} \approx 6 .$$

The superiority of the 4P/6P system is lowered by a factor of 2 if in the 2P system both hyperfine levels are used. An additional reduction of the signal-to-noise ratio occurs due to the flop-out operation and the less favourable oven temperature of the 4P/6P System under discussion. There seems to be no fundamental difference between the two systems with respect to the S/N ratio.

Specific technical design and operating practice of CS1

In the following, information concerning the specific design and operation of CS1 which is not related to the two-dimensional beam deflection, is reviewed from the papers referred to.

Beam reversal is performed every 6 weeks (= 42 d). Each calibration interval of 80 d contains both beam directions of almost the same durations. The oven chamber (containing the oven and the polarizer) and the detector chamber (containing the analyser and the detector) are directly exchanged. This method ensures the application of the same beam in both beam directions. Operation of CS1 can be continued 1 h later after beam reversal.

The multiple line-width modulation method /3, 4, 9/ is applied on a routine basis. The application of this method is favoured by the specific form of the Ramsey resonance shown in Fig.3.

So-called "full evaluations" of the primary standards are performed at the NBS and the NRC from time to time, e.g., every year. The operating practice used at the PTB consists of an almost continuous supervision of all important operational parameters. Further information on the operating practice can be found in /7/.

Measurements with the standard CS1

Fig.4 shows a frequency comparison between the Canadian standard NRC:CsV and the standard PTB:CS1. The standard deviation of independent measurements is about $6 \cdot 10^{-14}$. Since it contains contributions from propagation changes of the LORAN-C links, this result of a 4-year-comparison is considered to be very satisfactory.

Frequency measurements of some time scales including the free time scale EAL of the BIH from which TAI is derived by frequency corrections (steering) are shown in Fig.5. Seasonal frequency changes of free time scales produced with industrial Cs clocks can be seen from the measurements with CS1 since 1969. An analysis of the free time scale of the PTB revealed seasonal frequency changes with an amplitude of $4 \cdot 10^{-14}$ /7/. It is estimated at the PTB that a change of the environmental temperature of +1 K may cause a frequency change of about $-1 \cdot 10^{-13}$. However, the clocks differ in their behaviour. Measurements of the temperature coefficient of an industrial Cs clock performed in Japan /16/ resulted in a value as small as $-0.2 \cdot 10^{-13}$ /K.

Fig.6 shows a time comparison between the Canadian and the German primary clock. The slope of the regression line indicates that the frequency of the standard NRC:CsV is higher by about $4 \cdot 10^{-14}$ which is within the uncertainty limits claimed.

The deviations Δt of the measured time differences from the regression line are primarily due to time transfer changes of the LORAN-C link between North America and Europe. Δt has a standard deviation of about 160 ns. This is an unexpectedly small value since it is based on four LORAN-C time comparisons: one each at the NRC and the PTB and two performed by the USNO. Time comparison results using the NTS-1 and NTS-2 satellites had a considerably larger standard deviation /17/.

To the first approximation Δt represents the fluctuations of the USNO time comparisons with the Norwegian Sea LORAN-C Chain (LC/7970) published in /18/. The interpretation of TAI as consisting of two components is justified, a North American one and a European one, fluctuating against each other by Δt .

Since the clocks of North America and of Europe contribute almost to the same amount to TAI, about 50% of a change of Δt should appear on the European component of TAI and, with the opposite sign, on the North American component of TAI*. This can be seen from Fig.7 showing a comparison of TAI with the time scales of the Canadian primary clock CsV and the German clock CS1, using the data published by the BIH in its Circ.D (curves A). In most cases the fluctuations of the curves A have in fact opposite signs; the amount of the TAI changes with respect to the primary clocks is, however, not quite the same for both curves: the fluctuations of the North American TAI component are by about 50% stronger. Applying 40% of Δt as a correction to the European TAI and 60% of Δt as a correction to the North American TAI results in the curves B which are much smoother: the Δt corrected TAI has a better frequency stability; the splitting of TAI into two components is reduced.

Fig.6 shows that Δt may have a systematic deviation from the average over a few months. The deviation between October 1978 and February 1979 is probably a seasonal effect. A consequence of a systematic change of Δt with time is that determinations of the TAI frequency in North America and in Europe result in two different values, even when the standards used, do not differ. As shown in Fig.8 the frequencies (80 d averages) of the two TAI components may differ by as much as $7 \cdot 10^{-14}$. The standard deviation between the two TAI components for 80 d frequency averages in the interval investigated is $3.5 \cdot 10^{-14}$ and $4.3 \cdot 10^{-14}$ for 60 d averages.

* The existence of this "mirror effect" of the fluctuations has, as far as the author remembers, already been mentioned by Granveaud (BIH) at the CIC 1974.

With regard to the steering of TAI, the effect of the TAI frequency splitting is not negligible. It is also important to understand the reasons for possibly divergent TAI calibration results in order to be able to develop confidence in the capabilities of primary clocks that is necessary if allowing them to assume greater influence within the international time-keeping system.

Due to the (assumed) seasonal fluctuation of Δt erroneous seasonal frequency fluctuations on time scales of the other continent are observed. The rules for applying the Δt corrections are as follows:

For a comparison of a North American (NA) time scale with a European (EU) time scale:

$$(TA(NA)-TA(EU))_{\text{corr.}} = (TAI-TA(EU))_{\text{Circ.D}} - (TAI-TA(NA))_{\text{Circ.D}} - \Delta t.$$

For time scale comparisons with TAI:

In Europe:

$$(TAI-TA(EU))_{\text{corr.}} = (TAI-TA(EU))_{\text{Circ.D}} - p_A \cdot \Delta t$$

In North America:

$$(TAI-TA(NA))_{\text{corr.}} = (TAI-TA(NA))_{\text{Circ.D}} + p_E \cdot \Delta t$$

p_E is the relative European weight, and p_A is the relative North American weight. By definition $p_E + p_A = 1$.

$p_E = 0.6$ (and correspondingly $p_A = 0.4$) seems to fit best up to now. In principle, the TAI data published by the BIH in the Circ.D could already include the propagation corrections.

Fig.9 and 10 show some Δt -corrected measurements. It should

be noted that TA(NBS) is not a free time scale but a steered one. The comparison with TA(NBS) suffers from additional link fluctuations.

Due to the noise on the Δt corrections optimum smoothness of the curves is sometimes observed if only 50 to 80% of the corrections are applied.

Future role of primary clocks

A few years ago it was thought that the calibration of the TAI frequency with a primary standard (with an assumed calibration uncertainty of about $1 \cdot 10^{-13}$) necessitates not much more than one measurement a year considering that the EAL frequency drift turns out to be less than $1 \cdot 10^{-13}$ per year. The situation has since changed: the calibration uncertainty is now about $1 \cdot 10^{-14}$ (utilizing the propagation corrections made available by primary clocks) and the newly detected seasonal effects of the EAL frequency are larger than the calibration uncertainty by about a factor of 10. As a result, it can be said that the information available from a continuously running standard is of considerably more value than that of a standard which is switched on only once a year.

The present international time system necessitates a great deal of effort (e.g., daily LORAN-C time comparison measurements) to keep its synchronism to a few tenths of a microsecond. Two primary clocks with a maximum instability of e.g., $5 \cdot 10^{-15}$ over unlimited time intervals require comparisons only very rarely for the synchronization uncertainty quoted, e.g., once a year. This may be of importance for countries which have no access to TAI and UTC when LORAN-C is not available.

At present there are only two primary clocks, though a number of laboratories throughout the world are dealing with the construction of Cs clocks. Since it appears that in the future too, the number of primary clocks will increase only very slowly the question arises as to how to make the best use of existing primary clocks for the establishment of TAI.

It should be realized that the accuracy and stability of the time scale of a primary clock (assuming the performance discussed in this paper) is much superior to that of EAL or TAI.

At its meeting in 1979 the CCDS "Working Group on the Steering of TAI" discussed the question of whether TAI could be based totally on the primary clocks of the NRC and PTB. A decision of this kind cannot be taken by the Working Group but only by the CCDS. Nevertheless, this proposal is an indication of the interesting development which lies ahead of us.

The PTB is in favour of this proposal. We believe that a solution can be found to combine the superiority of the primary clocks with the operational reliability of the present TAI system.

With respect to steering methods /19/, primarily three types of steering can be distinguished:

1. Correction of a TAI frequency departure from nominal; "accuracy steering"
2. Correction of the TAI frequency in order to compensate a frequency change which has occurred; "stability steering"
3. Correction of the TAI frequency in order to keep approximate time synchronism of TAI with the time of a superior clock or clock ensemble; "time steering"

The first method has been in operation since 1977. Due to the delays caused by the time necessary for the computation of EAL and the evaluation of the TAI frequency calibrations, the necessary frequency corrections are applied rather late. The TAI frequency may have changed meanwhile. A frequency correction is only justified if the departure from nominal is outside the 1σ uncertainty limit of the calibration. In the case of a systematic frequency drift of TAI this causes a systematic frequency deviation of about 1σ from the primary standards as well as an increasing time difference with them.

For the second method only the stability and not the accuracy of a contributing standard is important. Stability steering in the form of a correction applied later is not in use. It is more reasonable to incorporate the standard in the clock ensemble as the basis for the computation of EAL. The present ALGOS computation method of the BIH limits the weight of a contributing clock to 100. The total weight of the clocks is at present about 5500. Since the stability of EAL is significantly smaller than that of a primary clock, the clock should receive an ALGOS weight which is significantly higher than 5500.

The opinion has been expressed that the weight given to a primary clock could be determined with ALGOS. This, however, is not possible, because the weight given to a clock is, in principle, derived from the instability of the clock as measured by the rest of the clock ensemble. It is, of course, impossible to measure the instability of a very stable clock using unstable clocks.

When ALGOS was established, the specialists thought that a new type of clock could be given a specific upper limit weight to be determined from statistics based on a suffi-

ciently large number of these clocks. There are not enough primary clocks, of course, to apply this principle to them.

Objections have been expressed to giving the primary clocks a high ALGOS weight because this could result in discouraging those contributing to TAI with industrial standards. The advantage of having the primary clocks included in the ALGOS computation with a high weight would be that they would immediately contribute to the stability, whereas all steering methods with later corrections cannot prevent the fluctuations due to the control system. A possible compromise would be to start with a primary clock weight of, e.g., 500 and to increase the weight later when sufficient experience has been gained. A reasonable weight would presumably stimulate the work on primary clocks. The present ALGOS weight for primary clocks is only 100.

If those operating primary clocks derived their UTC(i) from their primary clock at the same rate, UTC(i) would drift away from UTC(BIH) when the first two steering methods are applied. To maintain approximate agreement between UTC(i) and UTC(BIH) the quality of UTC(i) could either be decreased and steered to conform with UTC(BIH) or the TAI frequency could be steered to avoid an increasing departure of UTC(BIH) from the UTC(i) produced by primary clocks. This latter method is what has been called "time steering". In the case of several slowly diverging primary clock time scales, TAI could be adjusted to follow their time average.

At its 1979 meeting, the CCDS Working Group requested the BIH to steer TAI in a way that would avoid a systematic time departure from the primary clocks. This corresponds to a time steering method.

It seems that in the future, we shall see primary clocks greatly influencing international time keeping, resulting in a reduction of the principal role of the industrial Cs clocks in some cases. The practical role of these clocks will certainly not be reduced, as they ensure the accessibility to TAI. Concerning the role of the metrological institutes operating primary clocks, it should be noted that it is quite normal that a comparatively small number of them ensures the availability of the reference standards of international metrology.

REFERENCES

- /1/ G.Becker, B.Fischer, G.Kramer, E.K.Müller, "Neuentwicklung einer Cäsiumstrahlapparatur als primäres Zeit- und Frequenznormal an der Physikalisch-Technischen Bundesanstalt", (New development of a cesium beam device as a primary time and frequency standard at the PTB), PTB-Mitt. 79 (1969), pp.77-80
- /2/ G.Becker, B.Fischer, G.Kramer, E.K.Müller, "Neukonstruktion eines Cäsiumstrahl-Zeitnormals an der Physikalisch-Technischen Bundesanstalt", (New construction of a cesium beam time standard at the PTB), Proc.Int.Congress Chronom.1969, CIC 69-A1 and Jb.Deutsche Ges.Chronom. 20/I (1969) DGC - A 1
- /3/ G.Becker, "Recent progress in primary Cs beam frequency standards at the PTB", IEEE Trans.Instrum.Meas, vol. IM 25, (1976) pp.458-465
- /4/ G.Becker, "Research on Cs-Beam Frequency standards at the PTB: Beam Optics, Majorana Transitions", IEEE Trans.Instrum.Meas., vol.IM 27, (1978) pp.19-325
- /5/ G.Becker, B.Fischer, G.Kramer, E.K.Müller, "Diskussion der inneren Unsicherheit des neuen Cäsiumstrahl-Zeitnormals der Physikalisch-Technischen Bundesanstalt", (Discussion of the inherent uncertainty of the new cesium beam time standard of the PTB), Proc.Int.Congress Chronom. 1969, CIC 69-A2 and Jb.Deutsche Ges. Chronom. 20/I (1969) DGC - A 2
- /6/ G.Becker, "Das primäre Zeit- und Frequenznormal CS1 der Physikalisch-Technischen Bundesanstalt", (The primary time and frequency standard CS1 of the PTB), Proc.Int. Congress Chronom.1974, CIC 74-A1.1 and Jb. Deutsche Ges.Chronom. 25 (1974) DGC - A 1
- /7/ G.Becker, "Das Cäsium-Zeit- und Frequenznormal CS1 der PTB als Primäre Uhr" (The Cesium Time and Frequency Standard CS1 of the PTB as a Primary Clock), Proc.Int. Congress Chronom. 1979, CIC79, vol.2, pp.33-40, edited by the Société Suisse de Chronométrie, 3294 Bueren, Switzerland

- /8/ G.Becker, "Frequenzvergleiche mit dem primären Zeit- und Frequenznormal CS1 der Physikalisch-Technischen Bundesanstalt zwischen 1969 und 1973", (Frequency comparisons with the primary time and frequency standard CS1 of the PTB between 1969 and 1973), PTB-Mitt. 83 (1973) pp.319-326
- /9/ G.Becker, "Frequenzverschiebung beim Cäsium-Frequenznormal durch die Rabi-Resonanz", (Frequency shift at the cesium frequency standard due to the Rabi resonance), PTB-Mitt. 87 (1977), pp.288-295
- /10/ A.G.Mungall, H.Daams, D.Morris, C.C.Costain, "Performance and operation of the NRC primary cesium clock, CsV". Metrologia 12, (1976) pp.129-139
- /11/ D.J.Wineland, D.W.Allan, D.J.Glaze, H.W.Hellwig, S.Jarvis, "Results on Limitations in Primary Cesium Standard Operation", IEEE Trans.Instr.Meas., vol.IM 27 (1978), pp.453-458
- /12/ A.G.Mungall, "A new concept in atomic time keeping; The continuously operating long-beam primary cesium clock", IEEE Trans.Instr.Meas.vol.IM 27, (1978) pp.333-334
- /13/ J.H.Holloway and R.F.Lacey, "Factors which limit the Accuracy of Cesium Atomic Beam Frequency Standards", Proc.Int.Congress Chronom. 1964, CIC 64, vol.1, pp.317-331, edited by the Société Suisse de Chronométrie, Neuchâtel, Switzerland
- /14/ G.Becker, "Performance of the Primary Cs-Standard of the Physikalisch-Technische Bundesanstalt", Metrologia 13 (1977), pp.99-104
- /15/ P.Kartaschoff and P.-E.Debély, "Résonateur à césium de conception nouvelle" (Cesium resonator of a new conception), Proc.Int.Congress Chronom.1969, CIC 69-A3
- /16/ S.Iijima, K.Fujiwara, H.Kobayashi and T.Kato, "Effect of Environmental Conditions on the Rate of a Cesium Clock", Annals of the Tokyo Astronomical Observatory Second Series, vol. XVII, Number 1 (1978), pp.50-67

- /17/ J.Buisson, T.McCaskill, J.Oaks, D.Lynch, C.Wardrip and G.Whitworth, "Submicrosecond comparisons of time standards via the Navigation Technology Satellites (NTS)", Proceedings of the Tenth Annual Precise Time and Time Interval (PTTI) Application and Planning Meeting, Nov.1978, edited by NASA, Goddard Space Flight Center, Greenbelt Maryland 20771, USA, pp.601-624
- /18/ U.S.Naval Observatory Washington, D.C. 20380, "Daily Time Differences and Relative Phase Values, Series 4"
- /19/ G.Becker, "Problem of the steering of the International Atomic Time Scale with primary standards", PTB-Mitteilungen 87 (1977) pp.465-467
- /20/ S.R.Wagner, "On the Quantitative Characterization of the Uncertainty of Experimental Results in Metrology", PTB-Mitt. 89 (1979), pp.83-89

Table 1*

Relative uncertainty and instability of the standard CS1 of the PTB in continuous operation, based on 80 d average

Parameter	Relative uncertainty 10^{-15}	Relative instability 10^{-15}
Resonator phase difference	<5	<5
Beam path	<9 +	<3
Beam velocity	<0.1	<0.1
Second order Doppler shift	<0.4 +	<0.1
Resonator detuning	<1 +	<0.1
Magnetic field strength	<1	<1
Magnetic field inhomogeneity	<0.1 +	<0.1
HF sidebands 50 Hz	<1.3 +	<1
Adjacent transitions	<1 +	<0.1
Demodulator	<1 +	<1
Shot noise	2	2
Square root of the sum of squares	<10.8	< 6.4
Sum of the amounts	<21.9	<13.5
1 σ value **	6.5	4.0

⁺Contributions to the systematic uncertainty

* Translation from /7/

** The 1 σ value is achieved according to an evaluation method published by Wagner /20/ and recommended by PTB: upper limit values of uncertainty contributions are divided by $\sqrt{3}$ resulting in an estimation of a 1 σ value of these contributions.

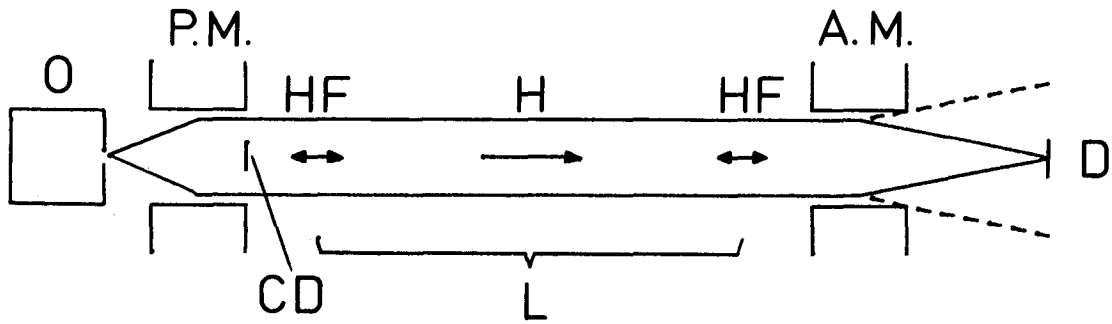


Fig. 1-Basic arrangement of the primary Cs standard of the PTB. P.M polarizer, A.M. analyser, both consisting of a combination of quadrupole and hexapole magnet, O, oven; F, detector; L, interaction length (0.8 m); CD, central disc as beam stop; HF, high frequency field; H, static magnetic field, both in beam direction. The dotted lines refer to the beam trajectory in case of resonance

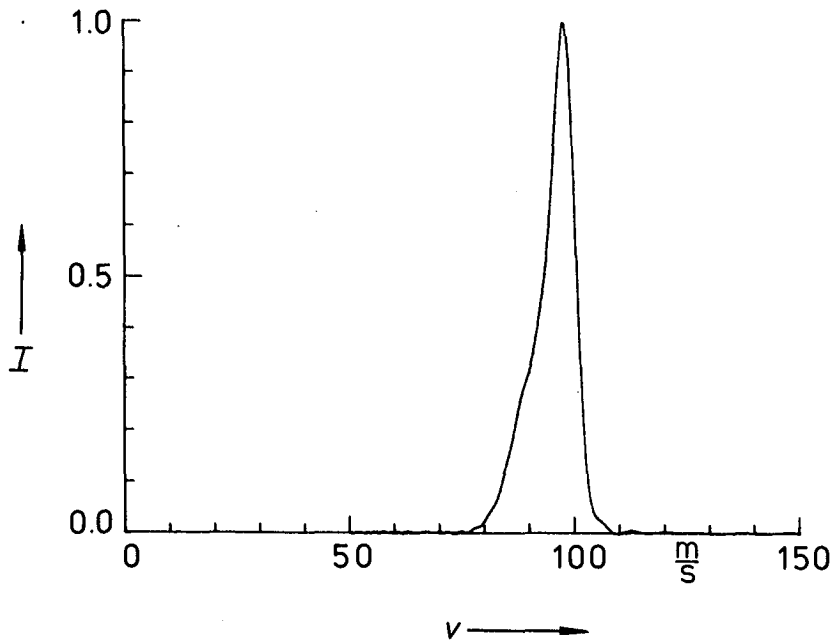


Fig. 2-Velocity distribution in the atomic beam of CS1 evaluated from the resonance curve Fig.3; intensity I in arbitrary units. The average velocity is now 93 m/s, lower than shown in the graph

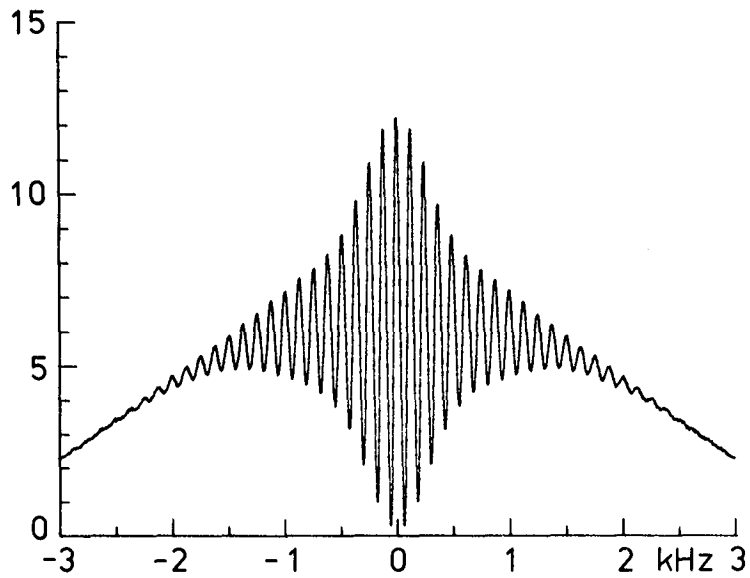


Fig. 3-CS1 resonance curve; line width 59 Hz

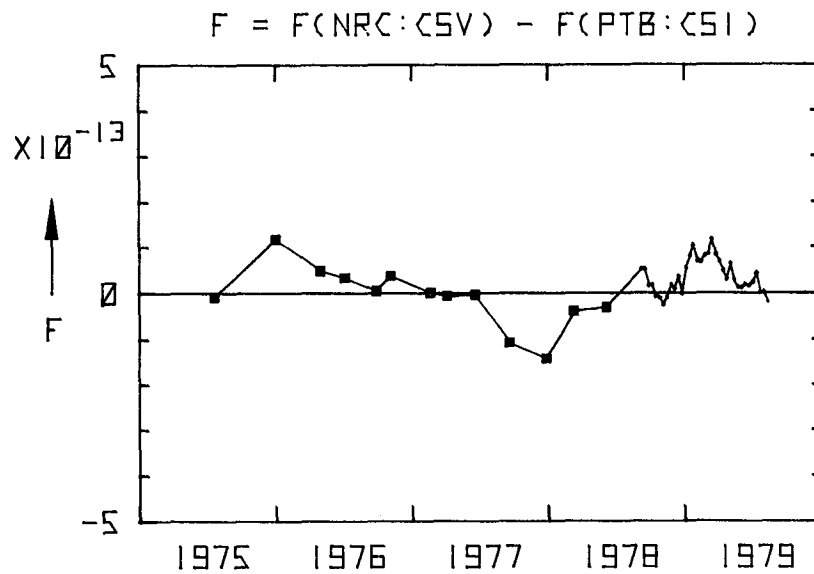


Fig. 4-Relative frequency difference F (80d averages) between the standards NRC:CsV and PTB:CS1 with reference to sea level. Since the beginning of the continuous operation of CS1 in 1978, sliding averages are shown, in steps of 10d

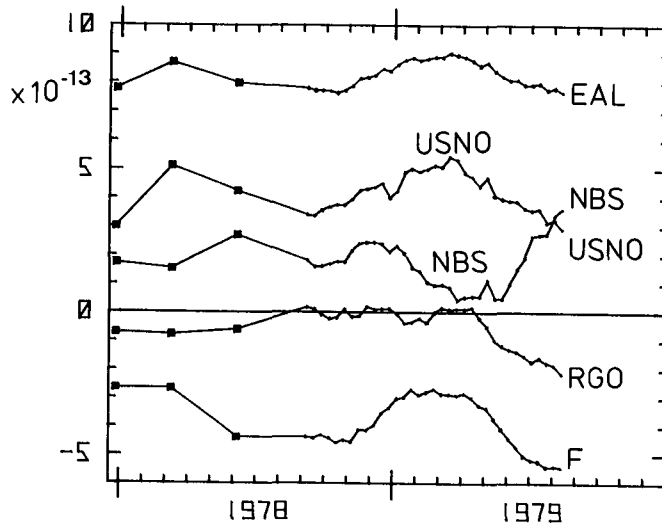


Fig. 5-Frequency measurements of some time scales $TA(i)$ and of EAL with the standard PTB:CS1. F refers to the French time scale and RGO to that of the Royal Greenwich Observatory. Seasonal effects of different sizes can be seen

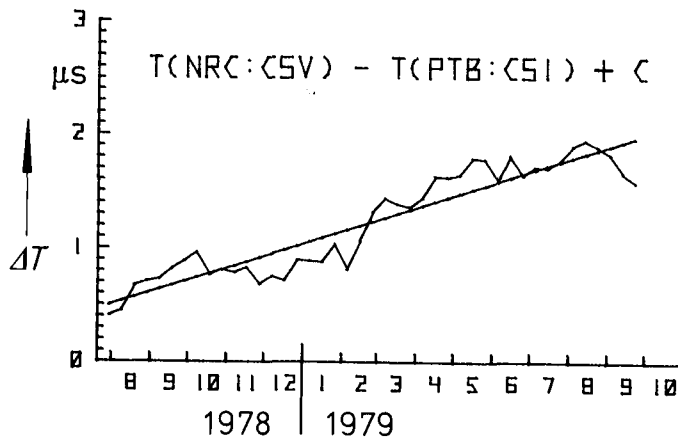


Fig. 6-Time difference ΔT (plus an arbitrary constant C) between the standards NRC:CSV and PTB:CS1 (with reference to sea level) evaluated using the Circ.D data of the BIH. The departure Δt from the regression line has a standard deviation of 160 ns

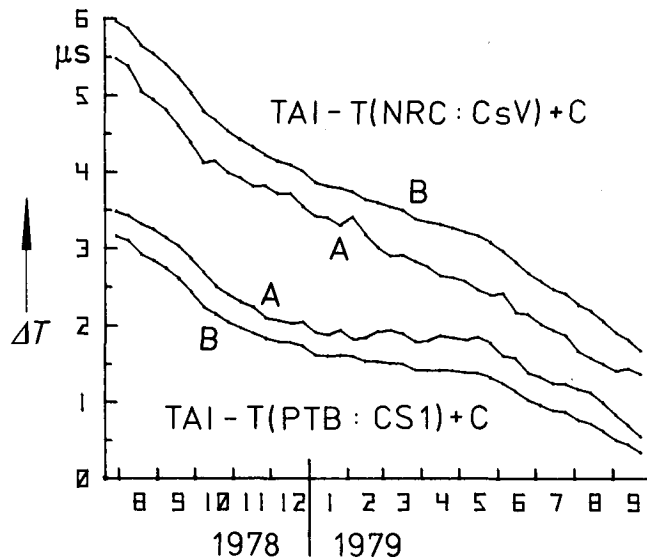


Fig. 7-The curves A show the time difference ΔT between TAI and the time $T(NRC:CsV)$ and $T(PTB:CS1)$ respectively, using the Circ.D data. Applying the propagation correction results in the curves B. A European weight of 60% and a North American weight of 40% of Δt was chosen for the corrections. An arbitrary additive constant C is chosen to separate the curves

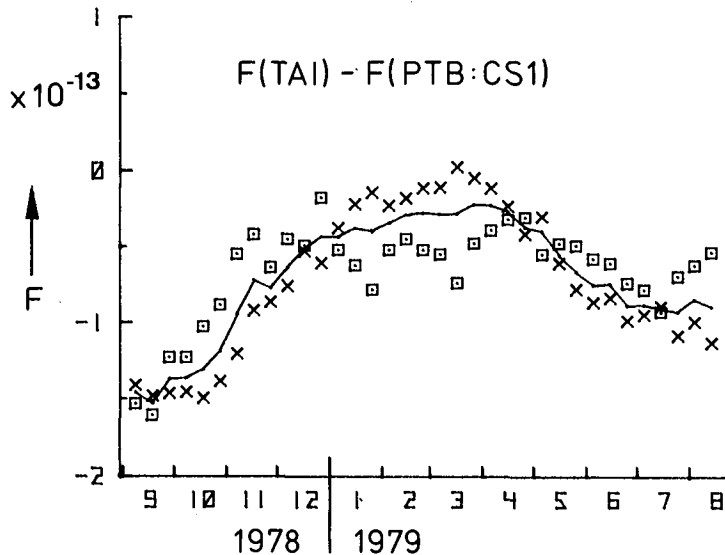


Fig. 8-Measurement of the TAI frequency (80d sliding averages in steps of 10d) with the standard PTB:CS1. Crosses: no Δt correction; squares: correction is 100% of Δt ; solid line: correction is 40% of Δt

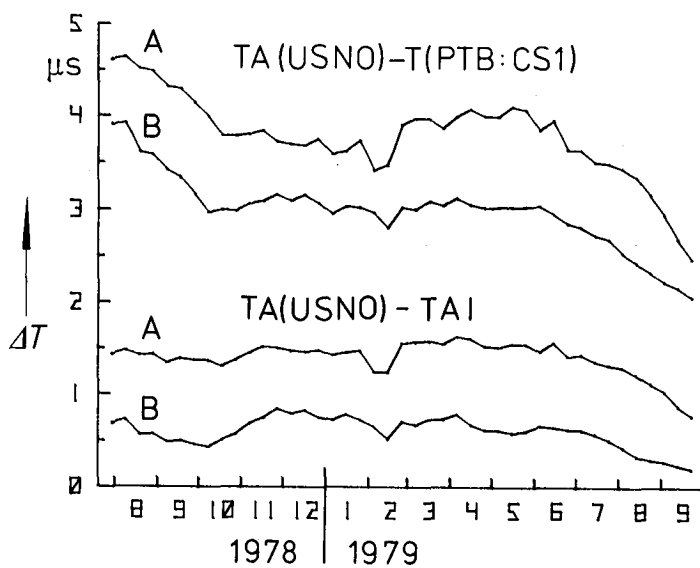


Fig. 9-Time difference ΔT of the time scale TA(USNO) (with rate corrections and arbitrary additive constants) from the time scales T(PTB:CS1) and TAI respectively. Curves A without Δt correction; curves B with Δt correction

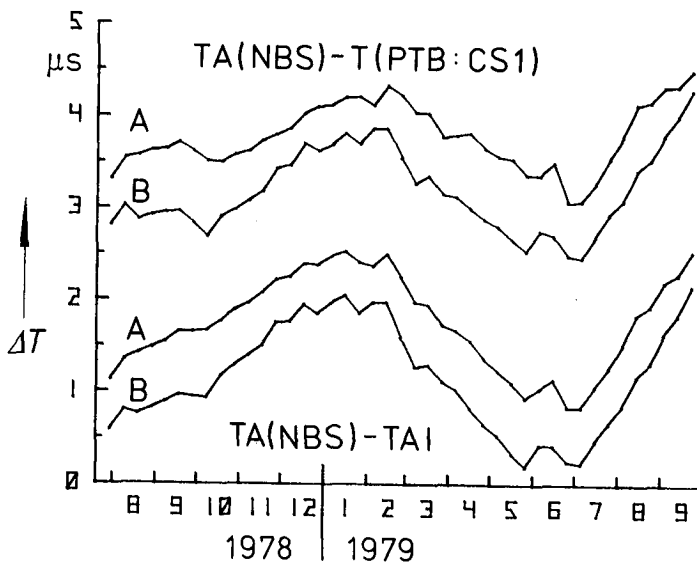


Fig. 10-Time difference ΔT of the time scale TA(NBS) (with rate corrections and arbitrary additive constants) from the time scales T(PTB:CS1) and TAI respectively. Curves A without Δt correction; curves B with Δt correction

QUESTIONS AND ANSWERS

MR. CHI:

Dr. Becker, I noticed in your final vu-graph you showed the time difference of about 2 microseconds for about 400 days, that is between PTB and NRC, which represents about 5 nanoseconds per day of 5 parts, 10 to the 14th. Is that systematic?

DR. BECKER:

This is in fact at present the difference between the two standards and it is within the uncertainty limits which are claimed by both institutes.

MR. CHI:

I have one more question. That is, in the other comparison of time when they use the Loran-C, there seemed to be a high peak, perhaps it is due to seasonal variation. In the case of comparison between NRC and PTB there is just a systematic straight line. How was that comparison made?

DR. BECKER:

You mean this one here?

MR. CHI:

In the systematic there is no peak. In the others, like NBS and NRC, there is always a peak on the comparison.

DR. BECKER:

Yes. This is Loran-C.

MR. CHI:

How about the first one. How is that measured? The one before that?

DR. BECKER:

The one before? Loran-C. The other one, from bulletins. That means I took the weekly bulletins which I get from Canada and from Dr. Winkler from the USNO and our own. And only one day is taken out. The specific day is every 10 days at one point and I took down these data.

MR. CHI:

There is no solution?

DR. BECKER:

If you take just the results which are published for that specific date then it looks like that. It is interesting to see that they are similar in type. That means maybe there is some kind of typical weather which changes slowly. It should be a temperature problem I think.

DR. FRED WALLS, National Bureau of Standards

Could I see the vu-graph showing the relative uncertainties and instabilities? I had a question about that.

DR. BECKER:

Can we have the slide once more?

DR. WALLS:

Two questions. One, under the relative uncertainty, under beam path you have 9 times 10 to the minus 15th. This is an estimate or a calculation of what the maximum uncertainty might be?

DR. BECKER:

This value is achieved in the following way. The theoretical consideration estimated the phase gradient to be expected and calculated the frequency change per millimeter, shifting beam per millimeter. Then, we did a beam shifting, an actual beam shifting and tried to verify this estimation and as it turned out it was the same order and so we relied on our knowledge and in this case I simply chose .3 millimeter, 10 percent of the beam. I think it is better but just because we didn't know it, then we chose .3 millimeter.

DR. WALLS:

I see. For statistical things, maybe dividing by the square root of 3 might be appropriate but for a systematic thing such as the beam path to quote a one sigma value less than the uncertainty there perhaps is a problem.

But let us talk about the relative instability, the column there on the right. These are, again, estimated rather than measured, is that true?

DR. BECKER:

Estimated. Yes.

DR. WALL:

When you compare against your commercial cesiums in your time scale, what kind of stabilities do you measure between season one and your--

DR. BECKER:

This is the value which is of interest. This is shot noise. We are using .3 grams here and there is an instability in a second of about 5.5 parts in 10 to the minus 12th.

DR. WALL:

So that it takes about 25 to 40 days in order to average down to that 6 or 7 times 10 to the minus 15 on both your standard and against maybe commercial standards. So that is a very long time to make a claim of stabilities of 4 or 5 or 6 times 10 to the minus 15 and to then base an estimate of weighting for TAI on a calculated stability rather than a measured one, I think, is quite risky.

DR. BECKER:

The method of evaluating an instability is up to the scientist. If he can measure it, the better. But if he cannot measure it because he has no comparable device, he is allowed to estimate it in the same way as he is allowed, and this is done also at NBS, to estimate the uncertainty. This is the same type of procedure.

By the way, this is a conservative estimation, more or less. Consider please that for commercial clocks the instability is much smaller than the so-called uncertainty. The same could also be for other clocks. But you can be quite sure that the instability is certainly not larger than the uncertainty is. As you see it is only a factor of two here taken. There is no other method of evaluating the instability by theoretical considerations.

Of course you have these things here, magnetic field strength. Well, this is based on regular measurements of the magnetic field and for 80 days we have 11 such measurements and you know how they fluctuate and this is not an estimated but a measured quantity.

DR. COSTAIN:

Dr. Becker, do you have any contribution from the power dependents? In other words your excitation power?

DR. BECKER:

This specific feature, the reason it is not in, the power shift is not an isolated effect and cannot be listed here. You have to go down to the roots of the physical behavior.

QUESTION:

Should it not be possible to use a long time running hydrogen maser which does exist, they run for hundreds of hours. You could use that maser as a direct method of measuring the changes that you have for instance due to beam path reversal and that would not require any estimates. You could really measure it.

DR. BECKER:

We are going to compare our hydrogen maser directly with this cesium. It is just going to be made. Yes. And as far as possibly we will try to measure what is possible.

DR. MICHEL GRANVEAUD, Bureau International de l'Heure

I would have two comments. The first one is about the annual term and I think we have to make the difference between the local time scale and the international one. It seems that in the case of PTB, for example, the local time scale of PTB it has some annual terms and this annual term can come only from the atomic clocks themselves or from the algorithm that is used. In the case of the international time scale, we have furthermore the transmissions using Loran-C.

My second comment is about the use of the difference in our cesium-5, minus cesium-1. Can I see the vu-graph?

DR. BECKER:

Let me first refer to the first question. In fact, if you refer to our time scale TA, is it?

DR. GRANVEAUD:

No. I refer to TA(PTB).

DR. BECKER:

Oh, TA(PTB). Those have a seasonal term yes.

DR. GRANVEAUD:

Please?

DR. BECKER:

Have a seasonal term, yes.

DR. GRANVEAUD:

And about the second comment? I was thinking of the differences in our cesium-5 minus cesium-1.

DR. BECKER:

Frequency or time?

DR. GRANVEAUD:

The curve. The plateau we saw.

DR. BECKER:

Yes. Frequency or time? Time difference?

DR. GRANVEAUD:

Time differences.

DR. BECKER:

Time differences. Das war das systematischen, wissen Sie, mit dem drien kurven. This one?

DR. GRANVEAUD:

Yes. And we think that it could be a bit dangerous to use the smoothing of the data in our cesium-5 minus PTB cesium-1, and it is better to use, when available, satellite data. As you can see there is a smaller frequency difference between the smoothing line and the satellite results.

DR. BECKER:

Yes. You are absolutely right. I said to the first approximation. If you have these data available then it is the best as you are doing, and have written me in your letter, that a combination of both informations is profitable, to use satellite data and these measurements of the standards. You are right.

DR. DAVID ALLEN, National Bureau of Standards

One note of clarification. I suspect there are many here who don't know what a weight of 5,500 means. The maximum amount a clock can

receive in the international time scale is the weight of 100, currently, in the ALGOS algorithm, and 5,500 means the total accumulated weight of all the clocks. And when Dr. Becker says that the weight of primary standards would be equivalent to all of those, he means to the total accumulated weight of 5,500 of all the clocks. In other words, if you look at the uncertainty associated with his error budget there that would be the resulting calculation.

The other point I would make is that a lot of the graphs that we see, especially those for NBS, as Dr. Becker pointed out, the Loran path across the NBS/Boulder is a significant problem in our communicating time and frequency to international atomic time. We are aware of that and are working strongly toward curing that problem. And as long as we use Loran-C we will be limited and so a lot of the data that we saw in his presentation is an analysis of Loran-C, not of primary standard.

THE LASSO EXPERIMENT

Bernard Serène (EUROPEAN SPACE AGENCY), Toulouse,
Pierre Albertinoli (CENTRE NATIONAL D'ETUDES SPATIALES), Toulouse

ABSTRACT

The LASSO experiment is an approach towards an internationally coordinated technical assessment of a system which promises to provide a synchronisation of clocks bound to time and frequency standard laboratories, with an accuracy of one nanosecond using existing or near ground-based laser stations via a geostationary satellite (SIRIO-2).

The purpose of this paper is twofold; to present the LASSO mission and the principle of the overall experiment, and to underline the system performance and the technical details concerning :

- on-board equipment,
- ground segment,
- operational configuration.

To conclude, we will show the future prospects of the LASSO experiment together with possible implementations.

1. INTRODUCTION

The permanent long baseline clock synchronisation presents many scientific and practical interests. From a scientific point of view, the standard of frequency or the very accurate synchronisation between clocks allows a correlation of phenomena in the same scale of frequency or time to be performed. The demand for greater accuracy has led to an improvement of the measurement of time and frequency by a factor of at least 10^8 over the past century. While the limiting accuracies are still confined to research laboratories and institutes dealing with time and frequency standards, commercial and scientific users are not far behind in their requirements :

- Digital communication	10 μ s
- International telephone communication	1 μ s
- Earth-based navigation	1 μ s
- Deep-space navigation	20 ns
- Radio-astronomy	1 ns
- Geodesy	} as accurate as possible
- Relativity	
- Astronomy	

Applications and research already planned for the next decade will require nanosecond accuracy of better. Present users of time and frequency information have access to a variety of services and techniques for disseminating this information. These include the well-known high and low frequency broadcast services operated by many different Administrations throughout the world, portable clock methods, the use of television transmissions, and satellite techniques (Table 2).

TABLE 1 : METHODS CURRENTLY USED FOR TIME SYNCHRONISATION		
Method	Accuracy	Remarks
Very long baseline interferometry (VLB) using pulsars	1 ns	Slow, expensive ground stations
TV-type transmission via satellite	10 ns	Requires a wideband spacecraft transponder
Symphonie B	20 ns	Requires two-way transponder
Portable clocks	30 ns	Slow
Timation-3	100 ns	Military
Loran-C	300 ns	Accuracy limited by propagation phenomena

Although available services can satisfy many of the present user needs in science and application, an increasing need is developing for services which are required to provide improved accuracy, coverage and reliability. For example, the rapid growth of technology as applied to such areas as precise navigation, high-precision geodetic position determination, multiple-access digital communication and metrology results in a need for intercontinental time synchronisation and comparison down to the nanosecond.

While existing services are undoubtedly capable of some improvements, experience with a number of spacecraft - albeit ones that were not specifically designed for dedicated timing missions - indicates that satellite techniques appear to be the best choice for meeting future requirements in the subnanosecond range. Following a proposal presented at the 1972 COSPAR meeting in Madrid, the European Space Agency accepted a proposal from the "Bureau International de l'Heure" (BIH) to implement an experimental space mission and decided to launch a payload package, LASSO (Laser Synchronisation from Stationary Orbit) on the SIRIO-2 spacecraft.

The objective of LASSO is to provide a repeatable, near-realtime method of long distance synchronisation with the nanosecond accuracy for a reasonable price to meet the above requirement.

2. THE LASSO MISSION OBJECTIVES

The mission objectives, backed up by a number of time and frequency standard laboratories, is to provide intercontinental synchronisation of clocks with an accuracy of one nanosecond or better, and is to be considered as an important approach towards an internationally coordinated technical assessment of such a system.

The mission will thus allow the establishment of an improved international network of reference clocks synchronised between themselves and with the Internationally adopted Atomically Time scale (IAT).

It will also impact on other practical applications, such as the tracking of deep space mission spacecraft, the dissemination of standard time and frequency signals to many users, and future generations of space navigation and telecommunication systems.

The LASSO/SIRIO-2 experiment is designed to employ laser techniques and is not only a significant breakthrough in synchronisation techniques but is also a unique opportunity to compare the performance of laser and microwave time synchronisation methods insofar as microwave timing results have become available from the Italian SIRIO-1 time synchronisation experiment started in 1978. Thus, two candidate techniques will be compared on the basis of identical link geometry and satellite type.

3. THE EXPERIMENT

3.1. Principle

The LASSO experiment is based on laser stations emitting, at a pre-defined time, monochromatic light impulses which are directed towards a geosynchronous spacecraft (figure 1).

On-board the spacecraft :

- an array of retro-reflectors sends back a fraction of the received signal to the originating laser stations;
- an electronic device detects and time tags the arrival of laser pulses.

Each station measures the two-way travel time of the emitted laser pulses and computes the one-way travel time between station and spacecraft, taking into account the station's geographical coordinates, the spacecraft position and the Earth rotation.

The difference between the clocks, which provide the time reference for each of the laser stations, is deducted from the data coming from the spacecraft and the stations (figure 2).

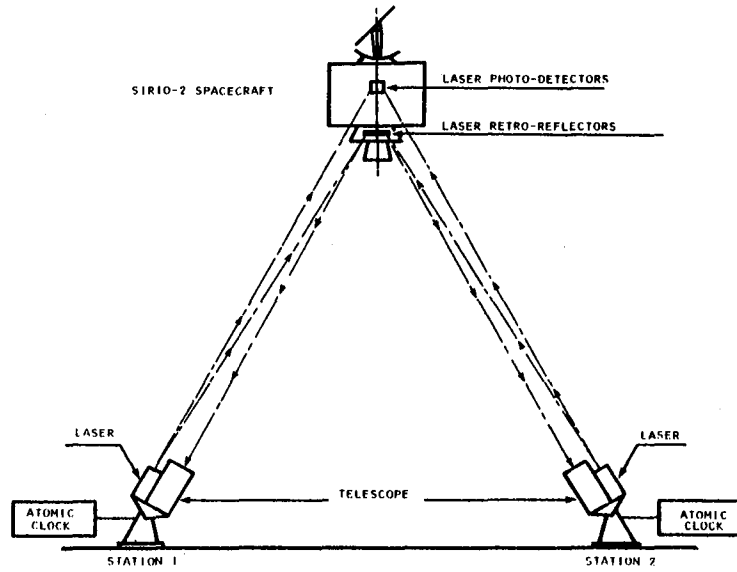


Figure 1. Schematic Diagram of LASSO Experiment

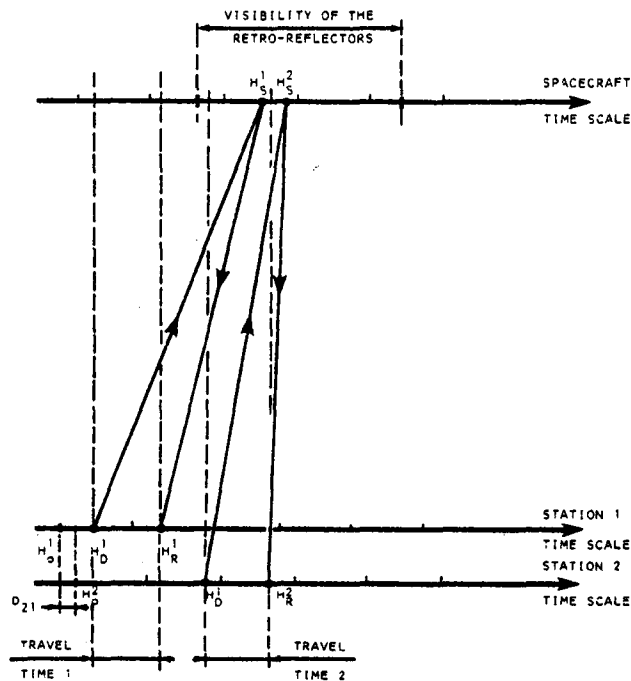


Figure 2. Time Scale Comparison

Consequently, for two stations we have :

$$D_{21} = (H_D^2 - H_D^1) + (T_2 - T_1) - (H_S^2 - H_S^1)$$

where : D_{21} = Time difference between the clocks of stations 2 and 1.

H_D^1 and H_D^2 = Departure time of laser pulses from stations 1 and 2.

T_1 and T_2 = Travel time between stations and spacecraft

$$\text{with } T = \frac{H_R - H_D}{2} + \epsilon$$

H_S^1 and H_S^2 = Arrival times on-board the spacecraft of the laser pulses from stations 1 and 2.

H_R^1 and H_R^2 = Return time of laser pulses from stations 1 and 2.

ϵ = Corrective factor depending on station and satellite positions.

The formula becomes finally :

$$D_{21} = \left(\frac{H_D^2 - H_D^1}{2}\right) + \left(\frac{H_R^2 - H_R^1}{2}\right) + (\epsilon_2 - \epsilon_1) - (H_S^2 - H_S^1)$$

3.2. Performance

Error Analysis

Using the above formula, the global error is :

$$\Delta D = \Delta H_D + \Delta H_R + 2\Delta\epsilon + 2\Delta H_S$$

with : ΔH_D : error on the departure time

ΔH_R : error on the return time

$\Delta\epsilon$: error on the corrective factor

ΔH_S : error on the arrival time on-board the spacecraft.

The error budget is detailed in table 2 for three different numbers of measurements (1, 15 and 30). In addition, all the laser firing times are in a time window of less than 100 msec.

TABLE 2

ANALYSIS OF ERROR FACTORS		NUMBER OF MEASUREMENTS		
		1	15	30
H_D	.Accuracy of cesium clock $\leq 10^{-11}$	± 1 psec	± 1 psec	± 1 psec
	.Short term stability $\leq 2 \cdot 10^{-11}$	± 2 psec	Negligible	
	.Chronometer resolution 0.1 nsec	± 50 psec	± 50 psec	± 50 psec
	.Detection system 0.1 nsec	± 100 psec	± 26 psec	± 18 psec
	$\Delta H_D \leq$	± 153 psec	± 77 psec	± 69 psec
H_R	.Accuracy of cesium clock $\leq 10^{-11}$	± 2 psec	± 2 psec	± 2 psec
	.Short term stability $\leq 2 \cdot 10^{-11}$	± 4 psec	± 1 psec	± 1 psec
	.Chronometer resolution 0.1 nsec	± 50 psec	± 50 psec	± 50 psec
	.Detection system 1 nsec	± 1000 psec	± 258 psec	± 183 psec
	$\Delta H_R \leq$	± 1056 psec	± 311 psec	± 236 psec
Σ	.Spacecraft position ± 1 km			
	.Station position ± 50 km			
	$\Delta \epsilon \leq$	± 40 psec	± 40 psec	± 40 psec
H_S	.U S O accuracy* $\leq 10^{-9}$	± 100 psec	± 100 psec	± 100 psec
	.U S O stability $\leq 10^{-10}$	± 10 psec	± 3 psec	± 2 psec
	.Chronometer resolution 0.1 nsec	± 50 psec	± 50 psec	± 50 psec
	.Detection 1 nsec	± 1000 psec	± 258 psec	± 183 psec
	$\Delta H_S \leq$	± 1160 psec	± 411 psec	± 335 psec
D	$\Delta D = \Delta H_D + \Delta H_R + 2\Delta \epsilon + 2\Delta H_S \leq$	± 3.6 nsec	± 1.3 nsec	± 1 nsec

* U.S.O. : Ultra Stable Oscillator

Liaison Budget

Considering the two planned positions in orbit of the spacecraft (25°W and 20°E), the parameters of the on-board equipment and the assumed characteristics of a certain number of laser stations, we have used different algorithms to compute :

- P_r which is the power density received by the spacecraft,

$$P_r = K \frac{J}{T} \cdot \frac{T_A}{\frac{4}{\pi} \theta^2 D^2}$$

using the following unit :

J (Joule) emitted energy

T (nsec) pulse width

θ (second of arc) beam divergence

D (km) distance station - spacecraft

$T_A = (0.7)^{1/\cos z}$ atmospheric transmission coefficient
(z = zenithal distance)

K = 0.7 coefficient of energy distribution

The formula becomes :

$$P_r \text{ (mW/cm}^2\text{)} = 3.79 \cdot 10^{12} \frac{J}{T} \frac{1}{\theta^2} \frac{1}{D^2} T_A$$

- \bar{N}_d which is the mean value of photons received by the photo-detector

$$\bar{N}_d \text{ (photons/nsec)} = \frac{N_d}{T} = P_r A_{op} s \frac{\lambda}{hc}, \text{ with :}$$

$A_{op} = 2.25$ gain of optical detection

s = 0.2 mm² photodiode sensitive surface

$\lambda_R = 694.3$ nm (Ruby)

$\lambda_N = 532.0$ nm (Neodyme)

h = 6.6256 $\cdot 10^{-34}$ J.sec

c = 2.998 $\cdot 10^8$ m/sec

consequently :

$$\bar{N}_d = k P_r \begin{cases} k_R = 15730 \\ k_N = 12050 \end{cases}$$

- S/N which is the signal to noise ratio,

$$\frac{S}{N} = C \cdot P_r^2$$

with C being a coefficient depending on the optics, the photodiode noise and preamplifier noise.

$$\left(\frac{S}{N}\right)_{dB} = 20 \log_{10} P_r + 10 \log_{10} C,$$

where $10 \log_{10} C = 32$ for Ruby and $= 26$ for Neodyme.

- N_e which is the number of photo-electrons collected at the laser station using the Fournet formula :

$$N_e = E \cdot TR_1 \cdot R \cdot TR_2 \cdot D$$

where $E = KJ \frac{\lambda}{hc}$ photons emitted by the laser station

$$TR_1 = \frac{T_A}{\frac{\pi}{4} \left(\frac{\pi}{180} \cdot \frac{\theta}{3600} 10^5 D \right)^2}$$

travel effect
station - spacecraft

$$R = R_{cc} \Sigma f (G_i)$$

retro-reflectors
effect

$$R_{cc} = 0.75 \text{ (coefficient of reflection)}$$

$$\Sigma f (G_i) = 14 \text{ (minimum efficacy)}$$

$$TR_2 = 0.328 \frac{T_A}{D^2}$$

travel effect
spacecraft - station

$$D = A T_r \rho$$

station detection
effect

$A(\text{cm}^2)$ is the receiving surface of the telescope,

T_r is the transmission coefficient of the telescope optics ($T_r = 0.8$ without interferential filter, and 0.4 with interferential filter of 3\AA),

ρ is the quantum efficacy of the P.M. (20% for Ruby and 25% for Neodyme).

All the computed values are reported in table 3, where the nominal value of the laser beam divergence θ has been considered equal to 15 seconds of arc.

STATIONS GEOGRAPHICAL LOCATION	CHARACTERISTICS				25° W				20° E			
	Laser Type	Ener gy	Pulse Dura tion	Teles cope Aper ture	P _r	\bar{N}_d	S/N	N _e	P _r	\bar{N}_d	S/N	N _e
		Joule	nsec	cm	mW/cm ²	Photon/nsec	dB	Photo electron	mW/cm ²	Photon/nsec	dB	Photo electron
CAGLIARI (Italia)	R	1	5	50	1.18	18560	33	4	1.42	22340	35	6
DIONYSOS (Greece)	R	4	15	45	1.18	18560	33	7	1.96	30830	38	20
GRASSE (France)	R	15	10	100	8.40	132130	50	211	9.84	154780	52	290
GRASSE (Lune) (France)	R	6	2	154	16.80	264260	57	200	19.70	309880	58	275
KOOTWIJK (Holland)	R	3	4	50	3.40	53480	43	7	4.03	63390	44	10
METSAHOVI (Finland)	R	1	20	63	0.06	944	.8	0.2	0.20	3150	18	3
SAN FERNANDO (Spain)	R	3	6	60	3.55	55840	43	24	3.36	52850	43	22
WETTZELL (Germany)	N	0.25	0.2	60	5.0	60250	40	0.4	6.83	82300	43	0.8
ZIMMERWALD (Switzerland)	R	5	17	50	1.52	23910	36	15	1.81	28470	37	21
AREQUIPA (SAO) (Perou)	R	6	15	50	2.38	37440	40	24	OUT OF VISIBILITY			
NATAL (SAO) (Brazil)	R	6	15	50	3.61	56790	43	55	2.0	31460	38	17
WASHINGTON (USA)	N	0.25	2	50	0.48	5780	20	0.4	OUT OF VISIBILITY			
WASHINGTON (USA) Mob.las. 1.3	R	0.75	5	50	0.58	9120	27	1.2	OUT OF VISIBILITY			
WASHINGTON (USA) Mob.las. 4.8	N	0.25	5	75	0.19	2290	12	0.9	OUT OF VISIBILITY			
WASHINGTON (SAO) (USA)	R	6	15	50	1.54	24220	36	10	OUT OF VISIBILITY			

TABLE 3

4. THE EQUIPMENT

4.1. General Description of the Spacecraft

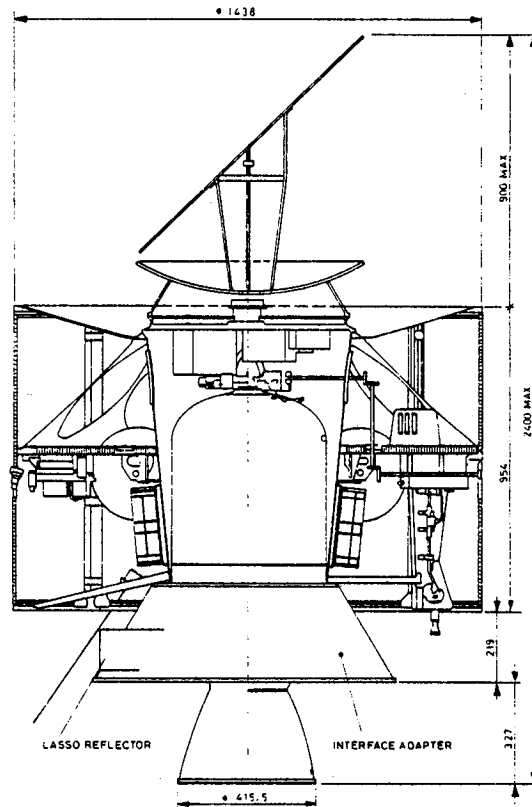


Figure 3. SIRIO-2 Spacecraft

A cross-section of the SIRIO-2 satellite is shown in figure 3. It consists of a drum-shaped central body covered with solar cells, on top of which is mounted a mechanically despun S-Band antenna. The apogee boost motor, which is to be retained after burn, protrudes from the bottom of the spacecraft. While the directional S-Band antenna supports a Meteorological Data Dissemination (MDD) function and transmits the housekeeping telemetry, the omnidirectional turnstile antenna serves telecommand, ranging and back-up telemetry functions in the VHF. As the satellite is to be spin-stabilised at 90 rpm and will act as an inertial gyroscope, attitude re-orientation is achieved by torque-induced precession of the spin axis using axial micro-propulsion thrusters in a pulsed firing mode. North-South stationkeeping is performed by the same thrusters in a continuous firing mode, while a pair of radial thrusters allows the satellite to be displaced in an East-West sense.

The monopropellant hydrazine fuel is contained in four symmetrically located spherical tanks. The telemetered readings from on-board infrared earth and V-slit sun sensors are used to determine the satellite's attitude in space. The satellite is powered by the solar cells and by a battery sustaining a minimum load configuration during eclipse transits.

The LASSO payload is comprised of retro-reflectors, photodetectors for sensing ruby and neodyme laser pulses, and an ultra stable oscillator/counter to time-tag the arrival of the pulses. These time-tags will be encoded in time-division multiplex with spacecraft house-keeping information before transmission to the ground.

The overall block diagram is given in figure 4.

The industrial effort for the SIRIO-2 project is led by the Compagnia Nazionale Aerospaziale (CNA) in Rome.

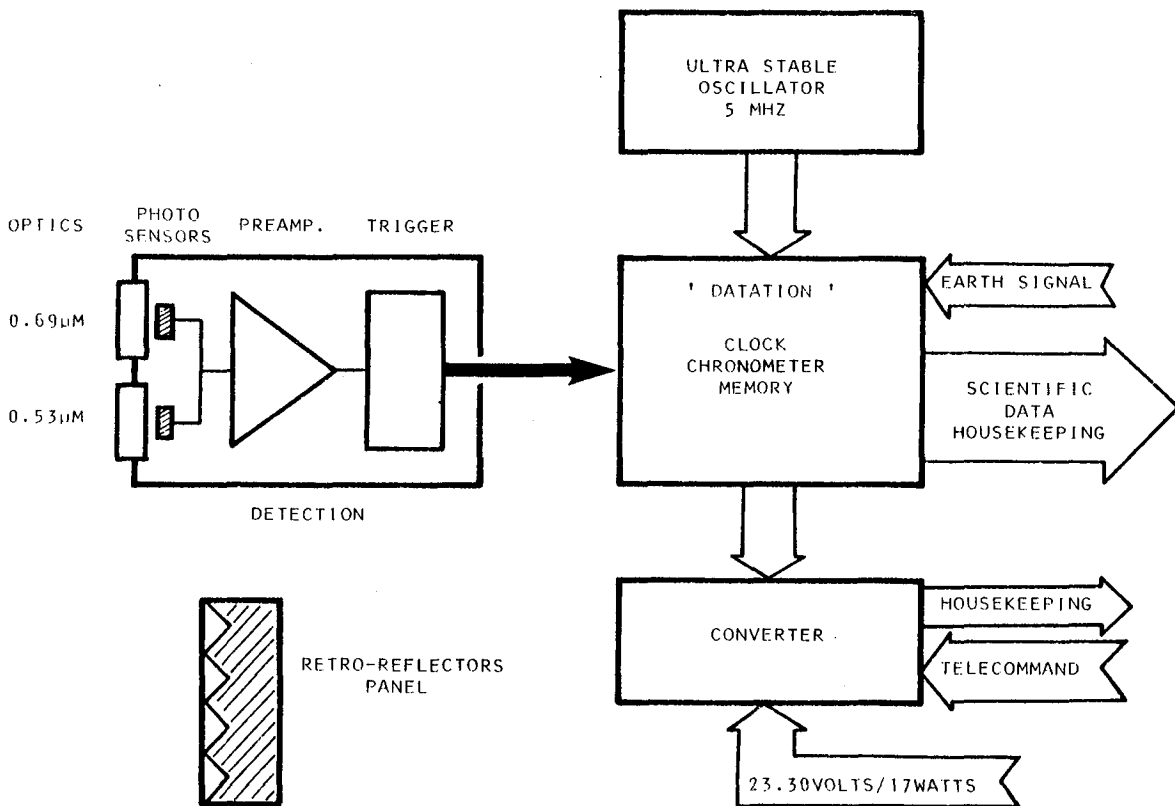


Figure 4: LASSO Equipment Block Diagram

The figure 5 gives the simplified industrial organisation of the SIRIO-2 programme.

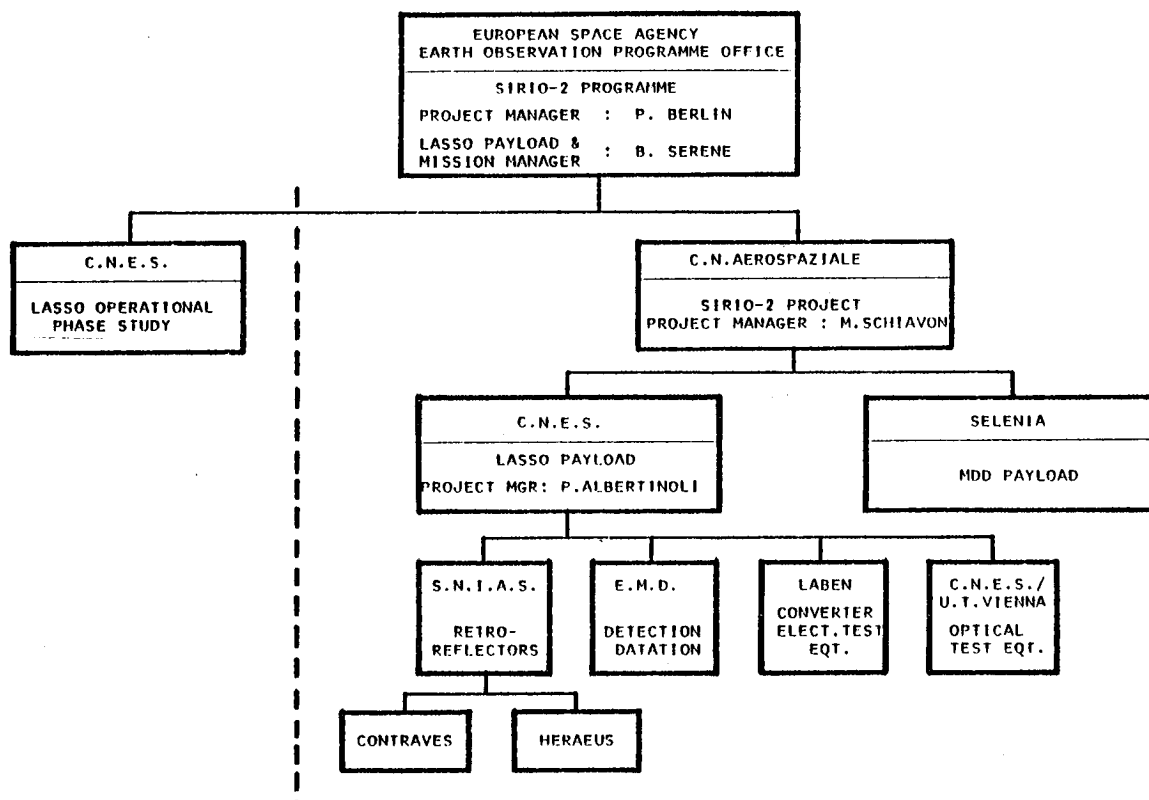


Figure 5 : Industrial Organisation

4.2. Details of the On-board LASSO Equipment

Retro-reflectors

The retro-reflector panel is an assembly of 98 aluminised corner cubes which are held by a mechanical structure thermally coated and decoupled from the spacecraft (figure 6). The panel, which is mounted on the launch interface adaptor and aligned with the field of view of the photo-detectors, has the following characteristics :

- weight : 2,5 kg
- dimensions : 155 mm x 340 mm x 35 mm
- minimum global efficacy : 14.

Each corner cube presents a diameter of 20 mm, with a reflection factor of more than 75%.

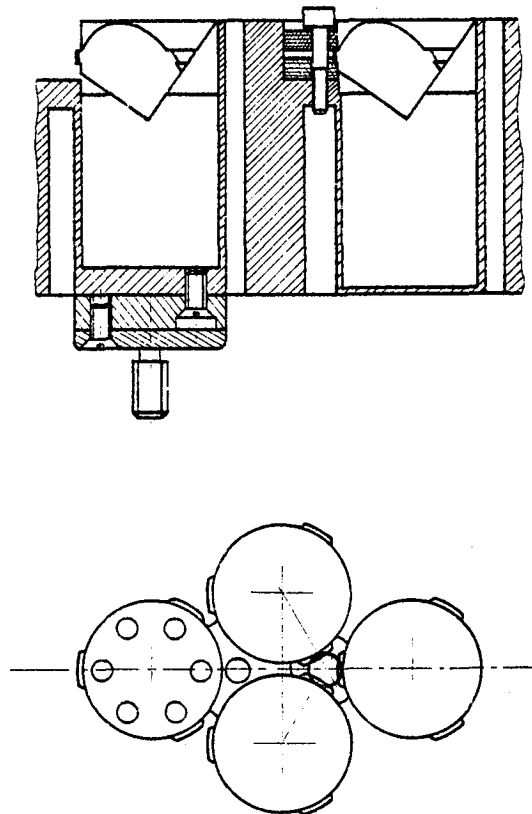


Figure 6. Mechanical Detail of the Retro-Reflectors

Photo-detection

The detection box is located on the main platform near the skin of the spacecraft and views through an aperture in the solar panels. This unit detects laser pulses and converts them into electrical signals which are transferred to the time-tagging unit.

The block diagram given on figure 7 shows :

- the optics (one for each laser type) including interferential filter, focusing lens and the avalanche photodiode,
- the broadband pre-amplifier (1 GHz),
- the threshold amplifier with the AGC system.

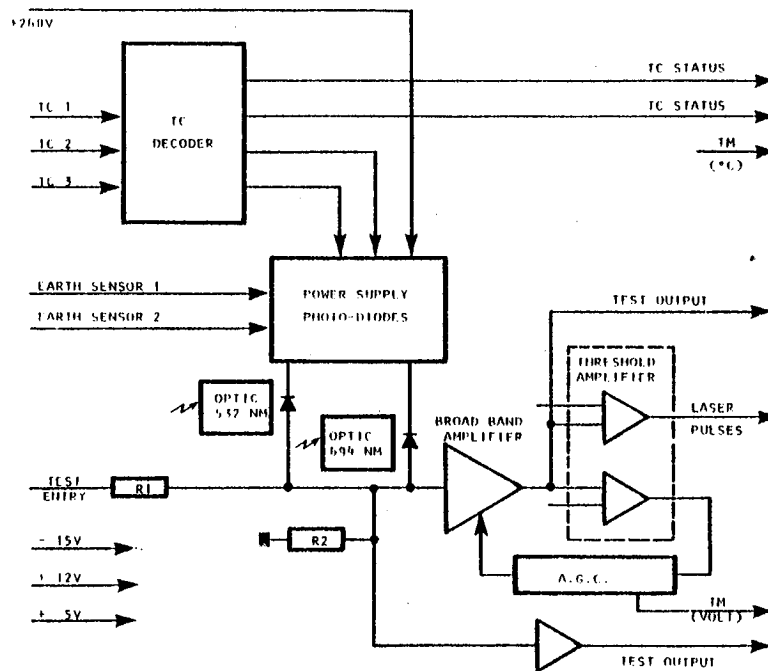


Figure 7 : Photo-detection Block Diagram

The main characteristics of the unit are :

- interferential filter bandwidth : 100 \AA
- optical incident angle : $\pm 10 \text{ deg}$
- minimum detectable power density
 - . ruby : 0.25 mW/cm^2
 - . neodyme : 0.50 mW/cm^2
- false detection : $\leq \text{one per minute}$
- non detection probability of a laser pulse : $\leq 1/100$

Time Tagging

The time tagging unit, which is time-synchronised by an ultra-stable oscillator, clocks in the pulses coming from the detection unit.

The time events are buffered in a memory before being sampled and transferred to the ground via the spacecraft telemetry. The block diagram given on figure 8 shows :

- the ultra stable oscillator (USO)
- the clock counter (clock of minutes)
- the chronometer (0.1 nsec)
- the memory (1 kbits)

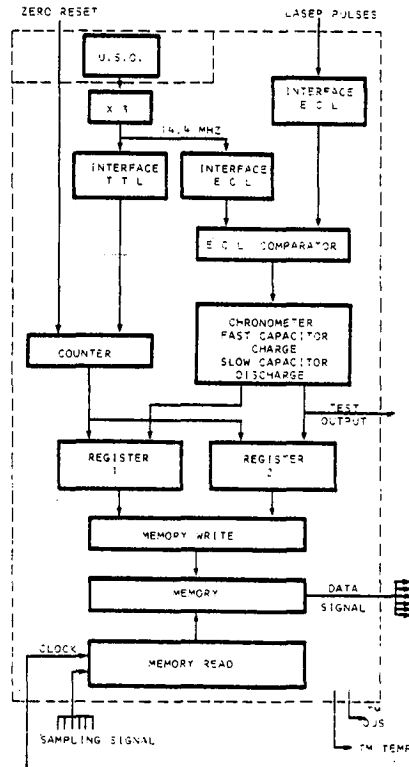


Figure 8. "Datation"
Block Diagram

The main characteristics of this subsystem are :

USO

nominal frequency	4.804434 MHz
short term stability (100 msec)	$\sigma \left(\frac{\Delta F}{F} \right) \leq 1.10^{-10}$
medium term stability (3 days)	$\left \frac{\Delta F}{F} \right \leq 5.10^{-10}$

Clock and Chronometer

chronometer resolution	# 100 psec
dead time	$\leq 200 \mu\text{sec}$
time tag encoding	42 binary digits

The overall statistical accuracy (over 100 couples of events) on the elapsed time between two events in the same time window of 70 msec will be better than 0.5 msec.

5. THE GROUND SEGMENT

The LASSO experiment consists of a space and a ground segment with the aim of obtaining a very high-precision synchronisation between remote clocks at intercontinental distances and will be used in a pre-operational mission in order to demonstrate the validity of the LASSO concept and overall performance.

In addition, the laser stations should fulfil a certain number of requirements to participate in the LASSO experiment.

The modes of operation described here are only tentative and should be frozen at the beginning of 1980.

5.1. Mission Duration and Duty Control

A total duration of two years for the LASSO mission is planned, with two positions in orbit : 25°W and 20°E.

During its useful life in orbit, the LASSO experiment will perform "working sessions" with an average duration of one hour per day. There will be no technological constraints on the time of the day when one or more sessions will be performed.

5.2. Mode of Operation

Each daily working session comprises 2 periods :

1st period : synchronisation of laser pulses
Synchronisation of pulse transmission of each station participating in the session with respect to the rotation of the spacecraft, and to other stations.

2nd period : time measurements
Due to LASSO on-board equipment, laser pulses of the various operating laser stations must arrive at the spacecraft with the time distribution shown on figure 9.

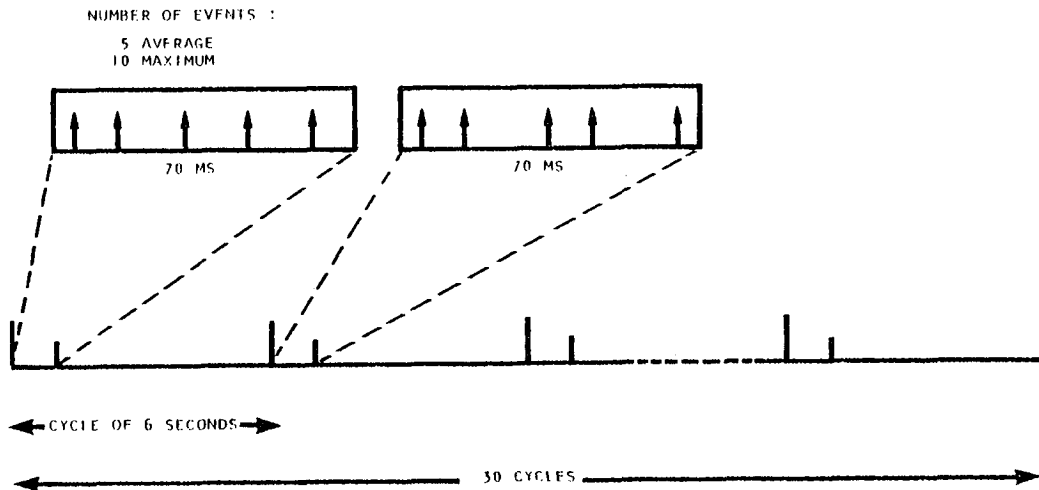


Figure 9 : LASSO Operation Mode

Each sequence of measurements lasts approximately 6 seconds (bound to the minimum pulse rate of laser stations).

In each sequence a certain time slot of $5 \cdot 10^{-3}$ sec. is reserved for the arrival of the laser pulse from a given laser station to the spacecraft (this figure is bound by the accuracy of the time of departure of the pulse from the station and by the accuracy of the computation of the time of transit of light from the station to the spacecraft).

Successive sequences differ one from the others since not all of the laser stations send pulses at each sequence. This permits ground processing by pattern recognition techniques to eventually discard false pulses detected by the on-board equipment.

Presently another mode of operation is investigated : the asynchrone mode.

Following each daily working session, measurements made by spacecraft equipment and laser stations are used for data processing. Currently, several data processing modes are under study, and before final implementation, the different principal investigators will be consulted.

5.3. Laser Stations Requirements

Localisation

Because of the necessity to correct the transit time of light from the laser station to the spacecraft, the laser station should be located in a common earth reference frame with an accuracy of :

- latitude : $\pm 10''$ (or ± 300 m)
- longitude : $\pm 10''$ (or ± 300 m)
- altitude : ± 50 m

Performance

Two conditions are imposed on laser station characteristics :

- one by the satellite detector and retro-reflector characteristics,
- one by the laser station detector system.

Conditions for detection on-board the spacecraft :

In order to have sufficient energy flux to be detected on-board the spacecraft, the laser station must deliver a sufficient energy in a sufficiently narrow beam during a maximum time.

- If (J) is the total energy of the light in the beam during one pulse of the laser station in Joules,
 (T) is the equivalent pulse duration in nanoseconds,
 (θ) is the laser station beam divergence in second of arc,
- and considering the link budget from the laser station to the spacecraft, and the sensitivity of the detectors on-board the satellite,

the laser station should satisfy the performance relationship shown in table 4 below :

TABLE 4

ELEVATION	DISTANCE STATION S/C	BEAM DIVERGENCE IN SECOND OF ARC	
		RUBY LASER	NEODYME LASER
90°	35786 km	$\theta \leq 128 \left(\frac{J}{T}\right)^{1/2}$	$\theta \leq 86 \left(\frac{J}{T}\right)^{1/2}$
55°	36780 km	$\theta \leq 120 \left(\frac{J}{T}\right)^{1/2}$	$\theta \leq 80 \left(\frac{J}{T}\right)^{1/2}$
25°	39070 km	$\theta \leq 92 \left(\frac{J}{T}\right)^{1/2}$	$\theta \leq 62 \left(\frac{J}{T}\right)^{1/2}$
15°	40061 km	$\theta \leq 69 \left(\frac{J}{T}\right)^{1/2}$	$\theta \leq 46 \left(\frac{J}{T}\right)^{1/2}$

Conditions for detection of return-pulse by the laser station :

In order to detect the return pulse with the retro-reflectors on-board of SIRIO-2 spacecraft (544 cm² of surface, reflexion coefficient=0.75, efficacy = 14), the laser station should :

- (a) transmit with sufficient energy J in a sufficiently narrow beam Θ ,
- (b) collect the light reflected by the spacecraft in order to get a sufficient number of photons on the laser station detectors.

If A (in square centimeters) is the effective area of the telescope used to collect the light,

T_R is the transmission factor of the telescope,

J (in Joule) is the energy of the laser flash,

Θ (in second of arc) is the beam divergence,

N is the number of photons collected by the telescope equipment, and considering the link budgets from the laser station and back to the laser station of reflection on the spacecraft,

the laser station should satisfy the relationship shown in table 5 below :

TABLE 5

ELEVATION	DISTANCE STATION S/C	NUMBER OF PHOTONS RECEIVED	
		RUBY LASER	NEODYME LASER
90°	35876 km	$N = 13 \frac{J}{\Theta^2} (T_R A)$	$N = 10 \frac{J}{\Theta^2} (T_R A)$
55°	36780 km	$N = 10 \frac{J}{\Theta^2} (T_R A)$	$N = 8 \frac{J}{\Theta^2} (T_R A)$
25°	39070 km	$N = 3 \frac{J}{\Theta^2} (T_R A)$	$N = 3 \frac{J}{\Theta^2} (T_R A)$
15°	40061 km	$N = 1 \frac{J}{\Theta^2} (T_R A)$	$N = 0.8 \frac{J}{\Theta^2} (T_R A)$

The number of photo-electrons detected is :

$$N_e = N \cdot \rho$$

$$\rho = (\text{quantum efficacy of photo-multiplier}).$$

Minimum beam divergence

A sufficient beam divergence is necessary for the laser station in order to ensure that the pulse arrives at the satellite, taking into account small errors in the satellite position (known within ± 1 km). Then the laser stations must have a beam divergence of :

$$\theta \geq 10'' + 2 \times (\text{angular error of tracking})$$

Performance of time-measurement devices in the laser stations

- Laser stations participating in the LASSO experiment should permit synchronisation with a standardised time of their zone (ex. IAT ...) by the terrestrial means on a daily basis with a precision of about a few microseconds.

Maximum error on the synchronisation between two laser stations participating in the LASSO experiment should be less than 1 millisecond before measurements by LASSO.

- Each pulse transmitted by the laser station should be able to be pre-programmed at T_0 . If T_1 is the real time at which the laser pulse was transmitted, one should have :

$$(T_0 - T_1) < 1 \text{ millisecond.}$$

T_1 should be measured with an accuracy of ± 0.1 nanosecond, "a posteriori".

- If T_2 is the time of arrival of the pulse back from the satellite, it should be measured with an accuracy of ± 1 nanosecond. Maximum time elapsed from start to return of a given pulse :

$$270 \text{ msec} > T_2 - T_1.$$

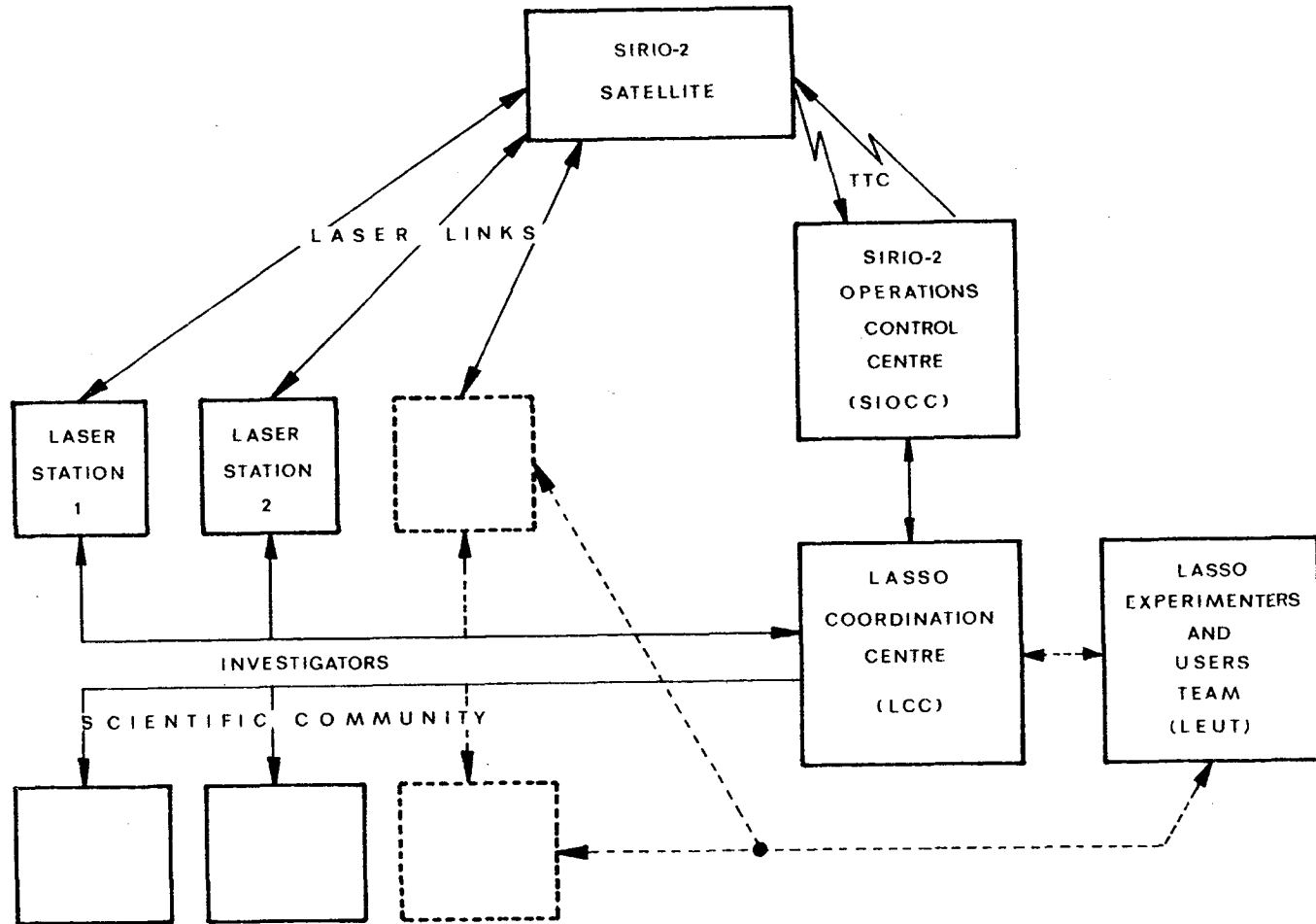
6. THE OPERATIONAL ORGANISATION

The overall possible organisation for the two-year period of LASSO operations is given on figure 10.

This diagram shows the inter-relations between four important bodies :

- The Scientific Community and the laser stations,
- The LASSO experimenters and users team (LEUT),
- The LASSO Coordination Centre (LCC),
- The SIRIO-2 Operations Control Centre (SIOCC).

Figure 10: Possible Organization of LASSO Operations



The Scientific Community, supported by laser stations, will submit to the LEUT their reply to the announcement of opportunity. After evaluation, principal investigators will be appointed and will become members of the LEUT for the duration of the proposed experiment.

The LEUT, attached to the ESA project group, is in charge of the international coordination of the LASSO experiment and the establishment of the utilisation schedule for the two-year life time of SIRIO-2. During the experiment phase selection, the LEUT is a nucleus of experts and will be enlarged afterwards by all the principal investigators.

The LCC, which is the key point between laser stations, SIOCC and LEUT, has the primary tasks to :

- exchange information with SIOCC (orbit parameters, spin phase and speed, telemetry data),
- compute laser firing times,
- exchange information with laser stations (pointing angles, firing times, time events, data),
- select the operational mode (synchronic, asynchronic, one way, ...),
- pre-process scientific data and ensure the dissemination,
- create and run the data bank,
- perform special data processing (on request).

The SIOCC is in charge of the spacecraft control and monitoring during two years under ESA's responsibility. In the frame of LASSO, SIOCC will be entrusted with :

- performing VHF ranging,
- providing attitude and orbit data for spin phase and speed computation,
- decoding of TM format to extract LASSO data,
- sending necessary LASSO telecommands,
- monitoring housekeeping information.

7. FUTURE PROSPECTS

In collaboration with CNES, the ESA project group will perform some preliminary investigations to evaluate the possibility of embarking equipment on board European spacecraft with the goal of achieving a 0.1 nsec synchronisation accuracy.

This evolution of LASSO might include :

- a three-axis stabilised spacecraft on geosynchronous or low polar orbits,
- a centroid detection system, self-adjustable, for laser pulse width from 50 psec to 25 nsec, with faster photodiodes,
- a digital chronometer with 10 psec resolution,
- possibly a space-qualified rubidium or cesium standard on board.

8. CONCLUSION

The LASSO experiment on-board the SIRIO-2 spacecraft aims at proving possibility to synchronise clocks over intercontinental distances by means of laser stations.

The pioneering aspect of this first experiment, the small amount of space and power available on-board, and the very tight schedule (18 months), have led us to maintain, for the design of the on-board equipment, relatively simple technical solutions.

In addition, the fact that SIRIO-2 is spin stabilised requires the laser stations firing times to be synchronised with the rotation of the spacecraft. This aspect makes the operational use of the system more complicated; however we are examining the possibility of using an asynchrone mode, and even a one way mode.

Taking into account the studies performed by CNES on the LASSO experiment and the results we have had during the testing of the breadboards, a certain number of improvements has led us to consider a second generation of LASSO.

- oOo -

QUESTIONS AND ANSWERS

DR. CARROLL ALLEY, University of Maryland

There are several things that those of us who are planning to participate in this experiment need to know a little more detail about. One would be an explicate value for the differential scattering cross section for the corner reflector array. Are you able to provide that at the present time?

DR. SERENE:

Not really. Actually, tests of the reflector are ongoing at CNES and each corner cube will be tested and all we can say is it is a bad one, which has a very bad, well, equivalent defraction pupil will be rejected, but I can give you actually only value. The only thing I can say, we ought to get a higher efficacy and to overpass the figure of 14 we gave in this presentation.

DR. ALLEY:

Yes. It is not 14. What is the actual cross section of individual corner reflectors? Circular reflectors?

DR. SERENE:

(Nods affirmatively.)

DR. ALLEY:

What diameter?

DR. SERENE:

Twenty millimeter. I think it is 20 millimeter diameter, the corner cube with a circular section, yes?

DR. ALLEY:

The second question. I have some concern about achieving even a nanosecond precision without some form of constant tracking discrimination for the received electrical signals. We have discussed this question before. Is there any possibility of including that kind of equipment on this first go?

DR. SERENE:

No. As I mentioned to you previously also, we are actually on a certain time schedule which is quite tight. We have to load the spacecraft. We are not the only passenger on-board and it will be the subject of LASSO number two on board of another spacecraft.

DR. ALLEY:

And one more. What will be the actual, with respect to receiver, area, including these additional objects that you have mentioned and what is the actual threshold of detection in terms of energy or photons for the detector?

DR. SERENE:

The threshold has been evaluated in terms of photon by something like 3,900 for Ruby and 2,050 for Neodyme I think. We have fixed the threshold because the threshold actually has been fixed to 20 dB as you have seen on the table for the different laser stations. Yes that is right. The number of photons per nanosecond riding up the detection element at the threshold is 3,900 photons per nanosecond arriving for Ruby lasers and 2,500 for Neodyme lasers.

DR. ALLEY:

What is the actual resolution of the on-board event timer?

DR. SERENE:

The actual-- The official one or the measured one?

DR. ALLEY:

The resolution. Can you resolve down to a tenth of a nanosecond or is it one nanosecond?

DR. SERENE:

Actually, I was two weeks ago in Paris where is Marcel Darseau and the breadboard was giving on the chronometer 50 picosecond for an average of 300 measurements. It is a statistical value.

DR. ALLEY:

What is the standard deviation of that? Do you know?

DR. SERENE:

Not really, because actually we are waiting for the last Hewlett-Packard counter to be able to perform a more accurate one because we are at the limit of the test equipment. The breadboard is looking better than all test equipment actually available, except this latest Hewlett-Packard counter.

SOME IMPLICATIONS OF RECIPROCITY FOR
TWO-WAY CLOCK SYNCHRONIZATION*

James L. Jespersen
National Bureau of Standards
Boulder, Colorado

ABSTRACT

Two common methods for synchronizing remote clocks are called one-way and two-way. Both of these methods, when operated in the traditional fashion are subject to a number of difficulties related to propagation perturbances. This paper points out however, that under certain circumstances, these difficulties can be circumvented for the two-way scheme. This possibility is explored theoretically, in some detail, with respect to the Loran-C navigation system.

*Contribution of the National Bureau of Standards, not subject to copyright in the United States.

INTRODUCTION

Radio signals are commonly employed to compare clocks at remote locations. The two most commonly used schemes are called "one-way" and "two-way." In the one-way scheme a signal is transmitted from location A, where clock A is located, to location B where clock B is located. The time, τ_{AB} , it takes the signal to travel from A to B depends upon the signal path distance, d , between A and B and upon the average signal speed, s , over the path. Or in simple mathematical terms

$$\tau_{AB} = d/s. \quad 1)$$

To accurately compare the clocks it is necessary to know τ_{AB} . Although 1) is mathematically simple its determination in the "real world" can be very difficult. There are a number of reasons for this. First, the signal may not travel a "line-of-sight" path between A and B. If the signal, for example, is ionospherically propagated the actual signal path is a complex function of the distribution of electrons in the ionosphere. Second, the signal speed may change along the path. Again, in the ionosphere, the signal speed is a function of electron distribution. Third, the signal may change its shape during propagation. This means that the point on the signal wave form that is "tagged" as the time reference point as the signal leaves A may be "washed out" by the time the signal arrives at B. Fourth, it is necessary to accurately know the geographic locations of A and B.

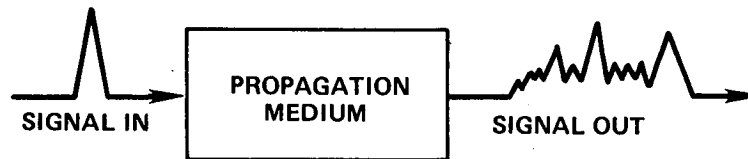
The first three factors are usually discussed in terms of:

- 1) homogeneity of the medium;
- 2) isotropy of the medium;
- and 3) frequency dependence of the medium (dispersion).

As mentioned earlier the ionosphere is not homogeneous because its

electron density changes with height, which leads to non-constant signal speed and to complicated signal paths. Furthermore, the propagation medium may be non-homogenous in the sense that it contains irregularities which scatter the signal. Thus, although only one signal is transmitted from A, several signals may arrive at B via several different paths.

Because of the presence of the earth's magnetic field, the ionosphere is also non-isotropic for radio waves. In general, this means that the signal speed and the attenuation of the signal depend upon direction of propagation. Finally, for radio waves, the ionosphere is frequency dependent because the signal speed depends upon signal frequency. This effect is usually referred to as frequency dispersion of the signal. All three of these factors lead to shape distortion of the signal, illustrated schematically:



Sommerfeld^[1] and others have considered dispersion in considerable detail. These treatments are highly mathematical, and I shall only briefly sketch the main results of these investigations. First, some very small part of the signal travels with the speed of light independent of the dispersive properties of the medium. This part of the signal called the "Sommerfeld precursor" is quite weak and oscillates very rapidly. A short time later the "Brillouin precursor" arrives with greater amplitude and longer duration. Finally, depending upon the structure of the transmitted signal and upon the detailed dispersive properties of the medium, the signal settles into some steady state value. The Sommerfeld and Brillouin precursors have been experimentally verified in the laboratory at micro-wave frequencies,^[2] although to my knowledge no one has investigated the possibility of using them in timing and navigation systems.

TWO-WAY MEASUREMENTS

To avoid some of the difficulties discussed in previous paragraphs, it is sometimes easier and perhaps even necessary to measure τ_{AB} when one wants to make a clock comparison. Usually a "two-way scheme" is employed to measure τ_{AB} in the following way. As in the one-way method, a signal is transmitted from A which arrives some time later at B. At the instant the signal arrives at B (or after some known delay time), it is returned to A. To determine the round trip path delay between A and B, an observer at A notes the transmission and reception times of the signal at A with respect to the clock at A. If the propagation medium is isotropic, then path delay reciprocity can be assumed; that is, the path delay from A to B equals the path delay from B to A. Thus, $\tau_{AB} = (\text{round trip delay})/2$.

This approach alleviates two problems. First, it is not necessary to know the geographic positions of A and B, and second, it is not necessary to know average signal speed. The disadvantage is that transmitting and receiving equipment are required at both ends of the path. There may also be a problem due to dispersion. If the signal arriving at B is a distorted version of the one transmitted from A, then it is no longer clear when the time reference point has arrived at B so it can be "reflected" to A. Similarly, the signal traveling from B to A will be distorted so there is again the problem of determining signal arrival time at A.

The problem of signal shape distortion can be considered from a somewhat different point of view. As stated above, if reciprocity holds and if there is no signal shape distortion, then the observer at A, using the two-way method, can determine the one-way path delay τ_{AB} from A to B. The concept of signal delay, τ_{AB} , involves

the notion of average signal speeds and path distance (as shown explicitly by equation 1). The two-way measurement only provides τ_{AB} , that is, it only provides the ratio of distance d to speed s . If either d or s is known by some independent means then the other quantity can be determined.

Consider the case now where there is some definite known path distance d , say a line of sight path, but there is dispersion along the path so that a distorted signal arrives at B and the return signal also arrives distorted at A. In this case, τ_{AB} cannot be measured, so no meaningful value can be assigned to s , even though d is known. We could say that the notion of signal speed or "group" velocity, as it is usually called, has failed. In a similar fashion suppose that there is not dispersion, but there are many irregularities in the path which scatter the signal so that although only one signal is transmitted from A, many overlapping but similarly shaped signals arrive at B. Again the composite signal at B is a distorted version of the one that left A, so that no meaningful arrival time can be assigned. For this case, s has a definite value (assuming isotropy), but d is not meaningful since no single path is involved. If a single path can be isolated (e.g. the Loran-C ground-wave signal), then the problem can be resolved.

Suppose now that τ_{AB} cannot be meaningfully determined by the two-way method, either because of signal shape distortion or because of a multitude of paths, or perhaps both. Are either one of these conditions sufficient to destroy the utility of the two-way scheme? That is, is the notion of definite path delay, τ_{AB} , and definite average group velocity, s , necessary for the two-way scheme to work?

Let's consider the following situation. The propagation medium between A and B is both dispersive and non-homogeneous, but isotropic. That is, the signals propagating between A and B are both dispersed and scattered identically in both directions because of isotropy. Suppose similar shaped signals are launched simultaneously from A and B. The signals arriving at A and B will have identical shapes, though very different from the transmitted shapes, and further, both signals, since they were launched simultaneously, will fluctuate in amplitude and phase identically as a function of time at A and B. If the signals are not launched simultaneously (and if the propagation medium remains constant with time), then the two signals arriving at A and B will still be identically shaped, but displaced in arrival time by an amount that is just equal to the difference in launch times of the two signals.

Thus, all that is required to compare the clocks at A and B is to determine the amount of time displacement of the two signals in spite of the fact that the notions of group velocity and definite path delay have no meaning. Thus, isotropy (with the two-way scheme) is the only condition required to compare clocks. Homogeneity and dispersionless media are not required.

This fact does not seem to have been explicitly pointed out before, perhaps because of the intimate association between timing and navigation systems where the notion of path delay is critical.

In summary then, if the medium is dispersionless, isotropic and homogeneous, the notion of path delay can be employed and the two-way scheme may be employed in the usual way. However, if the medium is dispersive and non-homogeneous, the two-way scheme can still be used if the received signals at the two ends of the path

are brought together to determine their difference in arrival time. In fact, we might say that bringing the records together is the extra price we must pay to remove the dispersion and non-homogeneity problems.

A practical implementation of this procedure would be to sample, at high rate, and store on magnetic tape, the amplitudes of the two received signals as a function of time with respect to the clocks at A and B. The tapes could then be brought together and lag cross-correlated to determine the clock offsets.

LORAN-C

Loran-C is the backbone of the system for international clock comparisons. Loran-C has the advantage that its signals are pulsed so that ground wave and sky-wave signals can be separated if the observer is sufficiently close to the Loran-C transmitter. However, at distances beyond several thousand kilometers, the ground wave weakens relative to the sky wave signal and the difference in arrival time between the sky and ground wave signals becomes small so that it is difficult to separate them. Even at distances where the separation can be made, international clock comparisons are compromised by the fact that the ground wave delay is subject to an annual variation with a magnitude of about one microsecond at sites as far removed as the NBS time scale in Boulder, Colorado.^[3]

The discussion in this paper suggests that more accurate clock comparisons could be made if Loran-C were employed in a two-way mode. First of all, variations in path delay (annual or otherwise) cancel out. Second, it is not necessary to separate the ground and sky waves if the cross-correlation technique is utilized. Third, the Loran-C sky wave has been detected at distances exceeding

5 thousand kilometers,^[4] so it would not be necessary to "bridge" large distances by intercomparing observations of Loran-C signals which were all within "groundwave" distance of each other. Fourth, to improve signal to noise, the signals could be averaged for long periods of time at both ends of the path, since signal path delay variations have no effect on the cross-correlation determination of clock offset.

Strictly speaking, for the two-way measurements, the observers at both ends of the path should be co-located with the transmitting antennas at A and B, but as a practical matter, this is not possible. However, other measurements^[5] suggest that the observer could be as far as a few kilometers from the transmitting antenna before any significant difference forward and return in the propagation paths developed. Another difficulty related to being near the transmitter antennas, is that the transmitter signals might interfere with one's ability to receive distant Loran-C signals. However, because of the short pulse width of the signals, it appears^[6] that gating procedures can be developed which will solve this problem.

The primary point that remains in question is the degree of an isotropy for Loran-C sky-wave signals. As stated earlier, the presence of the earth's magnetic field in the ionosphere makes it anisotropic. Using a procedure developed by Johler,^[7] some preliminary calculations have been made to determine the degree of anisotropy for Loran-C sky waves. Table I shows the results of these calculations for both local noon and local midnight at the mid-point of the path. When the observer is far enough from the transmitter station so that the signals reflect from the ionosphere at grazing incidence, i.e., at or exceeding 2000 kilometers, the table shows during the daytime that the path delay non-reciprocity

at 100 kHz is 49 nanoseconds for east-west propagation and 3 nanoseconds for north-south propagation. At night, the non-reciprocity amounts to 190 nanoseconds for east-west propagation. Other related calculations^[8] suggest that one can always expect a greater non-reciprocity at night.

Based on these results for grazing incidence, if the non-reciprocity component of the 100 kHz signal delay is ignored, the error in the two-way clock comparison would be half the total non-reciprocity or about 25 nanoseconds.

Of course these calculations depend upon a particular model of the ionosphere. However, as long as the signals reflect from the ionosphere at grazing incidence, I do not anticipate that the degree of non-reciprocity will be particularly sensitive to the details of the ionospheric model.^[9]

The table also shows that as the observer's distance to the Loran-C transmitter decreases the degree of non-reciprocity increases. This is probably due to the fact that, at shorter distances, the signal penetrates more deeply into the ionosphere during the reflection process, so that the signal path through the non-isotropic portion of the total path between A and B increases. My preliminary conclusion from these calculations is that two-way Loran-C comparisons should be made during the daytime over distances large enough for grazing incidence to hold.

It should be emphasized that these calculations apply only to the 100 kHz Fourier component of the Loran-C pulse. To determine in detail what happens to the entire pulse during propagation, requires making similar calculations for all of the significant

Fourier components of the pulse and then adding up these components with the proper phases at the observer's location. In addition, the degree of attenuation of the amplitudes of the Fourier components during propagation is also a function of Fourier frequency and propagation directions. Therefore, a complete analysis of what happens to the Loran-C pulse during propagation must take into account both amplitude and phase delay variations as a function of direction and Fourier frequency.

The advantage of such an analysis is that the full energy in the pulse at all Fourier components can be used. Such calculations are now under way and will be reported in a later paper.

As a final point, since the procedures discussed here imply that clocks comparisons in the tens of nanoseconds range be accomplished, relativity effects cannot be ignored. For example, in the east-west direction at 40° Lat., over a distance of about 4000 kilometers, non-reciprocity due to relativistic effects amounts to about 10 nanoseconds.^[10]

REFERENCES

1. A. Sommerfeld, Ann. Phys., 44, 177 (1914).
2. P. Pleshko and I. Palocz, Phys. Rev. Letters, 22, 1201, (1969).
3. Private Communication, D. Allan, P. Tryon, and G. Caldwell
4. L.D. Shapiro, IEEE Trans. Instrum. Meas., IM-17, 366, (Dec. 1968).
5. CCIR, Report 265-3, Geneva, (1974).
6. Private Communication, R. H. Doherty.
7. W. Hamilton and J. Jespersen, NBS Tech. Note 610, (Nov. 1971).
8. J. R. Jöhler and S. Horowitz, Office of Telecommunications Report 73-20 (1973).
9. *ibid.*
10. Private Communication, D. Allan.

TABLE I
THEORETICAL CALCULATIONS OF NON-RECIPROCITY

DISTANCE KILOMETERS	DIRECTION	FREQUENCY	LOCAL TIME OF DAY AT MID-POINT OF PATH HOURS	NON-RECIPROCITY NANOSECONDS
2000	EAST-WEST	100 kHz	0	190
"	"	"	12	49
1500	"	"	0	285
1000	"	"	0	360
"	"	"	12	67
800	"	"	0	458
"	"	"	12	86
700	"	"	0	427
"	"	"	12	129
600	"	"	12	343
2000	NORTH-SOUTH	"	12	3

QUESTIONS AND ANSWERS

DR. STEIN:

Any questions?

DR. VICTOR REINHARDT, Goddard Space Flight Center

What practical method do you propose to compare the two signals?
What correlation scheme do you think would be best for Loran-C signals?

DR. JESPERSON:

I think-- We have been considering several things. One of them is to maybe do something like the VLBI people do, put something on tape so we can bring the tapes together and do a lag cross correlation scheme between them.

So, we haven't gone into great detail yet, but some scheme of that sort.

DR. REINHARDT:

You then propose to look at the analog signals rather than measure the phase at zero crossing?

DR. JESPERSON:

What I would like to do is sample at a very high rate so we could get the whole signal. Then once we have got it we can do anything to it. We can Fourier analyze it and say pick out the 100 kilohertz component and look at the phased bit, and we can pick out all the other Fourier components and we can see then, in detail, how those components are matching up to our theoretical notions as to what should happen.

DR. REINHARDT:

Thank you.

DR. LESCHIUTTA, IEN, Turin, Italy

Thank you. The Loran-C is usually a one-way system, but in one case it is a two-way system. I refer to use made by the Loran-C station to control each other making reception time with the pulses coming from the other stations participating in the same network. And I am wondering if you think that if the data were

available, it would be available, I mean, in order to correct or to compensate some of the problems found across the Atlantic Ocean in order to correlate the clocks from both sides of the ocean?

DR. JESPERSON:

Yes. That is obviously one of the things that we are thinking about here that instead of using the ground wave over a number of short hops to span the Atlantic Ocean, in fact, one could use a one-hop sky wave essentially. Yes. That is one of the implications, I hope, of the work we are doing. As I say, it hopefully does away with some of the seasonal problems too, because whatever the seasonal part is, it disappears because you are not looking at the ground wave and even if there is some seasonal effect in the ionosphere, that also drops out.

EVOLUTION OF THE INTERNATIONAL ATOMIC TIME TAI
COMPUTATION

Michel Granveaud

Bureau International de l'Heure - Paris (France)

ABSTRACT

The International Atomic Time TAI is a worldwide time reference. Its computation has changed during the last 10 years. Further changes would essentially depend on the improvement of the atomic clocks.

The International Atomic Time TAI as computed by the Bureau International de l'Heure (BIH) is a worldwide time reference officially adopted in 1971 [1]. It has been made available for the scientific community for 24 years. The time signals transmit Universal Time Coordinated UTC which is closely related to TAI. The TAI computation has involved atomic clocks, comparisons between the clocks and mathematical algorithms. It is intended to outline the main recent changes concerning the above three points and to have a look to some future possibilities of computing TAI.

Atomic clocks

The computation of TAI has been performed from the data of cesium clocks*. Some significant modifications, quantitative as well as qualitative, must be noted in the devices involved in it over the last decade as shown by the Figure 1. In 1962, about 45 commercial cesium clocks entered this computation, all of them being manufactured by the Hewlett-Packard company-models 5060A and 5061A-. The Hewlett-Packard option 4 clocks were introduced into the TAI clocks ensemble at the end of 1972. Then the introduction of the Oscilloquartz

* Data from other devices with cesium comparable performances could be used.

cesiums -model OSA 3200- led to an interesting diversification of this ensemble. Nowadays, in 1979, TAI is composed of about a hundred cesium clocks. On the other part, three laboratory cesium clocks have been used in the computation of TAI: the NRC-CsV of the National Research Council since May 1975 [2], the NBS-4 of the National Bureau of Standards since the end of 1975 [3] and more recently the PTB-CS1 of the Physikalisch-Technische Bundesanstalt [4]. These clocks offer at the same time * very good stability for sample times up to several months and excellent accuracy.

Time intercomparisons between clocks

The time intercomparisons between distant clocks play an important role in the computation of TAI. In 1979, as 10 years before, the LORAN system ensures the connection between the clocks of various laboratories ; so the international time TAI appears strongly dependent on the qualities and defects of this system. The LORAN transmissions delays change with respect to time and they have to be calibrated from time to time by the clock transportations results. The US Naval Observatory carries out most of these transportations, especially between America and Europe ; it allows to limit the inaccuracy of the LORAN time comparisons down to about 1 microsecond, the precision being of the order of 300 nanoseconds or better. Many experimental time intercomparisons were performed during the last decade using satellites [5]. The NTS campaign results [6] showed interesting promises for the Global Positioning System; an inaccuracy of less than 100 nanoseconds is expected. Some precise time comparisons were performed between 2 or 3 laboratories through the satellites ATS-1 [7], Hermes and Symphonie [8]; precisions up to a few nanoseconds were obtained on a regular basis. As soon as precise time comparison results via a satellite system are routinely available, they will be used to compute the TAI.

Computation of TAI

From 1969 till 1979, the TAI computation was concerned with two main concept changes. The first one took place in 1973 as a conse-

*The NBS-4 works either as a clock or as a frequency standard.

quence of the 1972 Consultative Committee for the Definition of the Second (CCDS) meeting. A new TAI algorithm was implemented where each clock participates with a weight which is a function of its past and present frequency*. On a practical point of view, the mean frequency of each clock over a two-month interval is computed with respect to TAI ; and the weight of a clock is proportional to the reciprocal of the variance of 6 mean frequencies : it takes into account the changes of frequency or, generally speaking, the short term instability of the clock. The other change is concerned with the accuracy concept. The laboratory cesium standards give the best realization of the SI (International System) second. Their improvement has been quite remarkable during the last decade; in 1976, their accuracy capability was of the order of 1×10^{-13} or better and three laboratory cesium standards at NBS, NRC and PTB agreed that the frequency of TAI was too high by 10^{-12} . The International Astronomical Union, in 1976, recommended that the TAI frequency be corrected by exactly -10×10^{-13} on 1977 January 1. This adjustment was made and was the first direct input of the laboratory standards on TAI.

Taking into account the uncertainty of 1×10^{-13} of the laboratory standards and the possible change of the TAI frequency by 1 to 2×10^{-13} per year (already observed) if TAI is solely based on commercial cesium clocks, one comes to the conclusion that rather frequent adjustments of the TAI frequency could be required in order to avoid significant errors. It was recognized that a frequency steering by frequent small adjustments (of the same order as the variations which can be expected from random noise) were better than noticeable corrections at less frequent intervals. The implementation of the steering was recommended by the Consultative Committee for the Definition of the Second in April 1977 and it was immediately put into effect.

The current computation of TAI results from these concepts and is carried out in two steps as shown by the Figure 2. The first step introduces the short term stability concept. The algorithm ALGOS computes a "free" time scale from the data of the cesium clocks running independently from each other. The second step introduces the accuracy concept. Starting from the laboratory cesium standards

*the term frequency is used instead of normalized frequency

a frequency reference is obtained through the algorithm A. The inaccuracy of the "free" time scale is measured with respect to the reference and is partially corrected through a defined procedure. The correction of the inaccuracy leads to an improvement of the long term stability. The choice of the correction procedure is important to avoid any stability deterioration of the "free" time scale.

From now on

A worldwide time reference must be a) available for the users - b) reliable so that it is not upset or stopped by any local incident - c) stable for any sample times, i.e. uniform - d) accurate with respect to the SI second. The fulfillment of these qualities is strongly dependent on the clocks which are or could be involved in the TAI computation.

The current situation is given by the Figure 3. A hundred commercial cesium clocks contribute mostly to the availability, reliability and short term stability while the accuracy and long term stability are ensured by the 3 laboratory cesium clocks and 1 laboratory cesium standard. Development of new laboratory cesium clocks, such as the NRC-CsVI ones, is in progress. They are the first metrological devices for specific time purposes featuring stability and accuracy qualities. It could be imagined that a new situation for the TAI computation would arise when a large enough number -may be 6? - of such units would be running in various laboratories. It would be wise to utilize these devices to fulfill the stability and accuracy qualities as shown by the Figure 4. The commercial cesium clocks would ensure the availability and the reliability of TAI.

Another potential situation would appear if some clocks were developed whose stability in a limited range of sample times would be better than that of the cesium clocks -it could be, for example, H-masers (passive) [9] -. In this case, the qualities of availability, reliability, stability and accuracy would be fulfilled by three various kinds of clocks: commercial cesiums, superstable clocks and laboratory cesiums as Figure 5 indicates. There would be a clear similitude between this last situation and the current one.

The TAI results from the combination of the data of atomic clocks and/or standards. In the past decade, two changes occurred coming first from the algorithm itself and then from the introduction of the laboratory cesium standards data. Different modifications are possible in the future.

References

- [1] 14th General Conference for Weights and Measures, 19 (1971).
- [2] Mungall, A.G., Costain, C.C., "NRC CsV Primary Clock Performance", *Metrologia*, 13, 105 (1977).
- [3] Hellwig, H., Bell, H.E., Bergquist, J.C., Glaze, D.J., Howe, D.A., Jarvis, St. Jr., Wainwright, A.E., Walls, F.L., "Results in Operation Research and Development of Atomic Clocks at the National Bureau of Standards", 9th CIC A 1.7 (1974).
- [4] Becker, G., "Das Cäsium - Zeit und Frequenznormal CSI der PTB als Primäre Uhr", 10th CIC, A 1.5, 33 (1979).
- [5] 14th Plenary Assembly of CCIR, Vol VII, 52 (1978).
- [6] Buisson, J., McCaskill, T., Oaks, J., Lynch, D., Wardrip, C., Whitworth, G., "Submicrosecond Comparisons of Time Standards Via the Navigation Technology Satellites (NTS)", 10th PTTI, 601 (1978).
- [7] Saburi, Y., Yamamoto, M. and Harada, K., "High precision time comparison via satellite and observed discrepancy of synchronization", *IEEE Trans.*, IM.25, 4, 473 (1976).
- [8] Costain, C.C., Boulanger, J.S., Daams, H., Beehler, R., Hanson, W., Klepczynski, W.J., Venstra, W., Kaiser, K., Guinot, B., Azoubib, J., Parcelier, P., Fréon, G., Brunet, M., "Two-way Time Transfer via Geostationary Satellites NRC/NBS, NRC/USNO and NBS/USNO via Hermes and NRC/LPTF (France) via Symphonie", 11th PTTI, in this publication.

- [9] Hellwig, H., "Future Development of Atomic Clocks",
Séminaire sur les Etalons de Fréquence, leur caractérisation
et leur utilisation , Besançon (France), 14.1 (1979).

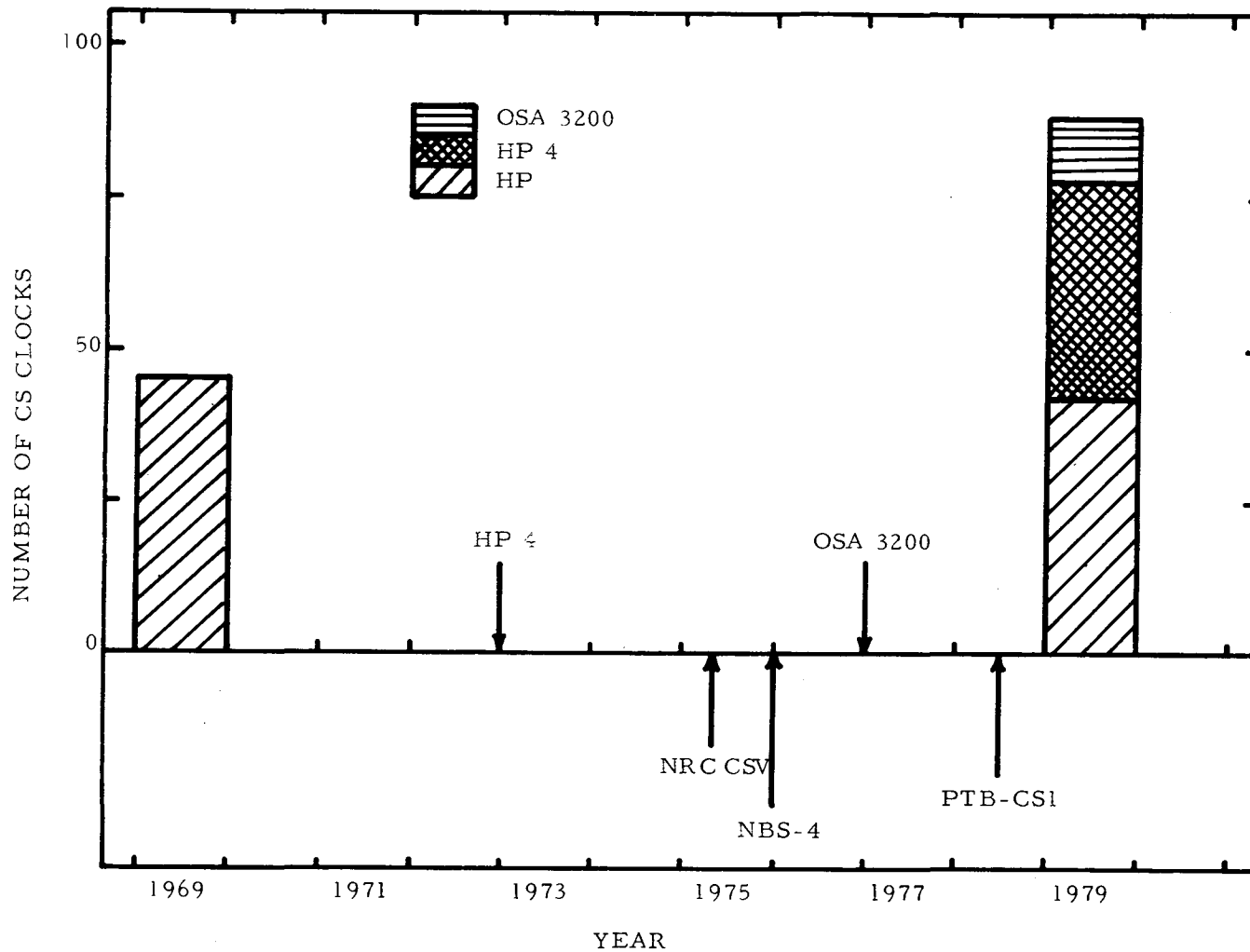


Figure 1. The Clock Ensembles of TAI in 1969 and 1979 are Shown and the Introduction of the New CS Clocks, Commercial and Laboratory. The Abbreviation HP 4 Means Hewlett-Packard Option 4 and OSA 3200 is the Oscilloquartz Model 3200.

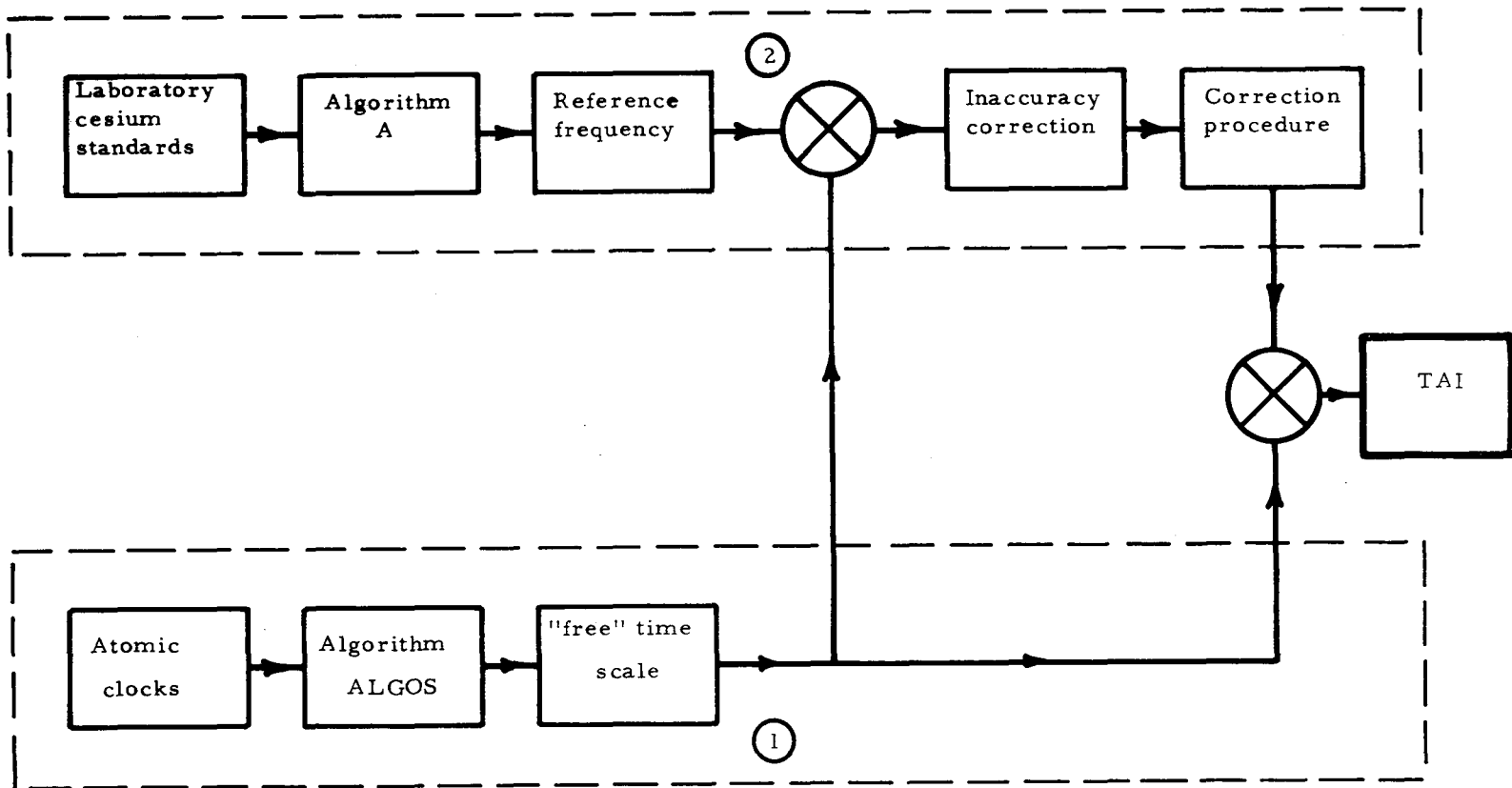


Figure 2. Schema of the TAI Computation in 1979. The Numbers 1 and 2 Refer to the Two Steps of the Computation

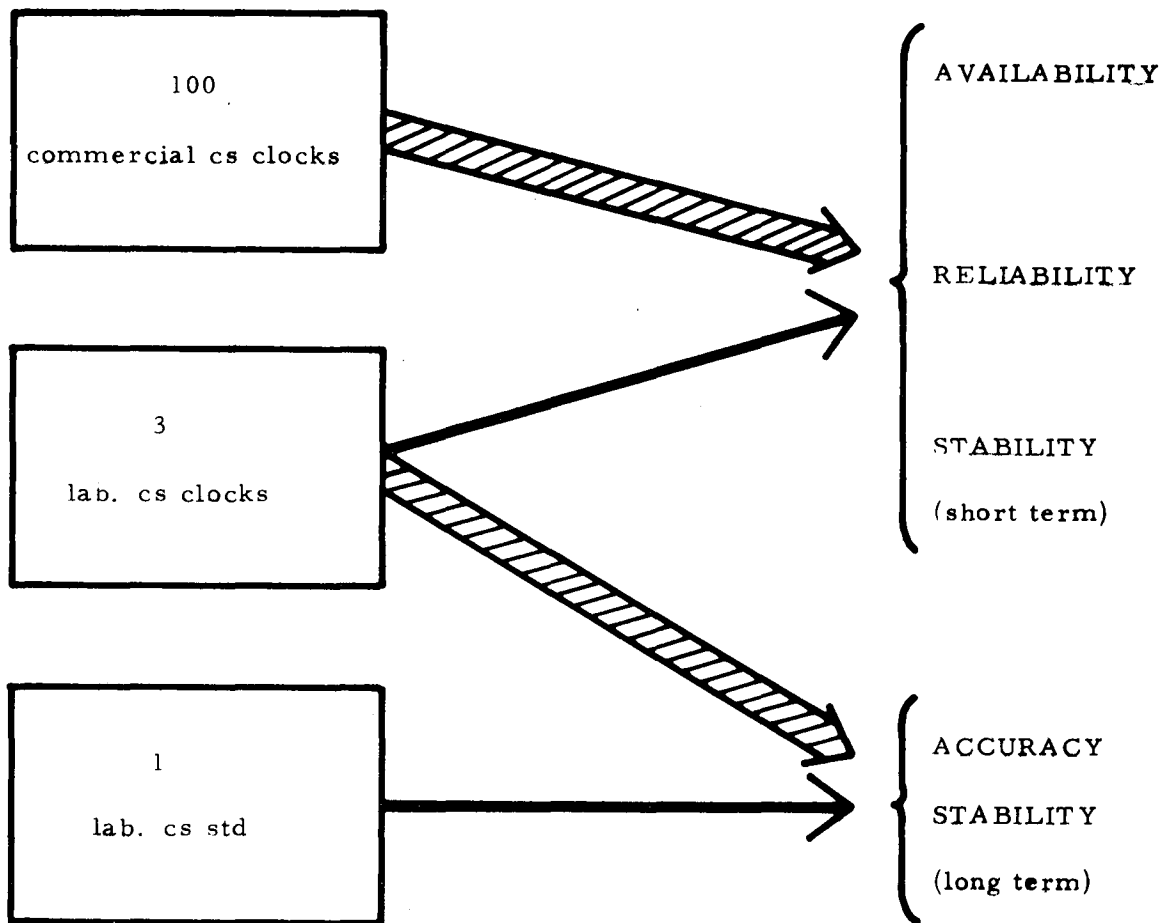


Figure 3. Current Computation of TAI. The Links Between the Available Devices and the Qualities Which are Looked for TAI are Shown. A Wide Line Indicates an Important Connection.

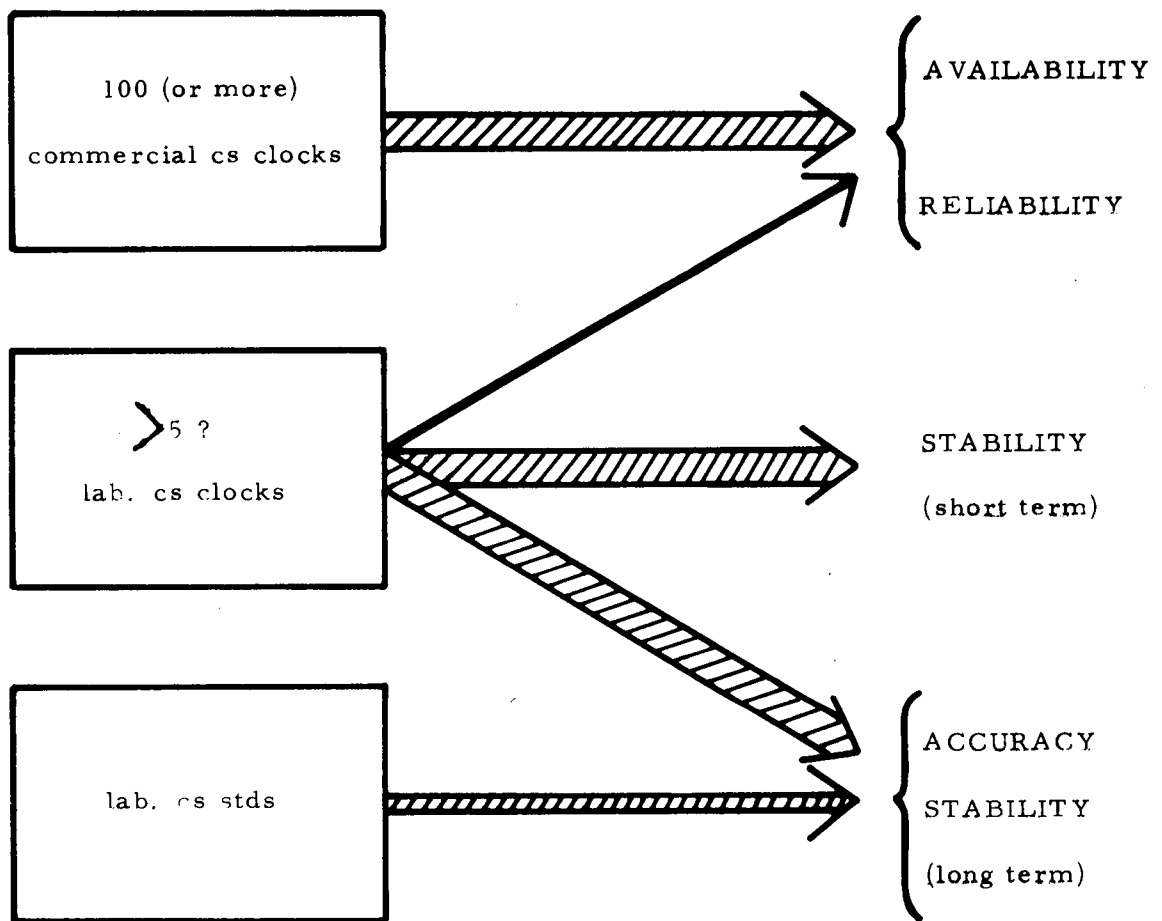


Figure 4. Foreseeable Computation of TAI. The Links Between the Available Devices and the Qualities Which are Looked for TAI are Shown. A Wide Line Indicates an Important Connection.

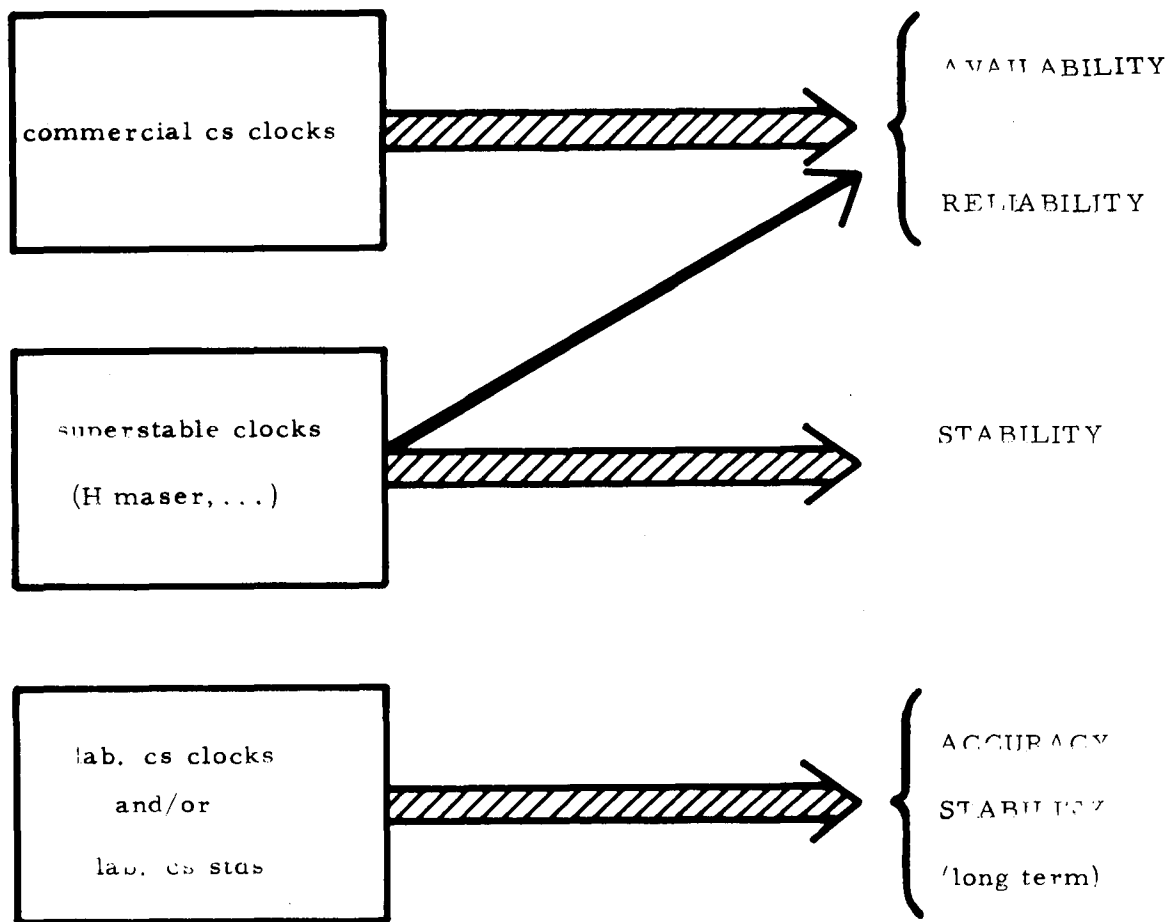


Figure 5. Potential Computation of TAI. The Links Between the Available Devices and the Qualities Which are Looked for TAI are Shown. A Wide Line Indicates an Important Connection.

QUESTIONS AND ANSWERS

DR. STEIN:

You made the distinction between, I think, what you called the laboratory cesium standard and, a laboratory cesium clock. Is that intended to represent the difference between a device which runs all of the time and a device which runs only a small fraction of the time?

DR. GRANVEAUD:

Yes.

DR. STEIN:

In that case I think it is probably important to add to your view of the future the fact that the kinds of developments that are going on right now in the cesium standard area will result in devices with full accuracy that is achieved without any interruption in the operation.

DR. GRANVEAUD:

Yes.

HYDROGEN MASER IMPLEMENTATION IN THE DEEP SPACE NETWORK
AT THE JET PROPULSION LABORATORY

Paul F. Kuhnle
Jet Propulsion Laboratory, Pasadena, California

ABSTRACT

Hydrogen masers (H-masers) are the most stable frequency standards in use today within the sampling intervals (τ) from 100 to 10^4 seconds. The Jet Propulsion Laboratory (JPL) employs hydrogen maser frequency standards in a variety of fixed and mobile applications, ranging from the 64-meter Deep Space Network stations to the 9-meter Astronomical Radio Interferometric Earth Surveying (ARIES) stations.

This paper describes the Frequency Standard Test Laboratory (FSTL) developed and implemented by JPL. This test laboratory has the capability to measure the frequency stability of five frequency standards including environmental parameters. Nine frequency standards may be evaluated simultaneously upon completion of the current instrumentation expansion program. Frequency stability measurements and environmental data on five H-masers are presented.

JPL is continuing hydrogen maser implementation plans by evaluating new H-maser designs for use during the 1980s.

INTRODUCTION

JPL supplies hydrogen masers as the prime frequency standard for navigation to the outer planets and for Very Long Baseline Interferometer (VLBI) experiments in both fixed and mobile ground stations. JPL has instrumented a Frequency Standard Test Laboratory to evaluate and test H-masers, other frequency standard types and reference frequency distribution equipment during development and prior to implementation in the user's facility. Selected representative test data recorded during the past two years is included in this report.

Hydrogen Masers at JPL

H-maser users at JPL have been using prototype and experimental H-masers for approximately 10 years for VLBI experiments and selected spacecraft tracking functions. In 1978, JPL formally installed one H-maser at each of the Deep Space Network (DSN) 64-meter tracking stations at Goldstone,

California and Madrid, Spain. A JPL DSN-type H-maser had previously been installed and has been in use at the DSN 64-meter tracking station near Canberra, Australia since 1976. In addition, JPL has operating H-masers at one DSN 26-meter tracking station at Goldstone, Owens Valley Radio-metric Observatory (OVRO) and the ARIES mobile ground station. Three H-masers are retained at the JPL Pasadena complex. Two of these are reference masers in the test laboratory; the third is used as the DSN spare and by the ARIES geophysical mobile ground station.

Currently JPL has a total of eight H-masers in continuous use. These have been supplied by two well-known manufacturers and JPL. There are three Smithsonian Astrophysical Observatory (SAO) model VLG-10B H-masers which were supplied to JPL by the NASA Marshall Space Flight Center. The NASA Goddard Space Flight Center (GSFC) has loaned JPL one model NX H-maser and has, until recently, supplied JPL with three model NP H-masers.

JPL has three of the DSN type and one prototype H-maser in use at this time. Figure 1 tabulates the location, manufacturer, model and serial number of each H-maser in use by JPL today.

Some Selected Test Data Results to Date

JPL established a Frequency Standard Test Laboratory at the Pasadena, California complex and subsequently tested five H-masers between May 1978 and April 1979. These five are currently in use as shown in Figure 1. The units tested were JPL model DSN, serial numbers 2 and 3 and SAO model VLG-10B, serial numbers P5, P6, and P7.

The tests scheduled were considered to describe fully the necessary operating parameters of each H-maser. Additional parameters were usually recorded to assist in diagnostics or help explain the erroneous behavior of a desired parameter. The desired parameters recorded during these test programs were frequency stability versus sampling time (Allan variance) and frequency shift versus the environmental parameters of temperature, barometric pressure and the Earth's magnetic field.

Temperature tests were conducted on the five H-masers for step frequency shift in the temperature range of 21 to 29°C and then repeated from 29°C to 21°C. A step change in temperature usually causes the frequency to start shifting in less than one hour and it will continue to shift for approximately 40 hours with an exponential decay. The temperature coefficient for each H-maser tested is tabulated in Fig. 2. Of the environmental parameters, temperature presents the greatest frequency stability perturbation. It is not uncommon to experience room temperature fluctuations of 1 to 2°C in a diurnal or longer time period, resulting in a $1-2 \times 10^{-13}$ frequency shift. At the 64-meter tracking stations, the H-masers are in separate temperature-controlled rooms. These rooms are controlled to the nearest 0.1°C, thereby minimizing the

problem and reducing the temperature-dependent frequency shift to typically 1×10^{-14} .

Response to changes in the local barometric pressure was tested on the same H-masers. The test chamber pressure was increased by 6 inches of water and after approximately one hour decreased to minus 6 inches of water, relative to the starting ambient pressure. Because the frequency shift responses are instantaneous, the pressure differential must only be maintained long enough to determine the resultant frequency shift. The barometric pressure coefficient for the five H-masers is tabulated in Fig. 2. The resultant barometric pressure data shows that four of the five H-masers exhibit approximately the same frequency shift for an incremental pressure change. The exception is model VLG-10B Number P6 which exhibited an excessive frequency stability fluctuation during test. This H-maser at Goldstone has not always responded to storm barometric pressure fluctuations. It is planned to schedule a barometric pressure retest on this unit when sufficient H-masers are available to temporarily remove this unit from the field. A typical barometric pressure shift at Goldstone is approximately 0.3 inch Hg. The resultant frequency shift of the other four H-masers would be approximately 1×10^{-14} .

Frequency shift response to static magnetic field disturbances was measured on the five H-masers. The results are tabulated in Fig. 2. The resultant normalized frequency shift per gauss is 1 to 5×10^{-12} for four of the five H-masers. Magnetic field perturbations in the test laboratory are typically less than one milligauss under controlled operating conditions of minimal movement of ferrous materials. The measured magnetic field perturbations are typically five milligauss at the H-maser installation location within the 64-meter tracking stations. The resultant predicted frequency shift during these disturbances would be typically a maximum of 1×10^{-14} . The fifth unit (JPL-DSN2) was several times more sensitive to magnetic field than the other four H-masers tested. Following these tests, this H-maser was installed in a moly-permalloy magnetic shield box, which improved the shielding factor by a minimum of 100 or a predicted magnetic field coefficient of 1.4×10^{-13} per gauss.

A selected sample of Allan variance curves for four of the five H-masers tested since June 1978 is shown in Fig. 3.

The sampling times (τ) of less than approximately 1000 seconds are controlled by the signal-to-noise ratio. Each manufacturer designs H-masers to operate within a desired output power range. The JPL model DSN H-maser's nominal output power is approximately -87 to -89 dBm. The SAO model VLG-10B H-maser output power range is approximately -95 to -100 dBm. Therefore the data between the two SAO H-masers measured in June 1978 is approximately as expected. Later tests have used one SAO H-maser compared against one JPL H-maser.

Measurements at sampling times greater than 1000 seconds depict a degradation of frequency stability. This is due to "systematics," which is a combination of environmental effects and oscillator aging. In this set of specific cases, the curves peak at the sampling time of 20,000 seconds (approximately six hours), the 1/4 diurnal temperature cycle. Note that two of four curves exhibit this effect. The other conclusion is that all of these H-masers, except possibly SAO serial number P6, are aging. Since installation, P6 has been nearly continuously compared against a cesium beam frequency standard bank traceable to NBS. There is no indication versus this bank that this H-maser is aging. The curve between serial numbers P5 and P6 in June 1978 indicates that the aging is considerably less than all the other H-masers tested. JPL H-maser DSN-3 is not shown on this curve, but the approximate same slope is apparent as with all H-masers except P6. Note that the frequency stability curves exhibit a broad "bright line" (degradation hump) on two curves for sampling times between 100 and 800 seconds. This is caused by the cooling cycling rate of the building air conditioner. The lower dotted-line curve was recorded during November 1979 after the FSTL temperature control was improved. This is discussed later in this report.

Figure 4 again shows the Allan variance versus sampling time curve in Fig. 3. This plot has the measurement error bars and number of data samples available written beside each bar. In this case, where the number of samples is not shown, the number is greater than 51. Since all sampling times are simultaneously recorded, the number of samples increases as the sampling time decreases.

Frequency Standard Test Laboratory

A Frequency Standard Test Laboratory (FSTL) installation was initiated in August 1977 at the Pasadena complex to determine the operational performance of H-masers. An isolated building was obtained and is located at one end of the "Mesa" antenna range above and behind the Laboratory. This location was chosen because it is isolated from man-made disturbances of the Earth's magnetic field and has sufficient floor space for five H-masers and all instrumentation required at this time. Figure 5 is a view of this building with the Angeles National Forest in the background. The floor plan of this 700-square-foot building (Fig. 6) depicts the location of H-masers, environmental chamber and instrumentation. This laboratory is now equipped with instrumentation to simultaneously measure 12 channels of Allan variance and 12 continuous recording channels of long-term frequency shift.

Figure 7 is a block diagram of a single channel of this frequency stability measurement equipment. Figure 8 is a block diagram of the test configuration for comparing the frequency of three H-masers using three sets of the instrumentation shown in Fig. 7. Local barometric pressure, room and equipment temperature and Earth's magnetic field disturbances are continuously recorded as ancillary data to the frequency stability

measurements. Instrumentation is available to record frequency standard anomalies as required. Several examples are: vacion pump current, oven heater temperatures and cavity tuning bias voltage.

Figure 9 is a photograph of the instrumentation room, which contains nine electronic instrument cabinets. The equipment description is as follows, from left to right: (1) cabinets 1 and 2 are for environmental and anomaly measurements; (2) cabinet 3 is for general spectral and waveform analyses; cabinet 4 contains the RF reference isolation amplifiers, mixers and zero crossing detectors shown in Fig. 7; cabinets 5 through 8 each contain three channels of frequency stability measurement and recording equipment, and cabinet 9 contains general instrumentation, a rubidium frequency standard and two spare H-maser receiver crystal VCO's.

A combined temperature and barometric pressure chamber was designed and fabricated by JPL with non-magnetic materials to prevent distorting and attenuating the Earth's magnetic field around the H-maser. A separate connected heat exchanger preconditions the chamber air temperature for barometric pressure and temperature tests.

A 7-foot-diameter double axially concentric Helmholtz coil is used to generate static perturbations of the Earth's magnetic field. Generally, these coils are mounted around the environmental chamber to expedite the schedule on separately measuring H-maser frequency shift versus temperature and magnetic field. The environmental chamber and Helmholtz coil are shown in the far right corner of Fig. 10.

Standby AC power was installed to prevent power loss to the test laboratory. This equipment consists of a 4.5-kVA uninterruptible power supply (UPS) and a 30-kVA automatic starting generator. All frequency standards and critical instrumentation requiring power without interruption are connected to the UPS. The balance of the instrumentation, UPS input power and most of the air conditioning equipment is connected to the generator during primary power outages.

H-maser test results between May 1978 and April 1979 showed that both the laboratory temperature environment and instrumentation required improvement for future test programs to determine the prospective improved long-term frequency stability performance. These revisions are now completed. Subsequent tests show the new computer floor plenum air temperature to be stable to within 0.1°C peak to peak and the room 5 feet above the floor to 0.5°C peak to peak. The previous air conditioning system controlled the room from 1 to 3°C peak to peak for diurnal and longer time periods, depending on the outside weather conditions. An Allan variance test recorded during November 1979 showed considerable stability improvement using the same two H-masers previously recorded in April 1979. Compare the two curves dated April 1979 and November 1979 in Fig. 3. Note that at the Allan variance at 2×10^4 seconds sampling time

(τ) the "bright line" peak is not evident and the overall noise at sampling times greater than 1000 seconds is much lower. Room temperature control is considered to be the major factor in this improvement.

Additions and improvements to the instrumentation expanded the Allan variance and long-term frequency shift measurement capability to 12 channels. Additional recording instrumentation to continuously measure equipment temperature, magnetic field and room humidity has been added. This is sufficient instrumentation to simultaneously measure the stability of five H-masers as shown in Fig. 11.

Frequency shift versus barometric pressure increments have been difficult to measure in the past. It is expected that newer H-maser designs will exhibit even less barometric pressure sensitivity; therefore the environmental chamber has been strengthened to double the barometric pressure stimulus range to ± 12 inches of water relative to the local barometric pressure.

It is intended to further improve the laboratory environment and instrumentation to meet the requirements from development and research of future frequency standards. Instrumentation improvements being considered and studied at this time are computerized automation of the data acquisition on a continuous basis, control of the test chamber humidity during environmental tests, and dual difference detection for frequency stability measurements of non-offsettable frequency standards.

Present Test Programs

JPL plans to continue use of the FSTL in the future to give frequency standard research and support to the JPL-operated Deep Space Tracking Station Network and other JPL-operated fixed and mobile ground stations.

An important task scheduled to start in December 1979 is the NASA-JPL program to evaluate the operating performance characteristics of two recently designed H-masers. These are the SAO Model VLG-11B and the GSFC Model NR.

Maintenance, repair and retest of all H-masers currently in field use by JPL is a continuing high priority project. The FSTL has done and will continue to do requalification after repair and diagnostics on non-obvious failures prior to repair. The FSTL has been and will continue to be scheduled to test other types of frequency standards (e.g., cesium beam), active reference frequency cable stabilizer equipment, frequency multipliers and synthesizers.

Recently the Laboratory scheduled and completed a series of tests on one superconducting cavity stable oscillator (SCSO) manufactured by Stanford University and purchased by Caltech. This was part of the JPL research program to evaluate new types of reference oscillators.

ACKNOWLEDGEMENTS

I wish to thank JPL engineers Albert Kirk and Roland E. Taylor for their participation in this program. Their task has been to operate the FSTL since inception. Both have been very involved in the recent upgrade of this laboratory and continued operation of the FSTL.

This paper presents the results of one phase of research carried out at the Jet Propulsion Laboratory, California Institute of Technology, under Contract No. NAS7-100, sponsored by the National Aeronautics and Space Administration.

<u>LOCATION</u>	<u>MANUFACTURER</u>	<u>MODEL</u>	<u>SERIAL NUMBER</u>
DSS 14 GOLDSTONE, CA	SAO	VLG 10 B	P6
DSS 63 MADRID, SPAIN	SAO	VLG 10 B	P7
DSS 43 CANBERRA, AUSTRALIA	JPL	DSN	1
DSS 13 GOLDSTONE, CA	JPL	PROTOTYPE	P2
OVRO BISHOP, CA	GSFC	NX	2
ARIES JPL	SAO	VLG 10 B	P5
FSTL, JPL	JPL	DSN	2
FSTL, JPL	JPL	DSN	3

MANUFACTURER CODE

GSFC: GODDARD SPACE FLIGHT CENTER

SAO: SMITHSONIAN ASTROPHYSICAL
OBSERVATORY

JPL: JET PROPULSION LABORATORY

Fig. 1. JPL H-Maser Deployment

	<u>VLG 10 B</u> <u>P5</u>	<u>VLG 10 B</u> <u>P5</u>	<u>VLG 10 B</u> <u>P6</u>	<u>VLG 10 B</u> <u>P7</u>	<u>DSN</u> <u>3</u>	<u>DSN</u> <u>2</u>
TEMPERATURE $\frac{\Delta F}{F} / ^\circ C$	-1.6×10^{-14}	-1.2×10^{-13}	-1.0×10^{-13}	7.0×10^{-14}	2.5×10^{-13}	-6.3×10^{-14}
BAROMETRIC PRESSURE $\frac{\Delta F}{F} / \text{HG}$	2.6×10^{-14}	2.6×10^{-14}	-3.4×10^{-13}	2.3×10^{-14}	-3.8×10^{-14}	-4.8×10^{-14}
MAGNETIC FIELD $\frac{\Delta F}{F} / \text{GAUSS}$	1.6×10^{-12}	3.0×10^{-12}	5.0×10^{-12}	2.8×10^{-12}	4.8×10^{-12}	1.4×10^{-11}

Fig. 2. H-Maser Environmental Parameters

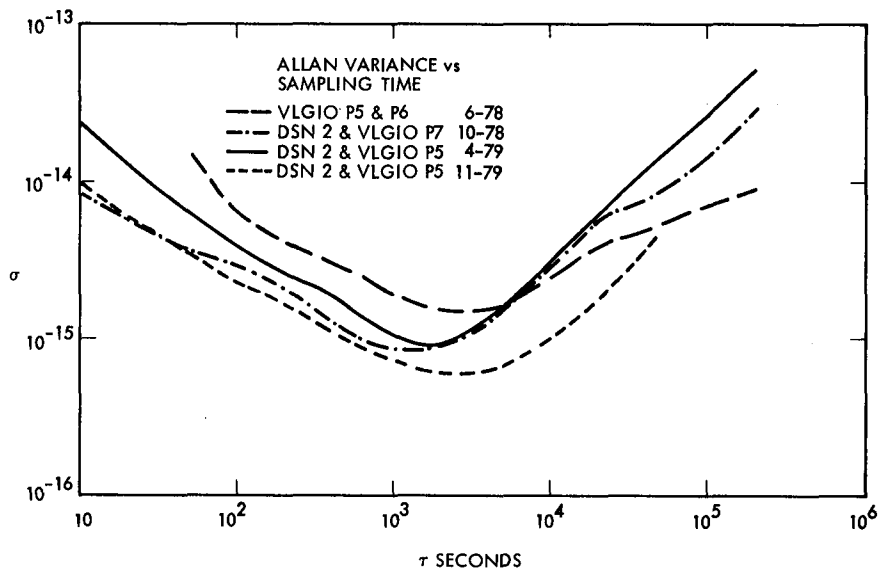


Fig. 3. Allan Variance vs. Sampling Time

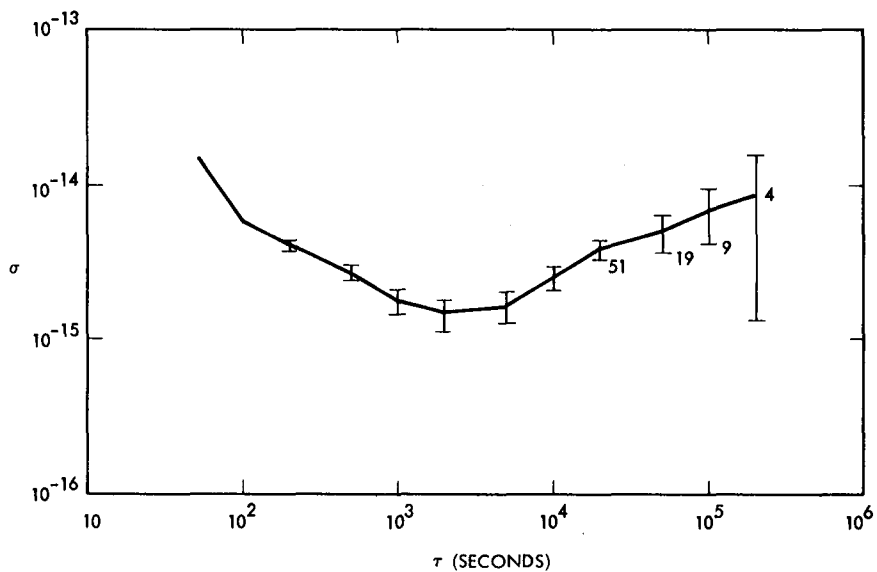


Fig. 4. Allan Variance vs. Sampling Time, with Error Bars

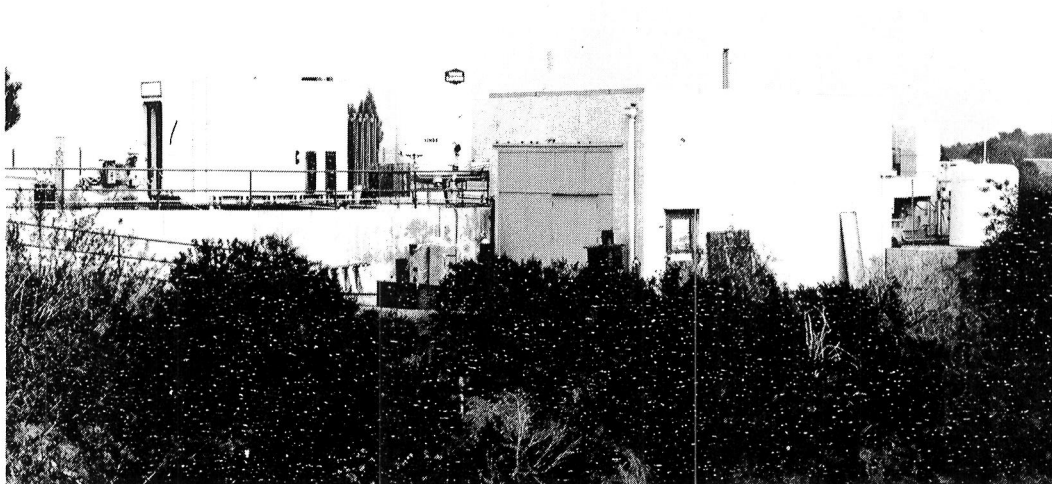


Fig. 5. JPL Frequency Standard Test Laboratory

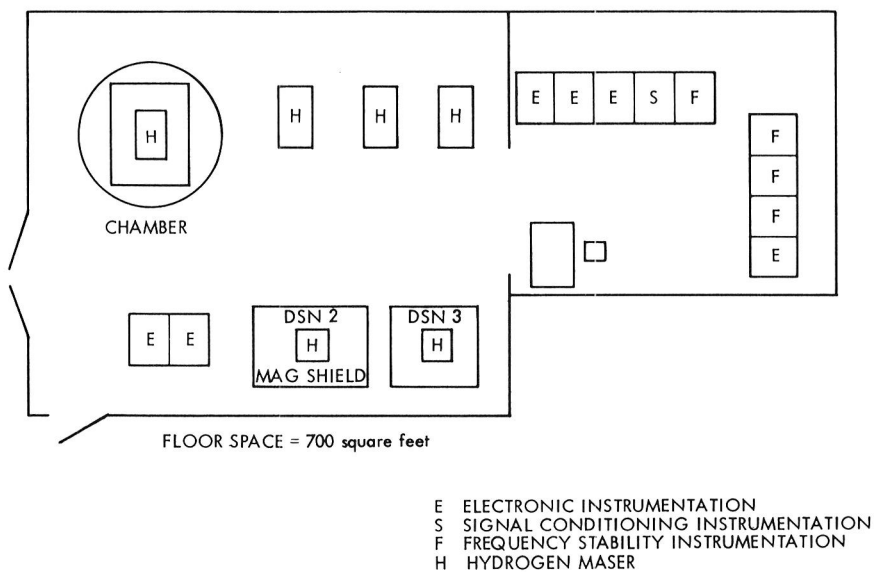


Fig. 6. Frequency Standard Test Laboratory Floor Plan

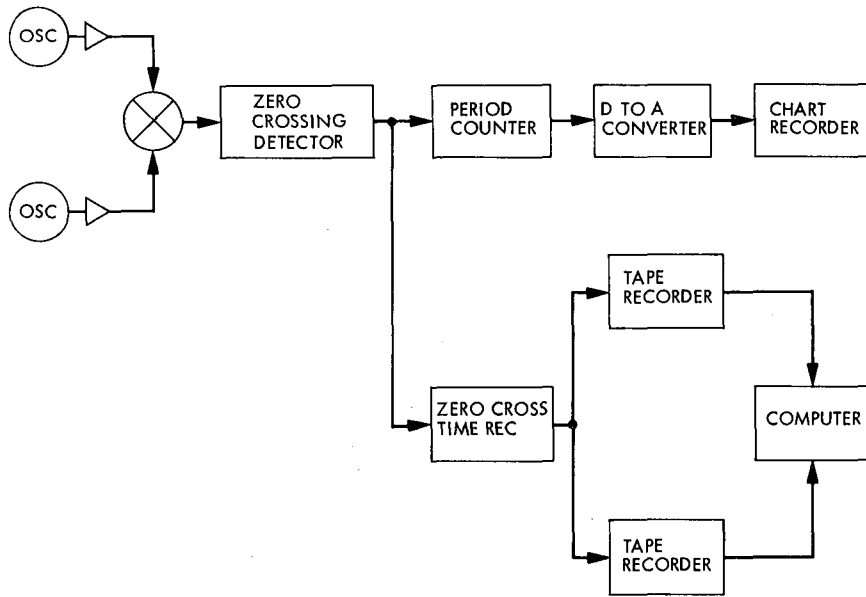


Fig. 7. Frequency Stability Instrumentation Block Diagram

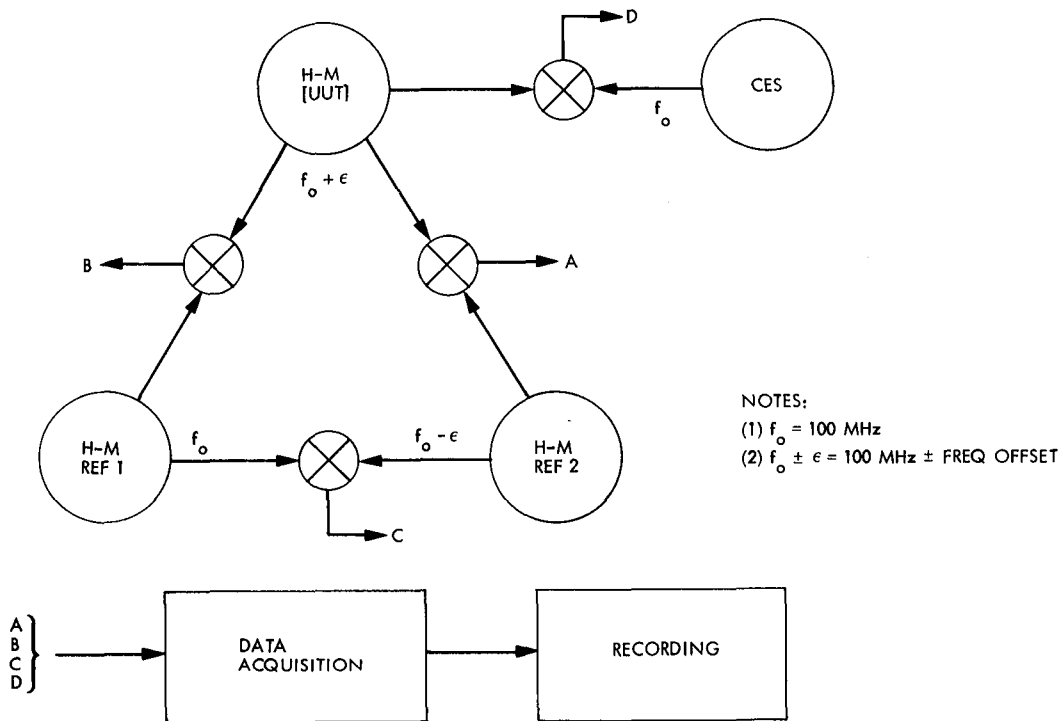


Fig. 8. Test Configuration for Stability Comparison of Three H-Masers

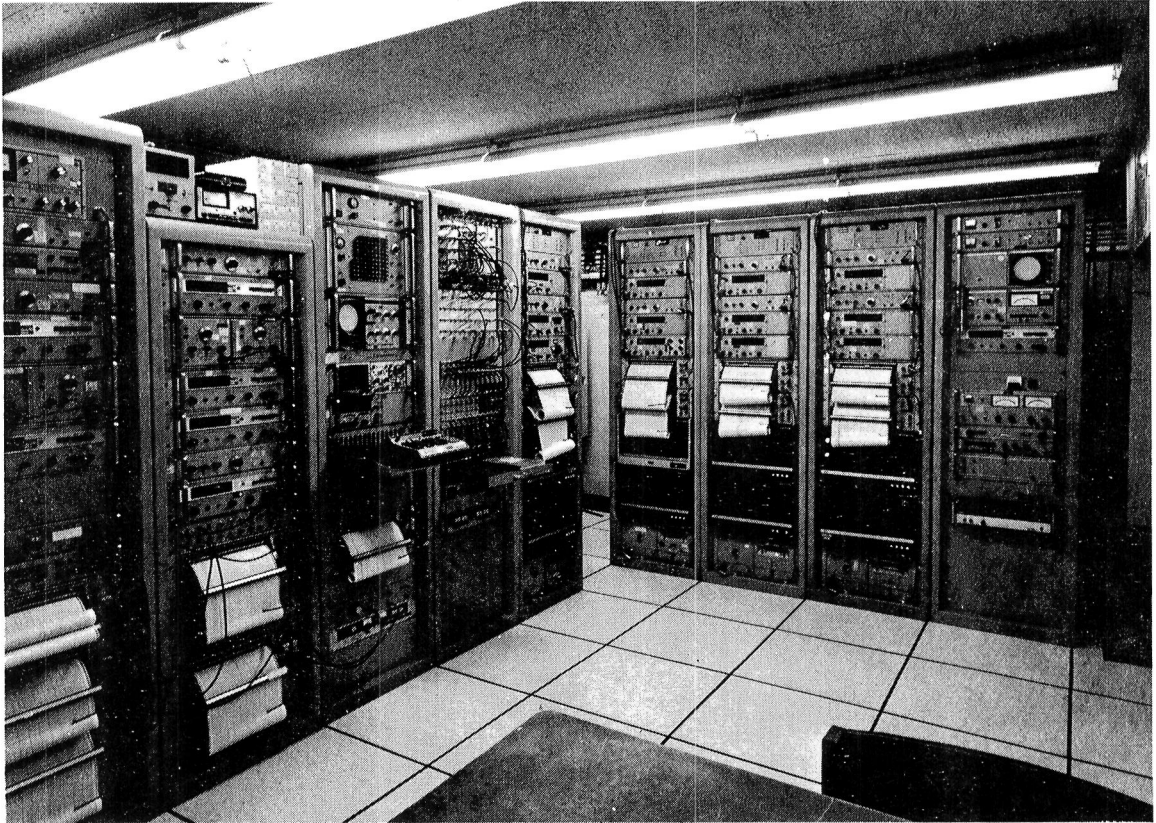


Fig. 9. Instrumentation Room Containing All Measurement Instrumentation

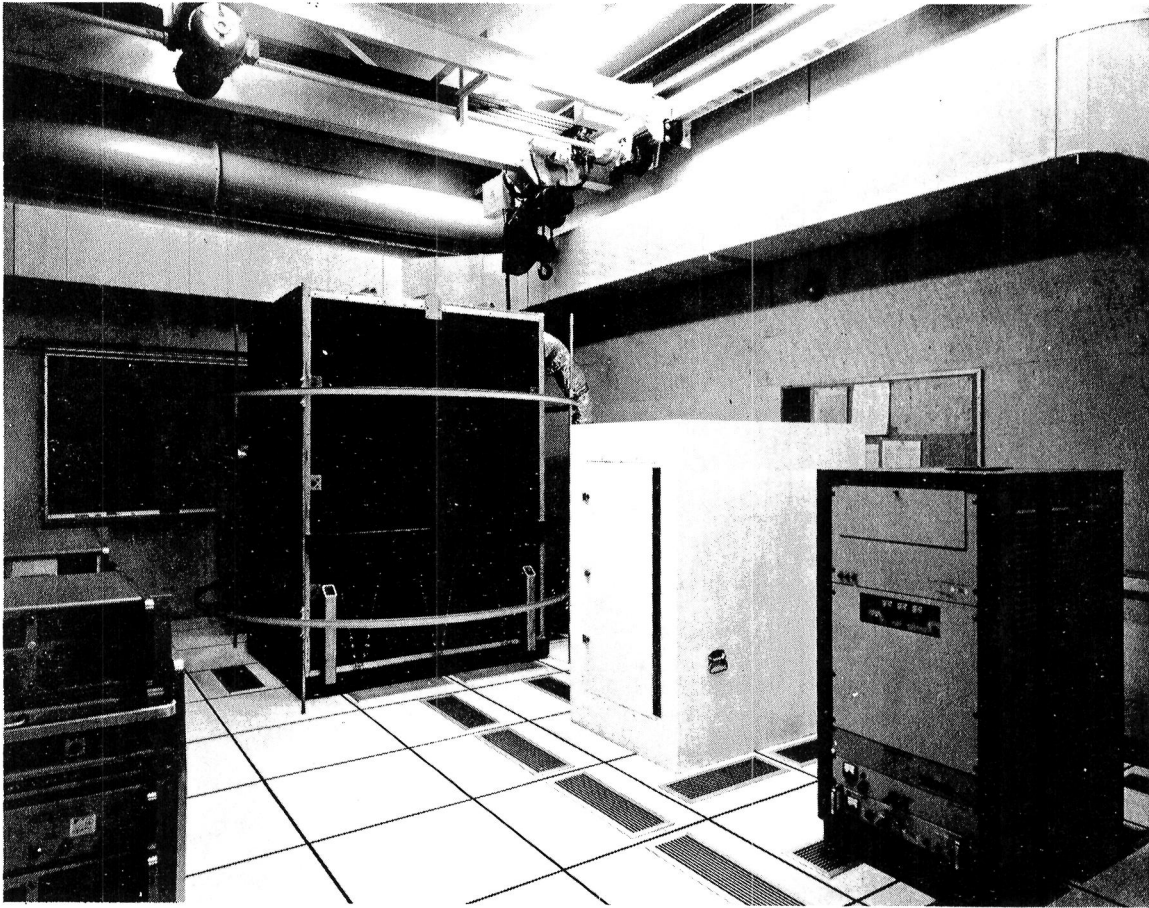


Fig. 10. Frequency Standard Room with Space on Right Side for H-Masers in Test and Environmental Chamber at Far Right

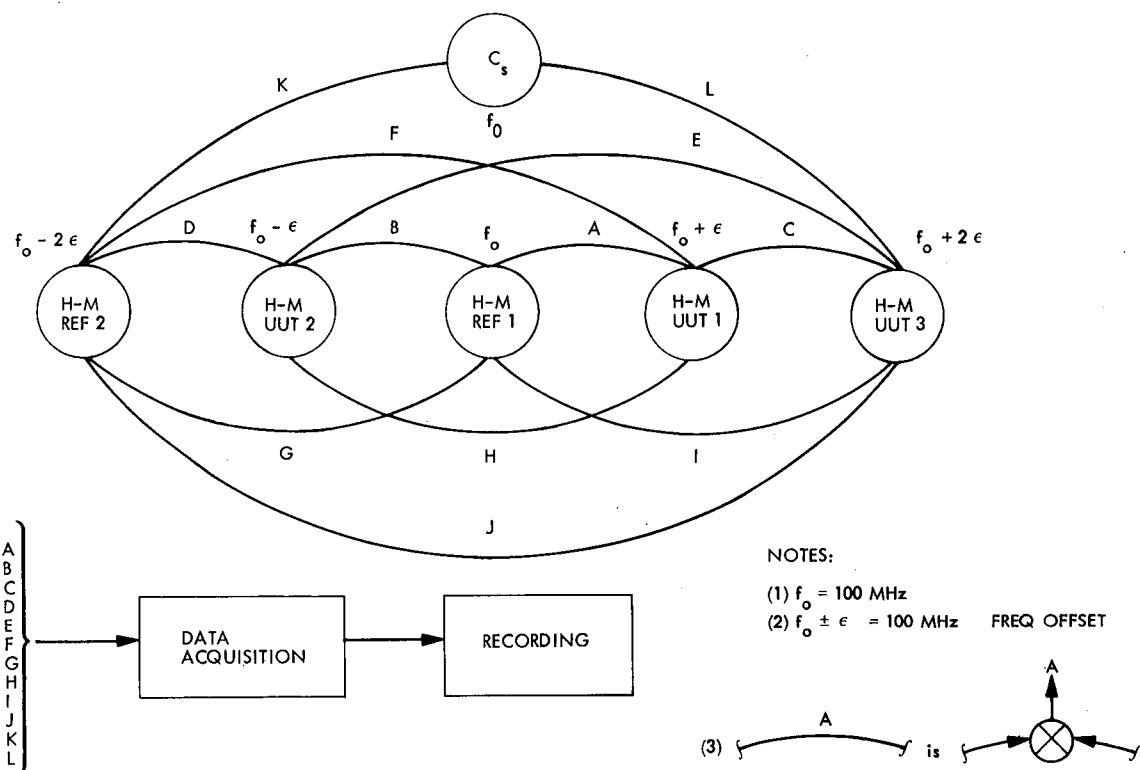


Fig. 11. Test Configuration for Stability Comparison of Five H-Masers

SESSION III

DISSEMINATION SYSTEMS I

**Prof. S. Leschiutta, Chairman
National Electrical – Technical Institute
National Standards Laboratory**

TIME DISSEMINATION - AN UPDATE

Kenneth Putkovich, U.S. Naval Observatory

Abstract

The original intent of this paper was to provide test results of the time transfers using a new Global Positioning System (GPS) Time Transfer Unit (TTU) developed for the U. S. Naval Observatory (USNO) by Stanford Telecommunications, Inc. (STI). As the TTU was not available for extensive testing at the USNO, only preliminary data were available at the time of the PTTI meeting. The scope of the paper was then changed to include several new developments in hardware and additions to services provided by the USNO in time dissemination in addition to reporting on results of time transfers utilizing the TTU and a new small portable atomic clock.

INTRODUCTION

The Precise Time and Time Interval Branch of the Time Service Division of the USNO is responsible for all of the hardware used in the monitoring and controlling of PTTI dissemination systems both local and worldwide. Included in this is the responsibility to publish and distribute the data gathered in a timely manner. In order to accomplish this within the constraints of limited available resources, the USNO relies heavily on the ingenuity and interest of specialists in the electronics industry to provide instruments that satisfy our stringent requirements. This paper provides a description of improvements that are being made to expand and enhance user services, a description of what is planned to improve the internal acquisition and reduction of data at USNO, a brief overview of new products that have become available due to USNO requirements and the initial results of tests conducted to determine the performance of two new time dissemination devices. These improvements provide the means to significantly improve time dissemination in a number of areas.

DATA AND SERVICES

In the past year or so several new or improved time data

distribution services have been implemented. In the coming year plans call for several more significant additions.

The Telephone Time Service [(202) 254-4950 or Autovon 294-4950] was inaugurated just prior to the 1978 PTTI Meeting. Since then over 750,000 calls have been logged on the system. System availability has been approximately 99.7% over that period. Modifications were made to increase the message length from one fifteen second cycle to four, thus making the service available for a full minute per call. Ten telephone trunk lines are installed so overloads are infrequent and occur only at times of high interest, i.e. Daylight Saving to Standard Time, leap seconds, etc. The system provides direct access to the USNO Master Clock. Fail-safe operation is provided by requiring that the digital input signals from separate reference clock systems be coincident to within a few microseconds before allowing calls to be answered. Any discrepancy which would result in an incorrect announcement causes the system to go off-line until the problem is corrected. The message consists of a one pulse per second tick (5 cycles of 1000 Hz) and a voice announcement and tone to identify particular seconds of both Coordinated Universal Time (UTC) and local time in the Eastern U.S. Time Zone. To prevent distortion due to interference, the voice announcement is blanked for a short period, during which, the tick occurs. Three simultaneous, fifteen second announcements, spaced at five-second intervals, are continuously on line and provide a caller access to an announcement within five seconds of his call being answered. The precision obtainable by measuring the time of arrival of the tick is on the order of one millisecond. Measurements of this signal, made in Switzerland by Dr. Peter Kartaschoff, showed delays of 55 milliseconds via cable and 251 milliseconds via satellite. Users utilizing multi-hop satellite links would have to exercise care in making measurements as delays of a half second or more could be experienced.

Timing coverage on the Loran-C system has been extended with the synchronization of two new chains, U.S. Northeast Coast (9960) and U.S. Southeast Coast (7980). The creation of two new chains from the combination of the stations of the now defunct U.S. East Coast Chain (9930) with five new stations has resulted in an increase in both coverage area and signal strength and, in many areas, gives users a number of signals to chose from.

The reconfiguration of the East Coast Chain also resulted in the loss of the Cape Race, Newfoundland station as a

dual-rated tie point for monitoring the North Atlantic chain performance. To alleviate this situation, the Observatory will install a monitor station at the Keflavik, Iceland SATCOM terminal to perform measurements on the North Atlantic and Norwegian Sea chains via the dual-rated station at Sandur, Iceland. Time transfers via SATCOM to Fort Detrick, Maryland and from there to the Observatory via TV Line 10 will provide the data necessary to accurately determine the timing performance of the two chains. Loran-C timing coverage will be further enhanced and expanded with the addition of the Great Lakes chain early in 1980 and the East Coast of Canada chain later that year.

The use of Earth satellites for time transfer and dissemination has always been of great interest to the Observatory. In addition to the routine operational use of SATCOM, Observatory personnel have been actively involved in nearly every satellite time transfer experiment performed (Telstar, Relay, Moon Bounce, ATS, Timation, Symphonie, etc.). Current efforts are centered around the Navy Navigation Satellite System, known as NNSS or Transit, and the Global Positioning System (GPS).

Although the Transit system has been in operation and available since the early 60's and the system's capabilities for precise time have been voiced by a number of proponents for a number of years, only recently, with the introduction of a commercially available Transit timing receiver, has the use of Transit time become realistic. The Observatory has published Transit timing information for a number of years in its Series 17, Transit Satellite Report. In recent years an effort has been made to improve the quality of the timing data available by seeking improvements in the satellite control procedures and by improving monitoring capabilities to allow the publication of data recovered from the satellite transmissions. The present generation of satellites (Oscars) provide a timing capability in the ± 25 microsecond region with global coverage on a daily basis. We hope that improved control procedures could reduce this to less than ± 10 microseconds for the Oscar satellites and to ± 1 microsecond for the new generation of satellites (Nova), two of which are scheduled for launch in 1980. Unfortunately, efforts to improve control procedures have been unsuccessful to date. The Observatory will continue its efforts in this area and is currently engaged in upgrading its monitoring capability to allow the daily publication of more useful and timely information on all satellites in view from Washington.

The GPS, when fully operational, will have the timing capability of worldwide coverage on a continuous basis to a level of better than ± 100 nanoseconds. Present proposals call for GPS time to be derived directly from the USNO Master Clock by means of a full GPS monitor station located at the Observatory in Washington. Monitoring by independent receivers will provide information for publication. The results of preliminary testing of the first receiver designed specifically for GPS timing will be presented later in the paper.

Another area in which the Observatory is currently engaged is the provision of access to Time Service data to users via a direct telecommunications link to our computers. This would provide real time availability of much of the data collected by the Observatory to any user who had a compatible modem and terminal.

COMPUTER HARDWARE AND SOFTWARE

The leading role that the Time Service Division has played in the development of automated systems for the collection and analysis of timekeeping information has continued and has become a major part of the Division's efforts. The now obsolete, but still operational, computer (IBM 1800) that is the mainstay of our automated system is being phased out and gradually replaced by two new minicomputers (IBM Series 1 and HP 1000). The integration of the new machines and the upgrading of the measurement system has turned out to be quite challenging. It is hoped that the two new machines, coupled to an IBM 4341 via a data communications link, will provide the improved performance, greater capacity and versatility and real time accessibility to data that is required. It is envisioned that the system will be able to accept data via a number of media (teletype, telephone, paper and magnetic tape, etc.) and will be able to output the processed information in printed form in several variations, electronically via telephone or teletype, in graphic form such as charts and view-graphs, on CRT terminals and so on.

The internal techniques and hardware for controlling the Master Clock system have been modified and refined to the point where the computer routinely adjusts the reference systems through a phase microstepper to a resolution of $\pm 1 \times 10^{-14}$. This is accomplished through a fail-safe interface designed and built at the Observatory. The programs for system control, the algorithms used in data analysis and the clock modeling techniques used in the predic-

tion process were also developed at the Observatory.

Work is also proceeding in two related areas. The first is a multiplexer for controlling the multilayered, coaxial switch system used for data collection on the Observatory grounds. When implemented, this will allow several computers and terminals to access any clock or data source as necessary. Access will be prioritized and the systems configured to extend the redundancy presently built into the clock system to the data collection system. The second is the development and implementation of computer controlled remote measurement systems which can be accessed via dial-up telephone lines. A pilot system has been installed in the Fort Detrick, Maryland SATCOM terminal as a test-bed. The system is based on IEEE-488-1975 compatible equipment operated by an HP 1000 computer over an autodialed, switched commercial line at 1200 baud.

SYSTEM HARDWARE

In the area of system hardware, the Time Service Division operates under a philosophy of utilizing off-the-shelf, commercially available equipment to as great extent as possible. If a product does not exist to fill a particular requirement, an attempt is made to interest a manufacturer in designing what is required and adding it to his product line. In house developments are limited to items which can't be economically procured by any other means. In the past several years there have been a number of requirements generated by the Observatory that are now being satisfied by off-the-shelf products whose origins can be traced to the Observatory. The following is a brief description of the more significant of these, including mention of specific characteristics which make them unique.

The first five instruments (designed by Mr. Leonard Shepard of ILC/Data Devices Corp.) are a direct outgrowth of requirements which developed over the last few years as a result of a general increase in the use of PTTI, an increase in the capability and sophistication of the user community and the availability of higher quality clock systems. As the stability of frequency standards improved and clock modelling improved, the need for improving the control mechanism at the frequency standard output become apparent. As a result, a new phase microstepper was developed which increased the range of operation from $\pm 1 \times 10^{-8}$ to $\pm 1 \times 10^{-7}$ at the low end and from $\pm 1 \times 10^{-14}$ to $\pm 1 \times 10^{-17}$ at the high end, reduced the size of the phase steps from 10 nanoseconds to 1 picosecond and reduced instabilities to

less than 500 picoseconds for a laboratory environment. This instrument is currently undergoing testing and should be in production early in 1980.

With the advent of measurement systems with subnanosecond resolution, the need to develop more well-defined and stable one pulse per second signals from the highly stable frequency standards came into existence. This need was satisfied with the clock/divider shown in Figure 1. It provides four independently buffered 50-ohm outputs (with port to port delay variations of less than 1 nanosecond) having rise times of less than 4 nanoseconds, jitters of less than 50 picoseconds and stabilities of better than 20 picoseconds per degree Celsius. In addition, a BCD output, a high visibility LED display and an audible tick are also provided.

As an adjunct to the above units, a pulse distribution amplifier (Figure 2), utilizing the same output circuits as the clock/divider, is available in configurations of up to 20 channels per unit. This allows the distribution of highly stable, isolated pulses over a large area without fear of system degradation due to line loading or other inadvertent interference.

Until recently, commercially available TV Line 10 time dissemination equipment suffered from a common fault. Television receivers designed for home use were used to recover the transmitted signal. The chief problems were due to the low quality of the components (compared to laboratory grade equipment) and the resultant instability and reliability. The TV Line 10 system offers an inherent capability for local time dissemination in the tens of nanoseconds under certain circumstances. In order to achieve this capability an instrument grade receiver (Figure 3) was designed and built. Utilizing these receivers, results well below 50 nanoseconds have been achieved. Efforts are currently under way to stabilize local TV transmissions using modified versions of the receivers to generate the required sync signals at the transmitter and thus achieve a stability below the 10 nanosecond level.

Time dissemination requires the ability to make high resolution, precise time interval measurements. Time interval counters used on portable clock trips have additional constraints in size and weight requirements. The most desirable situation is that of high resolution in a small package. After several unsuccessful procurement attempts, a counter designed specifically for portable clock appli-

cations has been built (Figure 4). The counter is contained in a package 1.75 inches high and 9 inches wide and weighs four pounds. It has a built-in digital voltmeter for setting the trigger levels, has a single shot resolution of 10 nanoseconds and an averaging resolution of 1 nanosecond.

TIME DISSEMINATION HARDWARE

The final two items, which have become available only in the last few months after several years of development, are a small portable atomic clock and a GPS Time Transfer Unit. Both are the result of requirements and support generated at the Observatory. As a large part of the Time Service Division's mission is concerned with the dissemination of PTTI, more efficient and accurate means of time transfer are of vital interest and a continuous effort is made to improve operations in these areas. Over the past twelve years the Observatory has conducted portable clock operations that have resulted in the synchronization of between 100 and 200 clocks yearly on a worldwide basis. The cost per clock synchronized can be anywhere between \$500 and \$1000 and three to four man-days of effort. Because of their size and weight, portable clocks presently in use pose logistical problems and require special handling to prevent injury to personnel handling them. Ways to reduce the physical and financial burden of these trips are constantly being sought.

The small portable cesium clock shown in Figure 5 is a product of Frequency and Time Systems, Inc., and it should have a significant impact on portable clock operations. Being slightly larger than a normal briefcase and weighing less than fifty pounds, it can be handled by one person and carried under most commercial aircraft seats. This makes possible an immediate cost reduction due to the elimination of the need for a seat for the clock and will allow the elimination of a second clock carrier on certain trips. As the clock has seven to eight hours of internal battery capability and provisions for operation from 115/230 VAC, 50 to 400 Hz, and 12 VDC it can operate in the same power environment as the larger clocks. The performance of the clock was recently evaluated on a seven-day trip to California. Two portable clocks were transported by auto and aircraft to a number of locations in and between Los Angeles and San Francisco. One was the small portable (designated FTS PC 101) and the other was a large portable (designated HP PC 1452). HP PC 1452 consisted of a Hewlett-Packard high performance cesium clock and standby power supply, a

combination that has given outstanding service for many years. At each site visited, measurements were made using both clocks. The results of these measurements are shown in Figure 6. The end points of the lines are measurements made at the Observatory at the beginning and end of the trip. The lines are interpolated estimates of clock performance during the trip. The data points plotted are the measurements made during the trip. If HP PC 1452 is assumed to be perfect and all the error assigned to FTS PC 101, we would assign the maximum deviation of approximately 50 nanoseconds to FTS PC 101. Since this is certainly not the case and since a curve fitted through the data points would be within 25 nanoseconds of the interpolation, the performance of the FTS PC 101 can be described as outstanding, well within the error one normally experiences on extended trips. The positive bias of the data indicates non-linear performance on the part of one or both clocks or some measurement error in the endpoint measurements. Efforts will be made to evaluate performance more fully in months to come.

The reason for this portable clock trip was to test a GPS/TTU at Stanford Telecommunications, Inc., Sunnyvale, California. The TTU was developed and built for the Observatory with funding from the Naval Electronic Systems Command. The GPS/TTU is intended to be a test-bed from which the timing performance of the present GPS phase can be evaluated, a monitor receiver from which operational GPS time dissemination can be carried out on an experimental basis, and a system prototype which will provide the information necessary to develop the next generation of GPS timing receivers.

The GPS/TTU is illustrated in the block diagram of Figure 7 and the photographs of Figures 8 and 9. The system consists of an antenna, preamplifier, receiver, processor, time interval counter, CRT terminal and power supply. After the equipment is powered up, the operating system and application programs are loaded in from magnetic tape cassettes and the time of day set. Execution of the application program begins with selection of various options for system operation and data collection, processing and recording. Data base parameters, such the geodetic location of the receiver, receiver delay and UTC-GPS time offset are entered from a tape or via the keyboard. The satellite acquisition procedure is then initiated by setting in the satellite identification number and an estimate of the expected doppler. Once initialized the system automatically acquires and tracks the selected satellite and records the data.

The receiver utilizes the C/A code on the L1 carrier frequency. The data from the C/A code is used to determine the satellite position and to estimate the time of arrival of the satellite subframe epoch. The estimate is corrected for ionospheric, tropospheric and relativistic errors and compared with the actual time of arrival as recorded by the counter. The difference between the actual time and the estimate is the difference between the local clock and the satellite clock. This process is repeated and data recorded for every six-second message received while the satellite is in view and the receiver is tracking.

The evaluation of TTU performance consisted of establishing the difference between GPS and UTC utilizing a high performance portable clock and then using the same clock as the input to the TTU and measuring the same quantity utilizing the satellites. The evaluation was performed during the period from November 14 to 19, 1979. Portable clock HP PC 1452 and FTS PC 101 were transported to the GPS Master Control Station (MCS) at Vandenberg AFB, to the contractor's plant in Sunnyvale, back to the MCS and then back to Sunnyvale. At each location measurements were made. The results of these measurements are shown in Figure 10. The data are presented with all clock biases and offsets removed and represent the actual measured differences between the GPS clock at the MCS and that same clock measured via the satellites. The two data points designated with an X are GPS time as defined by the atomic clock at the Vandenberg MCS receiver site. The circles and triangles are satellite values measured using the TTU in Sunnyvale. All data received via the satellite fall well within the ± 100 nanosecond limits established in the system specification.

CONCLUSION

This paper has provided a brief description of some of the improvements that are being made in the generation and dissemination of PTTI at the U. S. Naval Observatory. Details on some of the newer hardware developed for this purpose were presented. Data from tests of two of the more significant items, a small portable clock with performance approaching that of larger units and a GPS Time Transfer Unit capable of time transfers to an accuracy of less than 100 nanoseconds, were also given.

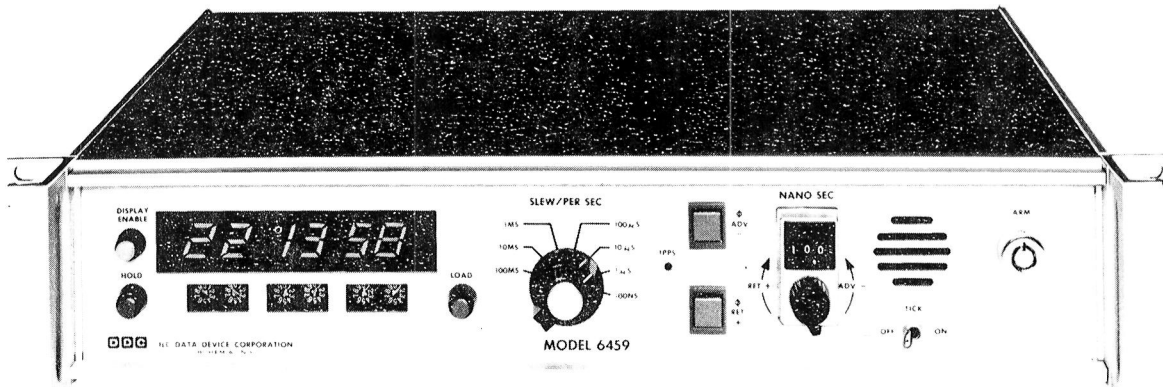


Figure 1. High Stability Clock/Divider

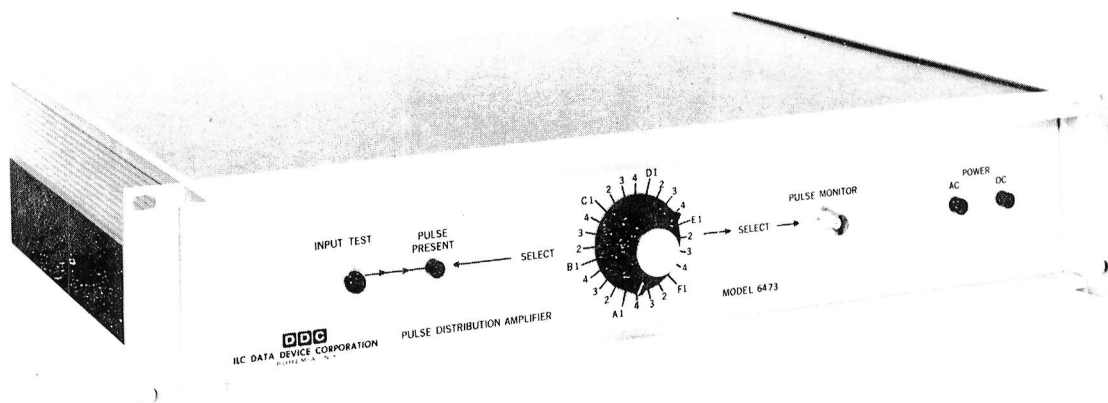


Figure 2. Pulse Distribution Amplifier

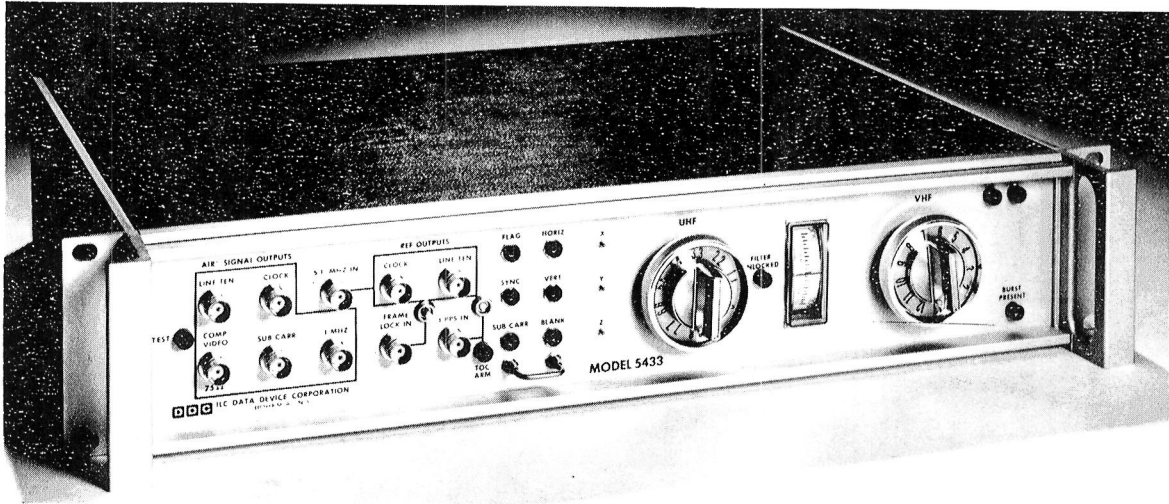


Figure 3. Precision TV Line 10 Receiver

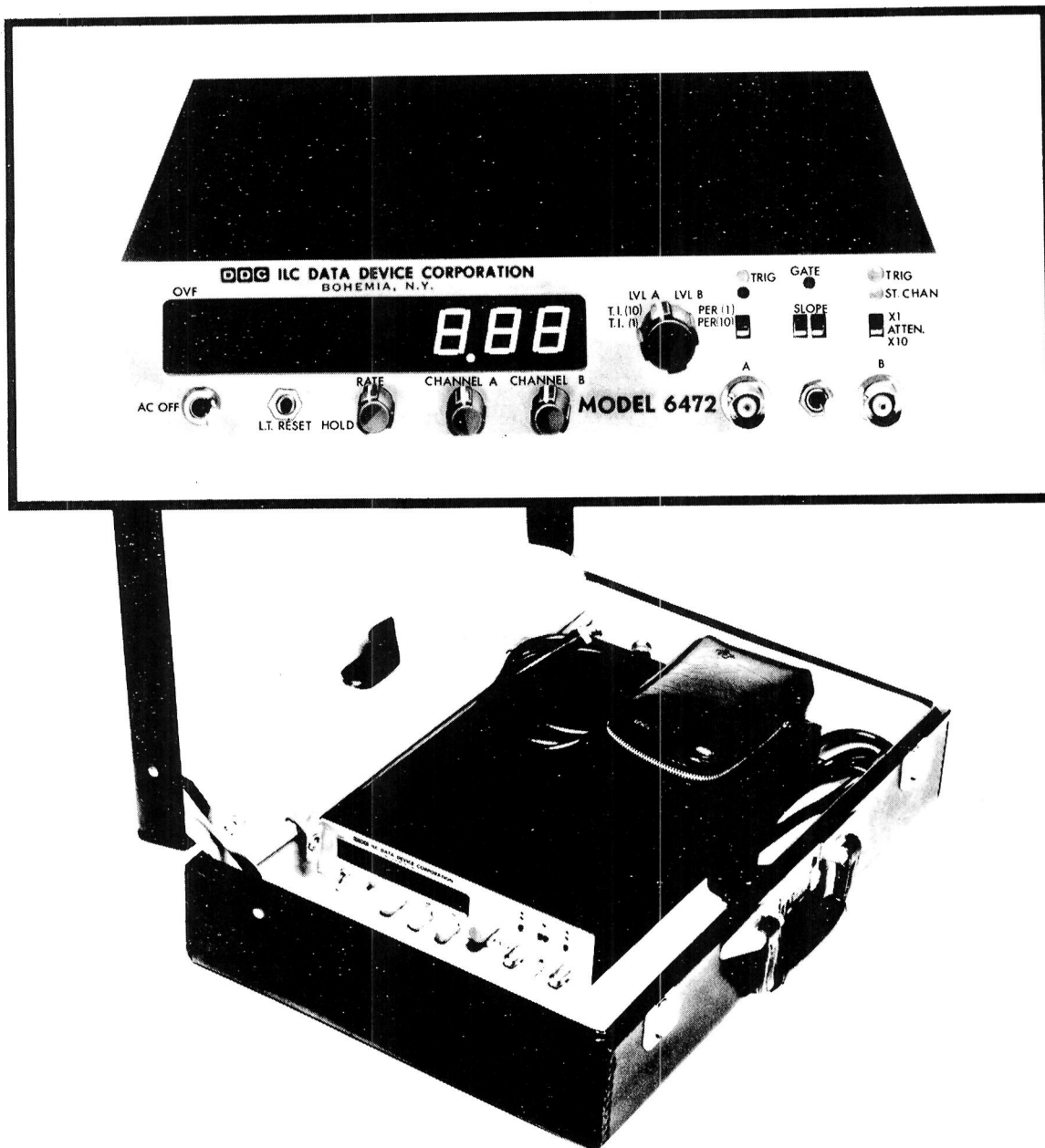


Figure 4. Small Time Interval Counter

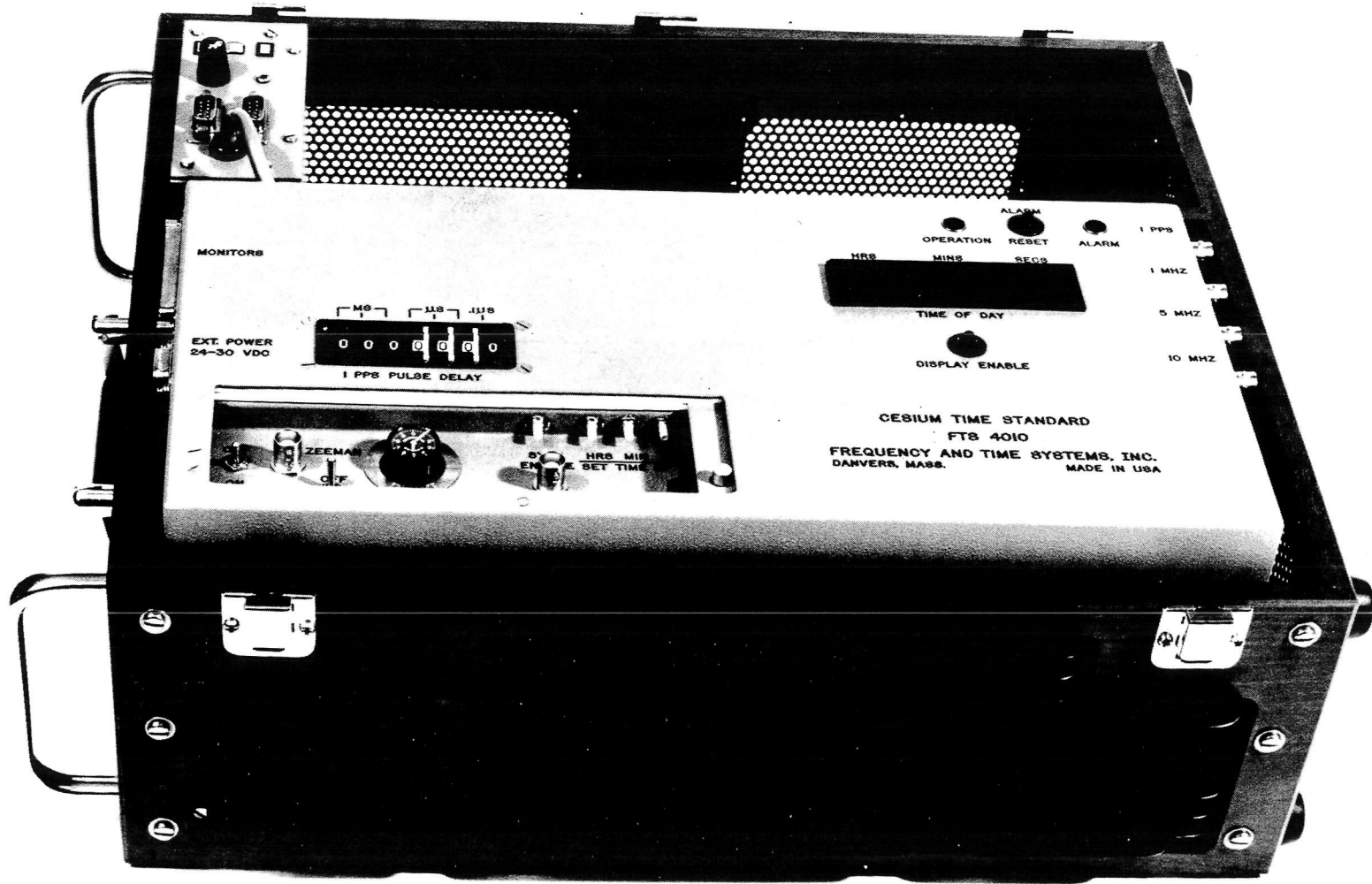


Figure 5. Portable Atomic Clock

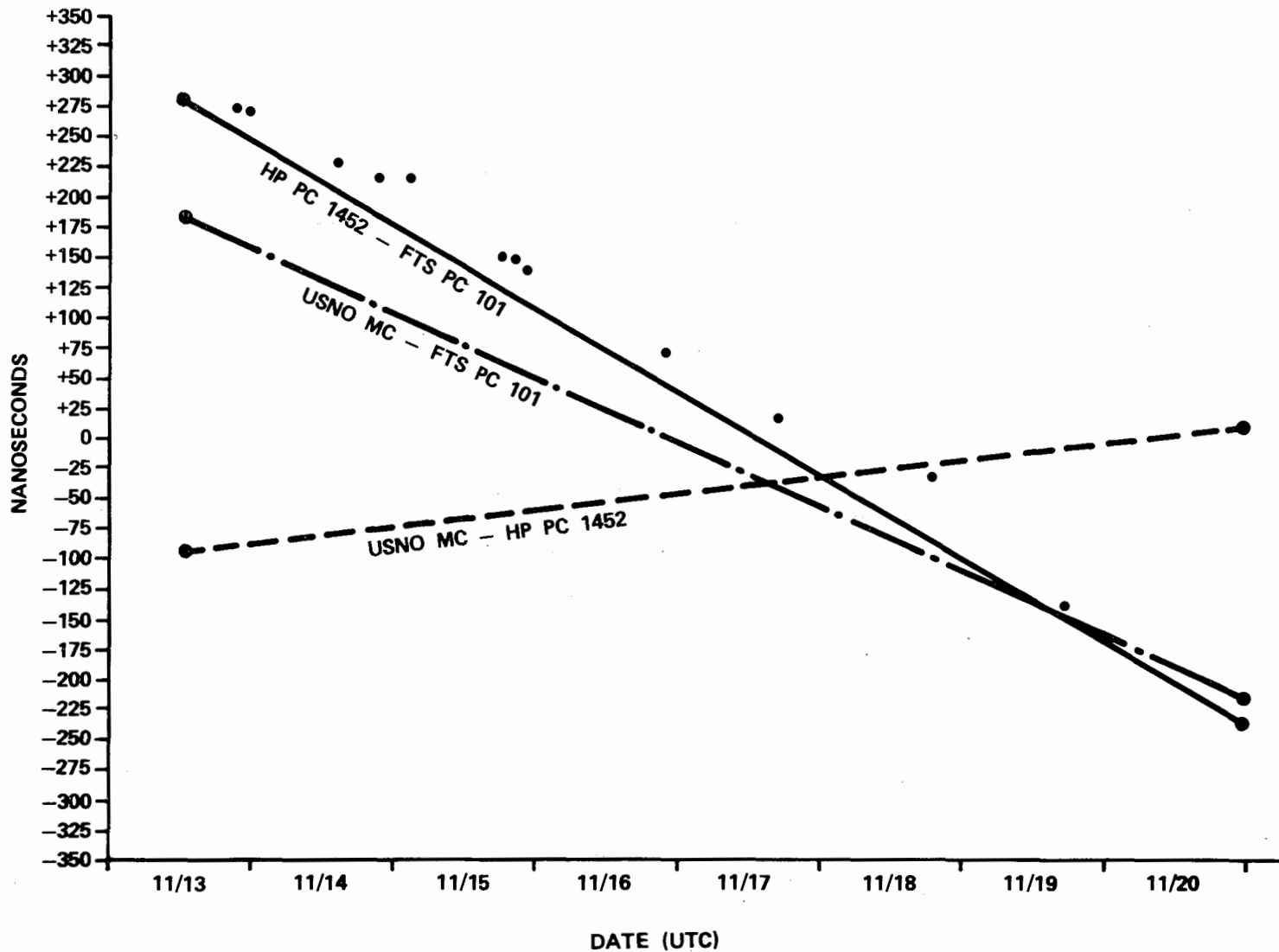


Figure 6. Small Portable Clock Performance

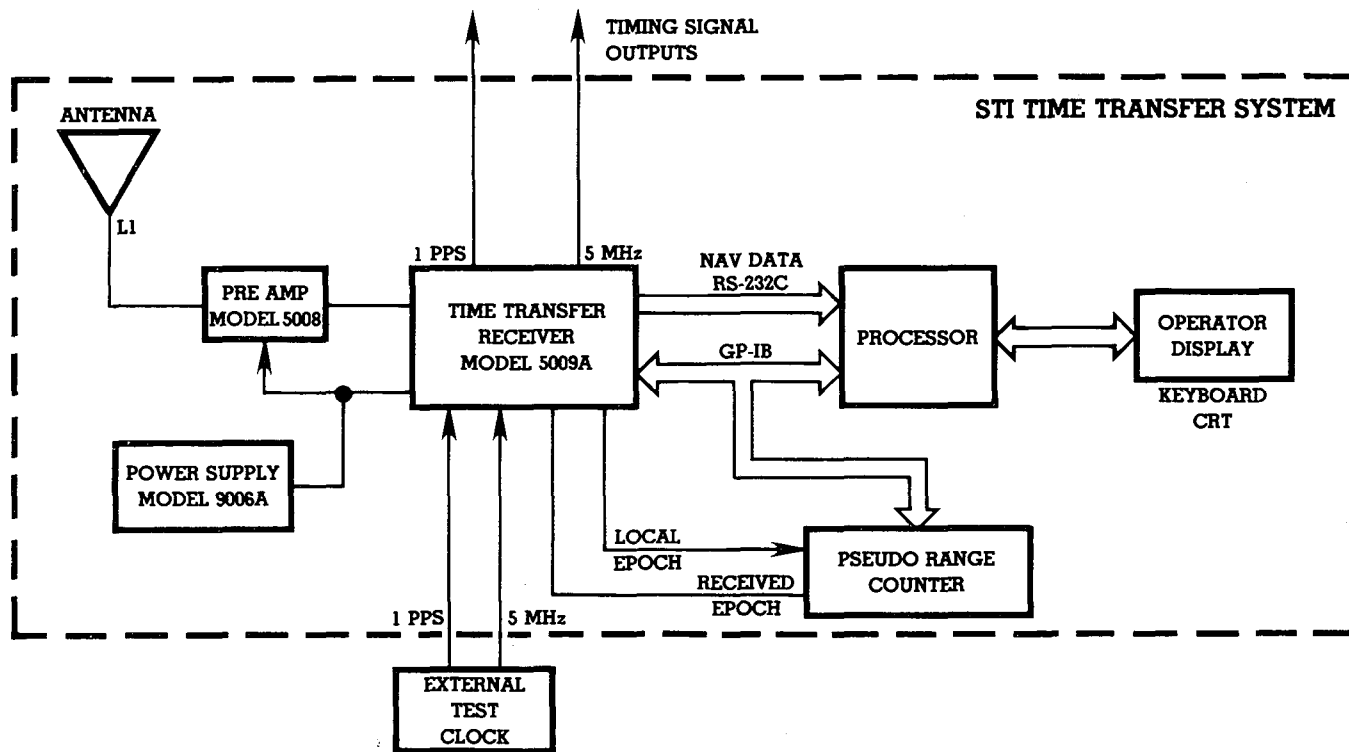


Figure 7. GPS/TTU Block Diagram

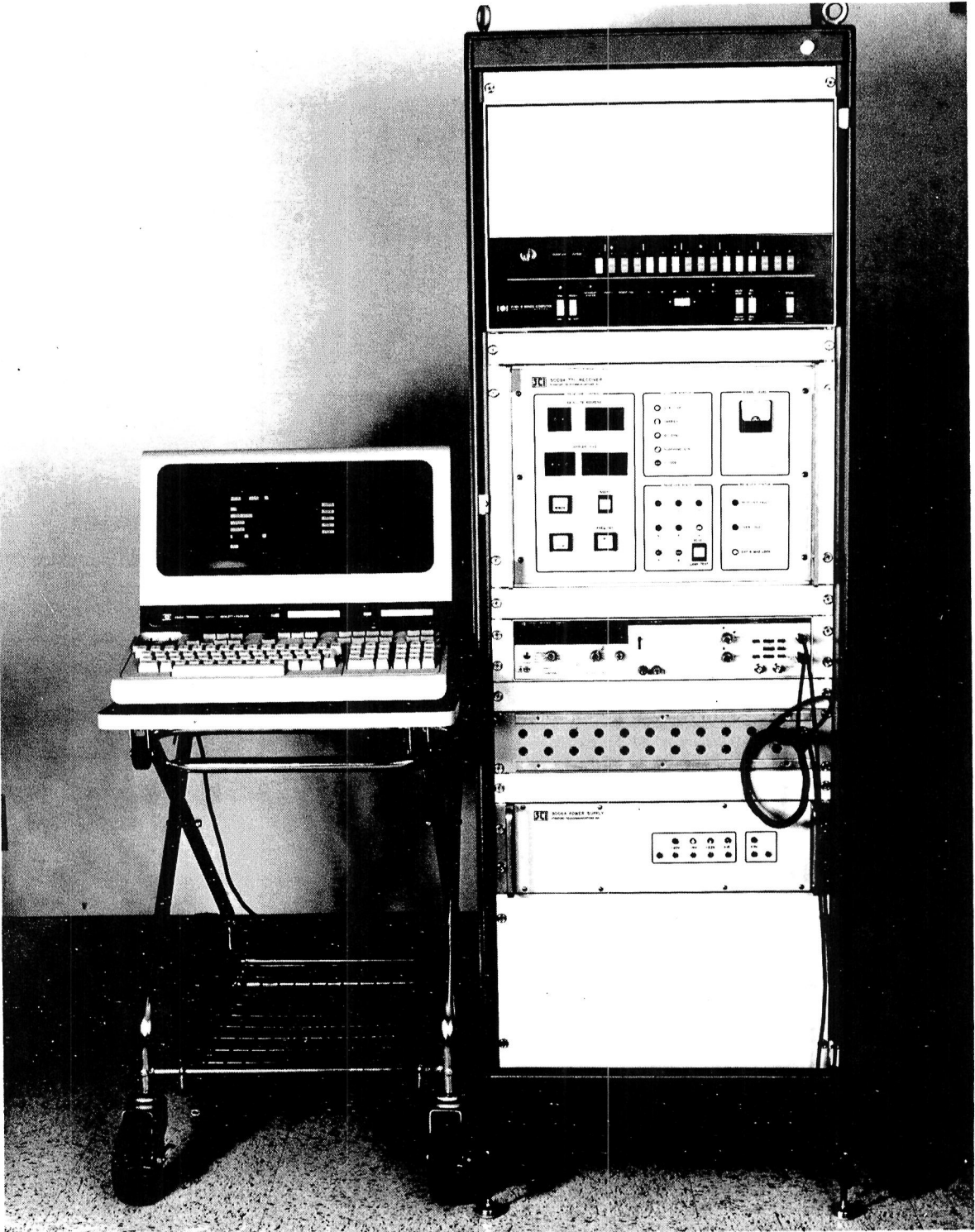


Figure 8. GPS/TTU System (Less Antenna)

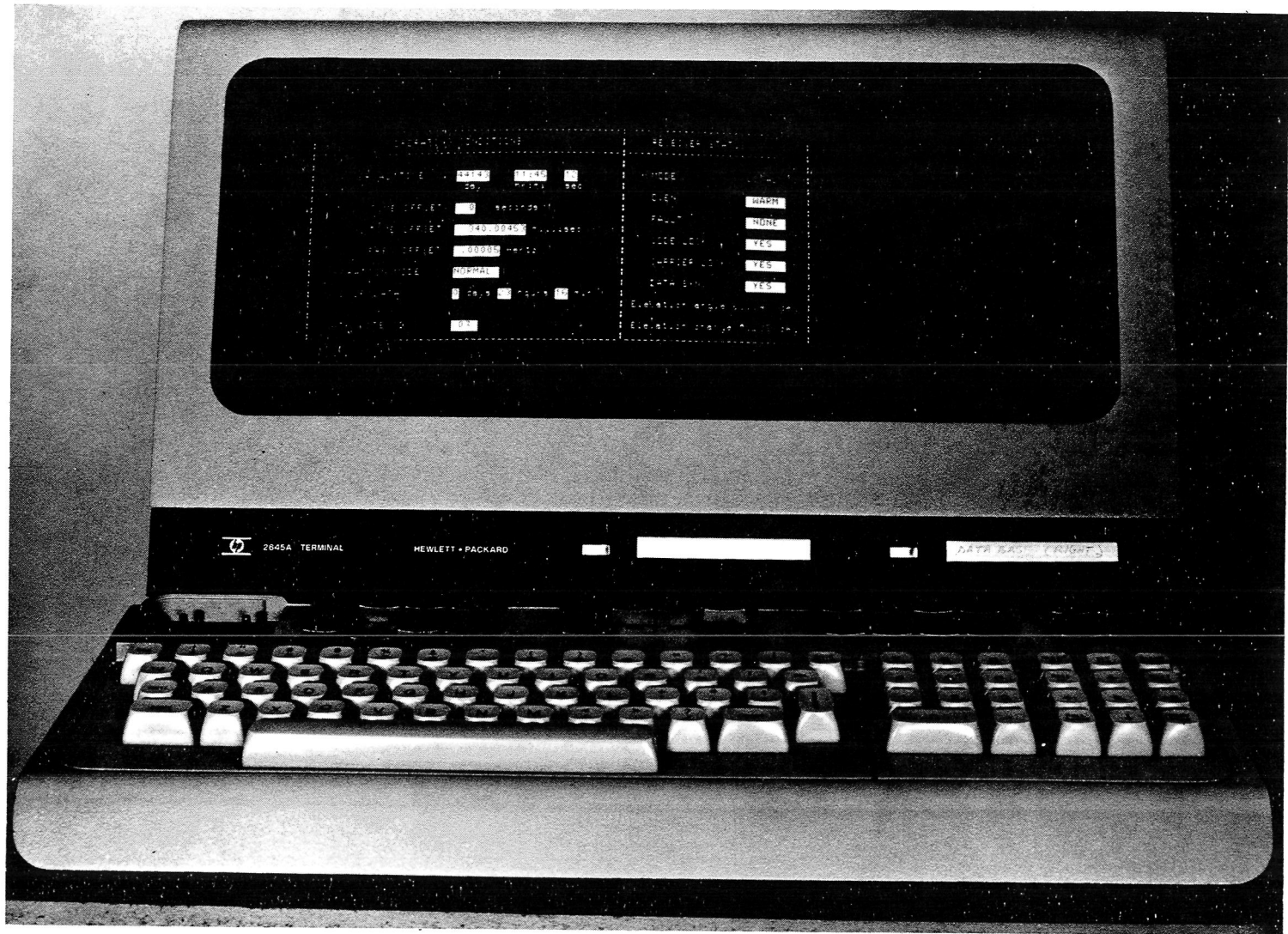


Figure 9. GPS/TTU Console and Display

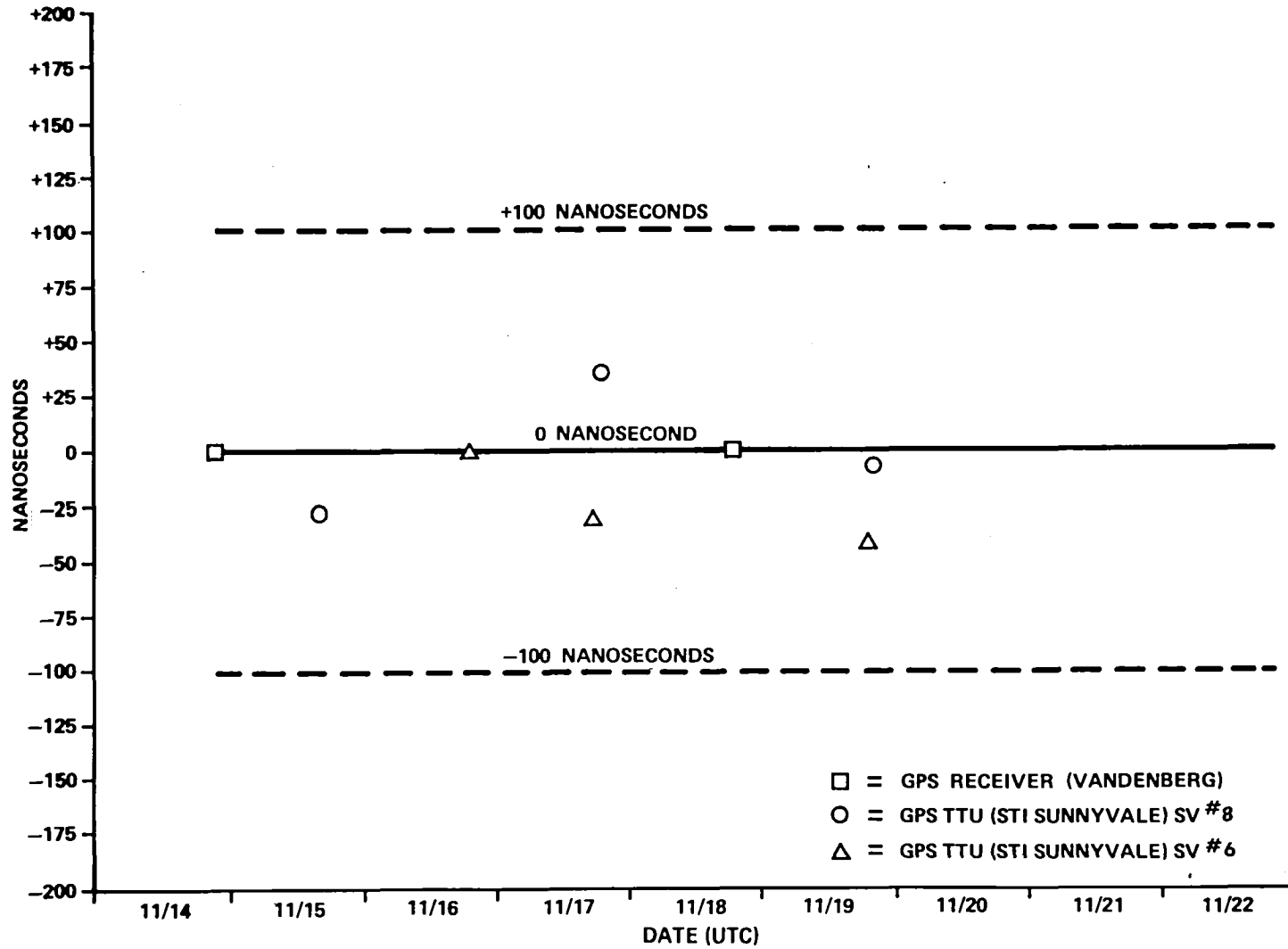


Figure 10. GPS/TTU Preliminary Test Results

QUESTIONS AND ANSWERS

MR. MYRON PLEASURE, Consultant Physicist, New York

In December of last year there was a paper published in "Physical Review Letters". It was a feature paper by a Professor Cohen of the University of Pennsylvania in which he suggested using your time dissemination methods from satellites and coordinating it with ground measurements which he said were easy, though they are not, and then you could use that to check the Einstein special relativity theory of what errors you would expect due to the satellite motion. Now, have you done any estimates of this yet? How well is it-- He has an approximate theory only. It was in the "Physical Review Letters".

DR. PUTKOVICH:

Could I defer the answer to Dr. Winkler here?

DR. WINKLER:

The corrections due to the general relativity are incorporated in the calculations or the algorithms which are used in the STI receiver. With all of that, you should have no visible effects if you put in your coordinates of the station, the receiver algorithm will take into account the relativity effects. There are some higher order effects which are incorporated in the second order corrections for the satellite clock so that the motion of the satellite itself is accounted for.

But in general the whole subject of relativity as it effects the GPS system has been reviewed repeatedly, the last time in a conference or a workshop organized by Dave Allan at the NBS which produced a report of that. And in the judgment of that group, also there were minor discrepancies found in various reports, but the effects seemed to be taken account in the existing algorithms. Thank you.

MR. RAULLO J. MCCONAHY, APL/JHU

We have a program at our laboratory that can use your timing recovery from GPS and I was wondering if you could give us a little more information about when you plan to disseminate those and how.

DR. PUTKOVICH:

We will be taking delivery of our GPS time transfer unit in, I would say, two to three weeks and we will have an initial testing period, but I would hope that sometime in January we would be able to start publishing differences between the USNO master clock and the received signal from the spacecraft that are now up there, the four GPS satellites.

MR. MCCONAHY:

Then you will be doing all four? The clocks on some of them are not too good, like GPS-2, for example.

DR. PUTKOVICH:

That is why we only took these two. We took the two best satellites that were recommended and operated on those two. But we will take a look at it and if the data is reasonable, I don't see any reason why we can't publish it. It is just a matter of scheduling people to take the passes at the proper time. If it gets to be too big of a burden we may have to make some choices as to what we publish. But initially I would hope that we could look at all four of them.

MR. MCCONAHY:

Could it be possible to request you to do passes on a given day for example?

DR. PUTKOVICH:

I don't see why not. If it is at 2:00 or 3:00 in the morning you will have problems getting me in there to do it, but I may be able to find somebody that is willing.

MR. MCCONAHY:

Yes. Our need is just periodic and we need it on a specific day.

DR. PUTKOVICH:

We have done that with TRANSIT with some people and there should be no reason why we can't do it with GPS.

MR. MCCONAHY:

Now another question is why did you choose the CA code rather than the P code to do your timing?

DR. PUTKOVICH:

I had nothing to do with that choice. I think that is a code that more than likely will be available other than the P code. I think Dr. Winkler can also give you more insight in that.

DR. WINKLER:

Cost. Because of the type of receiver we were looking at, and the possibility of using the existing equipment for a stationary location in contrast to an option on a type of navigation equipment which would have to look at four satellites and possibly use two frequencies for this purpose would be inherently more expensive.

MR. MCCONAHY:

Yes. But you could correct for the ionosphere.

DR. WINKLER:

We want a simple clock and that means that by confining yourself to just one frequency in CA code, a one megahertz code, it would be easier and less costly to decode. It is possible to obtain a time transfer which will satisfy all current operational criteria.

MR. MCCONAHY:

Thank you.

TIME TRANSFER WITH THE NAVSTAR
GLOBAL POSITIONING SYSTEM

Ben Roth (DMAHTC/SAMSO/YEUP), William Klepczynski and R.
Glenn Hall (U. S. Naval Observatory)

ABSTRACT

The Navstar Global Positioning System (GPS) is a space-based, radio positioning, navigation system which was authorized for development by DoD in December, 1973. The system will provide extremely accurate, three dimensional position and velocity information, together with system time, to suitably equipped users anywhere on or near the earth. Concept validation field tests were completed in the Spring of 1979. One of the objectives of these tests was to evaluate the performance by measuring the precision and accuracy of the transfer of GPS time to the static user.

INTRODUCTION

The Navstar Global Positioning System (GPS) is a space-based, Radio Frequency (RF), Navigation System that provides extremely accurate, three-dimensional position, velocity and system time information to properly equipped users anywhere on or near the earth. It is a Joint Services Program, managed by the Air Force, with deputies from the Navy, Army, Marines, Defense Mapping Agency, Coast Guard and NATO.

Concept validation, Phase I of the program, was completed in the summer of 1979. This phase of the program included extensive testing that was conducted at Yuma Proving Grounds (YPG), Ariz. The objectives of these tests were to address a variety of operational and technical issues which characterize the performance of the system. One of these issues was the ability of GPS to provide a properly equipped user with accurate system time.

Objectives

The objectives of the Phase I Navstar GPS Time Transfer Tests were: to evaluate the performance, to measure the precision and accuracy of the transfer of GPS time to the static user and to develop a base of information that would

support and expediate the United States Naval Observatory's (USNO's) efforts to develop and evaluate specialized user equipment to exhibit the operational GPS's precision timing characteristics.

System Description

GPS comprises three distinct segments: (1) the Control Segment (CS), (2) the Space Segment (SS), and (3) the User Segment (US). An inherent design property of the system is its precise and internally accurate time.

The CS comprises Monitor Stations (MS) and the Master Control Station (MCS) that are all very closely related in time (within a few nanoseconds). For the Phase I GPS there were four MS located at Guam, Hawaii, Alaska and Vandenberg Air Force Base, Calif., with the MCS at the same location as the Vandenberg MS. The function of the CS is to monitor the SS (GPS satellites) via measures of pseudorange, delta range (integrated Doppler) and satellite health. This information is processed in near real-time by the MCS to provide best estimates of each GPS satellite's ephemerides and clock performance. Using these estimates, very accurate predictions of the satellites' ephemerides and clock models are generated and uploaded to the satellites daily by the MCS.

The SS of the operational GPS comprises 24 satellites whose orbits are nearly circular, with 12-hour period and radii of 20,200 kilometers. These satellites will be configured into three equally spaced orbit planes that are inclined 63 degrees from the earth's equatorial plane. There will be eight equally spaced satellites in each plane. This configuration will provide continuous visibility to at least four satellites from any place on or near the earth. Each satellite will carry a system of redundant, high precision and highly predictable time and frequency standards. These standards will be used to generate the RF spread spectrum, Pseudo Random Noise (PRN), signals to the user segment. For the Phase I GPS there were four development model satellites that were equipped with redundant, precision, rubidium time and frequency standards, in orbit, for testing. These satellites were configured in operational orbit slots so that testers at YPG were able to observe them simultaneously for up to 1.5 hours per day. Just prior to this visibility at YPG, the satellites were uploaded with the newest ephemerides and clock prediction models by the MCS. In addition, if required, the satellites' standards were adjusted in phase and/or frequency so

that they provided the user segment with the necessary coherent navigation signals that are processed by the user equipment to obtain position, velocity and system time.

The user segment comprises a variety of User Equipments (UE's) and their associated host vehicles. The UE's are sets which are composed of PRN receivers and data processors. These sets are designed to meet the specialized operational requirements of the user which are generally characterized by the dynamics of the host vehicle. For the Phase I GPS there were four classes of UE: (1) high dynamic sets for fighter/bomber applications, (2) low dynamic sets for air transport applications, (3) low cost prototype sets for commercial aviation applications, and (4) man-vehicle sets for ground applications. In general, these sets all perform the navigation mission of GPS in the same manner. The receiver obtains measurements of pseudorange and delta range (integrated Doppler) to four satellites. These measurements are handed over to the data processor which computes the user's position, velocity and time, using a Kalman filtering technique. The rate of these measurements/computations is related to the dynamics of the host vehicle.

Test Description

The data for time transfer testing were collected in conjunction with static (point) positioning tests. These tests were conducted from January through March 1979 at YPG, Ariz. by Defense Mapping Agency personnel using the Mobile Test Van (MTV).

The MTV is a one-ton step van which provides an approved operational environment for an electronics pallet which contains a high dynamics user equipment (Magnavox X-Set) and instrumentation to monitor and record user equipment performance, measurements and navigation solutions. The X-Set comprises a four-channel, dual-frequency receiver, power supply and battery pack, navigation data processor (NAV DP), Control Display Unit (CDU), preamplifier and omnidirectional (volute) antenna. The instrumentation comprises a data processor, input/output extender, nine-track tape recorder with buffer formatter, cassette tape transport (memory loader), engineering display (CRT) unit and engineering control (keyboard) unit, power supply, power distribution unit, line filter, high performance cesium beam time/frequency standard with power supply and IRIG time code generator. Figure 1 provides a block diagram of the X-Set/Instrumentation.

The GPS satellites continuously broadcast PRN RF (L-band) signals at 1575.42 (L1) and 1227.60 (L2) MHz. Essentially, the process is as follows: the carrier frequency is combined with the PRN code and the low rate data stream, which contains the satellite's ephemerides and clock model to produce a modulated carrier frequency. To measure the range from the user to a satellite, the X-Set internally generates a PRN code which is identical to that of the satellite. This code is shifted until it is correlated with the received code and the amount that it is shifted can be interpreted as the difference in time between the X-Set's clock and that of the satellite. If the two clocks are synchronized, this time difference is the range to the satellite from the user, when multiplied by the speed of light and corrected for atmospheric effects. In reality, the two clocks are never synchronized exactly. This situation produces a pseudorange measurement which can be expressed by the following equation:

$$\bar{R} = R + c\Delta t_a + c\Delta t_o, \quad (1)$$

where

\bar{R} = pseudorange measurement from the user to the satellite,

R = true range from the user to the satellite,

c = speed of light,

Δt_a = propagation delays due to the atmosphere,

Δt_o = the user's clock offset from the satellite clock.

The X-Set's receiver is a four-channel, two-frequency unit which is implemented with internal process control software (firmware). The receiver is integrated with a high speed navigation data processor to provide a high dynamic user with navigation solutions at a 1.7 second rate. These solutions are obtained by processing the simultaneous measurements of pseudorange and include a first order ionospheric correction, 0.5 second duration delta ranges to four satellites, and a Kalman filter estimation process whose eight element state vector contains three dimensional position and velocity, and user clock offset and rate. In the context of the static user, the Kalman filter is cued so that the velocity state only reflects the noise of the delta range measurements. To clarify this process, the

determination of position and user clock offset can be determined in general mathematical terms as follows:

$$\bar{R}_i = R_i + c\Delta t_0, \quad (2)$$

where

$i = 1, \dots, 4$ and identifies measurements to the four satellites,

$R_i = [(X_u - X_i)^2 + (Y_u - Y_i)^2 + (Z_u - Z_i)^2]^{1/2}$ are the true ranges from the user at X_u, Y_u, Z_u to the four satellites at X_i, Y_i, Z_i ,

\bar{R}_i = the X-Set's simultaneous measurements of pseudorange to the four satellites,

Δt_0 = the user's clock offset from satellite's clocks. Notice, this assumes that all of the satellites' clocks are synchronized. In reality, the satellites' clocks are not exactly synchronized in terms of their pulse trains but the broadcast navigation messages contain the predicted clock models that are generated by the MCS, which mathematically synchronize the satellite clocks to the GPS Master clock, which resides in the Vandenberg MS. In the X-Set's computational process, the pseudorange measurements are corrected with these clock models prior to their entry into the estimation process so that one must solve for only the common clock offset.

In the above system of four equations there are four unknowns to be determined: three for the user's position (X_u, Y_u, Z_u) and one for the user's clock offset (Δt_0). Notice that the satellites' positions (X_i, Y_i, Z_i) are provided via the broadcasted navigation message which contains the predicted ephemerides that are generated by the MCS. For the testing, real time solutions of the user's clock offset were obtained as a part of the navigation solution. In addition, postprocessed solutions of the clock offset were obtained by assuming the users' position and this results in a one equation system with one unknown.

In order to maximize the precision of the pseudorange measurements and to provide a test configuration which would support time transfer tests, the X-Set was implemented as follows: the receiver's oscillator was syn-

chronized in a phaselock loop to the 5 MHz output of the instrumentation's cesium standard via a hardware upgrade in the receiver, and the receiver's clock phase was synchronized to the one pulse per second (PPS) output of the cesium standard by implementing specialized navigation software. This use of the cesium standard actually makes it the receiver's clock. Thus, the internally generated PRN code is equally or more precise than the satellite generated code.

To provide an independent monitor for the cesium and system redundancy, two additional cesium standards were installed in the MTV and the three cesium standards were integrated into an ensemble which was monitored hourly using a computer controlled time interval counter which measured the difference in time between the one pulse per second outputs of the cesium standards. These differences were automatically recorded on magnetic tape in a small cassette. The instrumentation cesium standard was considered the master for all testing. Figure 2 illustrates the timing ensemble.

The test site at YPG was located in the immediate vicinity of the Inverted Range Control Center (IRCC) and the antenna was precisely referenced to a permanent survey station mark. The position of the mark was determined in the WGS 72 earth centered/earth fixed coordinate system by the Defense Mapping Agency (DMA), using precise conventional and Geociever-Transit satellite surveys. The MS's have been positioned in the WGS 72 system by DMA, using the same methods, and their locations form the reference frame for GPS. Given the above, it is clear that we can use the position of the station mark as the user's position to implement the single satellite time transfer.

Up to this point, time transfer has not been defined explicitly, but it is now possible to provide this definition. Time transfer is the process whereby GPS time is transferred to a user's clock. In these tests, the transfer of time is to the instrumentation's high performance, cesium, time/frequency standard. To realize the transfer, the navigation (real-time) solution of the user's clock offset, error in clock phase (ECP), is applied to the user's clock time so that, effectively, the user's clock is in synchronization with GPS time. In the case of the postprocessed solution, the clock offset is determined and applied to the user's clock time to provide a GPS time scale for the user's clock.

Results

For the time transfer tests, the time reference was provided by the United States Naval Observatory flying clock trips, which established the difference in time between the GPS Master Clock at the Vandenberg MS and the MTV clock ensemble.

During the period from early January to early March 1979, the USNO flying clock made five trips from Washington DC to YPG and Vandenberg. Each of these trips consisted of flying a high performance, cesium beam, time/frequency standard and time interval counter from the USNO, Washington, D. C. to YPG, to the Vandenberg MS to YPG and back to Washington in approximately two days. Prior to the clock's departure and after its return to Washington, it was calibrated with the USNO ensemble of more than 20 high performance cesium standards. When the clock was at YPG and the MS, the time interval counter was used to measure the time difference between the flying clock and the local clock. The calibrations and the time difference measurements were processed at USNO to provide the relationship between the clocks at the Vandenberg MS, YPG, and the USNO. Figure 3 and Table I provide the results for these flying clocks.

For the period of 1 February through 1 March 1979, real time, time transfer, test data were collected at YPG. During this period, 14 days of data were collected. Each day's data consisted of approximately six samples which were collected over 20-minute time periods after the satellites were uploaded by the MCS with appropriate ephemerides and clock models. Each sample was the real time, Kalman Filter solution of the error in the X-Set's clock phase. This error in clock phase (ECP) is the difference between the user's local time and GPS time, and in this case the user's local time is obtained from the MTV instrumentation's high performance, cesium, time/frequency standard. To obtain values for the accuracy and precision of real time, time transfer, the ECP was compared with the accepted true difference in time between the MTV and GPS as determined by the flying clock and USNO's analysis of the MTV clock ensemble data. Before the comparisons were made, the ECP was corrected for hardware delays. These delays are due to the length of the X-Set's receiver calibration cable and to the difference between the six-second pulse offset of the Vandenberg MS and that of the MTV X-Set receiver from their respective time/frequency standards' one pulse per second references. The values for these delays are listed and explained in Appendix A and B. Table II contains the ECP/

USNO comparisons.

To provide additional checks of the time transfer and to look at the case in which the user's position is known, the MTV magnetic data tapes containing the pseudorange measurements, satellite broadcast ephemerides and Kalman Filter solutions for February 5-7 were post processed by the Aerospace Corporation. The results of these efforts are presented below.

Case I is a four satellite solution of the ECP which used the broadcast ephemerides/clock models and the Geceiver/Transit determined WGS 72 position of the X-Set's antenna. The ECP was determined by differencing the measured pseudoranges and the given ranges and then fitting these differences to a second order polynomial with a constant (bias) term, drift term and aging term. This polynomial was then used to generate the ECP for the same times that real time ECP data were obtained during MTV operations.

Date Polynomial: $A_0 + A_1 \cdot (t-t_0) + A_2 \cdot (t-t_0)^2$
 5 Feb 79 $A_0 = 8952.753$ mtrs
 $A_1 = -0.00042236$ mtrs/sec
 $A_2 = 0.00000023$ mtrs/sec²
 $t_0 = 50519.25$ sec

Time (sec)	Real-Time ECP (mtrs)	Post Processed ECP (mtrs)	Real-Post (mtrs)
50700	8951	8952.684	-1.684
50820	8951	8952.647	-1.647
51000	8952	8952.603	-0.603
51300	8954	8952.563	+1.437
51600	8951	8952.565	-1.565
51900	8949	8952.608	-3.608

Mn -1.278
 (-4 nanoseconds)

S 1.652

<u>Date</u>	Polynomial:			
6 Feb 79	$A_0 + A_1 \cdot (t-t_0) + A_2 \cdot (t-t_0)^2$ $A_0 = 8991.612 \text{ mtrs}$ $A_1 = 0.00376515 \text{ mtrs/sec}$ $A_2 = 0.00000042 \text{ mtrs/sec}^2$ $t_0 = 52256.48 \text{ sec}$			
Time (sec)	Real-Time ECP (mtrs)	Post Processed ECP (mtrs)	Real-Post (mtrs)	
52500	8992	8990.963	+1.037	
52800	8991	8990.901	+1.099	
53100	8990	8991.652	-1.652	
53400	8991	8993.219	-2.216	
			Mn	-0.433
			(-1 nanosecond)	
			S	1.749

<u>Date</u>	Polynomial:			
7 Feb 79	$A_0 + A_1 \cdot (t-t_0) + A_2 \cdot (t-t_0)^2$ $A_0 = 9042.962 \text{ mtrs}$ $A_1 = 0.00148212 \text{ mtrs/sec}$ $A_2 = 0.00000042 \text{ mtrs/sec}^2$ $t_0 = 50509.02 \text{ sec}$			
Time (sec)	Real-Time ECP (mtrs)	Post Processed ECP (mtrs)	Real-Post (mtrs)	
50700	9044	9043.260	0.740	
51000	9044	9043.791	0.209	
51300	9044	9044.397	-0.397	
51600	9041	9045.079	-4.079	
51900	9040	9045.836	-5.836	
52200	9040	9046.669	-6.669	
52500	9040	9047.598	-7.578	
				-3.373
			Mn	(-11 nanoseconds)
			S	3.505

Case II, is a single satellite (Navstar 4/PRN Code 8) solution which was obtained using the same technique as in Case I.

Date Polynomial: $A_0 + A_1 \cdot (t-t_0) + A_2 \cdot (t-t_0)^2$
 7 Feb 79 $A_0 = 9044.438$ mtrs
 $A_1 = 0.00162105$ mtrs/sec
 $A_2 = 0.00000003$ mtrs/sec²
 $t_0 = 50449.12$ sec

Time (sec)	Real-Time ECP (mtrs)	Post Processed 4 Satellite	ECP (mtrs) 1 Satellite	Real-Post (mtrs) 1 Satellite
50700	9044	9043.260	9044.847	-0.847
51000	9044	9043.791	9045.340	-1.340
51300	9044	9044.397	9045.839	-1.839
51600	9041	9045.079	9046.304	-5.304
51900	9040	9046.836	9046.853	-6.853
52200	9040	9046.669	9047.368	-7.368
52500	9040	9047.578	9047.889	-7.889
				-4.491
			Mn (-15 nanoseconds)	
			S	3.063

Case III, is a combined solution of the three days' data from Case I. In this case, Aerospace Corporation generated post flight ephemerides and satellite clock models for the four satellites by post processing MS measurement data, which covered the period of 29 January to 12 February. These ephemerides and clock models were then processed with the MTV measurements in a batch, least squares process which provided solutions for the MTV's position, clock offset and rate. In addition, solutions were obtained by using the MTV measurements without applying first order, ionospheric corrections.

Date & Time (sec)	Real-Time ECP (mtrs)	Post Processed ECP (mtrs)	Real-Post (mtrs)
5 Feb @ 51000	8952	8953.4 (8961.4*)	-1.4
6 Feb @ 52500	8992	8993.4 (9000.0*)	-1.4
7 Feb @ 51000	9044	9044.9 (9050.9*)	-0.9

*These are the ECPs determined without using the 1st order ionospheric corrections.

Review of the Results

The Case I data verify the real time solution data and indicate only marginal (approximately 10 nanoseconds) improvement is obtained when the pseudorange data is post processed.

The single satellite results illustrated in Case II and and ECPs determined without ionospheric corrections in Case III provide an indication that a single satellite time transfer without ionospheric correction would degrade the result by approximately 30 nanoseconds, depending on the individual satellites' broadcast ephemeris and clock model quality.

The Case III data indicate that processing with post fit ephemerides does not significantly improve the real time results except in terms of confirmation and greater statistical significance due to the amount of data employed to obtain the results, that is, the confidence level is greatly increased.

Conclusions

The comparisons of the real time and post processed ECPs show that GPS will be able to provide better than 20 nanosecond time transfers in real time, but the real time ECPs which were corrected for X-Set synchronization errors and calibration delay line errors indicate that there are hardware delays which must be accounted for if the user actually is to obtain a physical transfer of time in terms of his UE's clock output pulse. In this context, tests are now in progress that have been designed to address the delay issues so that the Phase II GPS UE will provide the user with a time transfer capability that is more in conformance with the system's real capability which has been demonstrated via the real time/post processed ECP comparisons.

Table I

USNO Master Clock - MTV Clock

11 January to 1 March 1979

The offsets are determined from USNO's adjustment of flying clock trip and MTV timing ensemble data.

<u>Date</u>	<u>Time</u>	<u>Offset (μs)</u>
1 Feb	1445	-8.210
2 Feb	1425	-8.298
3 Feb	1355	-8.366
5 Feb	1412	-8.482
6 Feb	1442	-8.535
7 Feb	1420	-8.591
8 Feb	1425	-8.646
9 Feb	1415	-8.705
12 Feb	1318	-8.890
13 Feb	1328	-8.951
15 Feb	1310	-9.078
21 Feb	1252	-9.452
28 Feb	1220	-10.014
1 Mar	1212	-10.086

Table II

Time Transfer at Yuma Proving Ground AZ
Mobile Test Van w/Magnavox X-Set

all data in nanoseconds

Date	Time (UT)	ECP	Correc- tion	ECP'	USNO TR†	ECP' - TR†
1 Feb	1430-1500 (7) [*]	29351±3	177	29528	29596	-68
2 Feb	1345-1505 (8)	29505±13	211	29716	29741	-25
3 Feb	1345-1405 (10)	29579±5	165	29744	29866	-122
5 Feb	1400-1425 (7)	29859±5	185	30044	30094	-50
6 Feb	1435-1450 (4)	29991±3	161	30152	30203	-51
7 Feb	1400-1440 (9)	30160±6	219	30379	30315	+64
8 Feb	1420-1430 (3)	30193±5	185	30378	30425	-47
9 Feb	1400-1430 (7)	30338±7	205	30543	30539	+4
12 Feb	1300-1335 (8)	30708±6	197	30905	30886	+19
13 Feb	1320-1335 (4)	30808±8	197	31005	31001	+4
15 Feb	1300-1320 (5)	30959±4	241	31100	31234	-134
21 Feb	1240-1305 (6)	31750±7	161	31911	31917	-6
28 Feb	1205-1235 (7)	32700±3	163	32863	32825	+38
1 Mar	1200-1225 (6)	32784±3	163	32947	32945	+2

†Time Reference

* these are the number of samples obtained during the time period.

ECP, is the mean of samples and is characterized by its standard deviation.

Corrections are derived from the material presented in Appendix A and B.

ECP' is the ECP with corrections applied.

USNO Time Reference, these values were obtained from the data presented in figure 3 and Table I.

ECP'-Time Reference are the errors in the time transfer.

Analysis, investigations of clock trips, timing ensemble and the synchronization suggest that the quality of each test is ± 50 nanoseconds (one sigma). The mean of the 14 tests: -27 ± 56 nanoseconds confirms this and suggests that the major source of error is the nominal value of 170 nanoseconds of VMS synchronization delay.

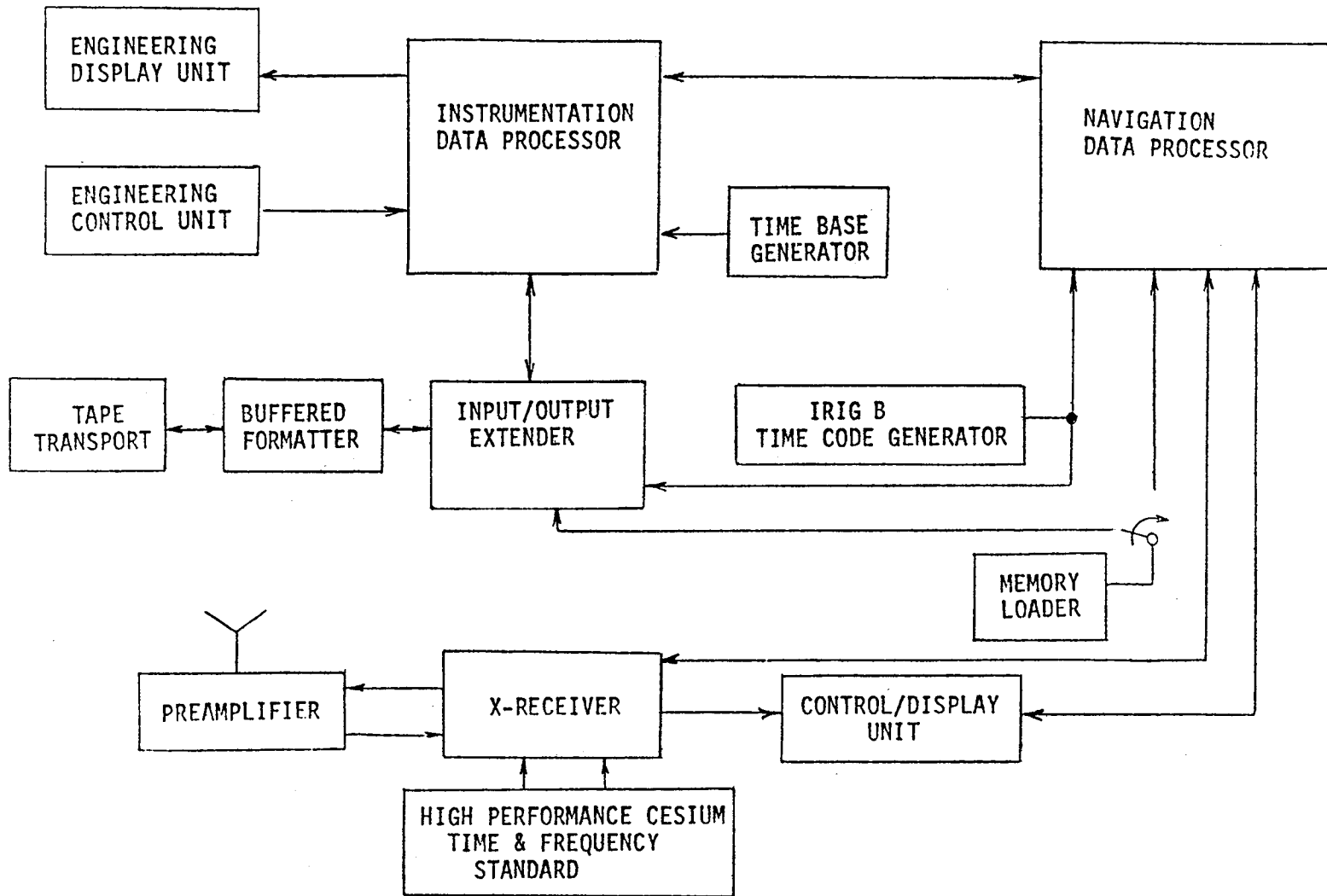
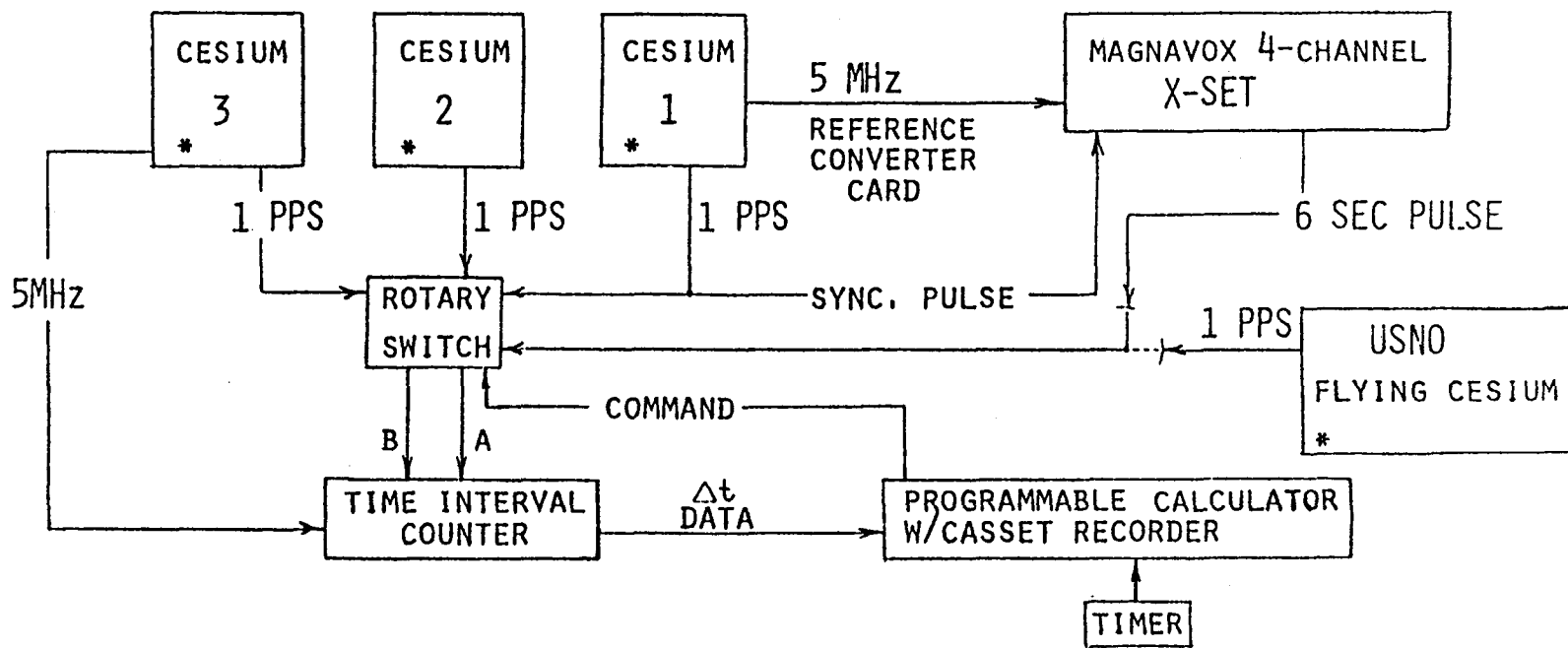


Figure 1. X-Set/Instrumentation



*ALL CESIUMS ARE HIGH PERFORMANCE TIME & FREQUENCY STANDARDS.

Figure 2. Time Transfer MTV's Timing Ensemble

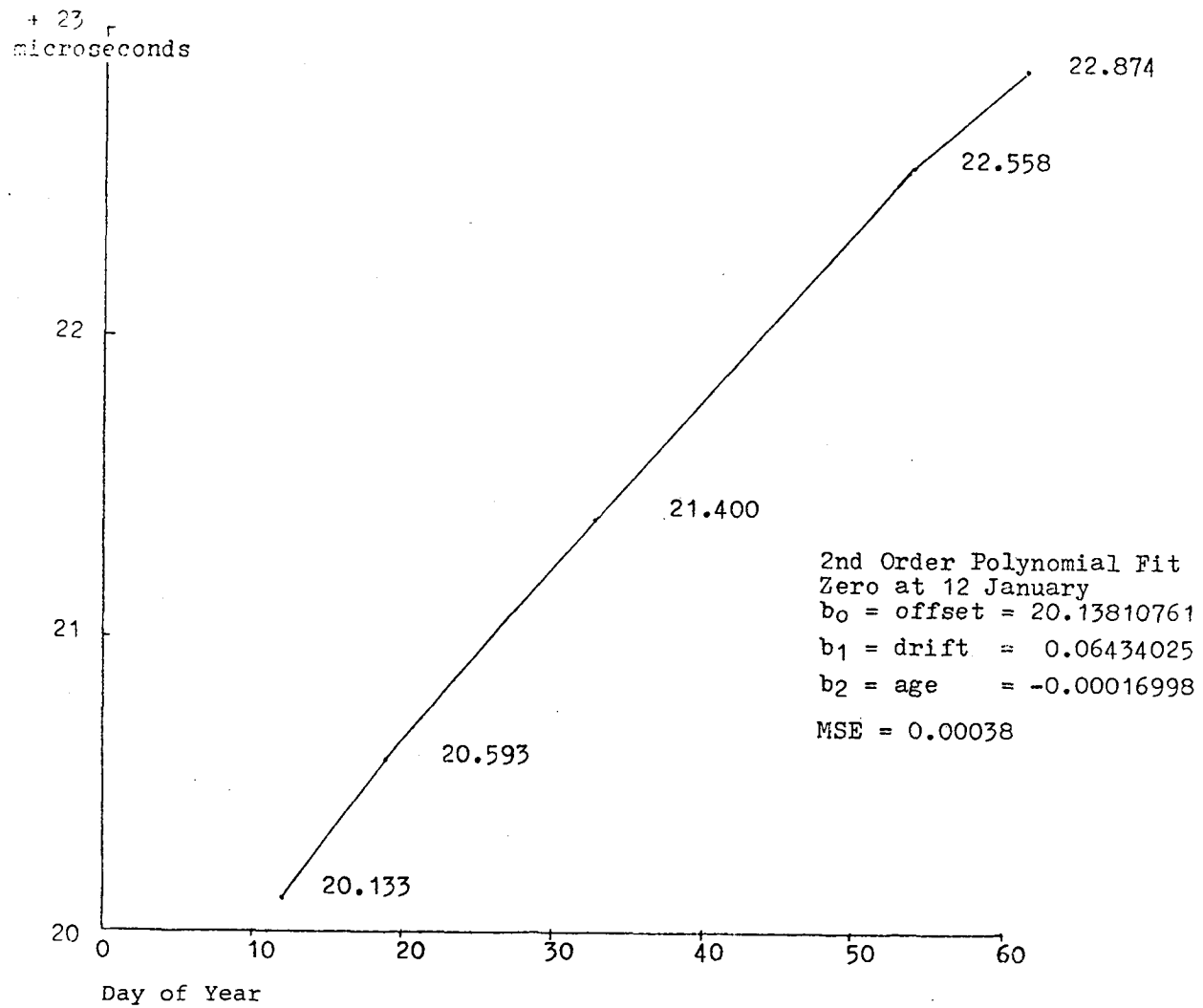
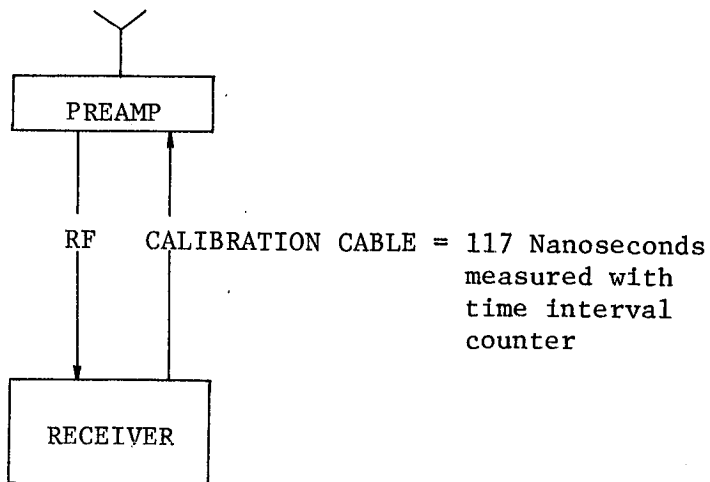


Figure 3. USNO Master Clock - GPS Master Clock, 11 January to 1 March, 1979

Appendix A

MTV X-Set Calibration Delay

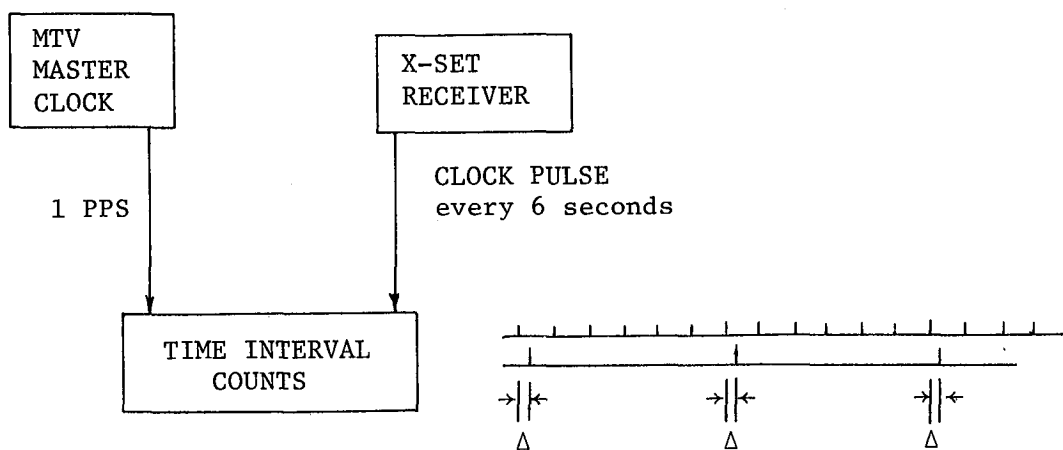


The X-Set's calibration procedure sends a signal out via a cable to its preamplifier and back to the receiver via the RF cable. The receiver measures the time it takes and the equivalent range is subtracted from the pseudorange measurements. This results in a measurement which is too short by the length of the calibration cable delay time. The calibration cable's delay was measured several times with a two-nanosecond resolution, time interval counter and found to be 117 nanoseconds. This delay is a plus correction and is added to the ECPs. Notice, MS's correct the pseudorange for this effect so this timing bias is not introduced into the SS. Further, the MTV's X-Set does not correct for this because the navigation solution is transparent to common timing biases and navigation was the primary test goal of the set.

APPENDIX B

X-Set Synchronization Delay

The X-Set's clock is synchronized to an external 1 PPS with software control of hardware. The procedure is as follows: the operator inputs the time which will be set via the CDU plus an estimate of the reference clock's (MTV Master Clock) offset from GPS time; this sets a gate in the receiver and the X-Set's clock to the time while freezing the epoch update of the clock; just prior to the Master Clock's epoch (1 PPS) of the set time the operator implements the time set with a CDU input command, which tells the receiver that the next 1 PPS it sees will be the synchronization pulse; when the receiver sees the 1 PPS at the gate it starts the epoch update of its clock carrying the set time. To determine the quality of the MTV synchronization, the difference between the reference 1 PPS and the X-Set's clock output pulse were measured during each test with a two nanosecond resolution time interval counter. Notice, the MS's use X-Sets for data collection and their clocks are set to an external reference. In the case of the VMS, this is accomplished similarly to the MTV while the other MS clocks are set from the MCS via the satellites. For the time transfer test it is important to know the offsets of the VMS and MTV synchronizations. In the case of the VMS, a nominal value of 170 nanoseconds has been determined. For the MTV, measurements were obtained and are listed on the following page.



Δ = X-Set's pulse lag

Notice, if the VMS and MTV synchronzation errors were equal, the errors would cancel. In this case, the VMS at 170 nanoseconds and the MTV at a lower level introduce a bias in the time transfer. The effect of this bias is to make the ECP smaller as the MTV clock is slightly ahead of the VMS clock. To correct for this, the measurements of the MTV synchronization error for each test are subtracted from VMS nominal value and the resultant value is added to the ECP. In terms of the VMS nominal value, we can characterize its quality by the statistics provided by the MTV measurements, which give us a nominal value of 170 ± 25 nanoseconds (one sigma).

Table B.1

Differences between Cesium 1 PPS and X-Set (Serial #12) 6 second pulse after synchronization. Measurements were obtained with the HP 5345A Time Interval Counter (2 nanosecond resolution).

<u>Date</u>	<u>Value (nanoseconds)</u>	<u>Date</u>	<u>Value (nanoseconds)</u>
1 Feb 79	110	1 Mar 79	124
2 Feb 79	76	2 Mar 79	140
3 Feb 79	122	5 Mar 79	100
5 Feb 79	102	6 Mar 79	114
6 Feb 79	126	9 Mar 79	138
7 Feb 79	68	12 Mar 79	94
8 Feb 79	102	13 Mar 79	132
9 Feb 79	82	14 Mar 79	54
12 Feb 79	90	15 Mar 79	134
13 Feb 79	90	16 Mar 79	124
14 Feb 79	140	19 Mar 79	140
15 Feb 79	146	20 Mar 79	92
16 Feb 79	112	22 Mar 79	90
19 Feb 79	86	23 Mar 79	134
20 Feb 79	66		
21 Feb 79	126		
28 Feb 79	124		

Mn = 109 ± 25 31 samples
 3σ = (34, 184) all values
 within this interval

Precise Time and Time Interval (PTTI) Measurements
From The
Navigation Technology Satellites and the GPS NAVSTAR-4 Satellite

J.A. Buisson, T.B. McCaskill, O.J. Oaks, M.M. Jeffries, S.B. Stebbins
Naval Research Laboratory, Washington, D.C.

ABSTRACT

Since the launch of the first NTS spacecraft in 1974, international time transfer experiments have been performed as part of the concept validation phase of the Global Positioning System (GPS). Time Transfer results from both NTS-1 and NTS-2 will be presented, including recent measurements from receivers located in South America, Germany, Japan and the United States. A time link to the DOD Master clock allows submicrosecond intercomparison of UTC(USNO,MC1) with clocks in the respective countries via the NTS link. Work is progressing toward a retrofit conversion of existing NTS receivers (located at NASA and foreign observatories) into GPS time transfer receivers.

Initial results will be presented on the long term rubidium frequency stability as measured from the GPS NAVSTAR-4 space vehicle (SV). Analysis has been performed for sample times varying from one to ten days. Using a 154 day data span starting on day 36, 1979, data was collected from the four GPS Monitor Stations (MS) located at Vandenberg, Guam, Alaska, and Hawaii.

A time domain estimate for the NAVSTAR-4 SV clock offset is obtained for each SV pass over the GPS monitor sites, using a smoothed reference ephemeris, with corrections for ionospheric delay, tropospheric delay, earth rotation and relativistic effects. Conversion from the time domain to the frequency domain is made using the two-sample Allan Variance; sigma-tau plots are used to identify the noise processes. Estimates of flicker and white frequency noise for the NAVSTAR-4 rubidium frequency standard are obtained. The contribution of the reference ground clocks and other error sources to the frequency stability estimates are discussed.

INTRODUCTION

The Navigation Technology satellites (NTS), developed by the U.S. Naval Research Laboratory (NRL), have provided on-orbit test vehicles for the basic satellite navigation technology^{1,2,3} currently used in the NAVSTAR Global Positioning System⁴ (GPS). Two satellites, TIMATION I and TIMATION II, were flown in 1967 and 1969 to demonstrate the concept of using synchronized clocks to provide time-ranging for time transfer^{5,6} and navigational^{7,8} purposes. Navigation Technology Satellite One (NTS-1), flown in 1974, introduced a rubidium⁹ atomic clock and NTS-2 (Figure 1), flown in 1977, a cesium¹⁰ clock. These spacecraft have demonstrated (Figure 2) a two order of magnitude improvement in timing precision from 300 ns in 1967 to a current value of near 3 ns!

Measurements from NTS-1 and NTS-2 will be presented that demonstrate the time transfer¹¹ capability, frequency offset and frequency stability¹² of the spacecraft clock. Measurements from NAVSTAR-4 (Figure 3) will be presented that estimate the long term frequency stability of the rubidium frequency standard from the pseudo range measurements. Time transfer results for the Hawaii, Guam and Alaska monitor sites have been made using the Vandenberg monitor site as the central station. These time transfer measurements are further processed to estimate the frequency stability of the Hawaii, Guam and Alaska clocks.

PTTI MEASUREMENTS

Two different types of time interval measuring techniques are used to obtain the results reported in this paper. The first is a sidetone ranging technique in which a set of tones is generated in the spacecraft, and then modulated onto the carrier; the receiver^{13,14} synthesizes the same set of sidetones and after detection and down conversion, compares the phase of the received tones to the phase of the synthesized tones. The set of phase difference measurements is then combined to produce observed range with progressively better resolution. Figure 2 presents the timing precision obtained as a function of time. The best precision¹⁵ was less than 5 ns with a resolution of 1.5 ns employing a 6.4 MHz sidetone.

A spread spectrum technique, first demonstrated on NTS-2 in 1977, is used for the Phase I NAVSTAR spacecraft. This ranging signal is comprised of two PRN¹⁶ (pseudo random noise) codes, biphasic modulated on the carrier frequency. A short 1.023 MHz C/A (coarse/acquisition) code is used for acquisition and a long 10.23 MHz P (precise) code is used for resolving range to at least 1.5 ns (46 cm). A navigation message¹⁷ is also modulated onto the signal and is available upon acquisition of the C/A code. Information exists in this message which enables acquisition of the P code. It also contains satellite ephemeris and health information.

Measurements of spacecraft doppler can be obtained by tracking the received carrier signal for a fixed amount of time or by counting a fixed number of cycles. The received frequency is mixed with standard frequencies generated coherently from the user's frequency standard. The respective difference frequency then enters a phase locked tracking filter. Measurements of doppler obtained from the PRN signal, called delta pseudo range, are taken every 6 seconds.

NTS Tracking Network

Figure (4) presents the four station network employed for tracking the NTS spacecraft. The limits of visibility for the Chesapeake Bay Division of NRL (CBD), Panama, Australia and England tracking stations are depicted by the symbols C,P,A and E, respectively. Reference to Figure (4) shows that the Panama station could track for 12 consecutive hours, or one complete revolution of the 2 rev/day NTS-2 orbit. This four station network provided 97% coverage of the NTS-2 orbit, averaged over one day.

Ground station timing was provided by cesium clocks which were inter-compared with other cesium clocks. Timing at the England NTS tracking station was coordinated with GMT and in Australia with the Division of National Mapping. The CBD tracking station had portable clock and TV links to the U.S. Naval Observatory DOD Master Clock. This arrangement provided control and timing checks for the time transferred by satellite.

Frequency Synchronization Results

Frequency tuning results from the first 150 days of NTS-2 operation are presented in Figure 5. For the first segment, beginning at launch on June 23, 1977, the transmitted frequencies were derived from the quartz oscillator subsystem of one of the two on-board cesium frequency standards. Using time difference measurements from the NTS network, the frequency offset with respect to UTC(USNO,MC1) was estimated. The quartz frequency was then tuned close to the cesium resonance frequency. The quartz frequency was then passively locked to the (nominal) cesium resonance at 9192 MHz.

The cesium resonators, which are primary standards, were expected to provide an absolute frequency reference to 1 part in 10^{12} while at rest on the earth's surface. The cesium frequency, in orbit, was expected to be influenced by the relativistic clock¹⁸ effect, which is (nominal prediction) 445 parts in 10^{12} for the GPS constellation. The frequency offset of each frequency standard was measured with respect to the DOD Master Clock before launch. The second segment presents the results of on-orbit estimation of the frequency offset,

which caused a (nominal) accumulation of time difference of 38,500 ns/day. By comparison of the theoretical and measured frequency offset, the Einstein relativistic clock effect was verified to less than one-half percent (0.5%).

Verification of this relativistic clock effect has resulted in a two part correction for GPS. The first part of this correction is obtained by (hardware) offsetting the transmitted frequency by $445\text{ppm}(12)$. This hardware correction accounts for more than 99.6% of the relativistic effect. The remainder of the correction is provided by software, with the necessary coefficients included in the navigation message.

Time Transfer Theory

Time transfer via satellite (Fig 6) is accomplished by measuring the time difference, beginning with the reference clock, for each of the time links and combining the results. Four links are necessary for GPS operation. These links are:

- (a) From DOD Master Clock to Master Control Station (MCS)
- (b) RF link from MCS to each GPS SV
- (c) SV clock update
- (d) SV to user RF link

These four links, and subsets thereof, have been used to analyze time transfer, navigation, SV clock and frequency stability, and orbital accuracy for GPS.

The link from the DOD Master Clock, which is denoted as UTC(USNO,MC1), has been demonstrated via portable clock and a TV time link to the NRL CBD (Chesapeake Bay Division) station. Measurements are then made at CBD to the NTS satellites for the second link. The third "link" is that of the satellite clock maintaining and carrying forward in time its measured offset with respect to the DOD Master Clock, through the CBD link. The fourth link is made by the user who makes the RF measurement to one or more satellites. Each satellite is synchronized, by combination of hardware and software, to a common time reference.

A GPS user who takes four simultaneous pseudo-range measurements to four GPS satellites can then use his assumed position and information in the navigation message to calculate four time transfer values. If the four time transfer values agree, his position is correct. If the four time transfers disagree, the four parameters (t, x, y and z) can be solved for simultaneously. Calculation of the time transfer value

first requires a coarse time synchronization of the user's receiver to GPS time, as maintained by the satellite clock. The satellite ephemeris, which is a function of GPS time, can then be used to calculate the geometrical range from the satellite to the user's assumed position. Corrections must be applied for antenna and equipment delays, the effects of ionospheric delay, tropospheric delay and earth rotation during the signal propagation time. The time transfer to the DOD Master Clock is obtained by a software correction which combines the offset of each GPS satellite clock with a relativity correction. This software correction is small because each GPS satellite clock is kept in near synchronization using an atomic frequency standard and most of the relativistic clock effect is hardware corrected.

The user's frequency offset and three dimensional velocity can be solved with four delta pseudo-range measurements to four GPS satellites. Alternately, frequency offset and three dimensional velocity can be obtained using a sequence of time transfers and successive x,y,z position estimates.

NTS Time Transfer Results

Time transfer techniques were first demonstrated by NRL in the formative development of GPS; by aircraft in 1964, by satellite in 1967 and on a worldwide^{19,20} basis in 1978 to the submicrosecond level of accuracy. Figure 7 tabulates a summary of those results from a six nation campaign as compared with portable clock measurements from USNO. The average accuracy obtained was 60 ns. The primary source of error was the lack of an ionosphere delay correction.

Recent time transfer results from South America, Japan²¹ and Germany (Figures 8 through 13) complement and confirm the previous time transfer results. These figures present continuous satellite time transfer results over a period of about 150 days through day 190, 1979. The entire worldwide net of stations participating since 1978 yields a history of worldwide submicrosecond satellite time transfer for the last two years.

Figure 14 presents time transfer to the NTS Panama Station over a 100 day span. During the first segment, NTS-1 was used to transfer time without the aid of an ionospheric correction. The last segment presents the NTS-2 results which had the benefit of an ionospheric correction and a cesium clock in the satellite. Figure 15 presents an 11 day segment of NTS-2 time transfer data. The 9 ns precision of these measurements indicates the potential of GPS to transfer time.

Long Term Frequency Stability

The Allan Variance was adopted by the IEEE as the recommended measure of frequency stability. Reference 22 presents a theoretical development which results in a relationship between the expected value of the standard deviation of the frequency fluctuations, for any finite number of data samples, and the infinite time average of the standard deviation. Eq (1) presents the Allan Variance²³ expression for M frequency samples with the sample period, T, equal to the sampling time, τ .

$$\text{Eq (1)} \quad \sigma_y^2(2, \tau) = \frac{1}{M-1} \sum_{k=1}^{M-1} \left(\frac{\bar{y}_{k+1} - \bar{y}_k}{2} \right)^2$$

The average frequency values \bar{y}_k are calculated from pairs of clock offsets, Δt , separated by sample time, τ , as given by

$$\text{Eq (2)} \quad \bar{y}_k = \frac{\Delta t_{k+1} - \Delta t_k}{\tau}$$

The clock offset is not directly observable from a pseudo range measurement; other variables must be measured or estimated. Figure 16 presents smoothed pseudo-range measurements that are evaluated at the Time of Closest Approach (TCA) of NAVSTAR-4 to the Vandenberg MS on day 177, 1979. Figure 17 presents the Long Term Frequency Stability²⁴ Analysis Flowchart which outlines the steps required to obtain estimates of $\sigma_y(2, \tau)$ for the NAVSTAR-4 rubidium clock. Pseudo range and delta pseudo range measurements, taken between NAVSTAR-4 and each Monitor Site, are transmitted to the Vandenberg Master Control Station (MCS) and are processed in real time to keep track of the NAVSTAR-4 clock and ephemeris. The measurements are collected and sent daily²⁵ to the Naval Surface Weapons Center (NSWC); once per week a reference ephemeris is calculated using the delta pseudo-range measurements in the CELEST²⁶ orbit determination program. Copies of the reference ephemeris are then transmitted to the Master Control Station, NRL and other GPS users. NRL then calculates the NAVSTAR-4 clock offset at the TCA for each monitor site pass, using the reference ephemeris and a smoothed value of pseudo range. This smoothed value of pseudo range, named SRTAP, is obtained from a 15 minute segment of 6 second pseudo-range and delta pseudo-range measurements which are used to sequentially estimate coefficients of a cubic equation. Corrections are applied for equipment delays, ionosphere, tropospheric delay, earth rotation and a small relativity correction. The significant effects which are not corrected are spacecraft orbit, clock offset and random effects remaining in the measurement.

The clock offset is estimated using the reference ephemeris and the a_0 coefficient from the cubic coefficients (a_0, a_1, a_2, a_3), which are reevaluated every 15 minutes of the NAVSTAR-4 pass. For a typical 6 hour pass, this procedure results in 24 values of clock offset; a subset of these values is used to estimate the clock offset at TCA.

Figures 18 through 21 depict the actual amount of information collected from each MS. Reference to Figure 18 presents 90 days (from day 036, 1979 through day 126, 1979) of observations from the Vandenberg MS. Figures 22 through 25 present the NAVSTAR-4 ground track, as observed at each MS on 4 Mar 1979.

Reference to Figure 22 shows that NAVSTAR-4 rose above the horizon at 2350 UTC on 3 Mar 1979 and set at 0410 on 4 Mar 1979. Consequently, NAVSTAR-4 could be observed for a maximum of 4 hours (h) and 20 minutes (m) for the first pass. The second pass is longer, with a pass duration of 5h 20m. In Figure 22 the dots along the SV ground track are placed at 10 minute intervals; the short bars perpendicular to the ground track are placed at 1 hour intervals. The TCA for each pass occurs approximately mid-way in the pass; the clock offset is calculated at this time. Reference to Figure 24 for the Guam MS shows that NAVSTAR-4 has only one pass each day, with a possible maximum pass time of 9h 50m. Reference to Figures 22 through 25 shows that the tracking network can track NAVSTAR-4 for as much as 66% of the time, averaged over the 2 rev/day orbit.

The SV pass time is a critical parameter in the orbit estimation; the $\Delta\rho$ (integrated pseudo range rate) reference trajectory orbit estimation assumes that the frequency offset (between the monitor site clock and the SV clock) will be constant for sample times varying from $\tau = 0.11$ days (Figure 23, Hawaii MS, second pass) to $\tau = 0.41$ days (Figure 24, Guam MS). Reference trajectory calculations are made one per week, using data collected for 7 days. The four monitor sites collect (typically) 49 passes per week, 7 passes from the Guam MS and 14 passes each from Vandenberg, Hawaii and Alaska.

The clock offset calculation at TCA produces a result that is independent of (small) along track orbit errors. This can be seen by reference to Figure 16; the pseudo range rate is zero at TCA. A similar statement applies for (small) normal to the orbit track errors. Radial (between the SV and the user) orbit errors behave differently; they look exactly like clock errors. Therefore, the capability of this technique to give significant $\sigma_y(2,\tau)$ estimates depends on the orbit smoothing to separate orbit errors from clock errors. The satellite dynamics have been extensively modeled; hence, the results are ultimately determined by the quality of the observations which are obtained by measurements between the spacecraft clock and the monitor site clocks.

NAVSTAR-4 Rubidium Frequency Stability Results

The clock offsets from the Vandenberg MS for a 90 day span are presented in Figure 26. During this time span, the clock offset of NAVSTAR-4 was within 100 μ s of the Vandenberg MS clock, except for a short time near day 055 when the cesium standard was activated. Two other clock resets are present, one near day 095 and another near day 118. The clock offsets for the other three monitor sites exhibit more frequent receiver resets.

The frequency stability of the NAVSTAR-4 rubidium frequency standard, referenced to the Vandenberg MS, is presented in Figure 27 for sample times from 1 to 10 days. A value of 6.1×10^{-13} was measured for $\tau = 1$ day. The frequency stability remains constant for up to $\tau = 4$ days, followed by an increase in frequency instability. These results were not corrected for aging rate, which averaged -8.7×10^{-14} /day for the 154 day span. Aging rate corrections were applied to each data segment and the $\sigma_y(2, \tau)$ was recalculated; the frequency stability with respect to the Vandenberg MS is presented in Figure 28.

$$\text{For } \tau = 1 \text{ day, } \sigma_y(2, \tau) = 6.1 \times 10^{-13};$$

$$\text{for } \tau = 10 \text{ days, } \sigma_y(2, \tau) = 2.4 \times 10^{-13}.$$

Frequency stability calculations were made for all four monitor sites; the results are presented in Figure 29. The influence of aging rate, which is quite evident in the Vandenberg MS measurements, is not as apparent in the Hawaii, Guam and Alaska monitor site data. Aging rate corrections were applied; the results are presented in Figure 30. These measurements indicate a constant trend for $\tau = 1$ day to $\tau = 6$ days, followed by an abrupt change for $\tau = 7$ days.

The frequency stability values from each monitor site were averaged; the four station average is presented in Figure 31 with no aging correction. Figure 32 presents the four-station frequency stability corrected for aging rate.

The four station average frequency stability for

$$\sigma_y(2, 1 \text{ day}) = 9.1 \times 10^{-13}.$$

The peak departure of any monitor site average from the four station average is indicated by the error bars. The frequency stability improves up to $\tau = 4$ days, followed by an increase with an apparent change in slope for $5 \leq \tau \leq 9$ days. The flicker floor is reached at $\tau = 9$ days, with $\sigma_y(2, 9 \text{ days}) = 2.5 \times 10^{-13}$. The coefficient for white frequency noise is estimated to be $(8.3 \times 10^{-13})/\sqrt{\tau}$, for $1 \leq \tau \leq 9$ days. Other factors are present in the data with the most notable being the change in $\sigma_y(2, \tau)$ slope for $\tau \geq 5$ days.

NAVSTAR-4 Time Transfer Results

Time transfer calculations for the three remote GPS monitor sites (Hawaii, Guam and Alaska) were made using the Vandenberg MS as the central station. The Vandenberg MS clock was linked to UTC(USNO,MC1)²⁷ by a series of portable clock trips. The SRTAP pseudorange measurements were used to obtain monitor station clock offsets with respect to NAVSTAR-4; the Vandenberg MS pseudo-range measurements were used to obtain the NAVSTAR-4 clock and clock rate values. Measurements were available from day 036, 1979 through Day 189, 1979, a 154 day time span. The internal receiver delay was not available; a value of zero was assumed.

Time transfer results from the Hawaii MS are presented in Figure 33 for a 25 day time span with an epoch of day 175, 1979. A time transfer value of 75031.121 usec was obtained for day 175 with a slope of $-4.80\text{pp}10(12)$ and a noise level of 17 ns. Each point in Figure 33, denoted by the symbol "X", was obtained using smoothed values for each of the four links involved in time transfer. The time transfer is given as the clock difference (UTC(USNO,MC1) - UTC(HAWAII)) which includes a 1 leap second correction since GPS time is not reset for leap seconds. The average frequency offset computed over the entire 154 day span was $[-4.05 \pm 0.41]\text{pp}10(12)$.

Time transfer results from the Guam MS are presented in Figure 34 for a 25 day time span with an epoch of Day 070, 1979. A time transfer value of 65660.025 usec was obtained for Day 070 with a slope of $4.24\text{pp}10(12)$ and a noise level of 72 ns. Inspection of Figure 34 shows an effect is present that increases the noise level of the Guam MS time transfers when compared to the Hawaii MS time transfers. The average frequency offset, computed over the 154 day span, was $[4.73 \pm 0.14]\text{pp}10(12)$.

Time transfer results from the Alaska MS are presented in Figure 35 for a 20 day time span with an epoch of Day 162, 1979. A time transfer value of 69314.634 usec was obtained for Day 162 with a slope of $-0.56\text{pp}10(12)$ and a noise level of 55 ns. The average frequency computed over the 154 day span was $[-0.14 \pm 0.11]\text{pp}10(12)$.

Further analysis indicates that the Alaska MS time transfer values change by 75 ns every 12 hours. Reference to the ground track (Figure 25) illustrates that this change corresponds to successive NAVSTAR-4 passes over the Alaska MS. This 75 ns change is responsible for the increased (55 ns for Alaska MS) noise level as compared to the Hawaii MS noise level of 17 ns.

The remote monitor site offsets, determined via NAVSTAR-4, vary from 65 ms to 75 ms. These values indicate that the remote monitor site

clock offsets approximate the 65 to 85 ms delay required for the signal to propagate from NAVSTAR-4 to the surface of the earth, assuming that the internal delay is small with respect to 85 ms (85,000,000 ns).

The monitor site frequency offsets for the Guam MS and the Hawaii MS differ from those expected of the cesium standards. The ground station cesium frequency standard manufacturer quotes an absolute frequency reference of 7pp10(12); however, user experience indicates that this is a conservative value. The difference frequency between the Guam MS and the Hawaii MS of 8.8pp10(12) is slightly larger than the expected value.

Remote Monitor Site Frequency Stability

The time transfer results were further analyzed by calculating the frequency stability of each remote MS (Hawaii, Guam and Alaska) cesium frequency standard, as determined through the time transfer measurements. This procedure involves all four links, similar to those given in Figure 6. Due to the relative position of the four monitor sites, the NAVSTAR-4 clock was required for an update of no more than 2 hours. In these calculations, the clock update time was from TCA at Vandenberg MS to TCA at each monitor site. This procedure involves NAVSTAR-4 clock and the orbital trajectory for a segment equal to the arc of the orbit traversed during the clock update time. Hence, the $\sigma_y(2, \tau)$ values computed via time transfer are sensitive to the short term stability of the NAVSTAR-4 clock and the difference in radial orbit error over a fraction of a revolution.

The frequency stability of the Guam MS cesium frequency standard, as determined by NAVSTAR-4 time transfer, is presented in Figure 36 for sample time varying from $\tau = 1$ to 10 days. For $\tau = 1$ day, a value of $\sigma_y(2, \tau) = 1.0 \times 10^{-12}$ was measured. The measured frequency stability decreases to a value of $\sigma_y(2, \tau) = 3.4 \times 10^{-13}$ for $\tau = 5$ days. For $\tau = 6$ through $\tau = 9$ days, a significant increase occurs; a peak value of 1.1×10^{-12} was measured at $\tau = 8$ days.

The frequency stability of the Alaska MS cesium standard is presented in Figure 37. For $\tau = 1$ day, a value of $\sigma_y(2, \tau) = 7.9 \times 10^{-13}$ was measured. A behavior similar to the Guam MS results (Figure 36) was noted with a peak value occurring at $\tau = 7$ days. The results for $\tau = 3$ days are less significant than the results from the Guam MS. A shorter arc of the orbit was required; also, more equipment resets resulted in a smaller sample.

The frequency stability of the Hawaii MS cesium frequency standard are

presented in Figure 38. For

$$\tau = 1 \text{ day, a value of } \sigma_y(2, \tau) = 6.7 \times 10^{-13}$$

was measured. An increase in $\sigma_y(2, \tau)$ which is less than that observed at the Guam MS, occurs for $\tau = 5$ days. The results from the Hawaii MS are the best of the three remote monitor sites.

The $\sigma_y(2, \tau)$ values for Guam MS reach a maximum at $\tau = 8$ days of 1.1×10^{-12} . The Alaska MS $\sigma_y(2, \tau)$ reach a relative maximum at $\tau = 7$ days; Hawaii shows an increased frequency $\sigma_y(2, \tau)$ value at $\tau = 5$ days as shown in Figure 37 and 38 respectively.

Two factors were considered as possible causes of this increased frequency instability. The first factor is the seven day reference trajectory orbit fit spans. A total of 22 seven day orbits were made during the 154 day data span. The time transfer results from Guam (see Figure 34) indicate small changes from the average slope that correspond exactly with the seven day orbit fit spans. The second factor considered was the once-per-week P code resets for the pseudo random code transmitter²⁸. If this was the factor it would have appeared at the same amplitude (1.1×10^{-12}) for the single station $\sigma_y(2, \tau)$ results presented in Figures 27-32. It is therefore concluded that "orbit mismatch" is present for the longer sample times, of five days or more.

The average value of the $\sigma_y(2, \tau)$ values for the Hawaii, Guam and Alaska frequency standards is 7.8×10^{-13} for $\tau = 1$ day. This value is considerably larger than the expected frequency stability for the HP5061A, Opt 004 standards. However, it is close to the 9.1×10^{-13} value measured for the NAVSTAR-4 rubidium frequency standard. These results indicate that NAVSTAR-4 rubidium is slightly less stable than the average remote MS frequency stability, as measured by time transfer.

CONCLUSIONS

- o Worldwide time transfer to the major time standards laboratories has been demonstrated with NTS-1 for the past two years. The average accuracy achieved was 60 ns. Ionospheric delay was the most significant uncorrected error source.
- o A time transfer precision of 9 ns has been demonstrated for an 11 day span with the NTS-2 spacecraft using a cesium clock and a first order ionospheric delay correction.

- o The NAVSTAR-4 rubidium frequency standard has a measured frequency stability, with aging corrected, of

$$\begin{aligned}\sigma_y(2, 1 \text{ day}) &= 9.1 \times 10^{-13} \\ \sigma_y(2, \tau) &= 8.3 \times 10^{-13} / \sqrt{\tau} \quad 1 < \tau < 9 \text{ days} \\ \sigma_y(2, 9 \text{ days}) &= 2.5 \times 10^{-13}\end{aligned}$$

referenced to a smoothed reference ephemeris calculated over 22 seven day orbits using delta pseudo-range measurements. For $\tau \geq 5$ days a change in the $\sigma_y(2, \tau)$ versus τ curve is present which correlates with the orbit fit span.

- o Time transfer to the three remote monitor sites indicates clock offsets near 65 to 85 ms. Time transfer noise levels of 17 to 55 ns were measured for the reported data span over a 154 day observed data span.
- o The frequency stability of the three remote GPS monitor sites has been calculated for $1 \leq \tau \leq 10$ days using NAVSTAR-4 time transfer results with the Vandenberg MS as the central station, linked by portable clock to UTC(USNO,MC1). These measurements indicate a seven day orbital effect.
- o Comparison of the on-orbit frequency stability of a rubidium frequency standard versus a cesium frequency standard indicates $\sigma_y(2, 1 \text{ day}) = 9.1 \times 10^{-13}$ for rubidium and $\sigma_y(2, 1 \text{ day}) = 3.7 \times 10^{-13}$ for cesium as presented in figure 39, details of which are in reference 12.

NRL, along with other agencies and contractors, is continuing development of advanced cesium and hydrogen maser frequency standards for use in future GPS spacecraft. Other proposed work includes a study to investigate the seven day orbit effect.

Acknowledgements

The authors acknowledge Roger Easton, Head of Space Applications Branch, for guidance and direction, Don Lynch for technical consultation, Kathy McDonald for data processing and Stella Scates for manuscript preparation. They are all of the Naval Research Laboratory. Acknowledgement is given to Hugh Warren and Jerry Mobley of Bendix Field Engineering and to Clark Wardrip of NASA for his international technical coordination efforts.

Acknowledgement is given to Dr. John Pilkington of the Royal Greenwich Observatory, England, and to Dr. Peter Morgan of the Division of National Mapping, Australia, for their efforts in the NTS tracking station operation for GPS concept validation.

Acknowledgement is given to the representatives from the Smithsonian Astrophysical Observatory (SAO), and from France, Germany, Canada, Japan and Brazil for their participation in time transfer experiments.

The authors acknowledge the support of CDR Ring, GPS Navy Deputy and CAPT Masson, JPO, for technical coordination.

Acknowledgement is given to Dick Anderle, Robert Hill, Michael Harkins and Jack Carr of NSWC for the reference ephemeris calculation.

The authors wish to acknowledge the continuing support, for more than a decade, of Dr. Winkler and his personnel at the U.S. Naval Observatory.

REFERENCES

1. R.L. Easton, "Optimum Altitudes for Passive Ranging Satellite Navigation Systems", Naval Research Reviews, Aug., 1970, pp. 8-17.
2. J.A. Buisson and T.B. McCaskill, "TIMATION Navigation Satellite System Constellation Study", NRL Report 7389, June 27, 1972.
3. T.B. McCaskill, J.A. Buisson, and D.W. Lynch, "Principles and Techniques of Satellite Navigation Using the TIMATION II Satellite", NRL Report 7252, June 17, 1971.
4. B.W. Parkinson, "NAVSTAR Global Positioning System (GPS)", National Telecommunications Conference, Conference Record, Vol. iii, 1976, pp. 41.1-1 to 41.1-5.
5. Roger L. Easton, "The Role of Time/Frequency in Navy Navigation Satellites", Proceedings of the IEEE, Special Issue on Time and Frequency, May, 1972, pp. 557-563.
6. R.L. Easton, D.W. Lynch, J.A. Buisson, and T.B. McCaskill, "International Time Transfer Between the U.S. Naval Observatory and Royal Greenwich Observatory via the TIMATION II Satellite", NRL Report 7703, Apr. 18, 1974.
7. T. McCaskill, J. Buisson, and A. Buonaguro, "A Sequential Range Navigation Altitude for a Medium Altitude Navigation Satellite", Journal of the Institute of Navigation, Vol. 23, No. 2, Summer, 1976.
8. J. Buisson, T. McCaskill, and J. Thompson, "Range Navigation Results Using the TIMATION I Satellite", NRL Report 7511, Feb. 12, 1973.
9. Stephen A. Nichols and Joseph White, "Satellite Application of a Rubidium Frequency Standard", Proceedings of the 28th Annual Symposium on Frequency Control, 1974, pp. 401-405.
10. J. White, F. Danzy, S. Falvey, A. Frank, and J. Marshall, "NTS-2 Cesium Beam frequency Standard for GPS", pp. 637-664 in the Proceedings of the Eighth Annual Precise Time and Time Interval (PTTI) Applications and Planning Meeting, 1976.
11. J.A. Buisson, T.B. McCaskill, H. Smith, P. Morgan, and J. Woodger, "Precise Worldwide Station Synchronization via the NAVSTAR GPS, Navigation Technology Satellite (NTS-1)", in the Proceedings of the Eighth Annual Precise Time and Time Interval (PTTI) Applications and Planning Meeting, 1976.

12. T. McCaskill, J. Buisson, J. White, and S. Stebbins, "NTS-2 Cesium Frequency Stability Results", NRL Report 8375.
13. G.P. Landis, I. Silverman, and C.H. Weaver, "A Navigation Technology Satellite Receiver", NRL Memorandum Report 3324, July 1976.
14. L. Raymond, O.J.Oaks, J. Osborne, G. Whitworth, J. Buisson, P. Landis C. Wardrip, and J. Perry, "Navigation Technology Satellite (NTS) Low Cost Timing Receiver", Goddard Space Flight Center Report X-814-77-205, Aug. 1977.
15. J. Buisson, T. B. McCaskill and O. J. Oaks, "Initial Results of Navigation Technology Satellite Time Transfer Receiver (NTS/TTR)", NRL Report, in preparation.
16. J.J. Spilker, "GPS Signal Structure and Performance Characteristics", Journal of the Institute of Navigation, Vol. 25, No. 2, Summer, 1978, pp. 121-146.
17. A. Dierendock, S. Russell, E. Kipitzke, and M. Birnbaum, "The GPS Navigation Message", Journal of the Institute of Navigation, Vol. 25, No. 2, Summer 1978, pp. 147-165.
18. "SAMSO Relativity Seminar", held at the National Bureau of Standards, March 8-9, 1979.
19. J. Buisson, T. McCaskill, J. Oaks, D. Lynch, C. Wardrip, and G. Whitworth, "Submicrosecond Comparisons of Time Standards via the Navigation Technology Satellites (NTS)", Proceedings of the PTTI, Nov. 1978, pp. 601-627.
20. J. Buisson, T. McCaskill, and J. Oaks, "A Comparison of Inter-continental Clock Synchronization by VLBI and the NTS Satellite", NRL Report, in preparation.
21. Y. Saburi, Y. Yasuda, S. Kobayashi, T. Sato and M. Imae, "T&F Comparisons via Broadcasting Satellite and Navigation Technology Satellite (NTS)", Proceedings of the 11th Annual PTTI, Nov. 27, 28, and 29, 1979.
22. David W. Allan, "Statistics of Atomic Frequency Standards", Proceedings of the IEEE, Vol. 54, No. 2, Feb. 1966, pp. 221-230.
23. David W. Allan, et al., "Statistics of Time and Frequency Data Analysis", Chap. 8, NBS Monograph 140, "TIME and FREQUENCY: Theory and Fundamentals", May, 1974.

24. T.B. McCaskill and J.A. Buisson, "Quartz- and Rubidium-Oscillator Frequency Stability Results", NRL Report 7932, Dec. 12, 1975.
25. "NSWC Interface Control Document", CP-CS-303, Part I, pp. 220-223, 14 July 1978.
26. J.W. O'Toole, "Celest Computer Program for Computing Satellite Orbits", NSWC/DL TR-3565, Oct. 1976.
27. G.M.R. Winkler, R.G. Hall, and D.B. Percival, "The U.S. Naval Observatory Clock Time Reference and the Performance of a sample of Atomic Clocks", International Journal of Scientific Metrology, Vol. 6, No. 4, Oct. 1970, pp. 126-134.
28. R.J. Milliken and C. J. Zoller, "Principle of Operation of NAVSTAR and System Characteristics", Journal of the Institute of Navigation, Vol. 25, No. 2, Summer, 1978, pp. 98.

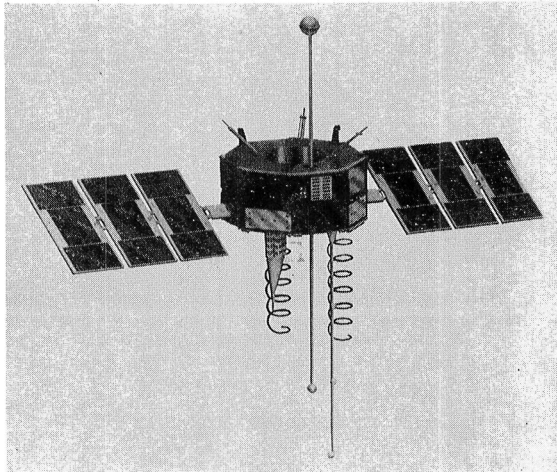


Fig. 1 — NTS-2

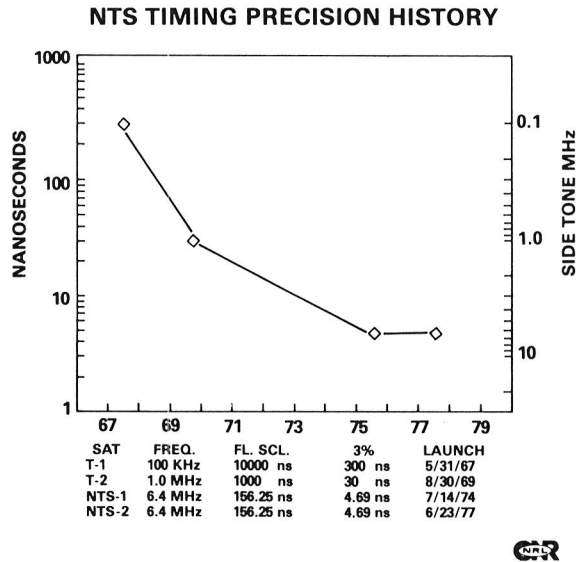


Fig. 2 — NTS timing precision history

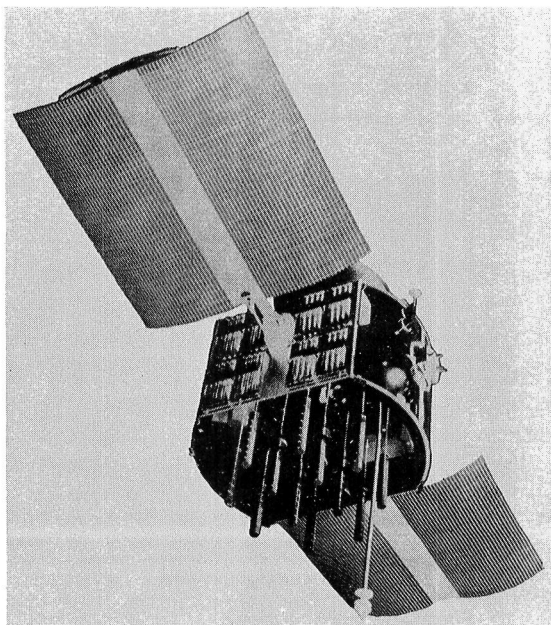


Fig. 3 — NAVSTAR-4

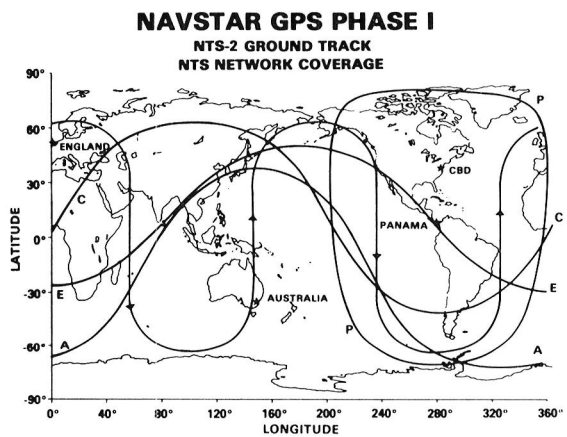


Fig. 4 — NTS network coverage

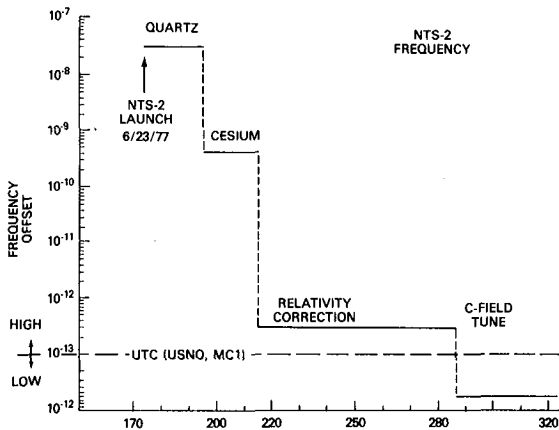


Fig. 5 - NTS-2 frequency history

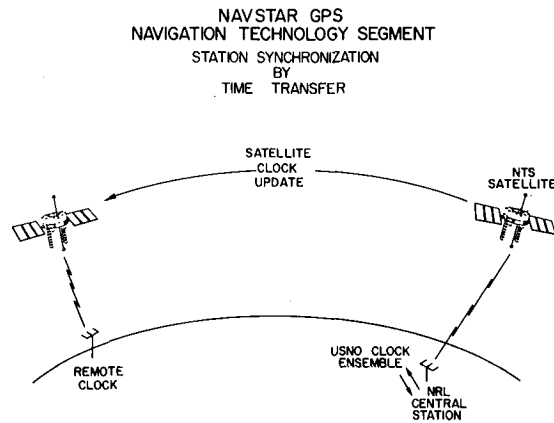


Fig. 6 - Time transfer via satellite

**SUMMARY OF
PORTABLE CLOCK CLOSURES
VS
NTS TIME TRANSFER RESULTS**

STATION	DAY (1978)	PORTABLE CLOCK - NTS TIME TRANSFER (μ S)
BIH	124	-.57
CERGA	117	.70
DNM	282	.09
IFAG	199	.03
NBS	221	.19
NRML	299	-.53
RGO	115	.44
RRL	303	.13
USNO	186	.04

Fig. 7 - NTS time transfer vs portable clock closures

**NAVSTAR GPS
NTS-1**

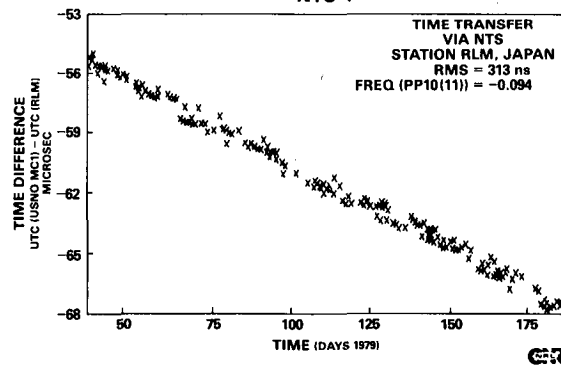


Fig. 8 - NTS-1 time transfer to RLM, Japan

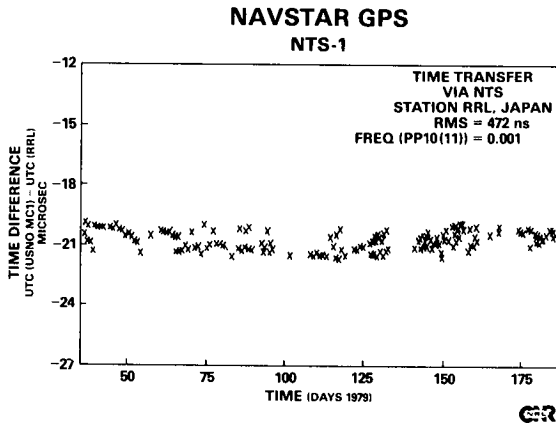


Fig. 9 — NTS-1 time transfer to RRL, Japan

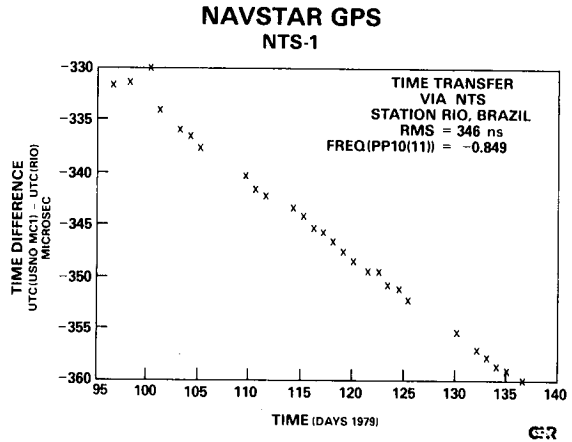


Fig. 10 — NTS-1 time transfer to Rio, Brazil

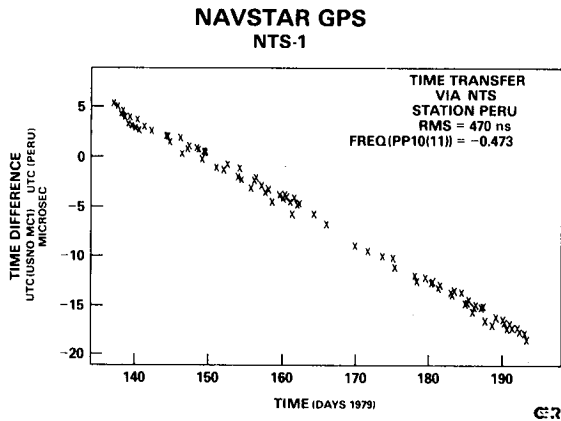


Fig. 11 — NTS-1 time transfer to Peru

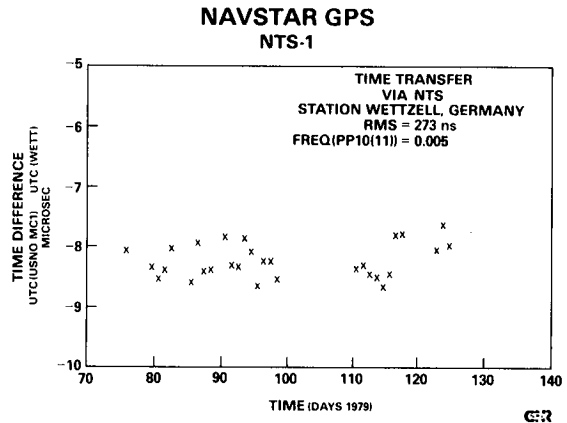


Fig. 12 — NTS-1 time transfer to Wettzell, Germany

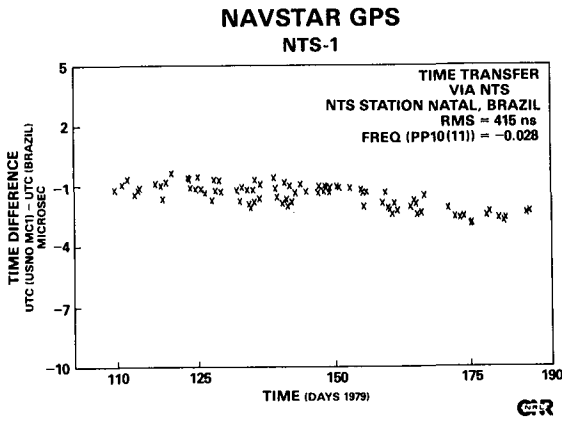


Fig. 13 — NTS-1 time transfer to Natal, Brazil

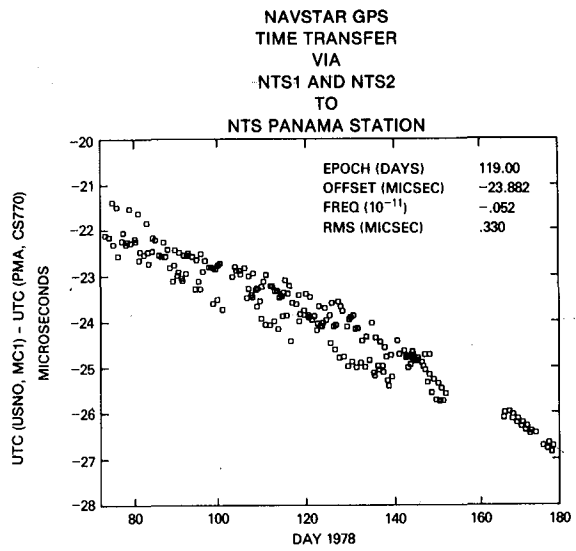


Fig. 14 — NTS-1/NTS-2 time transfer to NTS Panama tracking station

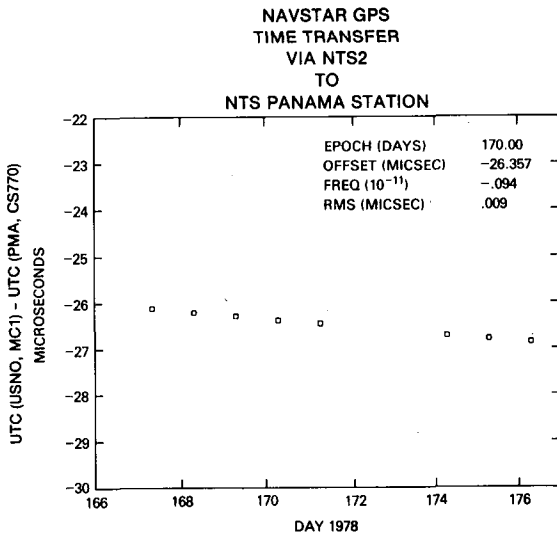


Fig. 15 — NTS-2 time transfer to NTS Panama tracking station

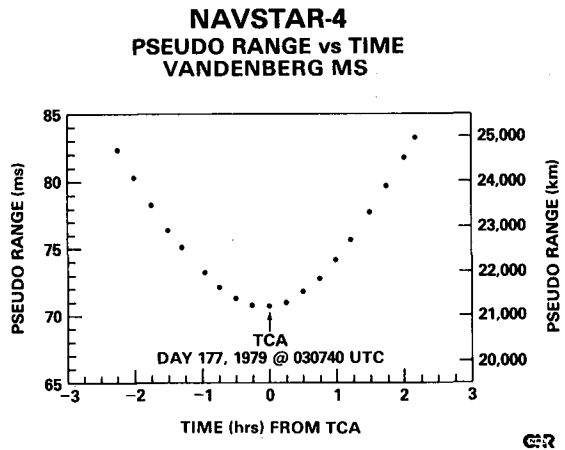


Fig. 16 — Pseudo range vs time, Vandenberg MS

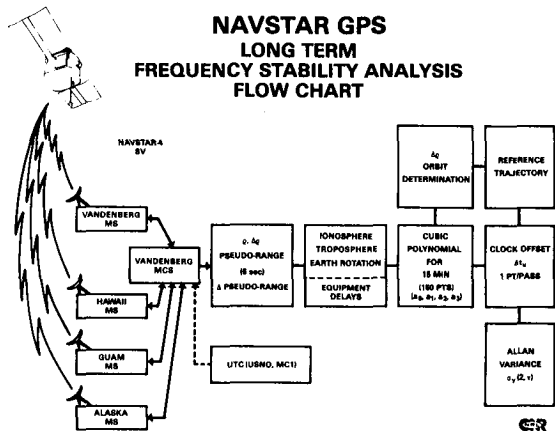


Fig. 17 — Long term frequency stability analysis flowchart

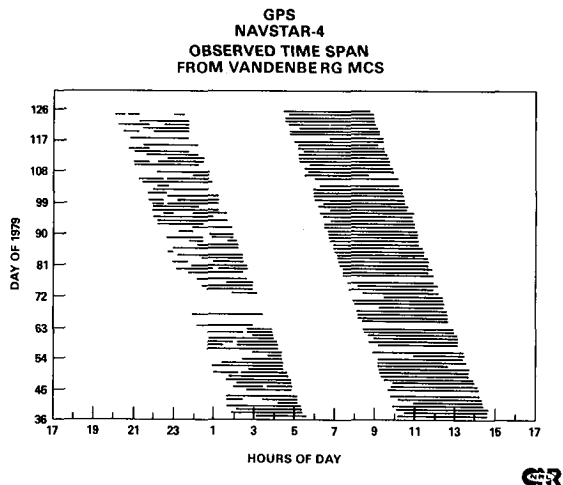


Fig. 18 — NAVSTAR-4 observed time span, Vandenberg MS

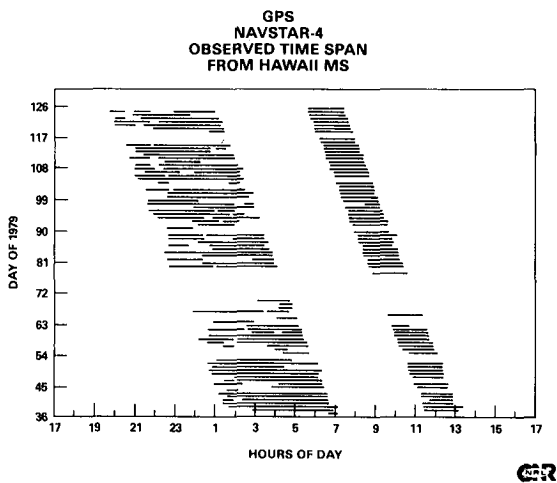


Fig. 19 — NAVSTAR-4 observed time span, Hawaii MS

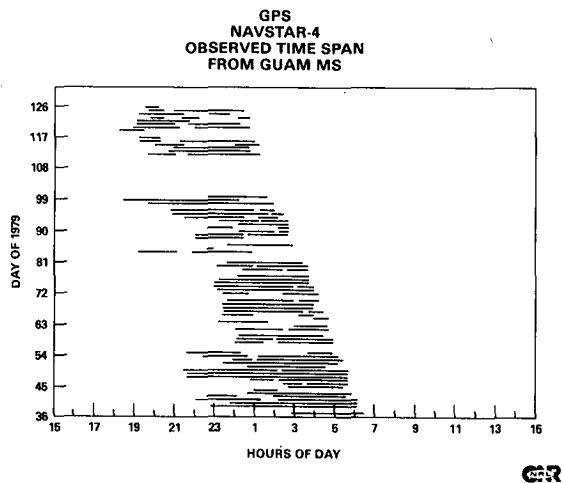


Fig. 20 — NAVSTAR-4 observed time span, Guam MS

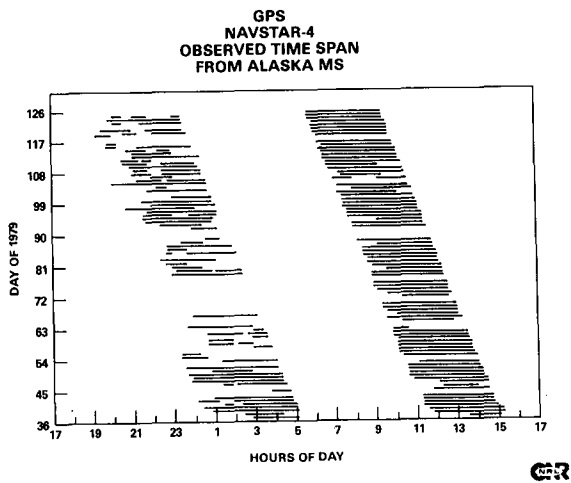


Fig. 21 — NAVSTAR-4 observed time span, Alaska MS

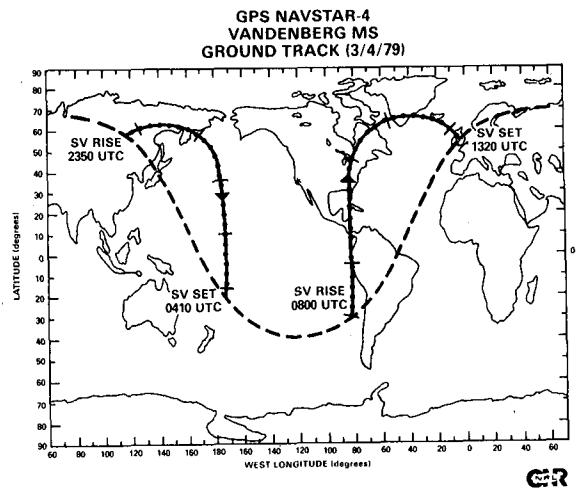


Fig. 22 — NAVSTAR-4 ground track on 4 March 1979, Vandenberg MS

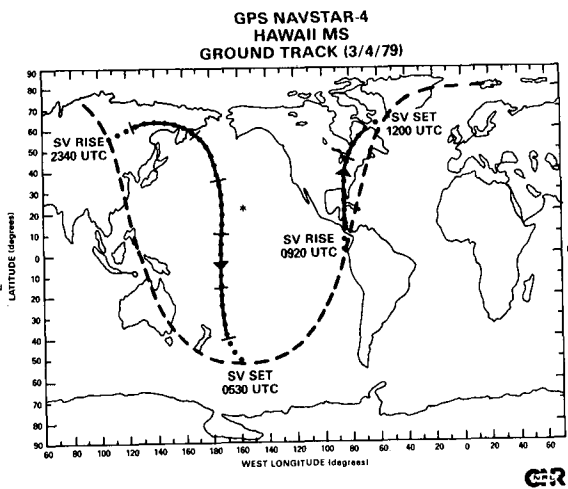


Fig. 23 — NAVSTAR-4 ground track on 4 March 1979, Hawaii MS

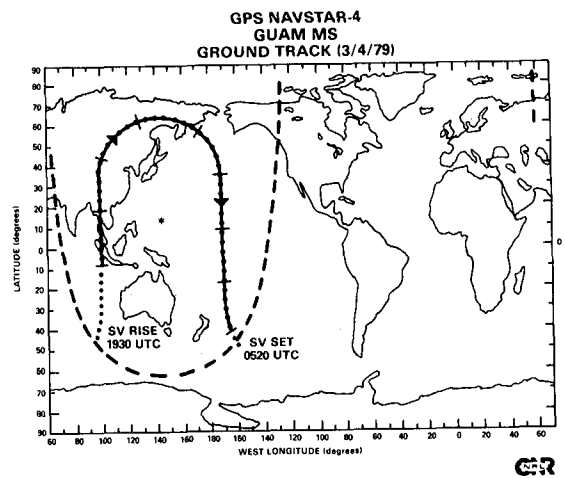


Fig. 24 — NAVSTAR-4 ground track on 4 March 1979, Guam MS

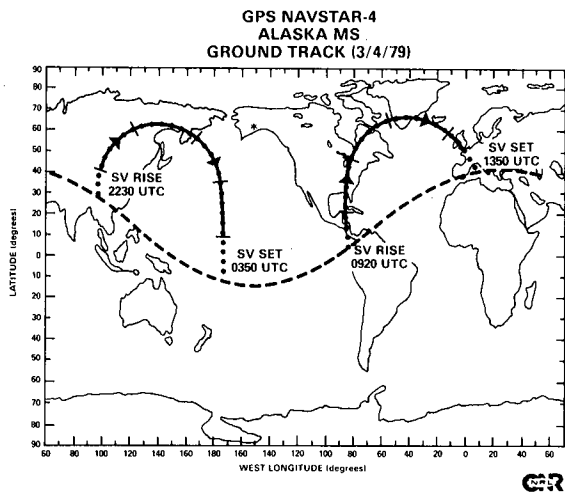


Fig. 25 — NAVSTAR-4 ground track on 4 March 1979, Alaska MS

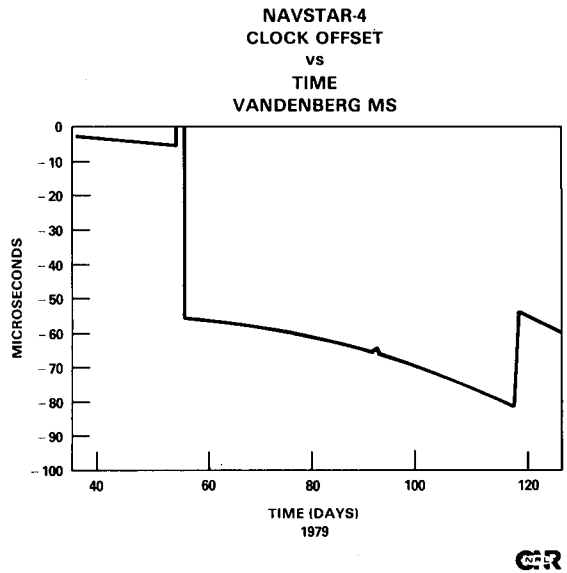


Fig. 26 — NAVSTAR-4 clock offset vs time, Vandenberg MS

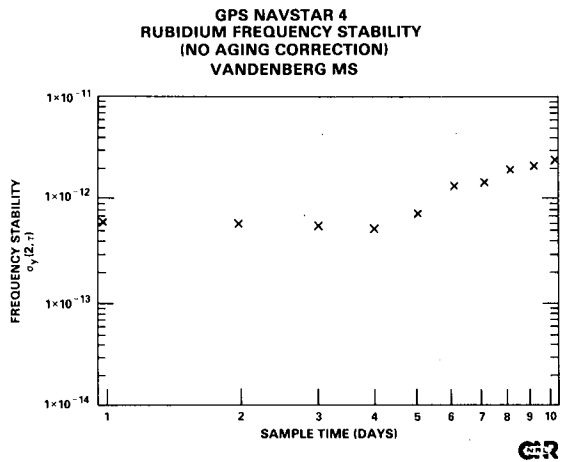


Fig. 27 — NAVSTAR-4 rubidium frequency stability (no aging correction), Vandenberg MS

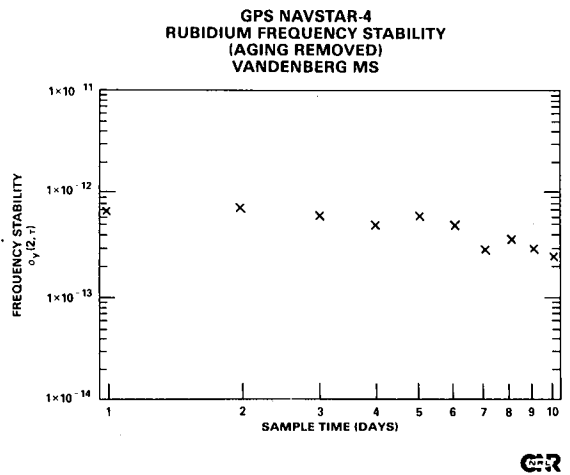


Fig. 28 — NAVSTAR-4 rubidium frequency stability (aging removed), Vandenberg MS

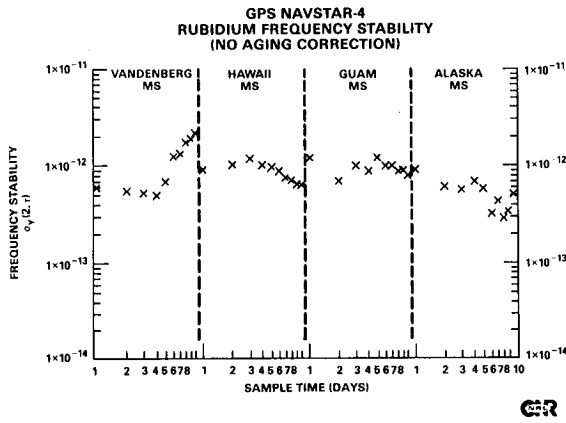


Fig. 29 — NAVSTAR-4 rubidium frequency stability four monitor stations, no aging correction

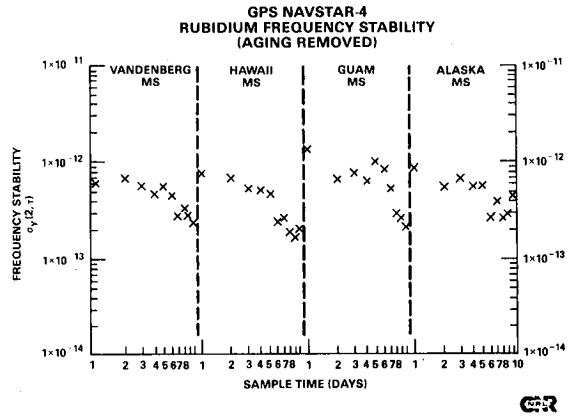


Fig. 30 — NAVSTAR-4 rubidium frequency stability four monitor stations, aging removed

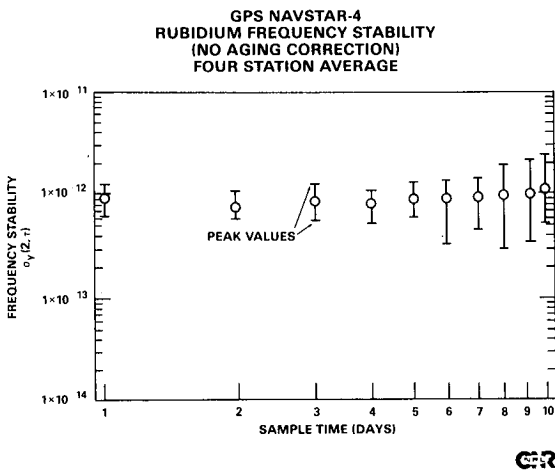


Fig. 31 — NAVSTAR-4 rubidium frequency stability four station average, no aging correction

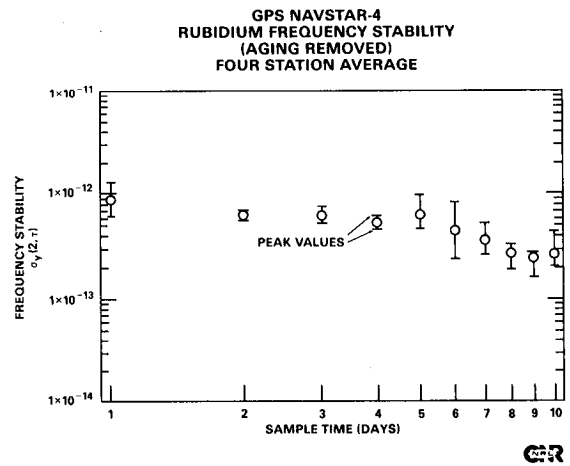


Fig. 32 — NAVSTAR-4 rubidium frequency stability four station average, aging removed

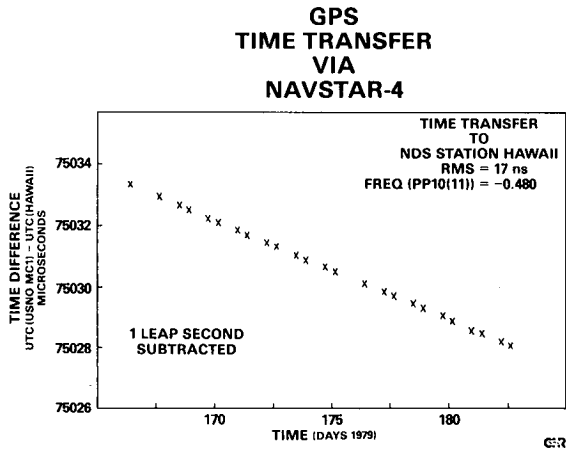


Fig. 33 — NAVSTAR-4 time transfer to Hawaii MS

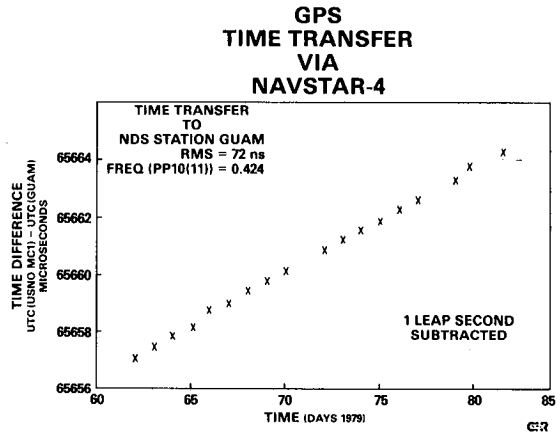


Fig. 34 — NAVSTAR-4 time transfer to Guam MS

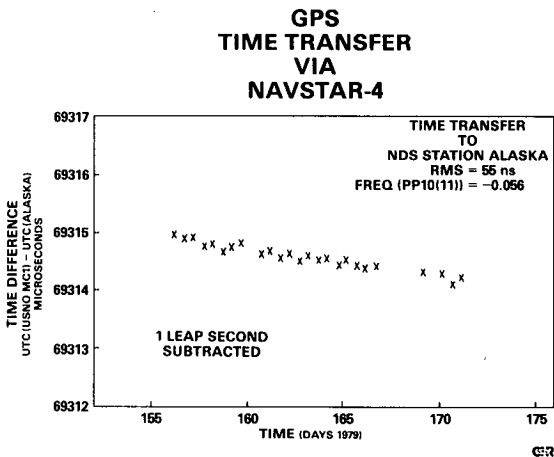


Fig. 35 — NAVSTAR-4 time transfer to Alaska MS

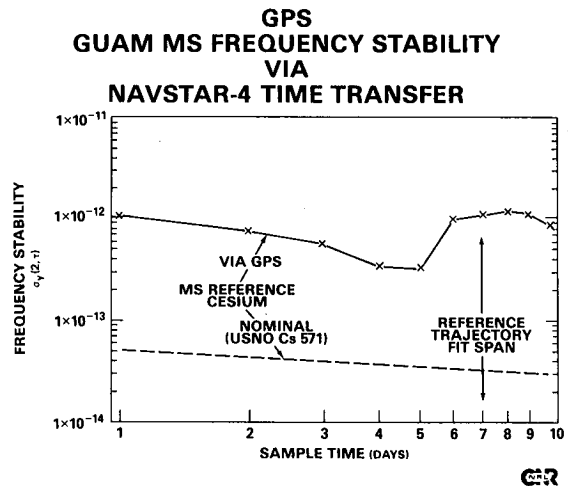


Fig. 36 — Guam MS frequency stability via NAVSTAR-4 time transfer

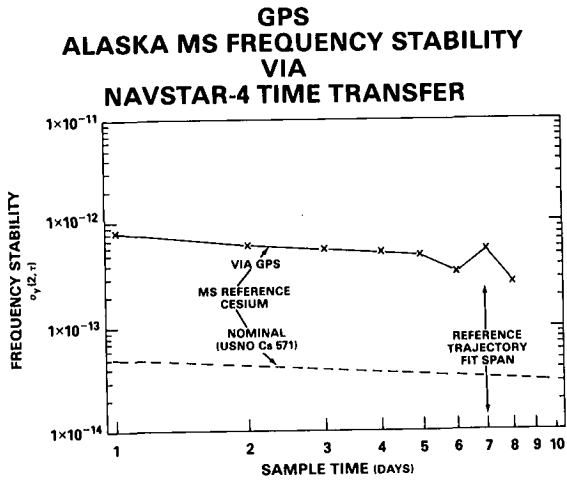


Fig. 37 — Alaska MS frequency stability via NAVSTAR-4 time transfer

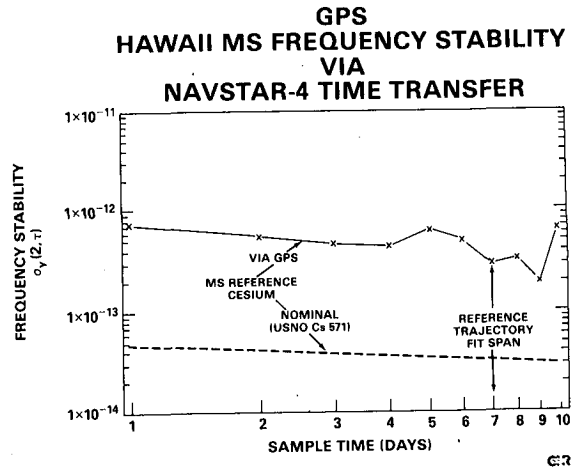


Fig. 38 — Hawaii MS frequency stability via NAVSTAR-4 time transfer

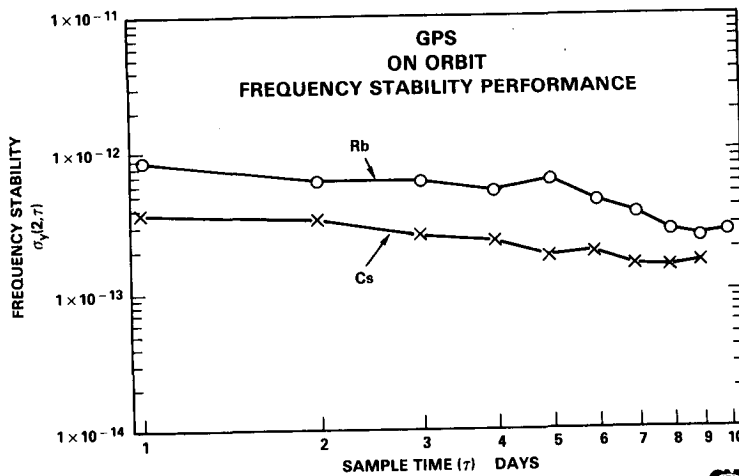


Fig. 39 — GPS on-orbit frequency stability performance

QUESTIONS AND ANSWERS

DR. VESSOT:

Are the rubidium data drift corrected in that instance?

DR. MCCASKILL:

Yes sir. The data are corrected for aging rate.

DR. ALLEY:

Could you say a few more words on just how the data will be extracted and did you use the full Kalman filtering process of the GPS code to get this?

DR. MCCASKILL:

The Kalman filter was not used at all. This was all done in a so-called post processing, batch type of mode. In the batch type of mode we used a week's worth of observation. If you had two passes per day from each station, you would have eight, you would have seven, because Guam only took one, so you would have around 50 complete passes, satellite passes of NAVSTAR-4 in order to estimate the orbit. So it is batch processing and it did not involve the on-line use of the Kalman filter.

MR. PLEASURE:

Are these algorithms for general relativity corrections, are they published in your literature or not?

DR. MCCASKILL:

As Dr. Winkler mentioned earlier, there was a workshop, I believe headed up by Dr. Dave Allan, who is here, on the relativity effects that would have to be accounted for for GPS and I know that the results are published. I do not know the availability of them. You might check with either Dr. Allan or Dr. Winkler to find out about the availability.

QUESTION:

Since when are they available?

DR. WINKLER:

They have been published.

TIME RECOVERY MEASUREMENTS USING
OPERATIONAL GOES AND TRANSIT SATELLITES*

R. E. Beehler, D. D. Davis, J. V. Cateora,
A. J. Clements, J. A. Barnes and E. Méndez-Quiñones
National Bureau of Standards
Boulder, Colorado

ABSTRACT

Users with requirements for timing signals available over wide geographical areas that are accurately referenced to UTC(NBS) or UTC(USNO) can conveniently access either of two operational satellite systems. Two geostationary GOES (Geostationary Operational Environmental Satellite) satellites located at 75° and 135° W longitude provide a continuous NBS-referenced time code to the Western hemisphere, including large portions of the Atlantic and Pacific Ocean areas. Five operational TRANSIT satellites provide timing signals referenced to UTC(USNO) from low-altitude polar orbits, resulting in worldwide coverage on a non-continuous basis. Convenient, fully automatic, microprocessor-based commercial receivers are now available for use with both satellite systems.

Results of regular monitoring of both the GOES and TRANSIT timing signals over a number of months at NBS, Boulder, CO are presented. The TRANSIT results include an analysis of how received timing accuracy and stability are affected by: (1) averaging over varying numbers

* Contribution of the National Bureau of Standards, not subject to copyright in the U.S.

of satellite passes; (2) averaging over different combinations of the 5 available satellites; (3) using several independent receivers of the same type; and (4) application of [TRANSIT-UTC(USNO)] published corrections to the received data. Based on monitoring experience to date at NBS, some pros and cons of using each of the available operational systems are discussed.

Updated information on recent improvements incorporated into the GOES time code generation and monitoring system at Wallops Island, VA is also included.

INTRODUCTION

Time transfer techniques using satellites are being investigated in one form or another by almost every major timing laboratory in the world. While much of the work reported on to-date has dealt with highly successful, experimental time transfers among international laboratories at the highest attainable accuracy levels, there are also very real needs for the more general dissemination of reliable timing signals at more modest accuracy levels in the 1-100 μ s range. Currently, there are two major satellite-based systems which offer such timing capabilities to general users on an operational basis. These are the U.S. Navy's TRANSIT satellite navigation system, also referred to as the "Navy Navigation Satellite System," and the Dept. of Commerce's GOES System, which is an acronym for "Geostationary Operational Environmental Satellites." Relatively low-cost timing receivers are available commercially for use with either of these operational satellite systems. The National Bureau of Standards has been systematically monitoring and evaluating both the TRANSIT and GOES timing capabilities over a period of about 8 months. The approach has been to use only

commercially available receivers, treating them essentially as a "black box" with a 1 pulse-per-second output that is analyzed and evaluated as a timing reference with respect to the UTC(NBS) time scale.

TIME DISSEMINATION RESULTS VIA TRANSIT*

There are currently 5 operational TRANSIT satellites providing timing signals in a one-way mode from nearly circular, polar orbits.⁽¹⁾ With this satellite configuration a user at a particular location has access to the TRANSIT signal for about 15 minutes each time one of the satellites flies over within range. Coverage is therefore worldwide, although at any particular location intervals between successive satellite passes might range anywhere from a few minutes to several hours. The TRANSIT signal format contains a fiducial time marker each 2 minutes derived from an on-board crystal oscillator and satellite ephemeris information that can be processed by the receiver to compute the path delay from satellite to user for each 2-minute interval. The receivers used in the NBS measurements, priced at about \$12,000 each, automatically acquire the 400 MHz TRANSIT signals, compute the path delays, and correct the output 1 pps to be on-time with respect to the satellite clock.⁽²⁾ Since the satellite clocks are carefully monitored and controlled by the Navy Astronautics group and the U.S. Naval Observatory, the receiver output can provide an excellent local representation of UTC(USNO).

The block diagram in Figure 1 indicates the way in which the commercial TRANSIT receivers available to NBS for these evalua-

*This work was supported by the Naval Electronics Systems Command under CCG Contract #79-142.

tions were used. Although these particular receivers include capabilities for averaging over any number of satellite passes from 1 to 100 and for selectively deleting one or more of the 5 operating satellites from the ensemble used to correct the output 1 pps, NBS chose to use a multi-channel data logger to accumulate data separately from each successful satellite pass. For each pass data were recorded providing a measurement of the TRANSIT receiver 1 pps relative to UTC(NBS), identification numbers for the particular satellite and receiver involved, the amount of correction computed and applied by the receiver, the date and time of correction, and the standard deviation of the individual 2-minute points as supplied by the receiver. After the fact the data file was completed by adding a "TRANSIT clock-UTC(USNO)" correction as published by USNO and the elevation angle for each pass. These data were then analyzed in various ways to show the dependence on the particular satellite ensemble used, the number of passes averaged, the particular receivers used, the application of the USNO corrections, and satellite elevation angle.

In all cases TRANSIT measurements deviating by more than 100 μ s from UTC(NBS) were discarded.

Dependence on Satellite Ensemble

Figures 2-6 present the received TRANSIT data from each of the 5 operational satellites separately for the 8-month period of the measurements. In each case, each plotted point is the average of 5 successfully received satellite passes (normally, there are about 2 satellite passes per day for each satellite). Also, on each plot are tabulated the mean values and standard deviations applicable to smaller time segments of the 8-month period.

UTC(NBS) is used as the reference, but since NBS and USNO differed by only 2 μ s during this period plots in terms of UTC(USNO) would differ only by that amount. Satellite #120, the oldest of the current group, consistently had the highest offset of about +30 μ s. #130, also one of the oldest TRANSIT's, was offset by only -0.5 μ s. Similarly, #140 was offset by about +14 μ s on the average, #190 by +3 μ s, and the newest satellite, #200, by -2.8 μ s. The standard deviations of the 5-pass averages ranged between 8 and 18 μ s for the 5 satellites. Figure 7 also shows the long-term behavior of each satellite over the 8-month period, where each plotted point in this case is an average over 60 days. It is apparent that for best accuracy with respect to either NBS or USNO during this period satellite #120, and possibly also #140, could have been excluded from the ensemble. This effect is shown in Figure 8 where the solid line refers to the complete 5-satellite ensemble, averaging 20 passes per point in this case, while the dashed line is the result if #120 is excluded. The ensemble mean offsets are about 8 μ s including all satellites and 4 μ s with #120 excluded.

Dependence on Number of Satellite Passes Averaged

Figures 9-11 illustrate how the measurement precision varies with the number of satellite passes averaged. As mentioned previously, the receiver can be easily set to average anywhere from 1 to 100 passes automatically. In the first case for illustration (Figure 9) all satellite passes are used and each plotted point is the average of 5 such passes successfully processed by the receiver. Since typically about 11 good passes per day were received in Boulder, this average corresponds to about one-half day. The standard deviation of the 5-pass averages is about 9 μ s. By comparison, a plot of 30-pass averages (Figure 10) corresponding

to about 3-day averages, shows that the standard deviation improves to about 5 μ s. When all of the data are analyzed in more detail, the plot in Figure 11 of standard deviation vs. the number of passes averaged results. One might interpret this as a dependence on the number of passes averaged, N, that varies as $N^{-\frac{1}{2}}$ down to a "flicker floor" level of about 3 μ s for N = 50 passes. The standard deviation for a single pass is about 20 μ s.

Dependence on the Particular Receivers Used

Although two independent, co-located receivers observing the same satellite pass occasionally disagreed by more than 50 μ s, their long-term agreement was excellent. Figure 12 compares two different receivers based on 30-pass averages. The tabulated mean values in the plot show that 50-60 day averages agreed to within better than 3 μ s for these receivers.

Dependence on USNO Published Corrections

Figure 13 illustrates the effect of correcting the observed data by applying the "TRANSIT-UTC(USNO)" corrections from USNO's Time Service Announcement Series 17. Data from all 5 satellites are included and each point is an average over 10 passes, or about 1 day. The dashed curve has the USNO corrections applied while the solid curve is the uncorrected output of the receiver. One reason that its hard to distinguish the two separate curves is that the means are essentially identical-in fact, applying the USNO corrections for this data sample actually moves the ensemble average farther away from UTC(USNO) by about a microsecond. From the tabulated standard deviations at the bottom of the plot, however,

it can be seen that applying the USNO corrections to the measurements does seem to reduce the standard deviation of the 10-pass averages by about 20%.

Dependence on Satellite Elevation Angle

The TRANSIT data were also analyzed for any correlation between the elevation angle of a pass and the scatter of the measurements. There was no significant correlation, which is probably not too surprising since the TRANSIT receiver automatically rejects any satellite pass corresponding to elevation angles of less than 10° .

Using TRANSIT Timing Signals to Control a Cesium Clock

Using the months of accumulated TRANSIT monitoring data as a starting point, one of the authors (JAB) developed a procedure for steering a cesium clock with the TRANSIT satellite signals in such a way as to realize a time accuracy of at least $20 \mu\text{s}$ at any time. The study involved (1) data analysis; (2) the development of computer models to simulate the performance of the satellite-receiver combination and cesium clocks; and (3) devising and testing different control algorithms using computer simulation.

The recommended algorithm is to use a TRANSIT timing receiver set to accept all TRANSIT satellites except #120. The receiver should be set to reject points in error by more than $150 \mu\text{s}$ and average for about one week. This should require averaging about 80 individual passes. Once per week an operator compares the cesium clock with the TRANSIT timing receiver output (i.e., the week's average) pulse using a time interval counter. If the ticks are within $\pm 10 \mu\text{s}$, the operator makes no changes. If the time difference exceeds the $\pm 10 \mu\text{s}$ tolerance, then the cesium clock

output is shifted exactly 10 μ s toward the output of the TRANSIT receiver. No use is made of the USNO published corrections.

While it is recognized that it is risky to extrapolate years into the future based on only six months of satellite data, still this data provides a reasonable basis to design a control algorithm. Assuming no deterioration in the operation of the satellites the models used should reasonably account for long-term trends in the clocks. The expected performance is an RMS time error of the cesium clock of about 7 μ s, with less than a 1% probability of exceeding \pm 20 μ s error relative to UTC. On the average, the cesium clock will be reset every two months.

TIME DISSEMINATION RESULTS VIA GOES

In contrast to TRANSIT with its 5 polar-orbiting satellites, the GOES system employs two operational geostationary satellites, backed-up by at least one in-orbit spare. The GOES satellites, designated GOES/East and GOES/West, are positioned over the equator at 75° and 135° W. longitude, respectively.⁽³⁾ From these locations they provide continuous coverage to most of the western hemisphere as indicated in Figure 14. Although their primary mission for NOAA involves the collection of large quantities of environmental data from many kinds of sensing platforms, the GOES signal format transmitted from satellite to Earth at 468 MHz also includes a digital time code generated and controlled by the National Bureau of Standards' equipment at the satellite control facility in Wallops Island, VA. In addition to complete time-of-year information referenced to NBS the transmitted code also contains satellite position predictions updated each 4 minutes, generated in Boulder from orbital elements supplied periodically

by NOAA and NASA tracking facilities. A two-way, dial-up telephone data link between Boulder and Wallops Island allows NBS to send updated position predictions and clock control commands to the automated system and to receive back on demand Loran-C and TV monitoring data and equipment status indicators.

Commercial GOES time code receivers are currently available in two basic versions, aimed at different accuracy levels. The more sophisticated type was used for most of the measurements being reported here. As in the TRANSIT case, it is microprocessor-based, enabling it to decode the satellite position data, compute the appropriate source-to-user path delay, and adjust its 1 pps output signal to be "on-time" with respect to the NBS-controlled atomic clock system at Wallops Island. Its base price is about \$4,000. A second receiver version used for some of the measurements ignores the satellite position data in the code and simply provides a time display and output timing signals usable at the ± 1 ms level at a cost of about \$2,000.

The GOES data to be discussed here resulted from monitoring the received timing signals in Boulder from both the GOES/East and GOES/West satellites, and recording the difference between the receiver 1 pps outputs and the UTC(NBS) time scale. During the full 8-month period occupied by the TRANSIT measurements, single measurements of UTC(NBS)-GOES/East and UTC(NBS)-GOES/West at a specified time each day were recorded. For a more limited 45-day period measurements of 1000-second averages were also recorded continuously from both satellites.

Medium-term (1000 seconds) GOES Performance

Figure 15 displays the 1000-second averages as received from GOES/East over a 45-day period. The Y-axis ranges from 0-1000 μ s so that essentially all of the several thousand data points - good and bad, can be included. (For comparison it should be kept in mind that the TRANSIT data plots discussed earlier excluded all outliers beyond $\pm 100 \mu$ s.) Figure 15 has at least 3 distinctive features. The first is the rather random sprinkling of outlier measurements with values mainly between the baseline at about 50 μ s and something like 500 μ s. At first it was assumed that these points correspond to offsets of the receiver 1 pps that occurred during periods of land-mobile radio interference in the local Boulder/Denver metropolitan area. Since the GOES frequency allocations near 468 MHz used for the NBS time code are coincident with communication frequencies assigned to the land-mobile service in the U.S., a significant potential for interference in large urban areas exists. During some such interference conditions our GOES timing receivers tended to go "out-of-lock" fairly often. According to the receiver manufacturer, however, such large offsets in the presence of noise are not normal and rather indicate a malfunction in the calculator circuitry which computes the path delay correction. Apparently this symptom has been observed on some other early models of this receiver. At least one of the NBS receivers with this symptom has been subsequently modified by the manufacturer with encouraging results.

The second distinctive feature of the plot in Figure 15 is the pronounced diurnal variations with an amplitude varying from nearly zero up to about 30 μ s. These variations are likely due to small imperfections either in the complex computer program used to compute the 4-minute updates of the satellite positions or in the

orbital elements. The changes in amplitude that obviously occur from time to time are generally correlated with new sets of position predictions and are believed to reflect the varying quality of satellite orbital elements supplied to NBS. The third noticeable feature of this plot is the generally flat trend of the GOES/East average baseline over the 45-day period in spite of the interference effects and orbital-element problems.

Figure 16 is the corresponding data for the GOES/West received time code. Again we see frequent outliers, diurnal variations which do not seem to be correlated with those on GOES/East, and a somewhat greater long-term variation amounting to about 50 μ s relative to UTC(NBS). Such variations are most likely due to imperfect orbital elements. Note the almost total absence of outliers during the first 10 days. Since the local interference conditions presumably weren't that much better, one possible explanation is that the receiver calculator circuitry was operating properly only during this period. In the next two figures an ARIMA-model filtering technique has been used to reject many of the obvious outliers and the remaining data points are plotted on an expanded 0 to 100 μ s scale. The GOES/East filtered data in Figure 17 show a fairly constant average value to within about 15 μ s over the 45 days. The GOES/West measurements in Figure 18 when filtered show about the same magnitude of diurnal variations but a larger systematic variation of the mean.

GOES Performance Averaged Over One Day

Figure 19 shows the improvement obtained by averaging the GOES/East filtered measurements over 1 day. The resulting daily means have a standard deviation of about 6 μ s.

Long-term GOES Performance

Figures 20-22 display some longer-term, once-per-day measurements during an 8-month period. Each point in this case is essentially just an instantaneous measurement of the receiver 1 pps vs. UTC(NBS) as recorded at 0000 UT each day. Such individual measurements are, of course, rather sensitive to local interference conditions. In the case of GOES/East (Figure 20) it's apparent that a shift of about 50 μ s in the mean value occurred sometime in April, 1979, but in general the average has been stable to within about \pm 50 μ s overall. Interestingly, the GOES/ West data in Figure 21 also shows about a 50 μ s shift at about the same time, and at present there is no clear explanation for this observation. As often seems to happen in such cases, an unrelated gap in the recorded data occurred at about that time that prevented pinpointing the shift more exactly. Aside from these few anomalies, however, the plots indicate that the long-term stability can be as good as \pm 10 μ s for many months.

Figure 22 is again based only on single, daily measurements of UTC(NBS)-GOES/West at 0000 UT. It differs from all the preceding ones in that these measurements are made with the simpler version GOES receiver that does not use the position information to compensate for path delay. Its output 1 pps rather fluctuates as the actual path delay changes due to various satellite motions. Note that the Y-axis in this case extends from 0 to 2 ms. The reason that the received signal ends up within 2 ms of UTC(NBS) even without any delay correction is that the time code as transmitted from Wallops Island is advanced by exactly 260 ms, which makes the signal arrive at the user's location nearly on time. This simpler receiver can provide a timing reference stable to a few tenths of a millisecond relative to a fixed mean delay bias that can be

calibrated out of the measurement. This bias for GOES/West is about 1.5 ms for the Boulder location. For many applications this level of accuracy may be sufficient and offers a reduced receiver cost of about \$2,000.

Recent Improvements in GOES Time Code Generation System

Very recently, the NBS time code generation and control equipment has been replaced with an upgraded system that provides the improvements listed in Figure 23. As a result, it can be expected that the GOES time code will be even more reliable in the future and will show improved stability relative to UTC(NBS), both at the transmitter and the receiver ends of the NBS-to-user-link. The preliminary data from the upgraded system suggests that the Wallops Island clocks can be maintained within a few microseconds of UTC(NBS) indefinitely.

CONCLUSION

To conclude, Figure 24 summarizes some of the more important advantages, as NBS sees them, of the TRANSIT and GOES time dissemination systems. The first group of advantages apply equally well to both these systems. In terms of long-term continuity it may be worth noting that new, improved TRANSIT and GOES satellites are scheduled for launch during the next year and there is every indication that both systems will be around for many years. In addition to these general advantages each system offers some special, more-unique features. For TRANSIT the coverage from the polar-orbiting satellites is global, clearly of great importance for some applications. Because the TRANSIT signals operate at different frequencies than GOES, they are not subject to the land-mobile interference problems. Based on the 8 months of data

monitored at NBS, received TRANSIT signals, when averaged over an appropriate satellite constellation, can provide a highly-accurate local time reference with respect to UTC(USNO) at the better-than-25 μ s level. Finally, the use of 5 operational satellites provides excellent service reliability. In the case of the GOES time code coverage is only hemispheric rather than global, but the signals are available continuously within this area. The code provides complete time-of-year information at two different accuracy levels, so that users have an option to accept lower accuracy with a cost savings of several thousand dollars per receiver. Even the full-accuracy user can find GOES highly cost-effective at a receiver cost of less than \$5,000.

REFERENCES

1. Theodore D. Finsod, "Transit Satellite System Timing Capabilities", Proc. 10th Annual PTTI Applications and Planning Meeting (Washington, D.C.), November 1978, pp. 511-537.
2. G. A. Hunt and R. E. Cashion, "A Transit Satellite Tuning Receiver", Proc. 9th Annual PTTI Applications and Planning Meeting (Washington, D.C.), March 1978, pp. 153-167.
3. D. W. Hanson, D. D. Davis, and J. V. Cateora, "NBS Time to the Western Hemisphere by Satellite", Radio Science, Vol 14, No. 4, July-August, 1979, pp. 731-740.

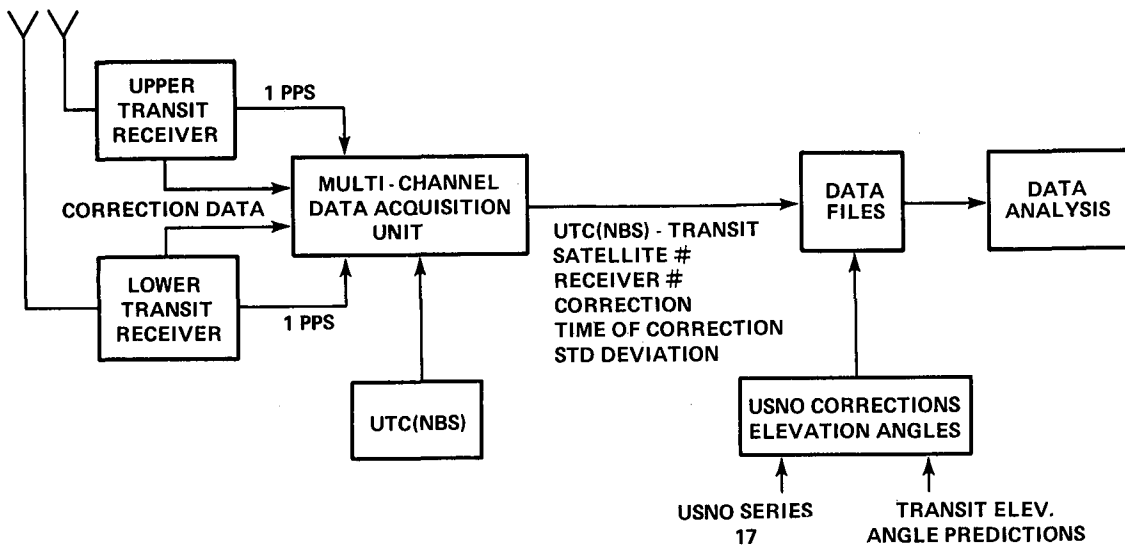


Figure 1. Block Diagram of Transit Monitoring System

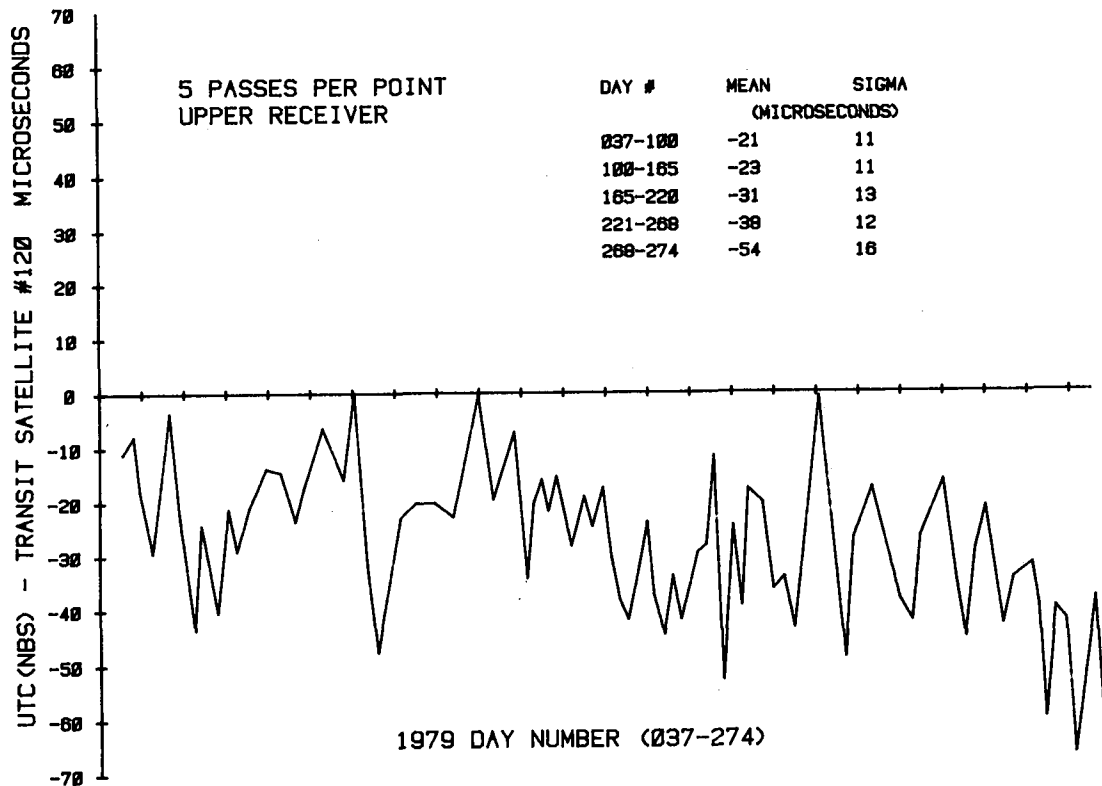


Figure 2. UTC (NBS) - Transit Satellite #120

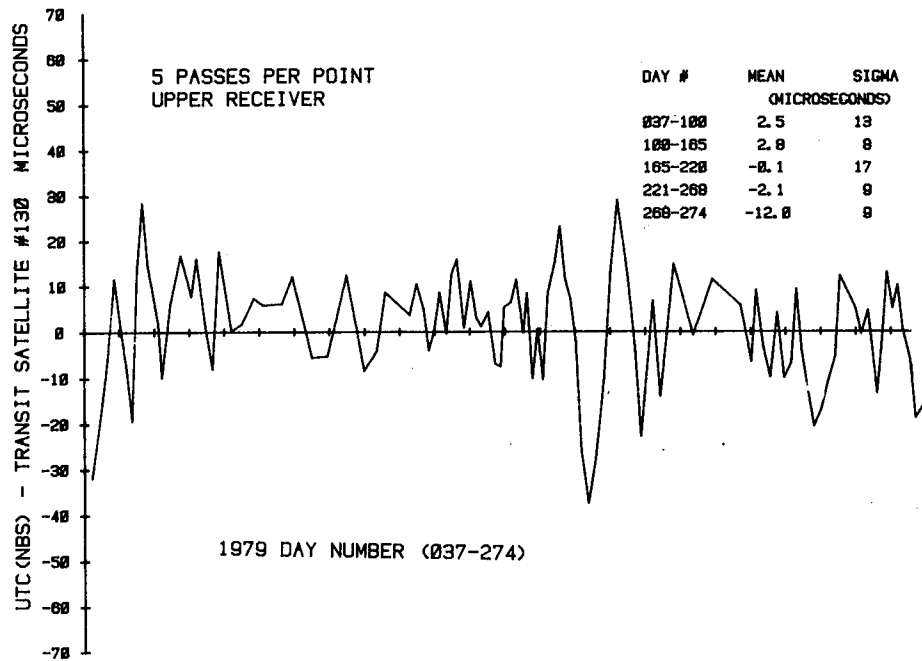


Figure 3. UTC (NBS) - Transit Satellite #130

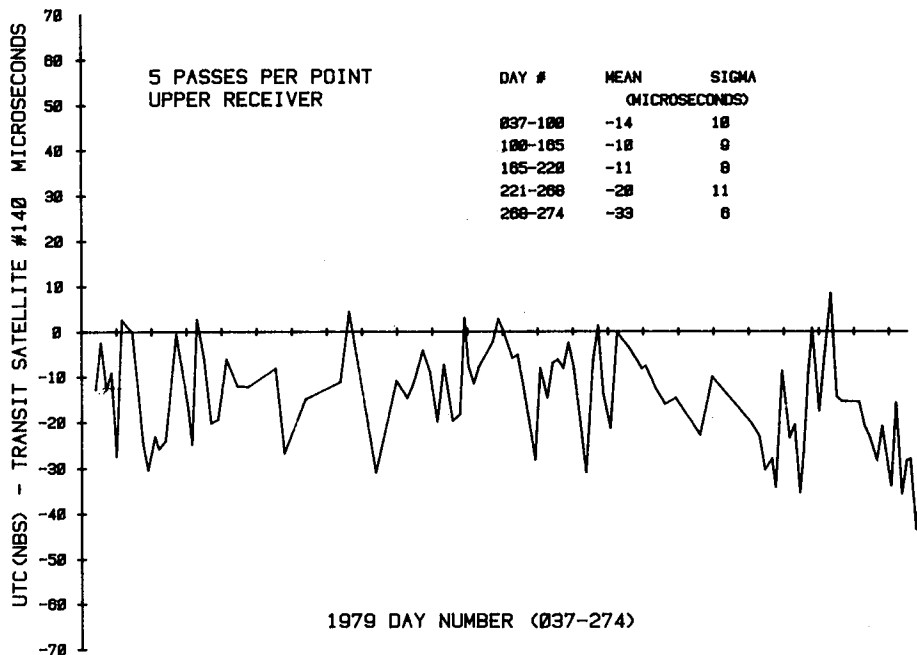


Figure 4. UTC (NBS) - Transit Satellite #140

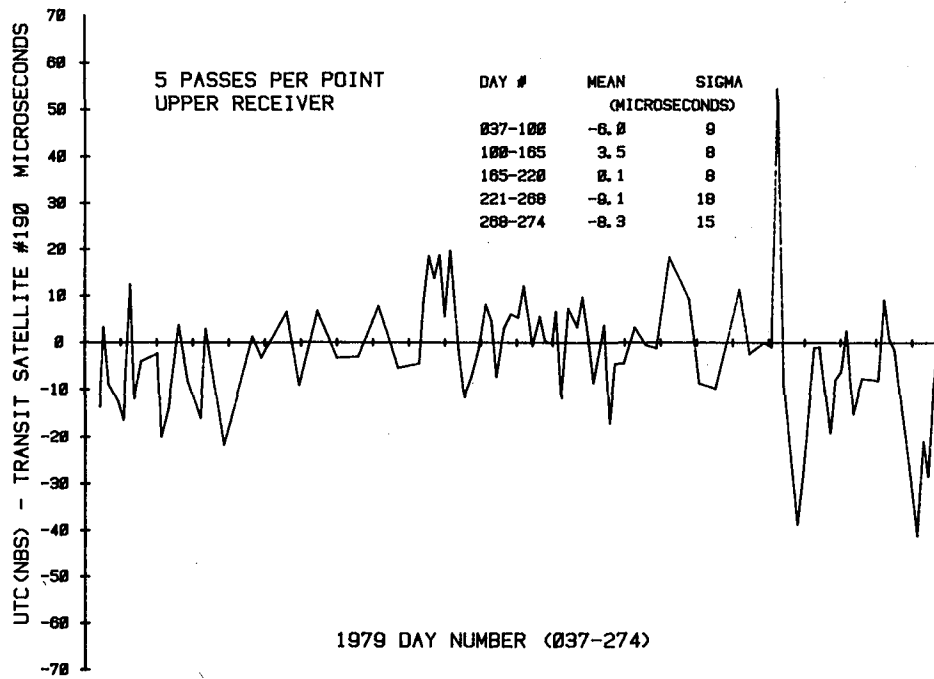


Figure 5. UTC (NBS) - Transit Satellite #190

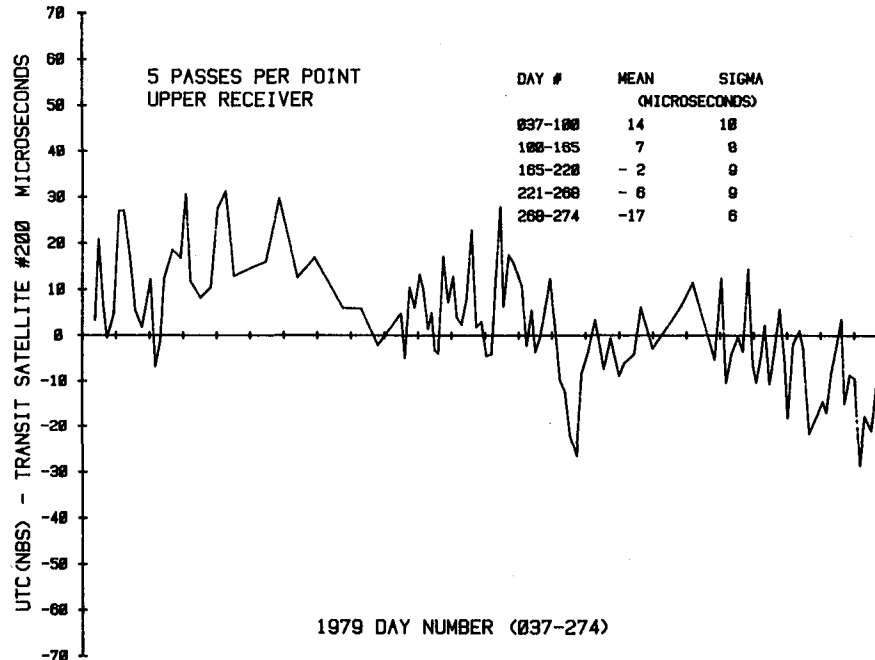


Figure 6. UTC (NBS) - Transit Satellite #200

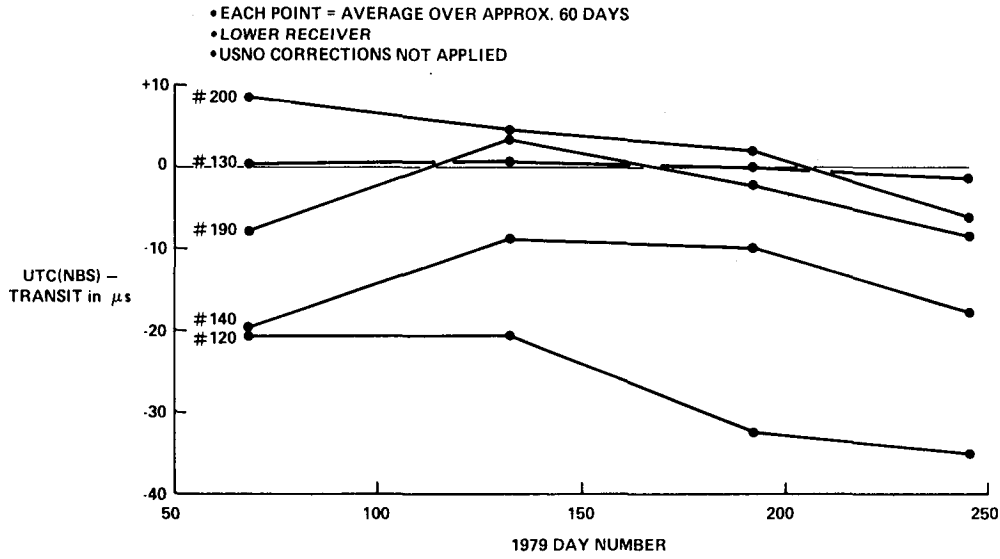


Figure 7. UTC (NBS) - Transit for Individual Satellites

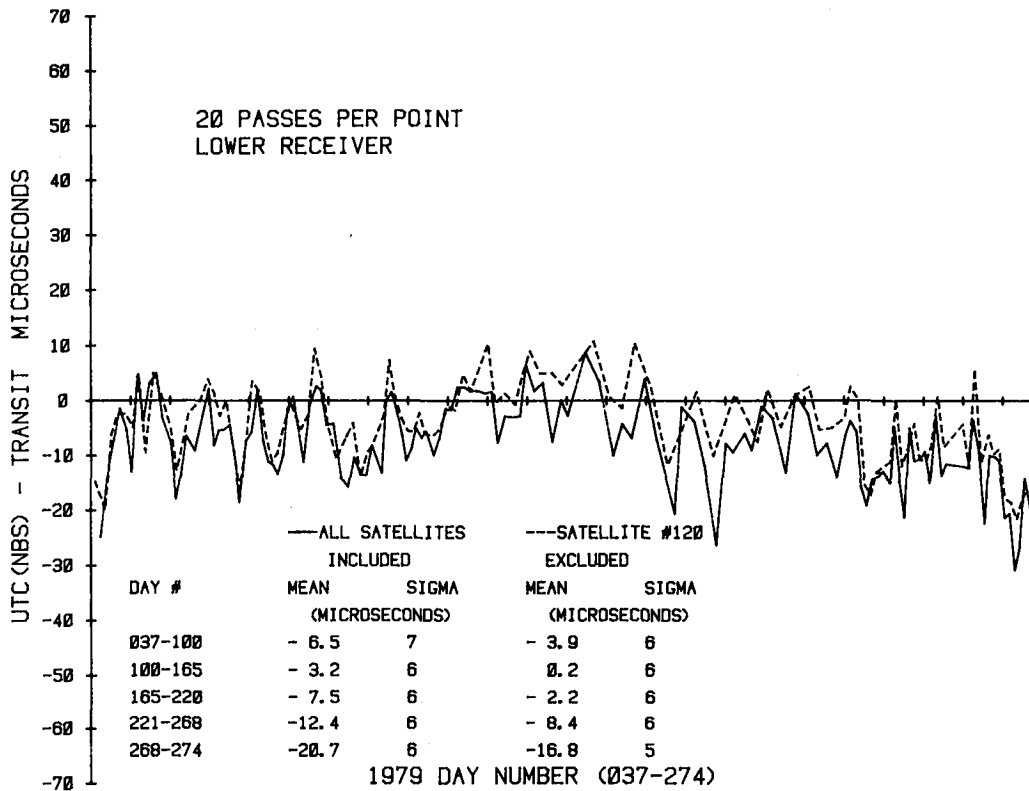


Figure 8. Effect of Deleting Satellite #120 from Ensemble

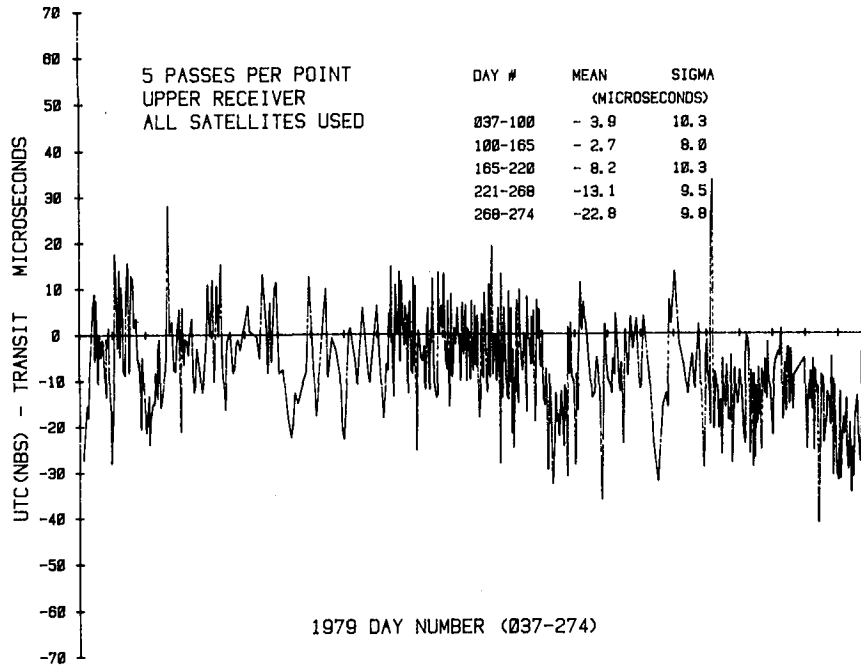


Figure 9. UTC (NBS) - Transit

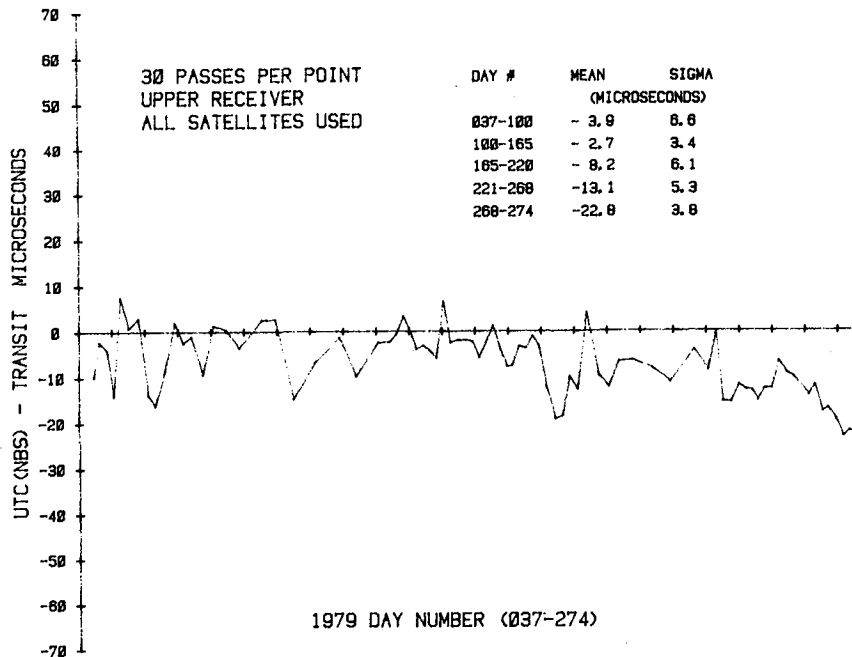


Figure 10. UTC (NBS) - Transit

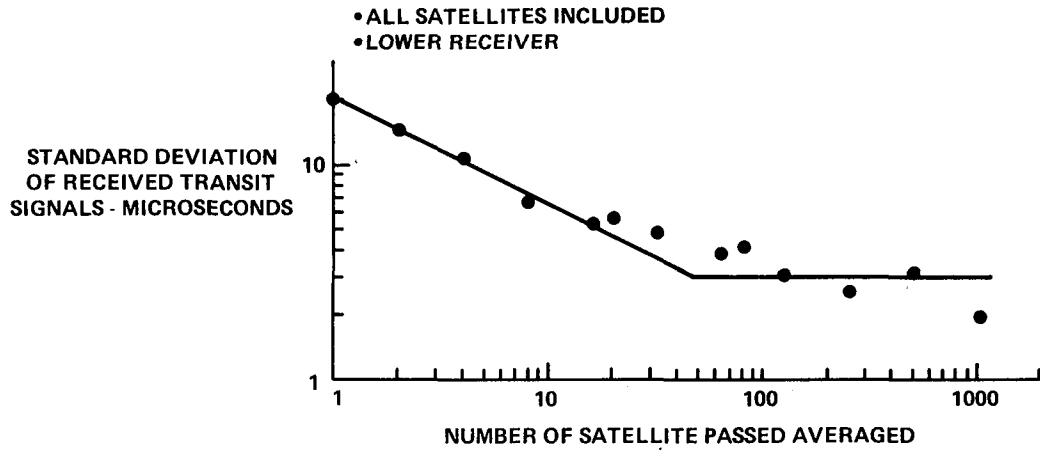


Figure 11. Standard Deviation of Received Transit Signals vs. Number of Satellite Passes Averaged

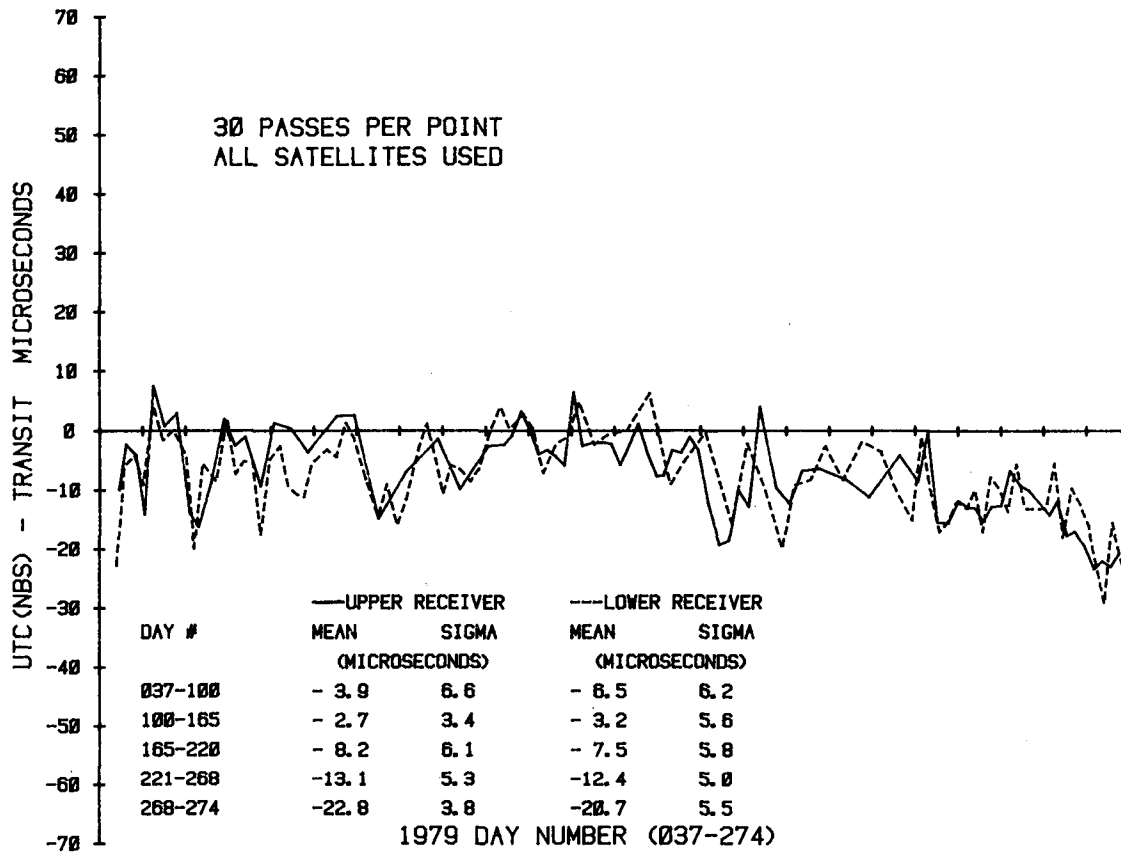


Figure 12. UTC (NBS) - Transit for Two Different Receivers

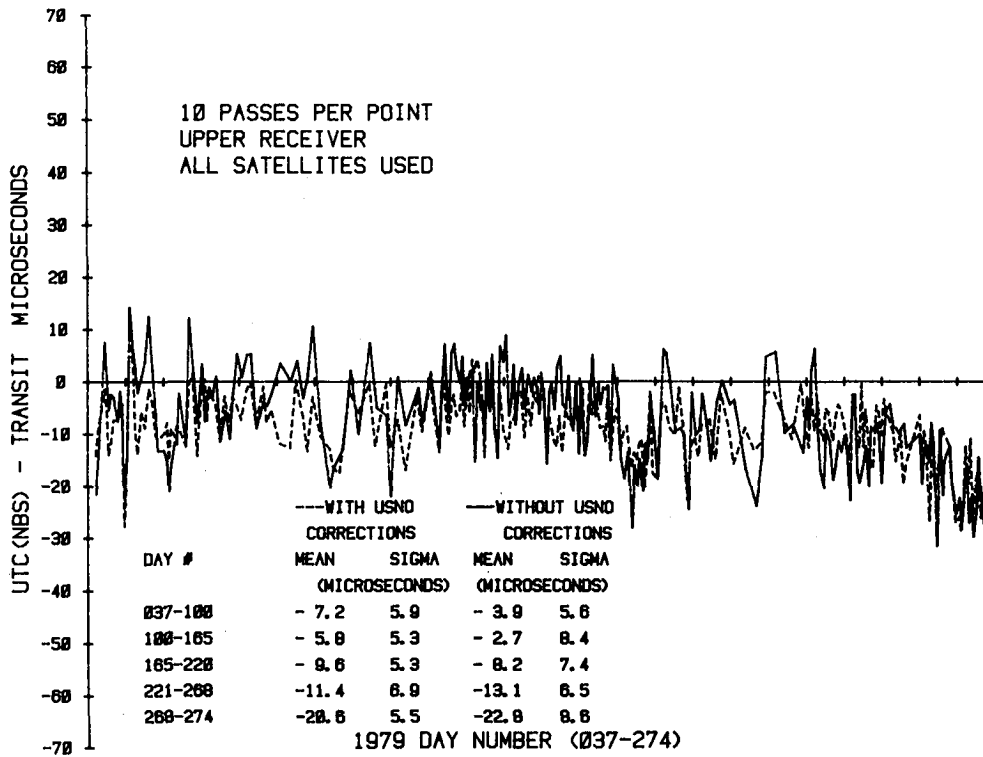


Figure 13. Comparison of Received Transit Data With and Without Additional USNO Corrections

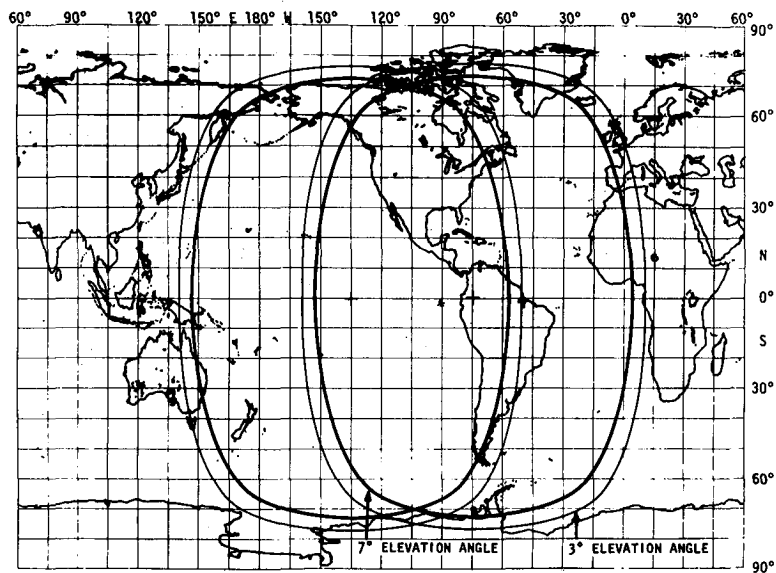


Figure 14. Coverage Areas for GOES/East and GOES/West Satellites

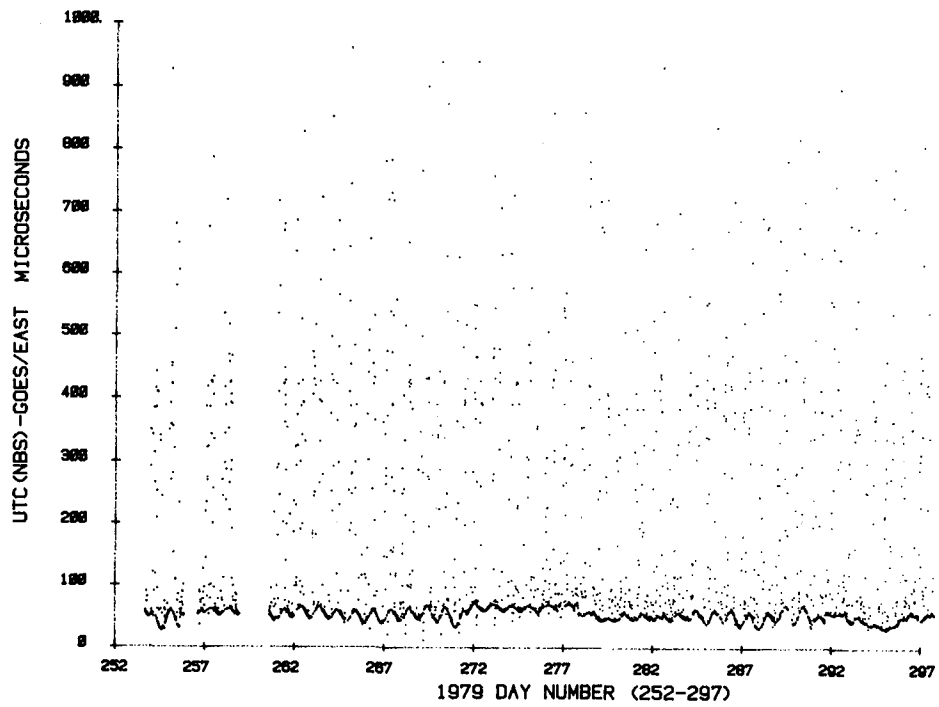


Figure 15. UTC (NBS) - GOES/East: 1000-Second Averages

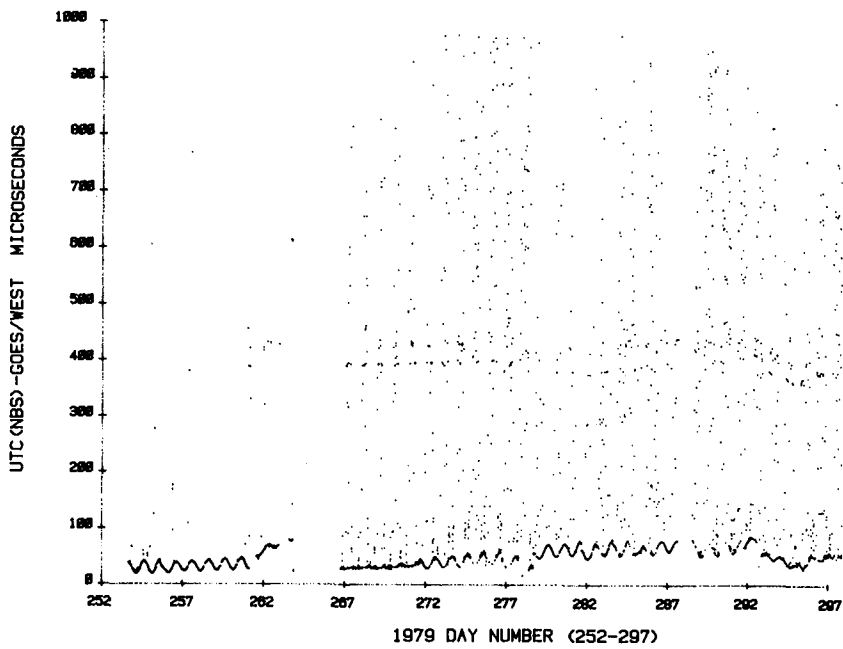


Figure 16. UTC (NBS) - GOES/West: 1000-Second Averages

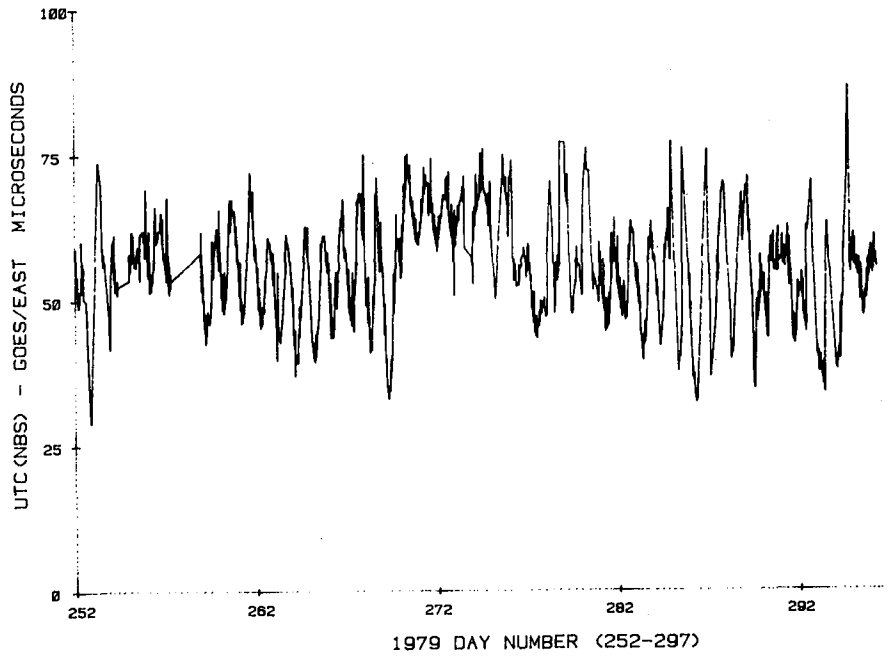


Figure 17. UTC (NBS) - GOES/East: 1000-Second Filtered Averages

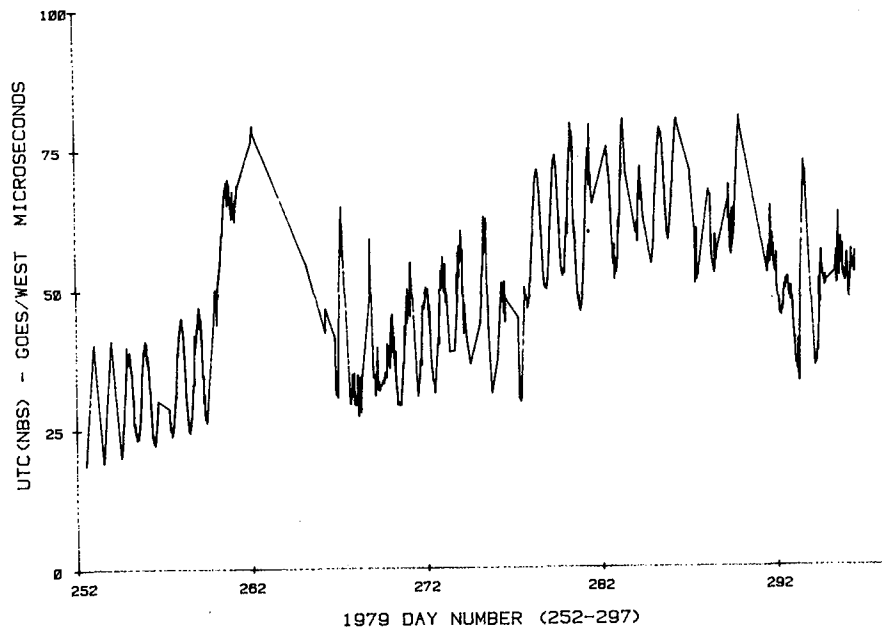


Figure 18. UTC (NBS) - GOES/West: 1000-Second Filtered Averages

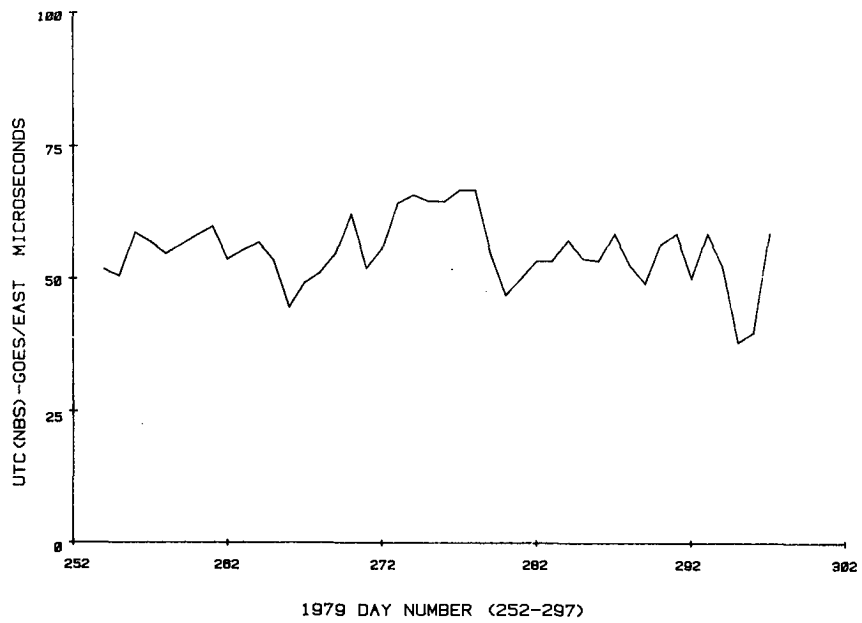


Figure 19. UTC (NBS) - GOES/East: Filtered Daily Averages

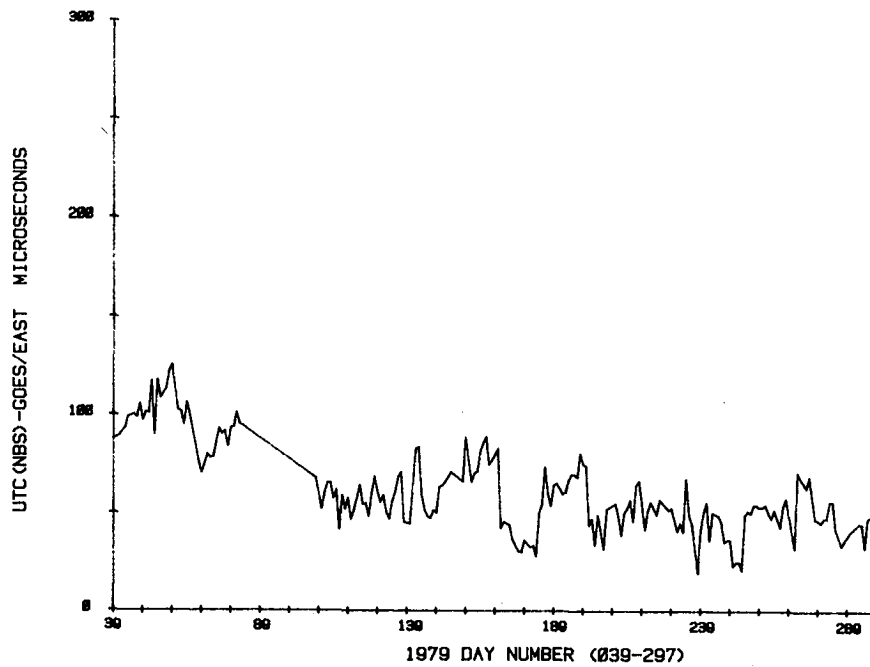


Figure 20. UTC (NBS) - GOES/East: Single Daily Measurements at 0000UT

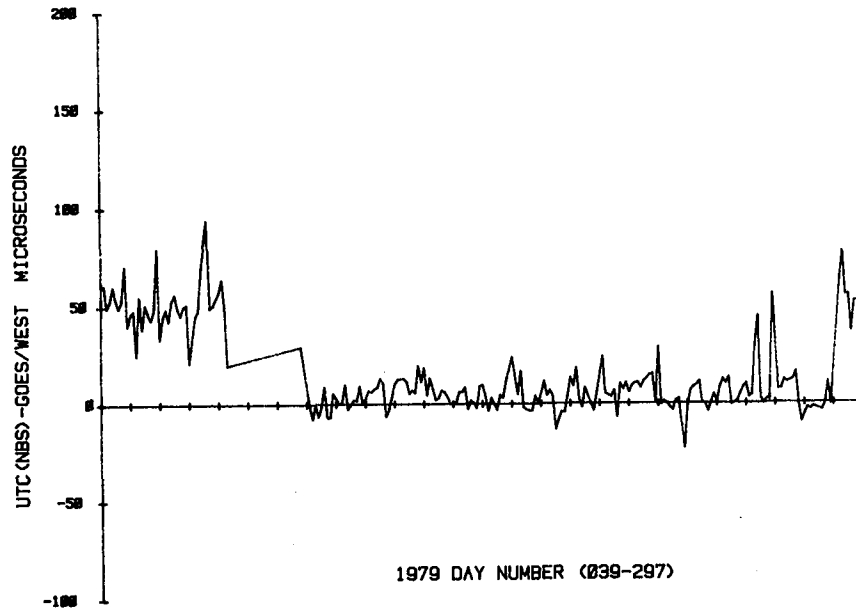


Figure 21. UTC (NBS) - GOES/West: Single Daily Measurements at 0000UT

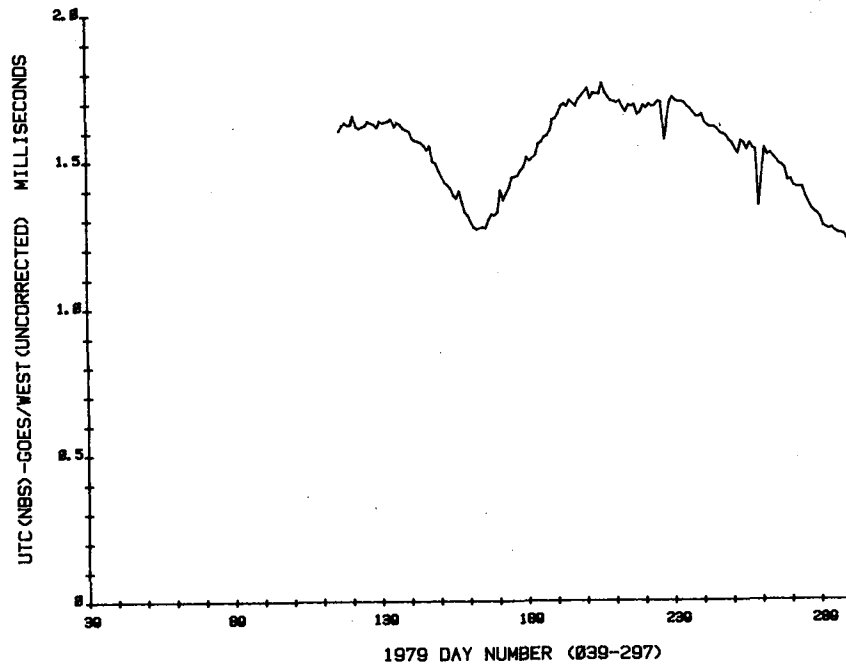


Figure 22. UTC (NBS) - GOES/West (Uncorrected for Path Delay): Single Daily Measurements at 0000UT

**GOES TIME CODE SYSTEM IMPROVEMENTS
AT WALLOPS ISLAND, VA**

- **SATELLITE - POSITION PREDICTIONS UPDATED EACH 4 MINUTES**
- **TRIPLE - REDUNDANCY TIME - CODE - GENERATION SYSTEM**
- **HIGHER RESOLUTION POSITION PREDICTIONS**
- **IMPROVED MONITORING CAPABILITIES**
- **COMPLETE SYSTEM STATUS AVAILABLE ON DEMAND TO
NBS/BOULDER VIA DIAL - UP LINK**
- **CAPABILITY FOR IMPROVED CONTROL OF CLOCKS**

Figure 23

ADVANTAGES APPLICABLE TO BOTH TRANSIT & GOES

- **RELIABLE TIME SIGNALS**
- **PROVIDES 100 μ s - OR - BETTER LINK TO USNO & NBS**
- **EXTENSIVE COVERAGE AREAS**
- **LONG - TERM CONTINUITY**
- **AUTOMATIC COMMERCIAL RECEIVERS AVAILABLE**
- **MINIMAL ANTENNA REQUIREMENTS**

SPECIAL ADVANTAGES : TRANSIT

- **GLOBAL COVERAGE**
- **INSENSITIVE TO LAND - MOBILE INTERFERENCE**
- **CAN PROVIDE <25 μ s LINK TO USNO**
- **FIVE OPERATIONAL SATELLITES**

SPECIAL ADVANTAGES : GOES

- **CONTINUOUS AVAILABILITY IN COVERAGE AREA**
- **COMPLETE TIME - OF - YEAR INFORMATION**
- **RECEIVER COST <\$ 5,000**
- **\pm 1 MS OPTION AVAILABLE FOR <\$ 2,000**

Figure 24

QUESTIONS AND ANSWERS

DR. LESCHIUTTA:

The paper is open to discussion, but before I open the discussion I would like to make a remark that in the European Space Agency there is a satellite named METEOSAT. This satellite is making basically the same work as the GOES satellite and there are some work in order to see if it could be possible to include a code very similar to the code of GOES satellite in one of the channels of the METEOSAT satellite. This is just as a general remark.

DR. GILLES MISSOUT, Quebec-Hydro

I have some comments about your measurement on GOES satellite. We have three clocks from one year ago now and also one improved model and we observed the same trouble as you and after receiving the new model we have the same trouble and we opened the black box and made measurement on it and we found most of the problem related to the RF filter, which has a rejection of only 50 dB instead of 90 dB we found on most mobile radios, commercial models. And we observed, by example, in Montreal, each time the signal from any radio mobile, even one or two megahertz apart comes with a value higher by 50 dB of the signal, the receiver saturates and doesn't work.

DR. BEEHLER:

Thank you very much. This is very interesting.

DR. MISSOUT:

One other point. We are waiting for a special filter having 90 dB, to install it and see what happens.

MR. RUEGER, APL/JHU

I wanted to compliment Roger Beehler on such a very thorough examination of the TRANSIT program for timing. I do want to point out to the rest of the audience that the specifications and requirements on that program start out at around a 10 millisecond requirement and we were so much better than the requirements that these applications are now possible.

As a matter of fact, about one year ago, the requirements on the system were altered so that it is now required to keep the TRANSIT satellite time within 200 microseconds of UTC. And with this effort and the new commercial receivers we expect to try

harder to keep the satellites still nearer to UTC time. They are ground controllable, so that some of the time excursions indicated were a part of the process of how the control is performed. In loading the satellite each 12 hours in the uploading cycle, if the loading is unsuccessful, we have a little quirk in the current satellites that they will put an extra 10 microseconds in their time error each time an extra load is attempted to get error-free uploads. This is why you will see these up and down excursions in quantas of 10 microseconds.

But I do believe the receivers, that you are evaluating do have time resolution limitations of about 7 microseconds because they are looking at a signal with a modulation rate of 50 Hz.

Thank you.

DR. BEEHLER:

Dr. Winkler?

DR. WINKLER:

I would also like to make some comments because in contrast to the GOES, which is more or less entirely under your control and where corrections can be introduced simply, the case with TRANSIT is exactly the opposite. It is a very large system and this brings me to the question of the corrections which are being published in Series-17, and the comment is prompted by the very poor correlation of the corrections which we publish and your observations at a different site.

Now, the corrections which we publish are not based on any measurements made at the Observatory as Series-17 says at the top. They are data which we receive from NAVASTROGRU, and I think on the basis of your investigations and also on the basis of what Ken Putkovich already has mentioned, I would like to tentatively say that maybe we should discontinue these Series-17s altogether. I think an improvement of some 20 percent in this caper is not worthwhile to go to the trouble. Really what that reflects is the correlation between what is the total set of monitor sets, all four monitor sets together, see, with what you see at a different time of day. And that correlation is very poor.

I think, however, that it may be more useful to the users to replace the present Series-17 with what Ken has mentioned with measurements, selected measurements, maybe only on the basis of the satellites, made in Washington and possibly at other sites. I think the correlations between these observations would probably

be greater. Would you have any comments to this proposal, to do away with the present Series-17 altogether, and instead, publishing measurements which are made at NAVOBS and possibly one other site for selected satellites at some given standard time of day?

DR. BEEHLER:

Well that certainly makes much sense to me. I think the thing to focus on, at least as a result of our data, is that even without these corrections and using a constellation that is averaging over more than one satellite, you certainly treat it as a black box and come out with a time reference that is very, very close to UTC/USNO, so I certainly think that would be a step forward.

MR. RUEGER:

I would like to respond a bit to the correction problem. Roger, did you, in the using of the data corrections of Bulletin-17, interpolate linearly or some other means between the times you observed and the times the corrections were applied?

DR. BEEHLER:

Yes, it was simply a linear interpolation.

MR. RUEGER:

I do want to point out that the time at which the Boulder Laboratory can see the satellites is the poorest in the cycle of the renewal of time in the satellite. It is just before we reinject or at about the time of reinjection of the satellite and this is the poorest place in the world so maybe your data are on the pessimistic side of actual performance.

DR. BEEHLER:

To each his own.

SESSION IV

DISSEMINATION SYSTEMS II

**Charles A. Bartholomew, Chairman
Naval Research Laboratory**

T & F COMPARISONS VIA BROADCASTING SATELLITE
AND NAVIGATION TECHNOLOGY SATELLITE

Y. Saburi, Y. Yasuda, S. Kobayashi and T. Sato

Radio Research Laboratoires
Koganei, Tokyo 184, Japan

ABSTRACT

The paper describes the results of a preliminary experiment of T/F dissemination via the Medium-Scale Broadcasting Satellite for Experimental Purposes (BSE) and those of the international time transfer experiment via the Navigation Technology Satellite (NTS-1).

(1) The preliminary T/F dissemination experiments have been made using the BSE, which has the down-link of 12 GHz and the up-link of 14 GHz. The measured short-term stability of the received TV sub-carrier frequency is as good as in the terrestrial TV broadcasting, e.g., $\sigma_y(10 \text{ sec}) = 3 \times 10^{-11}$. In order to establish the technique of the doppler shift canceling, the phase control servo including the satellite link, the pre-compensating frequency control using the measured values or using the orbital data of the satellite are tested. The amount of the residual doppler shift at the control station can be reduced to the order of 1 part in 10^{12} or less by use of the first and the second methods. The method using the orbit data is expected to give a control capability of a few parts in 10^{11} . Thus, the maximum value of the doppler shift at the farther-most place of the country is estimated to be $\pm 2 \times 10^{-10}$ without any correction. As to the time comparison, the experiment is now proceeding.

(2) The experiment of the international time comparison via the NTS-1 had been made for about one year since October 1978, by the support of the GSFC of NASA and the NRL. The data of time difference between UTC(USNO) and UTC(RRL) are in good agreement with those via the portable clock of the USNO. By applying the correction for ionospheric delay using the model developed by Bent, the standard deviation of the data can be reduced to about one-half.

1. T/F dissemination via broadcasting satellite

The sub-carrier frequency and the synchronizing pulses in the terrestrial TV broadcasting have been widely used for precise T/F comparisons for more than ten years. But the change of the delay time has been occasionally observed in the time comparison between two places remotely located from each other, because of the changes of the relay route, the repeater and the transmitter characteristics and others. This difficulty will be removed by use of a broadcasting geostationary satellite, because uniform high accuracy in the time comparison can be expected all over the service area, if the variation of the propagation time mostly due to that of satellite position around the geostationary orbit-Doppler effect can be precisely estimated and controlled [1].

Plan of T/F dissemination via BSE

The Medium-Scale Broadcasting Satellite for Experimental Purpose (BSE) was launched in April, 1978 to obtain the technical data necessary for establishing the future operational domestic satellite broadcasting system. The data of BSE spacecraft and the link budget (typical measured values) are given in Tables 1 and 2, respectively [2]. The satellite antenna has a suitable radiation pattern for providing high quality color TV broadcasting services to the whole Japan territory. Fig. 1 shows the BSE antenna radiation pattern (see Table 2) and places relevant to the plan of T/F dissemination. The value of 41.2 dB of the SN ratio in Table 2 corresponds to the TV picture quality of "Grade 4 (Good)" in the "5-grade assessment", which has been confirmed by the field tests with the receiving antenna of 1.6 m in diameter and a simple frequency converter (12 GHz to UHF). The tests with the receiving antennas of 0.75m and 1m in diameter have been made, too, showing the values of the "Grade" between "3 (Fair)" and "4", which correspond to comparatively high values of field intensity (approximately between 45 and 60 dB, 0 dB=1 μ V/m) in the terrestrial TV broadcasting. Thus the T/F comparison can be made by just adding the small size receiving antenna, whose diameter is 1 meter or less, and the simple frequency converter to the apparatus for the comparison via the terrestrial broadcasting.

To establish the technique of controlling the doppler effect and then to evaluate the accuracy of T/F dissemination, a countrywide experiment using BSE is planning to be made in 1980. At the RRL Headquarters in Koganei, the received sub-carrier and the pulse are measured with respect to the RRL master clock. The measured difference in time and frequency is the amount of control to be applied to the TV signals being transmitted from the transmitting station at Kashima to the BSE satellite. Thus the time as well as frequency of the subcarrier and synchronizing pulses are made synchronized with the UTC(RRL) as received in Koganei and its vicinity.

A transportable receiving station and a few simple receiving stations remotely located from Tokyo area are supposed to make the frequency/time measurement of the received subcarrier and synchronizing pulses with respect to their own cesium clocks.

Besides, a time transfer experiment has been planned, where displays of the standard time will be obtained by use of the time code inserted in the vertical blanking intervals of the TV signals.

Results of preliminary experiment

(a) Frequency stability as received: The short-term frequency stability of the received color subcarrier from the BSE is given in Fig. 2. The measurement was made on the output signal of 3.58 MHz from the TV synchronizing generator with the composite video signal from the simple receiving system with an antenna of 1 meter in diameter. As seen in the Figure, the values of $3 \sim 4 \times 10^{-11}$ and about 4×10^{-12} are obtained for the averaging times of 10 and 100 sec. respectively, which enables general users to make precise frequency calibration in a short time. The values of $\sigma_y(\tau)$ are a little better than those in a terrestrial TV broadcasting, the field strength of which is as high as 70 dB, which fact can be well understood from the foregoing discussion on the TV signal quality.

(b) Doppler shift; In order to enable the frequency calibration to be very accurate, it is essential to minimize the doppler shift. So the measurement of the doppler shift of the received color subcarrier from BSE was made at Koganei, using rubidium and cesium standards at Kashima and Koganei, respectively, which were synchronized in frequency to 1×10^{-12} via terrestrial TV signals.

An example of results of the measurement is shown in Fig. 3. Curve a gives measured doppler values at Koganei (dots), together with calculated ones at Kashima (solid line), by use of the predicted values of the satellite orbit. The doppler shift amounts to about $\pm 1 \times 10^{-8}$ before the maneuver and decreases to $\pm 2 \times 10^{-9}$ after it. The curves b and c show respectively the values of doppler shift, relative to the value at Kashima, at Wakkanai and Okinawa, the farther-most locations in the country (Fig. 1). These two curves show the amounts of variation of $\pm 2 \times 10^{-10}$, which means that it is possible to distribute standard frequency with the accuracy better than $\pm 2 \times 10^{-10}$ everywhere in the country without any correction if the transmitted frequency is controlled so as to cancel the doppler shift as received in Tokyo area.

In order to cancel the doppler shift, the following three methods were tested:

- (1) phase control servo including the satellite link,
- (2) pre-compensating frequency control using the measured values,

(3) pre-compensating frequency control using the orbital data.

Fig. 4 shows the block diagram of the experiments for these methods. In the first method, the phase-locked loop of the first order consists of the transmitter, the receiver, the BSE satellite and the VCXO. In the second and third methods, a calculator-controlled phase shifter pre-compensates the sub-carrier frequency to be transmitted by an amount of the estimated doppler shift using either the orbital data or the measured values. The phase recordings of the transmitted and the received sub-carrier are made on Recorder Nos. 1 and 2, respectively, with reference to the cesium frequency standard.

(c) Results of phase control servo; An example of the results on the first method are given in Fig. 5. As shown in Fig. 5 (a), the frequency departure of the transmitted sub-carrier, which is almost the same as the inverse of the satellite doppler shift, showed abnormally large values of about $\pm 1 \times 10^{-8}$, because the routine maneuver could not be done at an appropriate opportunity by some reasons. In fact, the doppler shift was reduced to within $\pm 2 \times 10^{-9}$ by the maneuver made a few-days after that time. Fig. 5 (b) shows the doppler shift measured at Koganei in the same period of Fig. 5 (a) when the phase-locked loop was closed at the Kashima transmitting station. The peak values are a few parts in 10^{11} , even in such an unfavorable condition of the satellite position control. The phase record of received sub-carrier with respect to the cesium standard at Kashima station is given in Fig. 5 (c), in addition to that of 100 kHz signal, which is coherent to the transmitted sub-carrier. The maximum value of the residual frequency error in this case can be estimated to be 2×10^{-13} , taking account of the maximum rate of frequency change of about $7 \times 10^{-13}/\text{sec.}$ in Fig. 5 (a) and the round trip delay of about 0.3 sec. via the satellite. In so far as seen on the record of 3.58 MHz, no phase variations larger than 3 ns could be observed.

(d) Result of pre-compensating control using measured values; The frequency measurements of the received sub-carrier are made at the transmitting station every 100 seconds. The fittings of polynomial of the second-order are made successively, each time using the past 20 data. The extrapolated value followed by the last measurement is used as the mean offset frequency to be transmitted for the next 100 seconds. The plot of Fig. 6 (a) shows the frequency departure of the transmitted frequency for 18 hours. Fig. 6 (b) shows the difference between the measured and the predicted values, of which standard deviation and mean value are 4.6×10^{-12} and -4.7×10^{-14} , respectively. The value of standard deviation is almost the same as that of short term stability of $\sigma_y(100 \text{ sec.}) = 4 \times 10^{-12}$ shown in Fig. 2, which means that the precision of the prediction in frequency is nearly limited by the short-term instability of the received signals. Fig. 6 (c) shows an example of the phase records of the received sub-carrier frequency and the transmitted frequency with respect to the Cs standard. The very small ripple on the

record of 3.58 MHz is due to the difference between the mean offset values and the instantaneous doppler frequency change, and this can be easily reduced, if necessary, by shortening the offset period. The small amounts of drift and variation may be the integrated phase errors due to the frequency instability of received signal and the predicted value.

(e) Pre-compensating frequency control using orbital data; To make certain the accuracy of prediction of the doppler shift in the third method using the orbital data of the BSE, the frequency comparison was made between the sub-carrier received at Koganei and the computer-controlled sub-carrier which is offsetted by the predicted doppler shift obtained from the orbit calculation taking account of the solar light pressure. The observed difference was within $\pm 3 \times 10^{-11}$ for the period of one day.

2. International time comparison via NTS-1

The time comparison experiment via NTS-1 has been made at the RRL for about one year since October, 1978. The measurements were made with respect to UTC(RRL) by use of Time Transfer Receiver developed by the NASA. The weekly and final values of the time difference between the USNO and the RRL, UTC(USNO)-UTC(RRL), were calculated by the NRL.

The precision and accuracy of the result was almost the same as those reported at the past PTTI meetings by the NRL and other institutes. It is thought, however, that a fairly large effect of the ionospheric delay may be included in the data, because the measurements for this period were made only at the carrier frequency of 335 MHz. As it is difficult to know the actual total electron content at the time of every measurement, the corrections of the ionospheric delay to the measurements both at the NRL and the RRL is examined using the first-order algorithm [4].

In this algorithm, the average monthly diurnal change of time delay at any location, as a function of local time of day, has been represented by a simple positive cosine wave dependence for day time, with an additional constant term for night time. The amplitude, phase and period of cosine model and the constant term are the functions of geomagnetic latitude, season and solar activity.

An example of application of this algorithm is shown in Fig. 7 for 4 months from January to April, 1979. Fig. 7 (a) shows the final data calculated by the NRL, of which standard deviation from the fitting line is 0.53 μ s. Fig. 7 (b) shows the corrected data for ionospheric time delay calculated by the algorithm, of which standard deviation is 0.34 μ s. Thus fairly good improvement of the result was made in precision, and also in accuracy with respect to the USNO portable clock data.

Conclusion

The preliminary experiments mainly for precision frequency distribution via the BSE satellite were made and some techniques of the doppler shift compensating methods were studied. The results showed that the doppler shift at one point can be canceled to the order of 10^{-12} . The experiments for time dissemination is now being planned to be held in 1980.

Acknowledgements

The authors wish to thank C. Wardrip and J. Perry of NASA Goddard Space Flight Center and J. Buisson and Dr. J. Oaks of Naval Research Laboratory and G. Whitworth of Applied Physics Laboratory, JHU for their valuable suggestions and support in the NTS experiment. They also wish to thank Y. Saito, M. Imae, H. Okazawa, T. Ito, and M. Aida for their work and interest in the BSE and the NTS experiment. They are very grateful to the staffs of BSE project in the RRL Headquarters and Kashima Branch.

References

- [1]. F. Takahashi, "A proposal of accurate time dissemination using TV signals from a broadcasting satellite", J. Radio Res. Labs. Vol.23, No. 112, pp 267-283. November 1976.
- [2]. M. Imai, S. Sonoda and Y. Ichikawa, "Experiment Results of Japanese BSE Program in the first year", AIAA (American Institute of Aeronautics and Astronautics) Journal 1980 (to be published).
- [3]. K. Tsukamoto, M. Kajikawa, S. Uchikado, M. Yokoyama, and T. Tanaka, "Main Transmit and Receive Station of BSE Program", Proc. 12th International Symposium on Space Technology and Science, pp 673-678, Tokyo, 1977.
- [4]. J. A. Klobuchar, "A first-order, world-wide, ionospheric time-delay algorithm", Tech. Rep. 75-0502 Air Force Cambridge Research Laboratories Bedford Mass. 1975.

Table 1 BSE Spacecraft Summary

1. Satellite location	110°E ($\pm 0.1^\circ$) on geostationary orbit
2. Life	3 years
3. Physical configuration	Rectangular solid (box type) with deployable solar array panel) Width 1.3 m Height 3.1 m Length 9.0 m (including deployed solar array panel)
4. Weight	350 kg (at the beginning of life on geostationary orbit)
5. Electrical power source of solar panel	780 W (at the end of life)
6. Size of solar array panel	1.5m x 3m (two sheets)
7. Attitude stabilization	Zero-momentum 3-axis stabilization using three momentum wheels
8. Communications	
Frequency	Receiving (up link) : 14 GHz Transmitting (down link) : 12 GHz
Capacity	Two FM color TV channels (Bandwidth : 25 MHz each)
Output power	100 watts/channel

Table 2 BSE Link budget

Up-link (Main Station)				
Main Station E.I.R.P.	(dBm/ch)			112.2
Free Space loss	(dB)			-207.4
Rx. antenna gain	(dB)			38.1
Noise Power	(dBm/25 MHz)			-92.9
Up-link C/N	(dB)			35.8
Down-link				
Service area		Main station	Mainland	Remote islands
Antenna of Rx.	(m)	13.0	1.6	4.5
Tx. power	(dBm/ch)		50.0	
Tx. feeder loss	(dB)		-1.7	
Tx. antenna gain	(dB)	37.6	37.0	28.0
Free space loss	(dB)	-205.9	-205.8	-205.4
Rx. antenna gain	(dB)	61.9	43.0	53.5
Rcvd carrier power	(dBm)	-58.1	-77.5	-75.6
Noise power	(dBm/25 MHz)	-96.4	-97.3	-96.6
Down-link C/N	(dB)	38.3	19.8	21.0
Total C/N	(dB)	33.9	19.7	20.9
TV signal quality				
FM improvement factor	(dB)		18.6	
Emphasis improvement factor	(dB)		2.9	
Unweighted S/N	(dB)	55.4	41.2	42.4

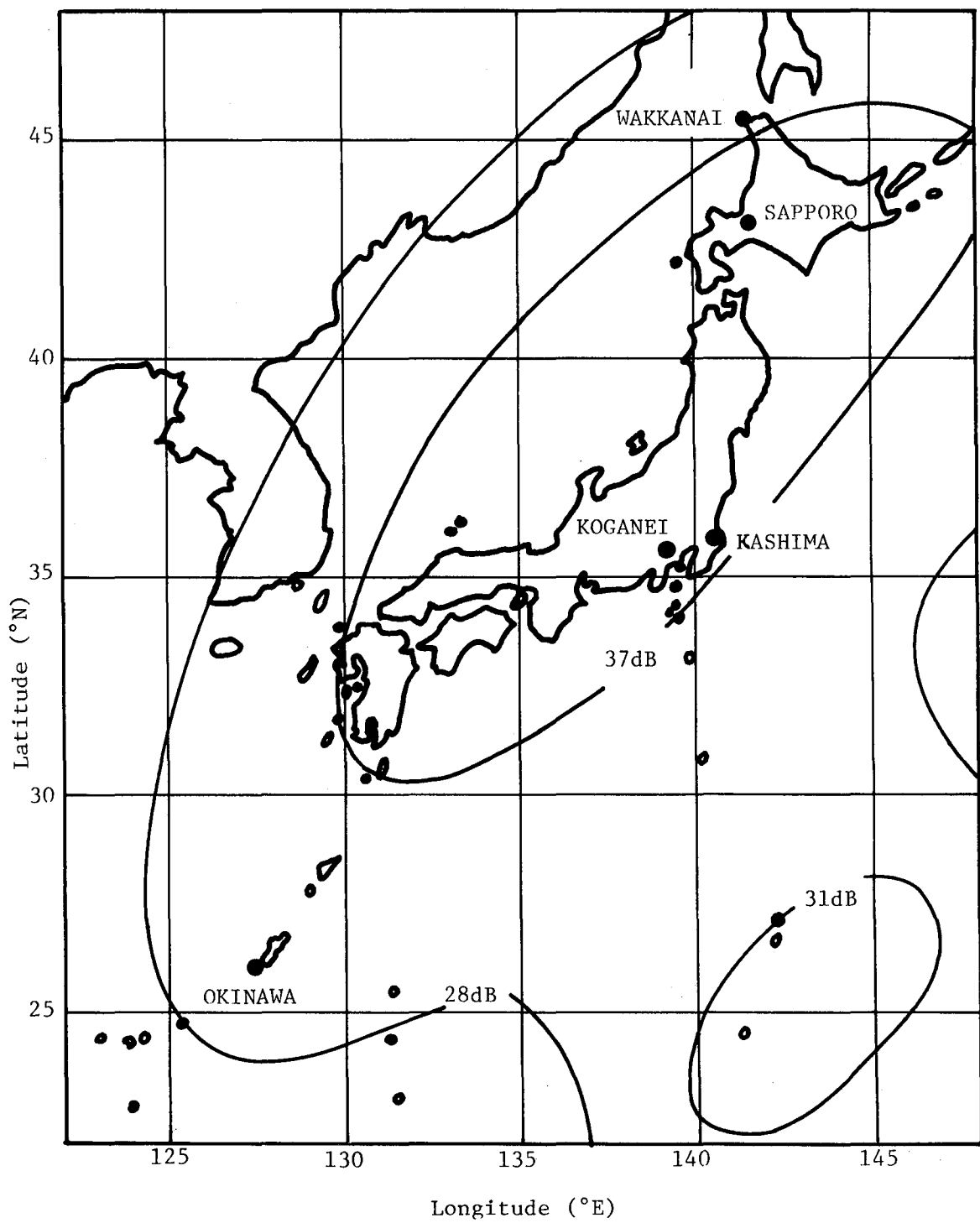


Fig. 1 BSE transmitting antenna pattern

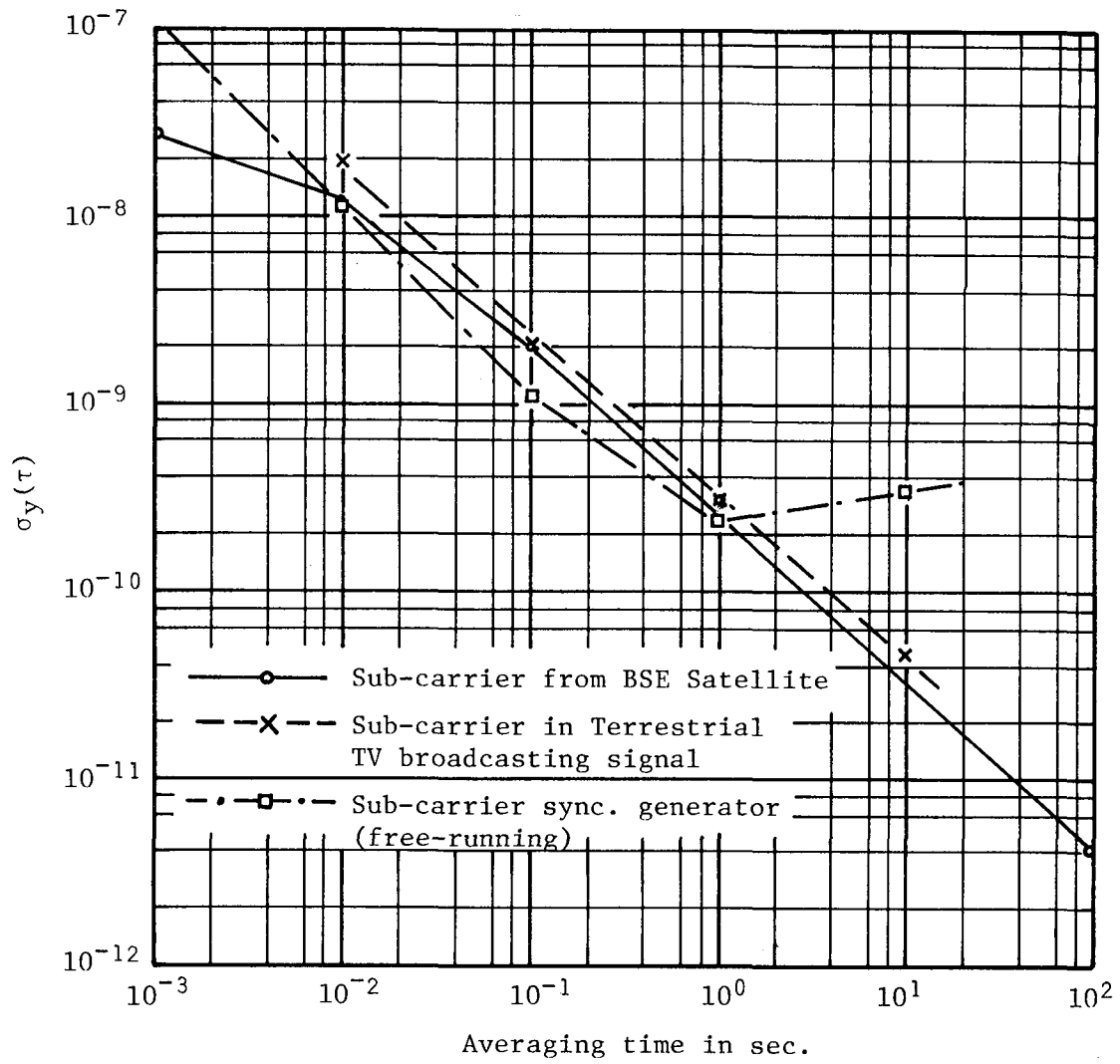
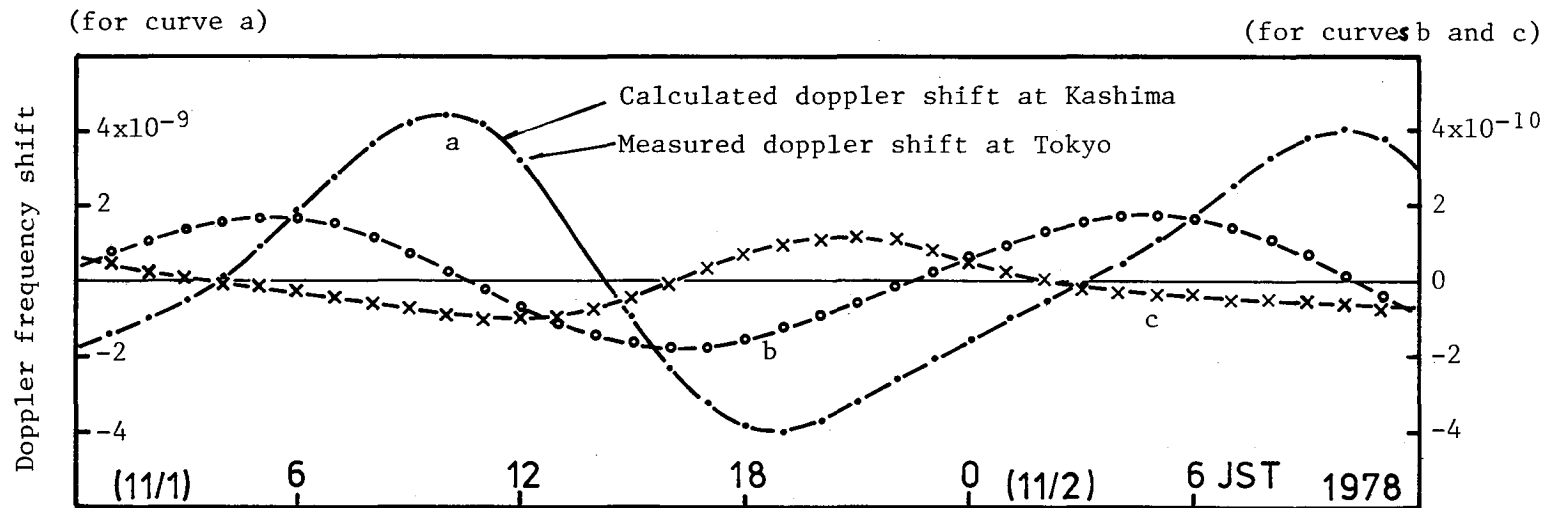


Fig. 2 Measured frequency stability



b: Calculated doppler shift at Wakkanai*

c: Calculated doppler shift at Okinawa*

*: Calculated frequency shift using orbit data, when compensated so as to cancel the doppler shift at the transmitting site.

Fig. 3 Doppler shift at Tokyo area and at the farther-most places in Japan

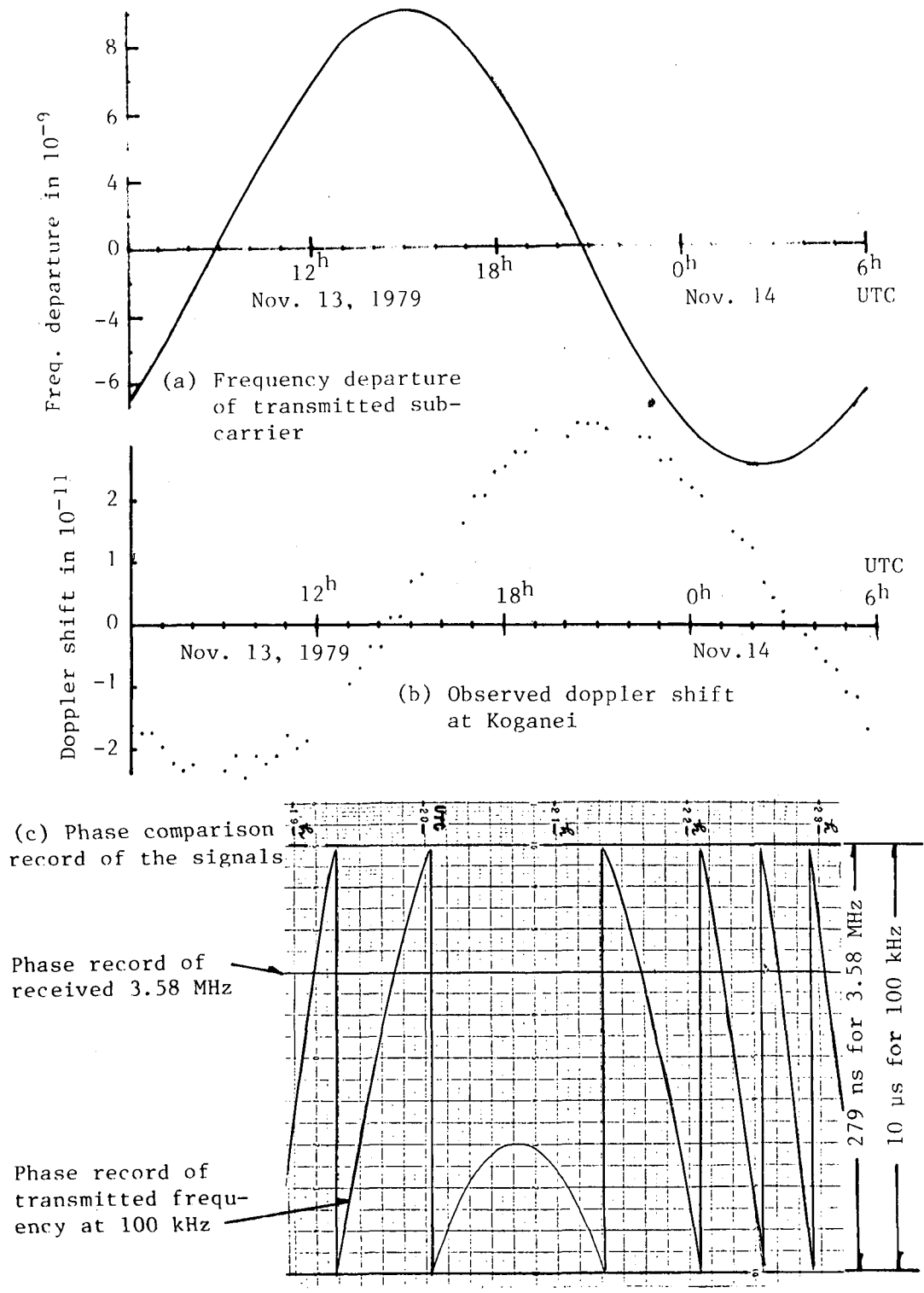


Figure 5. PLL-Controlled Data

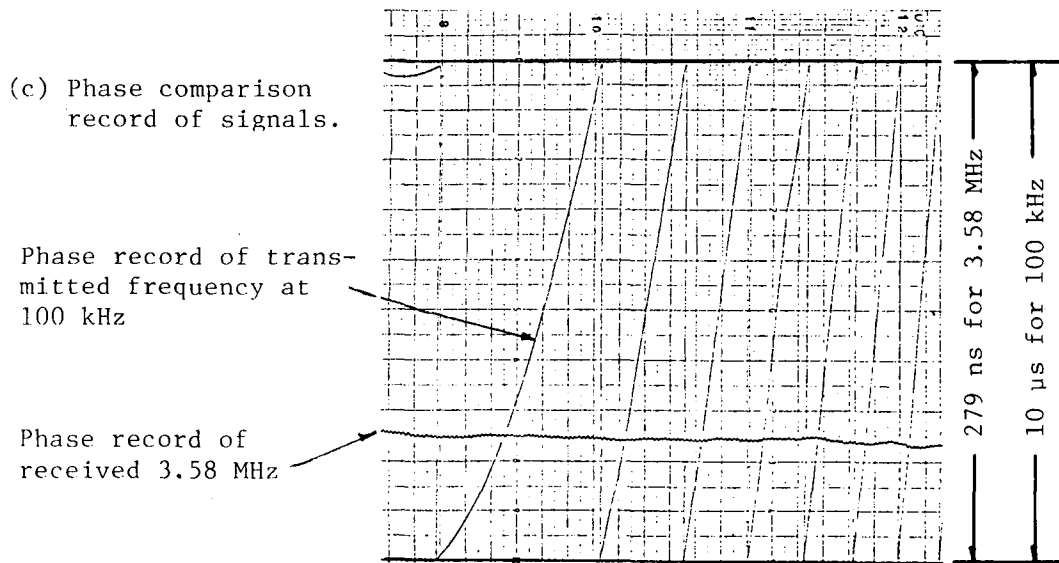
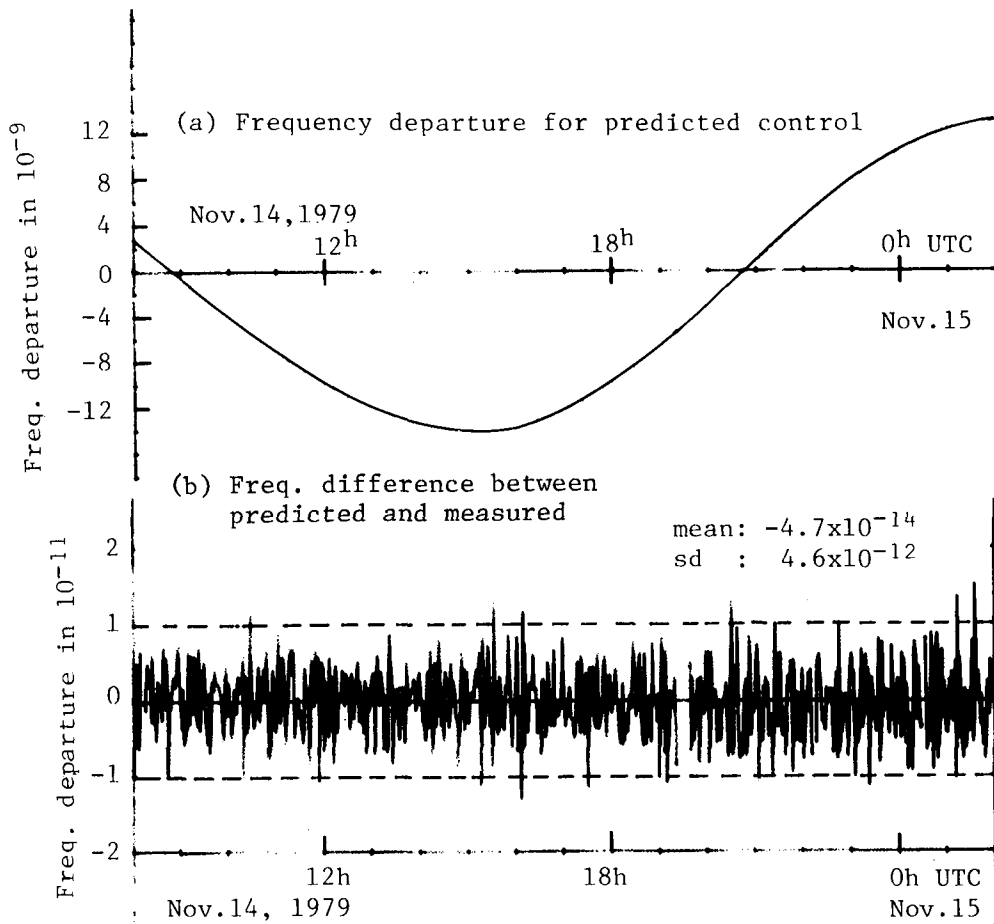


Figure 6. Pre-Compensating Control Using Measured Values

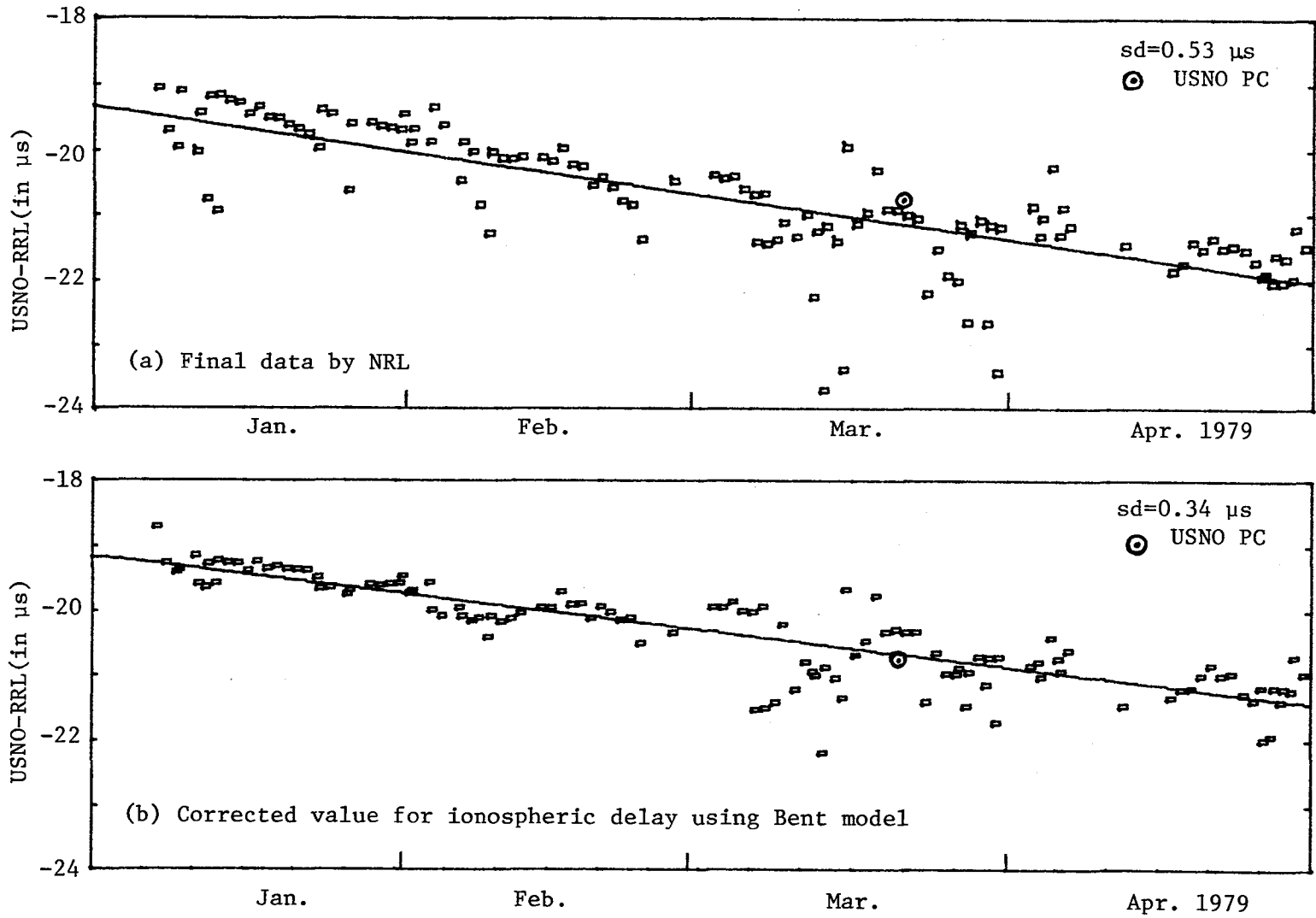


Fig. 7 UTC(USNO)-UTC(RRL) via NTS-1

ONE WAY TIMETRANSFER VIA METEOSAT
CAPABLE OF 30 NS ACCURACY

Klemens Nottarp, Wolfgang Schlüter
Institut für Angewandte Geodäsie (IfAG/Abt.II DGFI)
and Sonderforschungsbereich 78-Satellitengeodäsie
der TU-München
Frankfurt/M, Federal Republic of Germany

Udo Hübner
Physikalische Technische Bundesanstalt (PTB)
Braunschweig, Federal Republic of Germany

ABSTRACT

A pilot project under joint development of the Institut für Angewandte Geodäsie (IfAG) and Physikalische Technische Bundesanstalt (PTB) supported by the European Space Operation Center (ESOC) makes use of the METEOSAT ranging signal, available every 3 hours for about 1.5 minutes. The phase of the ranging signal is measured against the second pulses of the station clocks. A system study shows that the accuracy obtainable could be in the order of 30 ns. The receiver unit consists of a 2 m diameter fixed antenna, a low noise broadband receiver and a phase tracker and demodulator, the overall costs will be less than \$ 20 000 US.

1. ACKNOWLEDGEMENT

The authors express their gratitude to the European Space

Operations Center (ESOC) at Darmstadt, Federal Republic of Germany of which Gerhardus W. J. DREWES, ENNO E. LIJPHART and Sigmar PALLASCHKE cooperated in the system design described in this paper and which has agreed to cooperate in the execution of the experiment, notably in the receiver system development and in providing the satellite orbit data.

2. GENERAL REMARKS

Precise measurements for geodetic applications using space techniques such as laser ranging to artificial satellites or to the moon, very long baseline interferometry (VLBI) and Doppler observations require precise time and time interval measurements. Therefore the local clocks of the observation stations must be linked to a coordinated time scale such as UTC with high accuracy. The laser ranging technique which meanwhile achieved time interval measurements with an accuracy of better than 100 ps ($\sim 1 - 2$ cm) /5/ requires a real time determination of the epoch of the range-observations within a global frame better than 1 μ s /3/. As within short time routinely no time-transfer of high accuracy could be performed, except portable clock trips /1/, which are laborious, time-consuming and expensive, or time transfer via TV /1/ which could not be applied between Wettzell (IfAG) and Braunschweig due to the large separation and the non-existence of a common transmitter, the local clocks have to extrapolate the timescale within the desired accuracy up to the moment of observations. This procedure requires that the local clocks must be synchronised several days before to a high performance coordinated timescale of a time laboratory with an accuracy of better than 100 ns.

In Cooperation between the Physikalische Technische Bundesanstalt (PTB), the European Space Operation Centre (ESOC)

and the Institut für Angewandte Geodäsie (IfAG) it is planned to carry out a oneway **time transfer via the geostationary satellite METEOSAT /2/**. The accuracy could be expected to be better than 50 ns. As the position of METEOSAT is about 0° latitude and 0° longitude the application area is limited and the accuracy of the procedure is dependent on the location of the participating stations.

For this paper the procedure of the **time transfer is discussed** and an error budget for the transfer between Wettzell and Braunschweig is estimated.

3. PROCEDURE OF THE **TIME TRANSFER**

The principle of the procedure is similar to that used for **TV-time transfers with the main-difference that the transmitter is located in a satellite**. The main problem in one way time transmissions from a satellite is the accuracy with which its position must be known. A geostationary satellite offers the advantage of small relative movements but normally the mission requirements do not include a very accurate orbit determination. An exception in this field is the satellite METEOSAT of which the 2-point-ranging system allows orbit determination to the order of 100 m accuracy. A disadvantage is the long distance to the satellite which causes the received signal to be rather weak (in comparison to a TV signal). However, a special format of the timing signal allows averaging it for long periods of time and thus to reach the high accuracy in time coordination required. Investigation of the different transmissions from the satellite resulted in the conclusion that the "ranging signal" should be the best for the **time transfer**. **The carrier frequency of the ranging signal is 1.691 G Hz phase-modulated with a**

160 kHz sinewave. For the resolution of ambiguity of the zero-point crossings an additional pseudo-random-noise of 20 k bit/s (1000 bit Code; period 50 ms) synchronous with the 160 kHz-frequency is modulated onto the carrier (both signals are derived from a local atomic **standard**). Every three hours for a period of 1.5 minutes the ranging signal is transmitted from the ESA-ground station at Michelstadt (Fed. Rep. of Germany) for orbit determination of METEOSAT. For our application this ranging signal is also received at the ground stations Wettzell (W) and Braunschweig (B) after being transpondered by the satellite (figure 1).

For the time comparison the 160 kHz signal will be used. As the duration of one period is 6.25 μ s it is necessary to synchronise the clocks undergoing comparison within half of the duration (of 3.125 μ s) in order to identify the zero-point-crossings without decoding the pseudo-random noise. At the stations the **time interval T between the local second pulses and the subsequent zeropoint crossing of the received 160 kHz-signal** has to be measured. The time difference δ of two participating clocks, here the institutions in Wettzell (W) and Braunschweig (B), can be derived from figure 1 and 2. It has to be distinguished between the two situations (a) and (b) of figure 2 characterised by the fact of perhaps one unknown period P of the 160 kHz signal. The ambiguity of that one period can be resolved if the time difference between "B" and "W" is known to better than half the period P. From figure 2 the following formula can be derived:

$$\delta + T_W + \tau_{SB} - \tau_{SW} = T_B + n P,$$

with

T_W, T_B : measured time interval between the second pulse and the subsequent zeropoint-crossing of the 160 kHz

signals at Wettzell (W), resp. Braunschweig (B),
 τ_{SW}, τ_{SB} : propagation delay between the satellite and Wettzell,
resp. Braunschweig, derived from the coordinates of
the satellite and the earth station.

n : integral number of periods $P = 6.25 \mu\text{s}$ contained in
the difference of the propagation delays $(\tau_{SB} - \tau_{SW})$.

"N" (figure 2) characterises one **positive zeropoint-crossing**
of the 160 kHz signal transmitted at one point of time by
the satellite and received by the earth stations at **differ-**
ent points of time.

4. THE RECEIVING STATION

Figure 3 shows the block diagram of the receiving station.
The RF- and IF-portion of the receiver is of low noise phase
compensated, broadband design mounted in a weatherproof box
on the rear side of the antenna. The technical design of
that part of the receiver which extracts the 160 kHz tone
from the 70 MHz - intermediate frequency is closely related
to the design of the receiver ESOC is using for ranging.

The phase lock loop (PLL) for the 160 kHz tone at ESOC is
designed with a natural frequency of 15 Hz. With the signal
to noise ratio of 61.2 dB.Hz (table 1), estimated for a 2 m
diameter parabolic antenna that PLL causes a timing jitter
of 14 ns RMS. However, in view of the scheduled correlation
with the second pulses of atomic clocks a reduction to 2 ns
appears attractive and will not create technological prob-
lems. The overall cost of the receiving station is expected
to be less than \$ 20 000 US.

5. ERROR ESTIMATION

5.1 Random timing error of the ranging signal

As mentioned in chapter 3 the estimation of the signal to noise ratio leads, up to now, to about 14 ns RMS timing jitter. As during a period of 90 s up to 90 measurements will be available and about 90 values for δ (chapter 2) will be calculated the average of all will decrease the mentioned timing error of 14 ns for a single measurement to less than 2 ns, provided that the correlation between the data is as small as expected.

As the measurements are performed with different zeropoint-crossings of the 160 kHz signal (figure 2) there may occur the influence of the oscillator noise. As the 160 kHz tone is derived by local atomic frequency standards, it is expected that the influence is less than the other random noise contributions. If it is recognised in the first experiments that the noise is too strong, it will be simply omitted by identifying and using the same zeropoint-crossing ("N", figure 2).

5.2 Positioning errors

From the geometrical point of view errors in the coordinates of the stations and of the satellite will influence the accuracy. With the **Doppler technique point-positioning** for the observation stations and for the METEOSAT-tracking station with an accuracy of 1 m is possible. The position of METEOSAT will be known with an accuracy of the order of about 100 m. However, it should be kept in mind that the orbit determination is an order of magnitude better than the METEOSAT-mission requires and it is not self evident to be obtainable on follow-on spacecraft.

Expressing the range-differences $\Delta S = C (\tau_{SB} - \tau_{SW})$ in terms of coordinates of the station and of the satellite the differentiation of that expression permits the estimation of the influence of these inaccuracies. Assuming random errors the following formulae yield the estimations

a) for errors in the groundstation positions

$$m_{\Delta S}^{P_1 P_2} = \frac{1}{c} \sqrt{\sum_{i=1}^3 \left(\left(\frac{P_1^{X_i} - X_i^{Sat}}{S_1} \right)^2 dx_i^{P_1^2} + \left(\frac{P_2^{X_i} - X_i^{Sat}}{S_2} \right)^2 dx_i^{P_2^2} \right)}$$

b) for errors in the satellite position

$$m_{\Delta S}^{Sat} = \frac{1}{c} \sqrt{\sum_{i=1}^3 \left(\frac{X_i^{Sat} (S_1 - S_2) - S_2^{P_1} X_i^{P_1} + S_1^{P_2} X_i^{P_2}}{S_1 \cdot S_2} \right)^2 dx_i^{Sat^2}}$$

with

$X_i^{P_1}$: coordinates of the first groundstation

$X_i^{P_2}$: coordinates of the second groundstation

X_i^{Sat} : coordinates of the satellite

S_1 : range from station 1 to the satellite

S_2 : range from station 2 to the satellite

dx_i : errors in coordinates.

Inserting approximations for the coordinates of the stations (B and W) and the satellite position the geometrical influence is of the order of 5 ns from the observation stations and 5 ns from the satellite. In the period from 5th to 15th November a Doppler campaign including the participating stations and moreover some of the European time laboratories has been carried out with the objective of computing precise station coordinates.

5.3 Ionospheric refraction

The uncertainty due to the ionospheric refraction will be very small. The total influence of the ionosphere for a frequency of about 1.7 G Hz observed with an elevation of 30° is about 3 m. With the aid of an ionospheric refraction model this effect will partly be corrected in the computation of the propagation delays τ_{SW} and τ_{SB} . As it can be assumed that the influence in Wettzell and Braunschweig is similar the ionospheric effect can be neglected. It amounts to less than 1 ns.

5.4 Tropospheric refraction

The largest uncertainty will be due to tropospheric refraction as the meteorological conditions in Wettzell and Braunschweig can be expected to be different. In a study performed by "Stanford Telecommunications INC" /4/ for the production of the GPS-receiver for **time transfers, the uncertainty** due to the ionosphere and to the troposphere together was estimated to be 30 ns for a frequency of 1.575 G Hz. As the carrier frequency of 1.691 G Hz differs little from the GPS-frequencies, 30 ns for refraction can be assumed for this project. The influence of the ionosphere (~ 10 ns) is

to be subtracted thus only about 25 ns have to be taken into account for the tropospheric refraction.

5.5 Uncertainty due to the groundreceivers

The receivers used at the various sites should be identical in their IF-conception. Since this excludes the use of narrow filters in the signal (tone) path a stability requirement of 10 ns is expected to be feasible. Initially, and also at regular intervals it is possible to calibrate the receiving equipments at the ESA ground station where the received signal is much less contained with noise because it has a 15 m antenna. No influence can be expected to result from different temperatures at the stations between the high frequency part of the antenna and the preamplifier. The other parts of the receiver will be installed in a room, if possible with air conditioning, so that this influence should not be more than 5 ns. The total uncertainty should be less than 15 ns.

5.6 Error budget-Summary

Table 2 summarises the errors of the previous chapters. Assuming random influence of the estimated errors an accuracy of about 30 ns for a **time transfer during a ranging** period could be expected. As the measurements could be done every 3 hours (8 times per day) further averaging over a day probably leads to the total uncertainty of 20 ns for a daily **time transfer**.

6 REFERENCES

/1/ Becker, G.; Methoden zum Vergleich und zur

- Fischer, B.;
Hetzl, P.:
Verbreitung von Zeitskalen,
Kleinheubacher Berichte 16, S. 5 -
21, 1973
- /2/ Hübner, U.;
Nottarp, K.;
Schlüter, W.:
Verfahren für Einwegzeitvergleiche
hoher Genauigkeit via METEOSAT,
Veröff. der Bayr. Kommission f.
d. Int. Erdmessung, Astron. geod.
Arbeiten Heft Nr.39
München, 1979.
- /3/ Schlüter, W.:
Zeithaltung auf der Satelliten-
beobachtungsstation Wettzell (in
diesem Heft). Veröff. der Bayr.
Kommission f. d. Int. Erdmessung,
Astron. geod. Arbeiten, Heft 39,
München, 1979.
- /4/ Stanford Telecommunications Inc.: STI High accuracy GPS
receiver model 5007, Sunnyvale CA,
1978
- /5/ Wilson, P.:
A Short Pulse Satellite Ranging
System, Proc. of the Electro
Optics/Laser 77 conference
Anaheim, 1977.

1. Carrier frequencies	1691.00 MHz
2. Worst case effective radiated power	18.10 dBW
3. On board received signal to noise power density ratio	74.63 dB.Hz
4. Atmospheric loss (at $\approx 30^\circ$ ground antenna elevation)	0.07 dB
5. Ground antenna feed and cabling loss	0.10 dB
6. System noise : - cosmic noise	8K
- low noise amplifier, F=2.5 dB	233.5K
- atmospheric + cabling loss (0.17 dB)	11.5K
- Sidelobes, illuminating earth	15K
- TOTAL 268K	24.28 dBK
7. Propagation loss ($\frac{1}{4\pi d^2}$) d=39.000 km	162.81 dB
8. Receiver input power for a 2 m parabolic antenna with 50% efficiency	-142.92 dBW
9. Gain of above antenna at 1961 MHz	27.97 dB
10. Received signal to noise power density ratio, ignoring retransmitted up-link noise	61.4 dB.Hz
11. Overall signal to noise density ratio (from 3 and 10)	61.2 dB.Hz
12. Modulation loss	-7 dB
13. PLL Bandwidth	20.0 dB.Hz
14. Signal to noise ratio in the PLL	34.2 dB
15. Jitter	14 mrad.
16. RMS timing error	14 ns

Table 1, Estimation of the overall signal to noise density ratio.

uncertainty	in ns
1. random timing error	2
2. position of the ground station	5
3. position of the satellite	5
4. ionosphere	-
5. troposphere	25
6. ground receiver	15
	$\sqrt{\sum \mu_i^2} \approx 30 \text{ ns}$
	$\sum \mu_i \approx 50 \text{ ns}$

Table 2, error budget

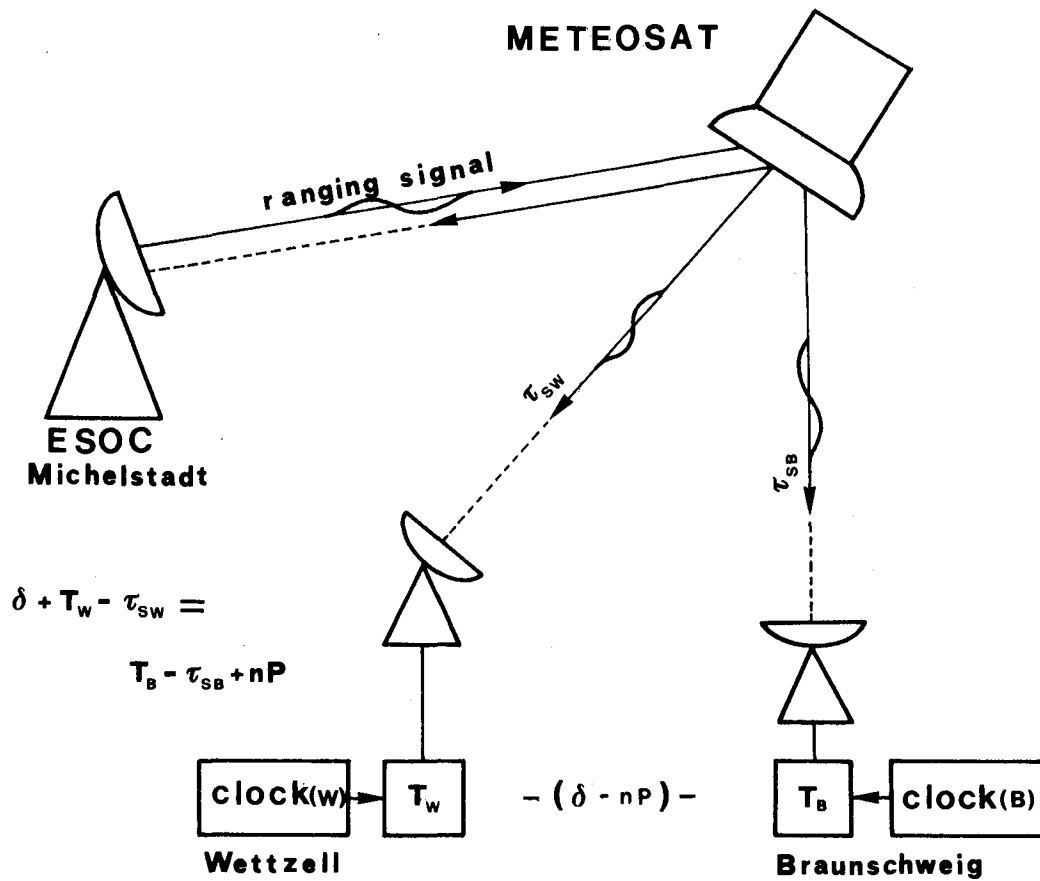


figure 1, scheme of the time transfer

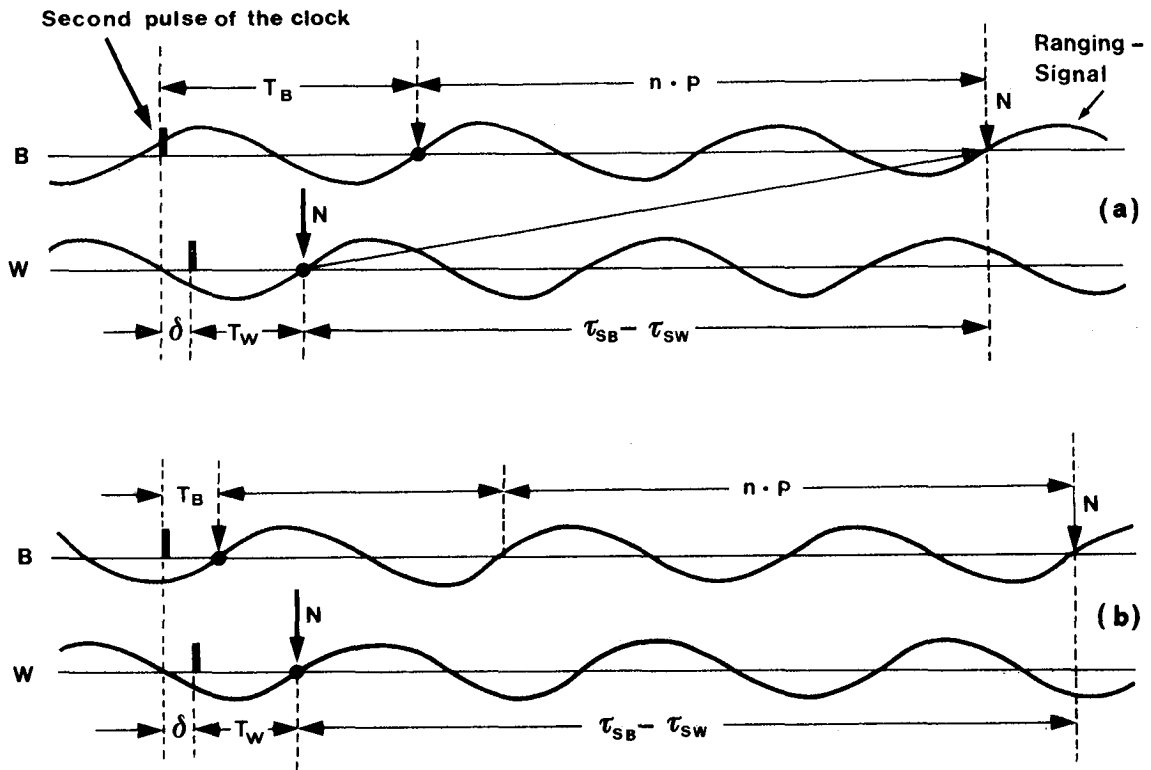


fig. 2, computation of the clock difference δ

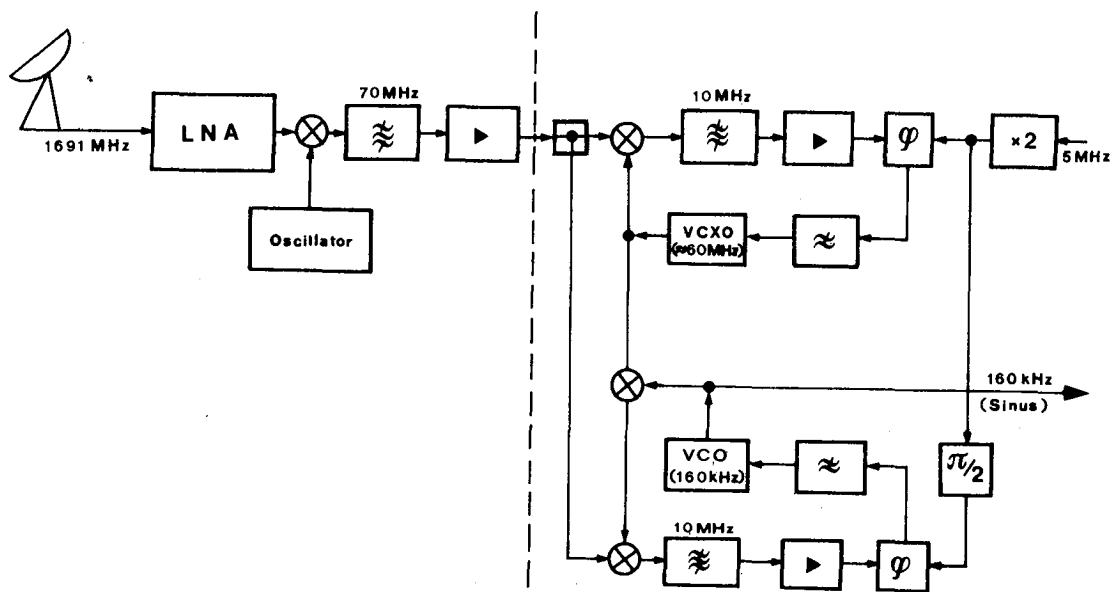


fig. 3, Block diagram of the receiver.

QUESTIONS AND ANSWERS

MR. PLEASURE:

You assumed random--

DR. SCHLUETER:

Yes.

MR. PLEASURE:

But have you made a spectrum analysis of the frequency given?

DR. SCHLUETER:

No, we assumed it. We assumed random errors.

MR. PLEASURE:

Yes. Well the standard technique is, for chemical engineering and most other types of engineering is to put a spectrum analyzer on it and you may find that you have got 60 cycle hum from nearby motors or something and if that is the case you are going to be in a larger error and then you have less than you were projecting.

DR. SCHLUETER:

Well this is a project we proposed that we have not yet experiences with it.

DR. BARTHOLOMEW:

In your error budget you showed 25 nanoseconds for a tropo uncertainty. That looks a little bit large to me. I didn't realize that.

DR. SCHLUETER:

If it isn't too large it is better for the error projections.

TIME DISSEMINATION IN THE HYDRO QUEBEC NETWORK

G. Missout, W. Le Francois, and Louis La Roche
Institut de Recherche Hydro Quebec
Varenes, P.Q., Canada

ABSTRACT

The ever increasing complexity of electrical networks combined with the increasing cost of power losses during a network failure has led public utilities to become equipped with more powerful and precise tools for pinpointing the causes of such a fault. Hydro Quebec has developed and is now using a time dissemination system which uses a modified IRIG B code transmitted on its own telecommunication network. The reasons for using such a system and the way it was carried out are discrete.

INTRODUCTION

After a fault occurs on a network it is at times difficult to reconstitute the chain of events without a means of precisely dating each one of these events. In fact when the fault is straightforward (the fall of a transmission line or bursting of a transformer) the cause and thus the remedy is easy to establish. In a lot of cases however the situation is not nearly so clear which leaves the analyst with a series of events which all took place within a few seconds or less (opening of a circuit breaker, alternator trigger off etc.) without him being able to determine precisely the cause or origin of these events.

The precise dating of each event has proved to be an effective tool in eliminating any doubt in those cases. Indeed the fact of being able to reconstitute the order of events allows to recover the origin and thus the cause of trouble to be pinpointed.

In practice each transport substation must therefore have the same time everywhere. The accuracy required is in the order of 1 ms or better.

Several tests with WWVB have proven that such exact timing could not be obtained, not to mention the fact that in the north east of Quebec and in Labrador the VLF station Rugby (united Kingdom) interferes with that of WWVB.

HYDRO QUEBEC IRIG B SYSTEM

Hydro-Quebec has thus decided to synchronise its clocks using an IRIG B code transmitted on its own telephone network.

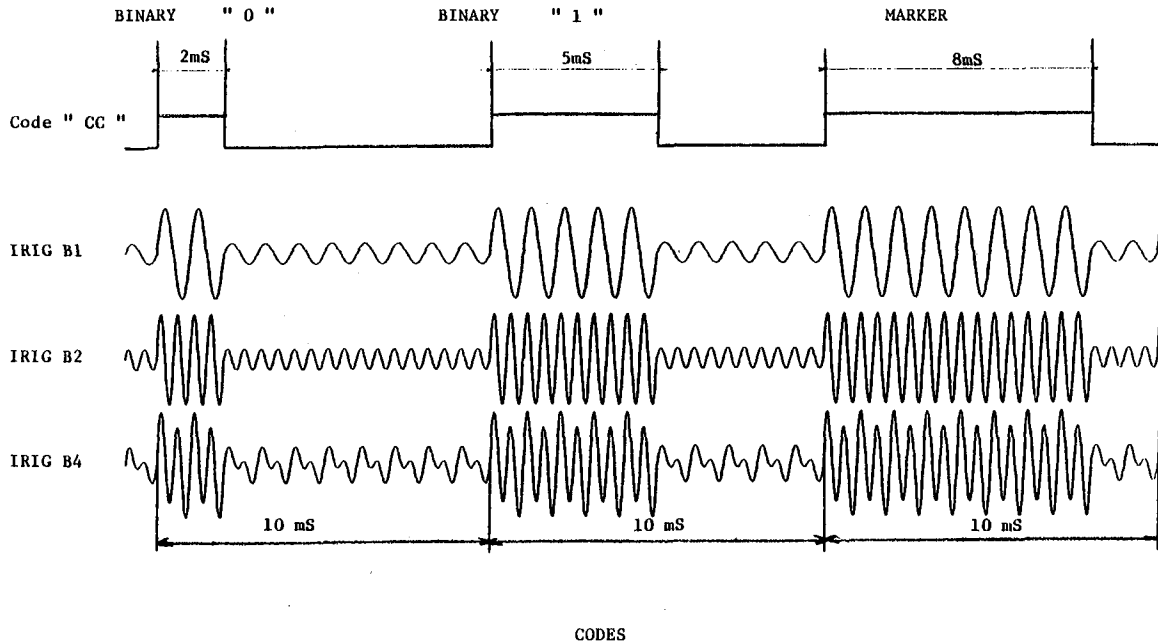


FIGURE 1

At first a 2 KHz carrier (Figure 1) (IRIG B2) was used in order to obtain a spectrum better centered within the telephonic band (300 Hz - 3 KHz). Closed loop measurements (go and return on the same telephone channel) have shown an excellent stability with this system (variations of less than 100 μ s over 728 miles - Montreal Churchill). However measurements between two points (go only) have shown that it is impossible to use such a method directly. In fact it was noticed that the phase of the 2 KHz signal varied in a random fashion giving a variation of $\pm 500 \mu$ s of the local hour as compared to the master clock and worse yet, that a normal decoder could not read the code about 20% of the time.

After a study it was discovered that this problem was related to the use of SSB in the FDM microwave system.

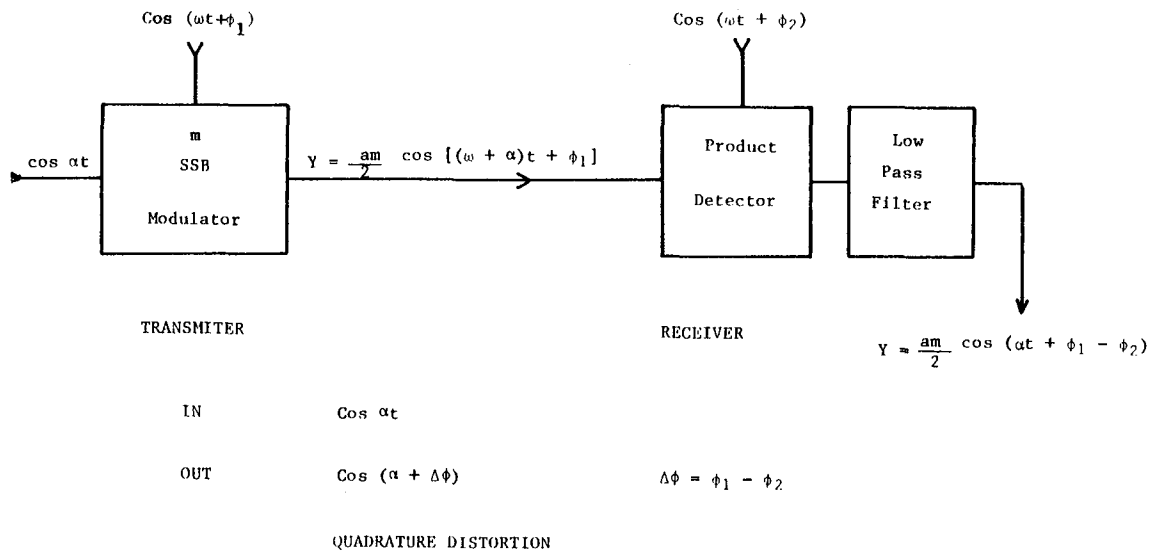
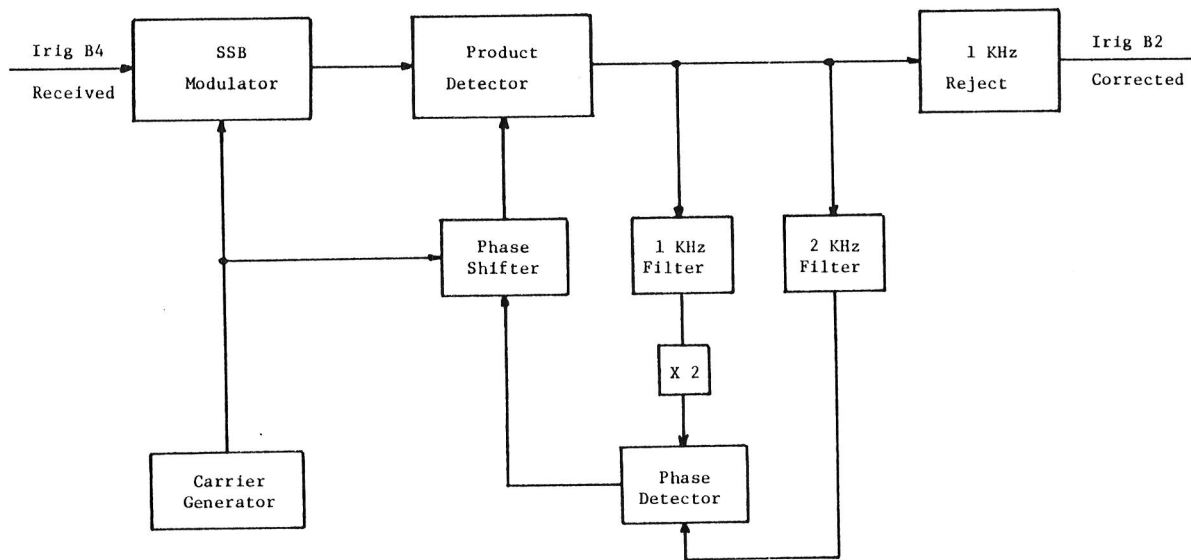


FIGURE 2

If we split the IRIG B signal in a Fourier Series, each component follows the equations of Figure 2. If $\Delta\phi$ is the phase difference between the two local oscillators of the FDM transmitter and receiver, the component will have a phase shift equal to $\Delta\phi$. The resultant from all these components gives a signal which can be deformed, inverted etc.

It was noticed that in a going and returning signal the error in the going signal is almost exactly corrected by the return error; thus the idea originated of simulating a return locally. For that purpose it was necessary to add a 1 KHz pilot to the IRIG B2 code which is in phase with the 2 KHz carrier of the B2 code giving IRIG B4 code (Figure 1).

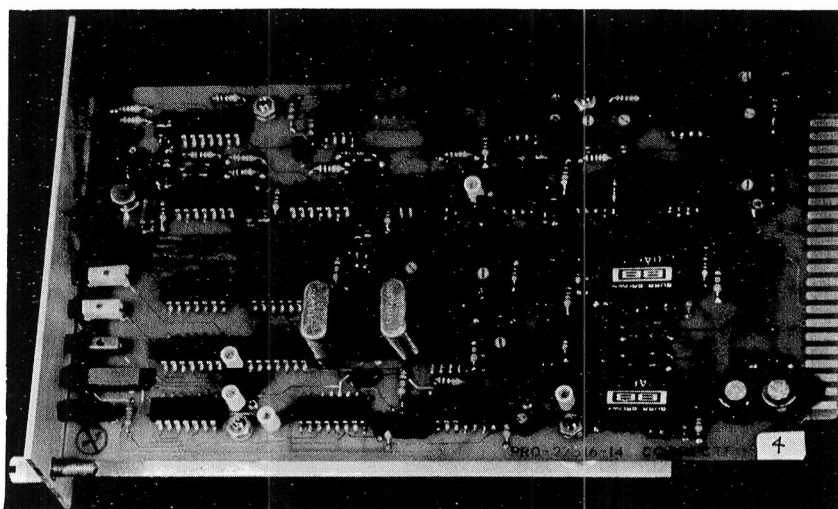
If locally at the arrival we split the signal by filtering its 1 KHz and 2 KHz components, each one will have a phase error of $\Delta\phi$. By multiplying the 1 KHz component we obtain a 2 KHz signal with a phase error of $2 \Delta\phi$ which there locally shows a phase difference $\Delta\phi$ between the two 2 KHz signals.



Corrector Bloc Schematic

FIGURE 3

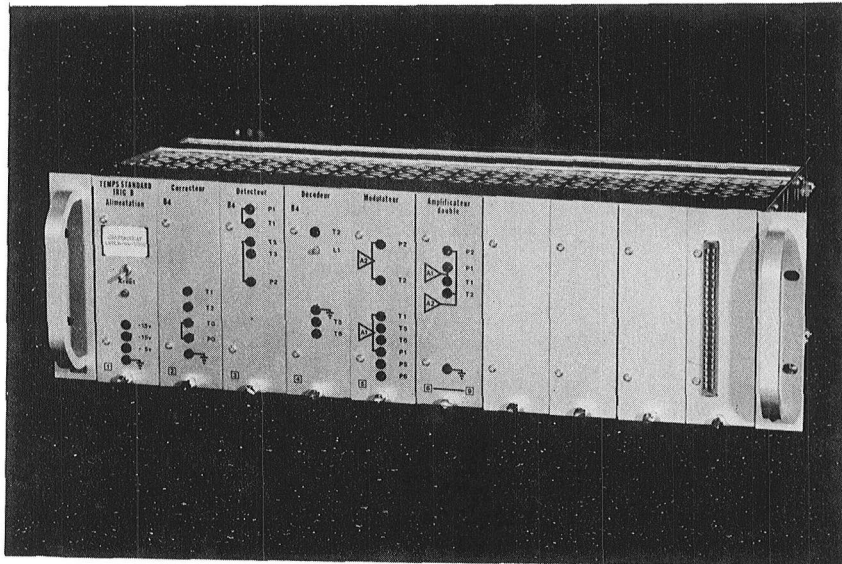
This particularity allows a corrector to be developed as seen on the Figures 3 and 4. This apparatus introduces the error $-\Delta\phi$ which now gives us a convenient signal.



Corrector

FIGURE 4

The reconstitution of an IRIG B1 signal (carrier at 1 KHz) is then assured by its allied circuitry (Figure 5).



Local Distributor

FIGURE 5

The apparatus also incorporates protection at its input and output which is necessary inside a high voltage substation.

Several measurements made in the Montreal region and between Montreal and 7 Island have shown the quality of the obtained results (Figure 6).

The method of measurements employed is shown on Figure 7.

The master clock used is a rubidium clock located in Montreal. The accuracy of the measuring clock is assured by a LORAN C receiver.

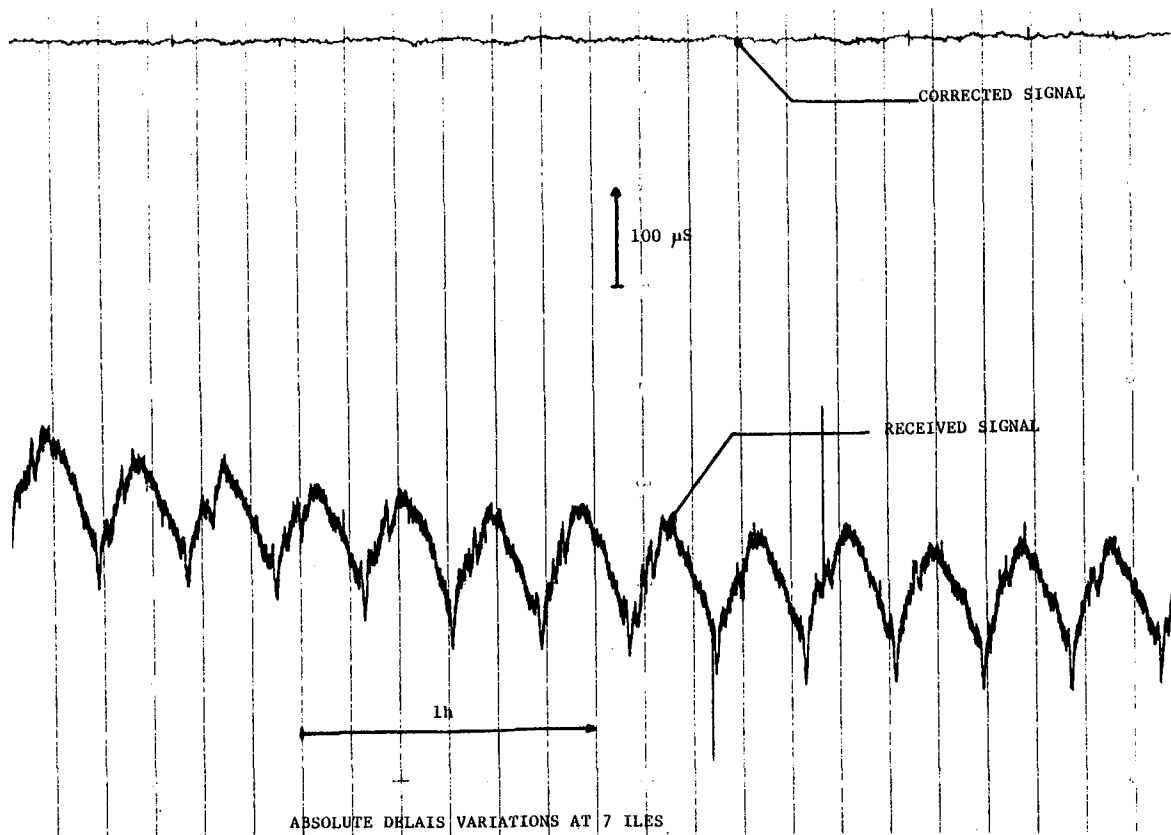
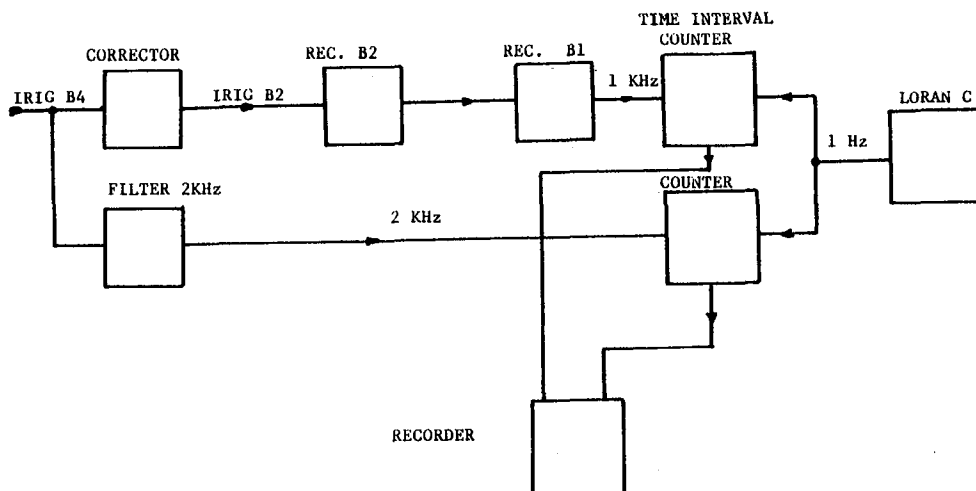


FIGURE 6

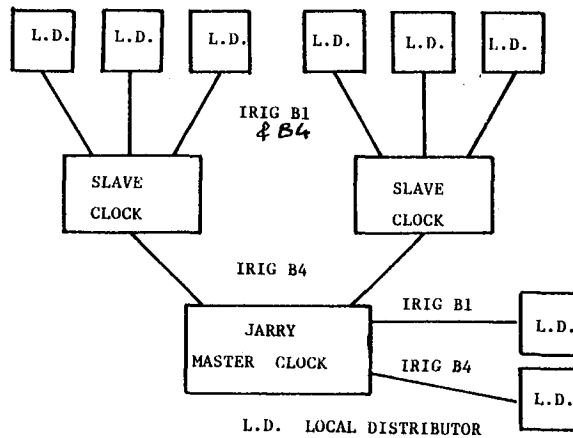


MEASUREMENT APPARATUS

FIGURE 7

Hydro-Quebec is presently installing a system based on a centralized master clock. A small number of slave clocks placed in some key areas of the network limits the number of necessary links by avoiding to join all the points to the master clock and also assures a permanent time code distribution in case of a link break between the master clock and a slave clock (Figure 8).

In Jarry Station we plan to have 3 clocks with an automatic Switch over based on a majority decision. One of the 3 clocks should be synchronized by GOES Satellite.



HYDRO QUEBEC TIME CODE GENERATION

FIGURE 8

QUESTIONS AND ANSWERS

DR. BARTHOLOMEW:

I would only observe that Hydro-Quebec, as a public utility, is not totally pre-occupied with fuel cost adjustments as some of our locals are.

TIME CODED DISTRIBUTION VIA BROADCASTING STATIONS

S. Leschiutta, V. Pettiti
Istituto Elettrotecnico Nazionale, Torino, Italy
E. Detoma⁽¹⁾
Bendix Field Engineering Corporation, Columbia, Maryland

ABSTRACT

The distribution of standard time signals via AM and FM broadcasting stations presents the distinct advantages to offer a wide area coverage and to allow the use of inexpensive receivers, but the signals are radiated a limited number of times per day, are not usually available during the night and no full and automatic synchronization of a remote clock is possible.

As an attempt to overcome some of these problems, a time coded signal, with a complete date information, is diffused by the IEN, via the national broadcasting networks in Italy.

These signals are radiated by some 120 AM and about 3000 FM and TV transmitters around the country.

In such a way, a time-ordered system with an accuracy of a couple of milliseconds is easily achieved.

INTRODUCTION

A national metrological Laboratory has to satisfy the requirements of many classes of users; it is also sometimes noticeable the tendency to concentrate the efforts on the primary metrology or on the most accurate or precise comparison systems, disregarding consequently the "low-precision" dissemination.

(1) The work was performed when the author was at IEN.

The aim of this paper is to illustrate how some of the latter problems are solved at the Istituto Elettrotecnico Nazionale (IEN), the Laboratory entrusted with the Time and frequency metrology in Italy.

In the following section some news is given about the so-called low-accuracy users and the requirements thereof. The third section deals with some dissemination systems all using the radio and television broadcasting stations, whereas the fourth section is devoted to a new time-code service introduced in the Country. Finally, in the last section some applications of the new code are outlined.

Medium to Low-Accuracy Users and their requirements

The larger set of the end-users of a national time and frequency dissemination service seems to be interested in knowing the time with accuracies between 1 s and 1 ms, and the frequency with a relative accuracy between 10^{-6} and 10^{-9} .

Some data about the classes of users and their requirements are to be found in a CCIR report (ref. 1), that is based on an enquiry performed by the National Bureau of Standards.

A similar analysis, albeit not so wide, was performed in Italy, only among technical and scientific users, giving similar results. But it turned out that for these users the most stringent requirements were not on the accuracy but in the format and the general characteristics of the signal that should:

- provide a complete date information,
- allow the use of automatic systems,
- be available on continuous basis, in order to avoid a local clock and,
- be available everywhere in the Country an adequate and stable signal-to-noise ratio.

In designing a new dissemination system, one is moreover confronted with some CCIR Recommendations (ref. 2) asking to use, as far as possible, the existing radio facilities, for obvious spectrum conservation reasons. On this line, some services (ref. 3) or proposals (ref. 4) were illustrated in recent years.

Some frequency and time dissemination systems via the broadcasting stations

In Italy there is one broadcasting Authority, the Radio Audizioni Italiane (RAI), with a network of microwave links connecting the major Studios, located in Rome, with all the AM, FM and TV broadcasting transmitters.

The standard time signals of the IEN are sent via a radio link to the above mentioned Studios to be hence distributed to the various transmitters.

At the moment about 120 AM transmitters operating in the MF bands and 3500 FM or TV transmitters operating in the VHF and UHF bands are linked to a common time source.

The standard time and frequency services via the RAI broadcasting transmitters are listed in Table I; some more services are under study or development.

As regards the standard Time signals, service 1 is a time signal, depicted in fig. 1, and distributed since the year 1942; this signal is radiated about 30 times per day. Service 2 is the new time code signal, to be described in what follows and attached to service 1. For the standard frequency dissemination, service 3 consists in the frequency stabilization of the carrier of an AM transmitter, located in North Italy and covering with its surface wave great part of the country during the day. The carrier at 900 kHz is obtained by synthesis from a rubidium standard and the corrections thereof are printed as a daily value, in a monthly instalment appearing on the review "Alta Frequenza".

The RAI, service 4, sends a standard frequency subcarrier at $16\frac{2}{3}$ kHz along the microwave links serving the FM transmitters.

This subcarrier is used in order to stabilize the frequency of the AM transmitters and to practice the so-called "precision frequency offset" between the carriers of some co-channel TV transmitters. The subcarrier can be easily extracted from any FM receiver and can be used in a number of well known techniques.

The new code

With reference to fig. 2 the new coded signal is sent along with the previous time signal at the second 52, and consists of an Audio-Frequency-Shift-Keying 1248+ code, whose characteristics are depicted in fig. 3, along with a sample information. The format and the AFSK frequencies were the result of a trade off between the time allotted (not more than one second), the information to be transmitted (32 bits), the bandwidths that are available on the AM receivers. the pleasantness to the ear, the compatibility with some existing decoders of the previous time signal, and so on. In order to enhance the "smoothness" of the signal, no phase jumps occur in the switching between the two frequencies.

In fig. 3, the presence of two "parity bits" at positions 16 and 31 can be noticed; the possibility to decode only one part of information, e.g. hours and minutes, is thus given. The bit at position 15 tells whether the "day-light saving time" is used in the Country or not.

Fig. 4 shows the set-up of the clocks and related instrumentation used in order to generate and to monitor the new service, whereas in fig. 5 a general view of the time-scale room is given.

As regards the decoding of the signal a number of approaches can be followed. In some receivers-decoders developed at the IEN Laboratories the following criteria were followed for the time signal of fig. 1: check of the frequency, of the length of the pulses, of the length of intervals, of the blank at second 59. For the new coded signal (fig. 3), tests are performed on: frequency, identification pulses, total number of pulses, parity checks.

For the date code, a correct decoding was observed with a **signal-to-noise ratio of 8 dB in simulated tests performed by the addition of white noise to the signal.** It must be taken into account that the BCD code can immediately follow speech or music, no silent interval being insured before the code. On the other hand at the output of a typical FM receiver the S/N ratio exceeds usually 40 dB.

Final remarks

Between the abovementioned requirements for a general-purpose time signal, the code described provides the date information, suits the automatic decoders, allows a good coverage of the Country, but fails the round-the-clock availability.

Consequently the receiver-decoder must be fitted, with one of the inexpensive quartz-clock modules now available.

The quality of the quartz depends obviously on the allowed departure of the local clock at the end of the maximum interval in which no time signals are radiated. One of the receiver-decoders available on the market not only sets the clock but tells how to correct the frequency of the local clock whenever the number of corrections exceeds a preset value. In other options, the drift of the local standard can be removed via a servo; after a few days of operation, the error is of the order of a few units of 10^{-9} .

As regards the time dissemination, the precision is of the order of one-two milliseconds. The propagation delay depends on the path of the signal, between Turin-Rome and the interested transmitters. These delays reach a maximum of about 15 ms and are fairly constant, since in the radio links carrying the voice programs no reroutings are usually performed. For some applications, such as the study of the dynamic behaviour of the power network, the propagation delays were measured with a portable clock within one millisecond.

Work supported by the Consiglio Nazionale delle Ricerche of Italy.

TABLE I

Service	RAI stations	Type of service	Availability
1	all AM, FM, TV transmitters	time signal + voice announc.	30 times/day
2	all AM, FM, TV transmitters	date code	30 times/day
3	one AM station	stabilized carrier	continuous
4	all the FM stations	standard sub-carrier	18 hours/day

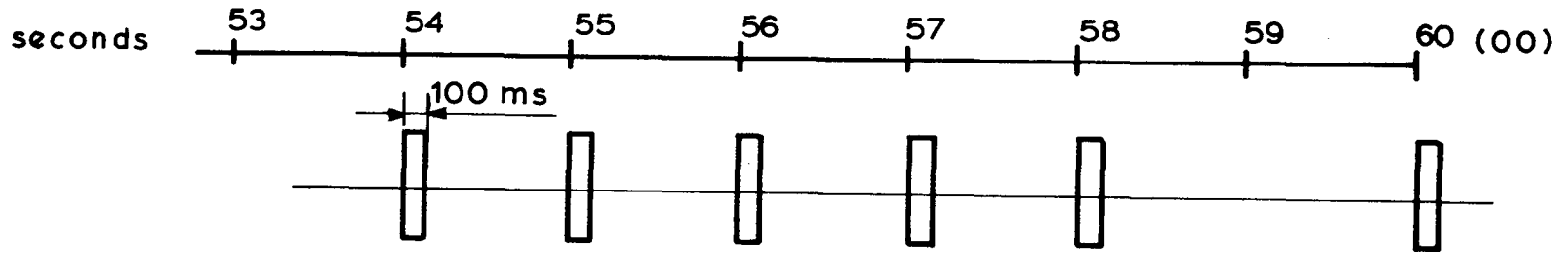


Figure 1. Time Schedule of the Old IEN Signal Radiated by the Italian Radio Company

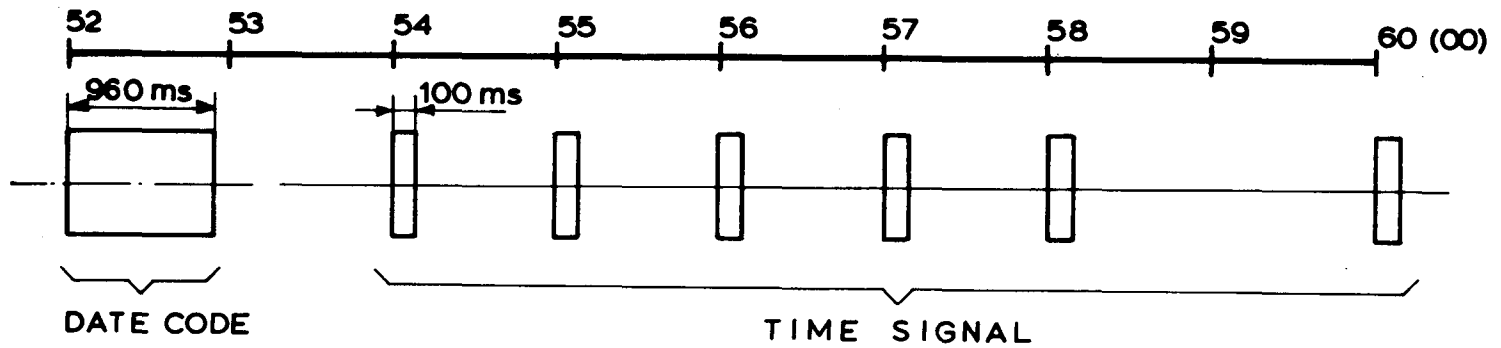
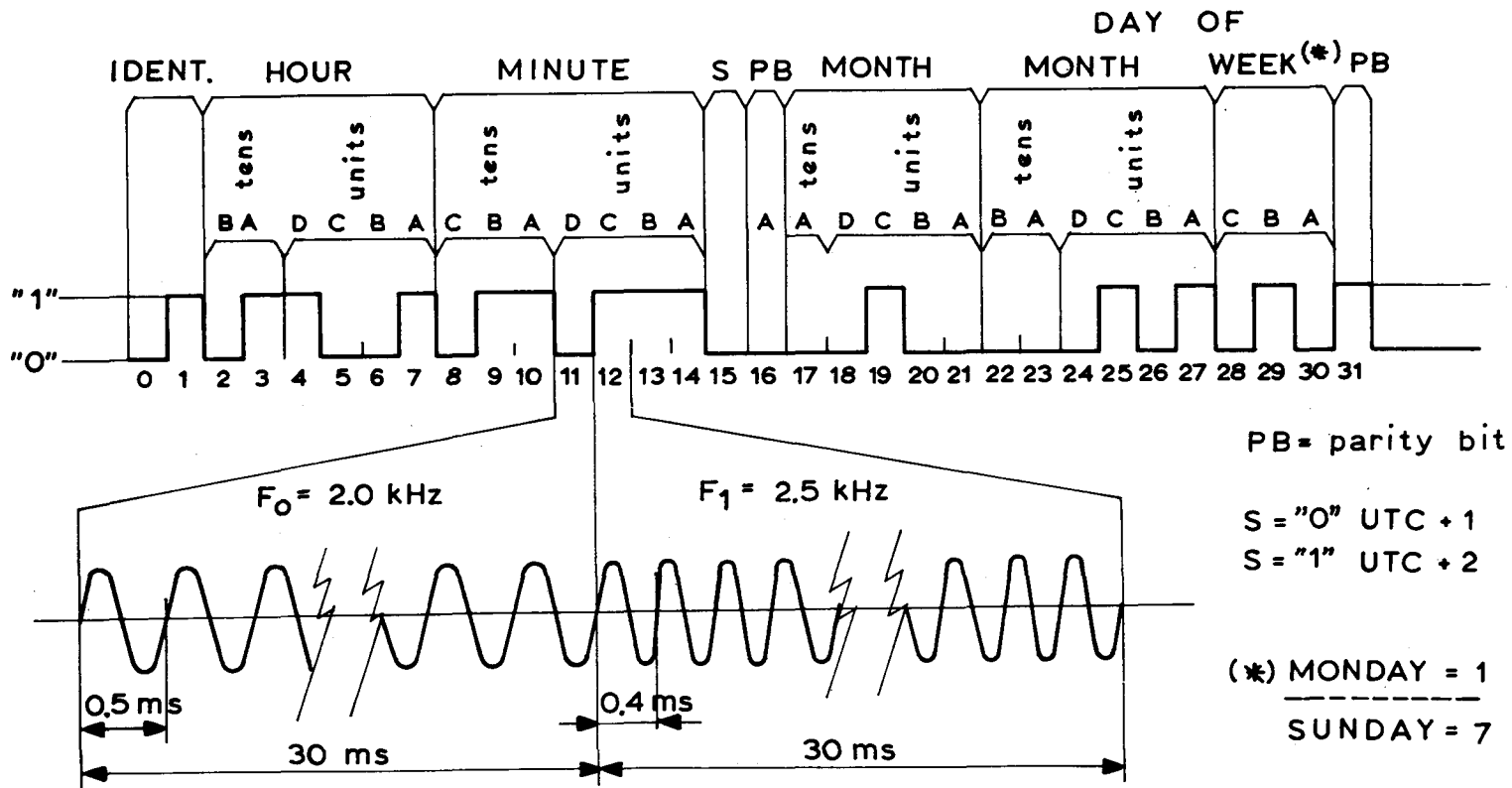


Figure 2. The New IEN Time Signal with a Complete Date Coded Information



DATE CODE AND DETAILS OF THE FSK MODULATION; THE DATE TRANSMITTED IS TUESDAY 5 APRIL, 19 HOURS 37 MINUTES, UTC +1

Figure 3. The Coded Information Seen in Details

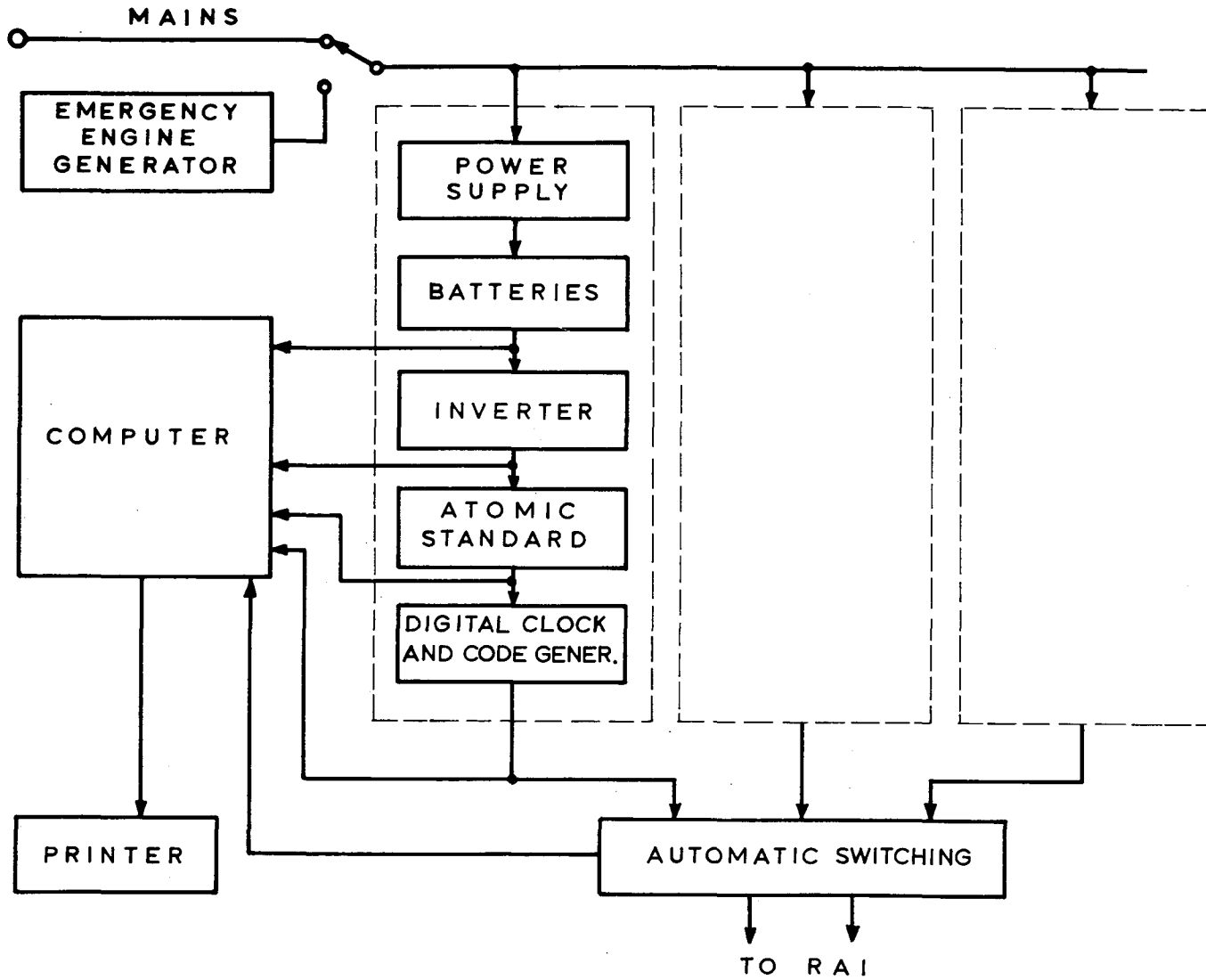


Figure 4. Equipment Set-Up Used to Generate and Control the New Coded Time Signal

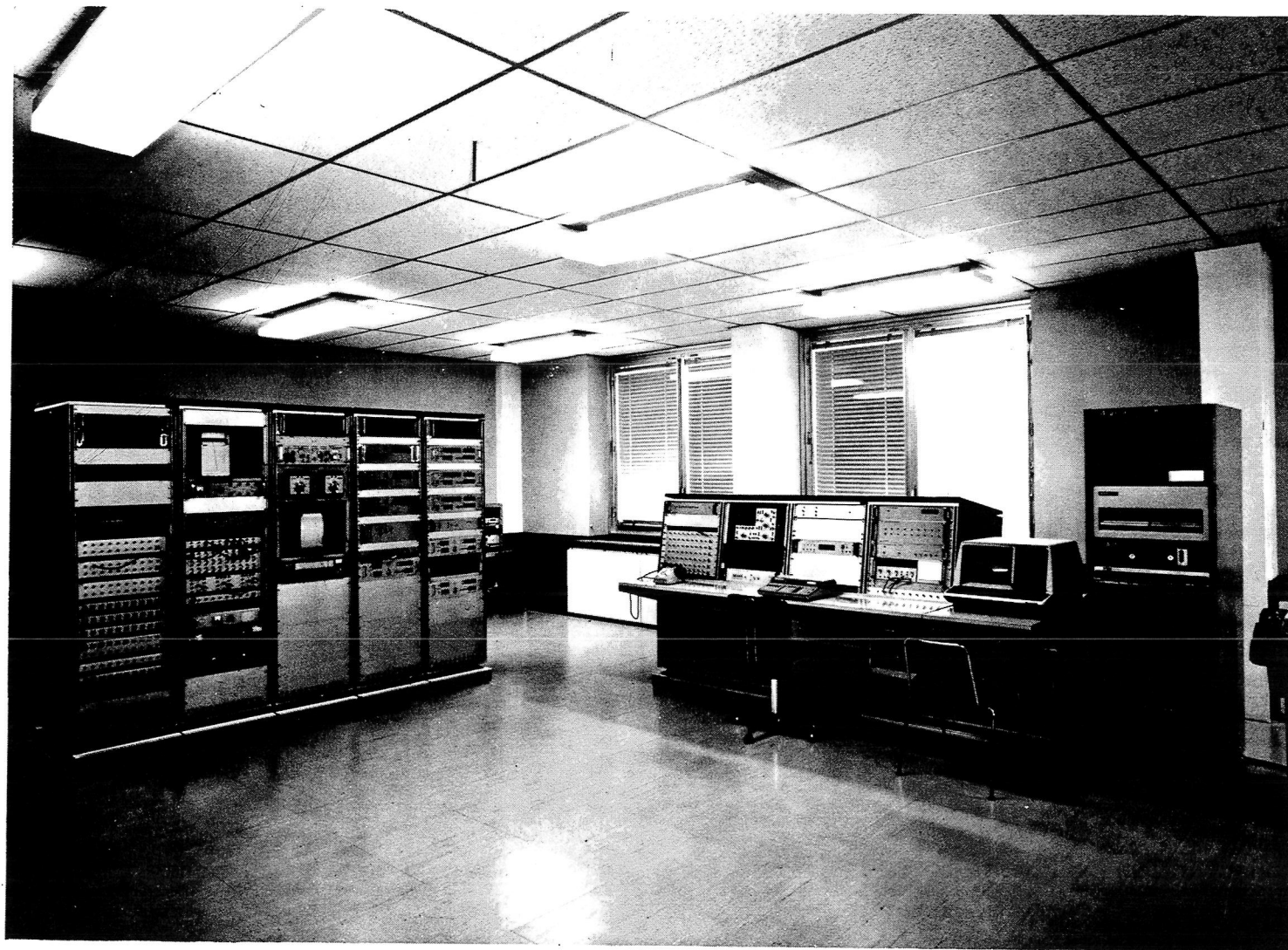


Figure 5. View of the IEN New Time and Frequency Laboratory

QUESTIONS AND ANSWERS

DR. BARTHOLOMEW:

We are being very economical of our time. Does anybody have any questions for the professor? How big a demand are you having for that day of the week time code?

DR. LESCHIUTTA:

Yes. Just to give you an idea, we have received about, when we made an inquiry three years ago, about 2,000 different people asking the day of the week. Those are, it is funny, are coming from banks or from supermarkets, from very, very strange peoples.

I don't know the reason why they need exactly also the day of the week, but this happens. So we were asked especially to insert also this information.

QUESTION:

Could you give an estimate of how inexpensive and reliable you expect the timing equipment will be?

DR. LESCHIUTTA:

Yes. At the moment the equipment we are seeing is on the order of \$1,500 dollars but this is development equipment. The problem is this one: you can buy a very inexpensive frequency modulation receiver, this is not the problem, \$20 or \$30 dollars, it depends upon the class of the receiver; or perhaps more, in the region of \$200 dollars if you want a receiver with the sort of control on your selector. And the decoder itself is about 4-5 IC's, can be done, and the rest is the display. So I think that that kind can come out with the price on the order between \$300 and \$500 dollars, just to give you an idea.

VOICE ANNOUNCEMENTS OF TIME: A NEW APPROACH*

J. Jespersen, G. Kamas, and M. Weiss
National Bureau of Standards
Boulder, Colorado

ABSTRACT

A recent survey by NBS reveals that the voice time announcements provided by radio stations WWV and WWVH are used more often than any other features of the time signals. It is the purpose of this paper to describe some recent NBS work aimed at exploring a different technique for generating voice time announcements. The idea is simply this--a time code from any source, such as those broadcast by WWV, WWVH, WWVB, CHU, or the GOES satellite is translated electronically into a voice announcement. This approach is attractive for several reasons. (1) In many areas voice time announcements are weak and noisy and it is difficult to understand them. In addition, there may be interference from other "standard time broadcast" stations. It is often easy, under such conditions, to detect and error correct a time code. The "cleaned-up" time code is then electronically converted into a noise-free voice announcement. (2) Normal time broadcasts provide voice announcements only at regular intervals of time such as every minute. With the code-voice conversion technique, a voice announcement is available on demand. (3) Any time code signal may be used. Thus, the GOES satellite which

*Contribution of the National Bureau of Standards, not subject to copyright in the United States.

broadcasts only a time code, can be made to "appear" to provide voice time announcements. (4) The same time code may be converted into one or more languages at the receiver. This may be important for solving "the problem" of what language or languages should be broadcast from a standard time satellite broadcast. That is, it may not be necessary to broadcast any voice announcement in any language from the satellite--only a code--and the receiver would contain the option to select the language desired.

NBS has developed equipment to convert time codes from several different sources into voice announcements. Although the emphasis in this development work was intended to demonstrate technical feasibility, rapid progress in the production of commercial electronic voice generation units will, no doubt, make the approach suggested here feasible both technically and economically in the near future.

INTRODUCTION

One of the most useful and popular services offered by the NBS is the shortwave time and frequency broadcasts from radio stations WWV (Fort Collins, Colorado) and WWVH (Kauai, Hawaii). Over the years these broadcasts have evolved from a simple service used primarily for frequency calibration, to today's signals which provide time and frequency information by codes and voice. A recent survey ^[1] reveals that the voice time announcements are used more than any other feature of the signal. It is the purpose of this paper to describe some recent work in the NBS Time and Frequency Division which is aimed at exploring a different

technique for providing voice time announcements. This approach, made more attractive by recent advances in solid state electronics, seems ideally suited for time broadcasts. The idea is simply this--a time code from any source, such as those broadcast by WWV and WWVH is translated, by electronic means, into a voice time announcement (See Fig. 1). Thus, although the input time information is in the form of a code, the output is a voice announcement. One advantage of this approach is that any coded time signal can be converted into voice. There are other implications, as we shall see in the next section.

PROBLEMS WITH PRESENT VOICE TIME BROADCASTS

Many time services, particularly those in the shortwave ranges, have difficulties. First, in many areas, signals are weak and noisy and it is hard to understand the announcement. Second, there are many world wide standard time broadcast stations operating at the same frequency, e.g., 10 MHz, so that a particular location may experience interference. Third, because of competition for radio spectrum space, pressures to reduce the bandwidth now allocated for standard time broadcasts may develop.^[2] Any such bandwidth reduction will tend to make the voice announcements even less clear, particularly if the present double-side-band, AM modulation (DSBAM) techniques are retained. Fourth, the need for voice time announcements is world wide, so announcements must be provided in many different languages, and in some cases in more than one language by a single stations. For example, the Canadian Standard Time signal station, CHU, broadcasts both English and French. Fifth, time voice announcements are available only at regular intervals of time. For example, WWV and WWVH provide voice announcements only on the minute. This means the user cannot obtain voice announcements on demand. The time-code-to-

voice conversion approach discussed in this paper addresses these five problem areas.

ADVANTAGES OF TIME-CODE-TO-VOICE CONVERSION APPROACH

In regions where voice reception is difficult, the human mind is usually the best and only "integrator" available to extract the voice announcement from noisy, fading signals. Although it is possible, in principle, to construct electronic devices to integrate voice signals it is not easy or cheap. Although many standard time stations broadcast at several frequencies simultaneously, there are many times when no static-free signal is available.

Compared to integrating voice signals, integrating a coded signal is relatively easy. Most time signals are coded in a straightforward way. As an example, the time codes carried by WWV and WWVH are a modified version of the IRIG-H format. Data is broadcast on a 100 Hz subcarrier at a one-pulse-per-second rate. The time frame is one minute long and each frame contains minute, hour and day information as well as the "UT1 correction", which is used primarily by navigators for celestial navigation. In the presence of noise, errors in this code can be detected by simply comparing several successive "decodes" of the signal. If, for example, three "decodes" step along in the proper time sequence, it can be assumed that the time code is being correctly decoded. If, on the other hand, there is a "misstep", the time code signal output can be made to "flywheel", on the receiver's internal clock, until there are successive, correct decodes.

INTERSTATION INTERFERENCE

The problem of interference between standard time broadcast stations operating at the same carrier frequency is serious and continues to grow as more stations start up in different parts of the world.^[3] Various solutions have been considered. One is to stagger the carrier frequencies at 4 kHz intervals within the allocated band. The bandwidth for these stations is ± 10 kHz at the standard broadcast frequencies of 15, 20, and 25 MHz and ± 5 kHz at frequencies 2.5, 5 and 10 MHz. The difficulty with this suggestion is that those stations assigned frequencies near either end of the allocated band would have to change from DSBAM to some other form of modulation to avoid "spilling" over into adjacent radio spectrum reserved for other purposes. In addition, some experiments have been conducted with these staggered allocations and there is still serious distortion due to interstation interference in commonly used shortwave receivers.

An alternative would be to have each standard time station broadcast a time code signal which is located in the time-frequency domain so that it can be selected without interference from other stations. As a simple illustration, suppose there are ten standard time broadcasts which might potentially interfere with each other, all operating at a nominal 10 MHz carrier frequency. We could imagine a 10 second segment, say, out of each minute during which each station broadcasts a time code for 1 second, or less, while the other nine stations are off the air. Each station broadcasts in turn throughout the 10 second sequence and the process is repeated throughout each minute. Such a routine would require time coordination among the participating stations, but this should not be difficult in view of the fact that these stations maintain time to within at least 1 ms of UTC.

A specific example of a code that could be used is one that is now being broadcast over the Canadian standard time station, CHU. A complete message is 0.365 seconds long and contains day, hour, minute, and second information--repeated twice for error checking. The code employs the standard commercial 300 baud FSK system with tones at 2025 and 2225 Hz. Since the message is short it does not interfere with the "seconds" ticks provided by CHU.

The time sharing scheme suggested here (or some variation on it) would provide interference-free time code signals part of the time out of each minute, and thus has some utility. But such a time-shared code coupled with a code-voice conversion unit could provide interference-free voice time announcements.

The time sharing scheme discussed here is not the only possibility. Frequency division multiplexing could also be employed. That is, each standard time broadcast station would be assigned a unique frequency in which to broadcast its time code, and other stations would be excluded from this spectral region. One of the difficulties with this approach is that if any aspect of the communication channel is non-linear then new frequencies will be generated which may spill over into adjacent channels. Thus, the spacing between adjacent channels would have to be increased to avoid overlapping signals.

A final example is spread spectrum techniques, which have the advantage that they minimize effects of nonlinear elements in the transmission channel (along with some other advantages) at the cost of a more complex receiver. While the time and frequency sharing schemes discussed in the previous paragraphs are widely employed and are essentially self explanatory, spread spectrum techniques may be less well known to the reader. Appendix I is a

rather elementary treatment of spread spectrum as it might apply to several standard time broadcast stations operating at the same frequency, f_c .

SPECTRUM CONSERVATION

The radio spectrum is a scarce natural resource and pressures to use it efficiently mount steadily. As pointed out, a voice time announcement uses considerably more bandwidth than is required to transmit the actual information content of the message. Thus an obvious advantage of a time-code-to-voice conversion approach is that the communication channel requirements are more in accord with actual information content of the message. Note there is presently an international allocation for the broadcast of time from a satellite. This allocation is ± 50 kHz wide and is centered at 400.1 MHz. Because of the worldwide need for voice time announcements and the large area covered by satellites a difficult question is raised: "What language or languages should be broadcast from the satellite?" In addition, there is a continuing worldwide need for improved time accuracy, beyond the accuracies shortwave broadcasts can provide. This means that a certain part of the allocated satellite band must be reserved for providing a signal whose time of arrival at the receiver can be measured precisely--the more precise this measurement the greater the signal bandwidth required for a given measurement interval. If the allocated band is used up by numerous voice announcements in a number of different languages, the ability to provide accurate time from a satellite is severely compromised. Aside from this technical difficulty is the political problem of deciding which languages to broadcast. If a code-voice conversion approach is adopted, the satellite decoder could be made to speak any language. The political problem is avoided and maximum bandwidth is available

to design a signal which can provide high accuracy time signals.

TIME ON DEMAND

Finally, the code-voice conversion approach allows the user to obtain a voice announcement on demand. He does not have to wait for the next voice announcement to "come up" in the time signal format. Although we have been discussing this feature with primary reference to the standard time broadcasts, it has potential application in other areas. For example, it is technically possible to insert, unobtrusively, time coded information into almost any kind of broadcast signal, e.g., AM, FM, and TV. In principle, all existing broadcast facilities are potential candidates to provide voice time announcements on demand.

One might wonder, why go to the trouble to convert the time code to a voice announcement? Why not simply display the time visually with LED's or perhaps use the code to keep an analog wall clock on time. Certainly in many cases this is desirable. On the other hand, there are many instances when people are processing several different information inputs at once. An airplane pilot may be scanning his instrument panel while he is listening to a voice announcement of the time, or perhaps watching his altimeter reading. Also, voice signals can be heard around corners while visual displays must be within line of sight of the viewer. In any case, for whatever reasons, the NBS survey clearly shows that the most desired feature of the standard time broadcasts is the voice announcements.

DESCRIPTION OF NBS TESTS

Basically, two different speech compression schemes have been investigated for time-code-to-voice conversion: waveform coding and source coding. In waveform coding a facsimile of the original acoustical signal form is retained. An example of waveform coding is to simply sample the acoustic signal at some specified rate, such as 32 k bits/sec, and store the bits in some memory device. To reproduce speech the process is reversed. The bits are read out of memory into a D/A converter which produces a replica of the original waveform. The degree to which the replicated waveform resembles the original waveform depends, of course, upon the sampling rate: the higher the sampling rate, the better the resemblance. Although this is conceptually a straightforward process, there are other related techniques which are easier to implement and which retain the same degree of fidelity, but use lower sampling rates. One such technique, called continuously variable slope delta (CVSD) encoding, was employed in the present tests. We shall describe this technique more thoroughly a little later.

The other technique, source coding, does not reproduce a replica of the original acoustical signal. When this technique is applied to speech it is called voice coding and the devices which perform the codings are generically termed "vocoders". The essential idea behind vocoding is that a model of the human voice system is created electronically or mechanically. A mechanical model might consist of a bellows, a vibrating reed, acoustical resonators resembling the mouth cavity, and so forth. This machine could be operated somewhat along the lines of a player piano to produce speech. The actual data required to generate speech with this machine is simply whatever data needs to be stored on the "piano

roll". Sophisticated electronic versions of this machine can produce intelligible speech with data rates as low as a few kilobits or less per second, although the speech sounds artificial. Sophisticated versions of the waveform coding technique, discussed earlier, succeed with rates as low as 5 k bits/sec or so, but speaker recognition is difficult at these rates. For time announcements speaker recognition is not important, but of course, intelligibility is essential.

A primary goal of waveform or source coding is, of course, to remove redundancies in the acoustic waveform so that channel communication requirements can be reduced, or in our application, to keep memory requirements in the time-code-to-voice conversion unit to a minimum. In the general case one would like to be able to send any arbitrary message. Here some arbitrary acoustic signal is coded (source or waveform) to remove redundancies. Since most real communication channels are subject to noise and other problems which introduce errors, the output of the acoustic coder will usually be recoded (channel encoded) to minimize errors introduced in the communication channel. That is, extra bits of information will be added to the data stream for error correction and detection. Thus, the acoustic coder removes redundancies and the channel coder introduces them again, but in a way that is designed to minimize errors introduced by the channel.

In the case of time signals it is not necessary to send arbitrary messages. A time signal message can be assembled in English from about 30 words: one, two, three, four, . . . minutes, hours, seconds, etc. Thus there is no need to initially code a voice announcement of time. The signal can originate as a code. We could at this point, if we wished, introduce extra bits of information for error detection and correction. But, because time

codes are by their very nature quite redundant, this redundancy in itself may be sufficient to overcome channel distortion.

The limited vocabulary also simplifies requirements at the receiver. The memory necessary at the time-code-to-voice conversion receiver need only be sufficient to store 30 words or so of vocabulary. In the next two sections we describe the use of both source and waveform coding to minimize memory requirements at the receiver.

DESCRIPTION OF NBS WAVEFORM CODER TESTS

This system consists of a receiver (WWVB, GOES Satellite, etc.), an A/D converter and storage system, an internal crystal oscillator clock and a processor. The processor performs several functions after receiving a time code from some source. First the processor sets its internal clock only after receiving three consecutive successful decodes. At this juncture the processor turns on the "Time Valid" light. The internal clock is accurate to 1/2 second in 30 minutes so that if 3 consecutive successful decodes are not obtained at least once every 30 minutes the "Time Valid light" goes off and the system will not output a voice announcement.

When time is requested, the processor decides which words, stored in the Read-Only-Memory (ROM), need to be assembled to provide the correct voice time announcement. These words are then converted to analog by the A/D converter. The voice announces time for begins 10 seconds after the initial request concluding with an "on-time" audio tone.

The A/D converter is a continuously variable slope delta (CVSD) modulator which samples the analog signal at 57.6 kbits/second.

The output of the converter is a string of 0's and 1's which indicate increases or decreases in the analog voltage. These bits are stored in memory. The amount of increase or decrease, of the slope, reflected by these numbers, depends upon the past history. At the beginning of a waveform the slope is always some fixed value. After 3 consecutive increases or decreases the slope is increased until the coded digitized output steps over the top, or under the bottom of the analog waveform (see Fig. 2).

When a voice announcement is requested, the CVSD turns the 0's and 1's back into an analog signal using exactly the same algorithm. At 57.6 kilo-bits/sec individual speakers are recognizable.

The necessary vocabulary and the tone have been digitized previously with the same CVSD modulator and stored in ROM. The vocabulary is: the digits "one", "two", . . . , "nine"; the words "twenty", "thirty", "forty", "fifty"; the word "teen", with special preambles, "fif", "thir", "fort"(for 14), and "ninet"(for 19); the single-use words, "zero", "ten", "eleven", and "twelve"; and, finally, the words for the beginning message, "National", "Bureau", "of Standards' Time". The memory required for the words and tone is 91,968 bytes or 735,744 bits. The digits are used both individually and as post-ambles for "twenty" through "fifty". In addition, "six", "seven", and "eight" are used as pre-ambles for "teen". Recording the words requires great care in maintaining a constant level, a continuous cadence, and a flat intonation so the different word "pieces" meld smoothly. It is important to carefully determine pause-time between words, and to notice that the "four" in "fourteen" and the "nine" in "nineteen" are different from the single digit sounds in creating natural sounding speech.

DESCRIPTION OF NBS VOCODER TESTS

As explained, the vocoder type of voice recording and reproduction depends on having prerecorded sound segments in the computer memory. Usually these sounds are simply the necessary parts of words that can be selectively joined by software to make a word. An example illustrates the problem of trying to form words in this manner. Using the common word "you", the programmer looks through the recorded options available in his set of sounds. After trying a number of combinations with various durations (long, short, etc) the programmer settles on EEUUU as best representing the spoken word "you".

Experience with voice generation in this manner soon leads to a rather extensive list of sounds with slight variations. A large list is necessary so that the final word sound is acceptable. Since pauses and sound duration are usually programmable, the number of possible combinations is very great.

This leads to the problems of using a Vocoder technique. The final sound is only as good as the programmer's ability and patience allows. Even if a single word is acceptable in quality, the following word may not sound acceptable when used in conjunction with the first. This problem plus the general one of being unable to completely overcome the machine-like sound of vocoders helped in making the decision to use a straightforward waveform digitizer for natural sounding words.

The NBS tests of a vocoder type of word generator used a commercial voice synthesizer. This was a proprietary instrument that had many variations of a single sound. The results did improve as the programming was altered after listening tests, but the final

output was felt to be unacceptable due to its machine-like sound qualities. Some thought was given to finding a very experienced programmer. Several companies that deal with such devices do offer to provide programs. This is apparently based on their experience and on having gained a repertory of words. This approach was considered, but rejected on the basis of cost and quality of the finished work.

Worth mentioning is the ability of listeners to adapt to slightly unfamiliar sounds. Listeners are almost always able to understand the spoken text after only a few practice sessions. The first time is hardest and it was felt that many users of a talking clock would be first time users, i.e. for a telephone time of day service.

Given such a comprehensive list of available sounds, any language can be output from the vocoder. Russian and French words were easily synthesized.

EXISTING CODED TIME SIGNALS

Throughout the world there are a number of coded time signals. We have already mentioned WWV, WWVH, CHU, and WWVB which was the time signal source for the NBS tests described in the previous two sections. Perhaps one of the best candidates for the time-code-to-voice conversion approach is the NBS satellite time code. This code is provided by two geostationary, meteorological data collection satellites (the GOES satellites) operated by NOAA. A time code is included as part of a satellite interrogation signal which is used to communicate with remote data collection devices. The time signal, which contains day, hour, minute, and second information allows the meteorological data to be tagged in time. But anyone within the coverage area can obtain the time signals

with receivers now commercially available. As shown in Fig. 3, the signals cover essentially the entire western hemisphere. The signal frequencies are near 469 MHz so they are not subject to the kinds of problems that plague broadcasts in the shortwave band: fading, interstation interference, etc. Thus a voice conversion unit driven by a GOES time signal would provide voice time announcements which are at least an order of magnitude more reliable than those now available from standard broadcasts in the shortwave band.

CONCLUSIONS

The tests discussed in this paper were primarily undertaken to demonstrate the utility of a code-voice conversion approach to time announcements. This approach leads to gains in a number of areas such as spectrum conservation, clear voice announcements in the presence of noise, and voice announcements on command and in any language. It was not our intent to design a device with minimum complexity, although this is obviously an important goal if the system is to be economically feasible. When the tests were first initiated component costs were in the hundreds of dollars. But devices are now coming on the market, in the \$10 or less range, providing several hundred words of vocabulary. This is more than adequate for time announcements which typically require a 30 word vocabulary. It seems apparent then that in the not too distant future a time-code-to-voice conversion approach to time announcements is entirely feasible.

REFERENCES

1. "Report On the 1975 Survey of Users of the Services of Radio Stations WWV and WWVH", NBS Technical Note 674, J.A. Barnes and R.E. Beehler.
2. Private Communication R.E. Beehler.
3. Ibid.
4. R. C. Dixon, Spread Spectrum Systems, John Wiley and Sons, 1976.

APPENDIX I

Consider stations broadcasting signals $s_1(t)$, $s_2(t)$, $s_3(t)$, . . . $s_n(t)$. Quite generally, the desired signal from the j th station is:

$$s_j(t) = A_j(t)\cos(2 f_c t + \phi_j t)$$

where $A_j(t)$ represents amplitude and $\phi_j(t)$, angle modulation. Before broadcasting, $s_j(t)$, it is multiplied by a time function $g_j(t)$ which has the property of spreading the original signal $s_j(t)$ over a bandwidth considerably greater than the original. Each standard time broadcast station would be assigned a unique $g_j(t)$. Now suppose we are located in an area where all n signals can be detected and we wish to extract, say, $s_1(t)$ from the others. If we multiply the incoming composite signal by $g_1(t)$ we obtain:

$$g_1(t)^2 s_1(t) + g_1(t)g_2(t)s_2(t) + g_1g_3s_2(t) + g_1(t)g_3(t)s_3(t) + \dots g_1(t)g_n(t)s_n(t).$$

If the $g_j(t)$ signals have the property that $g_j(t)g_j(t) = 1$ and $g_j(t)g_k(t) = 0$, then the only output of the multiplier is $s_1(t)$, the wanted signal, while all others are suppressed.

As a final point, we have assumed that all n signals entering the multiplier are spread at the transmitter by some function $g_j(t)$, which in actual practice will probably not be the case. But even here, unspread or cw type signals will be spread by the multiplier $g_j(t)$ at the receiver, so that spread spectrum technique still yields an advantage. [4]



Figure 1. Code to Voice Converter

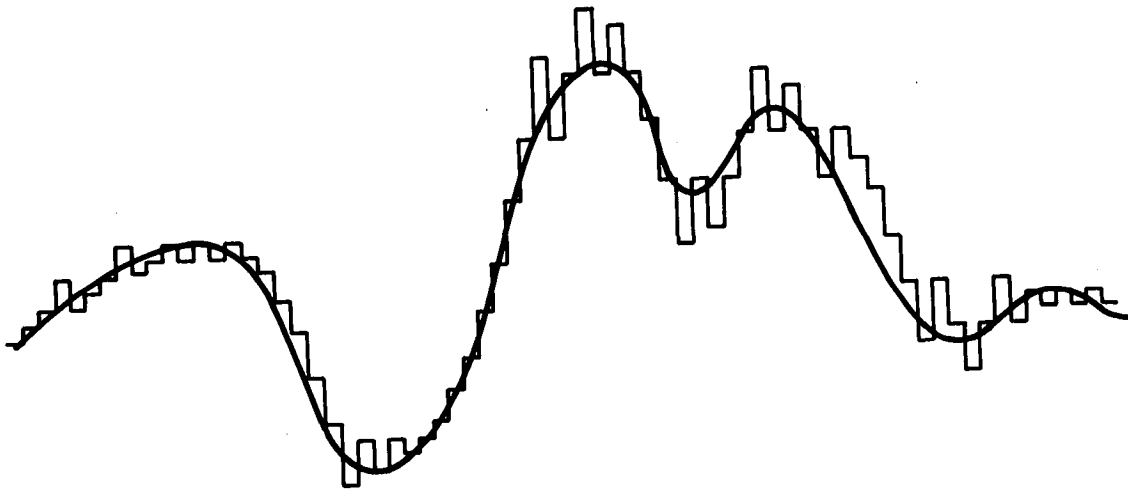


Figure 2. This Figure Demonstrates How the Magnitude of the Converter Output is Related to the Slope of the Waveform

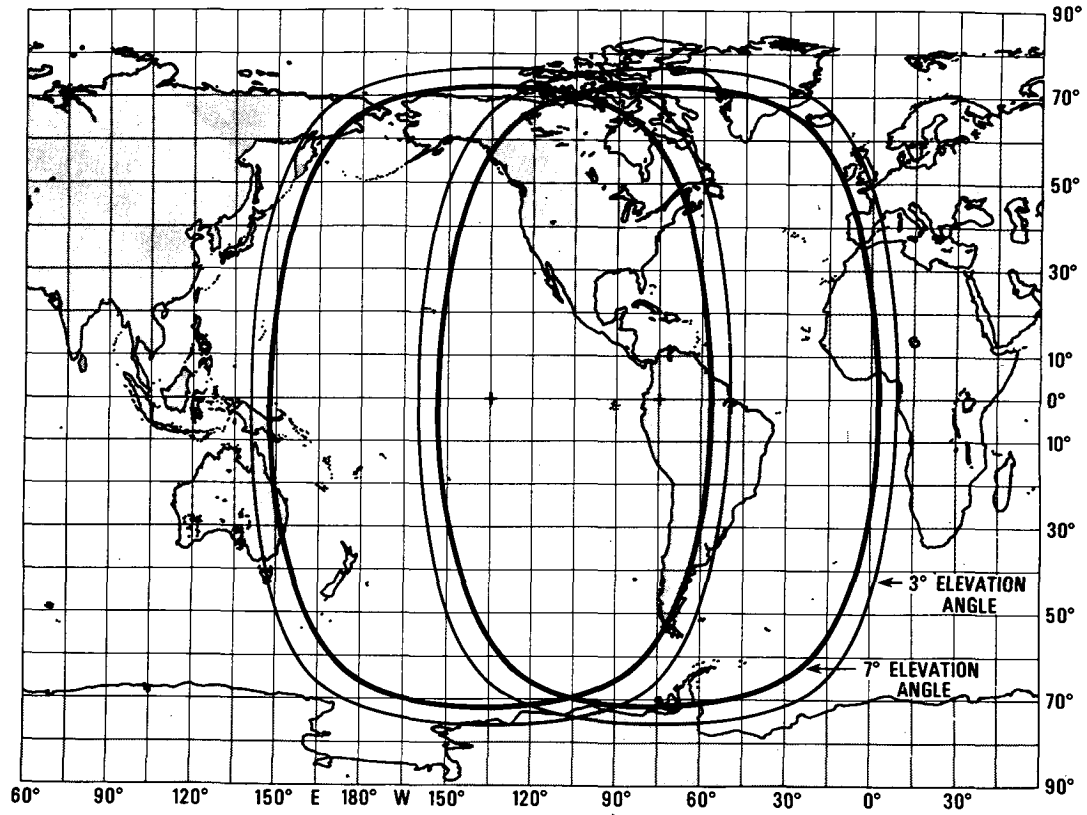


FIG. 3. Coverage of the GOES Satellite.

QUESTIONS AND ANSWERS

QUESTION:

Does this work and tell all about time in any language or is that in it?

DR. JESPERSON:

I think about any language. You need to record the numbers 1, 2, 3, so that you can say, "One two hours, zero three minutes, one five seconds".

QUESTION:

Will that do it? Is that true?

DR. JESPERSON:

I am not claiming that is true, but I think the point I am trying to make is let us suppose it is 100 words in some language. Even at that, I think with the price that these so-called talking devices are going to be, it is not going to make a lot of difference whether it is 30 words or 100 words.

For example, the weather forecast, it looks like it is going to take about 200 words, in English, to assemble the kind of weather forecast that the Weather Bureau normally puts out.

Yes?

QUESTION:

One problem that you might mention with the \$30 dollar vocoders are in fact that due to its linear position it is not a high-quality sound recording.

DR. JESPERSON:

Right. I think this is one of the questions that I think has to be sort of cleared up and I don't know how you do this exactly except to try it. I think it boils down to the question of what is more important in a time announcement or a weather forecast, is it being able to recognize somebody's voice or is it making certain the information gets there? I would tend to think that the people who really have need of this information would be more concerned about getting the information rather than being worried about whether they could recognize whose voice it was or even whether it sounds a little bit mechanical or not.

QUESTION:

Do you want to limit it to that?

DR. JESPERSON:

That is true. We are aware of that.

QUESTION:

We found that that is not true at all. We want it to sound pretty good.

DR. JESPERSON:

As I say, this technology is very rapidly changing. There are very sophisticated algorithms being produced. You mentioned linear predictive coding. Again, talking to some of the people who are working actively in this area, they think in the not too distant future they are going to come up with some very natural sounding devices that will be very low-cost.

They tell me that we are going to start seeing these things in consumer products fairly soon. You know, your oven tells you that the roast is done and there is going to be a huge market for these things.

QUESTION:

They are even going to be able to give lectures.

QUESTION:

I just wondered if you were aware of the FAA program in Washington where they are now giving weather reports via the phone by just pushbutton entry on the phone. I believe that is underway on phones.

DR. JESPERSON:

No, I wasn't aware of that.

QUESTION:

And you can just put in any three digit code for an airport and receive a computer talking to you, giving you the weather at that airport.

DR. JESPERSON:

And this is assembled from a vocabulary of words? No, I wasn't aware of that.

QUESTION:

It was initiated, I believe, approximately 6 months ago.

DR. JESPERSON:

Do you know, does the National Weather Service know about that?

QUESTION:

I wouldn't be surprised if they didn't.

DR. JESPERSON:

I won't comment on that.

QUESTION:

The National Weather Service knows about this thing, and they will need to build several thousand of these touch tone things for some of these facilities that are--

DR. JESPERSON:

How are those stored? On tape or something?

QUESTION:

Stored on magnetic tape for savings. Anybody that likes that though will find out that the Weather Bureau will not really like it.

DR. JESPERSON:

Thank you.

SESSION V

RECENT ADVANCES

**Dr. Donald L. Hammond
Hewlett Packard**

A STUDY OF TIME DISSEMINATION VIA
SATELLITE IN INDIA

B. S. Mathur, P. Banerjee, P. C. Sood,
Mithlesh Saxena, Nand Kumar and A. K. Suri
National Physical Laboratory, New Delhi, India

C. L. Jain and K. Kumar
Geodesy Division (RSA)
Space Applications Centre, Ahmedabad, India

ABSTRACT

The availability of French-German satellite Symphonie, coupled with the increasing demand on accuracy and coverage by the Indian users, provided an opportunity to carry out time transfer experiments with satellite, thus to enable us to have some gainful experience on the merits and demerits of different possible modes of time transfer via satellite. We report some of these observations and analysis in this paper.

A simultaneous two-way clock synchronization experiment between three Earth stations, New Delhi (DES), Ahmedabad (AES) and Madras (MES) was performed and improvements over the technique earlier attempted in India, where transmit/receive roles of the two stations were alternated at regular intervals, were studied.

The National Physical Laboratory, New Delhi (NPL) has been disseminating standard time and frequency signals, under the call sign "ATA," at three carrier frequencies, 5, 10 and 15 MHz. To study the improvements over the existing HF broadcast, a similar time format as used in HF "ATA" transmissions was disseminated via satellite Symphonie and was studied at DES, AES, MES and the mobile terminal TRACT located at Calcutta. The Time signals via these two modes (HF and satellite) were critically monitored at AES and analysed.

This time format was later modified to include the additional information about time of the day in year, month, day, hour, minute and second as well as DUT1 in BCD code and was disseminated via the satellite from DES. These signals were decoded, displayed and studied at DES, AES, MES and with TRACT at Calcutta, thus covering a very large cross-section of India.

Some preliminary work on time transfer via TV using direct satellite broadcast, is also reported. These studies, which yielded encouraging results, will be useful when different TV stations are linked via Indian satellite INSAT.

INTRODUCTION

In this paper we report a study of time dissemination over India, using French-German satellite Symphonie which was parked over equator at 49° East Longitude and was made available to India for two years, from June 1977 to June 1979, for doing telecommunication experiments. Three satellite Earth stations at Delhi (DES), Ahmedabad (AES), Madras (MES) and the Transportable Remote Area Communication Terminal (TRACT), stationed at Calcutta during the period of the experiments, participated in the experiments. In view of the vastness of the country and the Indian Space Programme, where an experimental satellite Ariane Passenger Payload Experiment (APPLE) and an Indian National Satellite (INSAT) are to be launched in 1980 and 1981 respectively, the aim of these experiments was to make preliminary studies on various time dissemination techniques via satellite which will provide helpful inputs and generate the desired expertise for the ultimate use of these by the Indian satellites APPLE and INSAT. These experimental studies were carried out during January - June 1979 period.

The experiments described in this paper include: simultaneous two-way clock synchronization between Delhi and Ahmedabad, Delhi and Madras and nearly simultaneous⁽¹⁾ three-way alternate transmit/receive clock synchronization experiments between Delhi, Ahmedabad and Madras; time dissemination, both in standard high frequency broadcast format (ATA) and time of the day coded format, and its studies and evaluation at Delhi, Ahmedabad, Madras and TRACT (Calcutta); and time dissemination using direct television broadcast via satellite.

SIMULTANEOUS TWO-WAY CLOCK SYNCHRONIZATION BETWEEN DELHI AND AHMEDABAD/MADRAS AND A NEAR SIMULTANEOUS⁽¹⁾ THREE-WAY CLOCK SYNCHRONIZATION BETWEEN DELHI/AHMEDABAD/MADRAS.

A block diagram of the experimental setup is shown in Figure 1. An experiment on clock synchronization where the transmit/receive roles of the two participating stations were alternated at regular intervals was reported from this group in the tenth PTTI meeting⁽¹⁾ last year. This limitation arose because out of the two C-band transponders aboard Symphonie, only one was made available for Indian Telecommunication Experiments. This, however, introduced uncertainties due to the satellite motion as extrapolations were needed to account for the satellite drift. A typical Symphonie range curve over the duration of 24 hours is shown in Figure 2. The straight line represents the range from satellite to AES and the dotted line represents the range from satellite to DES.

In view of these limitations, the interface units and modulator/demodulator systems at the Earth stations were modified to accommodate simultaneous two-way transmission within the available bandwidth of ± 10 MHz of the 70 MHz intermediate frequency. Bandpass filters centered at 70 MHz and 61 MHz with bandwidths of ± 1.1 MHz were used for the simultaneous two-way transmissions.

At Ahmedabad (AES), 1 PPS was modulated on the 70 MHz intermediate frequency. This 70 MHz was converted to 61 MHz using a 70 to 61 MHz frequency translator. This 61 MHz was up-converted to 6 GHz and transmitted to satellite. At Delhi (DES) the signal was received at 4 GHz, down-converted to 61 MHz and again

converted to 70 MHz, using a 61 to 70 MHz frequency translator. It was demodulated to extract 1 PPS. At DES the 1 PPS transmission was done at 70 MHz modulation, as normal, up-converted to 6 GHz and transmitted to satellite. At AES, this signal was received at 4 GHz, down-converted to 70 MHz and then demodulated after passing through 70 MHz ± 1.1 MHz bandpass filter to eliminate the reflected signal at 61 MHz.

There were, however, some inherent limitations in this mode of clock synchronization. Only a limited bandwidth (± 1.1 MHz) was available for each way of transmission and thus some advantage gained in simultaneous mode of transmission was lost due to sacrifice in the risetime. Also the 1 PPS amplitude was reduced to 0.5 volt as the 1 volt peak amplitude signal, which was used with the earlier system with full bandwidth of ± 10 MHz, caused a deterioration of SNR in the received signal due to excessive frequency deviation. The frequency translators and bandpass filters used at the Earth stations introduced fixed delays in the transmission path.

The data for simultaneous two-way mode of transmission between DES and AES for 28, 29 and 30 March is plotted in Figure 3. Simultaneous two-way clock synchronization experiments were also conducted between Delhi and Madras (MES) Earth stations with similar results. The precision obtained, even with the above limitations, was 4-5 times better than the earlier quoted results⁽¹⁾. A relative drift of the two cesium clocks at DES and AES is quite noticeable in this figure.

In absence of proper portable clock time comparisons between the three Earth station clocks, a three-way check on clock settings was obtained between DES, AES and MES by alternately one station transmitting and the other two receiving, as shown in Figure 4, and exchanging the data over the radio network or hot telephone lines among the three Earth stations. Discrepancies of submicrosecond nature were observed in these clock settings of the three stations. These were due to satellite motion not being accounted for properly and different propagation delays encountered at three Earth stations, even though the instrumentation at all ends was based on the same design. The lack of communication due to occasional break-downs of radio network and hotline channels between DES, AES and MES as well as limited experimentation time were the other limitations. As the system was not designed for simultaneous two-way transmissions, changing from one system to the other also presented some technical inconveniences.

As a practical use of this technique on 30th June 1979 a recently procured atomic cesium clock for the STARS project at Kavalur, near Madras, was brought to MES and synchronized to submicrosecond precision in the near simultaneous three-way alternate transmit/receive mode between DES, AES and MES.

DISSEMINATION OF HIGH FREQUENCY TYPE TIME FORMAT (ATA) VIA SATELLITE SYMPHONIE

The National Physical Laboratory, New Delhi has been transmitting standard time and frequency signals⁽²⁾ at 5, 10 and 15 MHz under the call sign 'ATA.' The time format transmitted is shown in Figure 5. The accuracy limitations of high frequency broadcast are quite well known. One-way time transmission technique via satellite provides not only wide coverage but also a more accurate

time synchronization means, due to a stable path, as compared to ionospheric propagation. In view of these and in accordance with the national plan to, ultimately, disseminate time via Indian Satellite INSAT, a time format similar to ATA (HF) was disseminated via satellite Symphonie and experimental studies were made at Delhi, Ahmedabad, Madras and with the mobile terminal at Calcutta. The major part of the studies were, however, concentrated between DES and AES. A block diagram for the experimental setup of ATA format dissemination via satellite is shown in Figure 6. At AES, ATA (HF) data via ionosphere was, side by side, recorded for the sake of comparison with the satellite data.

The ATA format data via ionosphere and satellite, as received at AES, are plotted in Figures 7 and 8 along with the standard deviation from the best line fit. In Figure 9 is shown comparison of ATA format via satellites with 1 KHz bursts; ATA format with 1 MHz bursts where 1 KHz signal of Figure 5 was changed to 1 MHz signal; and 1 PPS transmissions from a cesium standard. These signals were transmitted from DES and monitored at AES. The corresponding standard deviations are also shown in the figures. It is clear from these that the precision achieved by using 1 KHz signal is of the same order as that with 1 MHz or 1 PPS implying a great saving on bandwidth without sacrifice in the precision.

DISSEMINATION OF TIME OF THE DAY CODED FORMAT

The ATA format was later modified to include time of the day information in year, month, day, hour, minute and second and DUT1 information in BCD code. A slow code was used and is shown in Figure 10. The block diagram of the experimental setup is shown in Figure 11. The encoding scheme is shown in Figure 12 and the decoding scheme in Figure 13. Initially, rectangular pulses were tried but these got differentiated by the interface units and the information about time was lost. Later, sinewave pulses were transmitted and rectangular pulses were generated from the received signal.

The time via satellite along with DUT1 information was displayed and studied at Delhi, Ahmedabad, Madras and with the mobile terminal at Calcutta.

As in the previous case with ATA format, no corrections were applied for the propagation delays, neither the satellite orbit elements were disseminated along with the timing information. These will, however, be incorporated in the future satellite controlled clocks to be operated via Indian satellites APPLE and INSAT.

DISSEMINATION OF TIME VIA DIRECT TELEVISION BROADCAST BY SATELLITE

Time synchronization via television, using both passive and active techniques, is a common practice in many countries. A line 10 sync separator circuit was developed for using with land television systems. The availability of satellite Symphonie provided an opportunity to try this technique using the direct TV broadcast between Delhi and Ahmedabad. The scheme of pulses in vertical blanking interval of Indian TV format is shown in Figure 14.

The block diagram of experimental setup is shown in Figure 15. The circuit diagram for a TV line -10 pulse identifier is shown in Figure 16. The TV

signals were transmitted from Delhi to Ahmedabad via satellite. The TV sync separator identified line 10 of the odd field with an ambiguity of 40 milliseconds. As the propagation delay between DES and AES via satellite and between DES to satellite and back to DES were of the same order of 250 milliseconds, the time interval counter at DES was started with the local cesium clock 1 PPS and stopped with the reflected TV sync separated pulses from the satellite and the time interval counter at AES was started with local cesium clock 1 PPS and stopped with the same DES transmitted TV sync separated pulses received at AES. If C_{11} is the time interval counter reading at DES, C_{12} is the corresponding time interval counter reading at AES, T_1 is the propagation delay from DES to satellite and back to DES and T_2 is the propagation delay from DES to AES via satellite; all C_{11} , C_{12} , T_1 and T_2 correspond to the same TV sync pulse, then:

$$\begin{aligned} \text{Clock off set } (\tau) \text{ between DES and AES is} \\ &= (C_{11} - T_1) - (C_{12} - T_2) \\ &= (C_{11} - C_{12}) - (T_1 - T_2) \end{aligned}$$

The procedure adopted for the measurements was as follows: The DES and AES clocks were first synchronized to as close a value as possible, to within a fraction of a microsecond, by using nearly simultaneous technique⁽¹⁾. This was done to check TV synchronization results and to gain confidence in the TV measurements via satellite. In the beginning and at the end of TV measurements, the propagation delays of 1 PPS transmitted from DES were noted at DES for the reflected pulses via satellite (T_1) and at AES for the same transmitted pulses via satellite (T_2). From these measurements the ($T_1 - T_2$) data, corresponding to the respective TV line 10 measurement time, was deduced by using Lagrangian Extrapolation. The ($C_{11} - C_{12}$) and ($T_1 - T_2$) data of TV readings and the propagation delays at DES and AES for 27th and 28th April are plotted in Figure 17 along with the mean difference of the two sets of readings and the standard deviations. From this data it is clear that TV direct broadcast via satellite is capable of giving submicrosecond precision.

The propagation delay for the TV signals were taken care of by experimentally measuring ($T_1 - T_2$) rather than theoretically calculating it where a knowledge of satellite orbital elements is necessary. However, in routine calibrations, as in other cases, a knowledge of satellite orbital elements will be required for the clock synchronization purposes.

Due to limitation on satellite time, the experiments on active TV technique and time display via direct TV broadcast could not be carried out. The National Physical Laboratory, New Delhi is developing such a technique for use with land-line connected TV systems and will try these when next Indian satellite APPLE becomes available in 1980.

CONCLUSION

As the errors involved in time dissemination experiments via satellite are quite well known and are amply discussed in literature and in the earlier paper⁽¹⁾ presented at 10th PTTI meeting, we have not gone into these details. The standard deviations from the best line fit are calculated and shown in the respective figures.

A major limitation in these experiments has been that only one satellite transponder was available and simultaneous two-way transmission using full video bandwidth was not possible. Thus, a parallel experimental check on the precision of the measurements, in which satellite motion could be tracked simultaneously, was not possible thus necessitating extrapolations for the satellite motion.

Another limitation from practical use point of view was that satellite orbital elements were not disseminated along with the timing information. The reasons were two fold: firstly, the emphasis of these experiments was more on to develop and try out various possible time dissemination schemes via satellite and to study their merits and demerits rather than to push the limits of accuracy and precision of any single measurement; and secondly, that the satellite orbital elements were not readily available in advance and could be had only post facto.

The future Indian plans on time dissemination via satellite include some more experimentation in this direction when the next Indian satellite APPLE becomes available in 1980 with an effort to disseminate, simultaneously, satellite orbital information as well. The ultimate aim is to use Indian National Satellite INSAT, to be launched in 1981, for a general and wider time dissemination.

Towards the end of this series of experiments, a simultaneous two-way clock synchronization experiment using both the satellite transponders was performed between the National Physical Laboratory, New Delhi (NPL) and Physikalisch - Technische Bundesanstalt, Braunschweig, West Germany (PTB) in May and June 1979. These experiments were done using the facilities at Delhi Earth Station in India and Raistings Earth Station in West Germany. The results, which are under preparation, will be reported somewhere else.

ACKNOWLEDGEMENTS

The authors wish to thank the Directors STEP, ISRO and P&T for making the satellite Symphonie and facilities at Delhi, Ahmedabad Madras Earth Stations and TRACT available for this experiment. The encouragement and help received by the staff of Delhi, Ahmedabad, Madras Earth Stations and TRACT are duly acknowledged. The NPL's group will specially like to thank Mr. M. L. Hasija and his able group at Delhi Earth Station for their active involvement and keen interest in the experiments. The authors express their appreciation to Mr. G. C. Jain, Head, VIPED, RSA, SAC for developing and supplying TV sync separator. The help given by Head, TESC (SAC) by lending the atomic clock for the experiments at AES is acknowledged with thanks. The whole hearted cooperation of Telecommunication Research Centre, New Delhi through lending their sophisticated instruments, whenever needed, is thankfully acknowledged.

REFERENCES

1. Y. V. Somayajulu, B. S. Mathur, P. Banerjee, S. C. Garg, Lakha Singh, P. C. Sood, Tuhi Ram Tyagi, National Physical Laboratory, New Delhi and C. L. Jain and K. Kumar, Space Applications Centre, Ahmedabad, "Clock synchronization experiments in India using Symphonie satellite," Proc. Tenth PTTI Meeting, pp. 643-658, November 1978.

2. V. R. Singh, G. M. Saxena and B. S. Mathur, "Development of an atomic rubidium vapour frequency standard at NPL of India using indigenous sources," Proc. Ninth PTTI Meeting, pp. 437-461, March 1978.

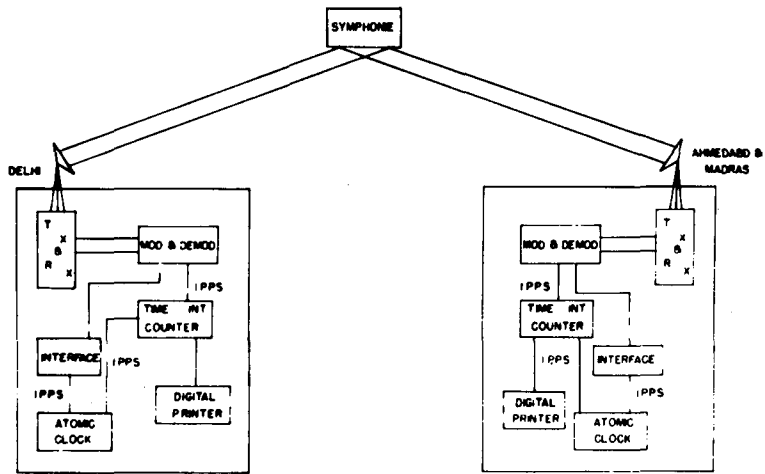


Figure 1. Block Diagram of Simultaneous Two Way Clock Synchronization Experiment

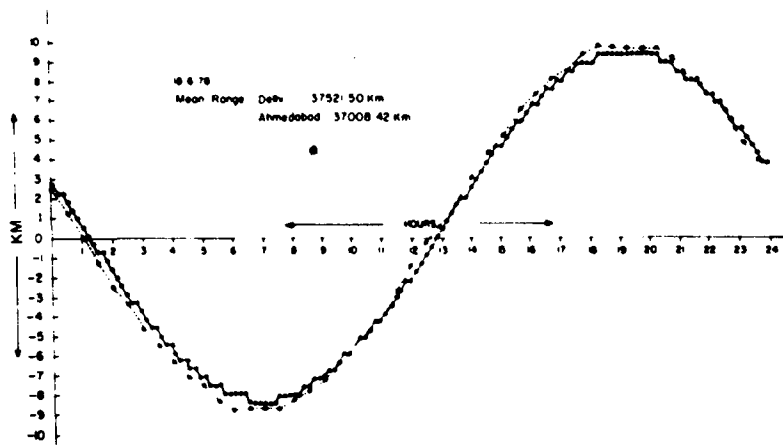


Figure 2. Variation of Satellite Range

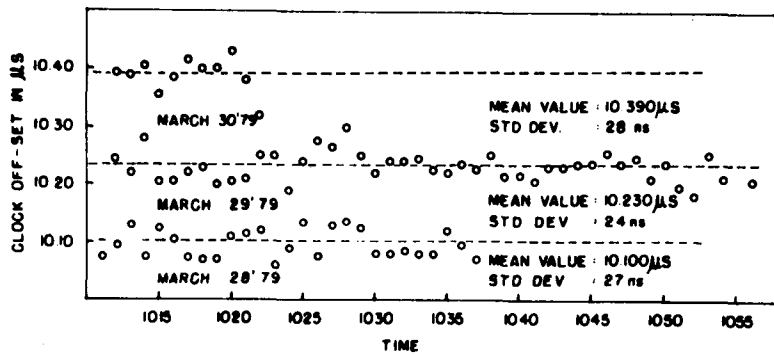


Figure 3. Simultaneous Two Way Time Comparison Between Delhi and Ahmedabad

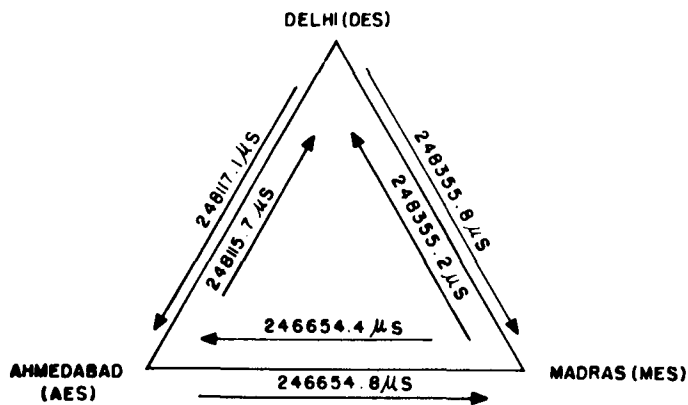


Figure 4. Three Way Time Comparison Between DES-AES-MES

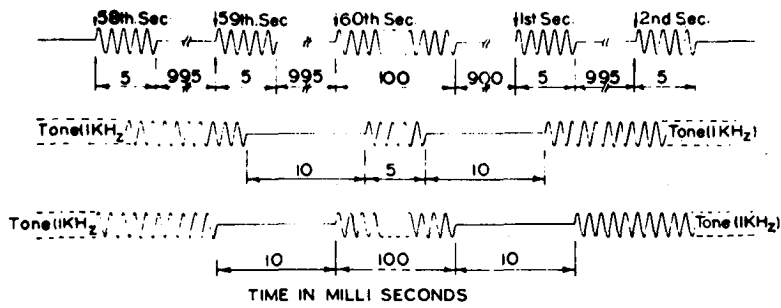


Figure 5. Time Format of ATA Signal

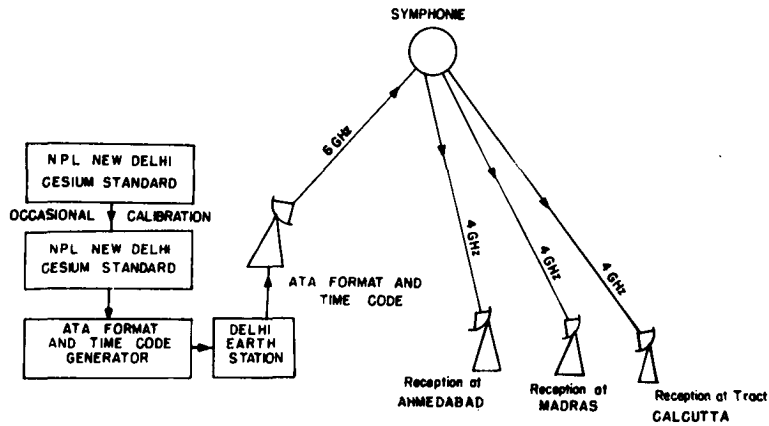


Figure 6. Block Diagram of Experimental Set-Up

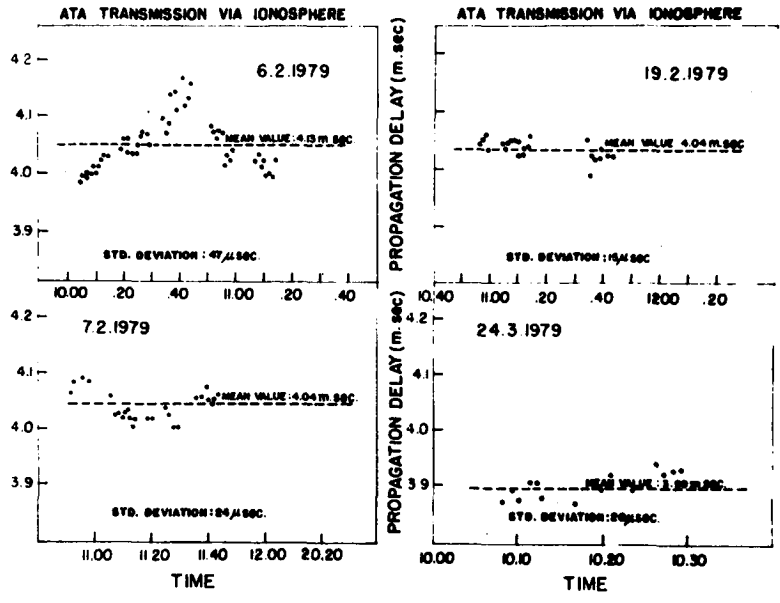


Figure 7

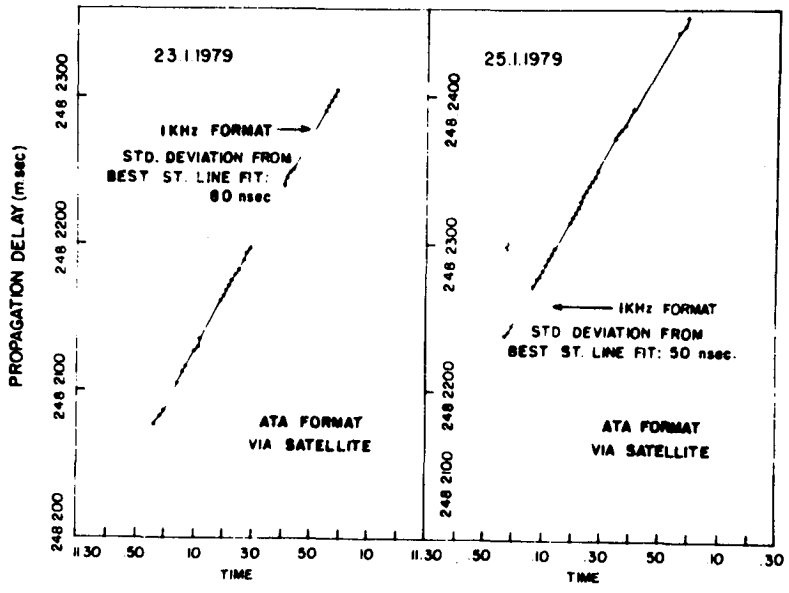


Figure 8

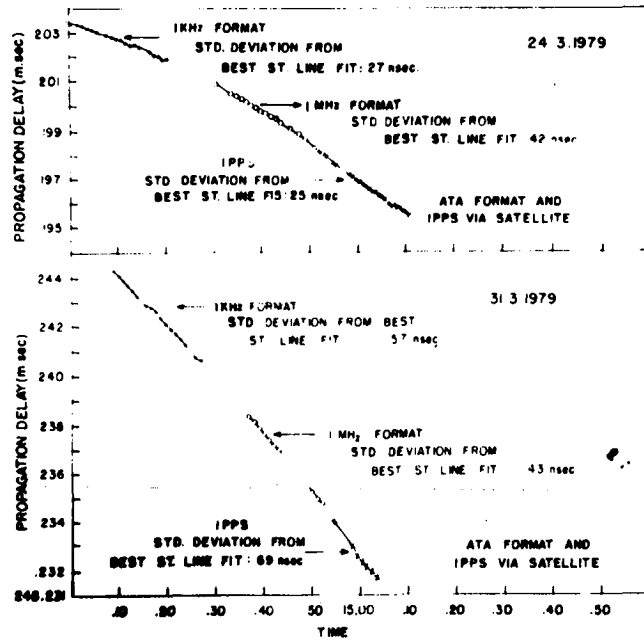


Figure 9. A Comparison of ATA Format Data Via Satellite with 1 kHz and 1 MHz Pulses and 1 PPS from a Cesium Standard as Recorded at AES

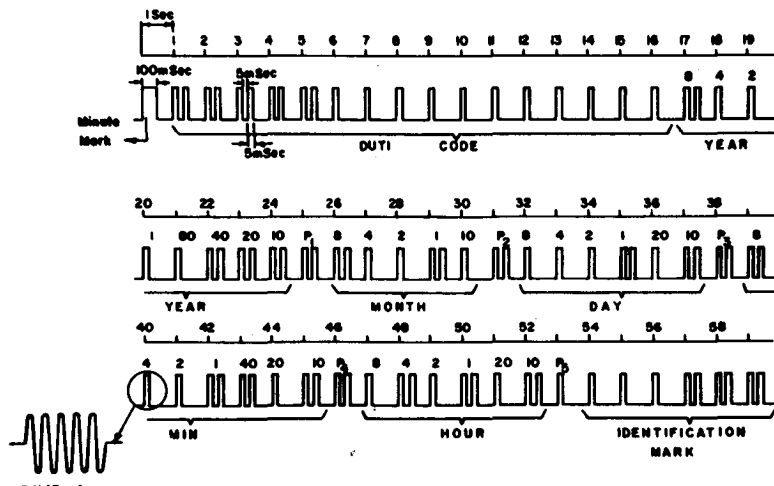


Figure 10. Code for Time of the Day Dissemination

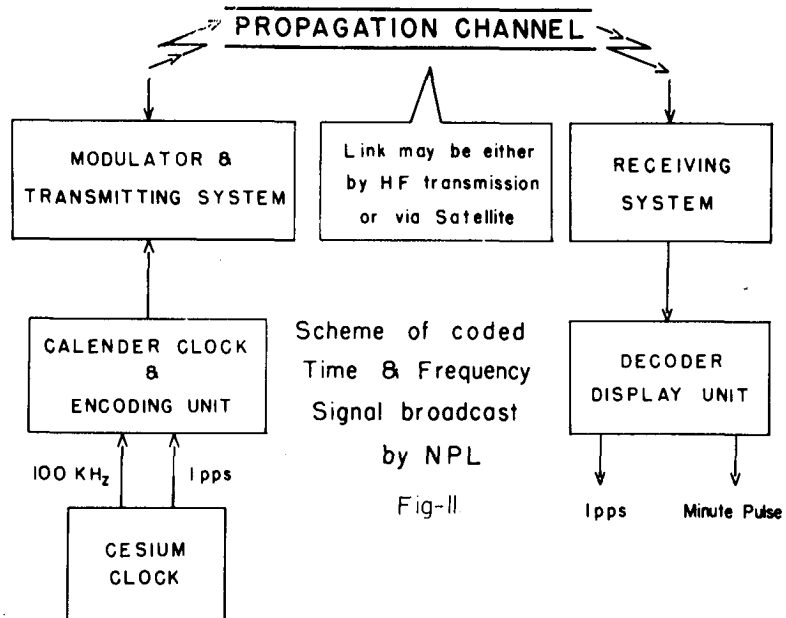


Figure 11. Block Diagram of the Experimental Set Up for Coded Time Signal Broadcast

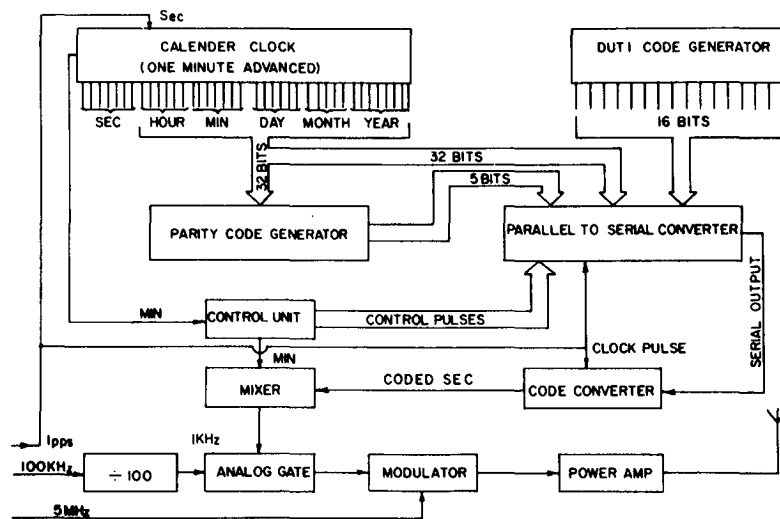


Figure 12. The Encoding Scheme for Time Signal Broadcast

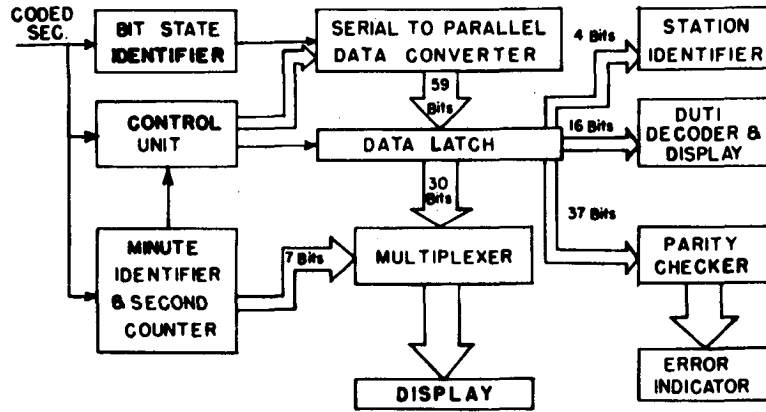


Figure 13. The Decoding Scheme for Time Signal Broadcast

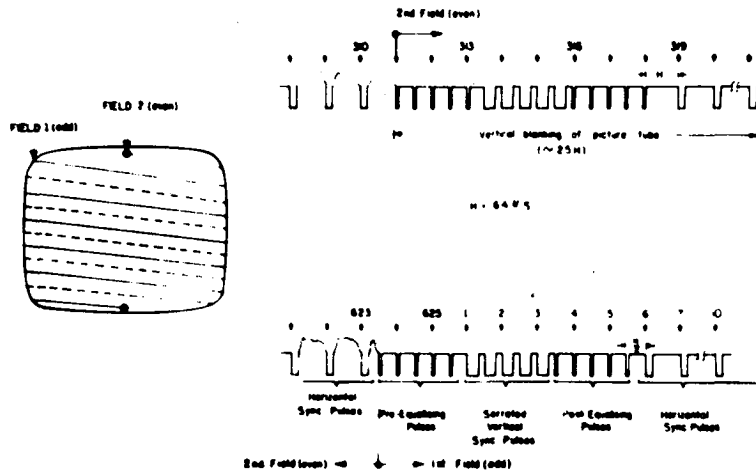


Figure 14. Pulses in Vertical Blanking Interval of TV Format in India

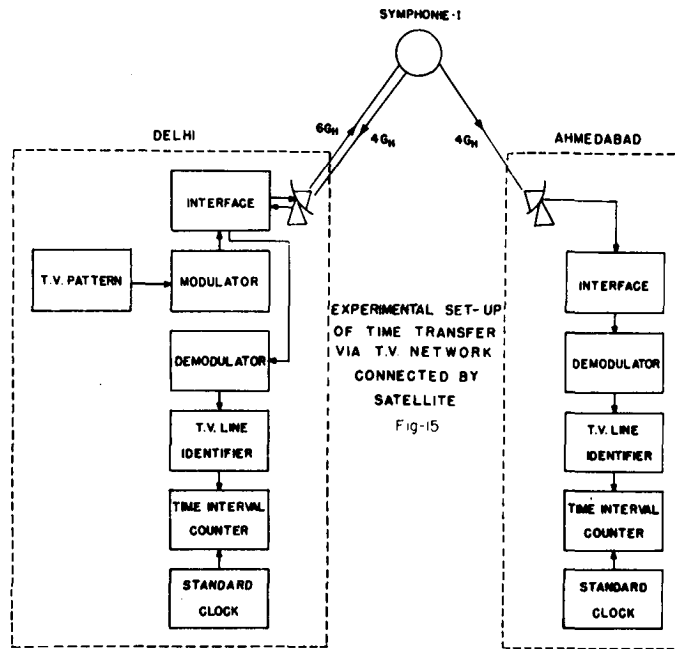


Figure 15. Block Diagram of Experimental Set Up for Time Dissemination Via Direct TV Broadcast by Satellite

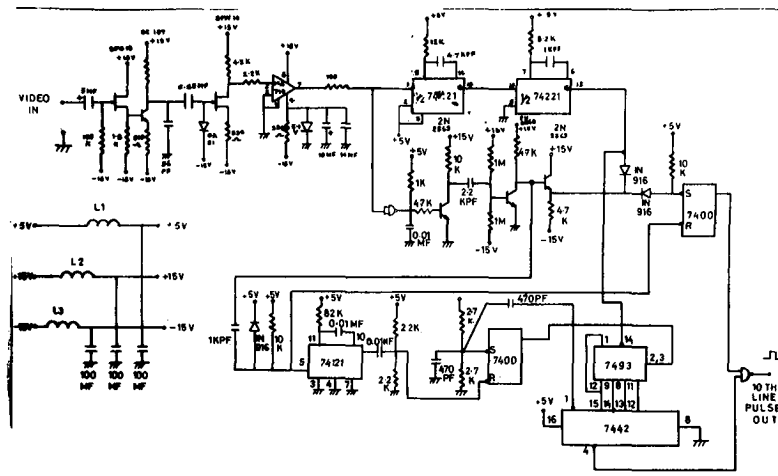


Figure 16. Circuit Diagram for a TV Line-10 Pulse Identifier

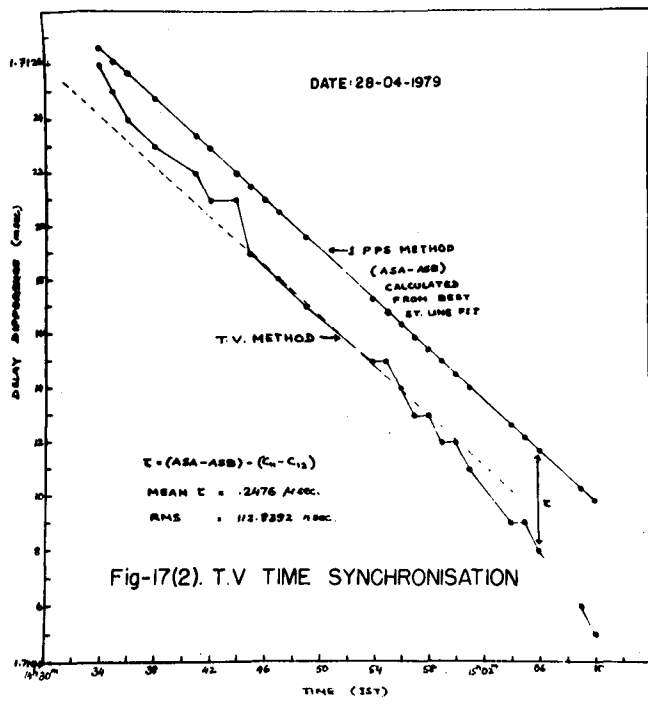
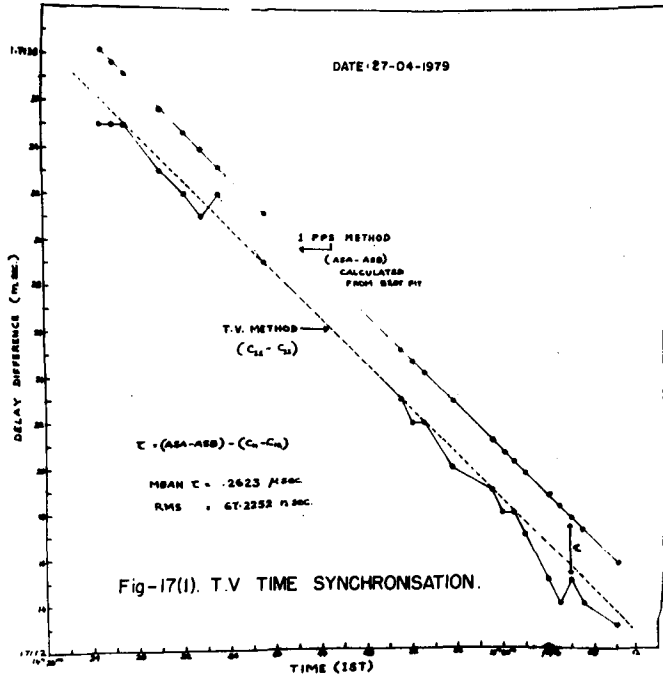


Figure 17. Data Plot for Time Synchronization Via Direct TV Broadcast by Satellite

ADVANCES IN THE STABILITY OF HIGH PRECISION CRYSTAL RESONATORS

Arthur Ballato & John R. Vig

US Army Electronics Technology & Devices Laboratory
USAERADCOM, Fort Monmouth, NJ 07703

ABSTRACT

This paper describes recent advances in technology directed toward minimizing the temporal changes in frequency of crystal resonators, as well as reducing their susceptibility to temperature, acceleration, and other environmental effects.

INTRODUCTION

Exceedingly stringent frequency control requirements follow from the performance specifications of the latest generations of communications, navigation and identification systems. Unfortunately, the present generation of crystal resonators, which are the stabilizing elements in the reference oscillators required in such systems, are frequency sensitive to acceleration fields produced by the dynamic environments surrounding land- and air- mobile use. These resonators are also susceptible to frequency shifts due to transient temperature variations and static stresses transmitted by their electrode and mounting systems. The acceleration effects lead to degradation of the short-term frequency stability, while the stress component contributes primarily to long-term aging and to distortions of the frequency-temperature behavior of oscillators.

This paper describes recent advances in quartz resonators that permit simultaneous compensation against both dynamic and static conditions, and that are compensated, moreover, against rapid temperature transients encountered in fast-warmup oscillators for manpack use.

Acceleration sensitivity is greatly reduced by utilizing novel monolithic compound vibrators having racemic* structures to nullify frequency shifts. Static compensation is achieved by means of unique lateral mounting contours, located so that nonlinear elastic constants cancel. Compensation of thermal transients comes about by use of a special, doubly rotated orientation of cut. We show that all three features may be realized at one time to yield a highly stable quartz resonator immune to accelerations in any direction, and to boundary stresses and thermal transients. No additional electronics are

* left- and right-handed combinations.

required, nor are increases in size, weight, and power requirements.

The aging is minimized through the use of: (1) the SC-cut, (2) ultraclean, ultrahigh vacuum fabrication techniques, and (3) packaging techniques which are capable of preserving the ultraclean surfaces. Additional concepts for high precision short-, medium-, and long-term frequency control are presented.

A crystal resonator is comprised of a piece of quartz, or other piezoelectric substance, together with a system of electrodes, mountings, and encapsulation. For the high precision units dealt with here, the form of the crystal vibrator is that of a thin disc with flat or lenticular major surfaces. The electrodes are most often deposited directly upon the major surfaces to form a capacitor-like structure; the connection to its external environment is made from the electrodes via the mounting supports, through the enclosure, to form a one-port device which is connected to the remainder of the oscillator circuitry.

Insofar as the external world is concerned, the mechanically vibrating element may be represented by means of the equivalent electrical circuit shown in Figure 1. The static capacitance C_0 is the actual capacitance of the crystal dielectric between the electrodes, plus additional stray capacitance due to the mount, etc. The C_1 , L_1 , R_1 combination arises from the mechanical vibration of the crystal as reflected at the output terminals by the piezoelectric effect. A knowledge of these four elements suffices in many instances to characterize the resonator in oscillator and filter design. The motional values C_1 , L_1 , R_1 , pertain to a single resonance of the system; if operation is not confined to the narrow vicinity of a resonance, then the equivalent circuit must be augmented by RLC series arms placed in parallel with that shown, one for each mode of vibration. We assume that a single motional arm suffices to characterize the resonators under discussion. Relationships between the critical frequencies associated with Figure 1, and definitions of other parameters, are given in [1].

Typical values for a high precision quartz resonator operating in the fundamental mode of thickness shear are

- $f_R = 5 \text{ MHz}$
- $Q = 750,000$
- $R_1 = 4\Omega$
- $r = 475 = C_0/C_1$
- $C_1 \approx 10.6 \text{ fF}$

- $C_0 \approx 5.04 \text{ pF}$

- $L_1 \approx 95.4 \text{ mH}$

These values will be used in subsequent examples. In the above,

$$(2\pi f_R)^2 L_1 C_1 = 1, \quad \text{and}$$

$$(QR_1)^2 = L_1/C_1.$$

In some oscillator applications, the resonance frequency f_R is adjusted to the "load" frequency f_L by means of a series capacitor C_L ; a typical value of which is

- $C_L = 100 \text{ pF}.$

This adjustment is necessary to bring the oscillator to a precise frequency, and to provide a means of correcting for subsequent frequency offsets. It is instructive to calculate the effect of changes in C_L itself on the frequency of a high precision oscillator. The load frequency is [2]:

$$f_L \approx f_R \sqrt{1 + \alpha/r}, \quad \text{where}$$

$$\alpha = C_0/(C_0 + C_L).$$

Therefore the sensitivity coefficient S is

$$S = C_L (\partial(\Delta f/f)/\partial C_L) = (-\alpha^2 C_L / 2r C_0 \sqrt{1 + \alpha/r}).$$

This is to be multiplied by the fractional change in C_L to obtain the fractional frequency shift $\Delta f/f$. Evaluating S for our resonator gives

- $S \approx -48 \times 10^{-6}.$

Temperature is one reason that C_L might change, and if C_L had a temperature coefficient of

- $TC_L \approx 2 \times 10^{-6}/K,$

then the resulting frequency shift would be

- $|S TC_L| \approx 10^{-10}/K.$

Thus changes in the temperature of only 10 millikelvins will change the frequency by parts in 10^{12} . In reality, the temperature coefficient of C_L is apt to be larger than 2 ppm/K, with correspondingly higher frequency excursions.

Reverting now to the physical quartz crystal plate, it has been known for many years that by cutting the plate at an angle to the crystallographic axes, the frequency-temperature (f-T) behavior could be greatly improved; in particular, that two orientations exist (the AT and BT cuts) where the temperature coefficient of frequency is zero. These cuts contain the crystallographic X axis and are referred to as singly rotated cuts. Figure 2 shows an example of such a cut as well as the more general doubly rotated cut, plus the locus of zero temperature coefficient (ZTC) as function of the two orientation angles θ and ϕ [3], [4].

For the orientations shown in Figure 2 by the solid line, the ZTC is obtained for the slow shear wave propagating along the plate thickness; the locus shown dashed is for the fast shear waves. These are distinguished by the terms "b-mode" (fast shear), and "c-mode" (slow shear); the thickness extensional mode is the "a-mode", but does not possess a ZTC for any orientation in quartz.

A ZTC means a flat f-T curve at some particular temperature. Over a wider temperature range, the curve is cubic in shape for those cuts on the upper portion of the locus (AT, FC, etc. branch), and parabolic for cuts on the two lower branches (BT and RT branches). The precise shape of the curve is dictated primarily by the elastic constants' behavior, and by the behavior of the piezoelectric, dielectric and thermoelastic constants. These are functions of ϕ and θ . Of smaller, but non-negligible influence on the f-T curve, are the load capacitance, the electrode mass-loading and the harmonic of operation.

In subsequent sections we will discuss parameters leading to resonator instabilities and point out how emerging technologies will minimize the various sources of frequency instability.

MAJOR PARAMETERS INFLUENCING FREQUENCY

Some of the major parameters that enter every discussion of high precision crystal resonators are given in Table 1. These will be addressed in turn.

1. Temperature

a. Static behavior

The overwhelming majority of conventional high precision resonators are fashioned of AT-cut quartz plates. The classical treatment of their properties was given by Bechmann [5]. These resonators have f-T curves similar in form to the cubic sketched in Figure 3. The curve is characterized by the three values a_0 , b_0 , c_0 :

$$\frac{\Delta f}{f} = a_0 \Delta T + b_0 \Delta T^2 + c_0 \Delta T^3;$$

$\Delta f/f$ is the fractional frequency change from the frequency at the reference temperature, and ΔT the corresponding temperature difference measured from the reference. The quantities a_0 , b_0 , c_0 are the first, second, and third order temperature coefficients of frequency, respectively; they are functions primarily of ϕ and θ , and are also weaker functions of resonator geometry, electroding and mounting.

Representative values for the AT and SC cut are:

	AT	SC	UNIT
a_0	0	0	$10^{-6}/K$
b_0	-0.45	-12.3	$10^{-9}/K^2$
c_0	108.6	58.2	$10^{-12}/K^3$
$\partial a_0/\partial \theta$	-5.08	-3.78	$10^{-6}/K, \text{ deg } \theta$
$\partial a_0/\partial \phi$	0	-0.18	$10^{-6}/K, \text{ deg } \phi$

These figures are for a reference temperature of 25°C . The inflection temperatures for the AT and SC cuts are 26.4 and 95.4°C , respectively. By changing θ slightly, the curves can be optimized for a given application. For wide temperature variations, as encountered in temperature compensated crystal oscillators (TCXOs), an AT cut can be made so that the total variation over a 0°C to 50°C range is less than 2.5×10^{-6} ; then the TCXO circuitry can compensate this variation further to less than 5×10^{-7} . When the resonator is used in an OCXO (oven controlled crystal oscillator), the temperature excursions are much smaller, and the θ angle is adjusted so that the f-T curve maximum or minimum is located at the desired oven temperature. If the oven temperature should coincide with, or be near to, the inflection temperature, then θ variations in the order of seconds of arc become very important as the slope changes rapidly in this region compared to its variation at the extrema when these are well separated. For OCXOs using AT cuts, the operating point usually is made the f-T minimum; for the SC cut the f-T maximum is used because of the high inflection point.

For cuts located on the upper locus of the graph in Figure 2 the inflection temperature monotonically increases as function of ϕ . Having the angle ϕ available, in addition to θ , allows the static f-T curve to be optimized for a given application. In high precision applications, however, the static, cubic, curve is found not to be invariant unless the temperature changes are made very slowly (quasi-isothermal = static). This problem did not become important until the past few years when requirements became increasingly stringent; this situation will be discussed further below; it has led to the necessity of using the doubly rotated SC cut.

b. Dynamic behavior

It has been known for many years that abrupt temperature changes produce in crystal resonators frequency changes that are unpredicted by the static f-T characteristic [6]. For the AT cut, an increase in temperature produces a negative-going frequency spike that slowly approaches the expected new frequency value; for BT cuts, the effect is reversed in sign. An example is shown in Figure 4, which shows the warmup characteristics for AT and SC cuts. Note the logarithmic ordinate. The oven warmup time is that required to approach within 10 mK of the final setting point, or operating temperature. Even with the oven at temperature, the AT crystal frequency is not constant for quite a while longer. Making the oven warmup shorter is of little help, because then the overshoot is larger. A typical figure with an AT cut is 20 minutes to get within 5×10^{-9} . The desirability of fast warmup oscillators has been stressed at PTTI meetings by systems users; a resonator unaffected by thermal transients is an urgent need. It is to be found in the SC cut. With its use the problem is determined by the oven alone, as seen in Figure 4, where the frequency is better than 10^{-9} in the oven warmup time.

The dynamic thermal effect has been given a phenomenological explanation by a modification of the cubic f-T curve to include a time-dependent term [7]-[8]. Evaluation of the added term using the results from thermal transient data enables one to simulate the effect of sinusoidal temperature variations about a fixed reference point. An example is shown in Figure 5. The nearly flat horizontal line is the static f-T curve for an AT cut, expanded about the frequency minimum. Superimposed are the ellipses that result from the dynamic effect having its basis in nonlinear elasticity, and characterized by the parameter $\hat{\alpha}$ in the modified expression

$$\Delta f(t)/f = (a_0 + \hat{\alpha} \dot{T}(t)) \cdot \Delta T(t) + b_0 [\Delta T(t)]^2 + c_0 [\Delta T(t)]^3,$$

$$\text{where } \dot{T}(t) = dT(t)/dt.$$

From Figure 5 it is seen that sinusoidal variations of temperature with magnitude $\pm \frac{1}{2}$ mK produce large frequency variations when the orbital period is hours long. With a period of 8 hours, the frequency change is about 3×10^{-12} ; when the period is lengthened to 1 week, the change is still about 1×10^{-13} , whereas the static f-T curve would predict a change of only a few parts in 10^{-14} , irrespective of cycling rate.

Recent results point to the necessity of including a second term \hat{a} in the equation:

$$\Delta f(t)/f = a_0 \Delta T(t) + b_0 [\Delta T(t)]^2 + c_0 [\Delta T(t)]^3 + (\hat{a} \Delta T(t) + \hat{a}) \cdot \dot{T}(t).$$

Since thermal transients, temperature cyclings, and fluctuations cannot be entirely avoided, the dynamic temperature effect is a very important consideration in high precision resonators. Means of reducing the effect are discussed in a subsequent section.

2. Time

The variation of resonator frequency with time is shown for a typical case in Figure 6 [9]. The curve has the over-all form of

$$\Delta f(t)/f = A \log (1+t/\tau),$$

with A an amplitude factor, and τ the time constant of the dominant rate-process leading to the frequency variation.

Superimposed on the long-range shape are perturbations having a distribution of time constants. The curve is somewhat arbitrarily broken up into three regimes: short term ($\tau < 10$ sec), intermediate term (~ 10 sec $< \tau < \sim$ several hrs.), long term ($\tau > \sim$ several hrs.).

a. Short term

This regime is characterized by noise effects whose origins are not fully understood [10]-[11]. Typical values of $\Delta f/f$, for 1-second sampling times, obtained with room temperature crystal oscillators (RTXOs), TCXOs, and OCXOs are

RTXO	2×10^{-9}
TCXO	1×10^{-9}
OCXO	1×10^{-11}

Contributing factors to short-term instability are

- fluctuations in temperature
- shock and vibration
- fluctuations in the active device, Johnson noise
- electromagnetic interference (EMI)
- circuit microphonics
- quartz plate to mount electrical noise
- fluctuations in surface contamination

Concerning this last point, consider the example of the 5 MHz, fundamental resonator. A monolayer of contamination will, by mass loading, reduce the frequency by approximately 1×10^{-6} . Since the relative fluctuation of the number of particles is proportional to the reciprocal square root of the number [12], for a disc 10 mm in diameter there will be about 3×10^{14} molecules / monolayer, and the relative fluctuation will be about 6×10^{-8} . Thus the frequency instability due to this cause is estimated at about 6×10^{-14} , which, coincidentally,

equals the best short term stability reported to date [13]. The discussion in the introduction concerning changes in C_L is germane here as well, as fluctuations in C_L and other circuit components contribute to the short-term frequency instability. A phase shift ϕ in the oscillator loop will give rise to a frequency change of

$$\Delta f/f = \phi/(2Q);$$

therefore, for the crystal parameters quoted in the Introduction, phase shifts of only 86 microdegrees (1.5 microradians) will produce $\Delta f/f$ shifts at the 10^{-12} level.

There is preliminary evidence that points to the quartz-electrode interface as a contributor to short-term instability. In a number of measurements, Healey [14] has found a $1/f^2$ phase noise dependence, close-in, in Cr-Ag-Ni plated units, and a $1/f^3$ dependence in Al-Al₂O₃-Au plated units.

Another contribution to short-term phase noise is bulk elastic nonlinearities. For example, when the b-mode of an SC-cut is driven simultaneously with the c-mode, an increase in the phase noise of the latter is found; although both modes would be independent if the crystal were linear, they are coupled by nonlinearities in the crystal.

b. Intermediate term

In this regime the greatest contributor to instability is probably the temperature control used. Ovens are normally of two general types: a switching controller type, and a proportional controller type. In the former, a snap action thermostat is used, where low cost and moderate performance are important. This type begets wear and sticking of the contacts, and contact arcing produces electrical noise. The proportional type uses a bridge circuit that provides constant adjustment because the heat supplied is proportional to the difference between the crystal temperature and the oven setting point. Some high precision oscillators use a double proportional oven so that inside the first oven the temperature never varies more than 1K, and this is reduced to less than 0.01K within the second proportional oven.

Other contributors to intermediate term variations are changes in crystal attitude, and low frequency vibrations. These will be considered under acceleration effects.

Additional causes are stress relief in mounts and electrodes, and changes in circuit reactance and drive level.

c. Long term [15]

Long-term frequency drift is called aging. It is usually found to

be a logarithmic function of time. When the oven and/or oscillator are turned off and then on, the oscillator typically experiences an offset in frequency and the onset of a new curve of the same form.

Typical values of aging are

RTX0	3×10^{-7} /month
TCX0	1×10^{-7} /month
OCX0	1.5×10^{-8} /month

A major contributor to long term aging is mass transfer due to contamination. Since, for a 5 MHz plate, one monolayer of contamination lowers the frequency by about 1×10^{-6} , to achieve high stability long-term performance, the mass transfer allowed must be a very small fraction of a monolayer. But, assuming that all molecules stick to the surface, the number of molecules adsorbed by a surface at a pressure of 10^{-6} torr would form a monolayer in approximately 1 second. It is obvious, therefore, that high precision resonators must be processed in a high vacuum to avoid contamination. This includes cleaning, handling and packaging.

Adsorption and desorption phenomena such as outgassing of surface contaminants from the electrodes and quartz are not the only causes of long-term drift. In back-filled units, changes in pressure due to atmospheric pressure variations produces oilcanning of the enclosure which will change the frequency by 10^{-7} per atmosphere; the oilcanning also produces time dependent stresses in the mounting structure. Permeability of the enclosure to gases is another contributor to aging.

Intrinsic stress relief with time changes the resonator's frequency as well. The stress relaxation takes place in the mounting structure, the bond between mount and crystal, and in the electrodes. As an example, a 5 MHz crystal of 14 mm diameter, mounted along the X-axis, would increase in frequency by 8×10^{-8} for a force produced by a mass of 1 gram applied to the mount [16]; microgram force changes are therefore perceptible in high precision applications. The observed aging is the sum of the aging produced by the various mechanisms, and can be positive or negative.

d. Thermal hysteresis

Thermal hysteresis, or thermal retrace is shown in Figure 7 [17]. This phenomenon is largely unpredictable, although Hammond, et al. [17] did find a variation with orientation angle θ about the AT-cut angle. It is a function of bonding, mounting and previous history, and as such is not a candidate for modeling in systems applications,

and ways to reduce it are discussed subsequently.

3. Acceleration

a. Attitude

Changes in the resonator's orientation with respect to the gravitational field produce frequency shifts because of the stresses set up in the resonator. For 180° changes one usually has a shift of about 2×10^{-9} . This is referred to as the "2-g tipover" value. This effect is equivalent to the acceleration effect next described.

b. Vibration

Valdois [18] established experimentally the behavior of resonators subjected to acceleration fields. His results are shown in Figure 8. It is seen that the frequency shift reverses sign with reversal of the direction of acceleration, and that the magnitude of the effect is dependent on which axis the acceleration is directed along. For a given system of mounting and direction of acceleration, the frequency shift will be given by

$$\Delta f/f = \bar{a}_0 \gamma,$$

where \bar{a}_0 is the acceleration (usually expressed in "g" units) and γ is the acceleration sensitivity coefficient of the crystal for that configuration. Values for γ normally run a few parts in 10^9 per g (AT-cut).

When the acceleration takes the form of vibration, the same considerations apply. If the vibration is sinusoidal, sidebands are produced at the carrier frequency + the modulation frequency. An example is shown in Figure 9 [19]. The ratio of single sideband to carrier powers follows from FM theory as

$$\mathcal{L}(f_m) \approx (\Delta f/2f_m)^2,$$

where Δf is the frequency shift under acceleration, and f_m is the modulation frequency. Measurement of $\mathcal{L}(f_m)$ yields γ from

$$\gamma = (2f_m/\bar{a}_0 f) \cdot 10^9 (\mathcal{L}(f_m)/20)$$

For high performance oscillators it is imperative that γ be significantly reduced; methods of attaining this end are discussed in the sequel.

c. Shock

Shock is distinguished from vibration and tipover only by its magnitude. If the shock level exceeds the elastic limit for the quartz or mounting structure, permanently offset frequency will result.

In certain sensor applications the crystals may be subjected to as many as 20,000 g's and be required to survive with minor frequency shifts; methods for shock-hardening will be described in a later section.

4. Radiation

a. Transient

Pulsed ionizing radiation produces frequency changes in quartz resonators by a mechanism similar to the dynamic thermal effect mentioned previously. Thermal gradients are set up in the quartz, leading to frequency changes brought about by the nonlinear elastic constants. The effect depends on the crystal cut, being negative for the AT cut, but is almost insensitive to the type (natural or cultured) of quartz used, and to the quality, although Q degradation and even cessation of the oscillation has been observed when impure quartz is used.

b. Permanent

Steady state or continuous radiation produces permanent frequency shifts in quartz resonators [20], [21]. The effect is due primarily to changes in the defect structure of the material, which changes, in turn, the effective elastic constants. Because the effect is very structure sensitive, the type and quality of the quartz material used is extremely important. Typical values for ionizing radiation are

natural quartz: $\sim -10^{-11}$ /rad
swept cultured quartz: $\sim <10^{-12}$ /rad.

For neutrons displacement damage occurs at the level

neutrons: $\sim 10^{-21}$ /n/cm².

Improvement of radiation insensitivity will be described in the next section.

TECHNOLOGIES AND TECHNIQUES IMPACTING STABILITY

In the last section some of the predominant parameters affecting frequency of resonators were described. In this section, technologies and techniques that are being brought to bear on the problem of resonator frequency changes will be reviewed in the light of latest developments. Some of these have been touched upon before at previous PTTI meetings [22], [23]. The "cures" to be described for the various effects already enumerated are surprisingly few in number; the most prominent of which is the substitution of the doubly rotated SC cut for the perennial AT cut. This is because many of the effects have their basis in nonlinear elasticity [24], [4]. The more important emerging/

improving technologies being brought to bear on the problem of improving high stability resonators are shown in Table 2. These will be briefly discussed in the same framework as the prior section. Cutting across the Temperature/Time/Acceleration/Radiation categories is the SC cut. Table 3 gives a preview of the sequel.

1. Temperature

The f-T behavior of SC cuts is shown in Figure 10, with adjacent curves separated by 1 minute of arc. The inflection temperature is about 95.4°C, as opposed to nearly room temperature for the AT, and the cubic parabola term is only about one half that of the AT. In many applications these are advantages over the AT cut, but relatively minor ones. The real advantage of the SC vis à vis the AT, as far as temperature effects are concerned, is that the curves in Figure 10 are nearly the dynamic as well as the static curves, because the SC-cut is compensated for thermal transients occurring in the thickness direction; lateral compensation of gradients does not in general occur, but very little experimental or theoretical work has been done on the lateral effect [10], [8]. Because of the compensation for temperature changes, setting an SC oscillator to its temperature operating point is rapid; anyone who has performed this feat with a high precision AT resonator will appreciate this practical advantage. More importantly, fast warmup oscillators are a reality with the SC cut, with warmup dictated solely by the oven, as shown in Figure 4; also highly important is the absence of the orbits of Figure 5 and the corresponding meanderings of frequency due to temperature fluctuations.

The consequences of eliminating dynamic thermal coupling are brought out dramatically in Table 4. The tabular entries pertain to an SC cut operated with its reference temperature at one of the two turning points. Refer to Figure 3 for the definitions of oven offset and oven cycle range with respect to oven setting point. For state-of-the-art ovens with cycling ranges in the millikelvin regime, resonator stabilities in the 10^{-14} range ought to be attainable. In fact, a stability of 6×10^{-14} for a sampling interval of 128 seconds has been reported for an SC cut [25].

Stabilities approaching those of Table 4 assume that the additional causes of instability can be sufficiently reduced or eliminated. As ambitious as such a program might appear at first to be, the path to doing just this is reasonably straight-forward and possible of accomplishment in the future for production quantities of high stability resonators.

The major drawback of the SC with respect to the AT is the increased criticality of the orientation angles ϕ and θ for oven operation near the inflection temperature; where a few minutes of arc suffice for the AT cut, the tolerance becomes seconds of arc for the SC cut. Fortun-

ately, an automated x-ray goniometer with microprocessor control is being developed under ERADCOM contract, and this should provide the necessary accuracy and precision.

2. Time

Under this category we will discuss just two areas of recent, significant progress: mounting and electrode stresses, and contamination control. Other areas discussed in this category in the last section will be addressed later on, in this section, or the next.

Figure 11 shows traditional metal enclosures, and the recently developed ceramic flat-pack enclosures [26]-[28]. The ceramic units have the advantages of cleanliness: they are cleaned more easily, can be baked at higher temperatures to remove contaminants, and the alumina enclosure is impervious to gaseous diffusion unlike metals and glasses. The flat-pack design also provides a geometric factor not possessed by the metal holders, and is microcircuit and hybrid circuit compatible. Within the ceramic enclosure, the resonators are attached to the mount with polyimide [29]. This material can be vacuum baked at above 350°C and thus has minimal outgassing. This means of attachment can be used from cryogenic temperatures to 350°C. The lid is sealed to the rest of the ceramic enclosure by metal-to-metal, clean surface adhesion.

The resonator blank sealed within the ceramic flatpack has gold electrodes deposited upon its surfaces. This provides a minimum of stresses and interface reactions. The interface between the gold and quartz must also be clean. Near-atomic cleanliness can be obtained by, among other things, UV/ozone cleaning [29]-[31].

Adherent electrodes are still subject to thermal stress cycles, and to stress relaxation, regardless of how ductile the electrode material may be. Means of obviating this problem are: 1. the use of the SC-cut, which is insensitive to electrode stress relief, and 2. the use of air gap designs [32], [33]. An embodiment of the air gap type of mounting/electroding design is the BVA of Besson [23]. The absence of electrodes directly on the vibrator surface rules out surface stresses and possible electrode asymmetry that would lead to couplings with even harmonics and with flexure. The BVA design also utilizes a ring structure with monolithic quartz bridges that isolate the vibrating portion from the quartz supporting ring.

The other area, contamination control, is best summed up by saying that all processing, from initial input of quartz blanks and ceramic enclosures, to finished resonator units, must be done under ultraclean conditions. The final, most critical fabrication steps must be performed in ultrahigh vacuum. An apparatus that accomplishes this is shown in Figure 12. This is the Quartz Crystal Fabrication Facility (QXFF) [34]. It consists of five separate chambers: 1. entrance,

2. UV cleaning-bakeout, 3. gold plating, 4. sealing, 5. unloading. Chambers 2,3, and 4 are under 10^{-8} to 10^{-9} torr continuously, and never see air after the initial pump-down. All chambers are separated by ultrahigh vacuum gate valves, and each chamber is separately cryo-pumped. The QXFF is being developed under ERADCOM contract; the pilot run for 22 MHz fundamental mode high shock crystals is scheduled to take place during 1980. The pilot production run for high precision 5 MHz and 10 MHz crystals is scheduled for 1981-82.

3. Acceleration

For accelerations out of the crystal plate plane, desensitization of the acceleration-induced frequency shift may be partially accomplished by use of ring-mounted resonators as shown in Figure 13 [35]. The improvement comes about by the alteration of the boundary conditions at the plate periphery as described at the bottom of Figure 13. When the acceleration is in the plane of the plate, one cannot make any a priori statements concerning the magnitude of the effect, except that it will be azimuth dependent. The ring-supported resonator may be fabricated of any cut.

It is an experimentally observed fact that SC cuts are considerably less sensitive to the effects of acceleration (attitude, shock and vibration) than AT cuts; the improvement may be as much as a factor of ten. Beyond this, one may use dual resonators with two crystal axes antiparallel [23], to obtain compensation along these axes, or one may use enantiomorphs in a three-axis antiparallel configuration to produce a dual resonator compensated against the effects of an acceleration field in any arbitrary direction [36].

The enantiomorphous composites may be fashioned as paired:

- conventional resonators
- ring-supported resonators
- BVA resonators
- stacked resonators
- ring-supported resonators with the ring structures stacked

Additionally, the electrical connections may be series or parallel, and the crystal cut may be singly (AT) or doubly (SC) rotated [36]. Examples of stacked crystal composites are given in Figure 14.

In order to render quartz vibrators capable of withstanding shock levels approaching the theoretical breaking strength of the material, it has been found that microscratches and imperfections left by the conventional mechanical polishing operation had to be completely removed. Otherwise, the stress magnification that took place as the stress wave passed over the scratch resulted in plate fracture. The

method newly introduced into quartz resonator fabrication for this purpose is chemical polishing [37]-[39]. Chemical polishing consists of etching the crystal to produce pure crystalline surfaces that reveal defects and makes the plate much stronger. The proper etchant and procedure is dependent on the orientation angles ϕ and θ . For $\phi \neq 0^\circ$, even though each surface may be chemically polished, the result is different on each side; this can be used as a polarity test of axes when using paired plates as enantiomorphous composites.

4. Radiation

Temperature gradient effects on resonator frequency, arising from pulsed ionizing radiation can be largely compensated by utilizing SC cut resonators. Steady state radiation effects depend strongly on defects in the material. Just as annealing has been used to increase the Q of quartz, and to attempt to reduce aging [40], a combination of high temperatures (below the α - β transition point) and strong electric fields (referred to as "sweeping") has been found to produce material with superior purity and thus superior radiation hardness [41]-[43], [21]. In addition, the sweeping process (done in a vacuum) has been shown [37] to produce material having many fewer etch channels than non-swept cultured quartz. Etch channels degrade the strength (shock resistance) and serve as repositories of etchant that can produce instabilities.

The use of tuned IR and UV to excite lattice vibrations, and impurities, respectively, to aid in the sweeping process has been proposed [44].

Further improvements in radiation hardness, Q, and long-term aging of the material itself due to diffusive phenomena will require further developments in crystal growth. Among these are use of defect free natural quartz seeds, special seed preparation, use of select high purity nutrient material, special cleaning of autoclaves, and use of precious-metal-lined autoclaves.

ADDITIONAL CAUSES AND CURES

1. Quasistatic forces

These include thermoelastic forces, and intrinsic stress relief mentioned under long-term aging. For in-plane forces applied to a circular plate as shown in Figure 15, it is found that there are azimuth angles such that applied force-pairs produce no frequency change [16]; this is true even for doubly rotated plates on the upper ZTC locus [45]-[48]. When this criterion is used to locate four mounting points [49], then thermoelastic forces will have no influence on the resonator frequency, as long as no asymmetry exists, i.e. so that bending moments are not generated. The structure is thus only

conditionally stable, that is, only as long as the forces are colinear in pairs. Another difficulty is that the force coefficient has an appreciable gradient with angle about the zero points. Two means of overcoming this difficulty are: 1. use of ring-supported resonators, and 2. use of special polygonal shapes instead of circular outlines. Ring-supported structures, which can be produced by chemical etching [49], absorb most of the forces and/or torques applied and are less sensitive than conventional resonators. Plates of special lateral contour have been developed [50] for singly and doubly rotated cuts that have the property of being frequency insensitive to in-plane forces applied normal to two pairs of edges. The edges are used for mounting, and the stress levels are greatly reduced over point-mounts. Moreover, the polygons are self-orienting in their holders. Examples of the plates are shown in Figure 16 (AT cut), and in Figure 17 (SC cut).

2. Line voltage changes

This is an oscillator, rather than a resonator, characteristic. Defining a voltage coefficient of frequency as

$$\bar{V}_f = \frac{V_0}{f_0} \cdot \frac{df}{dV} ,$$

one has the following typical figures for \bar{V}_f :

RTXO	10^{-6}
TCXO	5×10^{-7}
OCXO	10^{-9}

The RTXO figure of 10^{-6} means $\Delta f/f$ changes 10^{-7} for a 10% change in line voltage. Improvement of these figures depends mainly upon circuitry design and improvement.

3. Resonator drive level

The amplitude-frequency-drive level surface for a typical AT cut is given in Figure 18 in schematic fashion. For high power levels the surface becomes pleated, indicating a multiple-valued amplitude-frequency curve. A rule-of-thumb figure for the frequency change in an AT at low drive is parts in $10^9/\mu\text{W}$, but this depends on geometry. The BT cut bends in the opposite direction [4], [51], [52]. In the vicinity of the SC-cut the curve does not skew until much higher levels of drive.

Besides the amplitude-frequency effect, another nonlinear effect may occur, viz., the presence of a very high starting resistance at very low power levels [53], [54]. It is strongly suspected that surface

preparation is responsible; chemical polishing and processing under ultraclean conditions should eliminate this feature.

4. Static charge - dc field sensitivity [55]

The electric field coefficient of frequency is defined as

$$E_f = \frac{1}{f_0} \frac{df}{dE} .$$

In terms of this coefficient, measured values for three quartz cuts are [55]:

AT cut	0.04 pm/V
SC cut	2.3
LC cut	16.7

For rotated-Y-cuts, the effect should vanish for electric fields in the plate thickness direction; but any x component of field will produce a contribution for any cut. In a clean, dry environment, static charges on insulating surfaces can produce many kV with respect to ground. From the figures above it is seen that the SC cut is more susceptible to this effect than the AT cut. It is gotten rid of in a simple manner, by placing a high resistance in parallel with the vibrator.

5. Other nonlinear effects

- effect of bonding on f-T curve [56]
- piezoelectric hysteresis [57]
- nonlinear permittivity [58], [59]
- parametric excitation [60]-[62]

It remains to be seen if these effects are reduced in size for certain doubly rotated orientations. It has been established that the SC cut is remarkably free of another nonlinear effect-activity dips.

CONCLUSION

In many of the papers presented at the 1979 PTTI meeting that detailed system requirements, it was heard again and again that it was highly desirable or imperative that frequency sources be developed that possess fast-warmup capabilities, and that are insensitive to accelerations and other environmental effects.

This paper reports developments that make these requirements realistic for the future. The path is open for the realization; no "break-throughs" are required to reach the goal. This is not to say that the goal has been reached already! Ahead lies an exciting period consist-

ing of putting together coherently the developments reported in this paper. It will require time and support on the part of the interested systems users.

Table 5 shows a comparison relating to high stability oscillators. The first column gives figures derived from manufacturers' specifications as to what can be bought today off-the-shelf, in small quantities. The second column provides a "guesstimate" of the state-of-the-art in precision oscillators as of 1989 if the developments reported here are carried out. Prices are in 1979 dollars. The 50,000 quantity includes the sum of JTIDS, GPS, NIS, SINGARS, SEEK TALK, etc.

REFERENCES

Note: Many of the references were presented at the Annual Frequency Control Symposium, U.S. Army Electronics R&D Command, Fort Monmouth, NJ 07703. They are cited here as AFCS for brevity.

1. A. Ballato, "Resonance in piezoelectric vibrators", Proc. IEEE, vol. 58, January 1970, pp. 149-151.
2. A. Ballato, "Frequency-temperature-load capacitance behavior of resonators for TCXO application", IEEE Trans. Sonics Ultrason., vol. SU-25, July 1978, pp. 185-191.
3. R. Bechmann, A. Ballato, and T. Lukaszek, "Higher-order temperature coefficients of the elastic stiffnesses and compliances of alpha-quartz", Proc. IRE, vol. 50, August 1962, pp. 1812-1822; December 1962, p. 2451.
4. A. Ballato, "Doubly rotated thickness mode plate vibrators", in Physical Acoustics: Principles and Methods, vol. 13, W.P. Mason and R.N. Thurston, Eds. New York: Academic, 1977, Ch. 5, pp. 115-181.
5. R. Bechmann, "Frequency-temperature-angle characteristics of AT-type resonators made of natural and synthetic quartz", Proc. IRE, vol. 44, Nov 1956, pp. 1600-1607.
6. A.W. Warner, "Ultra-precise quartz crystal frequency standards", IRE Trans. Instrumentation, vol. I-7, pp. 185-188, Dec. 1958.
7. A. Ballato and J.R. Vig, "Static and dynamic frequency-temperature behavior of singly and doubly rotated, oven-controlled quartz resonators", in Proc. 32nd AFCS, May-June 1978, pp. 180-188.
8. A. Ballato, "Static and dynamic behavior of quartz resonators", IEEE Trans. Sonics Ultrason., vol. SU-26, July 1979, pp. 299-306.
9. "Fundamentals of quartz oscillators", Application Note 200-2, Hewlett-Packard Co., Palo Alto, CA 94304.
10. J.J. Gagnepain, "Fundamental noise studies of quartz crystal resonators", Proc. 30th AFCS, June 1976, pp. 84-91.
11. R.F. Voss, "1/f (flicker) noise: a brief review", Proc. 33rd AFCS, May-June 1979, pp. 40-46.

12. L.D. Landau and E.M. Lifshitz, Statistical Physics. Reading, MA: Addison-Wesley, 1969, Sec. 115.
13. F.L. Walls and S. Stein, "A frequency-lock system for improved quartz crystal oscillator performance", IEEE Trans. Instrum. Meas., vol. IM-27, Sept 1978, pp. 249-252.
14. D.J. Healey, III, Westinghouse Electric Corp., Baltimore, MD 21203, private communication.
15. J.R. Vig, "Resonator aging", Proc. IEEE Ultrason. Symp., October 1977, pp. 848-849.
16. A.D. Ballato, "Effects of initial stress on quartz plates vibrating in thickness modes", in Proc. 14th Annu. Frequency Control Symposium, May-June 1960, pp. 89-114.
17. D.L. Hammond, C.A. Adams, and A. Benjaminson, "Hysteresis effects in quartz resonators", Proc. 22nd AFCS, April 1968, pp. 55-66.
18. M. Valdois, J. Besson, and J.J. Gagnepain, "Influence of environment conditions on a quartz resonator", Proc. 28th AFCS, May 1974, pp. 19-32.
19. R. Filler, USAERADCOM, Fort Monmouth, NJ 07703, private communication.
20. W.J. Spencer and W.L. Smith, "Precision quartz crystal controlled oscillator for severe environmental conditions", Proc. 16th AFCS, April 1962, pp. 405-421.
21. J.C. King, "Vacuum electrolysis of quartz", U.S. Patent 3,932,777. Patented January 13, 1976.
22. E. Hafner, "Outlook for precision frequency control in the 1980's", Proc. 7th Annual PTTI Meeting, pp. 101-120, December 1975.
23. R.J. Besson, "Quartz crystal and superconductive resonators and oscillators", Proc. 10th Annual PTTI Meeting, pp. 101-128, November 1978.
24. E. Hafner, "Crystal resonators", IEEE Trans. Sonics Ultrason., vol. SU-21, pp. 220-237, October 1974.
25. S.R. Stein, C.M. Manney, Jr., F.L. Walls, J.E. Gray and R.J. Besson, "A systems approach to high performance oscillators", in Proc. 32nd AFCS, May-June 1978, pp. 527-530.

26. J.R. Vig and E. Hafner, "Packaging precision quartz crystal resonators", Technical Report ECOM-4134, US Army Electronics Command, Fort Monmouth, NJ 07703, July 1973, 18 pp.
27. P.D. Wilcox, G.S. Snow, E. Hafner, and J. Vig, "A new ceramic flat pack for quartz resonators", Proc. 29th AFCS, May 1975, pp. 202-210; Technical Report ECOM-4396, US Army Electronics Command, Fort Monmouth, NJ 07703, April 1976, 25 pp.
28. R.D. Peters, "Ceramic flatpack enclosures for precision quartz crystal units", Proc. 30th AFCS, June 1976, pp. 224-231.
29. R.L. Filler, J.M. Frank, R.D. Peters, and J.R. Vig, "Polyimide bonded resonators", Proc. 32nd AFCS, May-June 1978, pp. 290-298.
- 29' J.R. Vig, J.W. LeBus, and R.L. Filler, "Further results on UV cleaning and electrobonding", Proc. 29th AFCS, May 1975, pp. 220-229.
30. J.R. Vig and J.W. LeBus, "UV/Ozone cleaning of surfaces", IEEE Trans. Parts, Hybrids, and Packaging, vol. PHP-12, December 1976, pp. 365-370; Technical Report ECOM-4397, US Army Electronics Command, Fort Monmouth, NJ 07703, April 1976, 16 pp.
31. J.R. Vig, "UV/Ozone cleaning of surfaces: a review", in Surface Contamination: Its Genesis, Detection and Control, (K.L. Mittal, ed.), New York: Plenum, 1979, pp. 235-254.
32. D.L. Hammond and L.S. Cutler, "Crystal resonators", U.S. Patent 3,339,091. Patented Aug. 29, 1967.
33. L.S. Cutler and D.L. Hammond, "Crystal resonators", Reissue 26,707 of U.S. Patent 3,339,091. Reissued November 4, 1969.
34. R.J. Ney and E. Hafner, "Continuous vacuum processing system for precision quartz crystal units", Proc. 33rd AFCS, May-June 1979, pp. 368-373.
35. G.K. Guttwein, A. Ballato, and T.J. Lukaszek, "VHF-UHF Piezo-electric resonators", U.S. Patent 3,694,677. Patented 26 Sep 72.
36. A. Ballato, "Resonators compensated for acceleration fields", Proc. 33rd AFCS, May-June 1979, pp. 322-336.
37. J.R. Vig, J.W. LeBus, and R.L. Filler, "Chemically polished quartz", Proc. 31st AFCS, June 1977, pp. 131-143; Technical Report ECOM-4548, US Army Electronics Command, Fort Monmouth, NJ 07703, November 1977, 37 pp.

38. J.R. Vig, R.J. Brandmayr, and R.L. Filler, "Etching studies on singly and doubly rotated quartz plates", Proc. 33rd AFCS, May-June 1979, pp. 351-358.
39. P. Suda, A.E. Zumsteg, and W. Zingg, "Anisotropy of etching rate for quartz in ammonium bifluoride", Proc. 33rd AFCS, May-June 1979, pp. 359-363.
40. A.C. Prichard, M.A.A. Druesne, and D.G. McCaa, "Increase in Q-value and reduction of aging of quartz-crystal blanks", Proc. IRE, vol. 38, p. 314, March 1950.
41. J.C. King, "High temperature quartz piezoelectric devices", U.S. Patent 3,113,224. Patented December 3, 1963.
42. D.B. Fraser, "Electrolytic treatment of quartz", U.S. Patent 3,337,439. Patented August 22, 1967.
43. G.B. Krefft, "Effects of high-temperature electrolysis on the coloration characteristics and OH-absorption bands in alpha-quartz", Radiation Effects, vol. 26, 1975, pp. 249-259.
44. A. Ballato and J. Vig, unpublished.
45. E.P. EerNisse, "Quartz resonator frequency shifts arising from electrode stress", in Proc. 29th AFCS, May 1975, pp. 1-4.
46. A. Ballato, E.P. EerNisse, and T. Lukaszek, "Force-frequency effect in doubly rotated quartz resonators", in Proc. 31st AFCS, June 1977, pp. 8-16.
47. E.P. EerNisse, "Rotated X-cut quartz resonators for high temperature applications", in Proc. 32nd AFCS, May-June 1978, pp. 255-259.
48. E.P. EerNisse, T.J. Lukaszek, and A. Ballato, "Variational calculation of force-frequency constants of doubly rotated quartz resonators", IEEE Trans. Sonics Ultrason., vol. SU-25, May 1979, pp. 132-138.
49. A. Ballato, "Force-frequency compensation applied to four-point mounting of AT-cut resonators", IEEE Trans. Sonics Ultrason., vol. SU-25, July 1978, pp. 223-226.
- 49' J. Vig, unpublished.
50. T.J. Lukaszek and A. Ballato, "Resonators for severe environments", Proc. 33rd AFCS, May-June 1979, pp. 311-321.

51. A. Seed, "Development of a high Q, BT-cut quartz resonator", Brit. J. Appl. Phys., vol. 16, pp. 1341-1346, 1965.
52. J.J. Gagnepain, J.C. Ponçot, and C. Pegeot, "Amplitude-frequency behavior of doubly rotated quartz resonators", Proc. 31st AFCS, June 1977, pp. 17-22.
53. M. Bernstein, "Increased resistance of crystal units at oscillator noise levels", Proc. IEEE, vol. 55, pp. 1239-1241, July 1967.
54. J.E. Knowles, "On the origin of the 'second level of drive' effect in quartz oscillators", Proc. 29th AFCS, May 1975, pp. 230-236.
55. J. Kusters, Hewlett-Packard Co., Palo Alto, CA 94304, private communication, 1977.
56. R.L. Filler and J.R. Vig, "The effect of bonding on the frequency vs. temperature characteristics of AT-cut resonators", in Proc. 30th AFCS, June 1976, pp. 264-268; Technical Report ECOM-4433, US Army Electronics Command, Fort Monmouth, NJ 07703, September 1976, 15 pp.
57. R. Besson, "Phénomène "d'hystéresis" dans la déformation piézo-électrique du quartz α ," C.R. Acad. Sc. Paris, vol. 273, pp. 1078-1081, December 1971.
58. R. Besson and J.-J. Gagnepain, "Détermination des coefficients non linéaires de polarisation électrique du quartz", C.R. Acad. Sc. Paris, vol. 274, pp. 835-838, March 1972.
59. R.A. Graham, "Strain dependence of longitudinal piezoelectric, elastic, and dielectric constants of X-cut quartz", Phys. Rev. B, vol. 6, pp. 4779-4792, December 1972.
60. Y. Tsuzuki and M. Kakuishi, "Parametric excitation of contour modes of vibration in AT-cut quartz plates", Proc. IEEE, vol. 55, pp. 463-464, March 1967.
61. Y. Tsuzuki, "Parametric interaction between two contour modes of vibration in X-cut quartz bars", Proc. IEEE, vol. 56, p. 98, January 1968.
62. Y. Tsuzuki, Y. Hirose, and K. Iijima, "Holographic observation of the parametrically excited vibrational mode of an X-cut quartz plate", Proc. IEEE, vol. 56, pp. 1229-1230, July 1968.

Table 1
Some Parameters Influencing Crystal Frequency

1. TEMPERATURE
 - A. STATIC
 - B. DYNAMIC
2. TIME
 - A. SHORT TERM (NOISE)
 - B. INTERMEDIATE TERM (OVEN FLUCTUATIONS)
 - C. LONG TERM (AGING)
 - D. THERMAL HYSTERESIS
3. ACCELERATION
 - A. ATTITUDE
 - B. VIBRATION
 - C. SHOCK
4. RADIATION

Table 2
Emerging/Improving Technologies

1. SC-CUT
2. BVA DESIGN
3. NEW FABRICATION TECHNIQUES
 - A. SURFACE CLEANING
 - B. CHEMICAL POLISHING
 - C. ULTRAHIGH VACUUM FABRICATION
 - D. CERAMIC FLATPACKS
 - E. POLYGONAL PLATES
 - F. DUAL RESONATORS
 - G. AUTOMATED X-RAY ORIENTATION/ANGLE CORRECTION
4. QUARTZ GROWING AND SWEEPING
5. BETTER THEORETICAL UNDERSTANDING
6. LOW TEMPERATURE STUDIES

Table 3
SC-Cut vs. AT-Cut

ADVANTAGES

1. PLANAR STRESS COMPENSATED (LOWER AGING, LESS HYSTERESIS)
2. THERMAL TRANSIENT COMPENSATED (FASTER WARMUP)
3. LOWER ACCELERATION SENSITIVITY
4. LOWER DRIVE LEVEL SENSITIVITY
5. HIGHER CAPACITANCE RATIO (LESS Δf FOR OSCILLATOR REACTANCE CHANGES, HIGHER Q FOR FUNDAMENTAL MODE RESONATORS OF SAME GEOMETRY)
6. LOWER Δf DUE TO EDGE FORCES AND BENDING
7. IMPROVED STATIC F VS. T, WITH FEWER ACTIVITY DIPS
8. LOWER SENSITIVITY TO RADIATION

DISADVANTAGES

1. MORE DIFFICULT TO MANUFACTURE
2. FAST SHEAR (B-MODE) EXCITED
3. MORE SENSITIVE TO ELECTRIC BIASING FIELDS

Table 4
SC-Cut Frequency Change vs. Oven Parameters

$\Delta\theta \text{ \& } \Delta\phi$ = 5''		OVEN CYCLE RANGE (K)		
		0.1	0.01	0.001
OVEN OFFSET (K)	0.1	2.1×10^{-11}	2.1×10^{-12}	2.1×10^{-13}
	0.01	3.8×10^{-12}	2.1×10^{-13}	9.8×10^{-14}
	0.001	2.7×10^{-12}	3.6×10^{-14}	2.3×10^{-15}
	0	2.6×10^{-12}	2.6×10^{-14}	2.6×10^{-16}

Table 5
High Stability Oscillators

	1979	1989 GUESSTIMATE
STABILITY: 1 SEC	1 PP 10^{12}	PP 10^{14}
24 HOURS	2 PP 10^{11}	PP 10^{13}
5 YEARS	5 PP 10^8	PP 10^{10}
RETRACE	PP 10^9	PP 10^{11}
ACCELERATION	1 PP $10^9/G$	PP $10^{12}/G$
RADIATION	2 PP $10^{12}/RAD$	PP $10^{15}/RAD$
-40 TO +75°C	5 PP 10^{10} (TO 60°C)	PP 10^{12}
WARMUP	2 PP 10^8 IN 1 HOUR	PP 10^{10} IN 1 MIN
POWER AFTER WARMUP, AT -40°C	≈ 3 W	<250 MW
SIZE	>400 CM ³	10 CM ³
PRICE IN QUANTITY	>\$1,000	<\$300
OSCILLATOR CIRCUIT AND OVEN DESIGN	CRITICAL	LESS CRITICAL
QUANTITIES REQUIRED	FEW	≈50,000

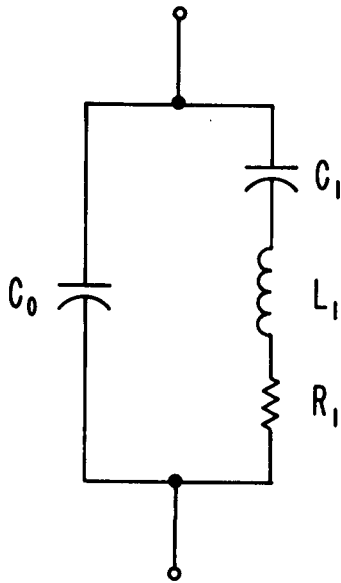


Figure 1. Crystal Resonator Equivalent Circuit

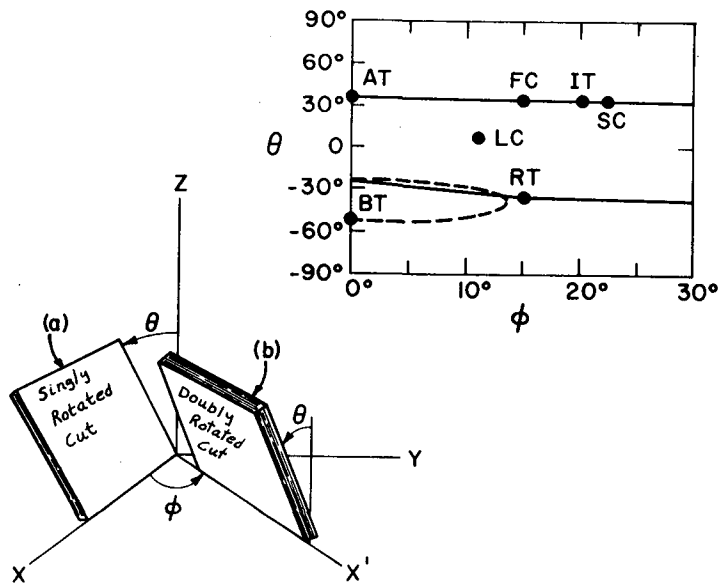


Figure 2. Doubly Rotated Quartz Cuts

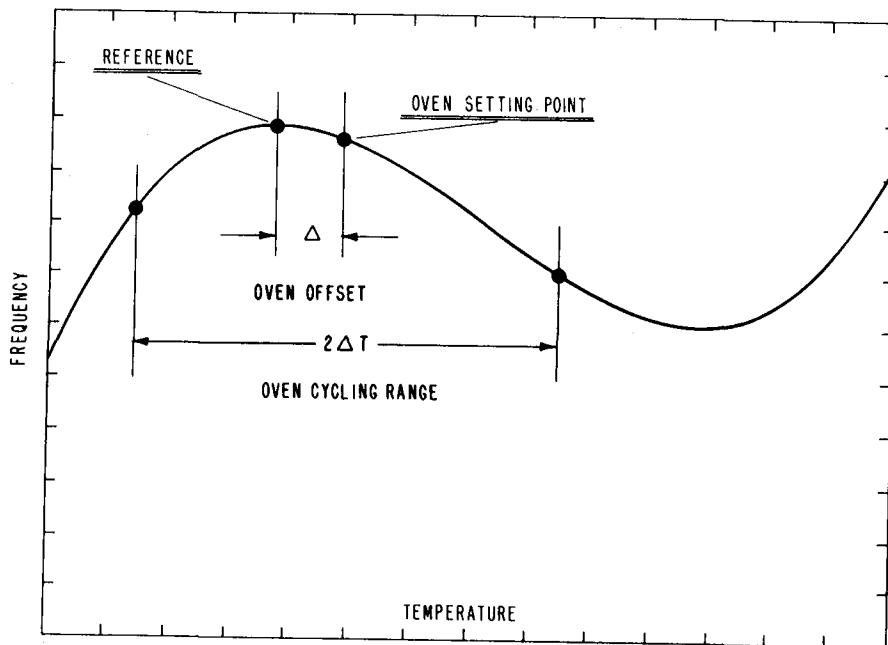


Figure 3. Static Frequency-Temperature Behavior

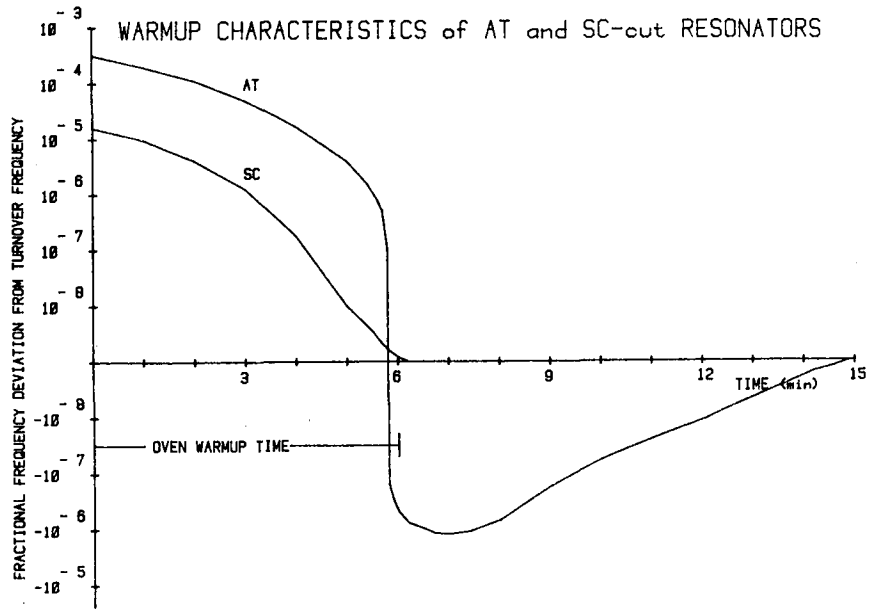


Figure 4. Warmup Characteristics of AT & SC Resonators

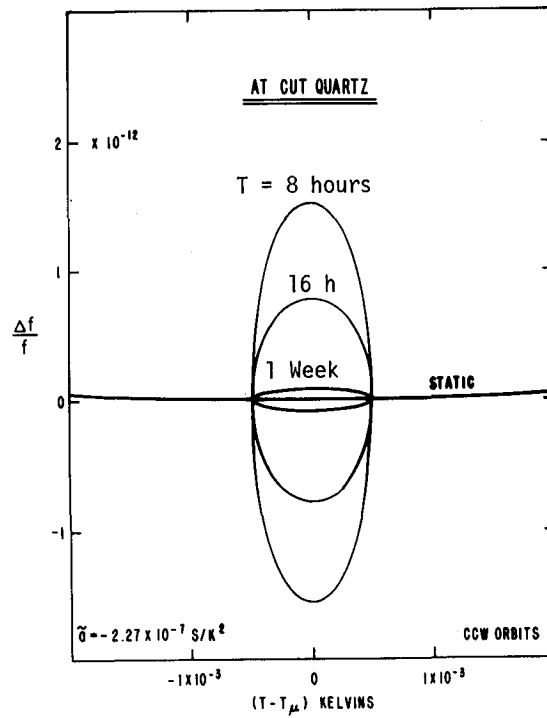


Figure 5. Dynamic Frequency-Temperature Behavior

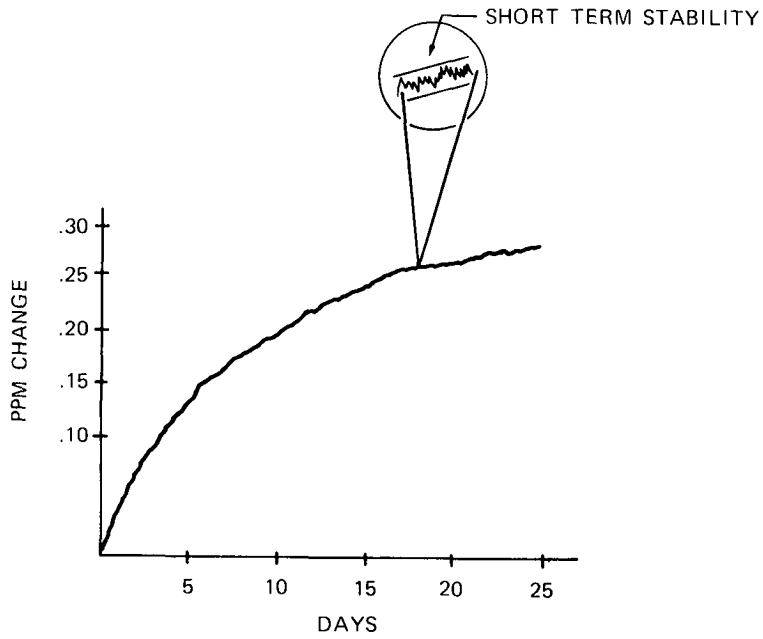


Figure 6. Resonator Frequency Versus Time

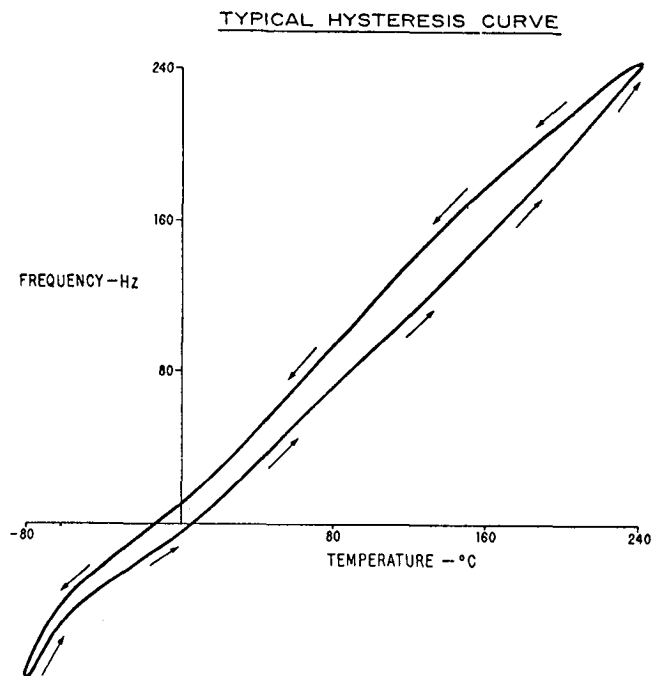


Figure 7. Thermal Hysteresis

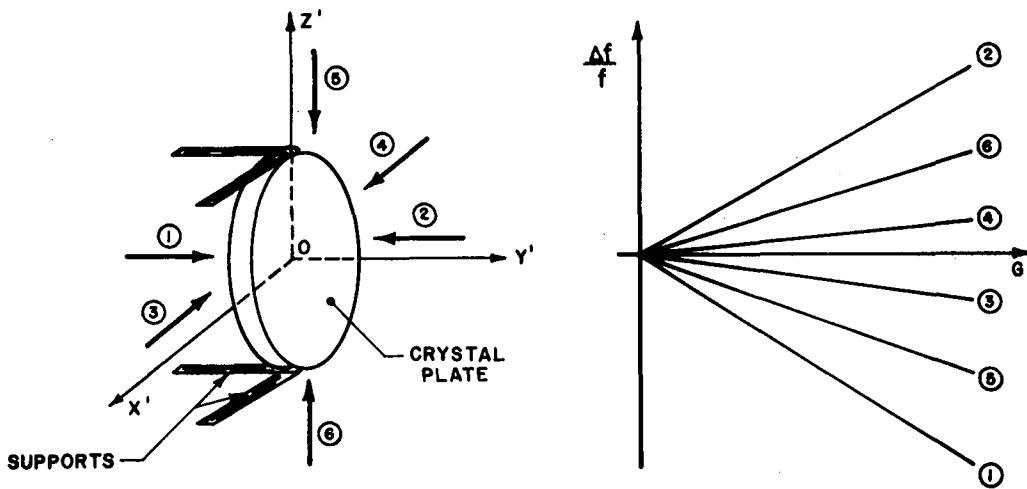


Figure 8. Acceleration-Frequency Behavior

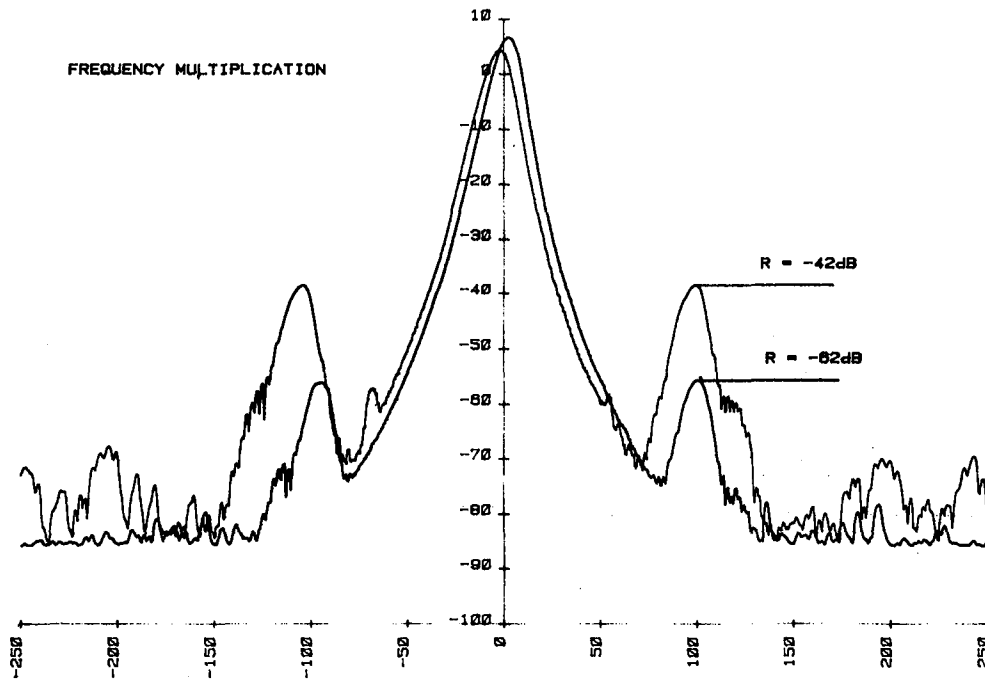


Figure 9. Resonance Spectrum Under Vibration, Showing 20 dB Sideband Increase Upon x 10 Frequency Multiplication

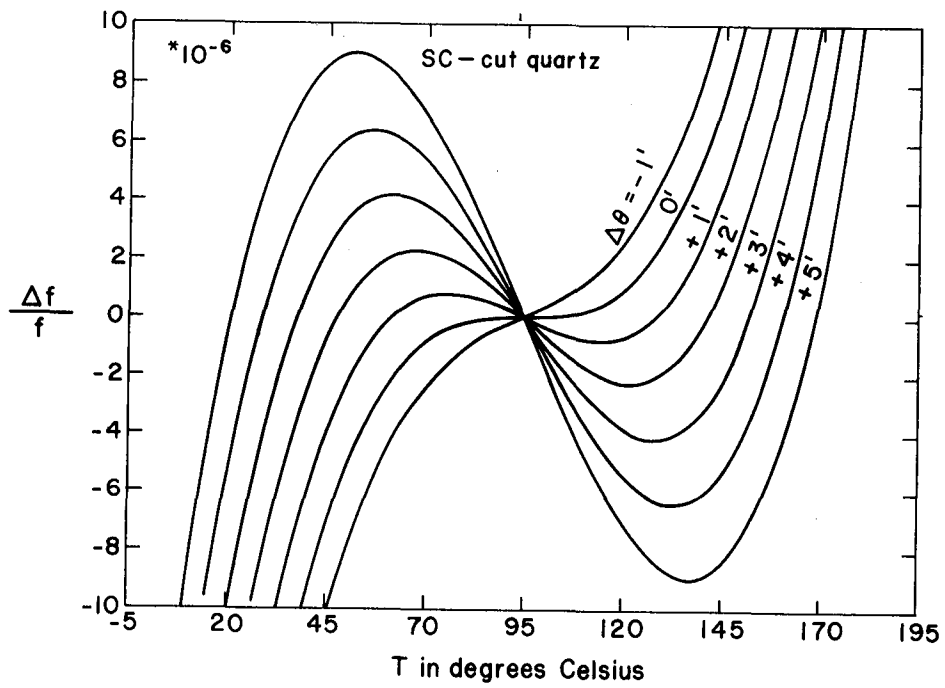


Figure 10. Frequency-Temperature-Angle Plots, SC Cut

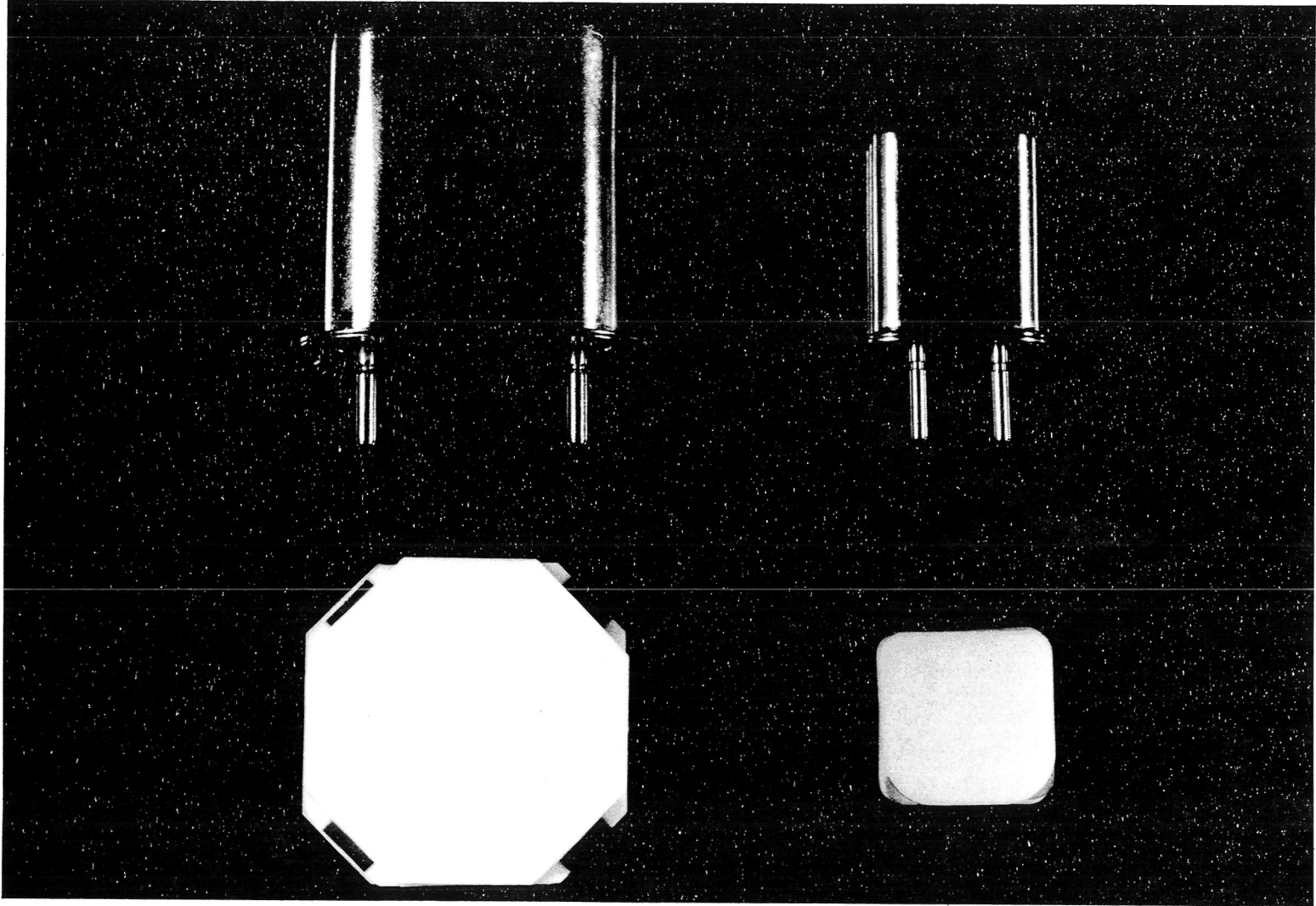


Figure 11. Metal and Ceramic Crystal Enclosures

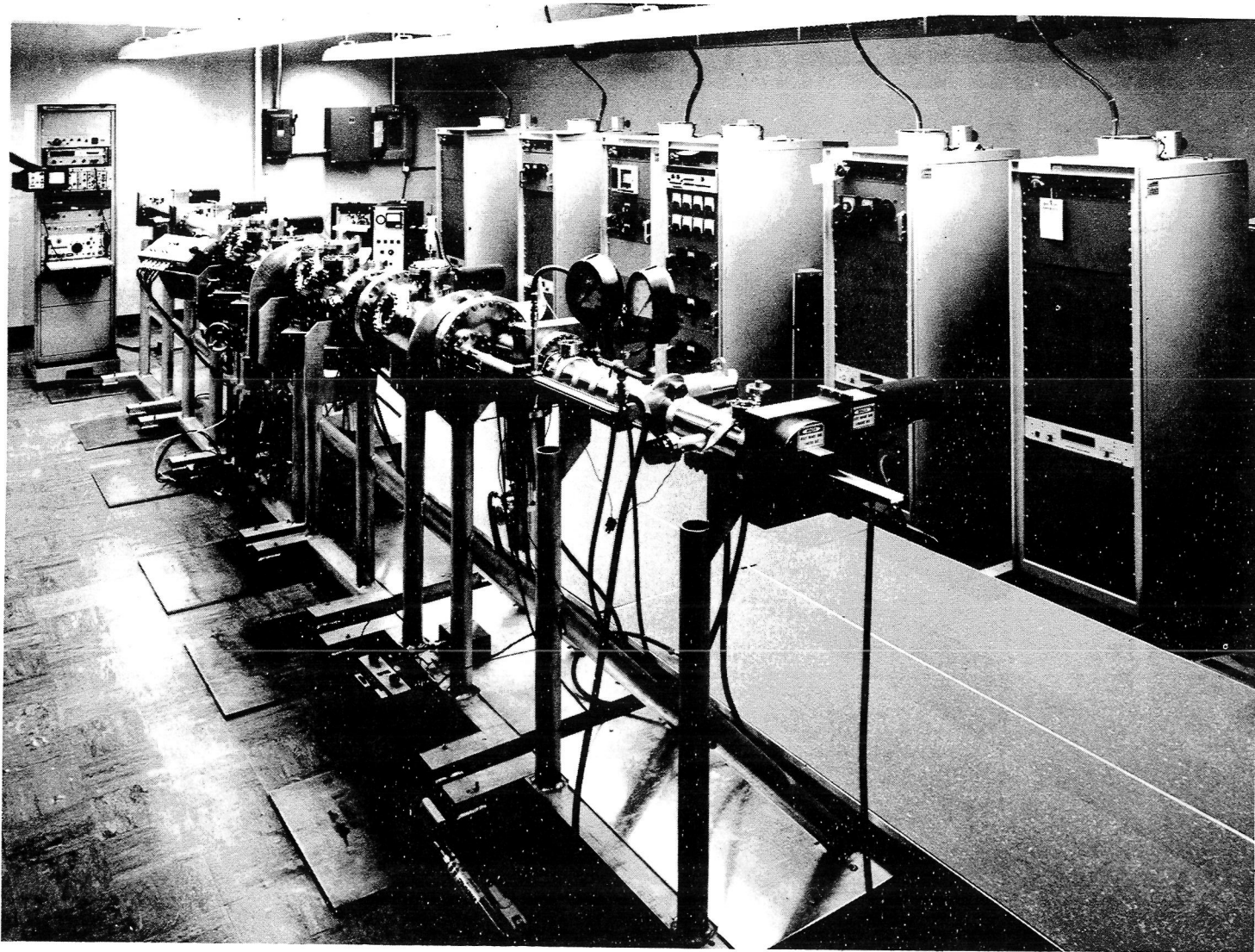


Figure 12. Quartz Crystal Fabrication Facility (QXFF)

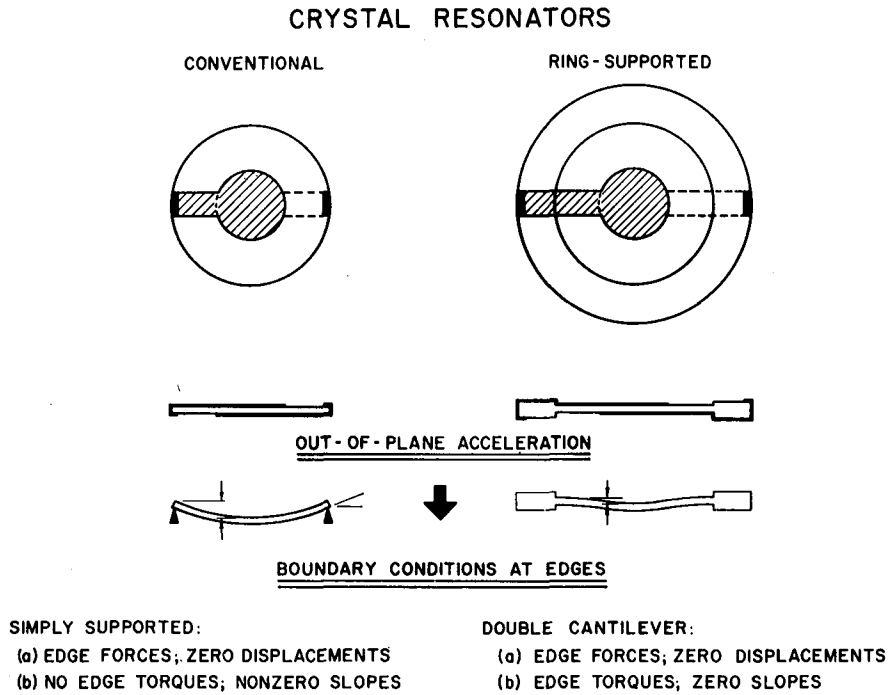


Figure 13. Conventional and Ring-Supported Resonators

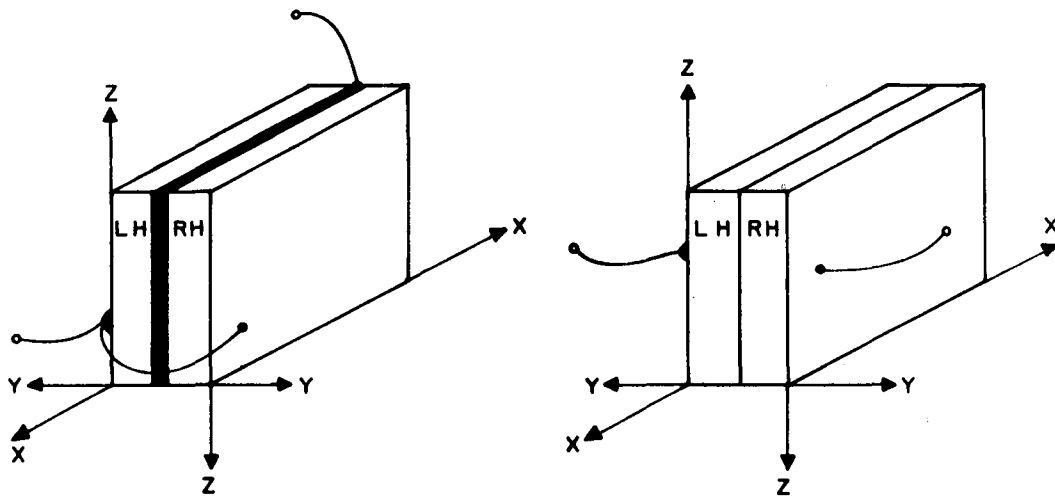


Figure 14. Stacked Crystal Enantiomorphs

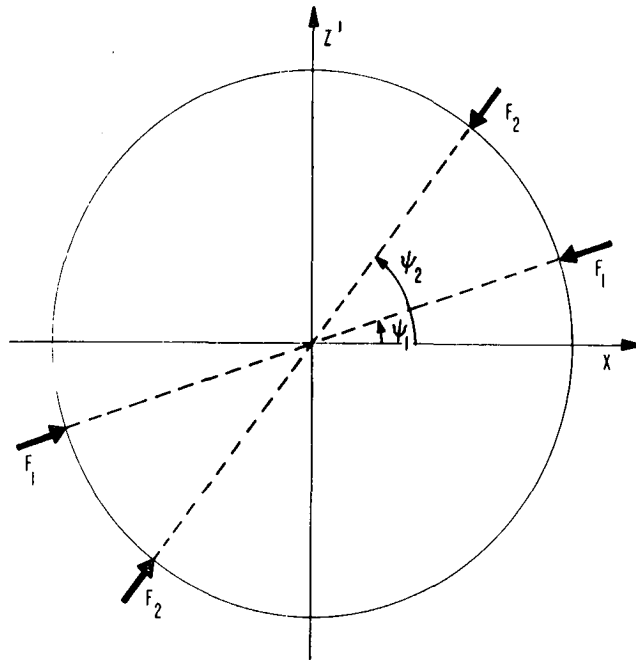
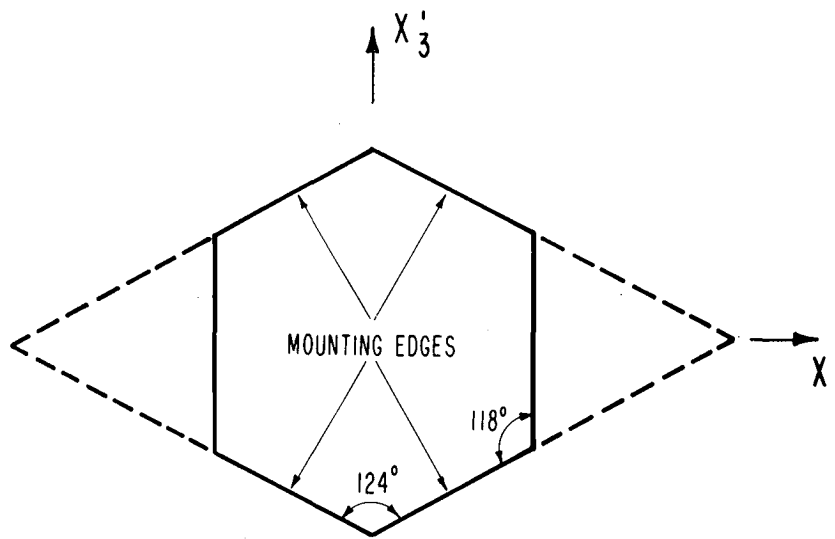
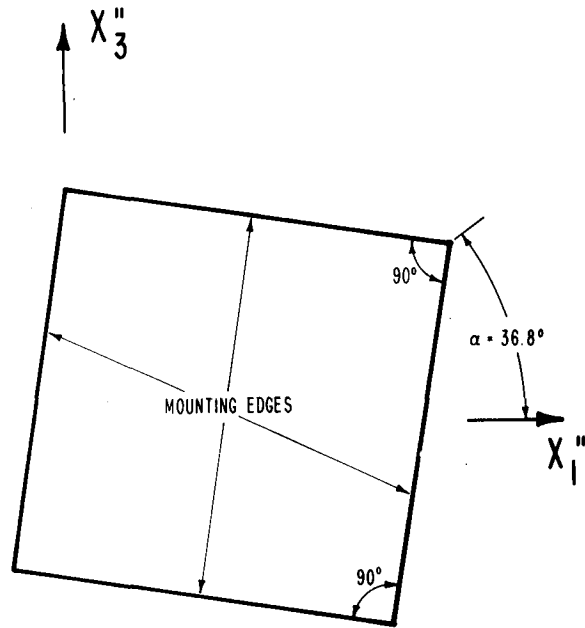


Figure 15. Crystal Disc with Edge Forces



AT CUT ($\phi = 0^\circ$)

Figure 16. AT-Cut Polygon



SC CUT ($\phi = 21.9^\circ$)

Figure 17. SC-Cut Polygon

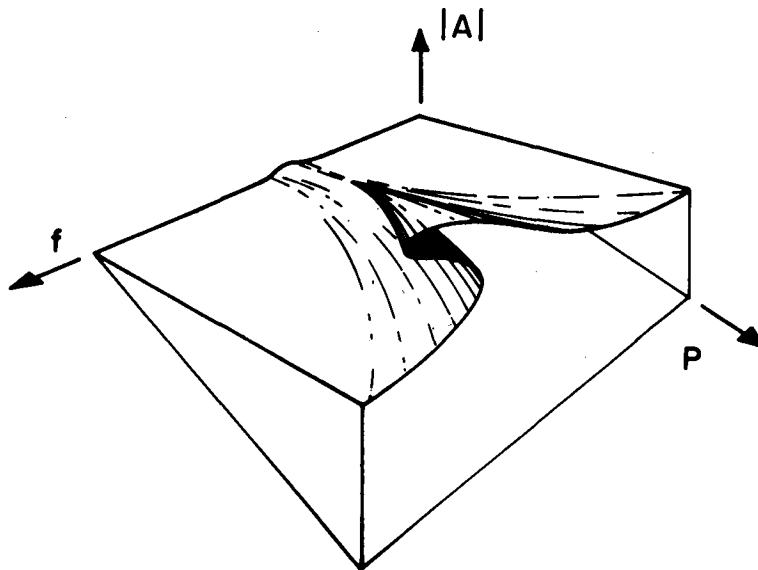


Figure 18. Frequency-Power-Amplitude Pleated Surface

QUESTIONS AND ANSWERS

QUESTION:

Is there any availability today commercially for SC cut crystals?

DR. BALLATO:

For SC cut crystals? Yes. They are-- Well, it depends upon the quantity. John, would you like to say a few words about that?

DR. VIG:

Yes. I would like to comment on the fact that, no, you cannot buy quantities of SC cut crystals and the ideas that are presented are, at this time, many of them are ideas, and they need to be reduced to practice and they need to be worked out, and there is a lot of work that needs to be done before we get to the point where we can mass produce SC cut crystals at a reasonable cost.

There are a couple of manufacturers who can provide very small quantities of SC cut crystals, whose angle controls is very poor. In other words, the turnover temperature is all over the place. There is no way you can buy an SC cut crystal with a turnover of 95 degrees, for example, if that is what you want. In order to get one of those, you might have to make a few hundred and select the one that meets your specification. So, there is a lot of work that needs to be done on manufacturing technology before we get to the point where we can afford to buy quantities of SC cut crystals.

QUESTION:

What about all the cases where they are needed, the majority. Not everybody needs 10, 11, 12, 13 crystals. If you need one today, what do you do?

DR. VIG:

If you reset your turnover temperature control, it doesn't make any difference. Okay? The SC cut plate is difficult itself to make today. You don't have the methods of angle control. As Art pointed out, you need to control both the Theta and the Phi angles to within a couple of seconds of arc. That is extremely difficult.

Okay? In theory the SC cut is going to be a beautiful cut. In practice, before you can buy it off the shelf, a lot of work needs to be done.

DR. WALLS:

Something of a comment I guess. From the work at the Bureau and work that we have done with Raymond Buisson and Jean-Jacques Ganupoint, I would guess that stress probably plays a greater role in frequency instability than what temperature contamination does and that the range between one second and a thousand seconds is dominated by temperature fluctuations in the AT as you have demonstrated in the last couple of talks and what we have seen. But beyond that, I would think that stress relaxation, stress in the mounting, stress in the plating is more important than contamination. Even at 10 to the minus 9 torr, you are still going to get monolayer exchanges of contamination within your enclosure at 1,000 seconds, so really it is an equilibrium between absorbed stuff on the inside of the enclosure and on the crystal blank. So I would guess that beyond 1,000 seconds it is really stress, and as we get better resonators, the aging and the long-term stability will be dominated by circuit parameters isolation in the output stage because of feedback and other things and it is my guess the architecture of our crystal oscillators must drastically change if we are going to achieve the stabilities of 10 to the minus 13 for long periods of time.

DR. BALLATO:

You are right, Fred. But stress is very very important, especially in the long-term. Also, some other rather subtle phenomena, that is to say diffusion of electrodes, if you have electrodes. Of course you don't need electrodes, or diffusion of impurities in the lattice. You need a lot of work on getting better quartz. Those will contribute significantly to long-term aging.

QUESTION:

How does the electromagnetic pulse change the frequency and stress?

DR. BALLATO:

How does that change the frequency? By heat effect.

QUESTION:

Heat?

DR. BALLATO:

Yes.

GALILEO QUARTZ CLOCK

M. Bloch, M. Meirs and M. Rosenfeld
Frequency Electronics, Inc., New Hyde Park, New York

P. Garriga
Hughes Aircraft Company, El Segundo, California

ABSTRACT

Frequency Electronics has developed and tested a quartz oscillator for use in the Galileo experiment (orbiter and Probe) for Jupiter mission 1982. This oscillator has achieved significant performance breakthroughs by the use of an "SC" cut, double rotated, crystal in a titanium Dewar flask. Some of the performance parameters are:

Radiation Sensitivity:	2×10^{-14} /rad
"g" Sensitivity	2×10^{-10} /g
Optimum Deceleration Sensitivity:	2×10^{-10} /425 g
Power Dissipation:	1.2 watts
Size:	1.8" dia. by 5.5"lg
Operating Pressure:	vacuum to 20 torrs
Short Term Stability:	3×10^{-12} /second

The quartz oscillator uses a double proportional control oven to achieve a temperature coefficient of less than 1×10^{-10} /10 degrees C. The results obtained on other "SC" cut crystals indicate the possibility of significant performance improvements in airborne, shipboard, missile timing, navigation and high speed communication systems.

INTRODUCTION

Jupiter, appropriately named for the most powerful god in the Roman Pantheon, is the largest planet in the solar system. Located 770 million km from the sun, Jupiter has an equatorial diameter of 140,000 km, approximately 10 times that of Earth. The planet, which is almost entirely liquid, takes nearly 12 years to complete a solar orbit, but a Jovian day is only of 10 hours duration.

The Pioneer 10 and 11 missions of the National Aeronautics and Space Administration (NASA) flew by the planet in 1973 and 1974 and verified that Jupiter emits more than twice as

much energy as it receives. Thus it is a source of high energy particles accelerated into space. In March 1979, Voyager 1 transmitted photographs of the planet's satellites and multicolored atmosphere, including the famous red spot. The photographs revealed a ring of material in equatorial orbit around Jupiter, a phenomenon previously observed only with the planets, Saturn and Uranus.

Scientists believe that Jupiter holds many clues to the origin and development of the solar system and that studies of its atmosphere, magnetic field, satellites, and radiation belts will be important keys in unlocking those secrets. To make these and other important observations, NASA has scheduled Project Galileo for launch on the Space Shuttle in early 1982. The program is named after Galileo Galilei, the Italian Renaissance founder of experimental physics and astronomy, who is credited with discovering four of Jupiter's 13 known satellites in 1610.

The program consists of an orbiter spacecraft which will arrive at Jupiter in 1985 and circle the planet for 20 months, and an entry probe that will descend into the planet's turbulent, hydrogen-rich atmosphere to a pressure of about 20 Earth atmospheres after withstanding an entry speed of 48 km/sec (107,000 mph).

The orbiter will accommodate eleven scientific investigations which will measure the magnetic, gravitational, and thermal properties of Jupiter and its satellites; determine their surface composition and morphology; and study their ionospheres, atomospheres, and gas emissions. The spacecraft will also study the magnetosphere-satellite interaction; define the topology and dynamics of the magnetosphere, magnetosheath, and bowshock; describe the nature of the magnetospheric particle environment; determine the distribution composition, and stability of trapped radiation and conduct a synoptic study of the Jovian atmosphere.

The interplanetary flight phase of the mission will take about 1290 days, or 3-1/2 years. The probe, which consists of a deceleration module and a descent module, will separate from the orbiter 150 days prior to Jupiter encounter. A timer will initiate probe operation about 6 hours before entry into the planet's atmosphere. During high speed entry, acceleration and heatshield performance data will be collected. No telemetry is planned prior to or during entry; all relevant information will be stored for playback during subsonic descent.

During the 60-minute descent the seven scientific instruments on the probe will determine Jupiter's atmospheric structure and composition, location of clouds and their structure and physics, hydrogen/helium ratio, lightning and radio emissions, energy absorption and radiation and energetic particle distribution. The probe mission will be completed at an altitude where the pressure is approximately 20 times that of Earth's sea level.

There will be stable oscillators located on both the probe and Orbiter spacecrafts. These stable oscillators will be used by the scientists to obtain data about the atmosphere of Jupiter as well as to transmit information. Both oscillators have been designed to be virtually identical although they will see somewhat different environmental conditions.

Design

The oscillator is housed in a 1.8" diameter by 5-1/2" long stainless steel enclosure. Stainless steel was chosen to allow the entire package to be a vacuum sealed welded enclosure capable of withstanding the vacuum to 20 bar pressure variation. The outline and mounting dimensions are shown in Figure 1. The internal construction is shown in Figure 2. The oscillator and amplifier printed circuit boards are located inside a titanium dewar flask. Titanium was chosen for the dewar flask for its low thermal conductivity and light weight to minimize both power consumption and weight and yet have the strength to withstand the 425 g deceleration force.

Figure 3 shows the construction for this Dewar flask. Inside the Dewar flask, we have a double proportional controlled oven. The quartz crystal and oscillator circuit are inside the inner oven. The output amplifier and oven control boards are located in the outer oven. The entire assembly is foamed in place to maintain stability during shock, vibration and deceleration. Figure 4 is a photograph of the first engineering model of this oscillator next to a larger Fltsatcom oscillator. The connectors used are ceramic to metal seals to withstand the large pressure variation. A special weldable r.f. connector was constructed by Tek-Wave, Inc. an FEI subsidiary to perform this function.

Figure 5 is the schematic of the oscillator circuitry. A Colpitts oscillator configuration was chosen for ease of use and minimization of components. The quartz crystal is an "SC" cut, 5th Overtone at approximately 24 MHz. The

"SC" cut was chosen because it is stress-free, and will give excellent warm-up repeatability. Q1 is the oscillator transistor, and both a fundamental and B Mode trap are used in the emitter. An output transformer couples the signal to the rest of the circuitry. Figure 6 is a circuit block diagram of the entire unit. The inner oven controller has an additional booster heater which is slaved to provide additional power during warm-up. Once the oven has reached its normal operating range, this booster heater is no longer functional. The A1 area represents all circuitry located inside the Dewar flask. The voltage regulator board A2A1 is located on the base of the unit. All of the components used in this oscillator are space qualified and goes through additional screening and burn-in requirements.

Performance

The oscillator was able to meet all of the specification requirements and performed considerably better than specified in some significant areas. Table 1 is a summary of these performance characteristics. The performance was such that under all conditions of environment, during the 30 minute descent phase of the probe, the oscillator was capable of maintaining the desired frequency accuracy. A composite curve is shown in Figure 7 which shows a total uncertainty of $+ 3 \times 10^{-10}$ at the end of this 30 minute interval. The warm-up characteristic of this oscillator is shown in Figure 8. The smooth and rapid warm-up is indicative of the SC cut crystal performance. The warm-up time to $PP10^{-9}$ occurred within 6 to 7 minutes and no overshoot or ringing was apparent in the frequency curve. This type of overshoot-free warm-up curve has been found in other oscillators which also used the SC crystals.

The oscillator performance in a radiation environment showed an improvement over typical AT crystal performance of 1 to 2 orders of magnitude. A typical AT cut crystal would exhibit a sensitivity of $1 - 2 \times 10^{-12}$ /rad whereas the SC cut crystals showed a sensitivity of $1 - 2 \times 10^{-14}$ /rad in the best case and 3×10^{-13} in the worst case. Radiation tests were performed using a Cobalt 60 radiation source. Figure 9 is a typical radiation response curve that was obtained from these oscillators. The radiation applied was at the rate of 10 rads/sec for 700 seconds. The initial response shows a positive offset which varied from 1 to 5×10^{-9} and was independent of radiation rate. After this initial positive offset a negative slope was obtained which was directly proportional to the radiation rate and whose sensitivity became less as the crystal was further preconditioned.

TABLE I
GALILEO QUARTZ CLOCK
TABLE OF CHARACTERISTICS

<u>PARAMETER</u>	<u>OBJECTIVE</u>	<u>ACTUAL</u>
SIZE:	1.75" DIA X 5.5"	1.75" DIA X 5.5"
WEIGHT:	14 OZ.	20 OZ.
INPUT POWER:	7 WATTS PEAK	7 WATTS PEAK
WARM-UP TIME:	300 MIN.	< 300 MIN.
FREQUENCY STABILITY:		
AGING:	1×10^{-10} /30 MIN.	< 1×10^{-10} /30 MIN.
VOLTAGE:	1×10^{-10} /VOLT	< 1×10^{-11} /VOLT
TEMPERATURE:	1×10^{-10} /10°C	1×10^{-10} /10°C
MOTION:	1×10^{-9} /G	2×10^{10} /G
SHORT TERM:	5×10^{-11} /SEC	1×10^{-11} /SEC
PHASE STABILITY:	0.016 DEGREES	0.003 DEGREES
RADIATION SENSITIVITY:	-2×10^{-12} /RAD	-2×10^{-14} /RAD

Figure 10 shows a radiation level of 150 rad/sec for 24 minutes. During this radiation exposure the change of slope as a function of radiation level is apparent. The retrace characteristic at the conclusion of the radiation exposure was random in nature and no conclusions have been drawn as yet.

Figure 11 shows an accumulated radiation exposure of 1 megarad after the initial 25 krad preconditioning. The variation was approximately 1×10^{-8} for 1 Mrad. Figure 12 shows the effect of radiation on the orbiter engineering model. Radiation levels of 10 rad/sec for 700 seconds was applied after initial preconditioning of 25 krads and shows a slope of 3.3×10^{-12} /rad. After a further preconditioning of 200 krads and with the same radiation level (as shown on Figure 13), we obtain a sensitivity improvement to 7×10^{-13} /rad. Data taken on these oscillators indicated that with a preconditioning of 500 krads to 1 megarad, radiation sensitivity of 10^{-14} /rad are obtained.

The two engineering models built on this program will be used to further determine radiation sensitivity and warm-up as a function of time. These units will be retested at 6 month intervals for the next two years to further characterize these parameters.

Conclusions

Tests on the engineering models of the Galileo oscillator have indicated that the SC cut crystal has achieved considerable improvements in both warm-up characteristics and radiation sensitivity. Five to ten minutes warm-up to within $1\text{pp}10^{-9}$ was achieved without overshoot and an order of magnitude improvement in radiation sensitivity was obtained. The use of the titanium Dewar flask has permitted the achievement of low power drain and high stability equivalent to that obtainable with glass, but has provided the capability to withstand the harsh environmental atmosphere that will be encountered during the mission.

Acknowledgment

We would like to thank both Ferdinand Euler and Lester Lowe of RADC for their help and assistance in making available both equipment and facilities to obtain the radiation data presented here. The experimental results in the paper were developed under the Galileo Probe Spacecraft subcontract with the Hughes Aircraft - Space and Communication Group and NASA/Ames Research Center. Special thanks are due to Al Kahane of RADC, Dr. T. A. Savo of HAC, and John Vig of ERADCOM for their technical support and encouragement in preparing this paper.

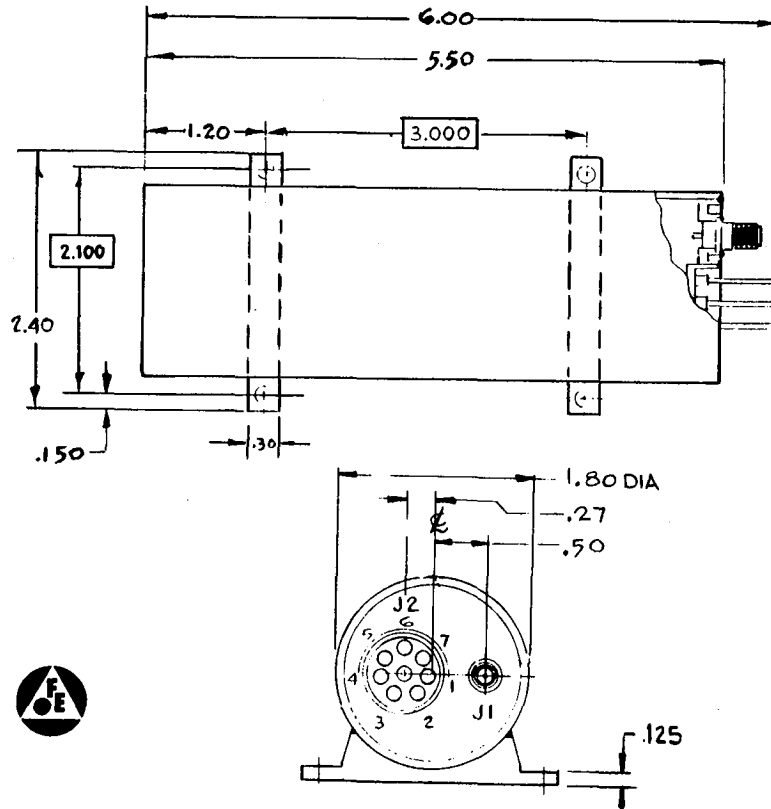


Figure 1. Outline Details

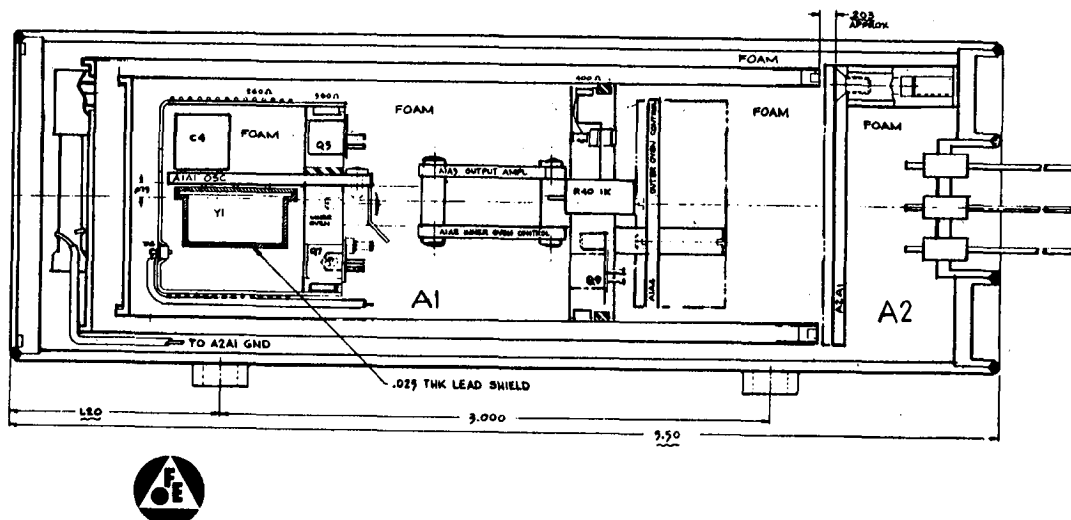


Figure 2. Unit Assembly

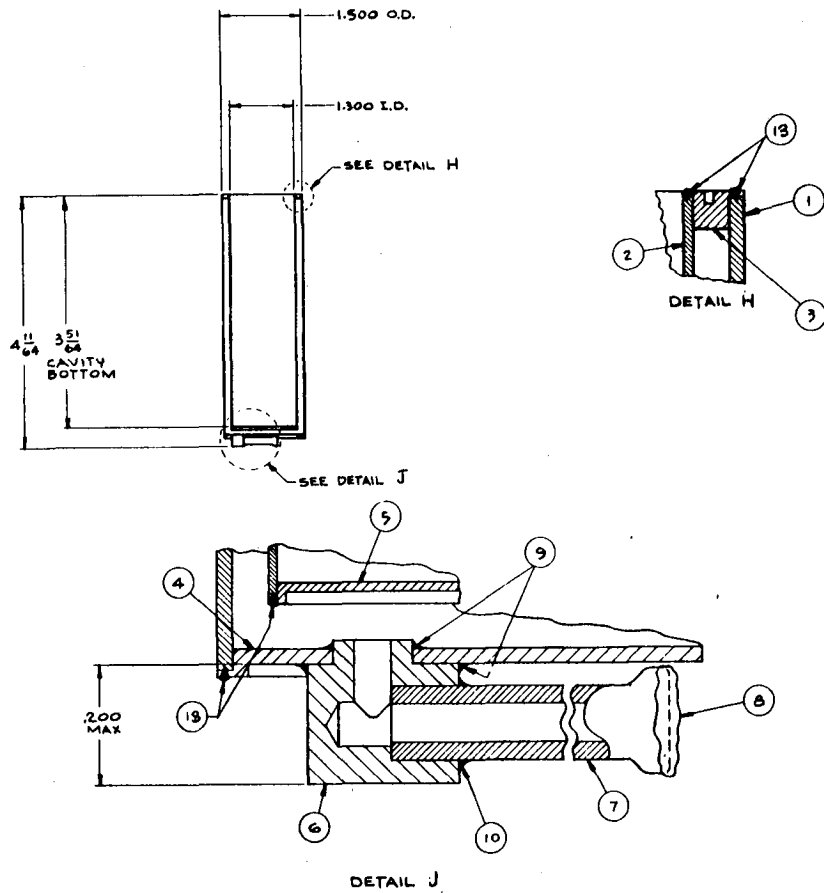


Figure 3. Dewar Flask Construction

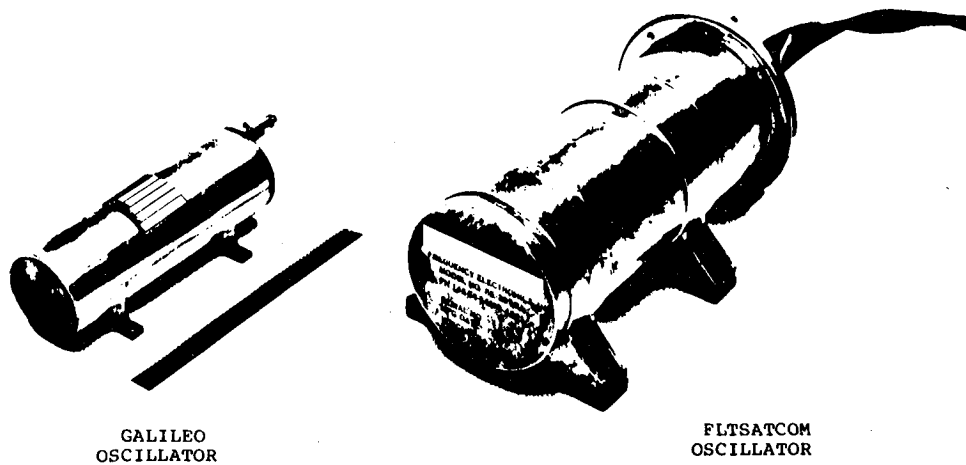


Figure 4. First Engineering Model

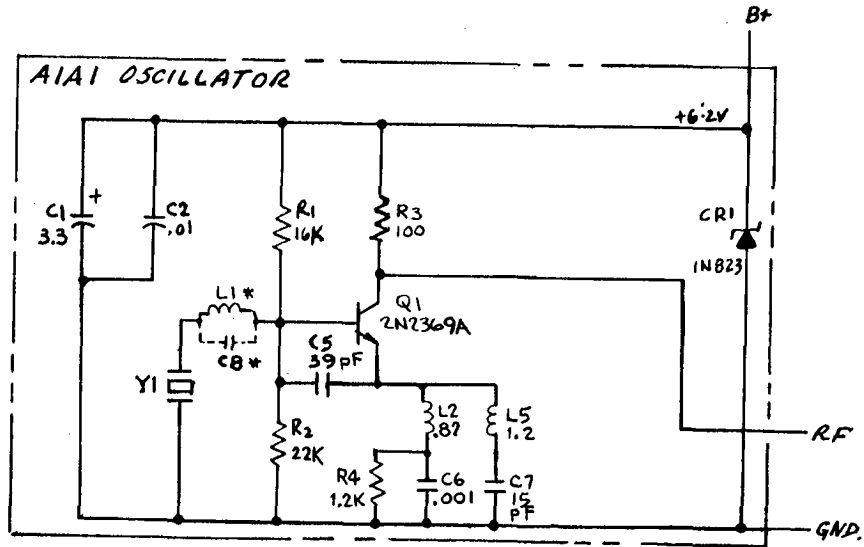


Figure 5. Oscillator Schematic

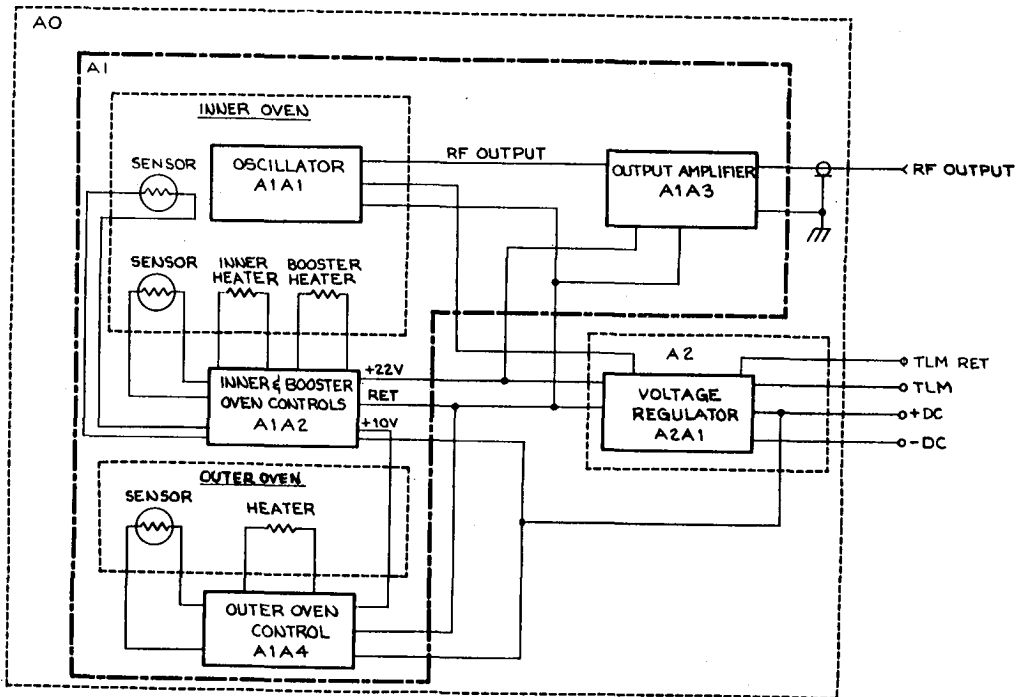


Figure 6. Circuit Block Diagram

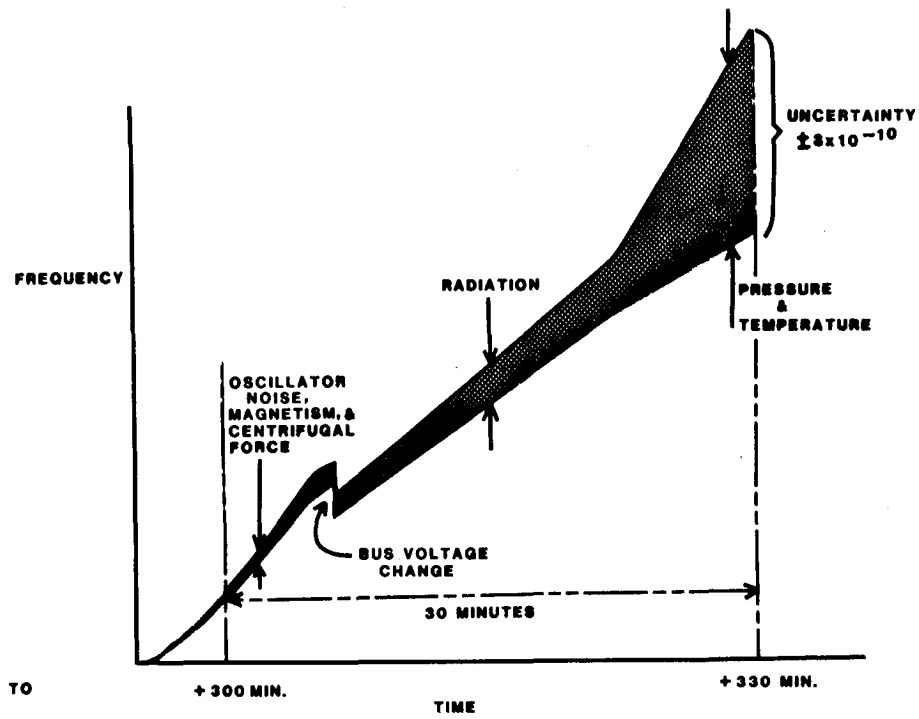


Figure 7. Typical Oscillator/Drift

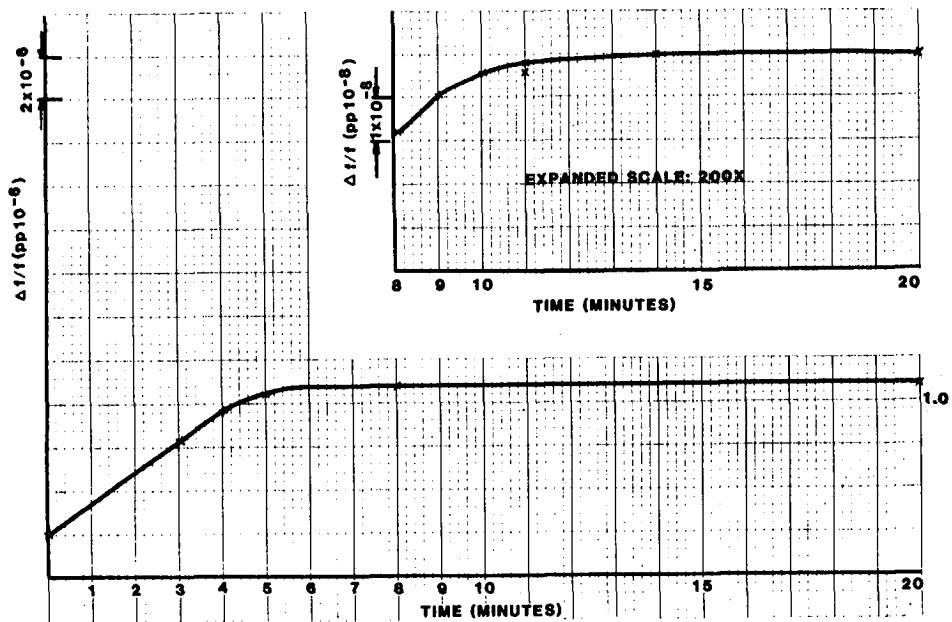


Figure 8. Galileo Warmup Curve

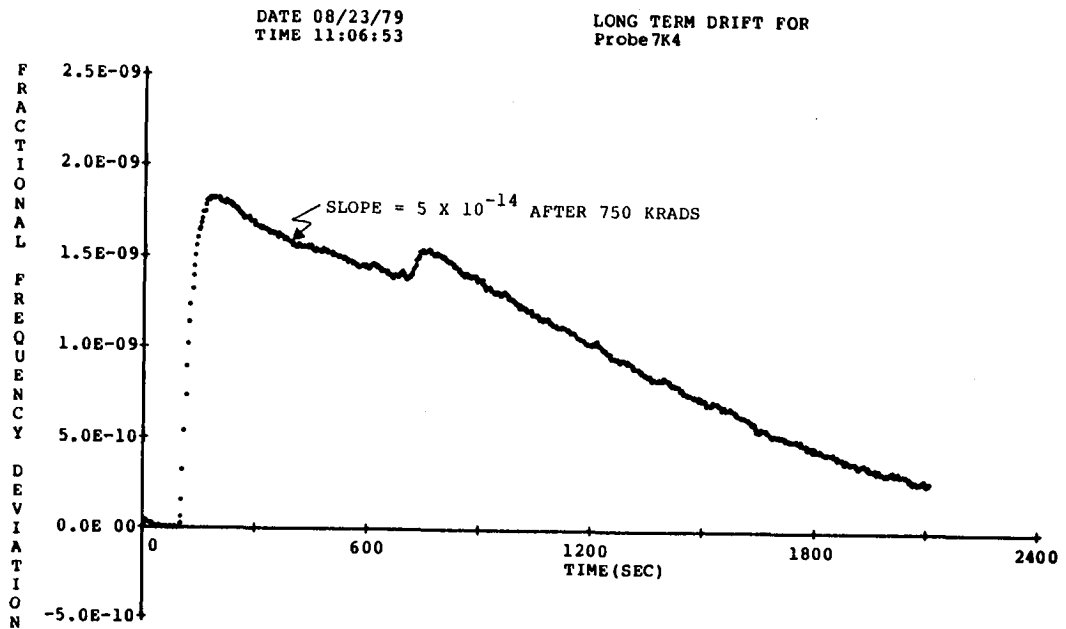


Figure 9. Probe Radiation, 10 RAD/Sec for 700 Seconds

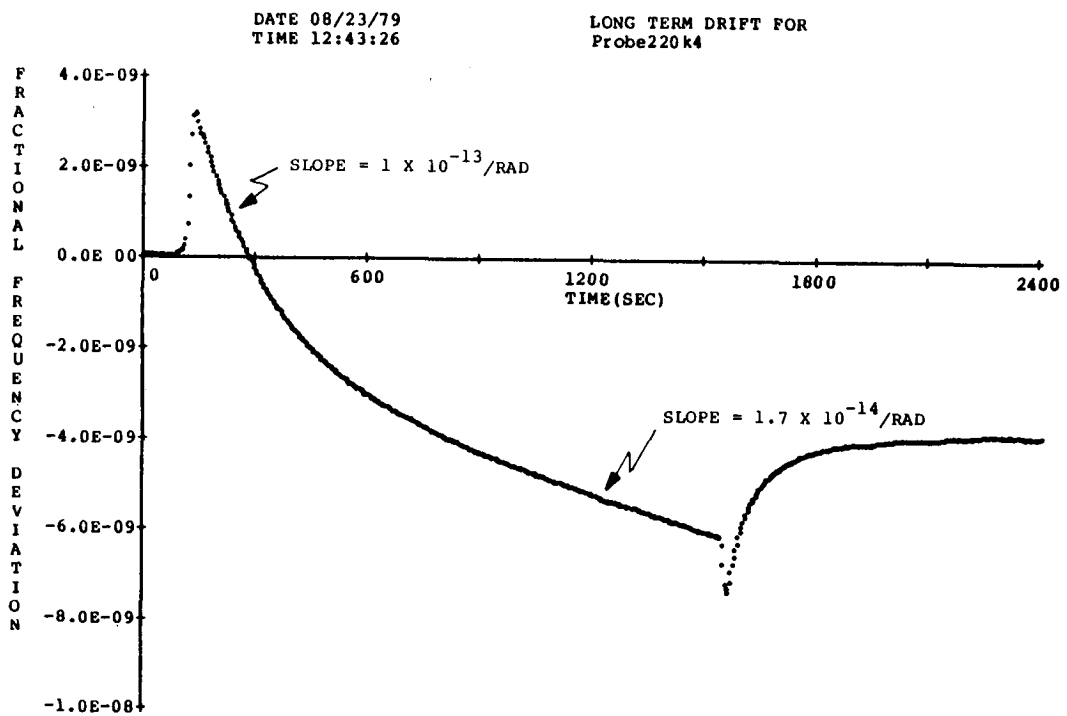


Figure 10. Probe Radiation, 150 RAD/Sec for 24 Minutes

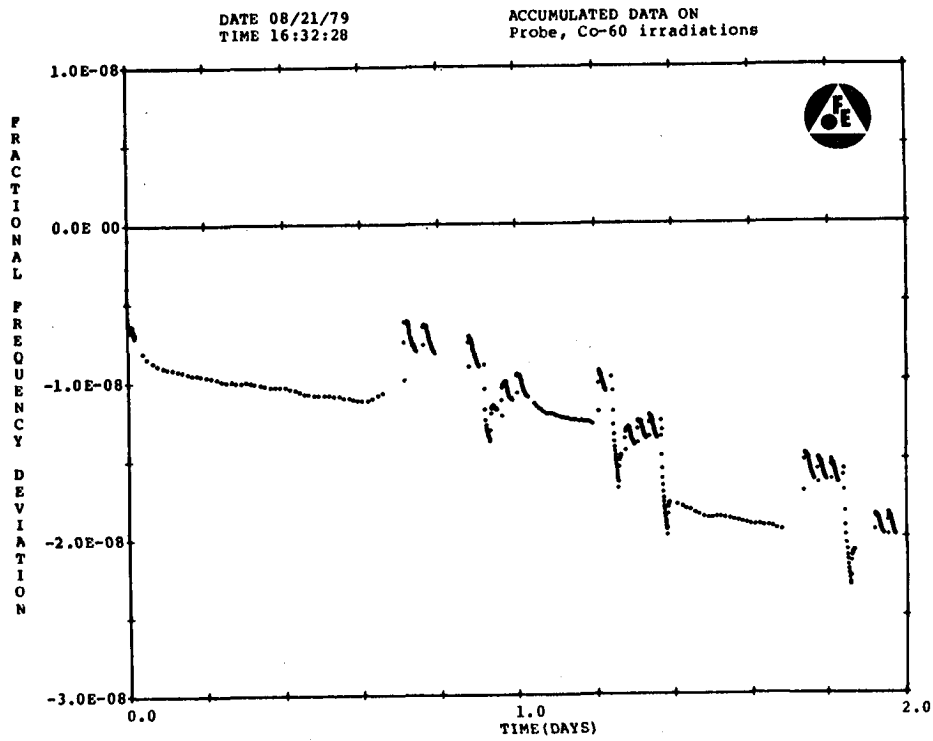


Figure 11. Accumulated Probe Radiation, 1,000,000 RADS

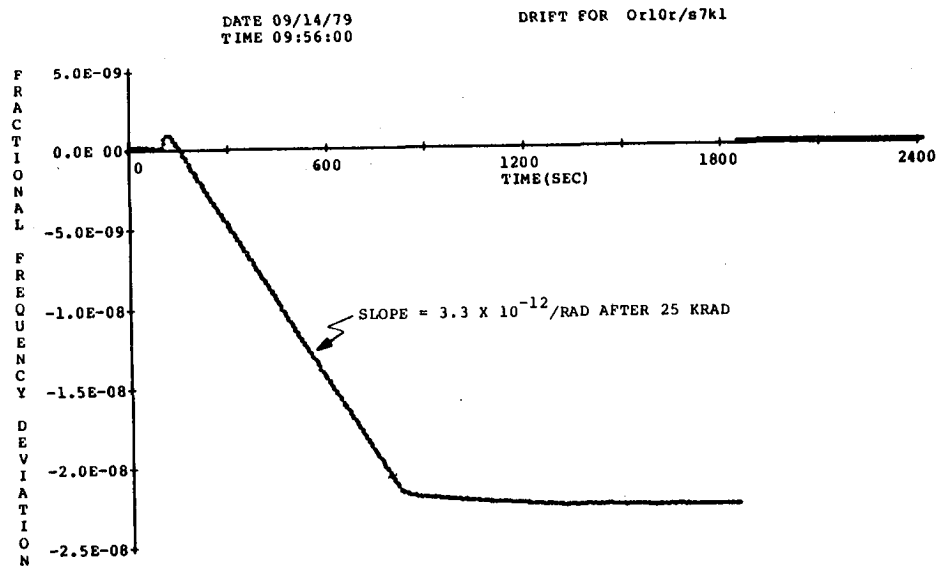


Figure 12. Orbiter Radiation, 10 RADOSEC for 700 Seconds,
25 KRAD Preconditioning

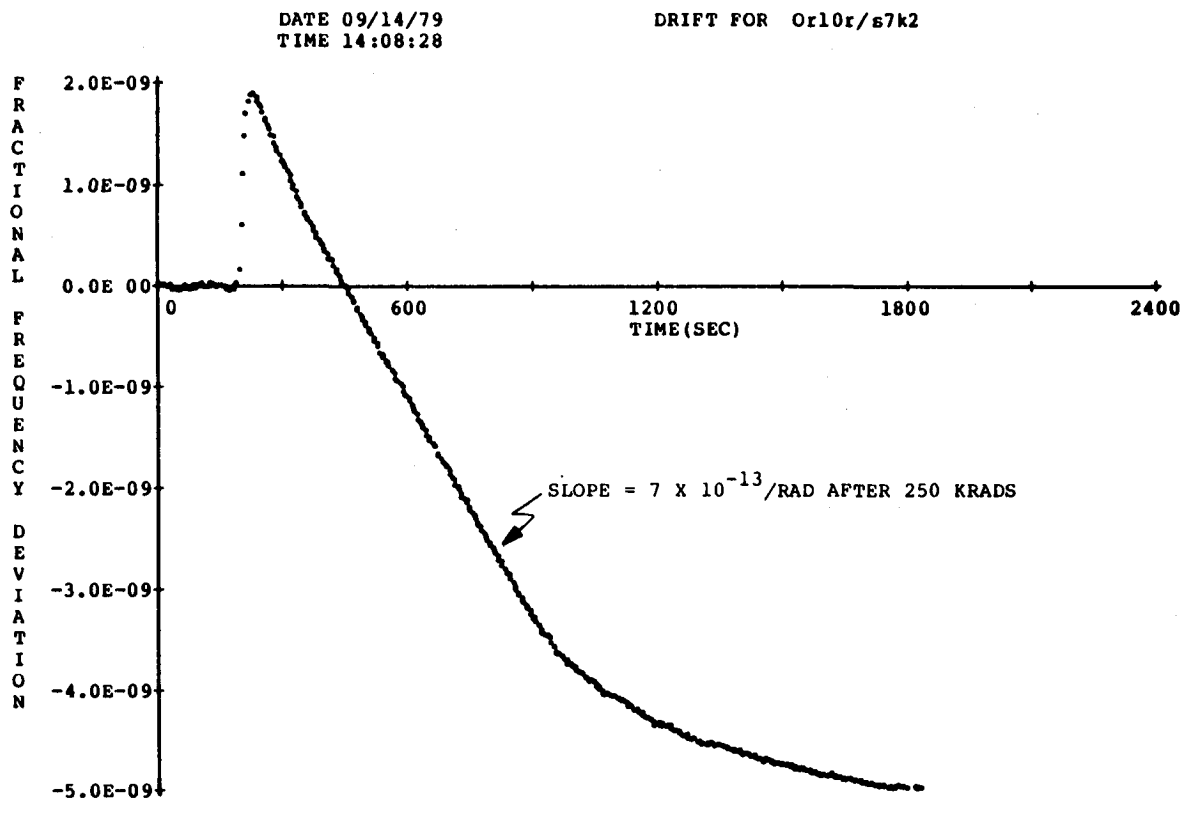


Figure 13. Orbiter Radiation, 10 RADOSEC for 700 Seconds,
250 KRAD Preconditioning

QUESTIONS AND ANSWERS

DR. WALLS:

Have you or do you plan to investigate the effect of chemical polishing versus mechanical polishing on radiation sensitivity because that may in fact involve some changes in the stress level of the surface?

DR. BLOCH:

No Fred. We did not intend to, but we have a study contract now on SC cut crystals and that might be a test that would be there. I have a feeling that it is something more simple. Unfortunately we didn't have the luxury to take apart the resonators, but we have seen in cutting quartz that the late vintage premium Q swept quartz there aren't two resonators cut right next to each other that have the same defects.

And another possibility Fred, it might be that one has more severe defects than the other. The quartz has been really a problem to us in handling.

MR. PLEASURE:

You seem to have a small resonator that is peculiar to the crystal itself. You showed a little L and a dotted little C, is that what you used to tweak in the final set of frequencies, the operating frequencies?

DR. BLOCH:

Yes. We use either inductance or capacitance to set nominal.

MR. PLEASURE:

And isn't that a temperature sensitive device?

DR. BLOCH:

It is really not, if you make an error budget analysis, it contributes less than a part in 10 to the 11th to the error budget. The SC cut crystal has a very low value of C-1, so the external effects, if you shift the frequency of a part in a million of let us say 20 picofarads, the effect of that capacitor is negligible, also with the inductor.

QUESTION:

Is it made on an air core so that it won't stretch and have a hysteresis in its characteristics?

Have you tried this?

DR. BLOCH:

Are you talking about the inductor? The inductors that we use for setting are all air core inductors so they have a very low temperature coefficient and the capacitors that we are using are all glass capacitors with about 20 parts per million per degree C. Since this is in an oven with about a 50 millidegree temperature control under the worst condition, it produces negligible effects.

QUESTION:

So you have a bad form, it will knock it silly.

DR. BLOCH:

It really doesn't, the glass capacitors do what we need. We have them to repeat to within a part per million and if you visualize a 20 picofarad capacitor changing by more than a part, that is far fetched change for a precision glass capacitor.

We have not experienced any such problem in the regime of parts in 10 to the 10th and 10 to the 11th. Maybe in 10 to the 14th.

QUESTION:

What is the error then?

DR. BLOCH:

There is an air core which has very similar retrace characteristic. It has very little hysteresis and again there is a large tolerance. You are talking many microhenries for one part per million change. It is a very stiff resonator. So there is a large tolerance on the effect of those parts.

INITIAL RESULTS ON 5 MHz QUARTZ OSCILLATORS
EQUIPPED WITH BVA RESONATORS

Raymond J. Besson
Ecole Nationale Supérieure de Mécanique
et des Microtechniques
25030 Besançon, France

Donald A. Emmons
Frequency and Time Systems, Inc.
Danvers, Massachusetts

ABSTRACT

The techniques of fabricating BVA resonators have yielded greatly improved performance in terms of aging, amplitude-frequency effect, and acceleration sensitivity.

Preliminary results have been recently obtained including Q factor of 3.5×10^6 , short-term stability of 5×10^{-13} at 1 second and aging of 5×10^{-12} per day measured at NBS. In addition, the frequency shift under acceleration (measured at ONERA) was found to be as low as 2×10^{-10} per g for AT-cut quartz, and a factor of 10 smaller for SC-cut, with no residual frequency shift after static g loading, to within a few 10^{-11} .

In this paper are presented new results on 5 MHz resonators concerning aging versus drive level, reduced amplitude-frequency effect, frequency and phase stability performance, and frequency retrace following power interruption.

The conclusion from aging and level of drive investigations is that a zero aging rate is possible at a drive level which depends on the quartz material used. For natural AT quartz, a level of 70 to 90 μW appears to be optimum, and for SC quartz approximately 160 μW .

Measurements of short term frequency stability and of the phase noise were performed using crystals mounted within a modified commercial oscillator model, FTS 1000. A 5th overtone crystal exhibits $S_{\phi}(f) = -127$ dB at 1.5 Hz from the carrier with close-in phase stability

being degraded very little as the drive level is increased. The white noise floor improves with drive level, as expected.

A stability $\sigma(\tau) < 5 \times 10^{-13}$ for averaging times of 1 to 30 seconds was measured for an SC, 3rd overtone resonator at 37 μW drive level. This is the square root of the Allan variance and represents the noise from both test and reference sources.

I. Introduction

New resonators have recently (1) (2) (3) (4) been developed in Besancon, France. Research type resonators have been developed covering approximately 10 different types or versions according to various goals of frequency range, type of mounting, size, environment, etc. At this point, some types are close to the industrial preproduction stage (5).

Results have been obtained at various frequencies including 100 MHz and ultrahigh frequencies (6). However the BVA₂ 5 MHz type resonator has been the most extensively studied.

In this paper, the most interesting results previously obtained are reviewed and some new results concerning oscillators and resonators are given. Particular attention is given to drive level capabilities and aging versus drive level questions. Frequency and phase stability performance and frequency retrace following power interruption are discussed. Of importance is the fact that BVA units have already been used in a modified commercial oscillator, FTS 1000; initial results with this configuration are presented and discussed.

This paper deals only with resonators of the BVA₂ design. Basically, BVA₂ resonator construction includes:

1. An "electrodeless" design. All problems of damping, stresses, contamination, ions migration, etc., which relate to electrode deposition are removed.
2. A crystal mounting made of quartz. Small "bridges" connect the vibrating part of the crystal to the dormant part. Key advantages are:
 - no discontinuities nor stresses in mounting points
 - very high precision in shape and location of "bridges"

- symmetry and reproducibility when needed
 - design of bridges very versatile according to goals.
3. Additional parameters. (when compared to classical designs).
The design exhibits additional construction parameters:
 - the electrode (and thus the electric field) can have a radius of curvature different from the radius of curvature given to the vibrating crystal.
 - heaters and sensors can be placed in a vacuum close to the crystal without contacting the vibrating crystal.
 - connecting "bridges" can have a great variety of shapes, locations and various other features.
 4. Provision for any material, crystal cut or frequency (including very high frequencies).
 5. Use of technological means (i.e. ultrasonic machining) which allow reproducibility or versatility (for example the external shape of the crystal does not need to be circular or rectangular).

II. Brief Review of Previous Results

In this section, only results dealing the 5 MHz AT or SC cut units will be discussed, to point out interesting figures already available. Very roughly speaking, the BVA design is capable of an order of magnitude improvement in short term stability (7), long term drift and acceleration sensitivity (8). More precisely, the following features can be listed from previous results:

1. Higher Q factor: A 5 MHz fifth overtone AT resonator (made at Oscilloquartz, Switzerland, ref. 3) yielded $Q = 3.5 \times 10^6$ together with

$$\begin{aligned} R_1 &= 80.7\Omega \\ C_1^1 &= 1.02 \cdot 10^{-4} \text{ pF} \\ C_0^1 &= 4.1 \text{ pF} \end{aligned}$$
2. Better frequency adjustment (by a factor of 2 to 5 depending on technology).
3. Better short term stability. 5.9×10^{-14} for 128 s has been achieved (7) and 10^{-13} (for integration time in the order of 100 s) has been reproduced since.

4. Lower drift rate. 5×10^{-12} /day drift has been measured at NBS Boulder and at ENSMM Besancon as well. Also important is the fact that final aging is established within days and remains constant (4) (9). Results recently obtained will be discussed in the next section.
5. Lower g sensitivity (8). A maximum sensitivity of the order of $10^{-10}/g$ can be achieved in the case of AT cut units. A sensitivity lower than $5 \times 10^{-11}/g$ can be achieved in the case of SC cut single crystals. There is no residual frequency shift after static g loading, to within a few parts in 10^{11} .
6. Reduced amplitude frequency effect: Reduction by a factor of 2 to 15 (9).

III. Recent Advances

1. Extremely high drive level:

The usual drive level for conventional units ranges from 0.1 μ W to some 20 or 30 μ W, at least in ultrastable 5 MHz oscillators. Precision oscillators with an aging rate lower than 10^{-10} /day usually operate at less than a few μ W. In the case of high spectral purity oscillators, the crystal can be driven slightly harder but this causes the aging rate to increase by an order of magnitude or two. If the crystal is driven harder, non-linear effects (10) occur and with still higher levels the crystal can even fracture.

On the contrary, BVA₂ resonators withstand drive levels in the mW range at 5 MHz. For instance, the BVA₂ 2-77, 5 MHz, natural quartz, AT cut fifth overtone unit has now been running for 11 months at a 1600 μ W drive level. The oscillator and the single oven are of very simple design. Nevertheless, the drift remained very constant at $3.3 \pm 0.2 \times 10^{-10}$ /day after 72 hours. Another similar resonator of artificial unswept material (BVA₂ 2-119) has been driven at 2.8 mW with an aging of approximately 10^{-9} /day.

2. Aging versus drive level:

The aging rate for BVA₂ resonators is a non-monotonic function of drive level. Although aging experiments require long time periods, preliminary results on 7 resonators, using various oscillator electronics, have been obtained. These data plus theoretical considerations show that the resulting aging, a_r , may be modeled by the following formula:

$$a_r = a_i + kP \left[1 + a \exp \left(- \sqrt{P/P_0} t/\tau \right) + \dots \right]$$

where: a_i is an intrinsic aging depending on material and cut

k is a constant depending on material and cut

P is the power dissipated in motional resistance R

P_0 is a reference power level

τ is a time constant; t is time

This formulation is valid for a first operation; there is some evidence that the exponential part decreases for further operations. At this point, it is premature to quote precise figures for each parameter. However, orders of magnitude can be given for AT cut natural-quartz fifth overtone crystals:

$a_i \rightarrow$ parts in 10^{11} per day (negative)

$k \rightarrow$ parts in 10^{13} per day, per μW (positive)

$a \rightarrow$ order of 10 to 100

$\tau \rightarrow$ several days

The numbers obtained with various units fabricated from the same material are consistent.

For these units the aging is predictable. Moreover it is possible to change the aging rate by changing the drive level. In particular it is possible to obtain, by slight changes of drive level, slightly positive or slightly negative aging. There is a drive level P_1 , called "zero aging drive level", since it yields an aging rate crossing zero. Three oscillators operating at this "zero aging drive level" were constant in frequency to within 2×10^{-10} over 3 months. For AT cut, natural quartz, 5 MHz, fifth overtone, four bridge units a drive level of 70 to 90 μW appears to be optimum. For SC cut, natural quartz, 5 MHz third overtone four bridge units a level of 160 μW is suitable for the so called "zero aging".

3. Internally heated crystals (11):

Using very high drive levels, it is possible to directly heat the crystal by energy dissipation in the motional resistance R_1 . Units specially devoted to internal heating have been designed (12). These special units are of special construction and will not be

described here. However, if a regular BVA unit is used at mW drive level, it is easy to see, through the mechanisms involved that important changes will occur. In particular, the internally applied energy can no longer be ignored; in other words, the energy exchange with the external environment will no longer uniquely go through the surface. As a consequence (11) the whole bulk crystal participates "in situ" in its own temperature control, and its sensitivity to external temperature fluctuations decreases.

4. Frequency retrace following power interruption:

Extensive retrace experiments have been conducted with resonator BVA₂ 2-77 already mentioned. This resonator retraced to within 2 or 3 x 10⁻¹⁰ following power interruption ranging between 12 and 48 hours. Some other experiments with similar resonators but different drive levels have been conducted yielding similar results. Nevertheless, one particular resonator has shown a frequency versus temperature hysteresis effect which at this point seems to be related to the old mounting structure and packaging of prototype BVA₂ units. If so, this is one more reason to use the low g design (8) which also carefully avoids mounting thermal stresses.

5. Results using commercial oscillator:

Several BVA₂ resonators have now been operated within modified commercial oscillators (FTS-1000 of Frequency and Time Systems, Inc., Massachusetts). Results have been obtained with both AT and SC cut, operated at various drive levels.

It has been verified that low aging rates are established quickly (in a few days), and that a "zero aging" drive level exists. However, since the first oscillator was operated for less than 200 days, more data must be collected for a more complete picture on aging versus drive level.

Figure 1 shows results for an SC-cut 3rd-overtone resonator (BVA 2-125) for which the drive level was progressively increased up to 284 μW, over an elapsed time period of 135 days. The aging rate changed from positive to negative in going from 124 μW to 284 μW. When the drive level was set to 160 μW approximately zero aging resulted and this is as predicted for SC-cut natural quartz.

This same resonator has yielded short term stability measurements shown in Figure 2. In one case the drive level is 37 μW and the reference is a standard FTS 1000 oscillator. The square root of the Allan variance for the two sources is better than 3.7 x 10⁻¹³ over 3 to 30 seconds averaging time.

Results for an AT-cut, 5th-overtone resonator (BVA 2-28) at 72 μW drive level are also shown. Figure 3 shows $S_{\phi}(f)$ phase noise results for this resonator versus the reference S/N 165. At 3 μW drive the phase noise floor is -142 dB (spectral density in 1 Hz bandwidth); for 72 μW the phase noise floor is -144 dB which is essentially the noise floor of the reference. At the same time, the close-in phase noise is degraded by not more than 1 dB for the higher drive level (indicating that a flicker floor of a few 10^{-13} is maintained). It should be noted that 72 μW is close to the theoretical "zero-aging" power level for this AT cut resonator.

Phase noise spectral density results for two other resonators are shown in Figure 4. Here two BVA resonators are directly compared, and assumed to contribute equally. A SC-cut, 3rd overtone resonator (BVA 2-131) is driven at a rather high power level of 265 μW . The other resonator (BVA 2-52) is an AT-cut, 5th overtone at 84 μW . Close-in phase noise is characterized as -118 dB at 1.5 Hz from the carrier, and -140 dB at 10 Hz. At 100 Hz, S_{ϕ} is -152 dB; at 5000 Hz, -154 dB. In this region the observed result is limited by the system noise floor shown as the dashed line.

IV. Conclusion

Initial results using a commercial modified oscillator have shown that it is possible to take practical advantage of the BVA resonator features. Especially the high drive level can provide extremely good spectral purity without degrading time domain stability. In contrast to results with conventional resonators, the aging of BVA resonators remains comparatively small even at high drive levels. Moreover, there are good hopes that the BVA technique can yield resonators with an aging modelable and settable through drive level.

Acknowledgements

The authors wish to thank D.R.E.T. Paris for sponsoring the research at the Ecole Nationale Supérieure de Mécanique et des Microtechniques, Besançon, France. They are also grateful to the Electronic Systems Command (RADC, Hanscom Field) for supporting part of the commercial oscillator interface experiment.

The authors also would like to thank Dr. H. Hellwig and R. M. Garvey of FTS, Dr. J. P. Valentin ENSMM and A. Wavre of Oscilloquartz for many helpful discussions and encouragements.

References

- (1) R.J. Besson, Proc. 30th AFCS pp78-83 (1976) and 31st AFCS pp 147-152 (1977).
- (2) French patents No. 7601035,7616289, 7717309, 7802261, 7828728, 7835631,7918553 and corresponding patent or patents pending in other countries.
- (3) R.J. Besson, 10th PTTI meeting pp 101-128 November 1978.
- (4) R.J. Besson, C.R. Acad Sc Paris t 288 (2 mai 1979) serie B 245-248.
- (5) R.J. Besson, V Peier Conf. A 1.8 Prodeedings Congres International de Chronometrie pp 57-61 September 1979.
- (6) J.P. Valentin, J.P. Michel and R.J. Besson, CR Acad Sc Paris 15 October 1979.
- (7) S.R. Stein, C.M. Manney Jr., F.L. Walls, J.E. Grey, NBS and R.J. Besson, ENSCMB Proc. 32nd AFCS pp 527-530 (1978).
- (8) R.J. Besson, J.J. Gagnepain, D. Janiauol and M. Valdois, Proc. 33rd AFCS (1979).
- (9) A. Berthaut and R.J. Besson, CR Acad Sc Paris, November 1979.
- (10) J.J. Gagnepain, R.J. Besson, Physical Acoustics Volume XI Acad Press pp 245-288.
- (11) J.P. Valentin and R.J. Besson, CR Acad. SC Paris B138 24 September 1979.
- (12) R.J. Besson, J.P. Valentin, French patent application No. 7918553.

APPROX. DRIVE LEVEL (MICROWATTS)	AGING RATE $\Delta f/f$ (per day)	TIME ELAPSED FROM 1st TURN-ON (DAYS)
10	$+ 4 \times 10^{-10}$	8
37	$+ 9 \times 10^{-11}$ (45 day avg.)	70
124	$+ 3 \times 10^{-11}$	120
284	$- 9 \times 10^{-12}$	135
160	approx. zero	165
Oscillator OFF 12 hours 160	$+ 4 \times 10^{-10}$ (after 1 day)	167
Oscillator OFF 12 hours		
160	$+ 2 \times 10^{-10}$ (after 4 days)	173
160	zero	177

Figure 1. BVA Resonator Aging Versus Drive Level

RESONATOR B V A	DRIVE LEVEL	REFERENCE OSCILLATOR	$\sigma_y(\tau)$ in units 10^{-13}				
			$\tau =$ 1 sec	3	10	30	100
2-125 SC, 3rd	37 μ W	1000 s/n 12	*6.5	3.6	3.5	3.7	5.1
	285 μ W	B5400 s/n 165	*8	6.5	5.2	7.4	
2-28 AT, 5th	72 μ W	1000 s/n 12	*8	6.0	6.4	6.8	

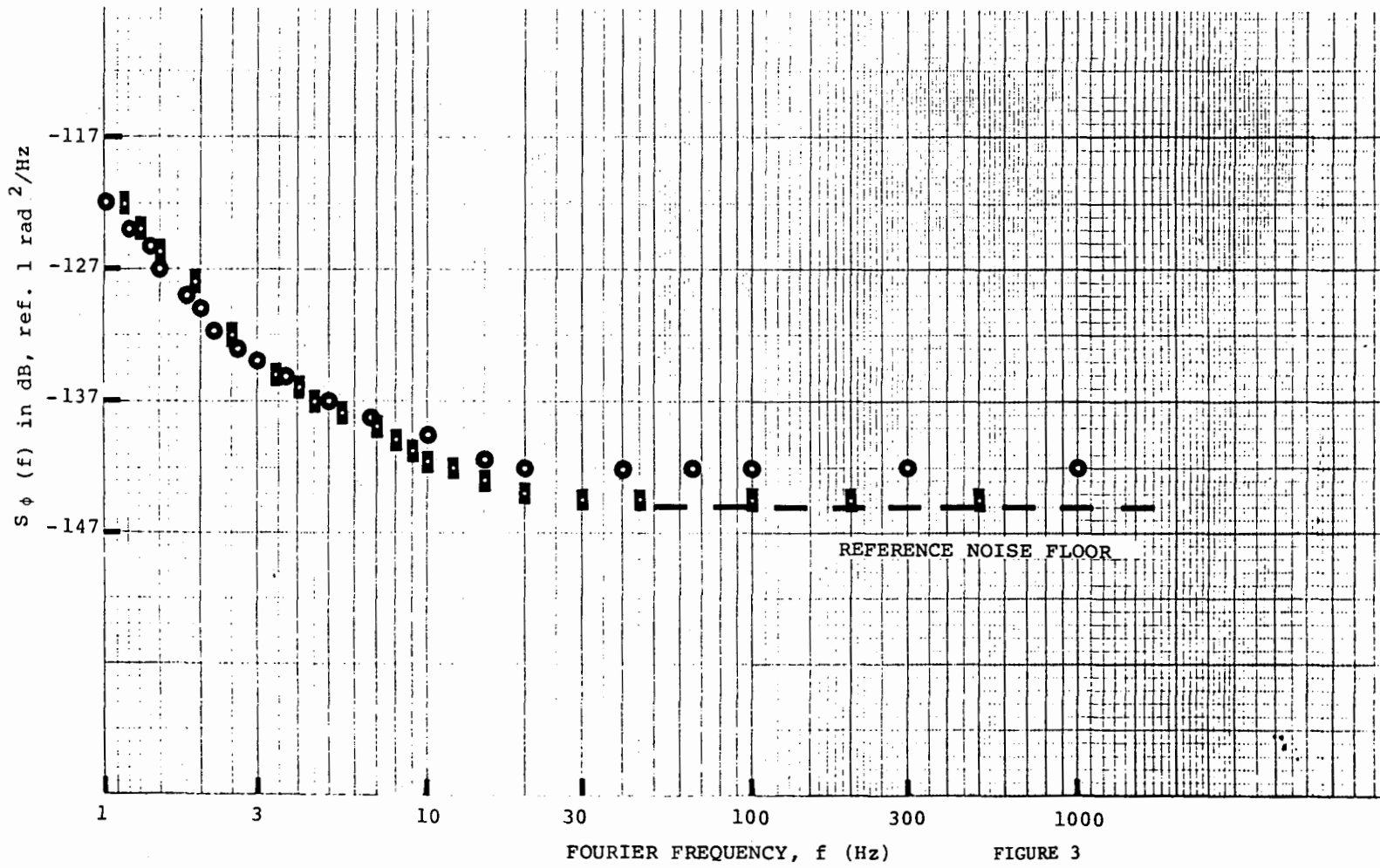
*Uncorrected for 50% dead time,
at 1 second only

Figure 2. Time Domain Stability - Allan Variance (Two Sources)

Resonator BVA 2-28 (AT, 5th): Drive Level 3 μ W \odot \ominus
in commercial FTS 1000

Reference: B5400 S/N 165

72 μ W \blacksquare \blacklozenge



467

Figure 3. Phase Noise Spectral Density, $S_{\phi}(f)$, in 1 Hz BW

FIGURE 3

BVA 2-131 (SC) (3rd) 265 μ W
 vs. BVA 2-52 (AT) (5th) 84 μ W
 Resonators in commercial FTS 1000 oscillators

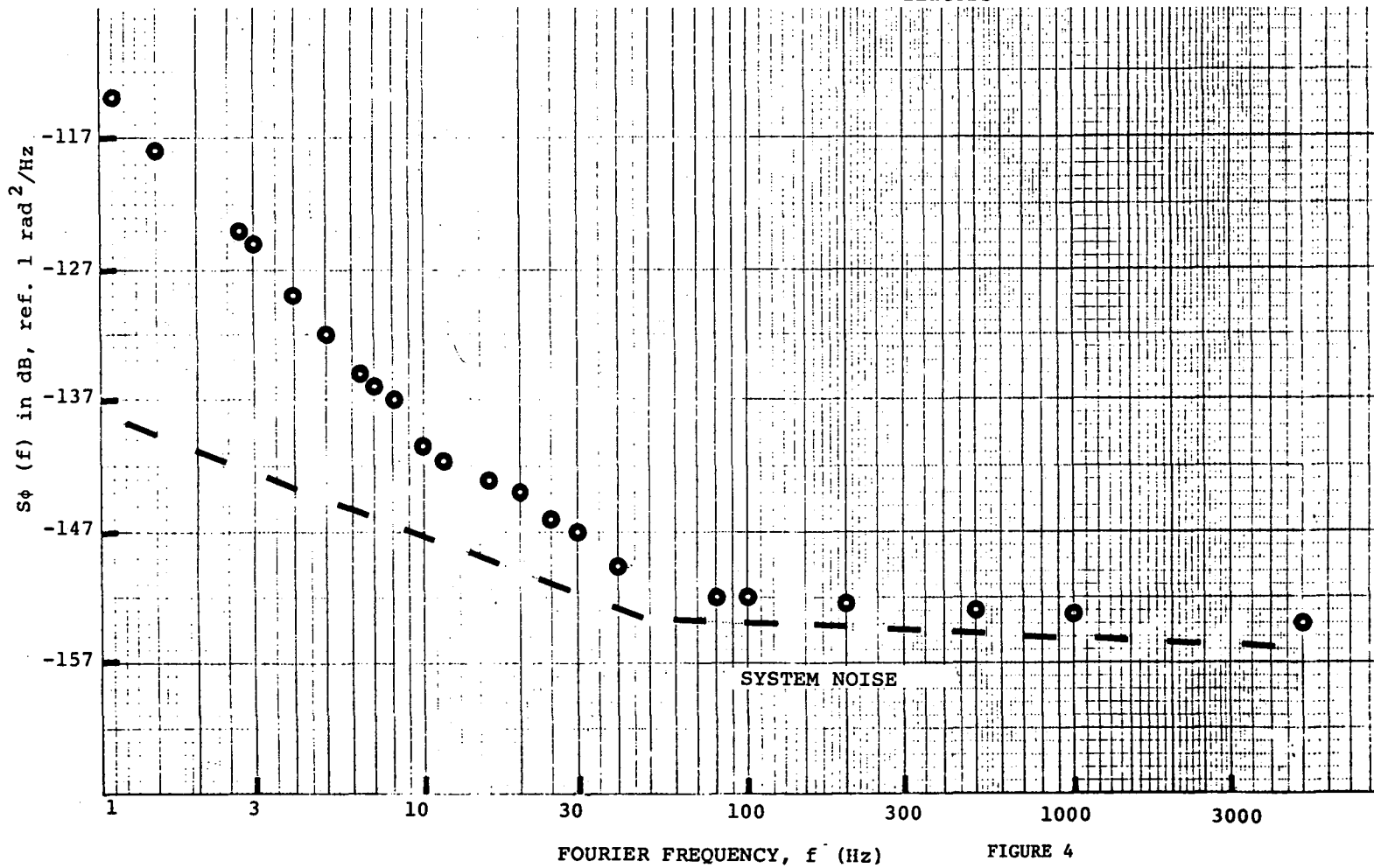


Figure 4. Phase Noise Spectral Density, $S_\phi(f)$, in 1 Hz BW

QUESTIONS AND ANSWERS

QUESTION:

Could you comment on the partial availability of and the quantities that they are available?

DR. BESSON:

You are talking about the resonators or oscillators or what?

QUESTION:

Resonators.

DR. BESSON:

Well, I don't believe I could, myself, answer that question, but however I believe that the resonator will be available with the oscillator.

DR. HAMMOND:

These three papers on quartz resonators, if you will pardon a few comments, in the thirty-some years that I have been following quartz, it has been interesting to track the progress of stability. If you go back to 1930, it was probably a part in 10 to the 5th, by 1950, a part in 10 to the 8th. Today we are looking at a part in 10 to the 12th. And watching that over the last 30 years that I have observed it, it has been an order of magnitude improvement in quartz about every 7 years and it looks like it is on track and it looks like, also, that the next order of magnitude is also possible. That that extrapolation-- It is always very dangerous to extrapolate into the future, but I agree with Arthur Ballato in his first comments that this is an exciting time in quartz. I know of no time that I have observed it when so many things have been coming together that showed so much promise.

Remember, you heard it here first.

TIME TRANSFER VIA SATELLITE-LINK RADIO INTERFEROMETRY

S.H.Knowles, W.B.Waltman (E.O.Hulburt Center for Space
Research, NRL, Washington, D.C. 20375)

J.L.Yen (University of Toronto, Toronto, Canada)

W.H.Cannon and W. Petrachenko (York University, Toronto,
Canada)

N.W.Brotten, C.Costain and D.H.Fort. (National Research Council,
Ottawa, Canada)

J.A.Galt (National Research Council, Penticton, B.C., Canada)

J.A.Popelar (Department of Energy, Mines and Resources,
Ottawa, Canada)

and

G.W.Swenson (University of Illinois, Urbana, Illinois)

ABSTRACT

Very long baseline interferometry using natural radio sources has been shown to be an excellent time transfer method. Our group has linked antennas using a synchronous communications satellite instead of the customary independent frequency standards and tape recorders. We have performed a successful preliminary time transfer using a wide-band data link that was accurate at the 100 nano-second level, and have compared frequency standards to a part in 10^{-13} over a 24-hour period using a phase coherent satellite link. The narrow-band phase coherent link method is potentially capable of timing accuracy of 10 picoseconds, and frequency comparison accuracy of 10^{-16} , and is in addition economical of spectrum usage. We plan to continue development of this latter method using the newly-launched ANIK-B satellite.

Our group's use of a synchronous satellite link between widely separated radio telescopes has demonstrated the feasibility of two related but separate approaches to accurate time transfer and frequency standards comparison. The first of these methods, reported by us previously¹, involves the use of the satellite as a wide-band data link to transfer the video signal used to cross-

correlate and thus determine the differential delay between radio source signals received at two separated stations. In our published work, we used the CTS or Hermes satellite to transfer a 20 megabit data stream between antennas in Greenbank, W. Va. and Lake Traverse, Ont. and to obtain differential clock measurements accurate to the 100 nanosecond level in real time. A joint M.I.T.-U.S.N.O. group has obtained results accurate to 20 nanoseconds². A similar accuracy should certainly be available via satellite link if a similar use of bandwidth synthesis and accurate equipment delay calibration is made. For any operational use, the simplicity of use of a real-time time indication is a significant advantage.

Our time data-link experiment used two large radio astronomy antennas and a wide-band (80 megahertz) satellite data channel. Either of these requirements can be considerably eased, however. The signal-to-noise ratio in a one-minute integration was considerably greater than 100 to 1 for either of the two strong radio sources (3C84 and 3C273) we used. Since the signal-to-noise ratio for a wide-band radio source is proportional to the square root of the signal bandwidth, it is possible to reduce the data rate to a low enough value to enable transmission via a telephone line (4 kilobits per second). This is in fact done as an equipment monitor by radio astronomy groups. The full (less than 10 nanoseconds) timing accuracy should be available by using the bandwidth synthesis technique even with a narrow signal bandwidth, although a greater number of programmed local oscillator settings would be necessary to compensate for the more severe ambiguity problem. An alternative possibility is the use of a portable antenna. For example, the diameter of one antenna could be reduced to a meter or two if used together with a large master antenna.

The delay-calibration method, then, is a relatively well-proven method with a potential for time comparisons to several nanoseconds accuracy. Another method we are presently developing has the ultimate potential for time measurements between separated stations accurate to 10 picoseconds. This is the two-way transfer of a phase-coherent carrier between stations. Although this concept may seem unfamiliar, it is in fact an extension of the coherent doppler tracking used on deep-space probes. In the simplest theoretical realization a signal at frequency f_0 is transmitted from station A via the satellite to station B and compared with the station B standard. Similarly the signal from B is transmitted to A and compared. In this case, we have at either station:

$$\begin{aligned}\phi_{mB} &= \phi_{sB} - \phi_{sA} \\ \phi_{mA} &= \phi_{sA} - \phi_{sB}\end{aligned}\tag{1}$$

where ϕ_{mA}, ϕ_{mB} are the measured comparison phases and ϕ_{sA}, ϕ_{sB} are the phases of the frequency standards. If we now allow the satellite to move, we have:

$$\begin{aligned}\phi_{mB} &= \phi_{sB} - \phi_{sA} - \frac{2\Delta d}{c} \cdot f_0 \\ \phi_{mA} &= \phi_{sA} - \phi_{sB} - \frac{2\Delta d}{c} \cdot f_0\end{aligned}\tag{2}$$

where Δd is the component of the satellite's motion along the link path, so that $\phi_{mB} - \phi_{mA} = 2(\phi_{sB} - \phi_{sA})$ and the satellite's motion cancels out to give a direct measure of the phase difference between the two standards that should be precise to within a fraction of a cycle at the transmission frequency (typically 15 GHz); this corresponds to a timing accuracy of 7 picoseconds for 0.1 turn (1 turn = 360 degrees) phase measurement accuracy. The phase measurement made at B is of course transmitted as data to A via telephone line, satellite link or other convenient means. The satellite's motion in theory cancels completely if measurements are made in such a manner that they transit the satellite at exactly the same time. The satellite used does not have to be synchronous, although our first experiments have used such because of the lesser (although non-zero) motion and the simplified tracking problem.

Significant complications arise because of the necessity for frequency translation at each pass through the satellite to avoid regeneration. Most importantly, the characteristics of the satellite's translation oscillator enter the picture. An ideal satellite for this purpose would be the synthesiser type (Fig. 1) in which the translation oscillator is phase-locked to a sub-multiple of the incoming frequency, thus contributing no phase error. This is in fact done on certain deep-space probes; but ordinary communications satellites have not had provision for this. It is possible, however, to make phase-coherent link measurements in spite of the incoherent satellite oscillator under certain common conditions. If the frequency of the path from A to B is translated by exactly the same amount, using the same oscillator, as that from B to A, the satellite crystal will contribute no error if both signals transit the satellite at exactly the same time. Both the CTS and ANIK-B satellites have had this equal-translation property. For small differences in the transit time, an error will be produced in the amount:

$$\Delta\phi = f_t \cdot \Delta t \cdot \frac{\Delta f}{f} \cdot \frac{f_t}{f_0}\tag{3}$$

where f_t is the frequency translation, Δt is the timing error, $\frac{\Delta f}{f}$ is the satellite crystal stability and f_0 is the nominal link frequency. For typical values of crystal stability of 10^{-7} , timing error of 10 milliseconds, translation frequency of 3 GHz and link frequency of 15 GHz, the total phase error from this source can be kept to within about 100 turns. There is in addition a method of compensating for the satellite's oscillator, using either a separate beacon signal on the satellite derived from the same oscillator, or, if this is not available, transmission of a second pilot tone at a different frequency. In either case, the use of two signals traversing the same path enables one to solve for the phase change of the satellite oscillator as well as that due to the path, and thus eliminate it; reduced accuracy is expected in the case of two pilot tones transmitted with only limited separation. The first method was used by our CTS experiments, the second method is being used in our current series using the ANIK-B satellite.

Another complication is introduced by the fact that, again to avoid regeneration, the mean frequency of the path from A to B cannot be the same as that from B to A. This difference, typically about 1%, can be allowed for, assuming no dispersive effects, by multiplying the total observed phase count from the lower-frequency path by the appropriate ratio before subtraction.

The earth's atmosphere should, surprisingly, contribute a relatively small error. Dispersive phase shift due to the ionosphere is negligible at the 15 GHz frequencies used by our satellite links, and total excess phase delay due to the troposphere is only several hundred turns, and should be completely cancelled by the two-way link.

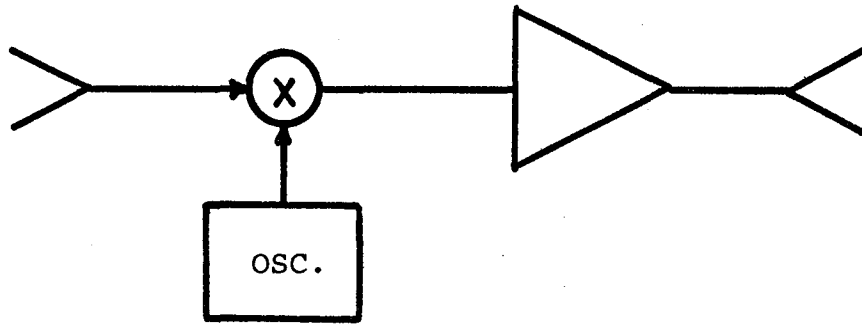
The largest practical error source is expected to be phase wind-up error in the electronics used for transmit and receive. This is similar to the delay error to be calibrated in delay VLBI measurements, but is made more serious here by the higher accuracy required, and by the use of electronics for both transmit and receive functions.

Preliminary experiments using this technique were carried out using the CTS satellite in May 1979. The short-term performance of the link is shown in Fig. 2. Longer-term phase stability is shown in Fig. 3, and a comparison of experimental results with the laboratory stability of different types of frequency standards is shown in Fig. 4. It is clear that short-term phase stability of a small fraction of a turn is attained, but that long-term phase drift with a period of a few hours is present degrading the phase-link measurements. If there were no long-term drifts in the phase-link its frequency measurement accuracy in Fig. 4 would have

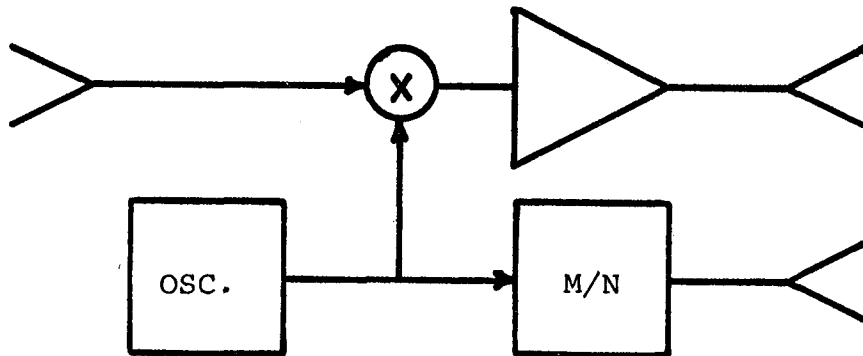
a 1/t slope. The most likely source of the phase drift that causes the slope of our very limited preliminary data to flatten is phase wind-up in our transmit and receive electronics.

We are presently instrumenting to continue experiments with a coherent link with the new ANIK-B satellite. We expect to obtain at least an order of magnitude better control over the behavior of the link over periods of 6-24 hours, and to obtain data on the performance of the link over periods of many days. This method should have the potential for comparing time bases maintained at different places on the earth to parts in 10^{-16} over periods of a year or greater. Our preliminary measurements correspond to a measurement of timing change with a precision of ± 5 nanoseconds over a 24-hour period; a potentially much higher accuracy should be available. For the CTS experiments we made no attempt to resolve our ambiguity interval of 100 picoseconds, and thus were unable to make absolute time comparisons. The transmission of appropriately spaced multiple tones within the typical communications satellite bandwidth of 100 MHz can reduce this problem, however. This method makes very economical use of the spectrum; all that is required is the transmission of a few pilot tones that occupy instantaneous spectral bandwidths of less than one hertz, and long-term bandwidths of less than one kilohertz allowing for satellite doppler. This narrow bandwidth increases signal-to-noise ratio, allowing for the use of small and thus inexpensive ground station antennas. The narrow bandwidth allows simultaneous multi-user use of the satellite (as is occurring on ANIK), unlike satellite pulse-transmission methods. For time- and frequency-standard comparison, it is important to note, radio astronomy antennas play no part and are not required. We hope during the next year or two to investigate and control sources of phase error in this method in order to realize its full potential.

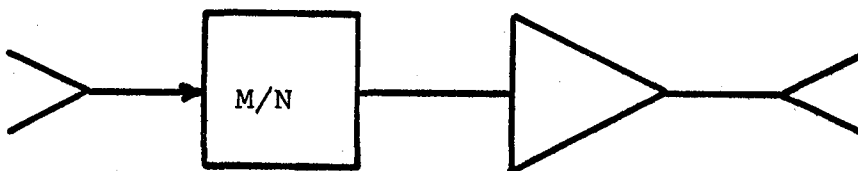
1. S.H.Knowles, W.B.Waltman, W.B.Klepczynski, N.W.Broten, D.H.Fort, K.I.Kellerman, B.Rayhrer, G.W.Swenson and J.L.Yen, "Real-time Accurate Time Transfer and Frequency Standards Evaluation via Satellite Link Long Baseline Interferometry", Proceedings of the 9th Annual PTII Meeting, p.135, Nov. 29- Dec. 1, 1977, NASA Tech. Memo. 78104
2. A.E.E.Rogers, A.R.Whitney, H.F.Hinteregger, C.A.Knight, T.A.Clark, W.J.Klepczynski, I.I.Shapiro, C.C.Counselman and L.B.Hanson, "Clock Synchronization via Very Long Baseline Interferometry", *ibid.*, p. 127



TRANSLATOR (ANIK-B)



TRANSLATOR WITH COHERENT BEACON (HERMES)



SYNTHESIZER

Figure 1. Types of Satellites

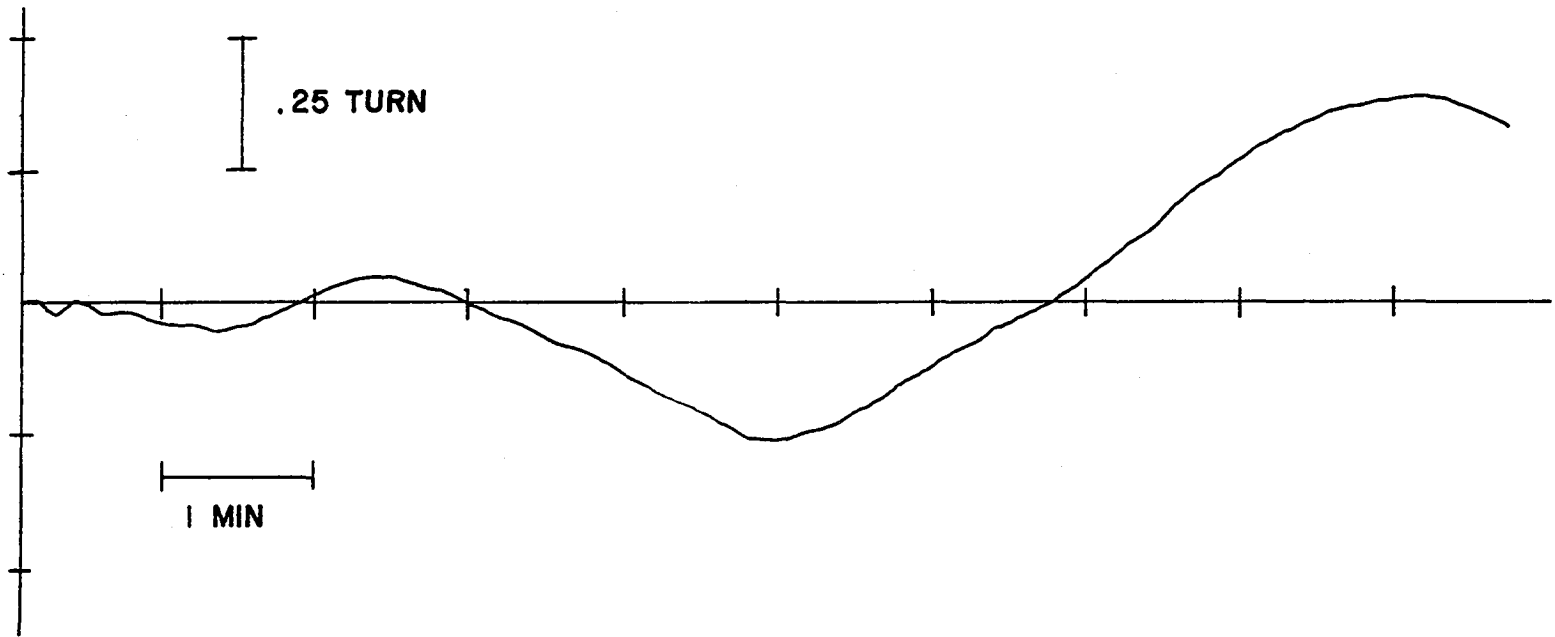


Figure 2. CTS Phase Link Results (Short-Term)

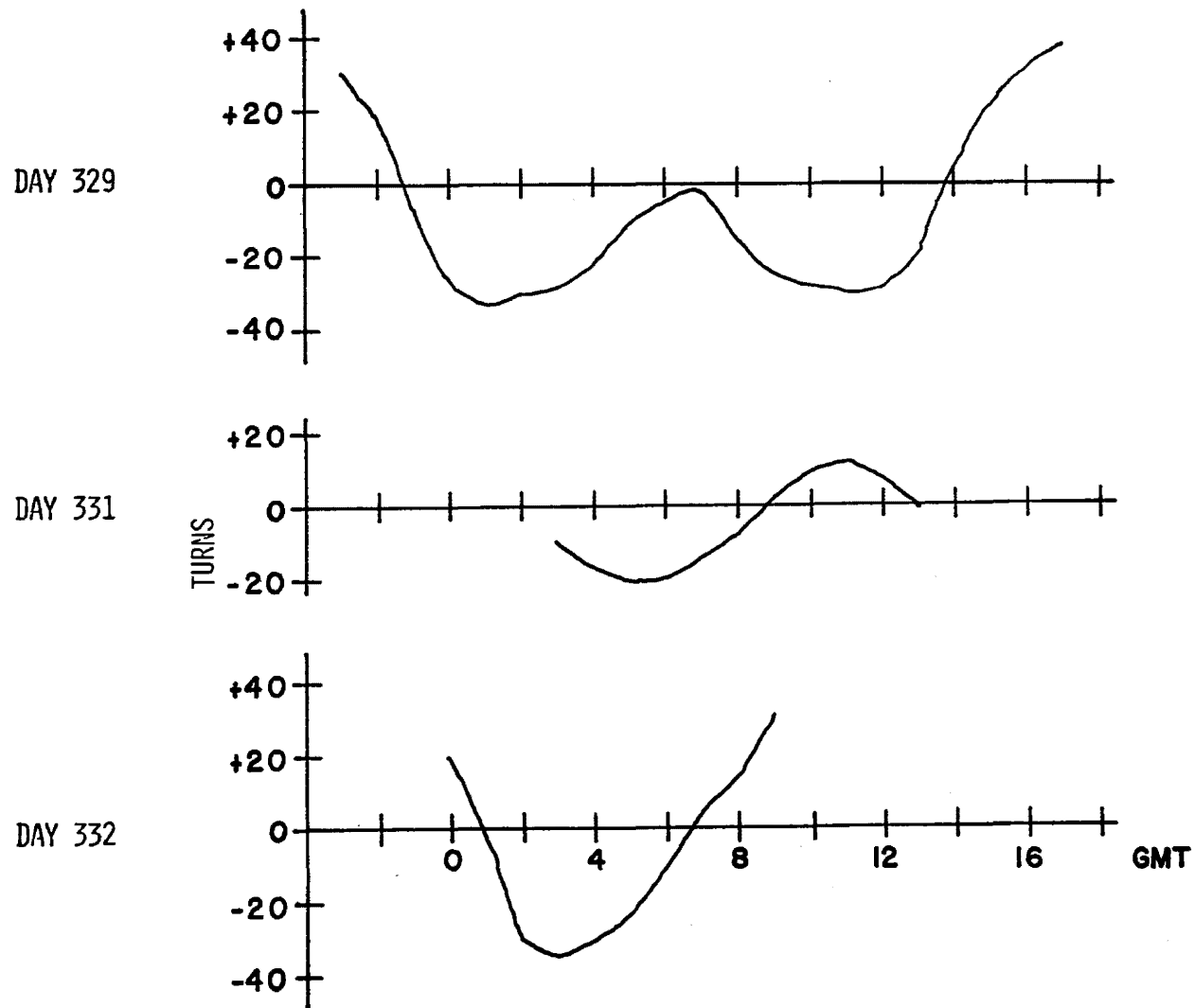


Figure 3. CTS Phase Link Results (Long-Term)

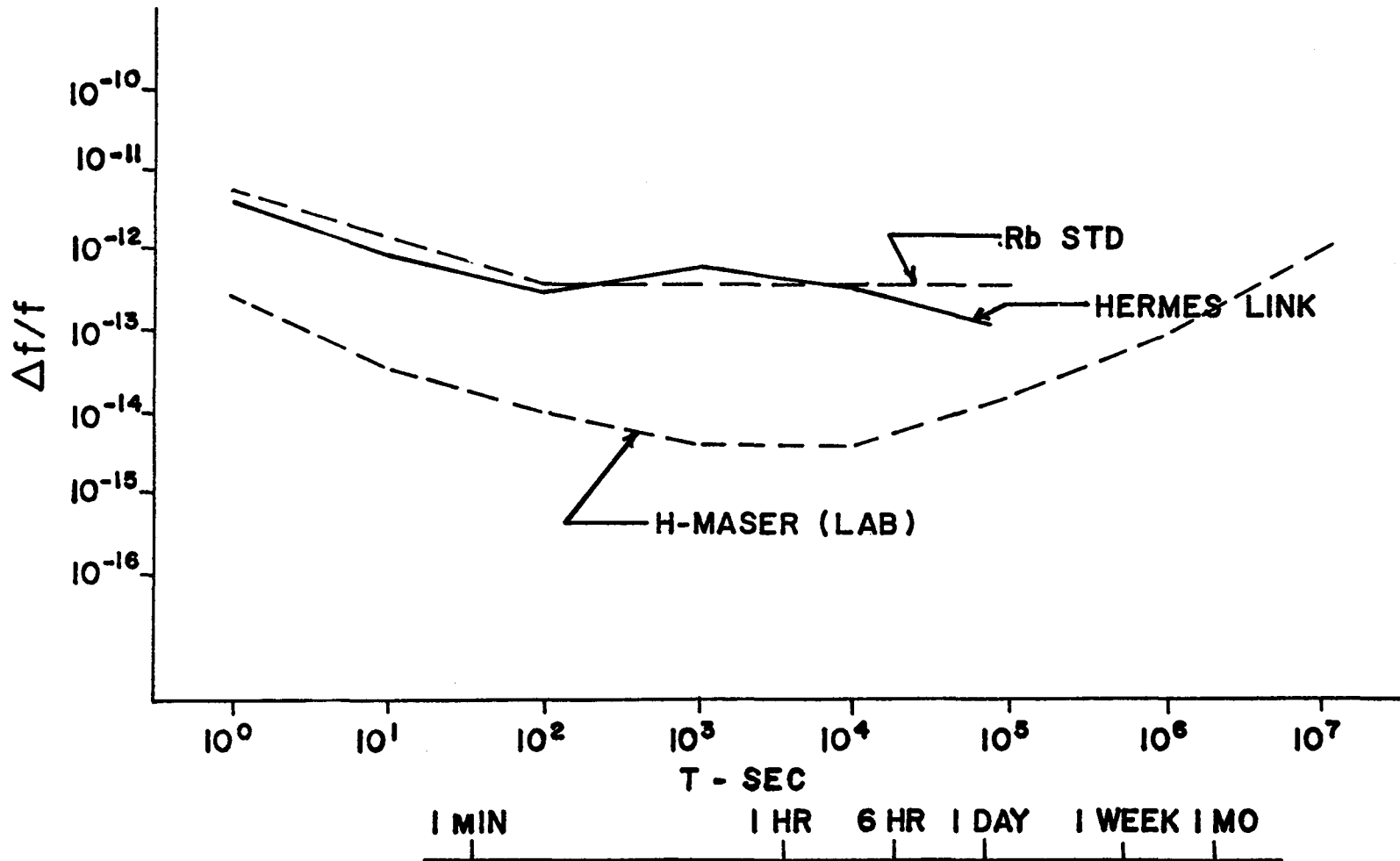


Figure 4. Comparison of Phase Stability

QUESTIONS AND ANSWERS

DR. KEN PUTKOVICH, Naval Observatory

Pardon my ignorance, but could you define the term "turn" for me?

DR. KNOWLES:

Yes. A turn is 360 degrees. I simply used it because it looks more impressive than saying our errors were 17,000 degrees. If you say it was 20 turns, it sounds better and is more appropriate.

DR. JIM JESPERSON, National Bureau of Standards

Really, what I have is more in the way of a comment. As you pointed out at the beginning of your speech, probably VLBI is one of the very best techniques that we know of for clock comparison. And in fact some of the ordinary ways that you can think of for checking these new techniques, such as carrying, say, a portable clock between the two sites as an independent check, perhaps isn't good enough, especially if there is a great separation between the two sites.

The only other system I can think of that might check the kinds of results that seem to be coming out here is the two-way satellite technique. And what I am wondering is that if at some future time you or perhaps some of the people here who are in a position to support a VLBI experiment with a two-way satellite, what about the possibility of doing the two-way satellite and the VLBI experiment simultaneously, because I think the kind of errors that contribute to the two systems are rather different. For example, the two-way satellite, the errors due to propagation effects, atmospheric delays and so forth cancel out, whereas in VLBI you have to make some assumptions, some guesses about what is going on now.

DR. KNOWLES:

In actual fact, we will do this routinely as part of the ANIK program because the major objectives of the ANIK program are to measure UT and polar motion, and for those purposes we do need to measure the position of a radio source using VLBI and we will completely reduce it according to the standard methods using the Canadian VLBI system and we will attempt to solve for several parameters. In the first place, we have to see to what extent our link works and measure UT, but we will have that comparison.

I do want to mention one thing, one slight point that I forgot to mention. The phase link for ANIK, I had no mention of avoiding the ambiguity problem. We haven't been concerned with that. In actual fact, if one is, the actual bandwidth of the ANIK transmitting band is 60 megahertz so one could think of transmitting multiple tones and alleviating the ambiguity problem from it so you could indeed lock in on the signal precisely.

DR. ROBERT KAARLS, Van Swinden Laboratory in the Netherlands

With respect to the question put by Dr. Jespersen, I can tell that we have some possibilities in our country because VLBI stations and stations which have possibility for two-way satellite links are very close to each other and we are looking into the possibilities to set up such an experiment. Thank you.

DR. KNOWLES:

Yes. I have talked to some of the people in the Netherlands, Dick Skilutsee in particular and I know there is an active effort to set up such a network in Europe. I think it is very commendable and I think you are ahead of current efforts in this country.

SESSION VI

SYNCHRONIZATION SYSTEMS

**Andrew R. Chi, Chairman
NASA Goddard Space Flight Center**

COMPARISON OF DIFFERENT TIME SYNCHRONIZATION TECHNIQUES

R. Kaarls and G. de Jong
Van Swinden Laboratory
Delft, Netherlands

ABSTRACT

The Van Swinden Laboratory (VSL) of the National Service of Metrology in the Netherlands has recently been moved to a new laboratory at Delft. The section Time and Frequency of the Division of Electromagnetism and Time is now housed in a laboratory, built as a cabin of Faraday, with well-maintained environmental conditions and equipped with different other provisions.

The cesium atomic clocks are put on heavy concrete blocks which are placed vibration free at sufficient distance from other objects to avoid mutual disturbing influences.

A microprocessor provides the automatic data registration of the complete system. The main international synchronization link is the Loran-C system.

Initially it was planned to set up an international TV-synchronization network between NPL/RGO, LPTF, PTB/DHI and VSL. For this purpose three 3 m-parabolic antennas should be placed at 90 m height on top of the main building of the Department of Electrical Engineering of the Technical University Delft.

A preliminary experiment between NPL and VSL during the years 1976 - 1978 showed the possibilities. The accuracy is 500 ns during most of the time. The link is about 240 km long, mainly across the North Sea. Also good reception of TV-syncpulses was found of a German TV-transmitter at a distance of 170 km from our laboratory. NPL is going to propose a new, improved TV-synchronization experiment. An accuracy of better than 200 ns seems to be possible. In both cases the receiver has been equipped with a phase locked loop TV-sync pulse detector.

However, instead of the planned three parabolic antennas, in the meantime the new laboratory has been equipped with a system of satellite receivers. A 3 m-parabolic antenna receives signals above 4 GHz and other antennas can receive signals in the frequency bands from 100 - 500 MHz and 1 - 2 GHz.

Close co-operation has been established within the Netherlands between the VSL and the laser-satellite groundstation of the Geodetic Department of the Technical University Delft at Kootwijk and the radio-astronomy station at Dwingeloo.

The mutual links make use of the TV-synchronization techniques, with which we can achieve an accuracy of about 8 ns to 10 ns (1σ) over links of 140 km.

It has been planned to join the ESA (European Space Agency) two-way laser satellite synchronization technique experiments -- where the Netherlands' ground station is one of the most powerful ones in Western Europe -- and to co-operate in VLBI-measurements. A proposal for such a VLBI-experiment between the UK and the Netherlands may be realised in 1980.

In this way a good comparison and synchronization can be performed between the different methods.

INTRODUCTION

The Van Swinden Laboratory (VSL) of the National Service of Metrology in the Netherlands has recently been moved from The Hague to Delft. In the old laboratory at the Hague the section Time and Frequency of the Division of Electromagnetism and Time was equipped for the reception of VLF/LF-, Loran-C- and TV-transmissions. In particular the standard frequency signal transmissions of DCF 77 (Mainflingen, FRG) were monitored daily. Daily measurements were done on the Loran-C transmissions of Ejde (7970-M and 7930-X) and Sylt (7970-W). Also every day measurements were carried out on the TV-synchronization system, in which way other laboratories in the Netherlands are synchronised to the VSL.

The new laboratory at Delft, about 17 km south of the Hague, also possesses the possibilities for receiving satellite transmissions, while by further co-operation with other institutes different techniques -- e.g. laser-synchronization and VLBI -- can be used and compared.

INTERNATIONAL TV-SYNCHRONIZATION NETWORK

Originally, it was planned to set up an international TV-synchronization network between NPL/RGO, LPTF, PTB/DHI and VSL.

For this purpose three 3-m parabolic antennae should be placed at 90 m height on top of the main building of the Department of Electrical Engineering of the Technical University Delft, directed to TV-transmitters in the UK, France and Germany. A special low attenuation coaxial cable of about 800 m should connect the antennae with the measuring equipment in the time and frequency standards laboratory of the VSL.

PRELIMINARY EXPERIMENT BETWEEN NPL AND VSL

An experiment between NPL and VSL during the years 1976 - 1978, when the VSL was still in The Hague, showed the possibilities.

The TV-transmitter to be received by the NPL as well as by the VSL, was located at Sudbury (Suffolk, UK), 85 km north-east of London. In this case no TV-relay stations should be involved. In principle NPL could receive this station without any special measures.

The transmitter frequency is 715 MHz (BBC 2).

The VSL, at a distance of 240 km of the transmitter and a transmitting path mainly over sea, installed a 21 element, 14 dB gain Yagi-antenna on the roof of a 60 m tall building next to the laboratory.

The NPL used a broad band antenna with broad band amplifier.

Because the transmission link from the TV-studio to the Sudbury transmitter is often different, it is strictly necessary to do the measurements at the same moment.

The difference in propagation delay between the transmitter and the respective laboratories showed up to be about 2200 μ s, what is much more than the theoretically calculated difference of 480 μ s.

It came out that the transmissions of Sudbury (at a distance of 100 km from NPL) were overruled by the transmission of a local transmitter at the same frequency and with the same program in Hemelhempstead (35 km from the NPL).

NPL could, however, very well receive another BBC 2 transmitter at Crystal Palace in South-London.

Taking into account that the BBC-program comes from studios in London and then is transmitted via a detour of about 500 km to the Sudbury transmitter, after which reception in The Hague is possible, the overall correction, which one has to apply, is 2470 μ s.

In figure 1 the result of the measurements UTC(VSL) - UTC(NPL) via TV is plotted over a period of 3 months (May - July 1978). For comparison is also plotted UTC(VSL) - UTC(NPL) via Loran-C (Sylt).

Except for throw-out measurements the average over these 3 months seems to be well within 500 ns.

The uncertainty in each measuringpoint is $\pm 1 \mu$ s as a maximum.

The VSL-measurements were carried out with the application of a phase locked loop, locked to the received synchronization signals. The variations in field strength in the troposphere over this distance can be 60 dB.

As a check a portable clock measurement was carried out between NPL and VSL on June 27, 1977. The difference $UTC(NPL) - UTC(VSL) = (30,05 \pm 0,05) \mu s$. Calculations in 1978 taking into account this value confirmed the delay of 2470 μs .

Also experimental TV-measurements were done between PTB and VSL.

The VSL could receive the German ZDF-transmitter at Wesel, 166 km away from our laboratory. The measurement data were calculated with the help of the measurements data $UTC(PTB) - ZDF$ as published weekly by the PTB in their Time Service Bulletin.

The TV-measurements were compared with the calculated time difference $UTC(PTB) - UTC(VSL)$ out of the Loran-C measurements.

Also in this case a correction had to be applied which was calculated out of the comparison of Loran-C differences and the averaged TV-differences.

The results are plotted in figure 2.

The dispersion over about 2 months is less than 1 μs .

CONCLUSION

The throw-out measurement results are mainly due to the fact that for direct TV-synchronization over such large distances there can be much disturbance, by which the signal levels can strongly change and thus the receiver will be upsetted and extra uncertainties of 1 to 1,5 μs are introduced.

Improvement for this can be achieved by applying a better antenna with a higher gain and a more narrow beam and placed on a greater height.

In this moment it is believed that in an international TV-synchronization network, as thought, one can achieve an accuracy of 500 ns, which possibly may be improved to 200 ns.

PROPOSAL

With respect to the feasibility study on long distance international TV-synchronization networks the NPL is proposing a continuation of the work in the year 1980.

THE NEW VSL - LABORATORY AT DELFT

In the mean time the VSL has been moved to a new laboratory at Delft, 17 km south of The Hague. Instead of the intended three 3-m parabolic antennae, one has installed on the highest point of the roof of the VSL satellite receiving antennae, so to have a good opportunity to link in in these synchronization systems.

INSTALLATION

The section Time and Frequency is now housed in a laboratory, built as a cabin of Faraday with a 135 dB screening up to 10 GHz. The environmental conditions are $(23 \pm 0,3) ^\circ\text{C}$ and $(45 \pm 5)\%$ R.H. An extra emergency air-conditioning is available.

The laboratory has been equiped with automatic fire alarm and halogen extinguisher.

The power supply consists of two different networks. One is a stabilized mains; the other network is connected via an emergency power generator. Further, an open NiCd battery power supply guarantees continuous and undisturbed functioning of the clocks and the other main electronics.

The cesium atomic clocks are put on heavy concrete blocks which are placed vibration free at sufficient distance from each other (1 m) and other objects to avoid mutual disturbing influences. Also was looked for a minimum magnetic field ($< 25 \mu\text{T}$).

All the measuring equipment, receivers, digital clocks, counters, microsteppers and other electronics are brought together in a large console.

A microprocessor provides the automatic data registration of the complete system.

The switching between the different standards and receivers is done by means of TTL-integrated switches.

The overall reproducibility in this switching system is about 1 ns.

The on tape gathered measurement data are further processed with the help of a microcomputer.

Further improvements on the system can be achieved and have been planned by providing a microprocessor controlled surveillance system.

The number of cesium atomic clocks, taking part into the BIH-program has been increased to four, while a fifth clock is under study.

Three of the clocks are located in our own laboratory.

The fourth clock is located at the European space Technology Center (ESA-ESTEC) at Noordwijk, Netherlands.

LORAN-C, VLF/LF AND DOMESTIC TIME SIGNALS

Also in the new laboratory the main international synchronization link is still the Loran-C system.

Received are the transmissions of Ejde (7970-M, 7930-X) and Sylt (7970-W).

The measuring data are sent by telex once a week to the USNO in Washington D.C. for keeping track on the North Atlantic and Norwegian Sea chains, and every period of 30 days to the BIH.

The standard frequency transmissions of DCF 77 are monitored as also the domestic time signals, which are disseminated by the telephone PTT, ± 10 ms, and the radiotransmitters Hilversum III, ± 1 ms.

TV-SYNCHRONIZATION

Daily measurements on the TV-synchronization system guarantee a very accurate synchronization of the time and frequency standards in other laboratories.

For the synchronization signal (point) one uses the middle of the trailing edge of the first field synchronization pulse.

The day by day variance in the difference UTC(VSL)-UTC(ESTEC) is about 15 ns, and is mainly limited by the instability of the standard tube of the cesium atomic clock used by the VSL.

Figure 3 shows the stability UTC(VSL)-UTC(ESTEC) via TV.

The variance of 6 measurements, spaced by 10 s each, is about 8 ns. This is mainly due to receiver noise.

TV-synchronization measurements done at other locations in the Netherlands show that over distances of 180 km, where one measures via other TV-relay transmitters, about the same variance of 15 ns can be expected.

A weekly time service bulletin is published by the VSL.

LASSO

For the successful operation of the two-way laser satellite synchronization technique, one needs very powerful laser ranging ground stations, which can give very accurate timed single shots and can detect the shot again after having been reflected by the satellite at a distance of 36000 km. One of the most powerful stations is located in Kootwijk, Netherlands.

After having applied some modifications and adaptations it is planned to join the BIH-ESA-Sirio II laser synchronization experiments, where we hope to achieve an uncertainty in the synchronization of 1-10 ns as a maximum.

The Kootwijk laser ranging station is linked to the VSL by means of TV-synchronization and portable clock measurements.

VLBI

Another possibility for time scale synchronization is to make use of the VLBI-technique.

The radio-astronomy station at Dwingeloo, Netherlands is located at a distance of 173 km from the VSL and has also a TV-synchronization link with the VSL.

An experiment which will make use of the VLBI technique has recently been proposed by the NPL and the VSL making use of the radio-astronomy stations in Chilbolton (UK) of the Appleton Laboratory and in Dwingeloo.

SYNCHRONIZATION VIA SATELLITE

The new VSL-laboratory at Delft has been equipped with different antennae.

It is now possible to receive signals in the frequency band from 100 MHz to 500 MHz. The antenna gain is 8 dBi; RH or LH circular.

Another antenna gives the possibility for receiving signals in the frequency band from 1 GHz to 2 GHz. The antenna gain is 8dBi; RH or LH circular.

Also a 3 m-parabolic antenna has been installed, which at present has been equipped with a receiving system for the frequency band 11 GHz - 12 GHz.

The noise figure is 4,5 dB. It gives the opportunity for looking into the time synchronization possibilities at a high accuracy level by receiving FM-TV-broadcasting. The parabolic antenna as also the 100-500 MHz antenna are remote controlled in azimuth and elevation from the console in the time standards laboratory.

At present apart from the 11 - 12 GHz receiver no other receivers has been installed or are available for measuring on other satellites.

The VSL might have also access to very large parabolic telecommunication satellite antennae of the PTT at Burum, Netherlands, 188 km north of our laboratory.

In the mean time the coordinates of the VSL as also of Kootwijk are together with the coordinates of other laboratories and institutions determined by means of simultaneous Dopplerobservations.

CONCLUSION

We hope to be able with the help of all the combined facilities to compare the different synchronization techniques among each other.

ACKNOWLEDGEMENTS

The authors are very much indebted to Mr. J. Mc. A. Steele(NPL), Dr. D. Sutcliffe (NPL), Dr. G. Winkler (USNO), Ir. J. van Neer (ESTEC), Dr. L. Aardoom (laser ranging station Kootwijk), Ing. F. Zeeman (Kootwijk), Dr. R. Schilizzi (radio-astronomy observatory Dwingeloo) and Ir. A. van Ardenne (Dwingeloo) for their fruitful contributions in hard-ware and soft-ware.

LITERATURE

1. J. McA Steele
Comité Consultatif pour la definition de la seconde:
Contribution by the National Physical Laboratory to
the 8th meeting, 26-28 April 1977, BIPM.
2. J.W. Stark
Simultaneous long distance tropospheric propagation
measurements at 560 Mc/s and 774 Mc/s over the North Sea.
The Radio and Electronic Engineer, October 1965.
3. CCIR
VHF and UHF propagation curves for the frequency
range from 30 MHz to 1000 MHz.
Proc. XII plenary assembly recommendation 370-1
4. M. Dumas, P. Joly
VHF and UHF propagation over the Mediterranean Sea
EBU review-technical part; 1972 no 131, February.
5. CCIR
Propagation statistics applied to broadcasting and
mobile services on frequencies from 30-1000 MHz
(study program 7A/5).
Proceedings XIIth plenary assembly report 239-2.
6. S. Leschiutta
Time and Frequency Panel - Chairman's report.
Proc. of the European Workshop on Space Oceanography,
Navigation and Geodynamics, ESA-SP-137, January 1978.
7. R.T. Schilizzi, J. Campbell
Very-long-baseline-interferometry in geophysics,
geodesy and astronomy
Proc. ESA SP-137, January 1978.
8. G.M.R. Winkler
Timekeeping and its applications.
Advances in Electronics and Electron Physics, vol. 44.
1977.
9. Sirio-2/Lasso experiment
Announcement of Opportunity
ESA - DP/PA/SH/AO 79-1, September 1979.

10. A feasibility study of a pre-operational meteorological data relay (MDR) and a laser clock synchronisation mission (LASSO) using the Sirio-2 spacecraft bus (ESA-information).

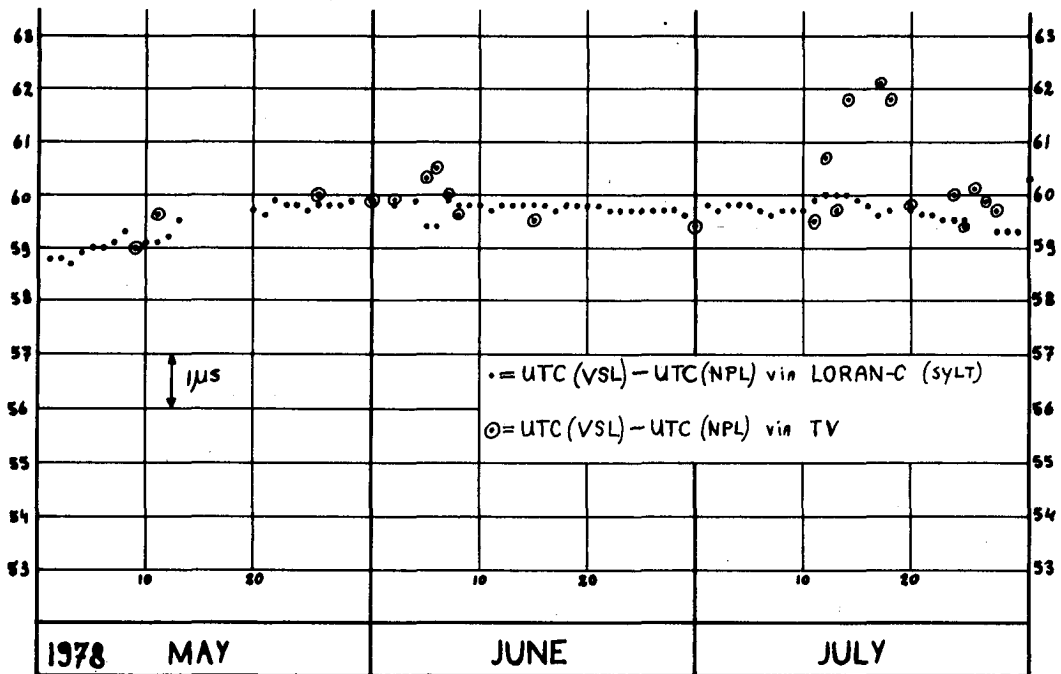


Figure 1

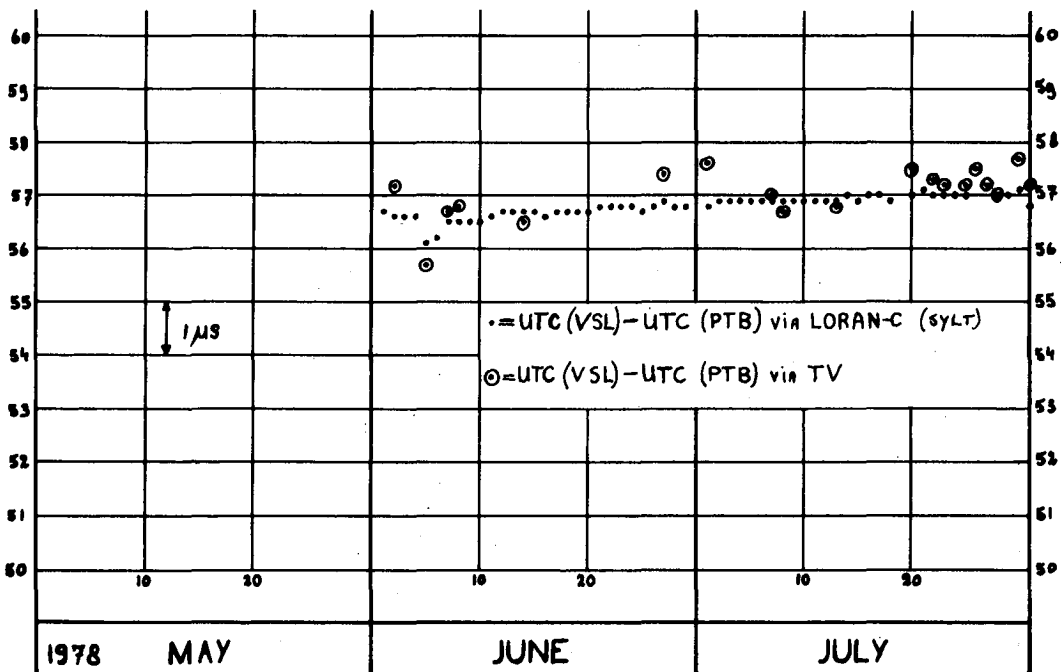


Figure 2

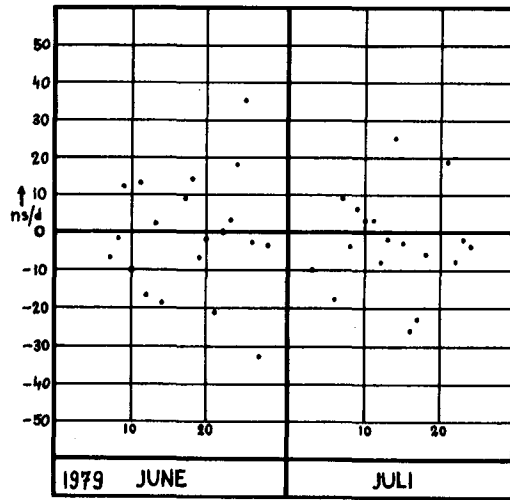


Figure 3. Stability of UTC(VSL)-
UTC(ESTEC) Via TV

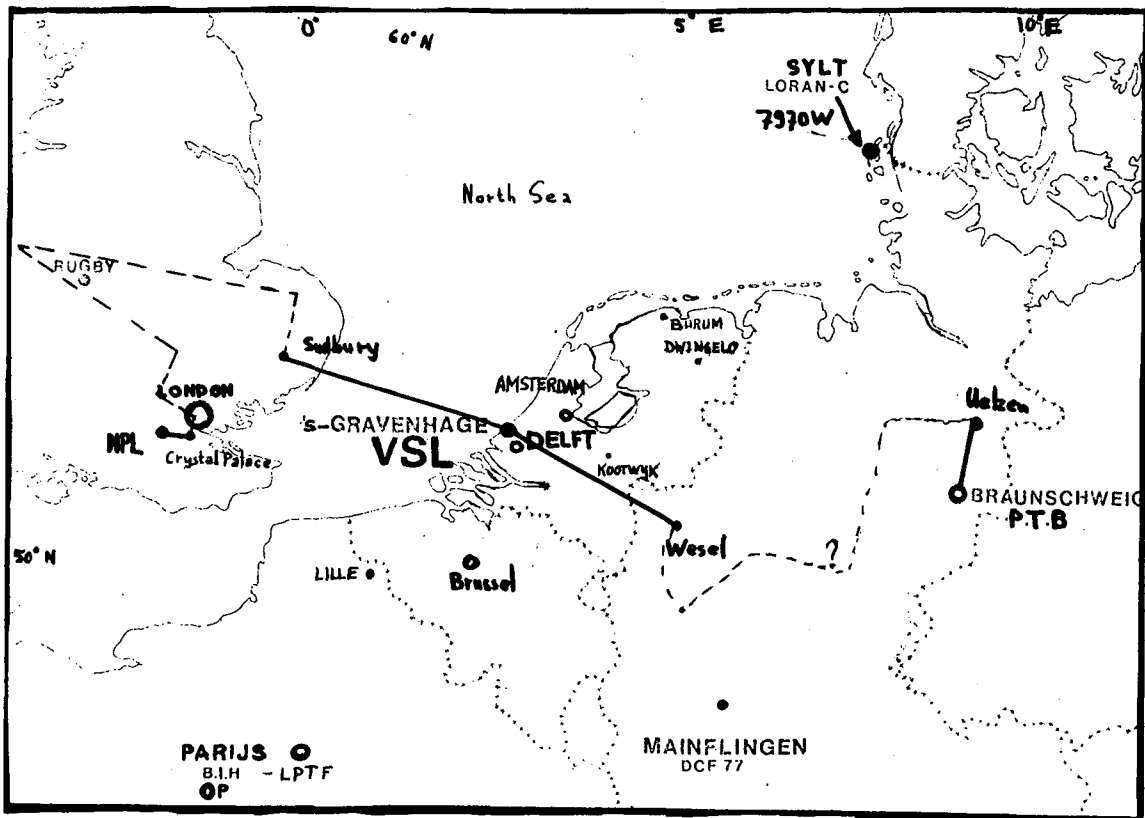


Figure 4

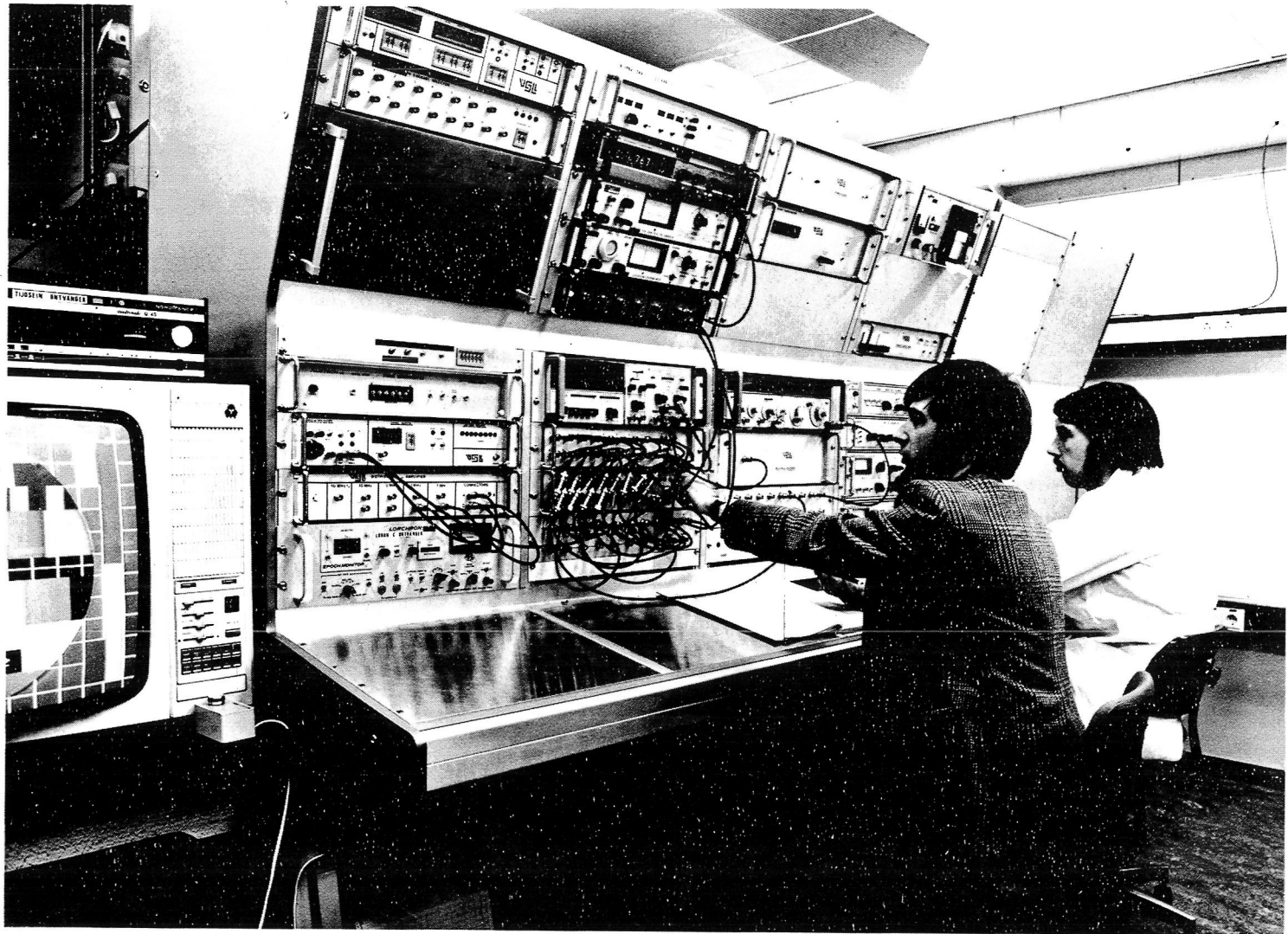


Figure 5

TWO-WAY TIME TRANSFER VIA GEOSTATIONARY
SATELLITES NRC/NBS, NRC/USNO AND NBS/USNO
VIA HERMES AND NRC/LPTF (FRANCE) VIA SYMPHONIE

C.C. Costain, J.-S. Boulanger, H. Daams, NRC
D.W. Hanson, R.E. Beehler, A.J. Clements, D.D. Davis, NBS
W.J. Klepczynski, USNO
L. Veenstra and J. Kaiser, Comsat Laboratories
B. Guinot and J. Azoubib, BIH
P. Parcelier and G. Freon, LPTF
M. Brunet, CNES

ABSTRACT

The two-way time transfer using the Hermes (CTS) satellite and the Symphonie satellite began in July, 1978. The Hermes experiment finished at the end of June 1979, and the Symphonie experiment will continue until the end of 1980. The N.R.C. uses terminals at the Communication Research Center about 25 miles from the N.R.C. laboratory, and the time transfer from N.R.C. to C.R.C. is made using line of sight TV reception with frequent checks by portable cesium or rubidium clocks. Initially the USNO used Goddard terminals, and the NBS a HEW terminal in Denver, and both relied primarily on portable clock synchronization. For the last eight months, Comsat terminals were used at the USNO and at NBS, so that no secondary time transfer was required. In France, the PBS Symphonie terminal is in Brittany, 300 miles from the Laboratoire de Temps et Fréquence (LPTF) at the Observatoire de Paris, and the time transfer to the terminal is made via the TV networks. The uncertainty in this latter link is about 20 ns, but for the other stations the uncertainty is 1 to 5 ns.

In most of the experiments, 1 pps pulses of the station atomic clocks were exchanged between the partners, and a cubic equation was fitted to the 1000 to 2000 second measurements. The equations were exchanged and subtracted to obtain the time difference of the stations. The standard deviation in the fit of the equations varied, depending on conditions, from 1.5 ns to 16 ns. For the last month of the Hermes experiment a 1 MHz signal was used, giving a standard deviation of 0.18 ns.

The comparison of the time scales via satellite and via Loran-C (BIH Circular D) show clearly that some Loran-C links are very good, but that the NBS link varies by 1 μ s. Via the satellite the frequencies of the time scales can be compared with an accuracy of 2×10^{-14} .

INTRODUCTION

A preliminary report on the two-way time transfer NRC/NBS and NRC/USNO via the Hermes (CTS) satellite was given at the PTTI meeting last year. The experiment finished at the end of June 1979, when the Hermes satellite was taken out of service, and this paper is the final report of the year's operation. The transfer NRC/LPTF (France) via the Symphonie satellite also began in July 1978, and is expected to continue until December 1980, but only the results of the first year will be presented for the purposes of comparison.

2. Satellite terminals

The NRC had the use of terminals at the Communication Research Centre in Ottawa, located about 25 miles from the NRC laboratory. The NRC rubidium clock and measuring equipment are housed at the 10 m Symphonie terminal. Initially for the Hermes experiment, the video signals were relayed via triax cables 1.5 miles to the 9 m Hermes terminal. After December 31, 1978 the signals were relayed an additional mile by cable with a 65 MHz carrier to a 2 m terminal, which operated until June 30, 1979. Time transfer from NRC to CRC was effected by line of sight TV reception calibrated periodically by portable clock transfers.

The USNO planned to operate using terminals at the Goddard Space Flight Center, but with various logistic and equipment problems, only one successful NRC/USNO transfer was possible. At the Wingspread Users Meeting, September 19, 1978 J. Kaiser suggested that portable 20 W 2.4 m Comsat terminals might be available, and one was installed at the USNO for transfers beginning November 14, 1978.

The Hermes satellite was a joint Canada/USA venture, with each country using the satellite on alternate days. The experiment was run on Canadian days up till December 31, 1978 after which time the Canadian allocation was dedicated to TV experiments. From January to June 1979, the experiment was run on USA days on time allocated to Comsat. The time transfers resumed on February 13, 1979 when the new CRC terminal was available and other arrangements were completed.

The NBS had the use of a HEW 200 W 3 m terminal on the top of a hospital in Denver from July 1978 to April 1979. Two portable Cs clocks were carried from NBS to Denver for each transfer, and TV transfer provided an additional check.

In April 1979, a second 2.4 m portable 20 W Comsat terminal was installed at the NBS laboratory at Boulder. The transfers NRC/Denver, NRC/Boulder and USNO/Denver, USNO/Boulder both

agreed to 30 ns, so no correction for the change in terminal delays was made.

In France, the Symphonie terminal (PBS) at Pleumeur Bodou in Brittany is used for the NRC/LPTF (Laboratoire primaire de temps et fréquence) transfer. The PBS/LPTF (Paris) transfer is made via the French TV network with calibration by portable clocks. The precision in the PBS/LPTF link is about 20 ns, and the accuracy via the portable clock trips is about 100 ns.

The network described above is given in Figure 1.

3. Experimental procedures

In the two-way time transfer, the second clock 1 pps pulses are beamed to the geostationary satellite, and provide the start signal for the local counter. The counter is stopped by the pulse received from the other terminal via the satellite. If it is assumed that there is reciprocity in the satellite transponders and in the paths for the slightly different frequencies, then the time difference between the clocks and the two stations is given, as in Figure 2, by

$$\Delta t = \frac{T_1 - T_2}{2} + \frac{t_1 - r_1}{2} - \frac{t_2 - r_2}{2} \quad (1)$$

$$= \frac{T_1 - T_2}{2} + \frac{t_1 - t_2}{2} - \frac{r_1 - r_2}{2} \quad (2)$$

To date, the transmitter delays t_i and the receiver delays r_i have not been measured. However, if a simple transmitter t^* and receiver r^* are built to measure $t_1 + r^*$ and $t^* + r_1$ at station 1, and the same measuring equipment is carried to measure $t_2 + r^*$ and $t^* + r_2$ at the second station, then it is apparent from Equation 2 that $t_1 - t_2$ and $r_1 - r_2$ can be determined with high accuracy. These measurements will be made for the present CRC and PBS terminals.

The 1 pps video signal, shown in Figure 3, includes the normal horizontal sync pulses of the TV format to maintain proper levels in the TV video circuits. There is a disadvantage in the simple 1 pps format in that the rise time of about 200 ns makes the readings dependent on the trigger level of the counters. There are also variations if the S/N is low. Normally runs about 15 minutes were made, giving 900 readings. A cubic equation was then fitted to the measurements, and the two equations subtracted to remove the effects of satellite motion. The time difference between the station clocks was then calculated for a particular second, and the necessary

transfers to the laboratory UTC scales included. The standard deviation in fitting the equation to the measurements varied from 1.5 ns to 16 ns depending on signal conditions.

For the month of June 1979, three modems built at NRC with the 1 MHz signal (Figure 3) were used at CRC, USNO and NBS. In the modem a crystal was locked to the incoming Doppler shifted 1 MHz wave train, and a wide band square wave was used to stop the counter. With these modems, a standard deviation below 0.2 ns was obtained.

In a later version of the modem, both 1 pps and 1 MHz signals are included, with the 1 pps at 0.7 volts and the 1 MHz at 0.3 volt level. The 1 pps is sent 0.5 μ s in advance, and is used in the modem to open a gate to allow the first 1 MHz cycle following to trigger the counter. This gives the same output as a 1 pps signal, but with the precision of the 1 MHz signal. On a double hop to France and back, CRC/PBS/CRC, a standard deviation of 0.25 ns was obtained.

Figure 4 is a reproduction of the computer output at NRC for a five minute NRC/NBS time transfer on June 27, 1979 using the 1 MHz modem. The output includes a plot showing the fit of the cubic equation to the data, and a histogram with 1 ns resolution. After the switching transients at the beginning of the run all of the measurements are within 0.5 ns of the equation. The constant term should read 256537709.67, the first two digits having been suppressed for convenience in computation. The linear term, showing a path length change of 51 ns/sec, is typical, and emphasizes the need to subtract the results for the two stations for a particular second. The sawtooth evident in the plot is a beat between the transmitted 1 MHz and the Doppler shifted received 1 MHz. The interference was due to inadequate decoupling in the modem, which would have been corrected had the experiment continued. It does not affect our present results, but it does partially mask real variations of about 0.5 ns at the beginning of the run. It appears that the precision of the experiment is sufficient to observe ionospheric effects of the order of nanoseconds.

Experimental results

The results of the time transfer experiments are given in Table I (NRC/NBS), Table II (NRC/USNO), Table III (NBS/USNO) and Table IV (NRC/LPTF). On January 1, 1979 NBS added a steering correction of 20 ns/day. This has been subtracted in the second column of the NBS tables to provide continuity for plotting the two six-month periods.

The terminal delays t_i and r_i were not measured, and therefore there is an unknown offset or error in the satellite time transfer, which hopefully is constant. Portable clock results NRC/USNO showed the satellite value about 300 ns high. For the NRC/LPTF the satellite error is about 200 ns.

There is therefore a fortuitous cancellation of the terminal delays, but the errors and the uncertainty in the errors are such that some smaller fixed corrections to the tables were not made. One correction that must be applied in future high accuracy transfer is that for the Sagnac Effect.

This correction for measurements made with geostationary satellites in the rotating coordinate system of the earth is significant. The true time difference is given by t (East clock) - t (West clock) = Δt (measured) - $\frac{2\omega A}{c}$

where ω is the angular velocity of the earth, and A is the projected area, on the equatorial plane, of the satellite and earth station network. The values* for the present experiment are given in Table V.

TABLE V

East	West	$\frac{2\omega A}{c}$ ns
USNO	NBS	75.5
NRC	NBS	67.6
NRC	USNO	-7.9
PBS	NRC	158.2

There is an interesting result for NRC/USNO, for while NRC is east of USNO, viewed from the satellite position it appears to be west.

The results of the Symphonie transfer to France are plotted in Figure 5. Transfers were made most working days until MJD 43913, and twice a week after that date. There was a break in the measurements during the eclipse period in the fall of 1978, and a shorter break following MJD 43913 when the antenna at CRC was changed.

There are occasional errors of about 200 ns which presumably arise from the time transfer to the laboratories, but the reason for these has not yet been identified.

*David W Allan, NBS, private communication

In Figure 6 the results for the NRC/NBS, NRC/USNO and NBS/USNO transfers are plotted (with the 20 ns/day adjustment for the UTC (NBS) value after January 1, 1979). The scale of the figure is such that detailed comparisons of the time scales is not possible, but some general conclusions can be drawn.

First, a comparison of the satellite results with the Loran C values obtained from the BIH Circular D show that the Loran C NRC/USNO is very good for most of the year. Unfortunately the one Hermes result in July cannot be used, because at Goddard separate transmitting and receiving antennas were used and the terminal delay errors are likely to be much different than those of the duplex Comsat terminal. Therefore, there is no comparison with the portable clock measurements possible for this period.

The NRC/NBS Loran C results show, as expected, variations of about $1 \mu\text{s}$ from the long land path to Boulder. Via Loran C there are apparent changes of 3×10^{-13} in the relative frequencies of the time scales for periods of 3 to 4 months.

In the satellite results, there are two dates when changes were made in the NRC terminal. The first in January 1979 was to a different terminal at a different site, and there must be some vertical shift in the scales at that point. However, from the NRC/USNO Loran C measurements it does not appear to be large. The second in March was an obvious change of 120 ns in both NRC scales that did not appear for the NBS/USNO results. This was not explained, but the correction was added to all subsequent measurements.

The best results were obtained for NRC/NBS in 1978, when the main 9 m CRC terminal was used and a 200 W terminal in Denver. As was mentioned before, the 1 pps results are dependent on S/N and the quality of the received pulse. Over the last four months of 1978, when routines had been established, frequency comparison between the NRC and NBS scales was better than 2×10^{-14} .

The same accuracy was obtained for NRC/USNO for the month of June 1979, using the 1 MHz modem. Unfortunately, the two mid June measurements with NBS using 1 MHz were in error by about 40 ns. A wrong deviation setting on the terminal at Boulder resulted in a 2.2 volt rather than the proper 1 volt video signal being received by the partners and this caused phase distortion in the receiving stations. However, all ended well, and on the last day of the experiment, on June 27, 1979 a 2 ns closure was obtained for the three two-way transfers.

There was some difficulty in 1979 at CRC in maintaining a constant video delay in the complex and long transfer system. On days when there was an obvious CRC error, the points were ignored in drawing the curves.

Another "closure" experiment was carried out on April 9, 1979. The allocation on Hermes and Symphonie satellites was at the same time, and the video signals from NBS and from France were patched through the CRC terminal to effect an NBS/LPTF two-way transfer. Immediately before and after this transfer an NRC/NBS and NRC/LPTF transfer was made, and the sum of these agreed to 4 ns with NBS/LPTF result. This agreement was perhaps fortuitous because in using two satellites the near simultaneity of the normal two-way transfer is lost. A further experiment, in which the NRC/NBS and NRC/LPTF transfers were carried out at the same time, had to be abandoned because one of the counters at CRC was not sufficiently reliable.

Near the end of the experimental period Comsat laboratory installed two PSK modems, which had been modified for time transfer, at the USNO and NBS terminals. This system demonstrated a higher efficiency in the time transfer, and achieved a sigma of 17.5 ns on a link of 100 kHz bandwidth.

The final comparison of the four time scales is given in Figure 7. In this figure the intercepts and slopes have all been altered to permit an expansion of the scale. Any factor that is common to the three curves arises from the NRC scale, and other individual changes can be determined by using the other two scales as controls.

Conclusions

There is no doubt that these long term experiments have shown the advantages of the two-way satellite time transfer. Our efforts must now be applied to the development of an economical operational system using commercial satellites.

Acknowledgements

We must acknowledge that we have had a great deal of assistance in these experiments. The Canadian Department of Communications has been most helpful in arranging the participation of NRC in both the Symphonie and Hermes experiments, and the staff of the Communications Research Center has given us excellent support with their terminal facilities. The joint French and German Secretariats have been generous in allocation of time on the Symphonie satellite,

and the PBS staff very cooperative. The CTS program office of NASA formalized the arrangements for NBS and USNO participation. The use of the Denver terminal of the Department of Health Education and Welfare for the first nine months of the Hermes experiment provided some of the best NRC/NBS results.

Table I UTC(NRC)-UTC(NBS)=dt ns Table II UTC(NRC)-UTC(USNO)=dt ns

MJD	dt	dt*
43717.83	2706	
43724.83	2674	
43731.85	2639	
43738.83	2643	
43759.84	2566	
43766.83	2558	
43773.84	2598	
43780.84	2684	
43786.83	2720	
43800.83	2891	
43807.83	2975	
43814.88	3009	
43821.88	3058	
43828.88	3087	
43842.88	3195	
43849.88	3233	
43856.88	3290	
43863.87	3322	
43870.87	3367	
43931.64	4938	3765
43952.68	5609	4015
43965.81	5990	4134
43972.61	6245	4253
43986.61	6566	4294
44002.60	7177	4585
44007.63	7265	4572
44028.73	7957	4842
44035.86	8126	4869
44044.67	8382	4949
44051.67	8642	5069

MJD	dt
43826.71	4938
43833.71	5033
43840.72	5053
43847.71	5129
43854.71	5191
43863.89	5207
43917.61	5363
43931.59	5420
43952.63	5474
43965.78	5548
43972.58	5574
43986.59	5586
43993.64	5710
44007.60	5690
44028.76	5911
44035.80	5939
44044.60	5987
44051.58	6053

Table III UTC(NBS)-UTC(USNO)=dt ns

MJD	dt	dt*
43917.65	989 (Denver)	1882
43938.64	354 "	1667
43945.63	44 "	1496
43952.70	- 123 "	1471
43965.83	- 436 "	1421
43972.66	- 613 "	1380
43986.68	- 998 "	1276
44002.63	-1477 "	1176
44002.64	-1446 (Boulder)	1146
44007.56	-1578 "	1113
44014.87	-1690 "	1142
44028.78	-2007 "	1106
44044.61	-2355 "	1077
44051.63	-2586 "	986

For dt*, the -20 ns/day change in UTC(NBS) frequency on January 1, 1979 (MJD 43874) has been removed to maintain consistency with the 1978 data. The dt* values are plotted in Figures 6 and 7.

TABLE IV UTC(NRC)-UTC(LPTF) = dT

MJD	dT	MJD	dT	MJD	dT
43701.80	4419	43839.78	5906	43959.64	6889
43702.81	4387	43842.75	5879	43962.66	6937
43707.80	4401	43843.75	5890	43966.60	6975
43708.80	4406	43847.79	5931	43969.62	6974
43709.79	4412	43850.77	5932	43972.64	7001
43710.80	4395	43853.77	5964	43973.60	6992
43713.81	4430	43854.80	5963	43980.60	7097
43714.80	4428	43855.80	5912	43986.64	7158
43716.80	4498	43862.70	6082	43993.59	7276
43717.80	4477	43863.76	6086	43997.56	7296
43720.80	4505	43864.76	6076	44002.56	7351
43721.80	4527	43869.71	6130	44007.64	7426
43722.80	4533	43870.76	6175	44010.65	7474
43723.80	4575	43875.69	6213	44011.63	7496
43724.80	4549	43877.76	6223	44021.62	7704
43729.80	4631	43878.69	6232	44025.61	7829
43730.79	4573	43881.76	6280	44029.60	7843
43731.80	4570	43882.69	6274	44032.62	7912
43734.80	4622	43883.69	6254	44035.62	7963
43735.80	4645	43884.75	6250	44039.60	8018
43736.79	4589	43885.76	6281	44042.64	8142
43737.79	4665	43888.76	6303	44043.54	8162
43738.80	4658	43889.69	6313	44044.56	8200
43797.76	5064	43891.75	6343	44046.62	8231
43799.71	5120	43892.75	6354	44051.60	8378
43800.76	5156	43897.66	6396	44053.61	8448
43801.75	5183	43898.62	6410	44057.60	8528
43804.75	5253	43899.62	6399	44060.62	8604
43805.67	5357	43902.62	6415	44063.62	8624
43806.67	5473	43903.66	6537	44067.61	8674
43807.77	5384	43904.66	6431	44071.60	8760
43808.77	5386	43905.60	6429	44074.60	8821
43813.70	5454	43906.60	6444	44078.61	8912
43814.76	5465	43909.61	6471	44081.61	9036
43818.75	5504	43910.66	6428	44085.60	9129
43820.70	5539	43911.66	6452	44088.62	9221
43821.75	5538	43912.61	6440	44092.60	9120
43822.74	5590	43913.62	6467	44095.62	9304
43826.70	5683	43931.66	6650	44099.61	9371
43827.70	5696	43934.66	6724	44102.61	9391
43828.75	5706	43937.66	6729	44106.60	9493
43832.73	5772	43941.66	6779	44108.62	9407
43834.70	5823	43945.64	6808	44113.81	9571
43835.74	5814	43948.66	6784		
43836.75	5687	43952.64	6881		

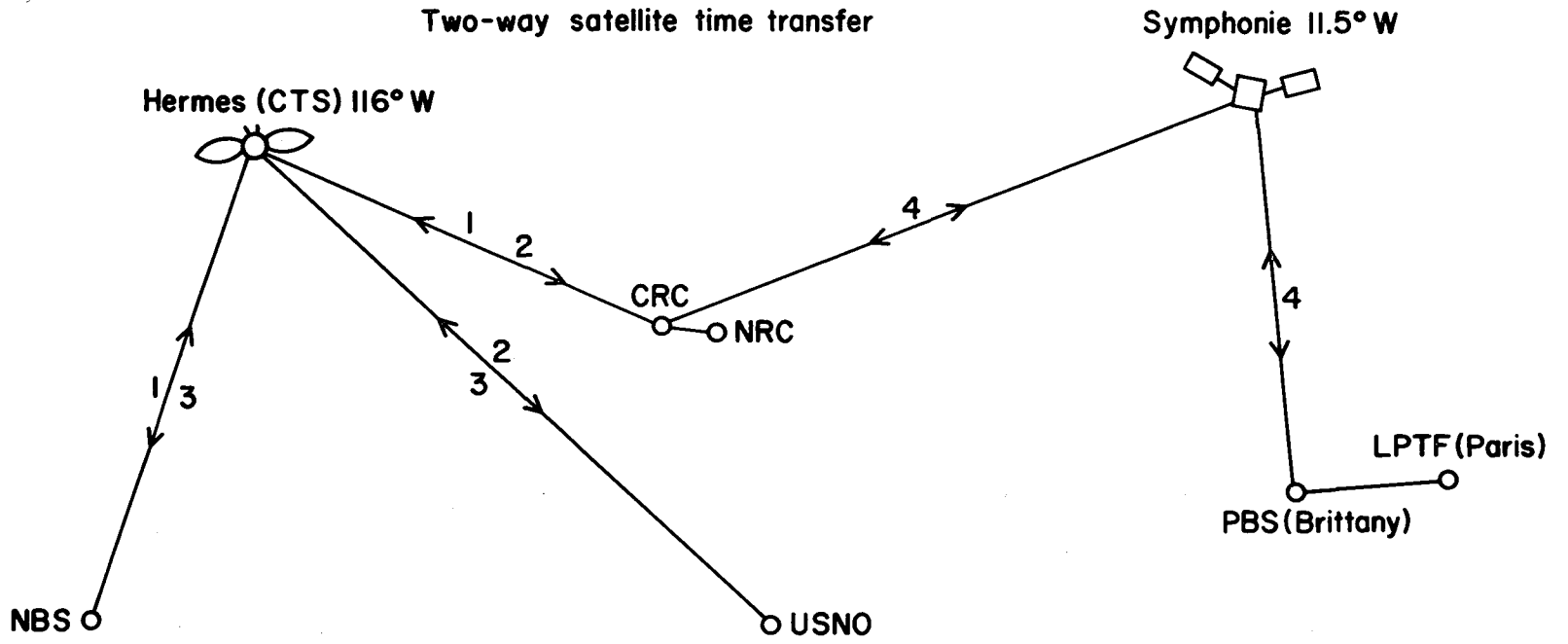


Figure 1. The Four Station, Two Satellite Network

Time transfer equation

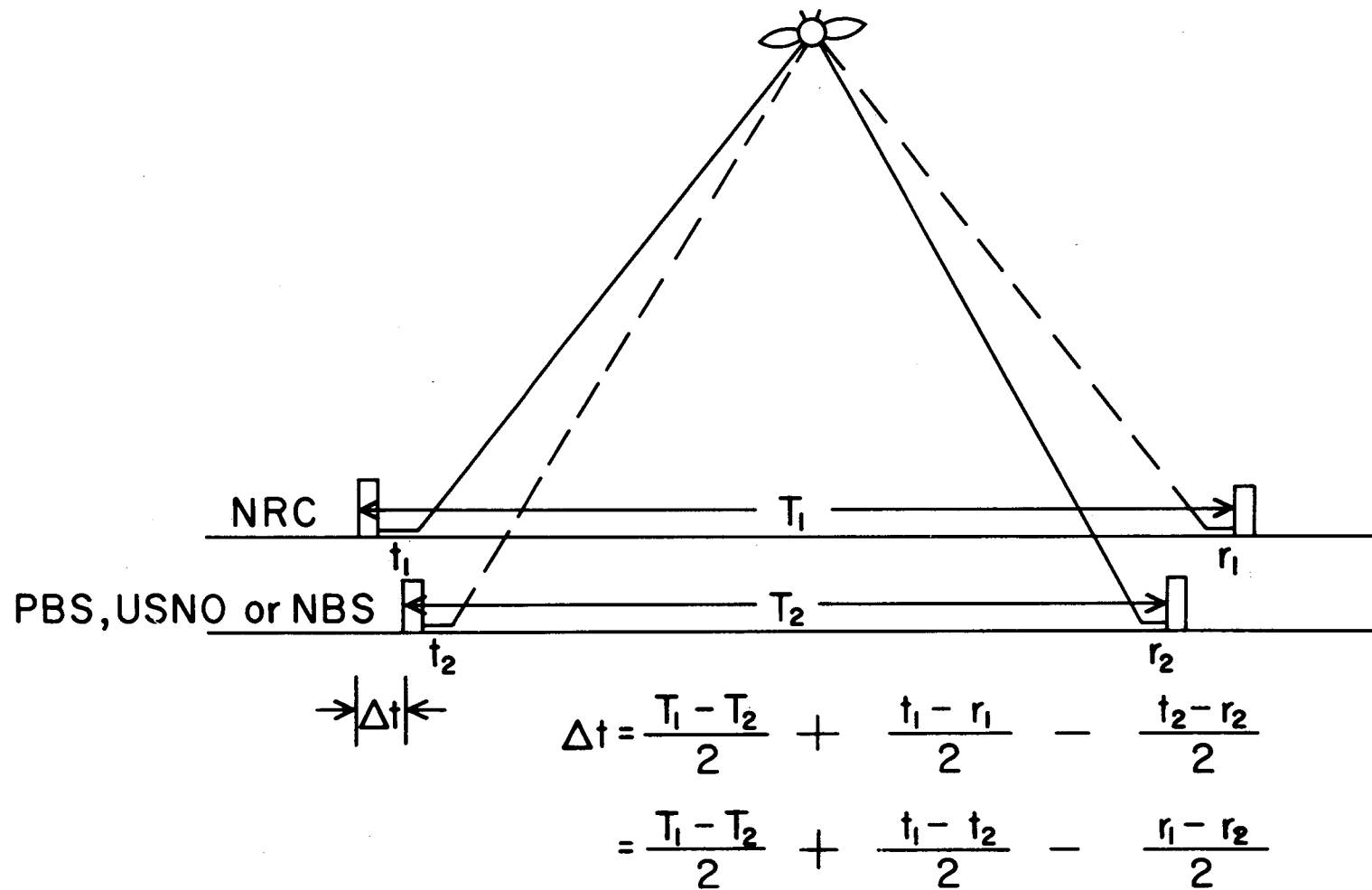
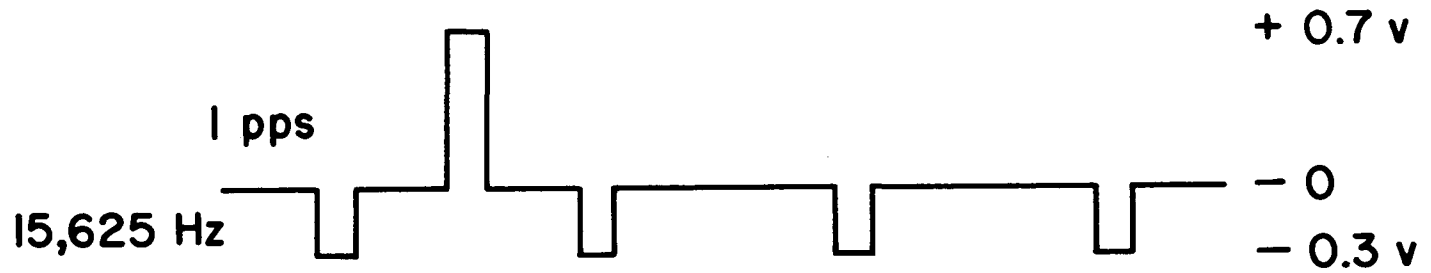


Figure 2. The Two-Way Satellite Time Transfer Equation



or

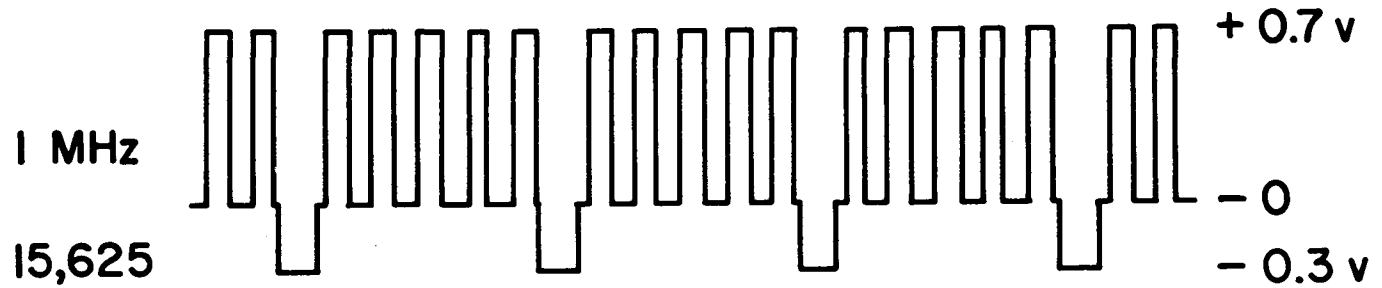
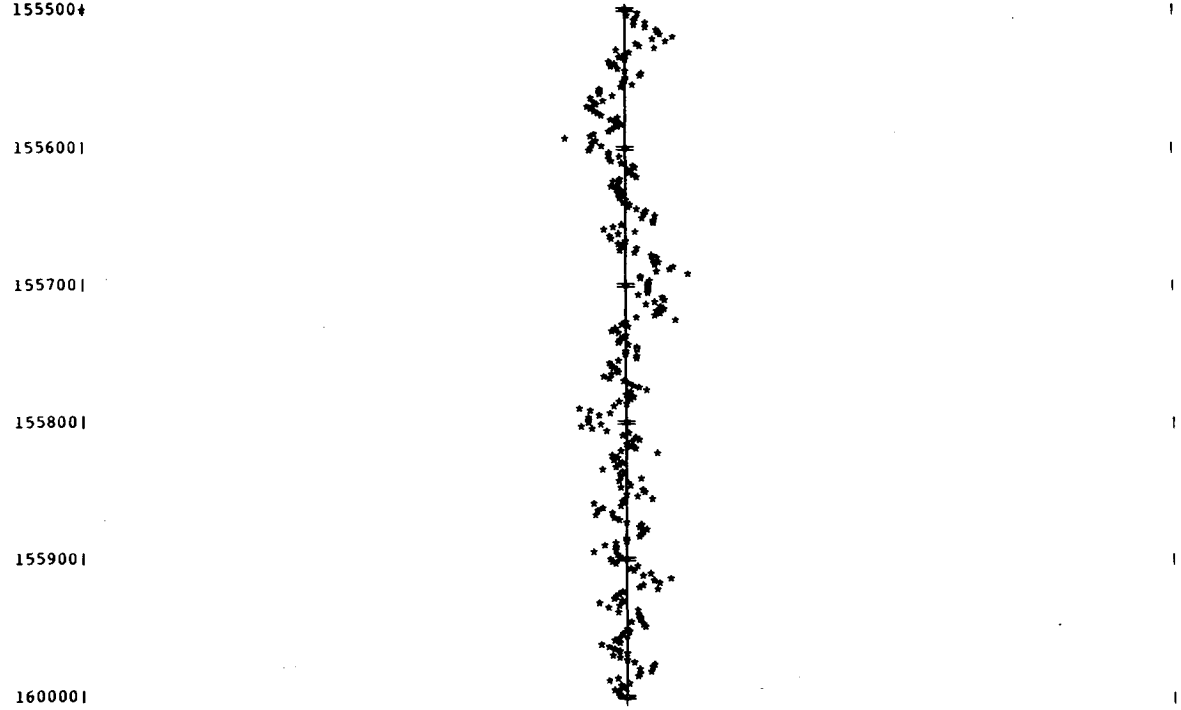


Figure 3. The 1 PPS and 1 MHz Video Format

The file is BOU178153935
 Scale is 1 ns per inch, from -5 to 5
 Curve from 155500 to 160000 : Data{tj}-Y{t}.



Histogram : scale = 3:1, computed from 155500 to 160000
 AT >24 : 1 |
 AT 1 : 1 |
 AT 0 : 297 |*****
 AT -1 : 1 |
 AT <-24 : 1 |

The file is BOU178153935: from 153938 to 161001
 Origin is 160000.
 UTC(NRC)-UTC(CRC)=7 ns. Trigger level is 0.25 VOLTS.
 $Y\{t\}(ns) = 6537709.67 - 5.1128137E+01*t - 1.7761167E-03*t^2 - 5.0445160E-08*t^3$
 Calculation includes 155502/155955
 Std dev = 0.19 ns (window = 2000 ns).
 0 pts rejected on a total of 294.

Figure 4. The Fit of a Cubic Equation to the Data at NRC for 1 MHz Modulation on June 27, 1979

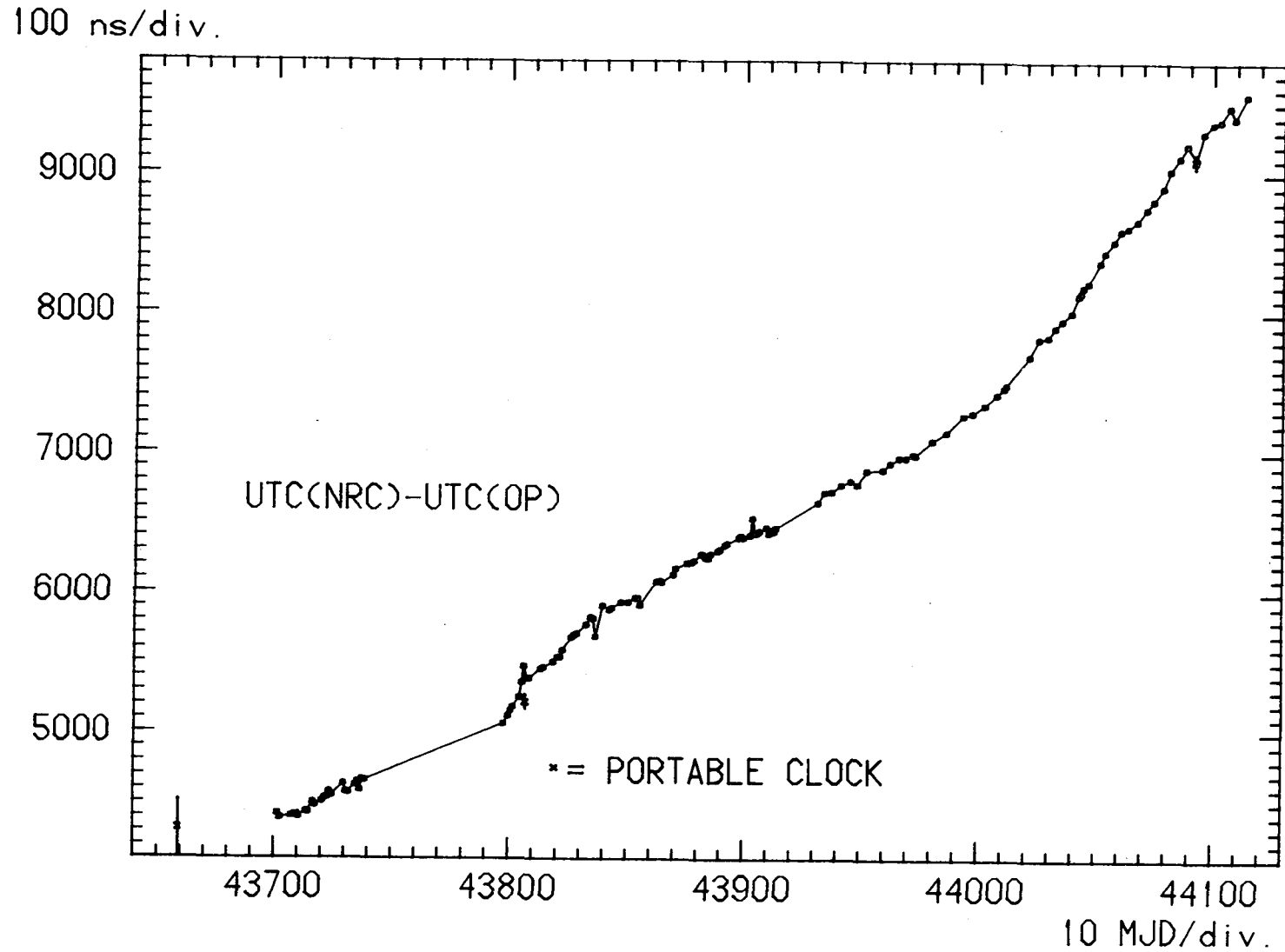


Figure 5. The Difference in the NRC and OP (or LPTF) Time Scales Via the Symphonie Satellite

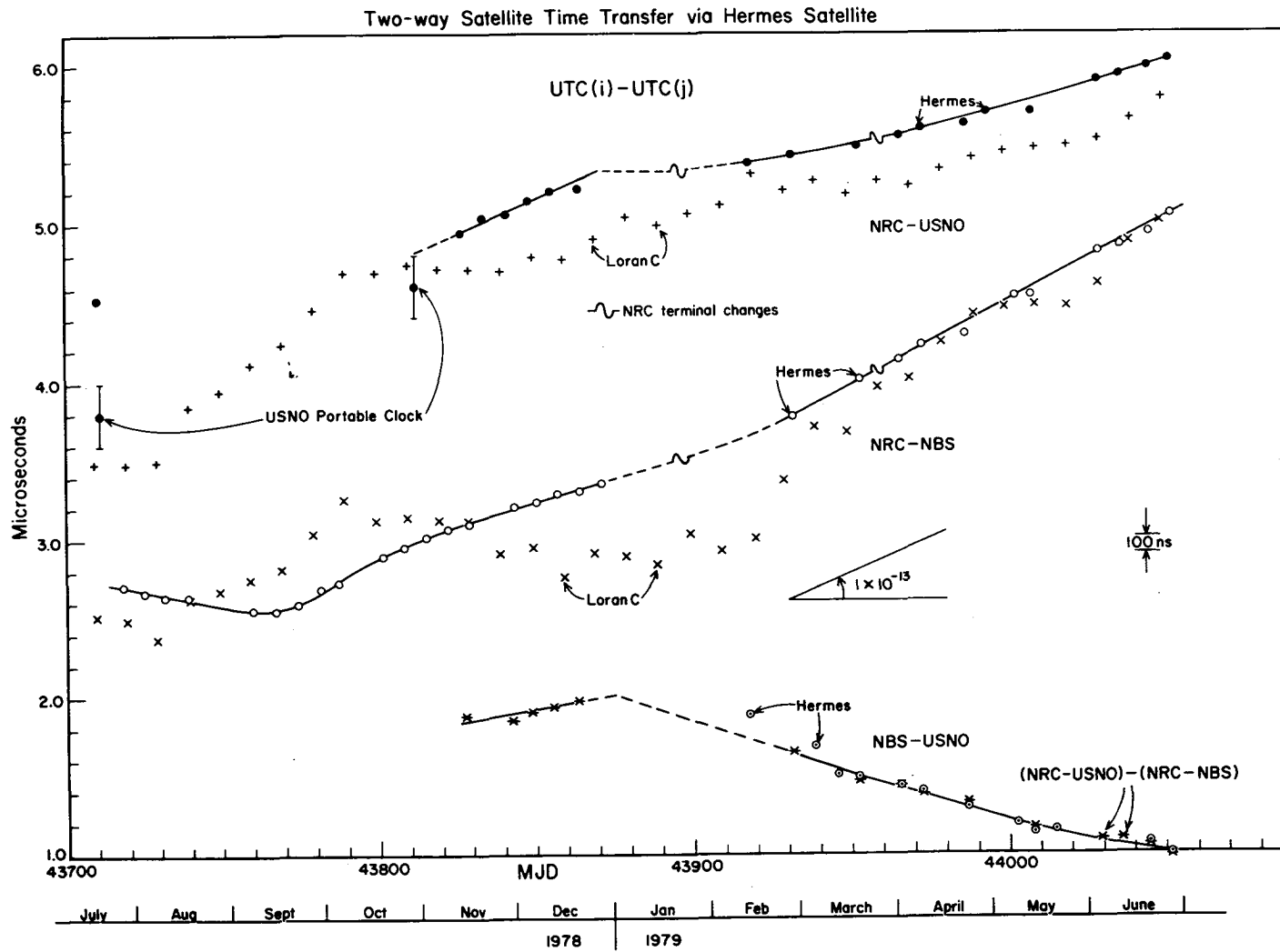


Figure 6. The Differences Between the NRC, NBS and USNO Time Scales Via the Hermes Satellite

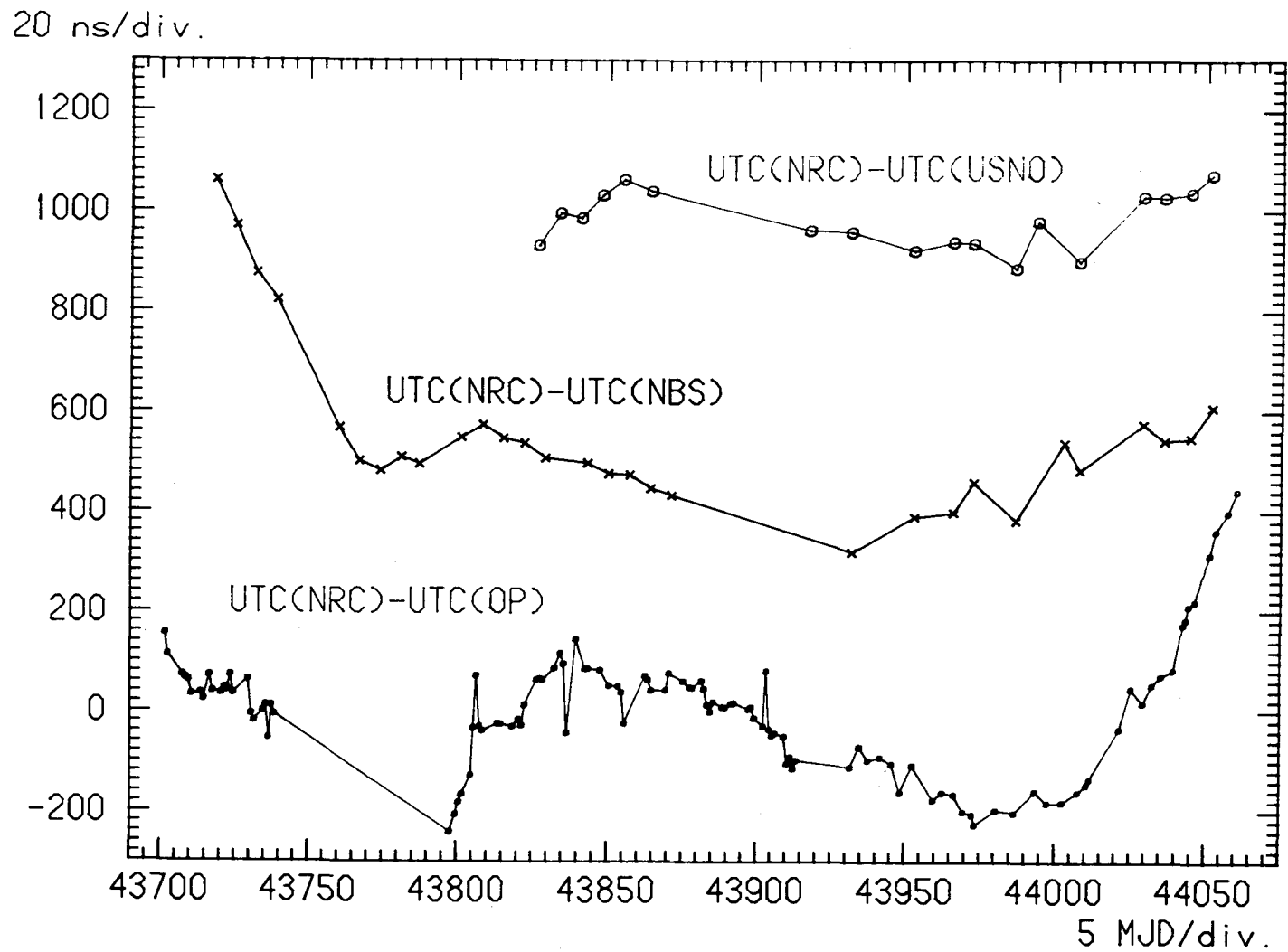


Figure 7. The USNO, NBS and OP Time Scales Compared to that of NRC. The Intercepts and Slopes have been Altered to Permit an Expanded Scale.

QUESTIONS AND ANSWERS

MR. CHI:

Are there any questions?

DR. COSTAIN:

Are there any answers?

MR. CHI:

Would you please use the microphone and identify yourself for the sake of recording?

MR. LAUREN RUEGER, The Johns Hopkins University, Applied Physics Laboratory

With all those precision measurements, what kind of a standard were you using out at the stations because we see in time order scatter a nanosecond kind of a variation in cesium standards?

DR. COSTAIN:

There was an HP Rubidium at the CRC site.

MR. RUEGER:

Okay. What about the standardization of the point on the pulses that you used for determining the epoch of a measurement? We have been hearing for a while that people use different places on these rise times and different rise time pulses and characterization. Have you some kind of standardization for this purpose?

DR. COSTAIN:

We try to operate at a quarter of a volt trigger level on the standard one volt pulses or .7 volt pulses. But of course with the one PPS it is very sensitive in fact to the quality of the received signal and the trigger level and somebody comes by and changes the trigger level from time to time. This is why we prefer the one megahertz. When you have got a wideband square wave it doesn't make much difference where the trigger is set.

The only thing is, is you have to make sure, and we did, that the megahertz is synchronized with your 1 PPS.

MR. RUEGER:

Does everybody in your network use exactly the same characteristics in this respect?

DR. COSTAIN:

We endeavored to. That was the main thing. The video treatment in the terminals was not always the same.

MR. CHI:

I would like to ask you one question if I may, and that is what is the variation of the corrections throughout the time of measurement? Is that variation large or fairly constant?

DR. COSTAIN:

It is a bit difficult to tell with the type of experiment we were running, I mean, and you were fitting a cubic equation and can cover a lot of faults. But I think we could see real variations of the order of nanoseconds.

I was going to say that my endeavor is, if I can persuade our authorities to get two terminals for Ottawa, to do a two-way time transfer to ourselves, eliminate clock errors and make a definitive evaluation of this satellite system.

DR. LESCHIUTTA:

Can you please tell us something about what techniques you are proposing to use in order to calibrate the ground stations? Calibrate the delay of the ground station?

DR. COSTAIN:

Yes. I should elaborate. While it is intentionally what we intend to do with Symphonie, first make a small transmitter, a little gun diode, that you use to measure the artificial transmit/receiver loop, then carry that to the next station and make exactly the same measurement and subtract it. I think that can be done to one or two nanosecond precision.

And the same with the transmitter. You build a small receiver and you carry that receiver, cables and everything and make the identical measurement at the other station. And it is the difference in those measurements that you want to know.

It is very difficult, I think, to measure precisely and separately the transmitter delay and the receiver delay at a station. If we can make the difference measurements between the two stations, then I think it can be much more accurate.

MR. PLEASURE:

Would you please comment on the technique suggested by Professor Cohen of the University of Pennsylvania in an article in "Physical Review Letters" where he has geostationary satellites communicating with one another and with ground stations and using that to calculate Einstein. Were you aware of that?

DR. COSTAIN:

I think I did read the paper. I don't know that any further verification to my knowledge is needed in relativity theory to the accuracy that we can make the measurements. You must, of course, take into account a rotating coordinate frame--

MR. PLEASURE:

But he could not do that accurately. He has an approximation that he would like to have measured.

DR. COSTAIN:

Well, if we can achieve nanosecond accuracy, this would be one percent verification on this SAGNAC effect. I would say that my objective is not that; my objective is a cheap commercial network. It is an interesting thing, but it costs money to mount a more elaborate satellite to satellite and we are at the moment searching for a way to make our communication network economical. And I think one of the things we have going for us is that I think the communications networks will need sub-microsecond times in their systems in the very near future.

DR. SERENE:

Are you planning to compare your result using the LASSO system, in the area of 1 nanosecond?

DR. COSTAIN:

The inquiries that we have made that we do not have access to a telescope for the two-way, and I am not sure, in fact, whether I would have the money or manpower for the one-way from Ottawa. We

are suffering a bit from retirements and it is going to be a bit complex in the next two years. We might know certainly before the experiment is finished. We might hope to be able to participate. At the moment, I cannot do so.

THE SIRIO-1 TIMING EXPERIMENT

E. Detoma
Bendix/NASA-GSFC(1)

and

S. Leschiutta
Istituto Elettrotecnico Nazionale "G. Ferraris"

ABSTRACT

During the 1979 a time synchronization experiment was performed via the SIRIO-1 satellite. The experiment is sponsored by the Italian National Council of Research (CNR) and was proposed and studied by the Istituto Elettrotecnico Nazionale, Turin, Italy.

The RF communication channels are in the SHF region, with the uplink carrier at 18 GHz and downlink at 12 GHz. The synchronization has been performed between two ground stations located in the northern and in the central part of the country. One-way and two-way techniques have been evaluated. Two modes of operation are tested in the two-way technique:

- sequential, time multiplexed, signal transmission on the same communication channel;
- simultaneous transmission using separate communication channel.

In the sequential mode of operation an advanced technique, using range and doppler measurements provided by the timing signals, is used, to take in account for the satellite motion.

A low cost, versatile, time transfer unit (TTU) was designed, to generate the timing signals and the functions (RF carrier and receiver switching, time tagging of the data, etc.) required to perform automatic time synchronization and data acquisition with a minimum of external components.

(1) The work was performed when the author was at IEN.

INTRODUCTION

During the 1979 a time synchronization experiment was performed in Italy via the SIRIO-1 satellite. The experiment was sponsored by the Servizio Attività Spaziali (Space Activities Service - SAS) of the Italian National Research Council and was proposed, studied and performed by the Istituto Elettrotecnico Nazionale (IEN), Torino (Italy).

One-way and two-way techniques have been evaluated. Two modes of operation are tested in the two-way technique:

- sequential, time multiplexed, signal transmission on the same communication channel;
- simultaneous transmissions using separate communication channels.

In the sequential mode of operation an advanced technique, using range and doppler measurements provided by the timing signals, is used, to take in account for the satellite motion.

The synchronization has been performed between two ground stations located in the northern and in the central part of the country. The results of the time comparisons have been checked using the TV method and portable clock trips.

The SIRIO-1 satellite

The SIRIO-1 satellite is a synchronous, spin-stabilized, experimental communication satellite, designed to conduct telecommunication experiments and study propagation phenomena at frequencies of 12 and 18 GHz, and was launched by NASA from the Kennedy Space Center on August 25, 1977.

The experimental SHF telecommunication payload consist of a transponder with three separate channels - one for propagation experiments and two for broad and narrow band communication experiments.

The broadband communication channel (34 MHz RF bandwidth at -1 dB) has been used for the time synchronization. The 17.10 GHz uplink carrier is frequency modulated; the available video (baseband) bandwidth used is 6 MHz. The downlink carrier frequency is 11.52 GHz.

Earth stations

The two ground stations, operated by Telespazio S.p.A. (the company is responsible in Italy for the operation of commercial telecommunication space links, mainly through the Intelsat satellites), are located in the northern part of the country, at the top of the Como Lake, near the Swiss border (Lario station) and near Rome (Fucino station).

The two stations, to operate with the SIRIO-1 satellite, are equipped with 17 m diameter azimuth-elevation mount autotrack antennas. The Fucino station serves also as the main control center of the operation of the satellite (tracking and command operations).

THE TWO-WAY TECHNIQUE

In the two-way time synchronization technique (ref. 1) two clocks, located in A and B (fig. 1a), exchange the time information through a satellite communication link.

The basic equation giving the time difference between the clocks is:

$$(1) \quad \varepsilon = \frac{[T_1 - T_0] - [T_3 - T_2]}{2} + \Delta\varepsilon (\text{corrections})$$

where ε is the time difference between the clocks in A and B [actually $\varepsilon = T(B) - T(A)$], T_1 and T_3 are the times of reception of the time signals transmitted at the times T_0 and T_2 by A and B (fig. 1b).

The corrections take in account several effects affecting the time synchronization process: the difference in the forward and return paths (from A to B and from B to A) due to the satellite motion and to the Earth rotation, the atmospheric propagation delays and the equipment delays.

Corrections due to the satellite motion

If the signals transmitted by A and B are relayed by the satellite at two different times t_1 and t_2 (fig. 1b) and the satellite changes its position in the time interval $(t_2 - t_1)$,

the two paths (r_{AB} from A to B and r_{BA} from B to A) are no longer equals; this results in a correction to be applied to eq. (1), that can be written as:

$$(2) \quad \Delta \epsilon_s = \frac{r_{BA} - r_{AB}}{2 V_p} \approx \frac{r_{BA} - r_{AB}}{2c}$$

where V_p (speed of propagation) is assumed to be nearly equal to c (light velocity)

Corrections due to the propagation effects in the atmosphere

Two types of effects have to be considered:

- a) tropospheric effects
- b) ionospheric effects

The tropospheric effects are frequency independent, so they nearly cancel out when performing the two-way time synchronization (in fact, they contribute nearly equal delays in the forward and return path).

The ionospheric effects (that are frequency dependent) are to be taken in account, again by adding to eq. (1) a second correction $\Delta \epsilon_p$ in the form:

$$(3) \quad \Delta \epsilon_p = \frac{\Delta \tau_B(f_u) - \Delta \tau_B(f_d)}{2} - \frac{\Delta \tau_A(f_u) - \Delta \tau_A(f_d)}{2}$$

where $\Delta \tau_N$ ($N=A, B$) is the additional delay (with respect to the free-space propagation) introduced in the path between the station N and the satellite; f_u is the uplink carrier frequency and f_d is the downlink carrier frequency for the station N (separate carriers may be employed in A and B).

At the frequencies employed in the SIRIO-1 experiment, the effects due to the eq. (3) are negligible.

Instrumentation delays - ground segment

The delays in the transmitting and receiving equipments must be taken in account; they contribute a correction $\Delta \epsilon_{eq}$ given by

$$(4) \quad \Delta \epsilon_{eq} = \frac{[\Delta \tau_{tr}(B) - \Delta \tau_{rec}(B)] - [\Delta \tau_{tr}(A) - \Delta \tau_{rec}(B)]}{2}$$

where: $\Delta\tau_{tr}(N)$ is the delay in the transmitting equipment and $\Delta\tau_{rec}(N)$ is the delay in the receiving equipment, at the station N (N = A, B).

Instrumentation delays - space segment

The correction $\Delta\varepsilon'_{eq}$ takes in account for the differential delay in the satellite transponder; if f_N is the frequency used by the station N, this correction can be written as:

$$(5) \quad \Delta\varepsilon'_{eq} = \frac{\Delta\tau_{transp}(f_B) - \Delta\tau_{transp}(f_A)}{2}$$

where $\Delta\tau_{transp}(f)$ are the group delays of the satellite transponder at the frequency f.

Modes of operation

Let we set (fig. 1b)

$$(6) \quad \Delta t = T_2 - T_1$$

Δt can be regarded as an arbitrary time interval (and we will make use of its arbitrariness in the following analysis) defining three possible modes of operation:

- a) $\Delta t > 0$: the two stations transmit sequentially in time;
- b) $\Delta t \approx 0$: the signal transmitted by A is simply transponded back by B;
- c) $\Delta t < 0$: the two stations transmit simultaneously to the satellite.

If the two stations transmit sequentially in time (case a), only one communication channel can be used, but in this case the satellite motion must be taken in account, to compensate the differences between the forward and return paths. In addition, if one channel is used, the correction due to eq. (5) vanishes.

If two channels are used, the two stations can transmit simultaneously, in order to have the signals relayed nearly at the same time by the satellite (case c), so that the change in paths due to the satellite motion can be neglected.

THE SIRIO-1 EXPERIMENT - SEQUENTIAL MODE OF OPERATION

The time synchronization SIRIO-1 experiment was designed to test and precisely measure the effects of the satellite motion.

Each ground station (fig. 2a), in addition to receive the signals transmitted by the other station, receives its own signal, relayed back to Earth by the satellite. This can be implemented easily, as shown in fig. 2b. We use a fixed synchronization sequence, that will be covered in detail later, so that the time of transmission for each station is at fixed times, according its own time scale.

With reference to the geometry depicted in fig. 2a, the basic synchronization equation, in which the corrections for the satellite motion are taken in account, becomes:

$$(7) \quad \varepsilon = \frac{(T_1 - T_0) - (T_3 - T_2)}{2} + \frac{(r_2 + r'_2) - (r_1 + r'_1)}{2c}$$

Now, we can write with good approximation [if $(t_2 - t_1)$ is small]:

$$\begin{aligned} r'_2 &= r_1 + \dot{r}_A (t_2 - t_1) + \dots \\ r'_1 &= r_2 + \dot{r}_B (t_1 - t_2) + \dots \end{aligned}$$

where \dot{r}_N is the range rate of the satellite with respect to the station N ($N=A, B$) and the higher order terms in the series expansion are negligible.

Let we define the pseudo-ranges $\bar{r}_1(t_1)$ and $\bar{r}_2(t_2)$ as:

$$(9) \quad \bar{r}_1(t_1) = \frac{T_4 - T_0}{c} ; \quad \bar{r}_2(t_2) = \frac{T_5 - T_2}{c}$$

so that, by having a sequence of n synchronization measurements, an estimate of the range rate can be obtained in the following form:

$$(10) \quad \dot{r}_A = \frac{\bar{r}_1(t_1)_{n+1} - \bar{r}_1(t_1)_n}{(t_1)_{n+1} - (t_1)_n}$$

$$(10) \quad \dot{r}_B = \frac{\bar{r}_2(t_2)_{n+1} - \bar{r}_2(t_2)_n}{(t_2)_{n+1} - (t_2)_n}$$

so that we finally obtain:

$$(11) \quad \mathcal{E} = \frac{(T_1 - T_0) - (T_3 - T_2)}{2} + \frac{\dot{r}_A + \dot{r}_B}{2c} (t_2 - t_1)$$

where:

$$t_1 \approx \frac{T_4 + T_0}{2}; \quad t_2 \approx \frac{T_5 + T_2}{2}$$

Obviously the determination of t_1 and t_2 is biased by the relativistic effect due to the Earth rotation (Sagnac effect) and by the non-reciprocity of the forward and return paths; however, these effects produce only a very small error on \mathcal{E} , so that they can be neglected.

But the time interval $(t_2 - t_1)$ is biased by a larger error: this is the same difference \mathcal{E} between the clocks, since t_2 and t_1 are measured in different time reference frames.

In principle, the two-way time synchronization technique sets no limits to the initial value of \mathcal{E} , that can be very large; the only limitation comes from the technical implementation of the synchronization procedure. It may be shown that for the fixed synchronization sequence implemented in the SIRIO-1 experiment, \mathcal{E} can be initially as large as 100 ms, without affecting the automatic operation of the equipment (mainly the data acquisition system).

Iterative solution

A simple iterative technique overcomes this problem. Let we neglect the offset \mathcal{E} , biasing the time interval $(t_2 - t_1)$; neglecting for now the other sources of error, it's easy to see that the error $\delta\mathcal{E}$, on the determination of \mathcal{E} , produced by the bias on $(t_2 - t_1)$, is given by:

$$(12) \quad \delta\mathcal{E} = \frac{\dot{r}_A + \dot{r}_B}{2c} \mathcal{E}$$

This suggests that an iterative procedure can be stated, the error $\delta\mathcal{E}_{k+1}$ at the $k+1$ iteration step being expressed by:

$$(13) \quad \delta \varepsilon_{k+1} = \frac{\dot{r}_A + \dot{r}_B}{2c} \varepsilon_k$$

The iteration converges very quickly to the resolution of the measurement system, since the term $(\dot{r}_A + \dot{r}_B)/2c$ is very small; usually one step is all that it is required to minimize the error due to ε .

Close form solution

A close form solution can be obtained by introducing ε in the right side of eq. (11), that now becomes:

$$(14) \quad \varepsilon = \frac{(T_1 - T_0) - (T_3 - T_2)}{2} + \frac{\dot{r}_A + \dot{r}_B}{2c} (t_2 - t_1 - \varepsilon) + \text{corrections}$$

from which it is easy to obtain:

$$(15) \quad \varepsilon = \frac{[(T_1 - T_0) - (T_3 - T_2)] + \frac{\dot{r}_A + \dot{r}_B}{c} (t_2 - t_1) + \text{corrections}}{2(1 + \frac{\dot{r}_A + \dot{r}_B}{2c})}$$

Corrections due to the propagation in the atmosphere and satellite transponder differential delay.

Only a very small bias is expected due to the propagation effects in the atmosphere; since it is quite small as compared with the resolution of the measurement system (based on the HP5345 counter, whose resolution is 2 ns), this bias can be considered negligible.

Since only one communication channel is used, the satellite transponder does not affect the synchronization accuracy. The satellite motion is precisely measured, so that, except for the Sagnac effect, that can be easily computed, no other effects, related to the space communication link (from one ground antenna to the other), affect the synchronization accuracy in the SIRIO-1 experiment, the main source of error still being represented by the uncertainties in the measurement of the ground communication equipments delays.

Corrections due to the Earth rotation (Sagnac effect)

This correction was computed and, due to the relative geometry of the satellite with respect to the ground stations, the total effect was evaluated to be about 15 ns.

A complete derivation of the equation giving this correction is reported in app. A, for reference.

THE TIME SIGNALS

The time signals used in the SIRIO-1 experiment consists in a burst of ten pulses (fig. 3); the duration of each pulse is 1 ms and the repetition period of the pulses within the burst can be manually set by the operator to be 5 or 10 ms (the time signal must be the same for both stations).

The received pulse repetition rate shows no relative doppler against the transmitted pulses, because of the small satellite motion in about 100 ms (that is the maximum duration of the burst), so that the repetition period between the received pulses can be considered constant and equal to the transmitted repetition period.

This allows ten measurements of the time T_n , since the relative time of occurrence of each pulse with respect to the first one is constant and well known. The time T_n is then computed as the mean over ten separate values; moreover, the standard deviation over this set of ten independent time measurements is related to the precision obtained in the determination of the time T_n . This allows to monitor the uncertainty in the determination of the time of reception of the signals in each station.

GROUND EQUIPMENT CONFIGURATION

The instrumentation installed in each station is shown in fig. 5. One cesium beam frequency standard (HP 5061 and Oscilloquartz 3200) generates the local time scale. The 1 MHz and 1 Hz output signals are fed into the time transfer unit (TTU), that actually controls the synchronization procedure.

The 1 Hz distribution amplifier provides several outputs that are used in the TTU calibration procedures and for the TV synchronization subsystem.

The time interval counter used is a HP 5345A, that receives the start and stop signals from the TTU; it is fully controlled (functions, trigger levels, output mode, etc.) by a HP 9815 programmable desk calculator, that acts also as a data acquisition system (via HP-IB bus), receiving the results of the measurements from the counter and storing the data on the built-in magnetic tape unit.

The TTU generates and receives the time signals from the communication equipment; the existing FM modulators-demodulators are used: the available video bandwidth is 6 MHz. The output of the modulator is the first 70 MHz IF, switched, under the TTU control, to provide the RF carrier suppression in the sequential mode of operation (while the gating of the received signal Rx is performed internally by the TTU itself).

The two cesium standards are also compared by using the passive TV synchronization system via the TV synchronization subsystem.

The time transfer unit (TTU)

The time transfer unit (TTU) controls the synchronization procedure by performing several functions:

- 1) generation, according the selected mode of operation, of the time signal Tx to be transmitted;
- 2) generation, in the correct sequence, of the start and stop signals to the counter;
- 3) time tagging of the data;
- 4) switching of the RF carrier in the sequential mode of operation, and gating of the receiving functions (to avoid noise related problems when the carrier is off).

Moreover, the TTU has a self-test capability (by simulating the signals received from the satellite in both the operation modes) and provides the internal switching to measure the internal delays (the results of these measures are also stored on tape with the data, in a separate file).

A block diagram of the TTU is shown in fig. 6.

The TTU receives the 1 MHz and 1 Hz signals from the frequency standard. All the other signals are generated from the 1 MHz signal; however, since the synchronization results are usually referred to the 1 Hz output signal from the clock, this is internally used to synchronize all the TTU functions.

The main purpose of the TTU is the generation of the time signals; this function is performed by the Signal Generation Subsystem (SGS); the repetition period of the ten pulses in the transmitted signal (fig. 3) can be set manually by a front panel switch to 5 or 10 ms.

The transmission time T_n (fig. 3) can be shifted over a 1 s time interval (that is the synchronization frame, see sect. 6) in 1 ms steps via a 3 digit thumbwheel switches; this is important when performing the time synchronization in the simultaneous mode of operation.

The generated signals are fed into the Logic Control Subsystem (LCS), that provides the signals to be transmitted (Tx) with the proper transmission rate; this rate can be set by another thumbwheel switch to generate a synchronization measurement:

- every second;
- every odd or even second (to avoid ambiguities in the switch setting at the two stations);
- every fifth second;
- every tenth second.

The LCS controls also the operation mode (sequential or simultaneous synchronization) and the status of the TTU (self-test or operation).

The LCS generates the start and stop signals to the counter and the control signals for the RF carrier switching and the gating of the received signals Rx (sequential mode of operation only).

In the self-test mode the LCS receives the simulated return signal from the satellite simulator subsystem (SSS), that is in turn controlled, according the operation mode, by the LCS.

The LCS receives also the time-of-the-measurement information from the internal clock, via a special subsystem called Time

Tag Interval Generator (TTIG). The TTIG receives a truncated time information (minutes and seconds of the measurement, the hours are omitted, the code is BCD parallel) from the clock and generates a variable length time interval (VLTI); the duration of the VLTI, in μs , corresponds to the digital read-out of the internal clock (i.e.: if the clock time is XX hours, 26 minutes and 56 seconds the duration of the VLTI is 2656.OYY μs , where X and Y are undefined digits).

The internal clock is driven directly by the 1 Hz signal generated by the SGS; this is obtained by dividing the 1 MHz signal from the frequency standard; 6 thumbwheel switches allow the time setting of the clock (hours to seconds); the residual setting (up to 1 μs) is performed automatically by the internal 1 Hz synchronization circuit.

The TV measurement subsystem

TV signals received in both stations are used to compare the two frequency standards after an initial and routine clock trips to measure the propagation delays have been performed.

A differential, passive method of comparing the two clocks against a common reference (a selected field synchronization pulse in the TV transmission) has been used; the measurements are performed when test patterns are radiated, once a day, from a central location (the television channel monitored is the state broadcasting television network), in order to minimize uncertainties and possible errors due to microwave links switching over different routes when local programs are transmitted. Moreover the test pattern provides a more stable and high quality signal.

The TV receiver (fig. 7) is a special, in-house built, receiver, designed to improve the separation of the signal of interest, that is performed digitally.

A programmer subsystem with an internal clock is provided; this controls the power switching of external equipment (HP 9815 calculator and HP 5345 counter), with the proper timing [to load and start the program (the 981.5 is in the autorun mode), to program the counter, to generate the proper signals to the counter, to record the data on the tape, to update the file name and other variables] to execute automatically, once

a day at the selected time, the TV synchronization procedure without any operator intervention in both the stations.

SEQUENTIAL MODE TIME TRANSFER

The time transfer in the sequential mode of operation is depicted in fig. 8.

The basic synchronization frame is 1 second; that means that it is possible to obtain one value of ϵ from the measured data over a 1 s interval.

The approach chosen is a fixed synchronization scheme, in which the two stations transmit at fixed times according their own time scale. The main advantages of this approach are:

- 1) the basic synchronization frame can be lengthened by simply rearranging the data, as we will show later;
- 2) the initial synchronization error (time difference ϵ between the clocks) can be as large as 100 ms without affecting the timing of the time transfer.

Since all the times shown are within a 1 s time interval, starting at the time T_0 , all the time measurements are unambiguously referenced to T_0 ; the time tag measurement resolves the second ambiguity.

The time transfer (fig. 8) is started by the transmission of the time signal at 0 seconds (T_0) by the station A. This signal is not expected, obviously, to be received in both stations within the next 0.2 s.

The first 100 ms are then devoted in both stations to time tag the measurement.

A start pulse is generated at 0.5 μ s (this 500 ns delay allows the setting of the internal clock counters after the count transition) and a stop pulse is generated after a time tag interval (TT), whose duration in μ s is equal to the clock reading at T_0 (minutes and seconds).

In this way, the first measurement obtained by the counter is the time tag of the measurement.

At 100 ms (from T_0) another start pulse is generated and now the counter in both stations will be stopped by the leading edge of the first received pulse.

This gives the coarse measurement of the time of arrival of the pulses relayed back by the satellite (T_4 and T_1). For example, at the station A the measured time interval will be ($T_4 - T_0 - 0.1$ s).

After the first pulse is received, nine start pulses are generated synchronously with the local clock and with the same repetition rate of the transmitted pulses. The corresponding nine stop pulses are provided by the remaining pulses of the received signal (fig. 4).

Since the doppler shift over these pulses can be neglected (see sect. 4) these nine measured intervals provide nine additional values to determine the time of arrival T_4 (or T_1) [modulo the repetition rate of the pulses, but any ambiguity is removed by the first measurement].

This allows $T_4(T_1)$ to be computed as the mean of the measured values and to obtain an estimate (based on the standard deviation of the measurements) of the precision related to the determination of the time $T_4(T_1)$ in each station separately and for each measured value.

At 0.5 s (according its local clock) the same time signal is transmitted by the station B; a start signal is generated in both sites at the time 0.6 s and the same procedure outlined before is repeated to recover the times T_3 and T_5 .

A total of 21 measured values is recorded at each station for every synchronization measurement in the sequential mode of operation.

RF carrier switching

A timing diagram of the RF carrier switching and the gating of the received signals Rx is shown in fig. 9.

The basic requirements that are satisfied by such an arrangement are:

- a) the carriers from A and B do not enter the satellite at the same time and a suitable time window is provided to

avoid any interference (since the propagation delay is not the same for the two sites and the timing is, in principle, based on clocks that are to be synchronized;

- b) a suitable time interval is allowed to stabilize the RF carrier before transmitting the time signals;
- c) the gating of the received signal is implemented in such a way that the Rx signal (that provides some stop signals to the counter, as shown in fig. 8) is enabled only after the RF carrier is received and stabilized.

The RF carrier switching is implemented at the first IF level (70 MHz); this simply shifts 70 MHz apart the RF carrier at 17 GHz, outside the bandwidth of the RF power amplifier.

Some considerations on the sequential time transfer

The fixed synchronization scheme as implemented is very useful to provide a variable length synchronization frame.

Suppose to implement the time synchronization over the basic frame (fig. 8) repeated every second (the TTU provides a selection of different repetition rates for the basic synchronization frame).

This provides a synchronization result $\xi(\tau = 1 \text{ s})$ every second, showing the relative behaviour of the two clocks. At this level the correction due to the satellite motion is negligible ($(t_2 - t_1) \cong 0.5 \text{ s}$) and we are perfectly aware of this (this is not an assumption) because we are able to evaluate the correction with the range-rate estimates (eq. 11); the correction, in this typical case, is in the order of 1 ns.

Now, let us consider the same basic sequence, but expanded over a 10 s interval; this can be obtained easily by simply taking the measured times of arrival T_4 and T_1 from the synchronization frame at T_0 and the times T_3 and T_5 from the synchronization frame at $T_0 + 10 \text{ s}$.

Now the time interval $(t_2 - t_1)$ is about 10.5 s and the correction is about 10 times greater (eq. 11). In this way we have another set of values $\xi(\tau = 10 \text{ s})$. We can compute these values without applying any correction. The difference between each $\xi(\tau = 10 \text{ s})$ and $\xi(\tau = 1 \text{ s})$ shows exactly the ef-

fect due to the satellite motion and, moreover, we are able to compute this correction and compare our estimate (based on a first order approximation of the satellite motion) with the measured values.

This procedure can be repeated for every τ of interest by using the same data. A reference set of values is always provided by the $\mathcal{E}(\tau=1 \text{ s})$ set.

SIMULTANEOUS MODE OF OPERATION

In addition to the sequential time transfer, a simultaneous mode of operation time synchronization has been planned. Using this well-known technique, the time signals emitted by the two ground stations are relayed by the satellite at the same time, thus avoiding any error on \mathcal{E} due to the satellite motion (see fig. 10).

The basic synchronization equation becomes now:

$$(16) \quad \mathcal{E} = \frac{(T_1 - T_0) - (T_3 - T_2)}{2} + \text{corrections}$$

where the corrections are due only to equipment delays, propagation delays and to the relativistic correction (app. A); as was shown, the corrections due to the propagation effects in the atmosphere can be considered negligible.

Two separate RF communication channels are obtained by splitting the available 40 MHz RF bandwidth in two 15 MHz bandwidth channels, at the expense of a reduced signal to noise ratio, while maintaining the same video bandwidth (6 MHz) as in the sequential mode of operation.

The two RF carriers are obtained with a change of the local oscillator frequency at the 2nd IF (transmission) and 1st IF (reception), so that the available 70 MHz modulators-demodulators are still used.

Since now two separate channels are used, the differential delay in the satellite transponder must be taken in account as a corrective term, given by eq. 5.

This delay has been measured by Telespazio (ref. 2) and re-

sulted to be about 0.5 ns/MHz. At a carrier separation of about 20 MHz, the value of the correction to the synchronization result ϵ is about 5 ns.

Procedure to obtain the simultaneous transmission from the satellite

A simple mean to adjust the transmission time in order to obtain the desired simultaneity of transmission of the time signals from the satellite is provided by adding an additional receiver (demodulator + IF) at one site (see fig. 5). This additional equipment receives back the signal transmitted by the same station, to allow a comparison to be made with the signal transmitted by the other site.

In this way the simultaneity is checked by observing the local pulses as received back from the satellite along an oscilloscope, the pulses coming from the other station. The transmitted signal is then shifted until nearly coincident (within a few ms) times of reception are achieved (fig. 11).

Even if the simultaneity error α (fig. 11) can be reduced in this way to less than 1 ms, usually a much larger error can be tolerated.

In fact, it can be easily shown by using the same equations as in sect. due to sequential mode of operation (where now $t_2 - t_1 = \alpha$) that the error $\delta\epsilon$ on ϵ due to α is approximately given by:

$$(17) \quad \delta\epsilon \approx \frac{\dot{r}_A + \dot{r}_B}{2c} \alpha$$

so that α can be as large as 100 ms without introducing a noticeable error on ϵ .

Simultaneous mode time transfer

The simultaneous time transfer is again obtained by using the same equipment described, and again a fixed synchronization sequence is easily generated by the TTU (refer to fig. 12) over a basic synchronization frame of 1 second.

The first 100 ms are devoted to time tag the measurement, so that any ambiguity is removed for later data processing; this

is the only constraint. The first 100 ms are not used in this case for time transfer; however this can be implemented freely in the following 900 ms.

In fact, in this case, the transmission times in both sites are not fixed and, moreover, can be changed during the operations to compensate for the satellite motion: so, the time of transmission T_0 (T_2) must be recorded and this is accomplished by generating a start pulse at 0.1 s and a stop pulse when the time signal is transmitted (T_0 or T_2); in this way the second time interval measurement recorded for each frame gives the transmission time.

After 10 ms (at the time T_0 (T_2) + 10 ms) a new pulse is generated; since T_0 is recorded, also the time of this pulse is known.

The leading edge of the first received pulse stops the counter at the time T_3 (T_1); this gives the coarse measurement of the time of reception of the pulses. Following the same procedure described above, nine start pulses are generated to provide additional nine values for the time of reception (modulo the repetition period of the pulses in the time signal).

A total of 12 measured values is recorded at each station for every synchronization measurement (1 s frame) in this mode of operation. The TTU provides as usual different repetition rates for the basic synchronization sequence.

CONCLUSIONS

The SIRIO-1 experiment was designed and implemented to measure and analyze the effect of the satellite motion on the accuracy of the two-way time synchronization and to demonstrate the feasibility of accurate time transfer using only one communication channel, time-multiplexed between the two stations.

The main features of the experiment are briefly summarized here:

- 1) the experiment tests and compares different techniques to implement the two-way time synchronization, and
- 2) precisely monitors the satellite motion;

- 3) a new technique has been proposed to correct for the satellite motion effect, while performing the time synchronization;
- 4) the experiment features a fixed synchronization scheme, allowing the flexibility of a variable length synchronization frame;
- 5) the synchronization in the sequential mode of operation is obtained by a time multiplexing technique, with automatic, fast RF carrier switching;
- 6) no effects affecting the accuracy at the 1 ns level are due to the space segment (from one ground antenna to the other) in the sequential mode;
- 7) the technique can be easily extended to a multiple site synchronization; inherent advantages of the methods tested are:
- 8) the low cost and almost automatic operation; moreover the time signals used
- 9) allow the independent determination of the uncertainties of the time-of-arrival measurements at the two stations, to separate the contribution of each station to the total precision.

This last feature can be important to understand the contribution of local phenomena (ground equipment, atmospheric condition affecting the signal attenuation, especially rain at SHF, etc.) to the synchronization precision.

Especially the sequential time transfer technique can be proposed as a useful tool to synchronize ground telecommunications stations; in addition to the time synchronization, it can provide also measurements related to the satellite orbital status (range and range-rate) with interferometric capabilities (since two stations are involved at the same time and the clocks offset is measured with high precision), that can be used to track the satellite or update the orbit elements with different techniques (i.e., differential correction of the existing parameters).

A complete analysis of the initial measurements is under way and the results will be available at a later time. The first

results show a precision between 5 and 10 ns (1σ) for rough (non filtered) data.

The accuracy is expected to be only dependent from the accuracy in the measurement of the ground equipment delays (see app. B).

ACKNOWLEDGEMENTS

The authors would like to thank the Telespazio personnel at the two ground stations, and particularly Mr. Marellò, Mr. Guerra and Mr. Saggese, for their generous assistance.

We wish also to acknowledge the work of the IEN personnel in performing the experiment; we are especially grateful to V. Pettiti, P.G. Galliano, E. Angelotti, F. Cordara, G. Moro, L. Canarelli, L. Pietrelli and V. Marchisio that actually carried on the measurements at the two sites, to G. Rietto for the software support, to E. Bava, A. De Marchi and A. Godone for the RF work, to Mr. G. Galloppa for the drawings and to Mrs. M. Castello for the typewriting.

This work was made possible by a grant from the Italian National Research Council.

REFERENCES

1. A.R. Chi, S. Cooper - Satellite time transfer and its applications - URSI, Measurement in telecommunications (Lanion, France - Oct. 1977) pp. 258-263.
2. L.A. Ciavoli Cortelli, B. Giannone, E. Saggese - Misure di verifica del funzionamento in orbita dell'esperimento SIRIO-SHF - Campagna prove 26+29-9-1977 - Telespazio, Servizio Sviluppo Telecomunicazioni, allegato 2, pp. 3-4.

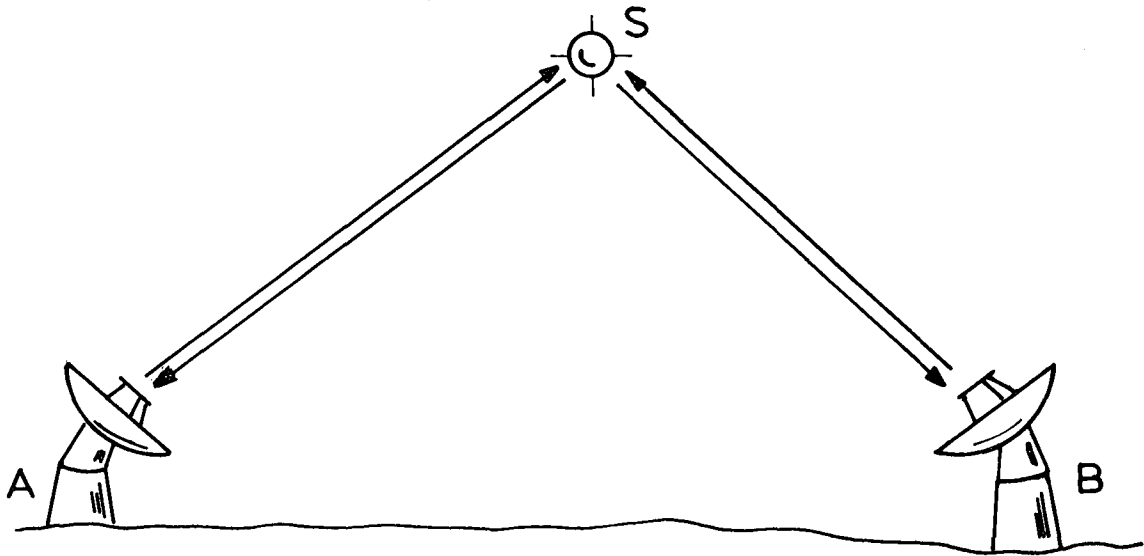


Figure 1a. Two-Way Time Synchronization Via Satellite

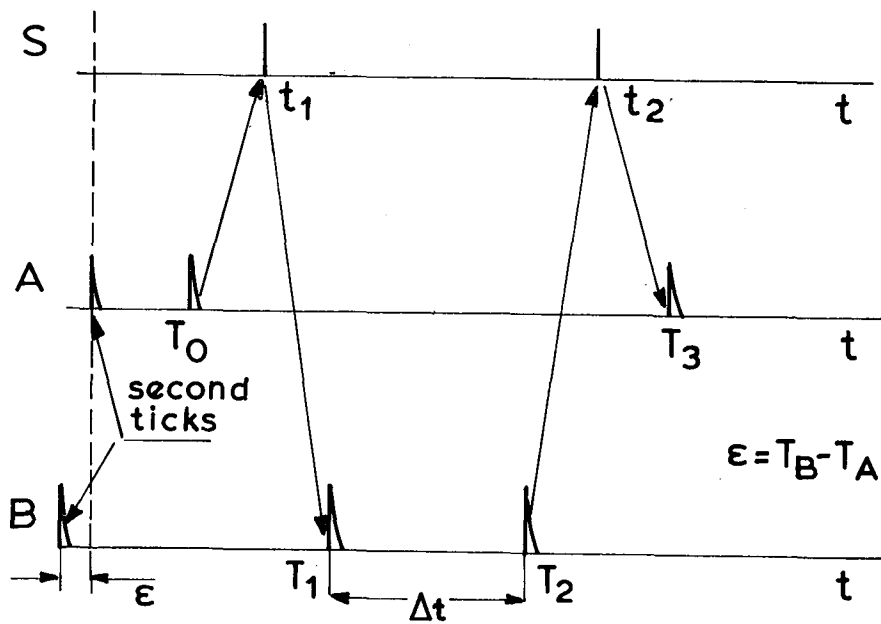


Figure 1b. Timing Diagram

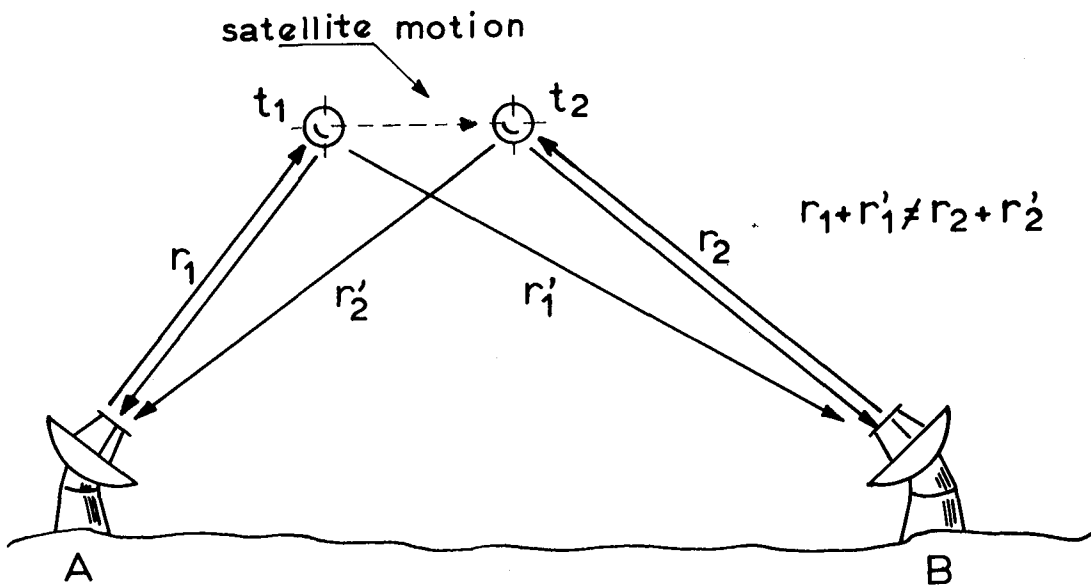


Figure 2a. Two-Way Time Synchronization - Sequential Mode

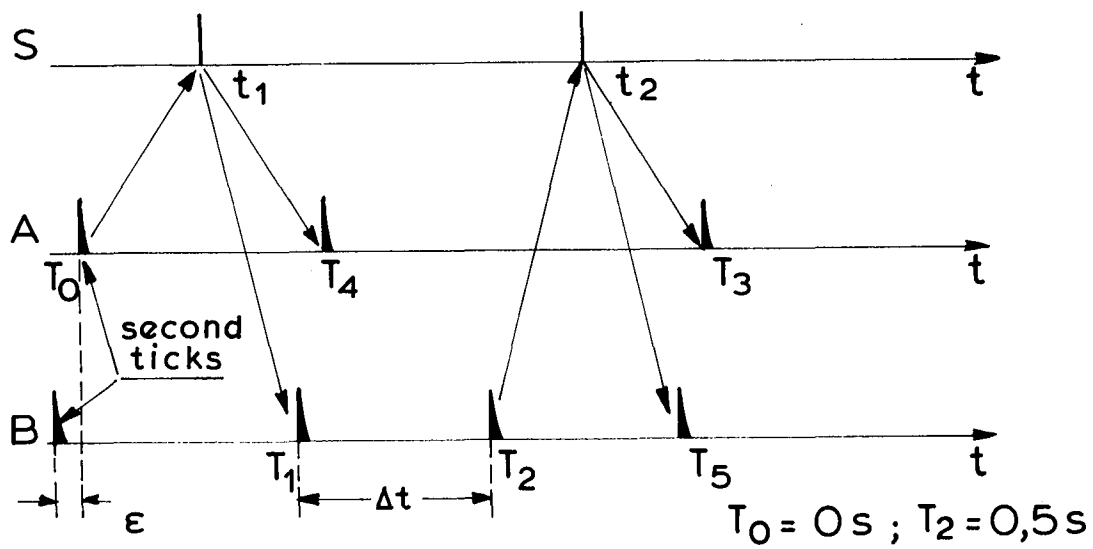


Figure 2b. Sequential Mode - Timing Diagram

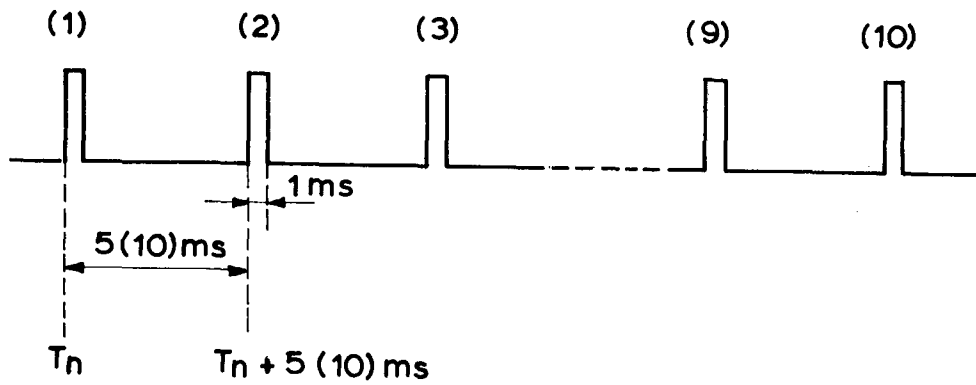


Figure 3. Timing Signal

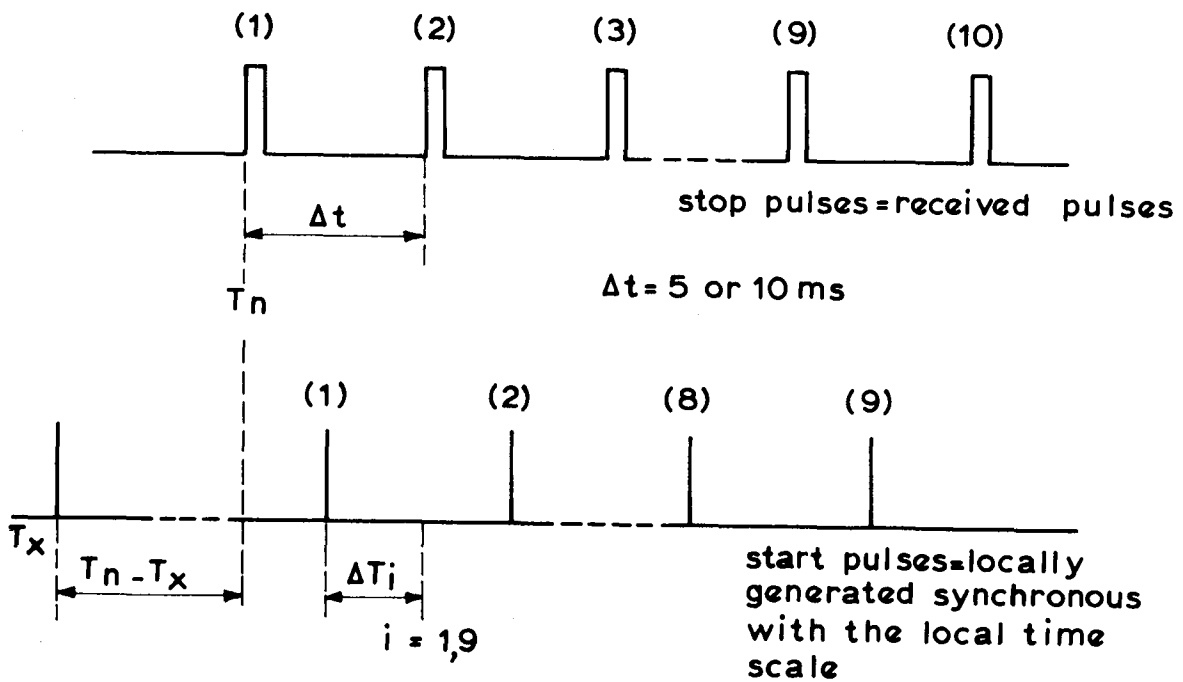


Figure 4. Time of Reception Measurements

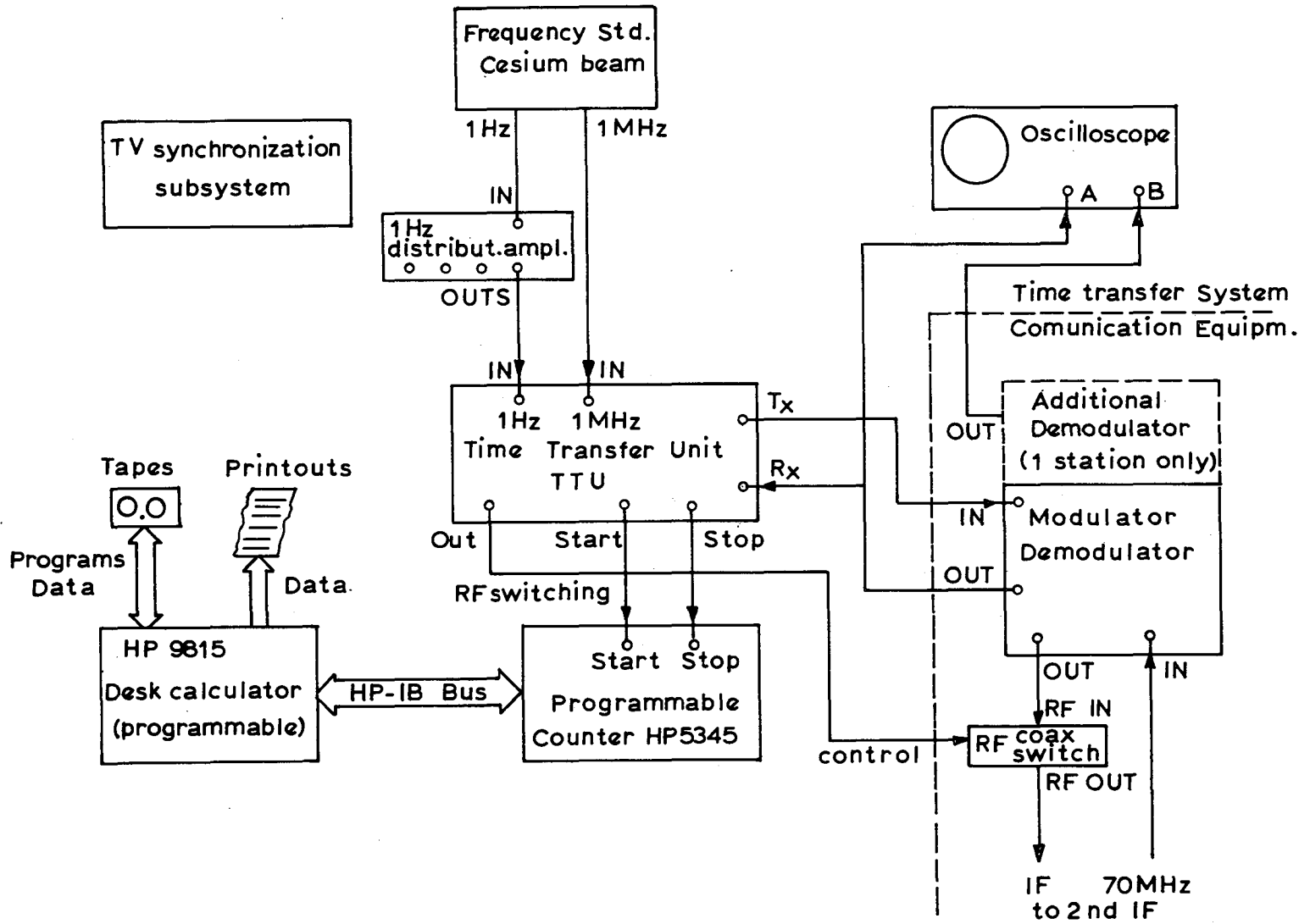


Figure 5. Experimental Set-Up

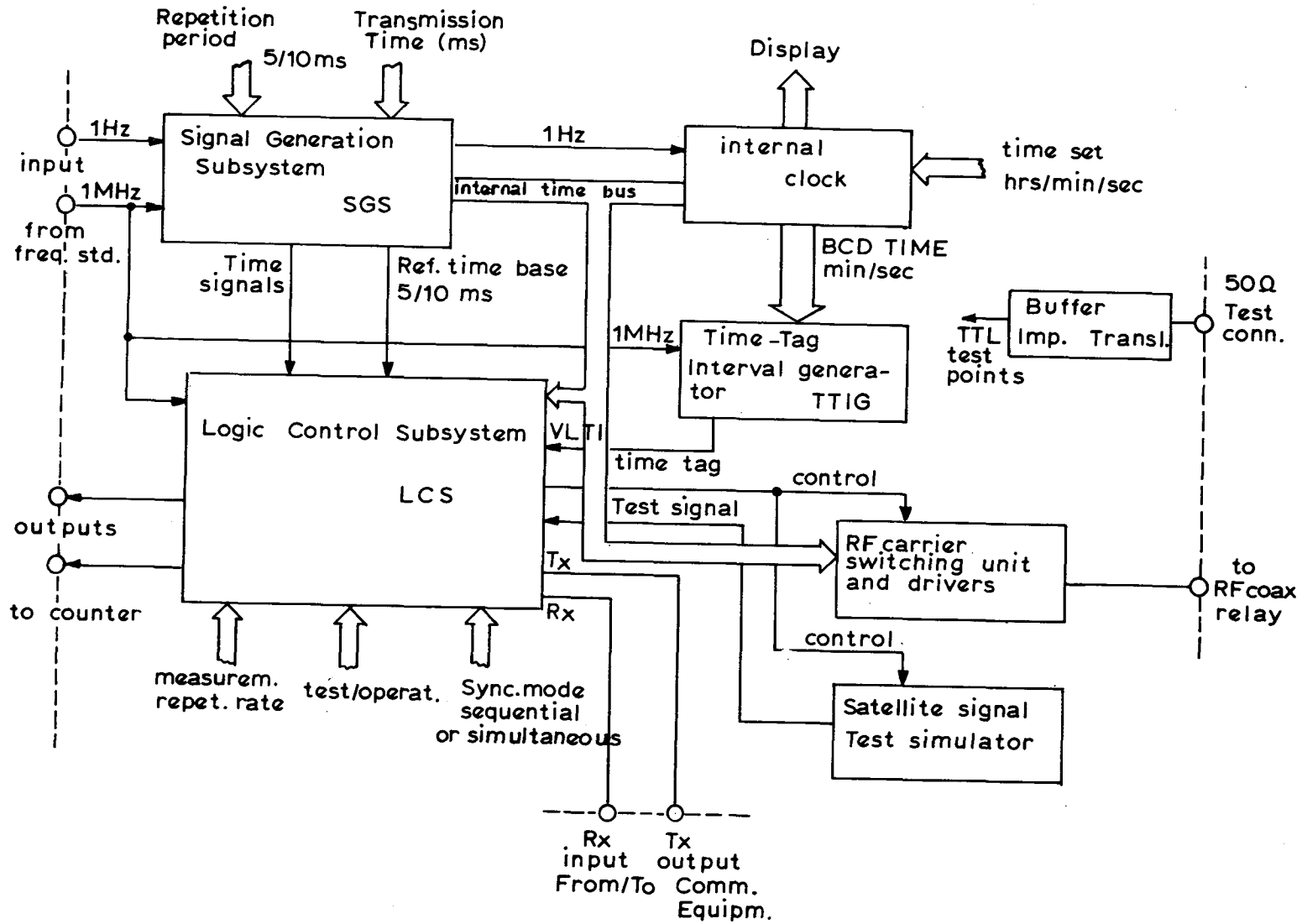


Figure 6. Time Transfer Unit-Block Diagram

545

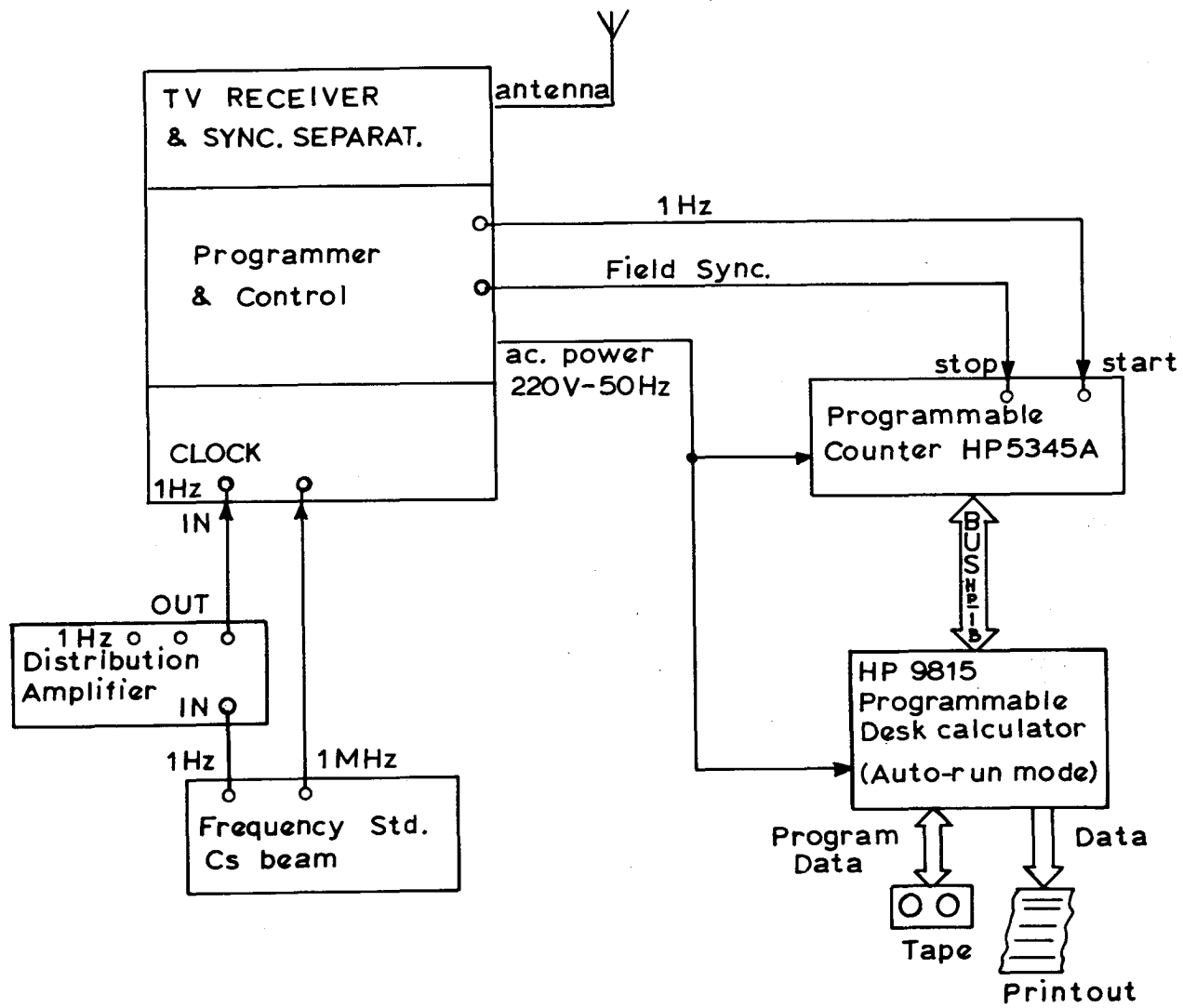


Figure 7. TV Synchronization Automatic Subsystem

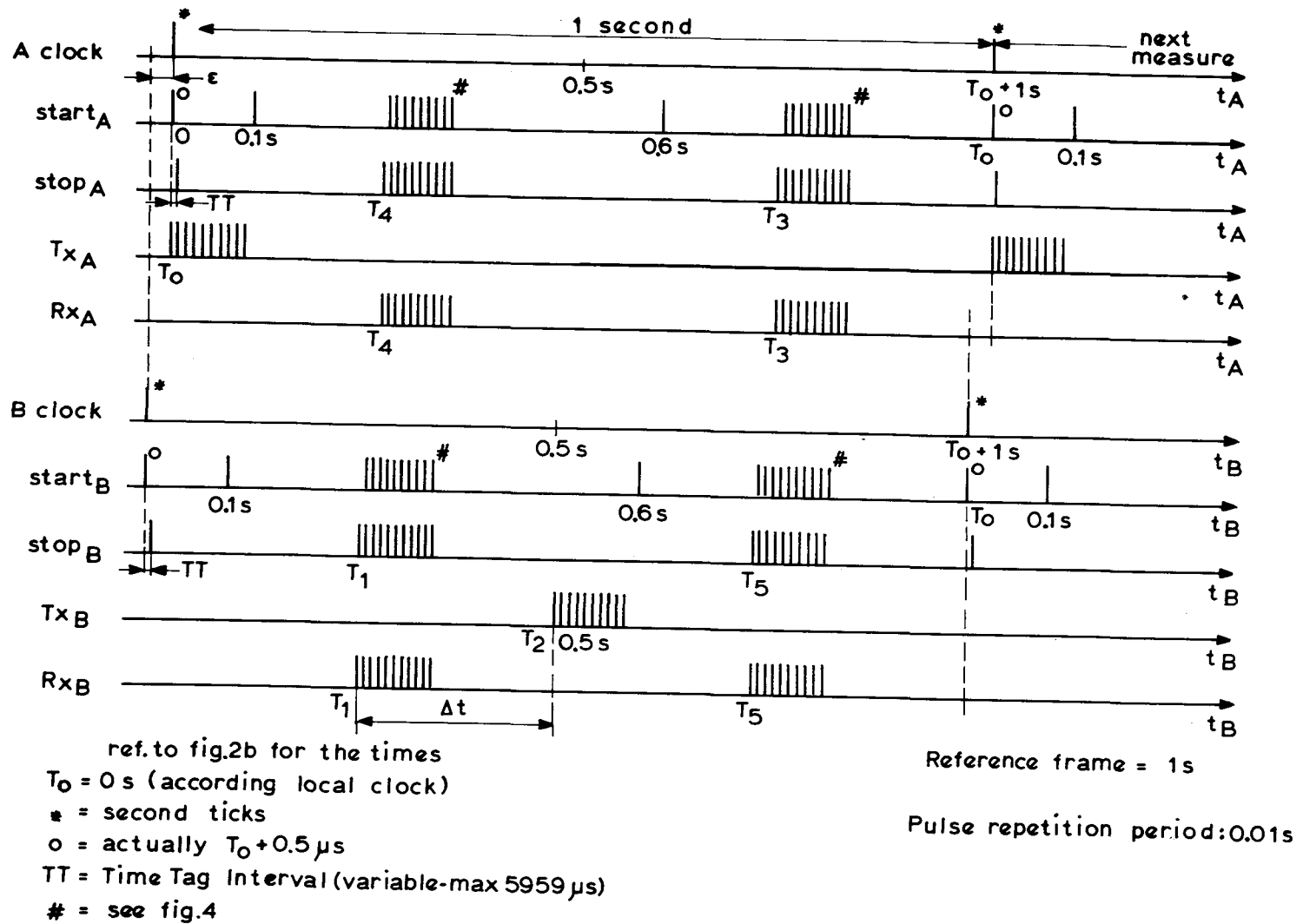


Figure 8. Sequential Mode Synchronization Frame

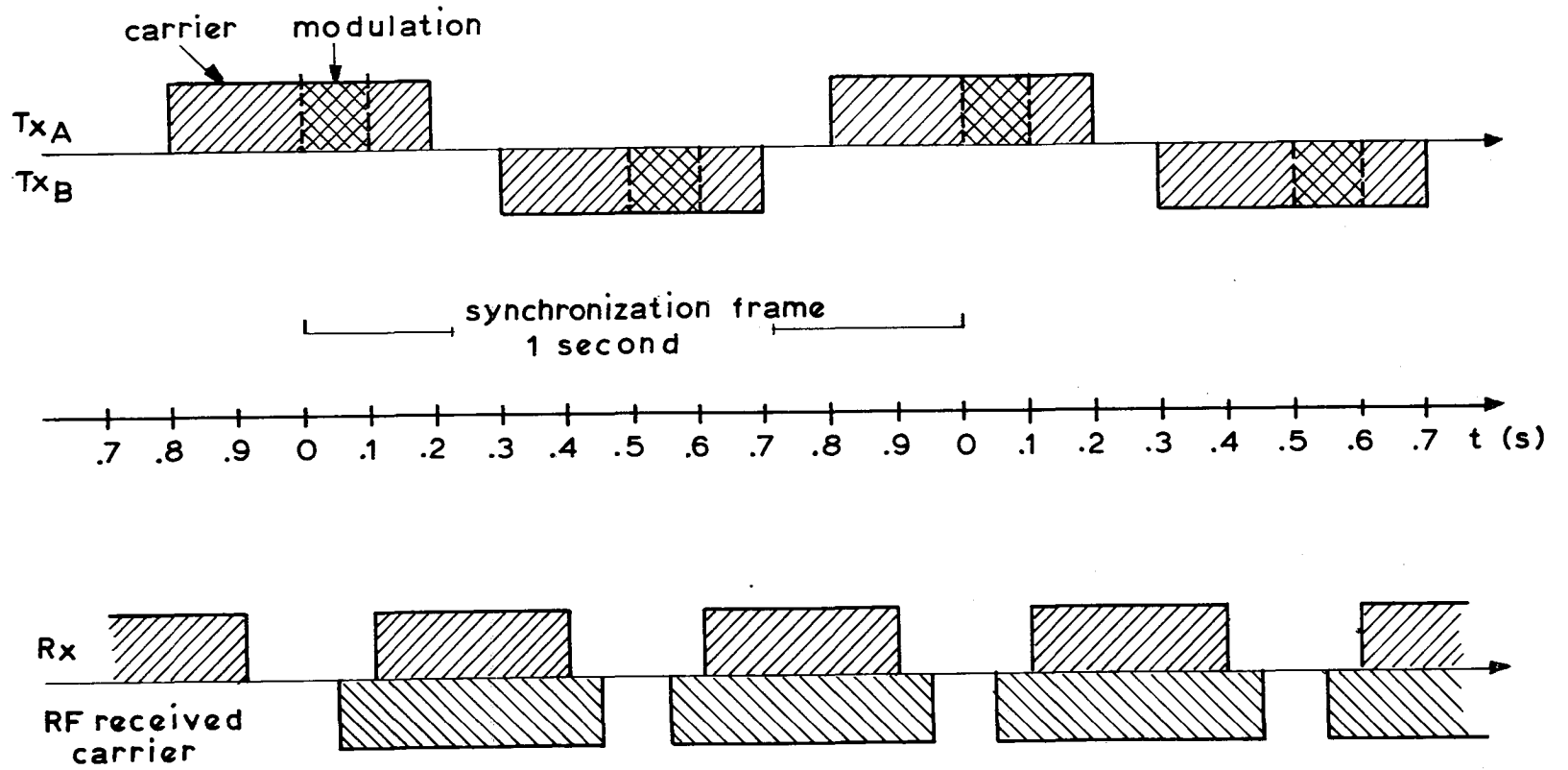


Figure 9. RF Carrier Switching

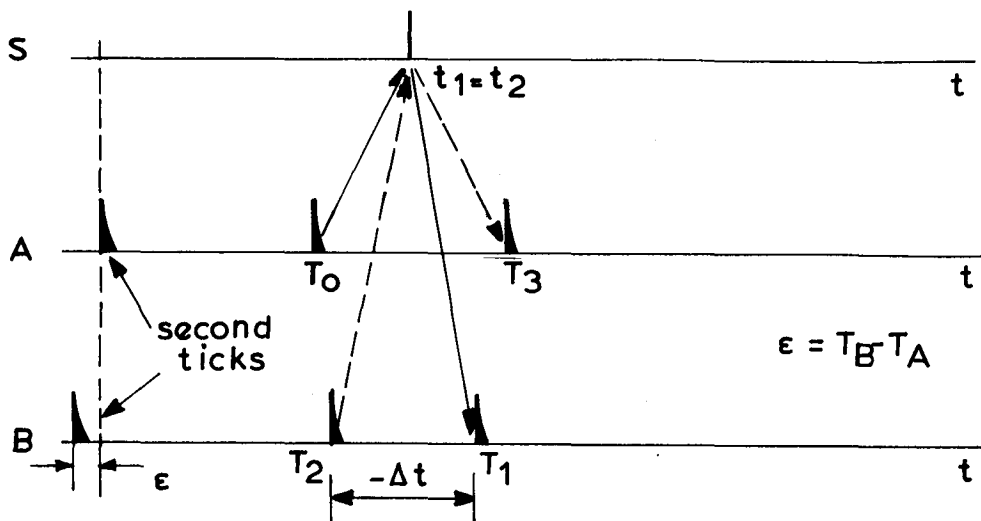
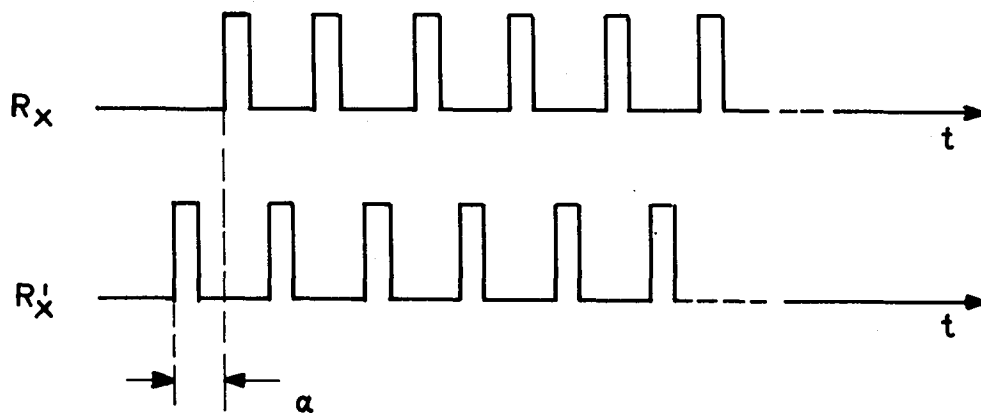


Figure 10. Simultaneous Time Transfer - Timing Diagram



R_X = signal received from the other station

R'_X = signal transmitted and received back (own signal)

α = simultaneity error = $|(t_2 - t_1)|$

Figure 11. Simultaneity Check

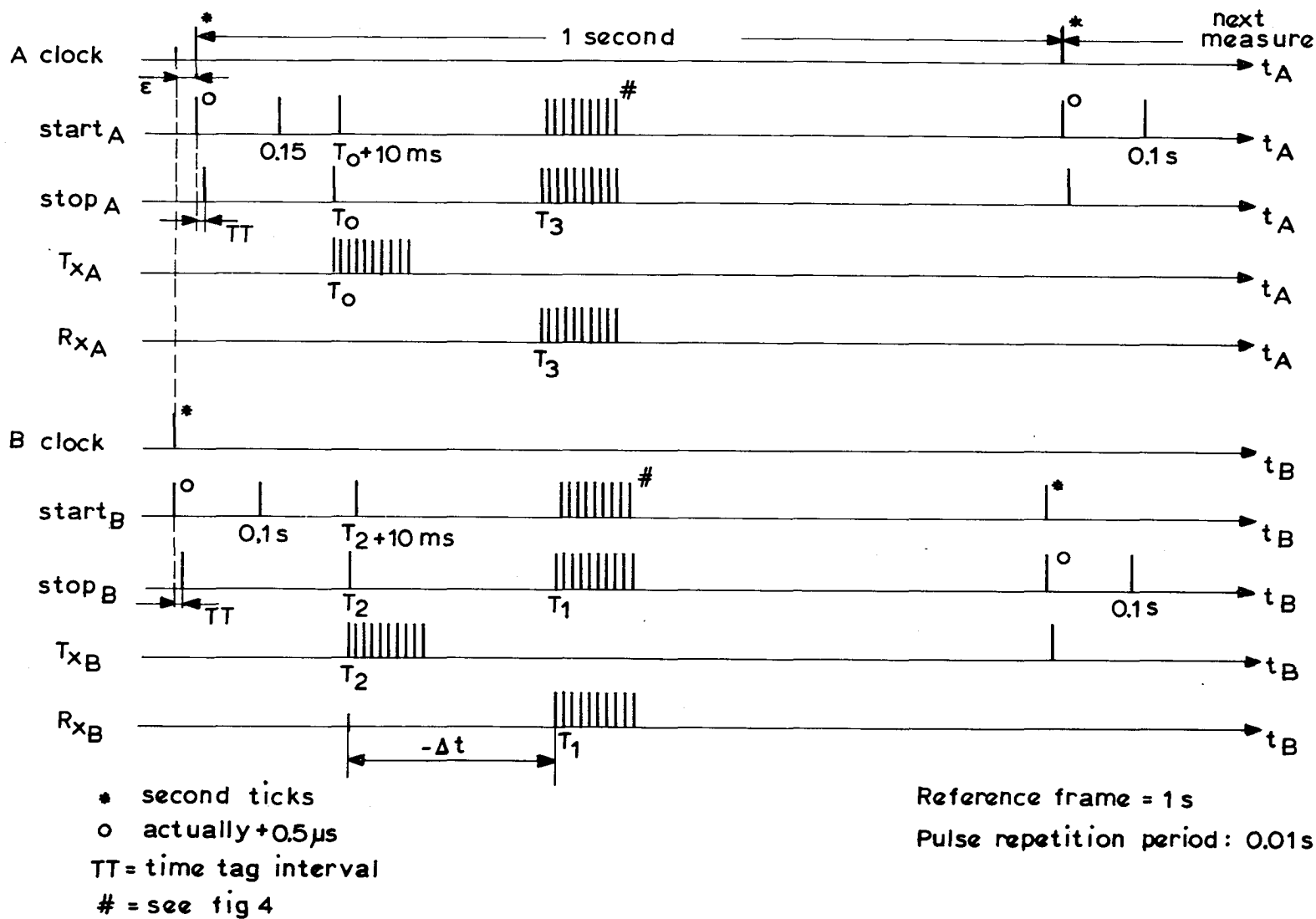
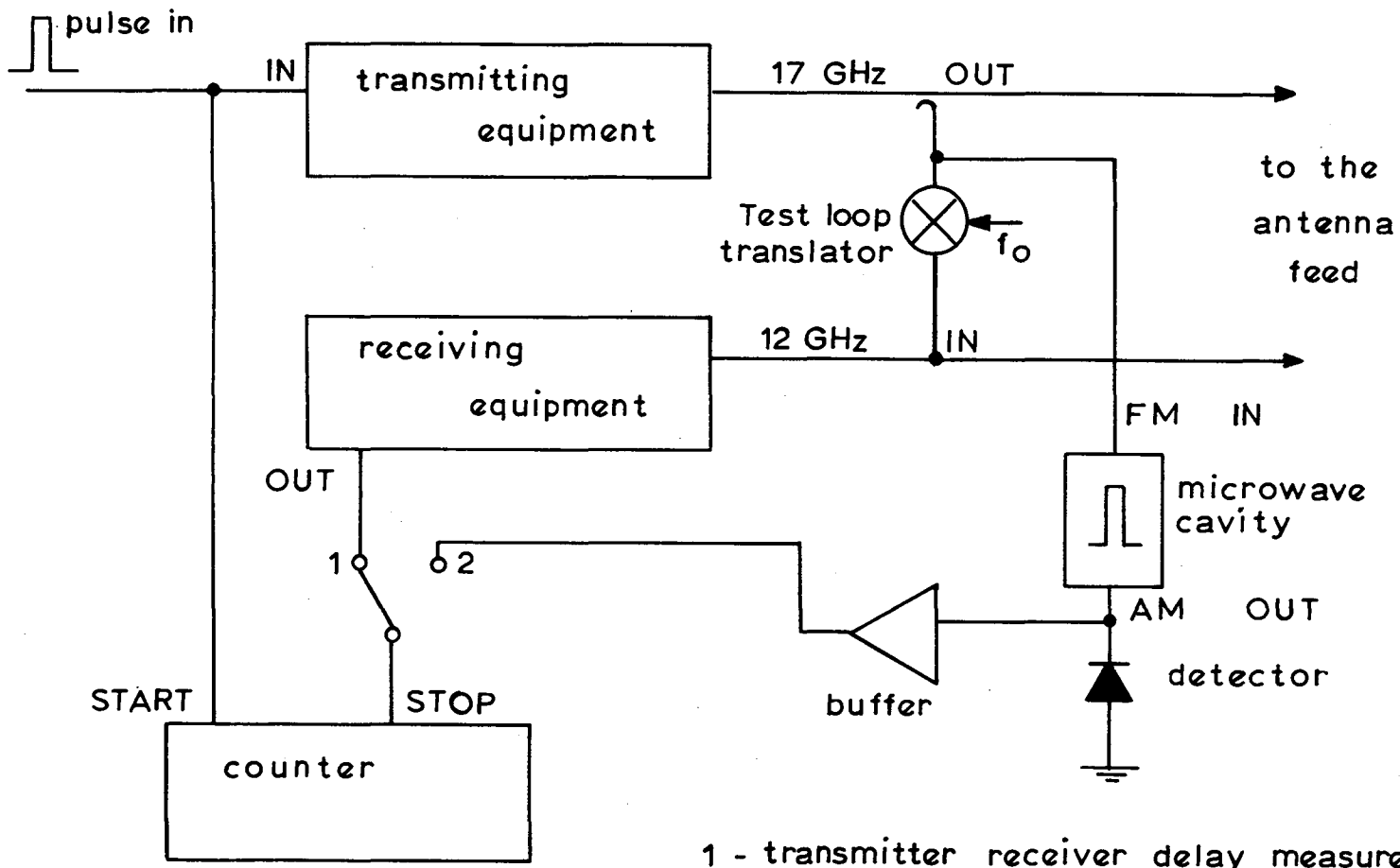


Figure 12. Simultaneous Mode Synchronization Frame



- 1 - transmitter receiver delay measurement
- 2 - transmitter delay only

Figure 14. Ground Equipment Delay Measurement

APPENDIX A

RELATIVISTIC CORRECTION DUE TO THE EARTH ROTATION (SAGNAC EFFECT)

This effect, due to the Earth rotation, introduces, if not properly taken in account, an error in the determination of the offset between the clocks using the two-way technique. The sign of the correction to be applied to compensate for this effect depends obviously by the relative longitude of the two stations. The magnitude of the correction can be easily derived (see ref. A1 and A2).

The metric in a flat Minkowsky space is given by:

$$(A.1) \quad ds^2 = dx^2 + dy^2 + dz^2 - c^2 dt^2$$

In a polar coordinate reference system we have:

$$(A.2) \quad \begin{cases} x = r \cos \lambda \cos \varphi \\ y = r \sin \lambda \cos \varphi \\ z = r \sin \varphi \end{cases}$$

Applying a uniform rotation with angular velocity ω (in the direction of the z-axis) we have:

$$(A.3) \quad \begin{cases} x' = x \cos \omega t - y \sin \omega t \\ y' = x \sin \omega t + y \cos \omega t \\ z' = z \end{cases}$$

By combining eq. (A.2) and (A.3), taking the differentials and squaring, after a few manipulations it's easy to obtain:

$$(A.4) \quad ds^2 = (\omega^2 r^2 \cos^2 \varphi - c^2) dt^2 + (2r^2 \cos^2 \varphi \omega d\lambda) dt + (dr^2 + r^2 d\varphi^2 + r^2 \cos^2 \varphi d\lambda^2)$$

The propagation of the electromagnetic signals at the speed of light c is obviously characterized by $ds^2 = 0$; so the eq. (A.4) is actually a simple second-order linear equation in dt , and again it's easy to obtain immediately:

$$(A.5) \quad dt = \frac{-(r^2 \cos^2 \varphi \omega d\lambda) \pm \sqrt{(r^2 \cos^2 \varphi \omega d\lambda)^2 - (\omega^2 r^2 \cos^2 \varphi - c^2)(dr^2 + r^2 d\varphi^2 + r^2 \cos^2 \varphi d\lambda^2)}}{(\omega^2 r^2 \cos^2 \varphi - c^2)}$$

By integration over the propagation path P (that is actually a round-trip path) we obtain:

$$(A.6) \quad \Delta t = \int_p dt = -2\omega \int_p \frac{r^2 \cos^2 \varphi}{2r^2 \cos^2 \varphi - c^2} d\lambda$$

that is the time difference in the propagation delays from one station to the other (via the satellite) and back, assuming a uniform speed ω of the Earth rotation.

The error $\Delta \epsilon_r$ in the determination of ϵ is actually half the magnitude of Δt , so we have a correction:

$$(A.7) \quad \Delta \epsilon_r = -\omega \int_p \frac{r^2 \cos^2 \varphi}{2r^2 \cos^2 \varphi - c^2} d\lambda \approx \frac{\omega}{c^2} \int_p r^2 \cos^2 \varphi d\lambda$$

where the term $\omega^2 r^2 \cos^2 \varphi$ can be neglected, since it is quite small as compared to c^2 .

A simple geometric representation (fig. 13) can be given for eq. (A.7) (according ref. A1). By assuming the term $r^2 \cos^2 \varphi = r'^2$ as the projection of the vector radius r on the equatorial plane, we have:

$$(A.8) \quad \Delta \epsilon_r = \frac{\omega}{c^2} \int_p r' d\lambda$$

The integral in eq. (A.8) is actually twice the area A generated by the vector radius r' (lying on the equatorial plane), so we can write:

$$(A.9) \quad \Delta \epsilon_r = \frac{2\omega A}{c^2}$$

According the geometry relative to the SIRIO experiment the $\Delta \epsilon_r$ correction was evaluated to be about 15 ns. This is not to be considered a constant, but a slowly varying term (period 24 hr) around 15 ns because of the satellite motion relative to an Earth fixed reference frame.

REFERENCES

- A.1. Y. Saburi - Observed time discontinuity of clock synchronization in rotating frame of the Earth - Journ. of RRL, vol. 223, N. 112, pp. 255-265 (November 1976).
- A.2. E. Detoma - Valutazione della correzione relativistica nell'esperienza di sincronizzazione via satellite SIRIO - Rapporto Tecnico IEN, SRT-678 (September 1978).

APPENDIX B

GROUND EQUIPMENT DIFFERENTIAL DELAY MEASUREMENT

The measurement of the delays of the ground communication equipment is performed at each station as shown in Fig. 14. A test loop translator is available at each ground station; this allows the measurement of the sum of the delays in the transmitting and in the receiving equipment at the same site.

However, in the time transfer the difference of these delays must be considered (eq. 4): a simple method to measure the transmitting equipment delay alone has been devised.

Since the RF carrier is frequency modulated, a microwave cavity is used as a frequency discriminator coupled to the feed of the antenna. The AM resulting signal (if a pulse is applied at the input of the modulator, the output signal is actually an on-off RF signal) is detected by a fast rectifier, which provides via an amplifier the stop pulse to the counter.

Two basic requirements must be satisfied by the microwave cavity: it must be able to detect the shift of the RF carrier as a result of the input pulse (this means that a high Q is required), while it must introduce the smallest delay as possible (low Q); a suitable Q value for our purpose is between 1000 and 2000.

In this way, measuring the delay in the transmitter alone and the sum of the transmitter and receiver delays, the eq. 4 can be easily solved.

DEMONSTRATION OF REMOTE CLOCK MONITORING BY VLBI,
WITH THREE BASELINE CLOSURE*

C. M. Cheetham, W. J. Hurd, and J. W. Layland**
Communications Systems Research Section
Jet Propulsion Laboratory, California Institute of Technology,
Pasadena, California

G. A. Madrid and T. P. Yunck
Navigation Systems Section
Jet Propulsion Laboratory, California Institute of Technology,
Pasadena, California

ABSTRACT

The capability of very long baseline interferometry (VLBI) to monitor the stability of remotely-located hydrogen maser frequency standards has been demonstrated by a series of experiments conducted from September 1978, through January 1979, between Deep Space Stations in Australia, Spain, and California. The measured stabilities of the clock systems, over approximately 10-day intervals, were 1 to 3 parts in 10^{13} , with the instabilities due to the oscillators, the clock distribution systems, the receiving system delays, and the VLBI measurement error.

Experiments were conducted independently using two different systems (BLOCK 0 and WBDAS). Later comparison shows agreement on the order of 1 part in 10^{13} . Closure was demonstrated on three separate occasions to 33, 10, and 13 ns with an error uncertainty of ± 42 ns. The results represent an important consistency check on VLBI measurements.

* This paper presents the results of one phase of research carried out at the Jet Propulsion Laboratory, California Institute of Technology, under Contract No. NAS 7-100, sponsored by the National Aeronautics and Space Administration.

** Now with TDA Planning Office.

I. INTRODUCTION

In order to improve the quality of radiometric observables at outer planet distances, the monitoring of time offsets and frequency standards at Deep Space Network (DSN) tracking stations has become a necessity. Very long baseline interferometry (VLBI) presents the most promising technique available to monitor clock epoch and rate offsets to the level required for advanced deep space missions.

A preliminary demonstration of clock synchronization via interferometry was performed using the DSN in 1967 by Goldstein (Ref. 1) over a short baseline. Early applications (circa 1972) of independent station interferometry to astrometry and geodesy (e.g. Cohen and Schaffer, Ref. 2, Hinteregger et. al., Ref. 3 and Wade, Ref. 4) have demonstrated the feasibility of VLBI and provided source position information. Also in 1972, Hurd (Refs 5, 6) and Thomas (Ref. 7) performed VLBI experiments on a short baseline using the DSN. In more recent work (circa 1977) by Counselman et. al. (Ref. 8), Clark et. al. (Ref. 9) and Hurd (Ref. 10), VLBI has been used to measure relative and absolute clock offsets. Clark and his associates (Ref. 9) demonstrated clock synchronization using a traveling clock to the 10-20 nsec level of accuracy on a relatively long 845 km. baseline. The works of Hurd (Refs 10, 11) and Thomas (Refs 12-14) form the basis for the experiments reported here. This work is based on relative clock offset measurements obtained over intercontinental baselines of 8 to 10 thousand km. The goals of the development work, of which these experiments are a part, are to develop an intercontinental VLBI capability which will measure relative clock offsets to 10 nsec and relative frequency offsets to one part in 10^{13} with a few minutes of observing time and to one part in 10^{14} over periods of approximately one week by differencing clock offset estimates.

This article reports the results of a series of clock synchronization experiments that were conducted from September 1978 through January 1979, between Deep Space Stations (DSS) in Australia, Spain, and California. During this entire time, the cesium clock at DSS 63 in Spain and the hydrogen maser clock at DSS 43 in Australia drifted only a few microseconds with respect to the DSS 14 hydrogen maser clock at Goldstone, California. The measured stabilities of the clock systems were 1 to 3 parts in 10^{13} , with the instabilities due to the oscillators, the clock distribution systems, the receiving system delays, and the VLBI measurement error.

On three separate occasions, measurements were made between the Spain and Australia stations — the first VLBI measurements ever made on this extremely long baseline. Unfortunately, these experiments could not be conducted concurrently with measurements on the other baselines. However, the data were compared to clock offsets on the other two

baselines, interpolated or extrapolated to the time of the Spain-Australia measurements. These experiments demonstrated closure to 33, 10, and 13 ns, with an error budget of ± 42 ns. This is an important check on the consistency of VLBI measurements, considering that they were performed at intercontinental distances under varying ionospheric conditions.

Two different VLBI systems were utilized in parallel in the reported experiments, thus providing both redundancy and a comparison of the two systems. The main distinction between the two systems lies in the manner in which the digitized received energy signals are recorded and correlated. One application records the digitized signal across the entire received bandwidth at distinct intervals of time, the other records selected channels across the bandwidth in a continuous stream of data from which the group delay across the passband is then reconstructed. The first mode has accordingly been termed the "Wide Band Data Acquisition System" (WBDAS) (Refs. 10 and 11) while the second is termed the "Bandwidth Synthesis" System (BWS). The BWS concept, originally developed by Rogers (Ref. 15), has been incorporated in the JPL system in modified form (Ref. 14). The WBDAS approach was developed for its ability to record and process VLBI data in near real-time for the purposes of obtaining quickly accessible clock epoch and frequency offsets. The BWS technique, on the other hand, with a more elaborate modeling and parameter estimation scheme was designed to provide astrometric and geodetic information in addition to more precise clock synchronization data. The intent of the latter is to use clock synchronization and improved timing and earth dynamics estimates in the support of increasing accuracy requirements for spacecraft navigation.

The specific BWS system used in these experiments is the Block 0 system, utilizing 4-Mbit/s digital recording on video tape recorders. This is an interim system leading to DSN implementation of a near-real-time Block I BWS System, and a wider bandwidth Block II System. At the time of these experiments, the DSN stations did not have phase calibrators (Ref. 16) and cable stabilizers that will be part of the Block I and Block II Systems, and that are required to do clock synchronization with the BWS technique. Thus clock synchronization with the Block 0 system could not use BWS, but used only the bit alignment of individual channels and therefore was similar in concept to the operation of the WBDAS.

II. Experiment Configuration

The two VLBI systems used in the experiments are briefly described in this section, and the configuration of the two VLBI data acquisition systems (Fig. 1) within the DSSs is discussed. It is argued that instabilities in the station 1-pps signal supplied to the VLBI systems,

and in generation of VLBI epoch references from the 1-pps inputs, are probably the dominant cause of discrepancies between results for the two systems.

A. Signal Path

The signal from the radio source passes through the antenna system and a traveling wave maser (TWM) amplifier, and is then translated from the RF center frequency to 55 MHz, using reference frequencies generated from the station frequency standard. Both VLBI systems receive 55 MHz IF signals, but there is one more stage of amplification and filtering for the WBDAS than for the Block 0 System. This restricts the passband to 55 ± 18 MHz, whereas the signal to the Block 0 System is bandwidth limited by the TWM or by a 55 ± 36 MHz filter. The difference in group delays between the two systems is consistent from experiment to experiment at a level considered to be insignificant. The total signal delay does vary significantly from experiment to experiment, however. Variations in tuning of the TWM amplifiers can cause group delay variations of ± 10 ns at each station, and the path length difference between the two TWMs at each station is as much as 52 ns, including waveguide lengths. Unfortunately, no accurate record of the TWM configurations was kept for all experiments, although each station was instructed to use the same TWM for each experiment whenever possible.

B. Block 0 System

Block 0 is a bandwidth synthesis VLBI system using 4-Mbit/s digital recording on video tape recorders and sampling sequentially up to eight BWS channels, each 1.8 MHz wide. The system is designed to measure fringe rates directly and group delay by either single channel bit stream alignment or bandwidth synthesis. Because, in BWS, unknown dispersive phase shifts can lead to large delay errors in the phase differences involved, the group delays produced by that method are not meaningful without the incorporation of phase calibrators to remove instrumental effects. Since operational phase calibrators were not available for these experiments, the group delays reported here were measured from the alignment offset of a single 1.8-MHz channel and are referenced to the Block 0 sampling clocks. As described below, the timing system implementation may have resulted in experiment-to-experiment delay changes which would not have occurred if the system had been in its BWS mode with phase calibrators. The system noise effects ranged from 3-20 ns, compared to the 0.1 ns which would be achieved with BWS.

For these experiments the system was configured to sample three S-band channels, spending 0.5 second in each. Although frequently X-band data were recorded as well; they were not included in these results.

C. Wideband System

The wideband VLBI data acquisition system utilizes a high instantaneous sampling rate in order to observe the entire signal bandwidth, as limited only by the receiving system. The receiver output is digitally modulated to baseband by sampling at 50 MHz in each of the two phase-quadrature analog-to-digital (A/D) converters. The time delay observable is the differential group delay to the A/D converter sampling clocks. The A/D converter outputs are low-pass filtered, by summing N consecutive samples in a digital integrate-and-dump filter. These experiments typically used $N = 3$, thus reducing the effective bandwidth to $16\text{-}2/3$ MHz. The filter outputs are quantized to 1 bit, and stored in a 4096-bit buffer. When the buffer is full, sampling is inhibited and the buffer is emptied onto magnetic tape. Fourteen bursts of data are taken each second, for an average data rate of 57 kbit/s. The WBDAS achieves a lower signal-to-noise ratio than the Block 0 system because of the lower data rate, but achieves a time-delay error due to system noise of 1-5 ns, because of the wider bandwidth.

D. Station Timing

The VLBI systems are referenced to the station frequency standards through the coherent reference generator (CRG) and the time format assembly (TFA). Power to the frequency standards, the CRG, and the TFA is nominally uninterruptible, so phase and timing is in principle continuous except when catastrophic failures occur. The function of the CRG is to generate various frequency references coherently from the station standard. For the purposes of this experiment, the CRG probably does not degrade the station standard. The station 1 pps is generated from 1 MHz in redundant divider chains. Because the divider chains are constructed of obsolete and slow circuits, the 1-pps signal is reclocked by 5 MHz in the TFA. This reclocking results in possible 200-ns glitches, which have been observed at DSS 14 during the course of these experiments. Both VLBI systems initially synchronize their internal 1-pps references to the TFA 1-pps signal, and then allow the internal clocks to free run until synchronization is lost. This loss of synchronization normally occurs only when there is an interruption in power to the TFA or to a VLBI system. Such interruptions did not occur within one day's experiment, but did occur between experiments.

E. WBDAS Timing

The WBDAS 1-pps reference is generated from a 50-MHz signal from the CRG, by dividing this signal to 1 pps using emitter coupled logic (ECL). The internal 1 pps is initially synchronized to the TFA 1 pps, and thereafter the WBDAS monitors the phase difference between the TFA 1 pps and the internal 1 pps, in increments of 10 ns. The 10-ns

resolution is achieved by observing the TFA signal both directly, and delayed by 10 ns. Normally the phase relationship does not change by more than 10 ns either within an experiment or between experiments. This 10-ns variation is expected, due to drifts in the WBDAS ECL circuits or in the TFA TTL circuits. Occasionally, jumps of 200 ns were observed at DSS 14; these jumps did not accumulate, but typically changed back and forth within an experiment on some days. We attribute this effect to the TFA. These jumps occurred only at DSS 14, and were always in the same direction. Therefore it is likely that the WBDAS clock was always consistently synchronized to the 50-MHz reference, within one 20-ns count interval, even when it was necessary to resynchronize due to power outages between experiments.

F. Block 0 Timing

The Block 0 VLBI System has a sampling rate of 4 Mbit/s, a frequency which is not available in the DSSs. The 4 Mbit/s is derived from 5 MHz in a phase locked loop synthesizer system. This system generates 1 MHz from the 5 MHz reference and from a 4 MHz voltage controlled oscillator (VCO), using digital dividers. The 1 MHz signals are then phase locked. A problem with this system is that the phase relationship between the 5 MHz and the 4 MHz can change up to 200 ns in increments of 50 ns upon resynchronization. Thus, power outages to the Block 0 System, and consequent resynchronization, may result in timing offsets in increments of 50 ns, in addition to the possible 200-ns TFA offset. This synchronization error is a likely source of discrepancies between the results from the two VLBI systems.

III. Results

A. Experiments

From 3 September 1978 to 21 January 1979, a total of 34 VLBI clock sync passes were scheduled. The pass durations ranged from approximately 2 hours to 25 hours. Each pass consisted of a number of runs, i.e., time spent taking data on a particular source, separated by antenna move time. Eight of the longer passes were scheduled by the Block 0 experimenters and consisted of 2.5-minute runs. The other passes were scheduled by the WBDAS experimenters and consisted of 9-minute runs. Because the time required for setup was uncertain, runs were scheduled from the start of the pass. Thus data was not always taken on the initial runs or the final runs. Some passes were not successful at all due to equipment failures in one or both VLBI systems, or in the DSS configuration. The results in this section are the estimates of the clock offset for the successful passes.

B. Processing and Results

1. Processing. The WBDAS results were produced in two stages. The first stage correlated the data from each separate run and produced an estimate of the clock offset and its rate of change, as well as estimates of the standard deviation for each parameter. The second stage combined the estimates for each successful run in a pass and produced an estimate for the clock offset and its rate for the pass.

Table 1 contains the results of the second stage. The column labeled Date contains the nominal date of the experiment, Epoch contains the time of the clock estimate, Clock contains the clock offset, Sigma clock contains the formal uncertainty of the clock offset, Residual contains the rms residual of the runs with respect to the clock estimate for the pass, Clock rate contains the rate of change of the clock offset, Sigma clock rate contains the formal uncertainty of the clock rate, No. of observations contains the number of runs or observations in the pass that were used to produce the pass estimates.

2. Closure Results. Three of the passes were performed on the 43/63 baseline, using only the WBDAS System. This provides a consistency check on the clock offsets, since the offsets between pairs of stations should sum to zero. Because the reference time for each pass is different and the clocks are all drifting, it is necessary to make some estimates to reference these clock offsets to the same epoch. Figure 2 shows the 14/43 and 14/63 clock offsets used to make these estimates. The clock offsets are modelled by straight-line, least-square fits to the data, based on the assumption that the clocks at the three stations have constant but different frequencies. On or about 16 November, the clock at DSS 43 apparently had a sudden frequency change and so two straight-line fits are made to the 14/43 clock offset. Table 2 contains the data used to calculate the 14/43 and 14/63 fits. The rms residuals to these fits are on the order of 70 ns. The closure is to about 10 to 30 ns. It should be noted that the 14/63 data has to be extrapolated to 14 October. The earliest 14/63 experiment used here was on 23 October since the preceding experiment of 1 October deviated considerably from the straight-line fit. The hydrogen maser at DSS 63 failed in September and presumably had not settled at its final frequency on 1 October. The fact that the closure is as good as it is suggests that it had settled before 14 October.

C. Block 0 Processing and Results

In the Block 0 System, the digital video tapes are shipped from the stations to JPL, then cross-correlated in quadrature on the hardware processor at Caltech. Postcorrelation analysis is performed on the IBM 3032 at Caltech and begins with a step called "phase-tracking" in which each source observation (typically 3-9 minutes) is divided into segments 20 to 60 seconds long. Each segment is fit by least squares to a complex sinusoid giving solutions for amplitude, phase, and fringe rate. Simultaneous interpolation of fringe amplitude in the lag domain with a $\sin x/x$ function yields the single channel group delay, while cross-channel differencing of phase solutions yields the synthesized delay for each segment. A priori values for the first segment solution are taken from an initial Fourier analysis, while those for the other segments are taken from the solutions for the segment preceding.

Segment solutions are then analyzed collectively to yield a solution for the entire observation. Amplitude and alignment delay are obtained by a weighted average of segment solutions, while fringe phase and rate result from a linear fit to segment phases. A linear fit to synthesized delays gives the final synthesized delay and a direct measurement of delay rate, which supplements the more accurate measurement obtained from the phase rate.

In the final processing step, solutions for all observations are supplied to a global fitting program which produces, for the entire experiment, single solutions for clock offset, fringe rate, and clock rate. In addition, when the number of observations is sufficient (typically >7), the program redetermines the baseline, thus providing some compensation for errors in the a priori UT1 and PM values. Although the program can also solve for selected source positions, we did not use that feature, electing instead to discard obviously bad data.

The Block 0 data reported here are from this final processing step. The clock rate reported is that derived from fringe rate rather than from delay rate, because this is more accurate. The rate accuracy is currently limited over the short term by systematic and random effects of ionosphere, instrumentation, and modeling errors.

Table 3 contains the Block 0 results and provides the accumulated "Allan Variance" stability estimates derived from the clock offsets. Note that the accumulation has been restarted at points of major breaks or jumps in the clocks.

D. Comparison of Results

Figure 3 shows the DSS 43 minus DSS 14 clock offsets versus epoch for both the WBDAS and Block 0 Systems. The offset is nearly linear from 17 September (Epoch 22.5) to 16 November (Epoch 27.7). The hydrogen maser failed at DSS 43 between the 3 September and 11 September passes and was put back on line just before the 11 September pass. Thus the early clock offsets are not colinear with those following. As mentioned above, the WBDAS data shows a rate change on about 16 November. This rate change is not as precisely located in the Block 0 data since there was no Block 0 result from 16 November. The frequency of the DSS 43 maser was intentionally shifted in late December and thus the offsets from 20 December (Epoch 30.7) to 12 January (Epoch 32.7) have a different rate than those previous.

Figure 4 shows the DSS 63 minus DSS 14 clock offsets versus epoch for the two systems. The DSS 63 hydrogen maser was not on line until January of 1979, thus only the last two points represent a comparison of two masers. However, the data is quite linear from 23 October (Epoch 25.7) to 24 December (Epoch 30.9) while DSS 63 was on the cesium standard.

The scale of Figs. 3 and 4 permits only a coarse comparison of the two systems. However, Fig. 5 shows the 14/43 data with a linear clock estimate removed, $\hat{c} = -26.71 + 1.35 \times \text{Epoch}$. In addition, a constant of 0.4 microseconds has been added to the Block 0 data, which represents an estimate of the difference of the signal and clock path lengths in the two systems. The rate change in the 14/43 offset mentioned above is quite obvious in Fig. 5, however it should be noted that the slope is not really negative past 16 November since the axis of Fig. 5 has a slope of 1.35×10^{-12} . There are 10 passes on the 14/43 baseline for which both systems reported results; the rms difference (after removal of the 0.4- μ s offset) is 64 ns.

Figure 6 shows the 14/63 data with a linear clock estimate removed, $\hat{c} = -11.4 + 0.29 \times \text{Epoch}$. In addition, a bias of 56 ns has been added to the Block 0 data. The rate of 0.29×10^{-12} reflects the rate observed from 23 October (Epoch 25.7) to 24 December (Epoch 31.0). Before 23 October, the points are outside the range of Fig. 6, due to station clock adjustments. A large clock jump occurred between 24 December and 16 January, so 1.1 μ s was subtracted from the passes on 16 January and 21 January to keep them on Fig. 6. There were 7 passes between 23 October and 24 December for which both systems reported results. The average difference between the two systems was 56 ns and after removal of this constant, the rms difference was 105 ns. Two days, 5 November and 3 December, disturb these calculations and may be the result of clock jumps.

IV. Analysis of Results and Error Sources

The principal objectives of VLBI clock sync experiments are to determine the offset and combined stability of the station frequency standards. In the present case, with near-simultaneous results from two different VLBI systems, we can also form some conclusions about the performance of the VLBI technique itself.

On the 14/63 baseline, over the period during which the cesium standard was on line at 63, the Block 0 results show a frequency offset of 3×10^{-13} and a stability (square root Allan variance) of 2×10^{-13} with a sample standard deviation on the latter figure of 0.9×10^{-13} . The WBDAS results show comparable values of 2.7×10^{-13} for the offset and 1.2×10^{-13} for the stability. On the 14/43 baseline both sets of results show a change in frequency offset sometime in the period from mid-November to early December. A lack of Block 0 results for mid-November prevents a more accurate determination of the time of the change. Block 0 data yield an offset of 1.7×10^{-12} before the change and 8.2×10^{-13} after, with a stability over the whole interval of 3×10^{-13} . The sample standard deviation is 1×10^{-13} . From the WBDAS data, the estimated offsets are 1.7×10^{-12} before the change and 1.2×10^{-12} after, with an overall stability of 1.9×10^{-13} . The average interval between samples is approximately 10 days; however, because the intervals vary, the Allan variances must be considered nonstandard.

Because neither S/X ionosphere calibration nor instrumental phase calibration were employed in these experiments, errors in the measured clock offsets are dominated by transmission media and instrumental effects. The stability values should therefore be regarded only as loose upper bounds on the instability of the clocks themselves.

Figures 5 and 6 show the differences between the WBDAS and Block 0 measured clock offsets, after the removal of a constant bias, on the days for which both systems obtained measurements. With the exception of a few greater discrepancies, the agreement is at about the 50-ns level. In all likelihood, the larger discrepancies are due not to large random errors but rather to real temporary changes in the instrumental delays of one system with respect to the other. For example, it has been observed that reinitializing the Block 0 clock, which is routinely done, can change its epoch with respect to the station clock by several hundred nanoseconds. The phase calibration systems now being installed will remove the effects of those jumps.

The VLBI systems described here have measured the combined instability over ~10-day intervals of frequency standards separated by intercontinental distances to low parts in 10^{13} with an uncertainty of 1 part in 10^{13} . It is known that well-maintained hydrogen masers will show a stability over such intervals of a part in 10^{14} or better. With VLBI systems now under development using dual-frequency ionosphere calibration, accurate measurement and modeling of the wet and dry components of the troposphere, instrumental phase calibration, and simultaneous solution for UTI and polar motion corrections, stability measurements of a few parts in 10^{14} should be attainable.

Although a thorough analysis of the error sources affecting the interferometer used for these experiments has not yet been completed, a preliminary set of mean value error estimates have been compiled based on prior experience with the instrument. These values are presented in Table 4 mainly to indicate the estimated relative magnitude of the errors at S-band. For the sake of consistency, the geometric effects have been scaled to a hypothetical 10,000 km. baseline and approximate worst case partials are provided as well as the corresponding one sigma error values. In the cases of "System Noise", "Instrumentation", "Ionosphere", and "Bandpass Shape", only those values footnoted by an "a" or a "c" are applicable to the current instruments. The other values presented in these categories represent an estimate of the level to which these error sources will be reduced once phase calibration and dual-frequency charged particle error cancellation have been introduced.

The system noise contribution ranges from 1 ns for strong sources with either system, to 20 ns with the Block 0 System for sources too weak to be detected with the WBDAS. The range of 10-40 ns for instrumentation effects depends on the station configuration integrity. The bandpass shape factor is smaller, about 1 ns, for the WBDAS than the 10 ns for the Block 0, due to system bandwidth utilized (Ref. 17). Since there are normally some strong radio sources in an experiment, the dominant error sources are instrumentation stability and the ionosphere, whose contributions cannot be accurately estimated. Overall, the error of the current measurements is believed to be in the range of 24-51 ns.

For the closure experiment, the expected error is $\sqrt{3}$ times the individual experiment error, or 42-88 ns, neglecting frequency stability induced errors. Thus the closures of 33, 10, and 13 ns were better than anticipated.

Acknowledgments

The authors express their appreciation to B. Bronwein, E. Cohen, R. Henderson, R. Shaffer, D. Spitzmesser, and the Deep Space Station personnel for their assistance in scheduling, configuring, and operating the stations, and processing the data.

References

1. Goldstein, R., "Clock Calibration via Quasar," in the Space Programs Summary 34-48. Vol. II, pp. 79-82, Jet Propulsion Laboratory, Pasadena, Calif., November 30, 1967.
2. Cohen, M. H. and Shaffer, D. B., "Positions of Radio Sources from Long Baseline Interferometry," *Astronomical Journal*, Vol. 76, No. 2, March 1971, pp. 91-100.
3. Hinteregger, H. F., Shaprio, I. I., Robertson, D. S., Knight, C. A., Ergas, R. A., Whitney, A. R., Rogers, A. E. E., Moran, J. M., Clark, T. A., and Burke, B. F., "Precision Geodesy via Radio Interferometry," *Science* 178, October 1972, pp. 396-398.
4. Wade, C. M., "Precise Positions of Radio Sources I. Radio Measurements," *Astrophysical Journal*, 162, November 1970, pp. 381-390.
5. Hurd, W. J., "A Demonstration of DSN Clock Synchronization by VLBI," in *The Deep Space Network Progress Report, Technical Report 32-1526, Vol. XII*, pp. 149-160, Jet Propulsion Laboratory, Pasadena, Calif., December 15, 1972.
6. Hurd, W. J., "An Analysis and Demonstration of Clock Synchronization by VLBI," *IEEE Transactions on Instrumentation and Measurement* Vol. IM-23, No. 1, pp. 80-89, March 1974.
7. Thomas, J. B., et al., "Radio Interferometry Measurements of a 16 km Baseline with 4 cm Precision," in *The Deep Space Network Progress Report, Technical Report 32-1526, Vol. XIX*, pp. 36-54, Jet Propulsion Laboratory, Pasadena, Calif., February 15, 1974.
8. Counselman, III, C. C., Shapiro, I. I., Rogers, A. E. E., Hinteregger, H. F., Knight, C. A., Whitney, A. R., and Clark, T. A., "VLBI Clock Synchronization," *Proc. IEEE*, Vol. 65, No. 11, November 1977, pp. 1622-1623.

9. Clark, T. A., Counselman, C. C., Ford, P. G., Hanson, L. B., Hinteregger, H. F., Klepczynski, W., Knight, C. A., Robertson, D. S., Rogers, A. E. E., Ryan, J., Shapiro, I. I., and Whitney, A. R., "Precise Clock Synchronization via Very-Long-Baseline Interferometry," Proc. 9th Ann. PTTI, Goddard Spaceflight Center, 1977.
10. Hurd, W. J., "Preliminary Demonstration of Precision DSN Clock Synchronization by Radio Interferometry," in the Deep Space Network Progress Report 42-37, Jet Propulsion Laboratory, Pasadena, Calif., February 15, 1977, pp. 57-68.
11. Hurd, W. J., et al., "Submicrosecond Comparison of Intercontinental Clock Synchronization by VLBI and the NTS Satellite," Proceedings of the Tenth Annual Precise Time and Time Interval Applications and Planning Meeting, NASA TM 80250, Goddard Space Flight Center, Greenbelt, MD., Nov. 28-30, 1978, pp. 629-642. Also in the Deep Space Network Progress Report, Technical Report 32-1526, Vol. 49, pp. 64-69, Jet Propulsion Laboratory, Pasadena, Calif., February 15, 1979.
12. Thomas, J. B., "An Analysis of Long Baseline Radio Interferometry," in The Deep Space Network Progress Report, Technical Report 32-1526, Vol. VIII, p. 37, Jet Propulsion Laboratory, Pasadena, Calif., February 1972.
13. Thomas, J. B., "An Analysis of Long Baseline Radio Interferometry, Part II," in The Deep Space Network Progress Report. Technical Report 32-1526, Vol. VIII, p. 29, Jet Propulsion Laboratory, Pasadena, Calif., May 1972.
14. Thomas, J. B., "An Analysis of Long Baseline Radio Interferometry, Part III," in The Deep Space Network Progress Report, Technical Report 32-1526, Vol. XVI, p. 47, Jet Propulsion Laboratory, Pasadena, Calif., August 15, 1973.
15. Rogers, A. E. E., "Very Long Baseline Interferometry with Large Effective Bandwidths for Phase Delay Measurements," Radio Science, 5(10), 1239, 1970.
16. Thomas, J. B., "The Tone Generator and Phase Calibration in VLBI Measurements," in The Deep Space Network Progress Report, 42-44, Jet Propulsion Laboratory, Pasadena, Calif., February 1978, pp. 63-74.
17. Layland, J. W. and W. J. Hurd, "VLBI Instrumental Effects, Part I," in The Deep Space Network Progress Report, 42-42, Jet Propulsion Laboratory, Pasadena, Calif., December 1977, pp. 54-80.

Table 1
WBDAS Results

Date	Epoch, secs past 1 Jan 1978 $\times 10^6$	Clock, ns	Sigma clock, ns	Residual, ns	Clock rate, $\times 10^{-12}$	Sigma clock rate, $\times 10^{-12}$	No. of observations
14/43							
11 Sep	21.9816	-3.551	0.4	5.3	0.78	0.08	4
17 Sep	22.518	3.744	23.9	62.8	3.0	0.7	7
23 Sep	23.0292	4.379	18.0	-	5.0	2.0	1
30 Sep	23.6304	5.292	0.4	5.4	1.41	0.06	6
14 Oct	24.8436	7.320	0.6	2.1	3.4	0.15	2
23 Oct	25.6176	8.591	0.7	7.9	1.8	0.1	3
27 Oct	26.0064	9.316	0.2	10.9	2.28	0.007	23
4 Nov	26.6724	10.659	0.4	11.5	0.98	0.04	9
16 Nov	27.6912	12.337	0.5	5.4	1.6	0.07	4
29 Nov	28.8072	13.688	0.6	11.2	2.1	0.2	3
12 Dec	29.9808	15.125	1.1	4.3	-2.8	0.9	2
31 Dec	31.5864	16.407	0.2	8.2	0.18	0.005	14
12 Jan	32.6628	17.423	0.5	14.2	0	0.15	6
14/63							
9 Sep	21.8484	-8.768	0.8	6.8	-1.8	0.2	5
1 Oct	23.7348	-2.443	0.15	14.8	0.7	0.4	4
23 Oct	25.6536	-3.845	0.8	7.6	-1.4	0.2	5
30 Oct	26.2008	-3.705	0.7	18.9	4.09	0.08	9
5 Nov	26.7984	-3.451	0.3	32.4	0.66	0.01	10
20 Nov	28.0044	-3.303	0.5	5.9	1.0	0.1	6
27 Nov	28.6092	-3.126	0.5	6.4	0.3	0.1	5
3 Dec	29.1996	-2.955	1.4	4.3	-0.7	0.3	5
24 Dec	30.9492	-2.368	0.3	6.0	-0.28	0.04	10
16 Jan	32.9472	-0.664	0.4	4.2	-0.5	0.07	6
21 Jan	33.3756	-0.564	0.8	4.5	-0.2	0.1	4
43/63							
14 Oct	24.858	-11.400	1.0	18.2	-3.4	0.3	5
3 Nov	26.604	-14.033	1.0	1.4	-4.0	0.2	3
28 Nov	28.7532	-16.643	2.0	6.3	-4.0	0.6	2

Table 2
WBDAS Closure Results

Date	Epoch	Clock	Residual to Fit		
14/43					
30 Sep	23.6304	5.292	0.070	$\hat{T}_{43-14} = -36.1159$ $+ 1.74937 \times \text{Epoch}$ rms residual = 0.076	
14 Oct	24.8436	7.320	-0.025		
23 Oct	25.6176	8.591	-0.108		
27 Oct	26.0064	9.316	-0.063		
4 Nov	26.6724	10.659	0.115		
16 Nov	27.6912	12.337	0.011		
16 Nov	27.6912	12.337	0.003	$\hat{T}_{43-14} = -21.386$ $+ 1.2177 \times \text{Epoch}$ rms residual = 0.004	
29 Nov	28.8072	13.688	-0.005		
12 Dec	29.9808	15.125	0.003		
14/63					
23 Oct	25.6536	-3.845	0.007	$\hat{T}_{64-14} = -10.669$ $+ 0.26574 \times \text{Epoch}$ rms residual = 0.062	
30 Oct	26.2008	-3.705	0.001		
5 Nov	26.7984	-3.451	0.097		
20 Nov	28.0044	-3.303	-0.076		
27 Nov	28.6092	-3.126	-0.060		
3 Dec	29.1996	-2.955	-0.046		
24 Dec	30.9492	-2.368	0.077		
43/63					
				\hat{T}_{43-14} \hat{T}_{63-14} RESID = T_{63-43} $+ T_{43-14} - T_{63-14}$	
14 Oct	24.858	-11.400	7.370	-4.063	0.033
3 Nov	26.604	-14.033	10.424	-3.599	-0.010
28 Nov	28.7532	-16.643	13.628	-3.028	0.013

Table 3
Block 0 Results

Date	Epoch	Clock, μ s	Sigma clock, ns	Rate, $\times 10^{-12}$	No. of observations	Square root Allan variance, $\times 10^{-13}$
14/43						
3 Sep	21.322339	4.368	5.2	-2.38	32	--
17 Sep	22.518534	3.377	9.7	2.22	7	--
30 Sep	23.629294	4.844	1.7	1.93	5	--
14 Oct	24.844771	6.910	1.0	3.82	3	2.68
23 Oct	25.618483	8.156	4.7	3.26	4	1.95
27 Oct	25.975236	8.744	2.4	2.31	117	1.60
4 Nov	26.670332	10.317	5.0	5.96	24	2.58
29 Nov	28.806020	13.397	1.6	2.91	4	3.47
13 Dec	29.981315	14.776	6.7	1.08	3	3.26
20 Dec	30.671408	15.361	2.0	2.23	3	3.14
31 Dec	31.543594	15.955	1.7	1.68	33	2.97
13 Jan	32.662017	16.984	14.6	2.32	6	2.86
14/63						
4 Sep	21.385637	-7.668	3.8	0.68	56	--
16 Sep	22.410587	-10.059	7.3	-5.15	59	--
23 Oct	25.655368	-3.965	8.0	-0.62	5	--
30 Oct	26.180608	-3.828	6.2	-1.82	57	--
5 Nov	26.754849	-3.672	3.9	0.24	127	0.08
20 Nov	28.005401	-3.329	9.3	0.13	7	0.06
27 Nov	28.611230	-3.184	18.9	0.09	5	0.15
3 Dec	29.202867	-2.800	7.5	1.05	3	1.45
16 Dec	30.249901	-2.604	8.0	0.16	17	1.96
24 Dec	30.942036	-2.385	5.3	0.16	15	1.82
16 Jan	32.947914	-0.582	2.1	-2.08	4	--
21 Jan	33.374313	-0.469	15.5	-0.84	5	--

Table 4
Estimated Magnitudes of Error Sources at S-Band for a 10,000km Baseline

Error Source	Delay			Delay rate, $\chi\omega$		
	Partial	1σ	Final value	Partial	1σ	Final value
Source position	130 ns/"	0.015"	2 ns	22 mHz/"	0.015"	0.33 mHz
Baseline	3.3 ns/m	1.0 m	3.3 ns	0.56 mHz/m	1.0 m	0.56 mHz
UT1	2.0 μ s/sec	0.003 sec	6 ns	0.32 Hz/sec	0.003 sec	1.0 mHz
PM (X)	3.3 ns/m	0.7 m	2.3 ns	0.56 mHz/m	0.7 m	0.4 mHz
PM (Y)	3.3 ns/m	0.7 m	2.3 ns	0.45 mHz/m	0.7 m	0.4 mHz
System noise			1-20 ns ^a			2.3 mHz ^a
	n/a ^b	n/a	3.5 ns	n/a	n/a	0.4 mHz
Instrumentation			20-40 ns ^a			1.0 mHz ^a
	n/a	n/a	3 ns	n/a	n/a	0.1 mHz
Ionosphere			10-20 ns ^c			4.0 mHz ^b
	n/a	n/a	~ 0 ns	n/a	n/a	~ 0 mHz
Troposphere			1 ns	n/a	n/a	0.2 mHz
Bandpass shape			1-10 ns ^a			
	n/a	n/a	~ 0 ns	n/a	n/a	~ 0 mHz
Root sum square			24-51 ns ^{a,c}			5.0 mHz ^{a,c}
			9.2 ns			1.4 mHz

^a Without phase calibration.

^b Not applicable.

^c Without S/X calibration of the ionosphere.

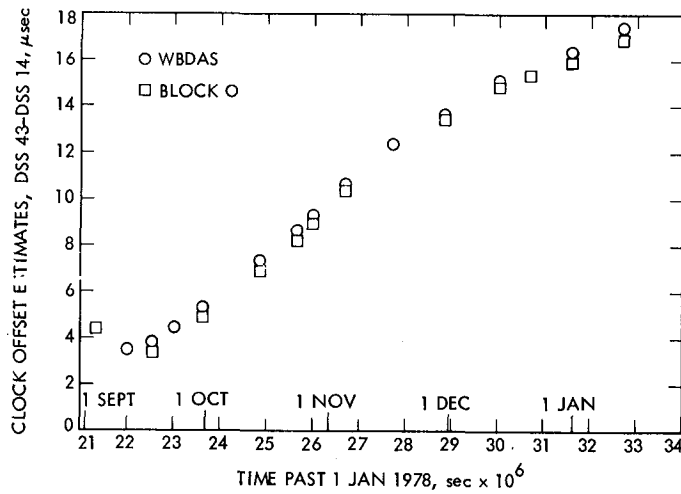


Figure 3. Clock Offset Estimates, DSS 43
Minus DSS 14

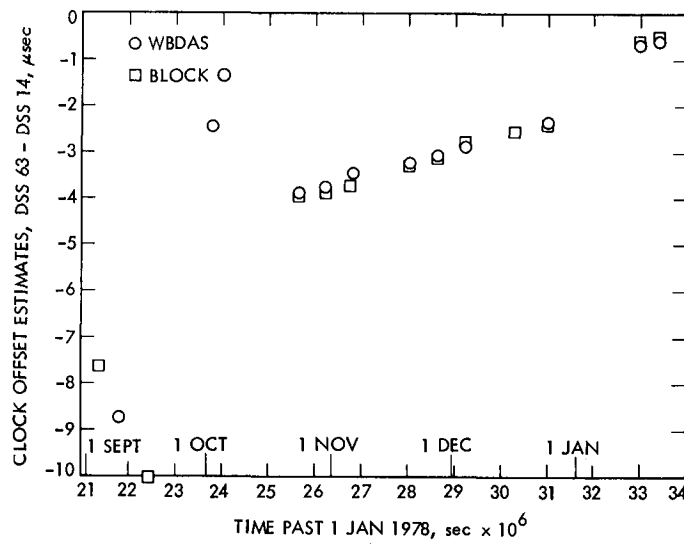


Figure 4. Clock Offset Estimates, DSS 63
Minus DSS 14

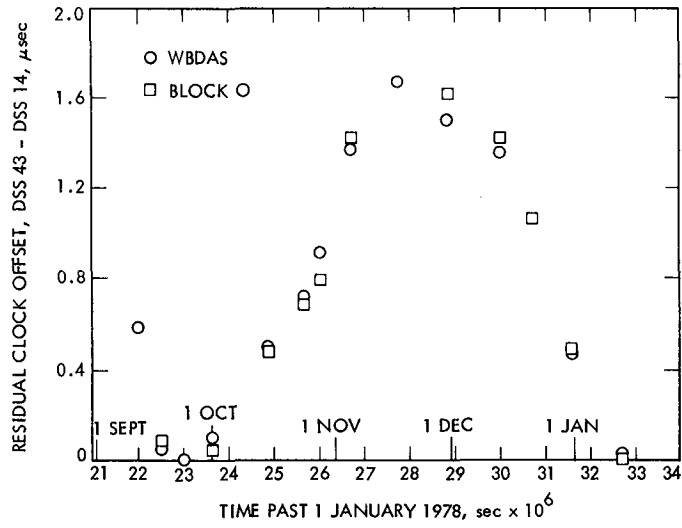


Figure 5. Residual Clock Offset Estimates,
DSS 43 Minus DSS 14

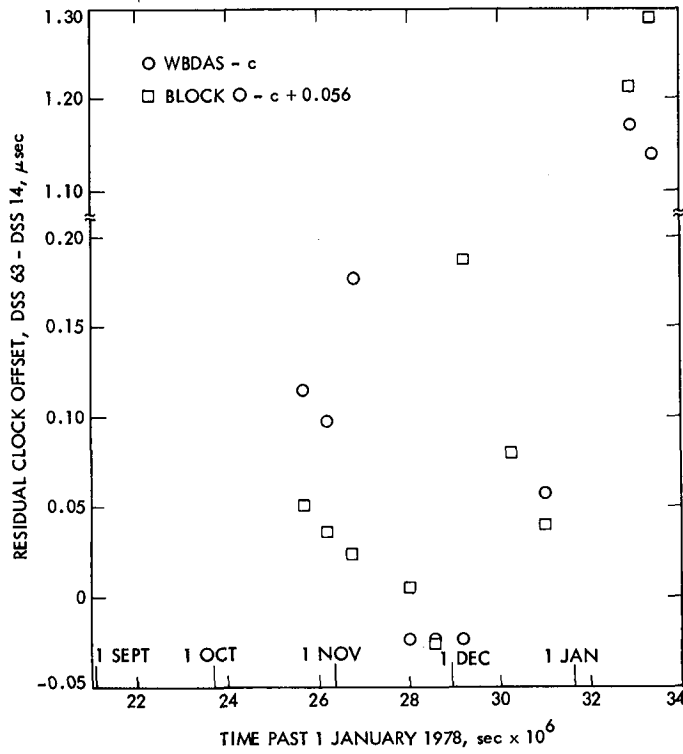
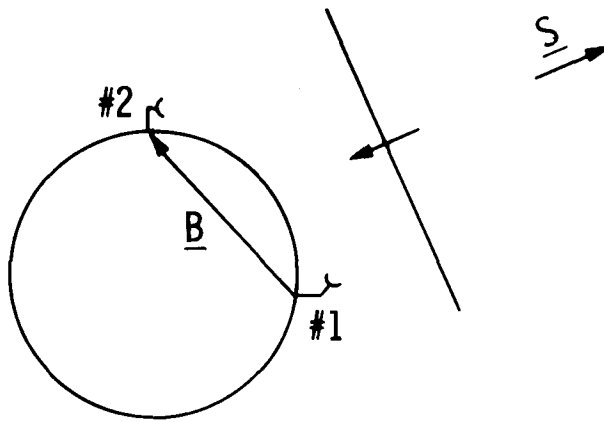


Figure 6. Residual Clock Offset Estimates,
DSS 63 Minus DSS 14



TRUE DELAY COMPONENTS

τ_G - GEOMETRIC DELAY

τ_P - CHARGED PARTICLE DELAY

τ_N - NEUTRAL ATMOSPHERE DELAY

τ_I - INSTRUMENTAL DELAYS

APPARENT DELAY COMPONENT

τ_C - CLOCK EPOCH OFFSET

Slide 1. VLBI Delay Components

QUESTIONS AND ANSWERS

DR. KEN YUGLO:

Mine is a clarification. I missed whether you are using the bandwidth synthesis or whether you are recording the whole bandwidth and possibly saving tape or something by taking pieces in time?

DR. YUNCK:

Yes. That is the difference between these two systems. The Block-0 system that Tom discussed in the last paper is a bandwidth synthesis system. This system does sample the entire bandwidth and throws away some samples.

DR. YUGLO:

And how long are those samples? The sequences rather.

DR. YUNCK:

Well, the samples are one bit samples and 4,096 samples are collected. Four thousand ninety six samples at 50 megahertz. Whatever that works out to be. Several microseconds. And then 14 samples per second or 14 bursts per second are recorded on the tape.

DR. YUGLO:

What noise?

DR. YUNCK:

Well it is all noise. The A to D converter is sampled continuously. It is just that some blocks of samples are thrown out and that is done digitally. These are digital signals.

TRAVELING CLOCK VERIFICATION OF VLBI CLOCK SYNCHRONIZATION

L. E. Young
Jet Propulsion Laboratory

ABSTRACT

Four experiments are described which involved measurements of clock offsets at two DSN stations. Both VLBI and traveling clock measurements were performed and the agreement between the two methods was within about 6 ns for all four comparisons.

INTRODUCTION

The Deep Space Network (DSN) plans to initiate a periodic program of very long baseline interferometry (VLBI) experiments in order to monitor the performance of the frequency standards used at its radio telescopes. In order to demonstrate the capability of accurate measurement of epoch offsets between DSN station clocks using VLBI, as well as to develop procedures to be used in the operational program, four VLBI experiments were performed from June 1979 to September 1979. During each VLBI experiment, a traveling clock was used to check the accuracy of the VLBI clock synchronization. In order to achieve a high degree of accuracy in the traveling clock measurement, a pair of DSN stations separated by a relatively short baseline was used. A previous short baseline VLBI/traveling clock experiment has been reported by C. C. Counselman III et al.¹ That experiment gave a reported difference of 9 ns \pm 11 ns in the clock offset obtained with the two methods, and it was suggested that a more accurate measurement would be desirable.

VLBI Experiment

The radio telescopes used were DSS 13 and DSS 14, with dish diameters

¹ C.C. Counselman III, I. I. Shapiro, A. E. E. Rogers, H. F. Hinteregger, C. A. Knight, A. R. Whitney, and T. A. Clark, Proceedings of the IEEE, Vol. 65, No. II, p. 1622 (1977).

of 26 and 64 meters, respectively. Both DSS 13 and DSS 14 are situated within the DSN complex at Goldstone, Ca., and are separated by approximately 22 kilometers. Each station used a Hydrogen maser as its frequency standard. The VLBI experiments were typically 5 hours long, incorporating some 40 observations of about 25 extra galactic radio sources.

Figure 1 illustrates the VLBI experiment in a schematic way. The plane wave represents an incoming burst of radio noise. Some incremental delay above that for free space is added by the media. Because of the proximity of the two radio telescopes used, and because the experiments were conducted during local nighttime, when media effects are at a minimum, the media delay is assumed to be the same at each site.

The wave front reaches the two antennas at times separated by the geometric delay, τ_g . At each station, phase calibrator tones derived from the frequency standard were injected into the data stream near the beginning of the receiver assembly. From this injection point on, the phase calibrator tones were imbedded in the data, and indicated the instrumental delays and phase shifts added to the data as it was down converted and recorded into three time multiplexed s-band frequency channels along with time tags from the station clock. These channels were later combined to synthesize a measured delay.

Each 2 MHz channel of data contained three phase calibrator tones. In order to use the unambiguous delay resulting from the correlation of a single 2 MHz channel at each station to remove the cycle ambiguities inherent in the delays determined via the bandwidth synthesis technique, it is necessary to know the instrumental delay characteristics of that single channel. The instrumental delay can be measured as a separate experiment, but this can prove difficult for a complex receiving system and must be re-done after station hardware changes which affect instrumental delay. In the interest of avoiding the need for extensive calibration measurements, the system of phase calibration used by the DSN allows a variable spacing of tones, with the narrowest spacing corresponding to an ambiguity of 19.8 μ s in the instrumental delay. As this is much larger than the 2 or 3 μ s delay typical for DSN radio telescopes, somewhat wider spacing can be used. In these experiments, for instance, a tone spacing of 0.5 MHz was used. With this system the instrumental delays added below the phase calibrator injection point never need to be measured separately, and the VLBI clock synchronization is not jeopardized if these delays change between experiments. Another advantage of the presence of multiple phase calibrator tones per channel was that it allowed a continuous monitor of the phase

versus frequency response of each channel.

When the video tapes from each station were brought together and correlated, the geometric delay, τ_g , known A priori, was removed analytically. The phase calibration correction was made, resulting in the following VLBI delay:

$$(1) \quad \tau_{\text{VLBI}} \approx (\tau_a^{14} - \tau_a^{13}) - (\tau_u^{14} - \tau_u^{13}) + (t_c^{14} - t_c^{13})$$

Portions of the antenna delays, τ_a^i , were measured and the rest were calculated from the physical dimensions of antennas and waveguides.

The results were $\tau_a^{14} = 119.2 \pm 1.0$ ns and $\tau_a^{13} = 53.4 \pm 2.0$ ns.

The uplink delays, τ_u^i , consisted largely of a stabilized cable whose delay was held constant with the use of a phase locked loop controlling a phase shifter in series with the cable. In addition to the fixed portion of the uplink delay, there was a 200 ns ambiguity in the timing generator.

τ_u^{14} and τ_u^{13} were 1321.0 ± 4.2 ns and 2015.2 ± 4.2 ns, respectively.

The remaining term in formula 1 is the clock offset term, which was solved for. The errors in the determination of the clock offset using VLBI were dominated by the estimated error of 6 ns in the determination of antenna and uplink delays. These errors were systematic, in the sense that they were not expected to vary among the four experiments. The errors in the determination of τ_{VLBI} were ≈ 0.1 ns.

Traveling Clock

During each VLBI experiment the traveling clock comparisons were made at station A, station B, back to station A, and finally back to station B. Each comparison involved about five offset measurements between the traveling clock and station clock over a 45 minute period. For each offset measurement, a Hewlett Packard 5360A computing counter with time interval plug-in was used to measure the offset between the 1 pps signal from the traveling clock and the zero crossing of a 5 MHz signal from the station clock. In order to remove the 200 ns ambiguity inherent in this measurement, the

traveling clock 1 pps was also compared with a 1 pps signal from the station clock. In all these measurements, a digital voltmeter was used to insure the appropriate and repeatable setting of trigger levels. As a result, the error attributed to the setting of trigger levels was less than 1 ns.

The error in the synchronization of station clocks by the use of a traveling clock was estimated by noting that the fit of a straight line to the approximately 10 offsets measured between each station clock and the traveling clock gave a RMS residual of about 1 ns. While the behavior of these residuals ruled out the existence of large unobserved jumps in the Rubidium clock during travel times, jumps of up to 3 ns could not be excluded. Therefore, the accuracy of the offset determined between the two station clocks was estimated to be ± 3 ns, which is expected to be a random error among the four experiments.

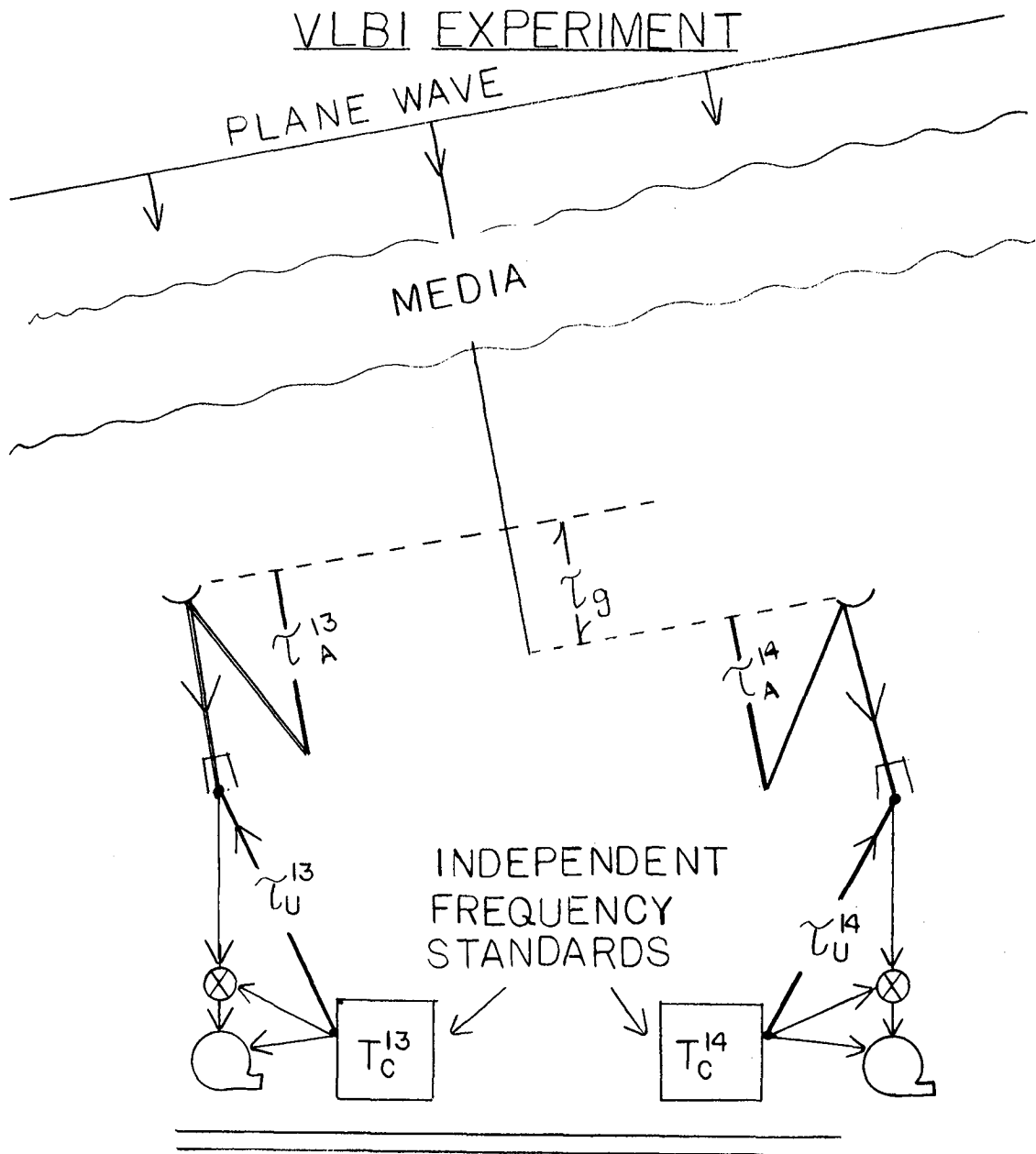
Results

The results of the independent measurements of clock offset, $t_c^{14} - t_c^{13}$, using the traveling clock and using VLBI are shown in table 1 for the four experiments. The frequency offsets between the two stations, $2 \times \frac{f_c^{14} - f_c^{13}}{f_c^{14} + f_c^{13}}$ are also shown. The epoch offset

measurements did agree within about 6 ns in all four cases. In fact, there was a systematic deviation of 4.6 ns between the two techniques, with a R.M.S. scatter of 1.4 ns about the average. The systematic deviation originates from the measurements of the antenna and uplink delays. The 1.4 ns scatter is primarily due to the traveling clock measurements. The fact that the scatter is less than the estimated value of 3 ns implies that there were no undetected clock jumps of this magnitude while the Rubidium Clock was in transit.

Acknowledgements

I would like to acknowledge the assistance given by Tom P. Yunck, Lyle Skjerve, and Tom Otoshi in the completion of this project. The research described in this paper was carried out at the Jet Propulsion Laboratory, California Institute of Technology, under NASA contract NAS7-100.



$$\tau_{VLBI} \approx (\tau_A^{14} - \tau_A^{13}) - (\tau_U^{14} - \tau_U^{13}) + (\tau_C^{14} - \tau_C^{13})$$

(AFTER REMOVAL OF τ_g)

Figure 1. This figure illustrates the instrumental delays, τ_a and τ_u , which must be measured at each station in order to use a VLBI experiment to synchronize station clocks. The use of phase calibration with multiple tones per channel eliminates the need for measurements of the receiver and downlink delays. It should be noted that, in practice, τ_a , and τ_u are defined relative to the intersection of the antenna axes.

Table 2

This table shows the results of four VLBI measurements of clock offset along with the results of concurrently performed traveling clock experiments. For each experiment, the clock offsets are given for a certain epoch chosen within that experiment.

RESULTS

	Traveling Clock	VLBI	VLBI - T.C.
6-6-79 Clock Offset $\frac{\Delta f}{f}$ Offset	+733.9 \pm 3. ns +2.3x10 ⁻¹² \pm 1.5x10 ⁻¹²	+740.1 \pm 6. ns +1.00x10 ⁻¹² \pm 0.03x10 ⁻¹²	+6.2 \pm 7. ns -1.3x10 ⁻¹² \pm 1.5x10 ⁻¹²
7-21-79 Clock Offset $\frac{\Delta f}{f}$ Offset	+874.2 \pm 3. ns +2.1x10 ⁻¹² \pm 0.6x10 ⁻¹²	+879.7 \pm 6. ns +2.31x10 ⁻¹² \pm 0.01x10 ⁻¹²	+5.5 \pm 7. ns +0.2x10 ⁻¹² \pm 0.6x10 ⁻¹²
8-26-79 Clock Offset $\frac{\Delta f}{f}$ Offset	-302.1 \pm 3. ns +0.4x10 ⁻¹² \pm 1.5x10 ⁻¹²	-299.7 \pm 6. ns +1.00x10 ⁻¹² \pm 0.01x10 ⁻¹²	+2.4 \pm 7. ns +0.6x10 ⁻¹² \pm 1.5x10 ⁻¹²
9-18-79 Clock Offset $\frac{\Delta f}{f}$ Offset	-1135.5 \pm 3. ns +2.9x10 ⁻¹² \pm 0.6x10 ⁻¹²	-1131.1 \pm 6. ns +2.04x10 ⁻¹² \pm 0.01x10 ⁻¹²	+4.4 \pm 7. ns -0.9x10 ⁻¹² +0.6x10 ⁻¹²

Mean difference between two methods VLBI - T.C. = +4.6 ns

RMS Scatter = 1.4 ns

QUESTIONS AND ANSWERS

MR. CHI:

Are there any questions? Yes?

DR. KAARLS, Van Swinden Laboratory

You use in your system a cable of several hundreds of meters, do you know if there is any influence of temperature on the delay?
I assume the cable is in the open air.

DR. YOUNG:

Yes. The cable is in the open air and is in the sun in some cases. However, the cable has a delay compensation network, in which, the total delay through the cable is held constant by a voltage controlled phase shifter, so that if the cable were to stretch, the voltage controlled phase shifter would have its delay diminished in such a way as to hold the total delay constant through this up-link.

MR. RUEGER:

In making your differential measurements of your traveling clock, did you use the same counter at both ends?

DR. YOUNG:

Yes. The same equipment.

MR. RUEGER:

Was the counter turned off in-between?

DR. YOUNG:

Yes. The counter was turned off in-between.

MR. RUEGER:

We found some problems in some of our work by having that counter stabilizing thermally between measurements.

DR. YOUNG:

Well, I have seen those problems too. And we have thrown away some data at the beginning of the measurements, during the warm-up time of the computing counter.

EARLY RESULTS FROM A PROTOTYPE VLBI
CLOCK MONITORING SYSTEM

T. P. Yunck and G. A. Madrid
Jet Propulsion Laboratory
Pasadena, California

ABSTRACT

Four sets of experiments were conducted to measure the relative epoch offsets between atomic clocks in California, Australia, and Spain by means of very-long-baseline interferometry (VLBI). The experiments were conducted using an incomplete R & D VLBI system with a number of inherent limitations. However, the results give us confidence that our measurement objective of epoch offset to 10 nanoseconds will be met using the carefully calibrated system to begin regular operation next year.

INTRODUCTION

With the increasing navigational precision demanded of future planetary missions comes the increasing need for precise monitoring of the atomic frequency standards at the deep space tracking stations in Goldstone, California, Canberra, Australia, and Madrid, Spain. To keep the clock contribution to range error at outer planet distances (beyond Mars) below 0.5 meters it will be necessary to know the relative frequency offsets to three parts in 10^{13} . In addition, the Deep Space Network (DSN), which is charged with operating and maintaining the stations, has a vigorous interest in monitoring the behavior of its clocks as precisely as possible. Consequently, a variety of methods for inter-continental clock comparison have been under evaluation at JPL for some time.

OBJECTIVES AND PLAN

In the Navigation Systems Section at JPL we plan soon to begin regular weekly monitoring of several clock and geophysical parameters by the technique of very-long-baseline interferometry (VLBI) [1-7]. Each weekly observing session will employ two baselines (sequentially), with eight to 10 observations of extra galactic radio sources on each, and will last approximately three hours. From the data gathered during one session we expect to determine:

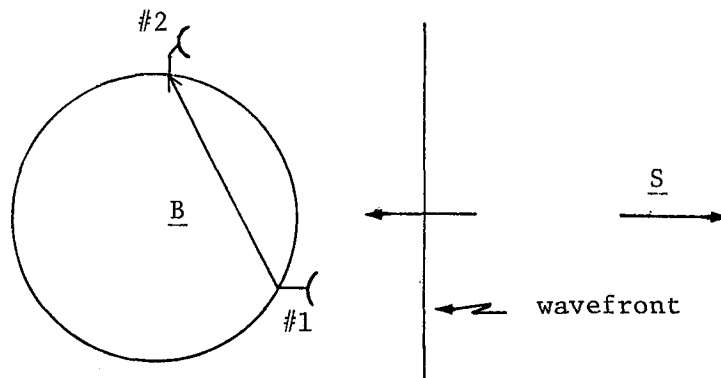
- UT1 to ± 0.7 msec
- Polar motion (X and Y) to ± 0.3 m

- Clock epoch offset to ± 10 nsec
- Clock frequency offset to ± 3 parts in 10^{13}

From the weekly epoch offsets we will be able to compute long-term clock stability to a few parts in 10^{14} . Within several years, when various pieces of dedicated hardware are in place, we will be able to produce those results within 24 hours of the onset of data taking.

THE VLBI SYSTEM

To obtain results of that quality we require both a very accurate prior knowledge of the VLBI geometry and the ability to remove a number of contaminating delays. The diagram below illustrates the VLBI geometry.



The signal arrives from a distant radio source and is received first at Station 1 and then, a time τ later, at Station 2. The received signals are sampled and recorded on magnetic tape with time-tags derived from the station clocks. The apparent delay can be very precisely measured by later cross-correlation of the two recorded signals. When all components of the true delay τ have been accurately modeled or otherwise calibrated and removed from the measured delay, what remains is the apparent delay due to clock synchronization error.

The components of the true delay include

- τ_G - the delay due to geometry
- τ_P - the delay due to atmospheric charged particles
- τ_N - the delay due to the neutral atmosphere
- τ_I - the delay due to instrumentation

Removing the geometric delay requires knowledge of baseline length to ~ 0.5 m and of source positions to $\sim 0.01''$. Such accuracies are now being achieved with VLBI measurements being made at JPL and elsewhere. The VLBI clock monitoring system to begin operation next year will include enhancements to remove the other delay components. They include:

- S- and X-band recording for dual-frequency cancellation of charged particle delay,
- More accurate modeling of the neutral atmosphere based on surface weather measurements and (later) water vapor radiometer measurements,
- Continuous calibration of instrumental phase and group delay [8,9].

In addition, the near-simultaneous observations on two baselines will permit solution for UT1 and polar motion, thereby improving the geometric model.

While this system has been under development, we have been conducting experiments with an earlier R & D system employing none of those enhancements. Consequently, the results presented here are substantially degraded by errors from the corresponding sources. Perhaps the most serious of these errors -- occasionally producing large apparent changes in epoch offset from one experiment to the next -- are a) changes in instrumental delays resulting from minor configuration changes, and b) spurious epoch jumps at the temporary clock reference point used for these experiments. Those effects would be removed by the instrumental calibration system.

In addition, the absence of instrumental calibration prevented our using the "bandwidth synthesis" technique to achieve large bandwidths and hence very precise delay measurements [10,11]. The delay measurements reported here were obtained with one comparatively narrow 1.8 MHz channel at S-band.

We must therefore be careful in defining the delay measurement error. The precision of the measurements -- that is, the random error due to such usual sources as ionosphere, neutral atmosphere, geometric modeling error, and system noise -- is estimated at 40 nanoseconds. However, because of the occasional changes in instrumental delay, the offset variation from one experiment to the next can be as much as several hundred nanoseconds. Finally, the large, uncorrected, but constant instrumental delay introduces a bias in delay measurements of up to one microsecond.

RESULTS

We have obtained epoch offset measurements between the California - Australia and California - Spain clock pairs for two experimentation periods lasting several months each. Figure 1 shows a set of 10 epoch offsets measured between California and Australia over the period 30 Sep 78 to 13 Jan 79. Both stations were using hydrogen masers as primary standards. The cause of the rate change, apparently in early December, is unknown. Because of the sparseness of points,

exact placement in time of the rate change is impossible. There is a clearly anomalous point in early November, indicating either a large (~430 ns) temporary instrumental glitch or a much earlier rate change not well-determined by the data. We interpreted it as the former and excluded it from the linear fit. Residuals to the two fitted lines are shown in Figure 2. The rms residual, excluding the anomalous point, is 39 ns. The irregular spacing of samples in Figure 1 and subsequent plots precludes the meaningful computation of the two-sample variance. However, as an item of information we have computed it and included it with the numerical data from those plots. The data for Figures 1 and 2 are given in Table 1.

Figure 3 shows a set of eight offsets measured between California and Spain over the period 23 Oct 78 to 24 Dec 78. Clearly evident is the onset of apparently aberrant clock behavior at the sixth point. The jump at that point is believed to be due to instrumentation local to our VLBI system, probably the sync mechanism of the temporary clock, as it did not appear in data taken simultaneously with another experimental JPL VLBI system, the "Wideband Data Acquisition System" (WBDAS) [12]. The smaller rise in the last two points has apparently other causes since it does appear in the WBDAS data. Note the switch at Spain from a cesium standard to a hydrogen maser before the last point.

To more clearly illustrate the changes at the later points, the line in Figure 3 was fitted to the first four points only. Figure 4 is a plot of the residuals to that fit. Table 2 gives the values from those plots as well as the residuals to a line fitted to all eight points.

Figure 5 is a plot of 13 offsets measured between California and Australia over the period 19 May 79 to 25 Sep 79. Note that Australia was operating with a cesium primary standard until the last point and that two different Australia antennas were used. Those antennas use a common frequency standard; however, there is a small unknown instrumental delay difference between them which is uncorrected in the data.

The outstanding feature of Figure 5 is the abrupt, temporary rate change in early August. As it happens, those responsible for maintaining the frequency standards had the rate at California adjusted on 1 August and then had it reset on 16 August. The two anomalous points fall on 6 and 11 August. Separate lines were fitted to the points before and after the disruption. Note that the reset did not restore the rate to precisely its original value. The residuals to the fit are plotted in Figure 6 and the numerical values given in Table 3.

Finally, Figure 7 shows a set of eight offsets measured between California and Spain over the period 23 Jun 79 to 25 Sep 79. Both stations employed H-masers as primary standards, however, again two different overseas antennas with a common clock were used. For a

number of reasons, including station configuration changes and scarce antenna time at Spain, there is a large gap in the data from the beginning of August to early September,

The two sets of points show markedly different slopes of -6.6×10^{-14} and 5.1×10^{-13} . Since there is no comparable rate change over the same period in the California - Australia data, we conclude that the change in slope is due to a rate change in the H-maser at Spain. However, we are unaware of any deliberate resetting of that clock. Residuals to the fits are shown in Figure 8 and the numerical values given in Table 4,

CONCLUSIONS

In view of the spurious clock and instrumental delay jumps inherent in the data, the fitting residuals from Tables 1-4 of 39 ns, 56 ns (8-point fit), 50 ns, and 43 ns are consistent with the quoted precision of 40 ns in delay measurements. Recent experience with operational phase calibrators and wide bandwidth delay measurements [13] suggests that the observed variability will be much reduced when those features are incorporated into the operational system. When, in addition, the planned enhancements to correct for propagation media and geodynamic effects become operational in 1980, we should have little trouble achieving the delay measurement accuracy required.

ACKNOWLEDGEMENTS

We are grateful to E. Cohen, R. Henderson, R. Shaffer, D. Spitzmesser, and the Deep Space Station personnel for their assistance in scheduling, configuring, and operating the stations, and processing the data.

REFERENCES

1. B. F. Burke, "Long Baseline Interferometry," Phys. Today, vol. 22, pp. 54-63, July 1969,
2. M. H. Cohen, "Introduction to Very-Long-Baseline Interferometry," Proc. IEEE, vol. 61, pp. 1192-1197, September 1973.
3. C. C. Counselman, III, "Very-Long-Baseline Interferometry Techniques Applied to Problems of Geodesy, Geophysics, Planetary Science, Astronomy, and General Relativity," Proc. IEEE, vol. 61, pp. 1225-1230, September 1973.
4. J. B. Thomas et al., "A Demonstration of an Independent-Station Radio Interferometry System with 4-CM Precision on a 16-KM Baseline," J. Geophys. Res., vol. 81, pp. 995-1005, February 1976.
5. I. I. Shapiro, "Principles of Very-Long-Baseline Interferometry," in Proc. of the 9th GEOP Conference, Applications of Geodesy to Geodynamics, October 2-5, 1978, Dept. of Geodetic Science Rept. No. 280, The Ohio State University, Columbus, Ohio, pp. 29-33.
6. C. C. Counselman, III et al., "VLBI Clock Synchronization," Proc. IEEE, vol. 65, pp. 1622-1623, November 1977.
7. T. A. Clark et al., "Synchronization of Clocks by Very-Long-Baseline Interferometry," IEEE Trans. Instr. Meas., vol. IM-28, pp. 184-187, September 1979.
8. A.E.E. Rogers, "A receiver Phase and Group Delay Calibration System for Use in Very-Long-Baseline Interferometry," NERO Haystack Observatory, Westford, MA, Haystack Technical Note 1975-6, 1975.
9. J. B. Thomas, "The Tone Generator and Phase Calibration in VLBI Measurements," DSN Progress Report 42-44, pp. 63-74, January - February 1978.
10. A.E.E. Rogers, "Very-Long-Baseline Interferometry with Large Effective Bandwidth for Phase-Delay Measurements," Radio Sci., vol. 5, pp. 1239-1248, October 1970.
11. J. B. Thomas, "An Analysis of Long Baseline Radio Interferometry, Part III," DSN Progress Report, Technical Report 32-1526, vol XVI, pp. 47-64, August 1973.

REFERENCES (Cont'd)

12. C. M. Cheetham et al., "Demonstration of VLBI Remote Clock Stability Measurements and Three Baseline Closure," these proceedings.
13. L. E. Young, "Traveling Clock Verification of VLBI Clock Synchronization," these proceedings.

Table 1

Clock Offset Data for California-Australia Baseline
30 Sep 78 - 13 Jan 79

Date	Epoch	Measured* offset, μ s	Residual to Fit, ns	Square Root Allan Variance, $\times 10^{-13}$
30 Sep	23.629294	4.844	-29	----
14 Oct	24.844771	6.910	33	----
23 Oct	25.618483	8.156	3	0.63
27 Oct	25.975236	8.744	3	0.49
4 Nov†	26.670332	10.317	430	2.54
29 Nov	28.806020	13.397	-11	3.64
13 Dec	29.981315	14.776	17	3.37
20 Dec	30.671408	15.361	48	3.21
31 Dec	31.543594	15.955	-58	3.01
13 Jan	32.662017	16.984	73	2.88
			RMS 39	

*Approximate sigma for all offsets is 40 ns

†Not included in fit or in RMS residual

Table 2

Clock Offset Data for California - Australia Baseline
23 Oct 78 - 24 Dec 78

Date	Epoch	Measured* Offset, μ s	Residual to 4-point Fit, ns	Residual to 8-point Fit, ns	Square Root Allan Variance, $\times 10^{-13}$
23 Oct	25.655368	-3.965	3	31	----
30 Oct	26.180608	-3.828	-2	8	----
5 Nov	26.754849	-3.672	-2	-11	0.08
20 Nov	28.005401	-3.329	2	-49	0.06
27 Nov	28.611230	-3.184	-18	-88	0.15
3 Dec	29.202867	-2.800	206	116	1.45
16 Dec	30.249901	-2.604	118	-7	1.96
24 Dec	30.942036	-2.385	149	1	1.82
			RMS 99	RMS 56	

Table 3

Clock Offset Data for California-Australia Baseline
19 May 79 - 25 Sep 79

Date	Epoch	Measured Offset, μ s	Residual to Fit, ns	Square Root Allan Variance, $\times 10^{-13}$
19 May	43.492585	26.438	71	----
1 June	44.611414	27.692	-64	----
8 June	45.214741	28.432	-75	0.75
15 June	45.823228	29.324	60	1.31
24 June	46.599963	30.205	-26	1.73
3 July	47.375655	31.205	8	1.59
16 July	48.512931	32.634	22	1.43
6 Aug	50.317639	33.487	---	----
11 Aug	50.743254	33.166	---	----
2 Sep	52.565956	38.348	-46	----
10 Sep	53.255908	39.158	54	----
18 Sep	53.945952	39.851	38	1.20
25 Sep	54.549574	40.391	-44	1.01
			<u>RMS 50</u>	

Table 4

Clock Offset Data for California-Spain Baseline
24 June 79 - 24 Sep 79

Date	Epoch	Measured Offset, μ s	Residual to Fit, ns	Square Root Allan Variance $\times 10^{-13}$
24 June	46.594296	7.641	7	----
3 July	47.370614	7.593	11	----
10 July	47.973634	7.562	20	0.07
16 July	48.484081	7.414	-95	1.19
23 July	49.089347	7.526	58	2.17
10 Sep	53.222916	8.645	-17	----
17 Sep	53.839622	9.010	32	----
24 Sep	54.518217	9.312	-15	1.04
			<u>RMS 43</u>	

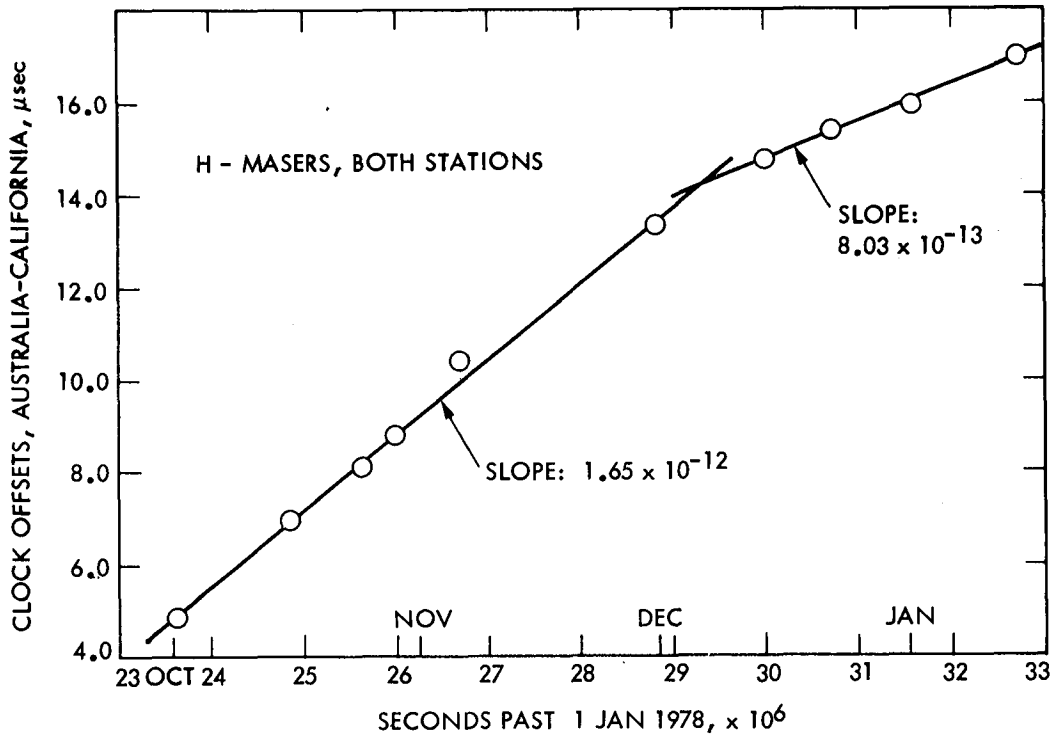


Figure 1. Clock Offsets, Australia Minus California, 30 Sep 79 - 13 Jan 79

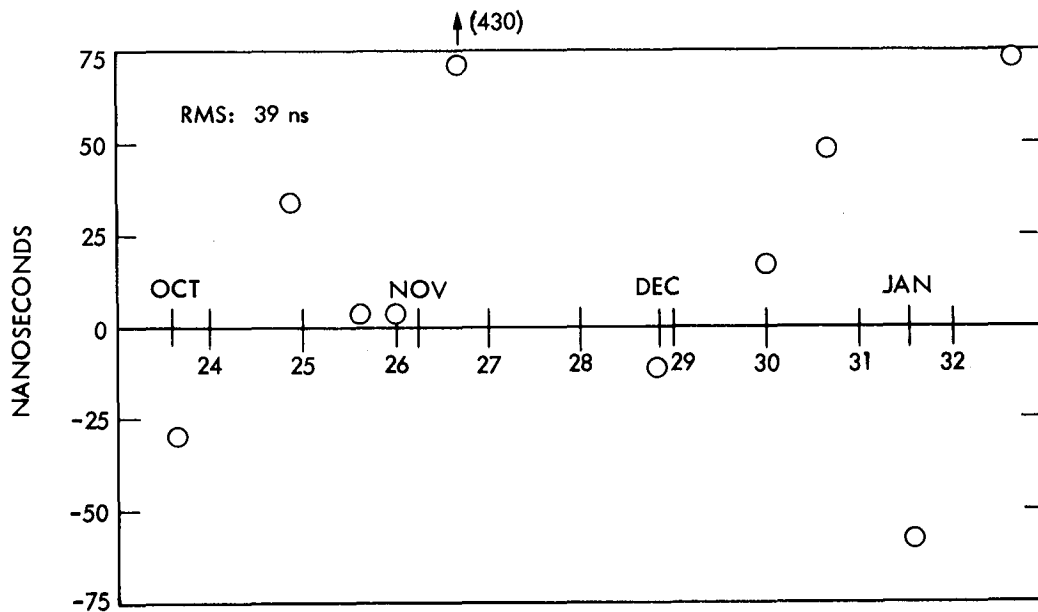


Figure 2. Residuals to Fits, Australia - California, 30 Sep 79 - 13 Jan 79

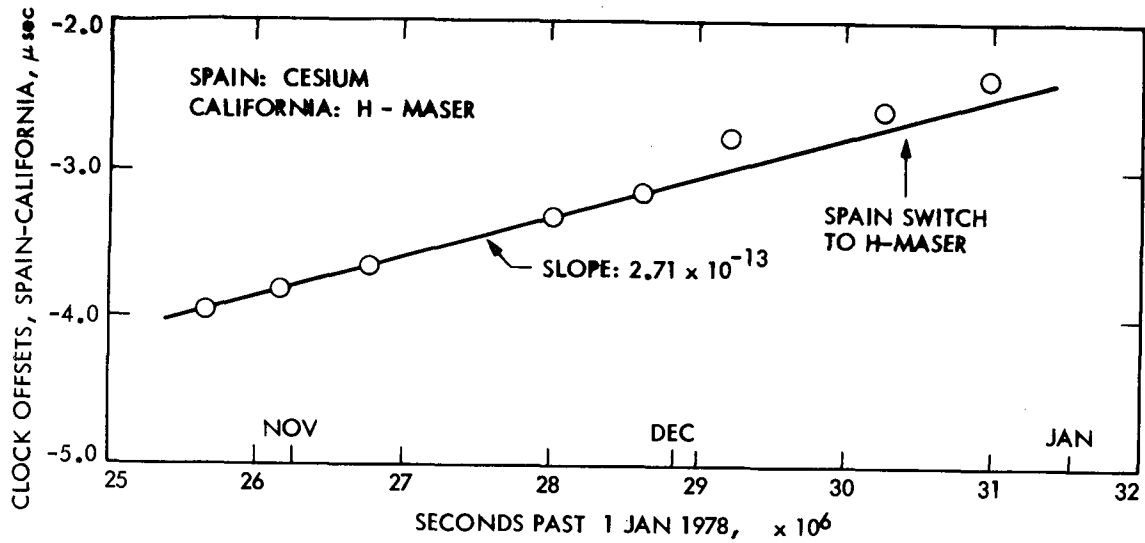


Figure 3. Clock Offsets, Spain Minus California, 23 Oct 78 - 24 Dec 78

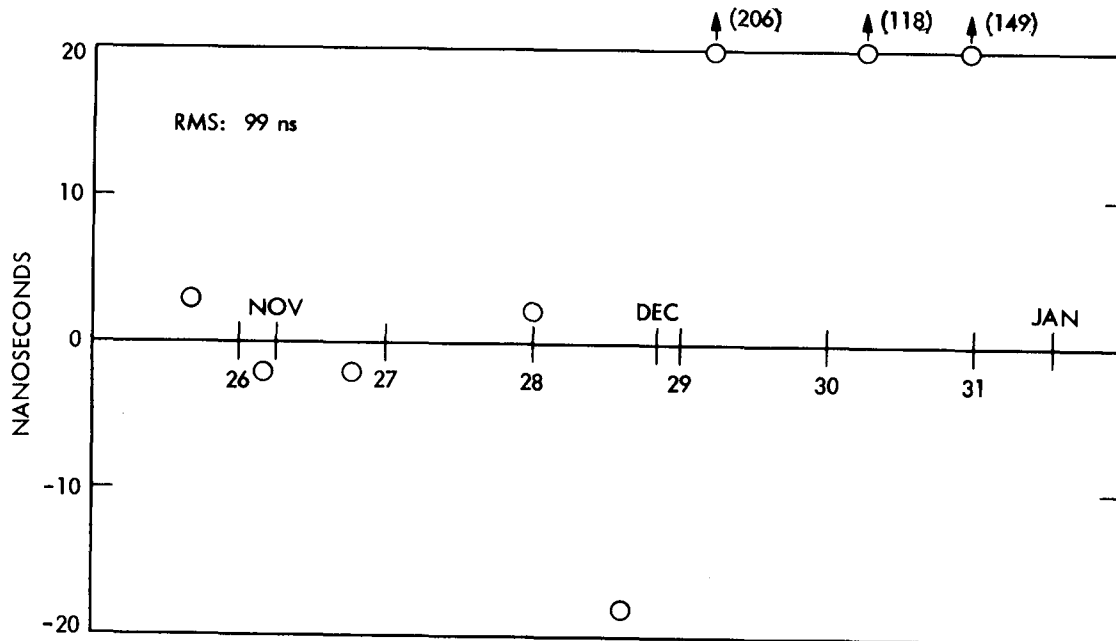


Figure 4. Residuals to 4-point Fit, Spain - California, 23 Oct 78 - 24 Dec 78

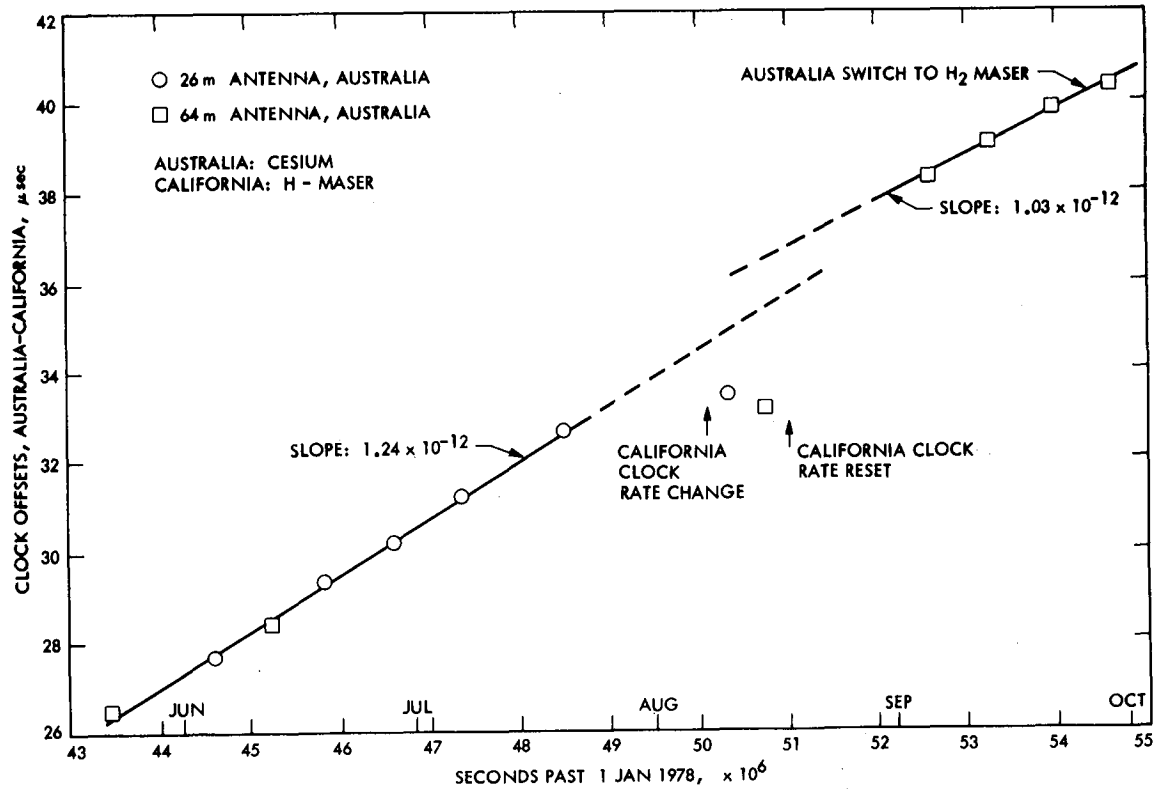


Figure 5. Clock Offsets, Australia Minus California, 19 May 79 - 25 Sep 79

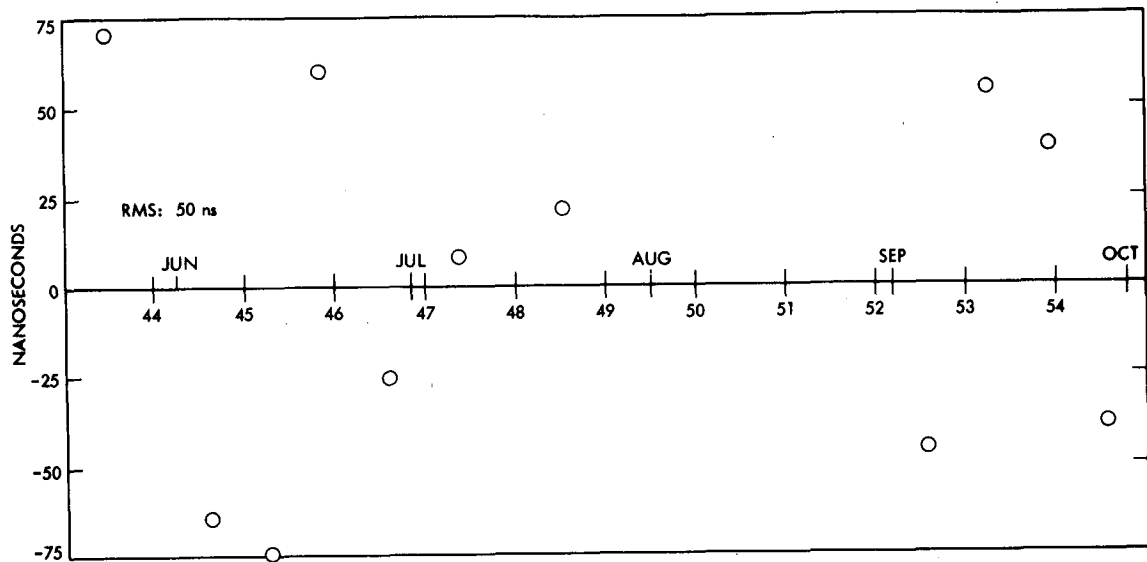


Figure 6. Residuals to Fits, Australia - California, 19 May 79 - 25 Sep 79

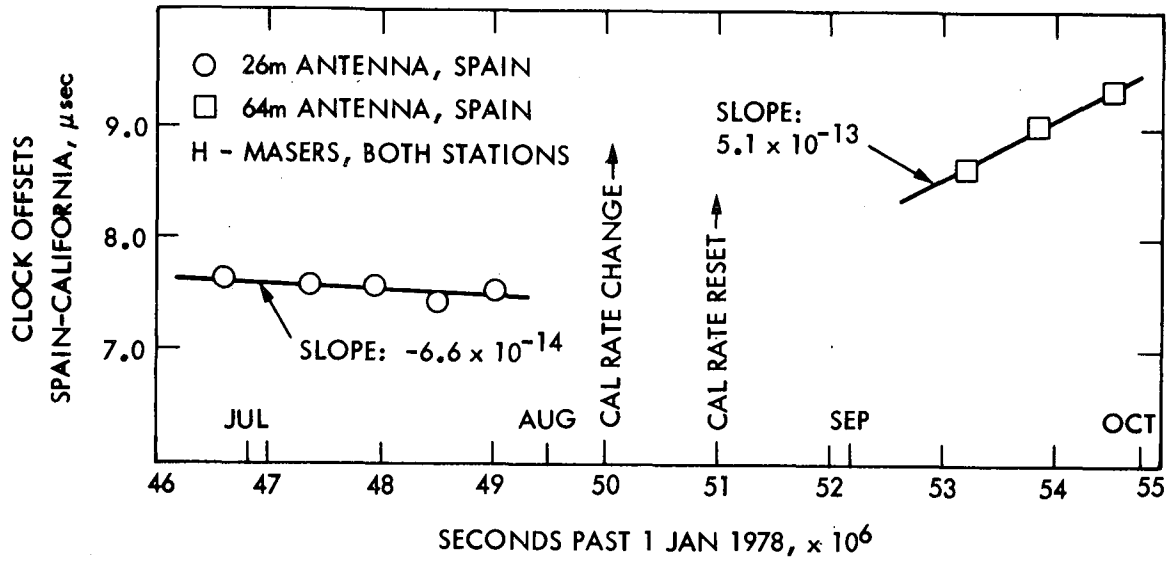


Figure 7. Clock Offsets, Spain Minus California, 24 Jun 79 - 25 Sep 79

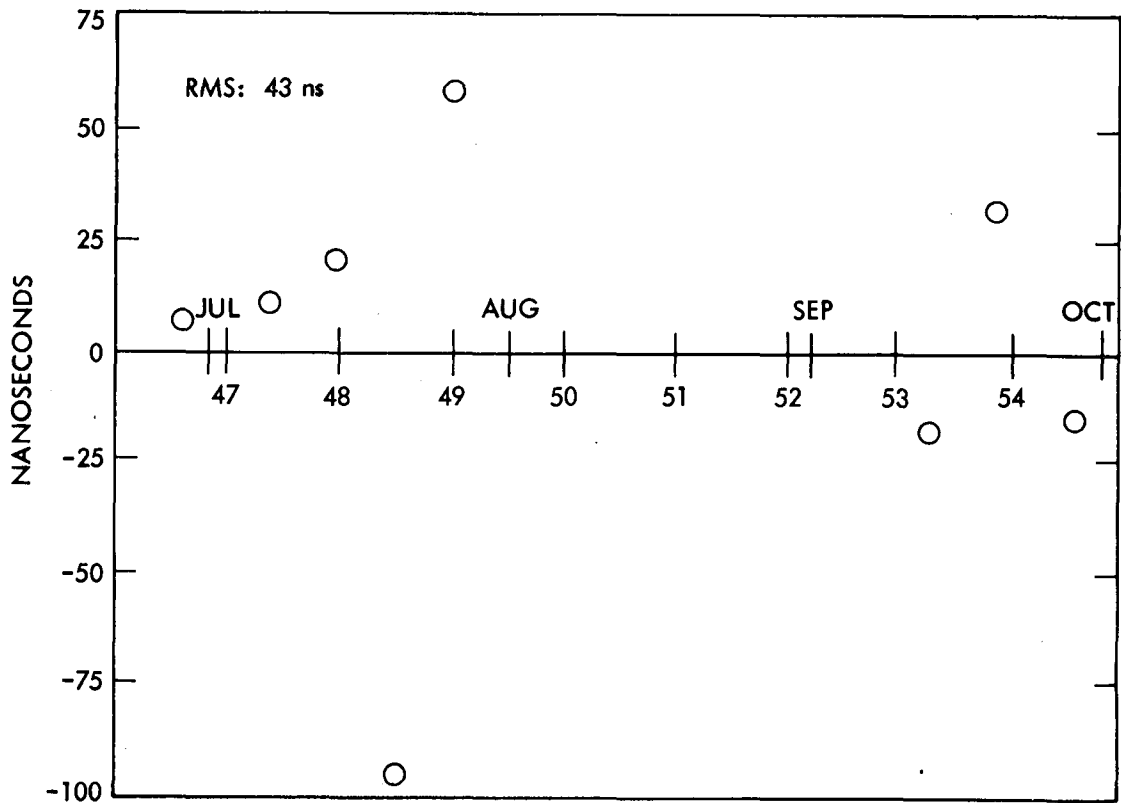


Figure 8. Residuals to Fits, Spain - California, 24 Jun 79 - 25 Sep 79

QUESTIONS AND ANSWERS

DR. CHI:

Are there any other questions? Yes. Would you please use the microphone and identify yourself?

DR. STEVE KNOWLES, Naval Research Laboratory

I would be interested in a few more of the specific details on bandwidth synthesis scheme being used or that you intend to use and how it fits this into the rather narrow bandwidth of your masers?

DR. YUNCK:

The bandwidth synthesis? Well, our receiver/amplifier will admit only a maximum of about 40 megahertz. The channels that we were using for this were 1.8 megahertz and that was purely a signal alignment measurement for delay. So when we use bandwidth synthesis we will go out to 40 megahertz and that is it.

SOURCE STRUCTURE ERRORS IN THE SYNCHRONIZATION OF
CLOCKS BY RADIO INTERFEROMETRY

J. B. Thomas
Jet Propulsion Laboratory, Pasadena, California

ABSTRACT

Radio interferometry has the potential of synchronizing clocks across intercontinental distances with accuracies better than one nanosecond. One of the potential error sources in such determinations is the spatial structure of the natural radio sources that provide the reference signals. Due to their extent, the effective position of these sources can vary as a function of the length and orientation of the baseline vector joining the two antennas. If they are not corrected, such variations can lead to errors in clock synchronization. This presentation discusses the theory of structure corrections and gives specific examples to illustrate the nature and size of the effect.

INTRODUCTION

Radio interferometry with natural radio sources has the potential for very accurately synchronizing clocks over distances up to intercontinental lengths, possibly eventually reaching accuracies of the order of 0.1 nsec. Comparisons of absolute clock synchronization by interferometry with the measurements obtained by traveling clocks have already been carried out at the 10-20 nsec level by the MIT VLBI group and at the 5 nsec level by the JPL VLBI group (see L. E. Young's presentation in this conference). One of the error sources that can degrade high accuracy synchronization measurements is the extended structure of the natural sources. In this talk, I will present the results of a study to estimate the size of this particular error source. Before the results of that study are outlined, a few slides of background explanation will be presented for those unfamiliar with the source structure problem.

INTERFEROMETRY THEORY

The first slide is a schematic representation of the basic geometry of the interferometry process and defines the baseline vector, source direction, and geometric delay. Given two antennas, the basic idea is to measure the difference in arrival times of a radio signal from a natural source. After appropriate calibrations, the measured delay will be equal to the geometric delay plus a clock synchronization offset. If the geometric delay can be removed on the basis of a priori knowledge of source direction, earth orientation, etc., then the offset between station clocks can be extracted. If the position of the source is uncertain due to extended structure, clock synchronization determinations will be impaired.

This same slide also presents the first step of the data reduction procedure used to extract delay. The analysis has been reduced to an ideal form and includes a simplified derivation of the fringes that would be obtained by perfect instrumentation when a monochromatic signal is recorded for a point source. A sinusoidal voltage signal is recorded at both stations but the signal at station 2 is offset in time by the geometric delay τ_g and by a clock synchronization error τ_c (relative to station 1). The signals recorded at the two stations are multiplied together (cross-correlated) to produce the sinusoidal cross-correlation function referred to as fringes. The fringe phase is extracted by post-correlation software and is equal to a product of observing frequency and $\tau_g + \tau_c$. As shown in the next slide (2), when the phase is observed at two frequencies (separated by about 40 MHz in JPL efforts), the two phase values can be combined as indicated to obtain the observed delay τ_{BWS} .

Integer cycle ambiguities in τ_{BWS} resulting from phase ambiguities can be removed on the basis of a priori information and/or the delays from other more closely spaced channel pairs. The resulting delay will be referred to as the bandwidth synthesis (BWS) delay. As indicated, the synchronization offset is obtained by subtracting from the BWS delay an a priori model for geometric delay. Synchronization measurements can be no more accurate than the accuracy of this geometric model. If the source is extended, the specification of source position, and therefore geometric delay, becomes uncertain.

To begin to explain structure effects, it is useful to present a simplified derivation of the fringes for a double-point source. As we shall see, these results can then be easily generalized

to an arbitrary brightness distribution. As shown in the next slide (3), suppose two points in the sky radiate with power a_1^2 and a_2^2 at positions \hat{S} and \hat{S}' . If the points radiate uncorrelated signals, the observed fringes will be the sum of the fringe expressions separately derived for each point (see slide 1). As shown, the sum can be rewritten as a product of a modulating factor R and the fringes from point source 1. The factor R depends on the difference of the source vectors $(\hat{S}' - \hat{S})$ and varies as a function of baseline \vec{B} , ranging between summed power $(a_1^2 + a_2^2)$ and difference power $(a_1^2 - a_2^2)$. Remember the form of these terms in R - power times a phasor - since they will be used later to generalize to an arbitrary distribution.

As suggested in the present slide (3) and stated in the next slide (4), the maximum constructive interference occurs when the difference in geometric delay for the two points is equal to an integral number of wavelengths of the observed signal. If the position difference $(\delta\hat{S} = \hat{S}' - \hat{S})$ is converted into an angular differential representing the corresponding change in angle (ψ) between baseline vector and source detection, one obtains an expression for the angular separation of adjacent lines on the celestial sphere between which constructive interference of source emissions would occur. (The meaning of $\delta\hat{S}$ is changed here to denote the vector difference between two possible points of radio emission on the celestial sphere). These lines are usually referred to as fringes on the sky. Note that, as baseline length increases or as wavelength decreases, the spacing of the sky fringes decreases. Further, minimum fringe spacing occurs when the source direction is perpendicular to the baseline vector ($\psi = 90^\circ$). For $B = 10,000$ km and $\lambda = 3.5$ cm ($f = 8.5$ GHz), the minimum fringe spacing (maximum resolution) is 3.5 nrad ($0''.0007$).

The next slide (5) schematically shows the changes in effective position for a hypothetical extended source as baseline length changes. The source is assumed to consist of a point source placed next to a diffuse component. For the short baseline, the fringe spacing is large compared to the size of the source. Since all components contribute to the cross-correlation without destructive interference, the effective source position will

be equal to the centroid of the two components. For the long baseline, the fringe spacing decreases so much that the diffuse component is much larger than the fringe spacing and different parts of that component destructively interfere with one another. Consequently, this component is "resolved out" to such an extent that it effectively does not contribute to cross-correlation. Thus, for the long baseline, the effective position moves and becomes the position of the point component. This example emphasizes the possible dependence of effective source position on baseline length and orientation.

As summarized on the next slide (6), one can easily generalize the analysis for the double-point source to an arbitrary brightness distribution. By adding more points to the sum in slide 3, and then converting the sum to an integral, one obtains the factor R for the general distribution. The factor R , usually referred to as the brightness transform or complex visibility function, becomes the complex Fourier transform of the brightness distribution. The reference position \hat{S}_0 , which was placed at the strongest point for a double-point source, is arbitrary at this point, provided it is near the source.

The next slide (7) shows how structure phase ϕ_B and fringe amplitude are defined from the complex brightness transform. When total fringe phase is measured, this structure phase will be one of the components. As shown in slide 2, the observed BWS delay is essentially the derivative of phase w.r.t. frequency. Thus the contribution of structure to the measured BWS delay will be approximately given by the partial of ϕ_B w.r.t. frequency. Such partials can be readily obtained for both analytical and measured (numerical) source distributions.

The next slide (8) presents without derivation the equation for computing the effective position of a source, given a brightness distribution independent of time and frequency. For computational convenience, the effective position is computed relative to an assigned reference position \hat{S}_0 .

One can show that, for a given observation, the extended source can be analytically replaced by a point source located at the effective position. With this and only this assigned position, the hypothetical point source will produce the same geometric delay and geometric delay rate as the actual source when the BWS delay and phase-delay rate are the observables.

As can be seen, the effective position is a relative of the ordinary centroid but is based on the quadrature components of the resolved distribution. Given a measured brightness distribution, this expression for effective position can be readily evaluated. One can easily show that the effective position becomes the ordinary centroid when the baseline approaches zero, as one would expect.

Before structure effects can be properly removed in clock synch measurements based on a single source, the absolute location of the brightness distribution for that source must be accurately determined relative to a global set of celestial coordinates. When obtained through multibaseline VLBI measurements, the brightness distribution for a source will be accurately determined relative to a set of local coordinates (structure coordinates) specific to that source but will not be accurately placed on the celestial sphere in one absolute sense. Accurate absolute positions are usually obtained by multiparameter fits to the delay values for many sources, where the delays are obtained through VLBI measurements independent of the structure measurements. For these solve-for locations to have meaning relative to the brightness distribution, each observation of delay for a given source must be corrected for the difference between effective position and some constant reference position, where both are computed in structure coordinates. The solve-for position of the source will then be the absolute location of the reference position for that source.

TWO EXAMPLES OF ANALYTICAL SOURCES

For the first example, the next slide (9) derives equations for the structure effects of a double-point source. As can be seen from slide 3, the brightness transform can be rewritten as a function of only two variables: the relative strength (g_2) of point source 2 and the projected separation (p) of the two sources in units of resolution. Both the phase and delay effects of structure become a function of these same two parameters. As explained in previous slides, the delay is obtained by taking the partial of phase w.r.t. frequency, but, for brevity, this operation is not shown.

The next slide (10) shows how the effective position of a double-point source varies as a function of p (the projected source separation in units of resolution) for selected ratios of the

point strengths. The plot can be constructed in this manner due to the fact that the effective position of a double-point source always lies on the line drawn through the two points. As shown, the effective position is equal to the ordinary centroid when the resolution is large compared to the source extent (i.e. when $p = 0$). As the resolution improves (i.e. as Δ decreases so that p increases), the effective position moves away from the ordinary centroid and can move far outside the extent of the source. In fact, for nearly equal point strengths, the effective position approaches infinity when $p = \text{integer}/2$. These nearly singular points correspond to points of large delay excursion as will be shown in the next slide.

This slide (11) plots the delay effect for a double-point source as a function of the same two parameters. The plotted values are referenced to the brightness centroid of the source rather than to the brightest component. This shift, which is not derived here, results in the subtraction of a simple term from the phase expression in slide (9). As can be seen in the plot, there can be critical values of baseline vector for which the delay effect becomes very large, even approaching infinity if the source strengths are nearly equal. These singular points occur when the component phasors sum to zero so that small changes in p can produce large changes in phase. These undesirable regions can be eliminated to a large extent by placing a lower limit on relative fringe amplitude. When the weaker source is 0.95 of the strength of the stronger source, the maximum delay effect at 8.5 GHz is 1.2 nsec for $p = 0.5$ cycle. This plot indicates that, except for the unusual case of very nearly equal point strengths, the structure effect of a double point source would be small relative to the present VLBI clock synchronization capabilities (~ 5 nsec). However, when clock synch accuracy reaches 0.1 nsec, structure effects will be very important.

For the second example, the next slide (12) presents the equations for the structure effects of a triple-point source. Note that phase and delay effects can be expressed as a function of four variables: the relative strengths (g_2, g_3) of point sources 2 and 3 and the two variables (p, q) that give the projected separations (in units of resolution) of point sources 2 and 3. When parametrized in this manner, the delay results can be used for any triple-point source with the specified values for (g_2, g_3) regardless of the point separations and directions. Two cases will be shown to illustrate typical delay behavior

for a triple-point source. The next slide (13) presents the first case and plots delay as a function of p and q for the strength values $g_2 = 0.2$ and $g_3 = 0.4$. Note that there are extrema in delay that occur with lattice-like regularity. It can be easily shown that these extrema correspond to points of minimum fringe amplitude. The extrema occur when p and q are multiples of 0.5, provided $g_2 + g_3 < 1$. For the example in this slide, the first delay extremum reaches 0.1 nsec at $p = q = 0.5$.

The next slide (14) presents the second case and shows the structure delay associated with a triple-point source with relative strength values $g_2 = 0.4$ and $g_3 = 0.8$. There are local regions in the (p, q) plane where the structure delay becomes very large and even certain points where it approaches infinity. In this slide, the delays are truncated above 1 nsec to improve the plots. As suggested by the sharp dips near the positive peaks, the delay goes to negative infinity next to each point of positive infinity. This behavior is demonstrated in the next slide (15) where the delay is inverted. These singular points occur whenever the amplitude drops to zero. One can easily show by means of three-phaser sums that, if $g_2 + g_3 \geq 1$, singular points can always be found on a lattice of points in the (p, q) plane. (We assume here that point source 1 has the greatest flux). One beneficial characteristic of such singular regions is that they can always be detected (and therefore avoided in large measure) through a drop in amplitude. Note that, in the regions between adjacent null points, the delay effect reaches 0.3 - 1.0 nsec for the plotted range of (p, q) .

SUMMARY AND CONCLUSIONS

The analytical examples presented here indicate that, if a source can be accurately represented by a double-point or triple-point model, it might be necessary to avoid certain critical values of the baseline vector. At the critical points, the delay effect can even theoretically approach infinity for a pure multipoint source. The effective position at these points can move far outside the extent of the source. However it is unusual for a real source to consist solely of two or three sharp points. Real distributions tend to possess extended component rather than point features and usually have additional weaker components or background features. These characteristics would blunt the truly singular behavior found in pure multipoint models. Nevertheless, it seems likely that the structure effect in BWS delay will

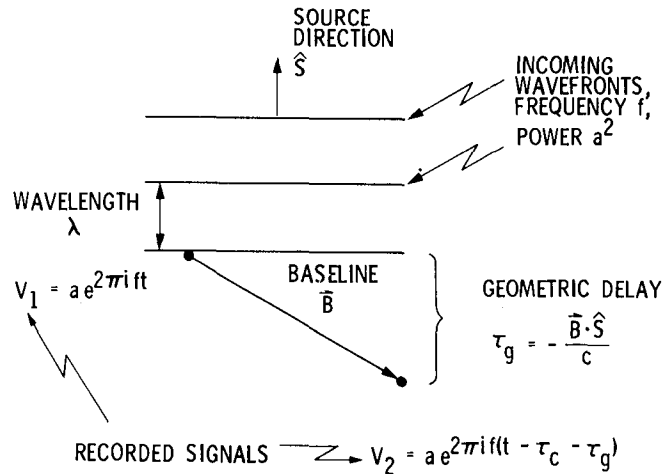
be of the order of 0.5 nanosecond for some real sources at some baseline values. At the nanosecond level, structure effects would be small compared to present VLBI clock synch capabilities (~ 5 nsec). When VLBI clock synch reaches the 0.1 nsec level, structure effects are likely to become an important consideration.

The analysis presented here has concentrated on the BWS-delay observable. Unlike BWS delay, phase delay does not diverge to infinity near points of zero amplitude. In such cases, the phase-delay observable will be subject to less extreme structure errors than BWS delay. Therefore, even though the development of a phase-delay system is more difficult, the phase-delay observable has important advantages with regard to structure effects.

In order to obtain a more accurate assessment of structure effects, an effort is underway to analyze measured brightness distributions for a number of real sources. That study will help to assess the feasibility of limiting the size of structure effects through judicious selection of sources and/or through enforcement of a lower limit on relative fringe amplitude.

ACKNOWLEDGEMENTS

I would like to thank Sue Finley for her enthusiastic assistance in generating the three-dimensional computer plots of structure delay for a triple-point source. This paper presents the results of one phase of research carried out at the Jet Propulsion Laboratory, California Institute of Technology, under contract No. NAS 7-100, sponsored by the National Aeronautics and Space Administration.



CROSS-CORRELATE TO OBTAIN FRINGES:

$$V_1 V_2^* = a^2 e^{2\pi i f (\tau_c + \tau_g)}$$

Figure 1. Interferometry with Perfect Instrumentation, Point Source & Monochromatic-Signal

PHASE EXTRACTED FROM FRINGES:

$$\phi = f (\tau_c + \tau_g) \quad \text{AT FREQUENCY } f$$

$$\phi' = f' (\tau_c + \tau_g) \quad \text{AT FREQUENCY } f'$$

COMPUTE DELAY FROM PHASE:

$$\tau_{\text{BWS}} = \frac{\phi' - \phi}{f' - f} = \tau_c + \tau_g$$

USE A PRIORI TO EXTRACT CLOCK SYNCH:

$$\tau_c^{(\text{obs})} = \tau_{\text{BWS}} - \tau_g^{(\text{model})}$$

Figure 2. Phase, Delay and Clock Synch from VLBI

GIVEN TWO POINTS WITH POSITIONS (\hat{S} , \hat{S}') AND STRENGTHS (a_1^2 , a_2^2)

GEOMETRIC DELAYS:

$$\tau_g = -\vec{B} \cdot \hat{S} / c \quad \tau'_g = -\vec{B} \cdot \hat{S}' / c$$

FRINGES FROM CROSS-CORRELATION:

$$\begin{aligned} V_1 V_2^* &= a_1^2 e^{2\pi i f (\tau_c + \tau_g)} + a_2^2 e^{2\pi i f (\tau_c + \tau'_g)} \\ &= R e^{2\pi i f (\tau_c + \tau_g)} \end{aligned}$$

WHERE

$$R \equiv a_1^2 + a_2^2 e^{-2\pi i f \vec{B} \cdot \delta \vec{S} / c}$$

$$\delta \vec{S} = \hat{S}' - \hat{S}$$

Figure 3. Fringes for a Double-Point Source

AMPLITUDE $|R|$ = MAXIMUM WHEN

$$f \vec{B} \cdot \delta \vec{S} / c = \text{INTEGER.}$$

IF

$$\vec{B} \cdot \hat{S} = B \cos \psi$$

SO THAT

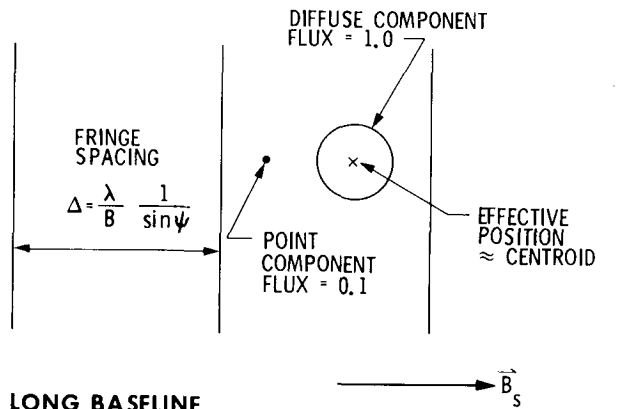
$$\vec{B} \cdot \delta \vec{S} = -B \sin \psi \delta \psi$$

THEN FRINGE SPACING (RESOLUTION) BECOMES

$$\Delta = \frac{\lambda}{B} \frac{1}{\sin \psi}$$

Figure 4. Fringes on the Sky

SHORT BASELINE



LONG BASELINE

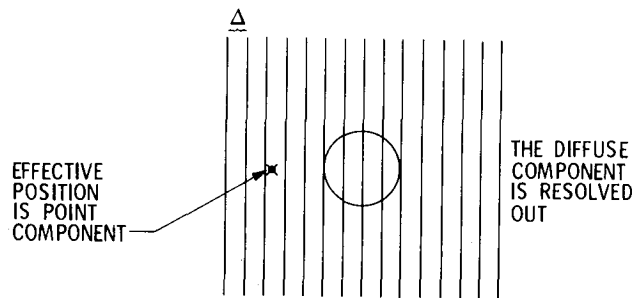


Figure 5. Schematic Example of Effective Position

FOR GENERAL SOURCE

$$R\left(\frac{\vec{B}_s}{\lambda}\right) = \iint D(\hat{S}) e^{-2\pi i \vec{B}_s \cdot \delta\hat{S}/\lambda} d\Omega_{\delta\hat{S}}$$

WHERE

$D(\hat{S})$ = BRIGHTNESS DISTRIBUTION

$d\Omega_{\delta\hat{S}}$ = "AREA" DIFFERENTIAL ON PLANE OF SKY

$$\delta\hat{S} = \hat{S} - \hat{S}_0$$

\hat{S}_0 = ASSIGNED REFERENCE POSITION

\vec{B}_s = SKY-PROJECTED BASELINE VECTOR

Figure 6. The Brightness Transform

REWRITE BRIGHTNESS TRANSFORM

$$R = |R| e^{i2\pi\phi_B}$$

WHERE

$$|R| = \text{FRINGE AMPLITUDE}$$

$$\phi_B = \text{STRUCTURE PHASE}$$

STRUCTURE EFFECT ON τ_{BWS} :

$$\Delta\tau \approx \frac{\partial\phi_B}{\partial f}$$

Figure 7. Structure Phase and Delay

$$\langle \delta\vec{S} \rangle_E = \frac{Z_c^2 \langle \delta\vec{S} \rangle_c + Z_s^2 \langle \delta\vec{S} \rangle_s}{Z_c^2 + Z_s^2}$$

WHERE

$$\langle \delta\vec{S} \rangle_c \equiv \frac{1}{Z_c} \int \delta\vec{S} D(\hat{S}) \cos(2\pi\vec{B}_s \cdot \delta\vec{S}/\lambda) d\Omega_{\delta\vec{S}}$$

$$\langle \delta\vec{S} \rangle_s \equiv \frac{1}{Z_s} \int \delta\vec{S} D(\hat{S}) \sin(2\pi\vec{B}_s \cdot \delta\vec{S}/\lambda) d\Omega_{\delta\vec{S}}$$

$$\delta\vec{S} = \hat{S} - \hat{S}_0$$

$(Z_c, -Z_s) = (\text{REAL}, \text{IMAG})$ PART OF BRIGHTNESS TRANSFORM

*FOR BWS DELAY AND PHASE-DELAY RATE

Figure 8. Computation of Effective Position* from the Brightness Distribution

REWRITE EARLIER RESULT AS

$$R \propto 1 + g_2 e^{-i2\pi p}$$

WHERE

$$g_2 \equiv a_2^2 / a_1^2 \quad \text{AND} \quad p \equiv \hat{B}_s \cdot \delta \vec{S} / \Delta$$

FOR WHICH $\Delta \equiv \frac{\lambda}{B \sin \psi}$ = RESOLUTION

\hat{B}_s = UNIT. SKY-PROJECTED BASELINE VECTOR

STRUCTURE PHASE BECOMES

$$\phi_B = \tan^{-1} \left[\frac{-g_2 \sin 2\pi p}{1 + g_2 \cos 2\pi p} \right]$$

Figure 9. Structure Effect for a Double-Point Source

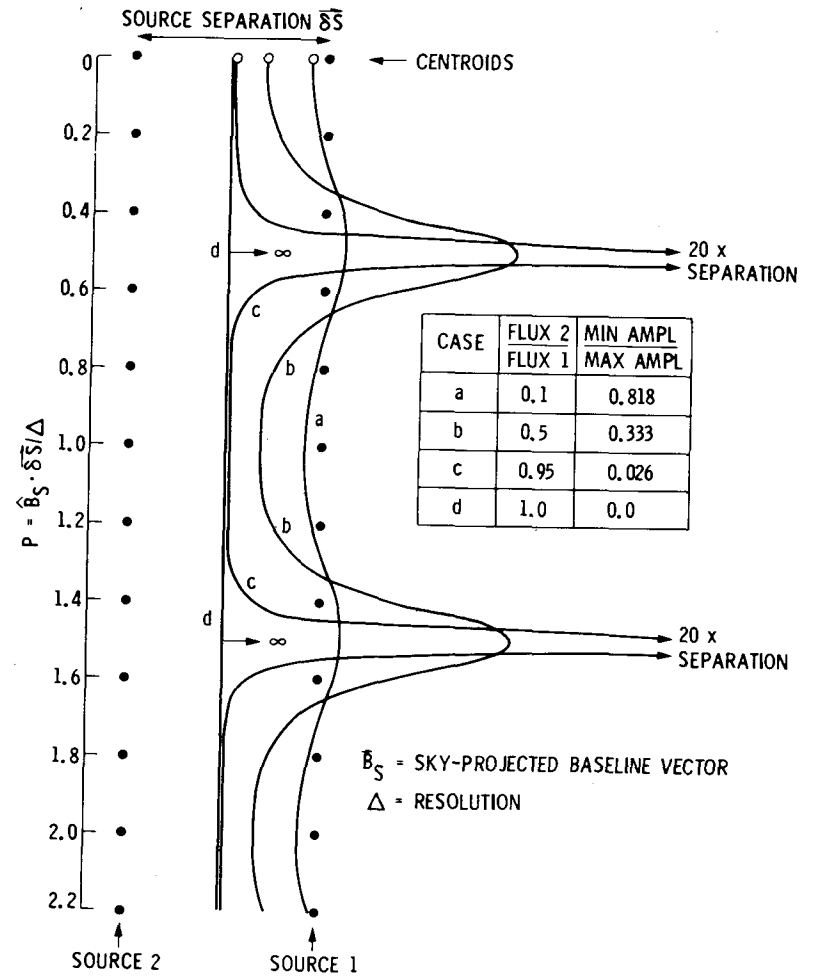


Figure 10. Effective Position for Frequency-Independent Double-Point Source: BWS Delay and Delay Rate

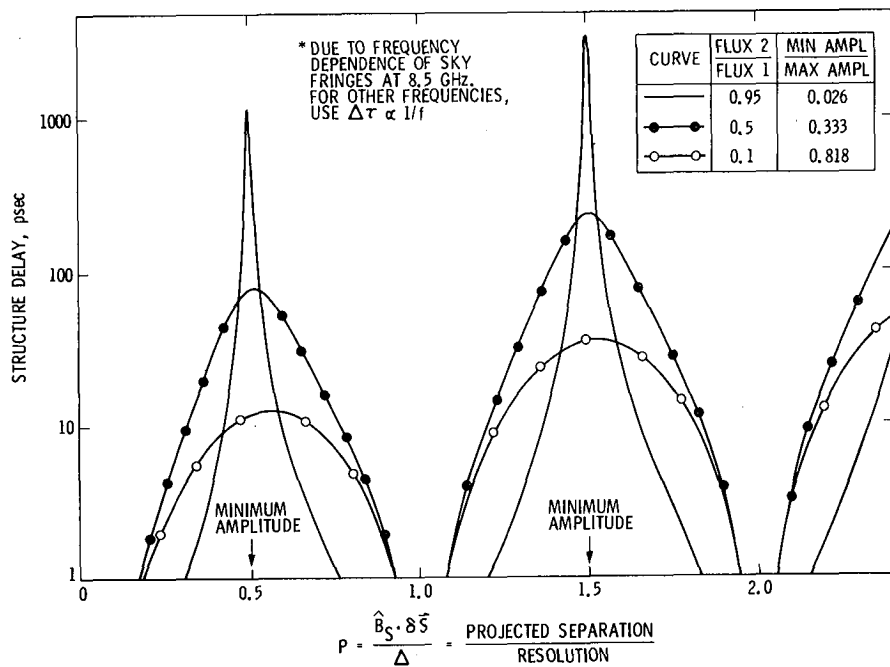


Figure 11. BWS Delay* Relative to Brightness Centroid for Double-Point Source

IN ANALOGY WITH DOUBLE-POINT SOURCE

$$R = 1 + g_2 e^{-i2\pi p} + g_3 e^{-i2\pi q}$$

WHERE

$$p = \frac{\hat{B}_s \cdot \delta \vec{S}_2}{\Delta} \quad q = \frac{\hat{B}_s \cdot \delta \vec{S}_3}{\Delta}$$

AND

$$\delta \vec{S}_K \equiv \hat{S}_K - \hat{S}_1 \quad g_K \equiv a_K^2 / a_1^2$$

STRUCTURE PHASE BECOMES

$$\phi_B = \tan^{-1} \left[\frac{-g_2 \sin 2\pi p - g_3 \sin 2\pi q}{1 + g_2 \cos 2\pi p + g_3 \cos 2\pi q} \right]$$

Figure 12. Structure Effect for a Triple-Point Source

FLUX1=1.0
FLUX2= .2
FLUX3= .4
FREQ= 8.5GHZ

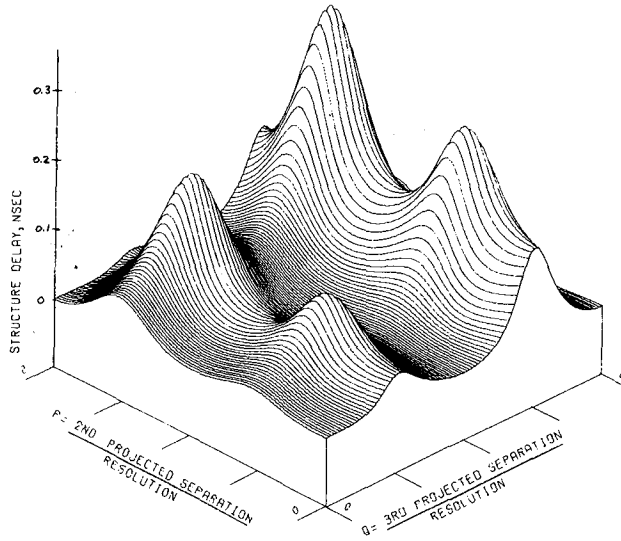


Figure 13. BWS Delay Relative to Brightness Centroid for a Triple-Point Source

FLUX1=1.0
FLUX2= .4
FLUX3= .4
FREQ= 8.5GHZ

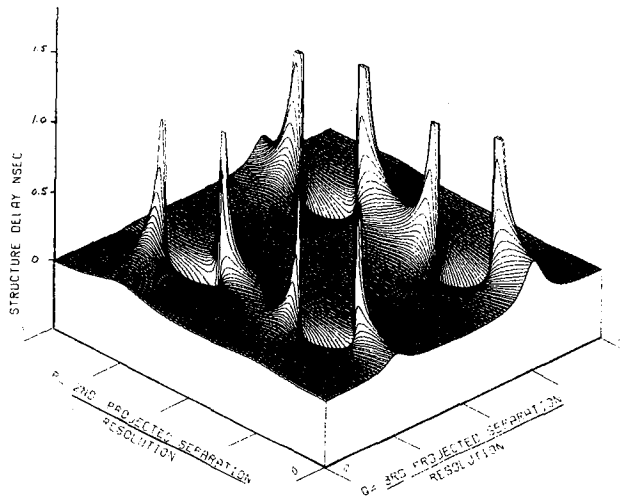


Figure 14. BWS Delay Relative to Brightness Centroid for a Triple-Point Source

FLUX1=1.0
FLUX2= .4
FLUX3= .8
FREQ= 8.5GHZ

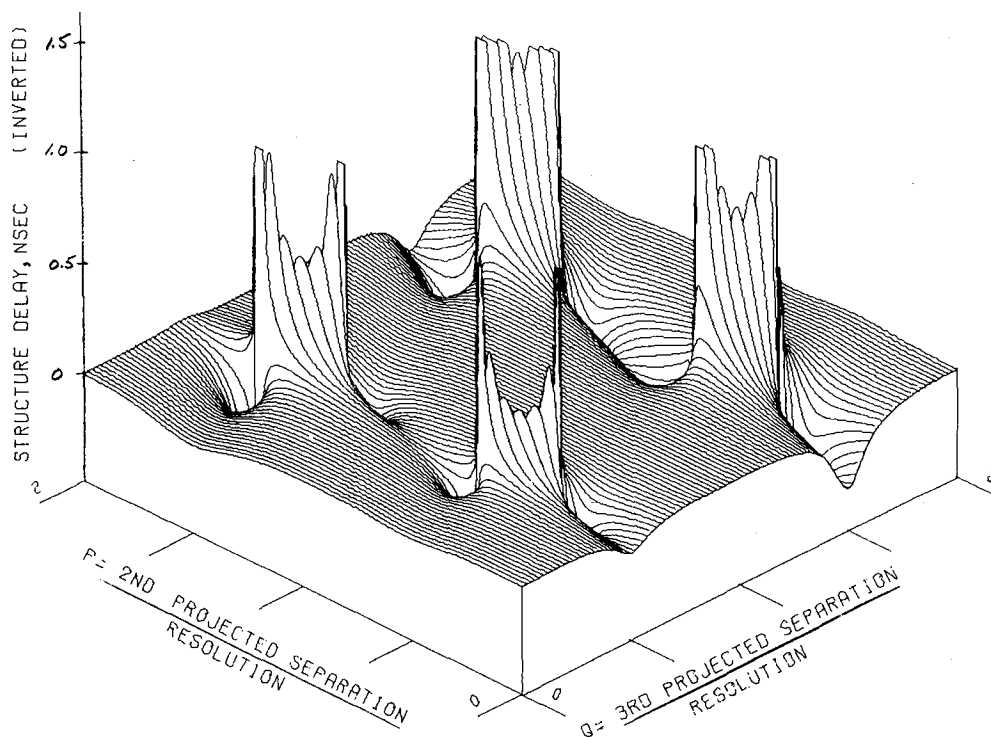


Figure 15. BWS Delay Relative to Brightness Centroid for a Triple-Point Source

QUESTIONS AND ANSWERS

DR. ALLEY:

Where is worldwide time synchronization at the level of the 1/10 nanosecond readily available, because this assists in the unraveling of the source structure of the interferometry measurement.

DR. THOMAS:

Yes it might, but there are better ways to approach that problem. One of the best tests for approaching whether the theory presented here will be useful in correcting for source structure is to do differential measurements between close adjacent pairs of sources and that way all the typical error sources in VLBI cancel out except for a very few minor ones and then you can look at the actual variations in delay at a very accurate level and can take measurements of brightness distributions to predict what those variations are and see if you get the same results. So we plan to try things like that, if possible, to check our structure calculations. Otherwise, the structure effects tend to get messed up in all of your other error sources in normal interferometry.

DR. TOM CLARK, NASA, Goddard

I just had a couple of brief comments, Brooks. First of all, the information that you show proves that one man's signal is another man's noise, because exactly the same source structure that poses problems in things like clock synchronization or geodesy is exactly what is of interest to the radio astronomer who wants to study these same objects for his other purposes.

One of the things which you might want to stress is that the typical VLBI observation, as was pointed out by Larry Young in his comments and so forth, does not involve just a single source or complex source whatever, but tends to involve anywhere from a half a dozen upwards of 50, depending upon the nature of the observing program, a number of sources on the sky. And although Nature may be a bitch and conspire against you on one source, the chances that she will also be conspiring against you on eight others at the same time is very small. So, in a real experiment, I think these, effects tend to go down much smaller.

There is one other thing which can be done in this to improve the situation and give you additional information. You, of course, pointed out that when the amplitude goes to zero that is the time at which the phase becomes undefined, hence the derivative of phase with respect to frequency becomes undefined and you can't define apocryphae when there are no fringes. That is sort of the summary.

One thing which you can also do at that time is if you are running an interferometer with more than two stations, let us say three, by summing the observed phases around the loop of three stations, all of the instrumental phases cancel out, but the structure phase, at least in its total, around the loop, is still unobservable, so by looking at the closure phase on a three-station interferometer, you can immediately pinpoint when you are having the bad apples problems that can foul up clock synchronization.

DR. THOMAS:

Okay. That is true. One has to be careful though, there may be cases when one wants to do clock synch with not many, many sources but maybe one or two and you want to go out and take a quick measurement of some sort with some limited antenna system or whatever. So it is not always true with clock synch you are going to have 50 sorters or so. It could be a case where you run with only one or two. And also with clock synch. I am not sure that there would always be the funds available to do a closure experiment with three antennas. I suspect it would be a lot more limited effort than that, where you will have a couple of antennas out just to do a clock synch between the stations in question. So, I mean, while your comments are true, I think they might be of limited use.

THE LASSO PROGRAM – AN OVERVIEW

**Professor S. Leschiutta
National Electrical – Technical Institute
National Standards Laboratory
Torino, Italy**

(PAPER NOT AVAILABLE FOR PUBLICATION)

PROSPECTS FOR ADVANCES IN MICROWAVE
ATOMIC FREQUENCY STANDARDS*

F. L. Walls
National Bureau of Standards
Boulder, Colorado

ABSTRACT

This paper will focus on conceptual and component developments which could have a major impact on the performance of microwave atomic frequency standards. Traditional microwave standards based on rubidium, cesium and hydrogen have been greatly refined over the past decade, such that the frequency stability of the current generation of devices is generally limited by the basic concepts on which they are based, as well as the performance of various key subsystems. Future advances in ultimate frequency stability and environmental performance will primarily come from new conceptual developments, and only secondarily from improved components. These new advances will be explored in some detail and projections for possible performance improvements made for microwave frequency standards based on rubidium, cesium and hydrogen. Brief mention of a new class of standards based on stored ions will be made.

*Contribution of National Bureau of Standards, not subject to copyright in the United States.

INTRODUCTION

The next few years will, in my opinion, bring significant changes in atomic microwave frequency standards. Traditional standards based on rubidium, cesium and hydrogen have been greatly refined over the past decade, such that that the frequency stability of the current generation of devices is generally limited by those basic concepts on which they are based. In my opinion, future advances in frequency stability will principally come from changes in the concepts on which the standards are based, and only secondarily from more careful engineering of the old concepts.

In the following, I will point out what I consider the fundamental limitations in these standards and indicate the important conceptual and component advances which could have a major impact on future performance of these standards. In addition, brief mention is made of a very promising new class of microwave standards based on ion storage techniques.

RUBIDIUM FREQUENCY STANDARDS

Fig. 1 shows a generalized block diagram of a rubidium gas cell frequency standard. Because of the small size, weight and cost, these standards are the most abundant of all atomic frequency standards. The short term stability is of order $5 \times 10^{-12} \tau^{-1/2}$ limited by shot noise in the background optical signal with the rubidium hyperfine signal being about 0.5% of the total detected signal.^[1] Long-term frequency stability is affected by many things; such as temperature of the buffer gas, density of the Rb, magnetic field gradients, microwave power variations, light spectrum changes, etc. The common contributor to most of these effects is the highly asymmetric hyperfine resonance caused by the presence

of the buffer gas, which essentially causes each interacting atom to sample a very small portion of the total cell volume. The buffer gas is primarily used to isolate the rubidium from the walls of the cell where it would normally relax, typically causing a frequency shift of order $\frac{\Delta\nu}{\nu} = 5 \times 10^{-7}$.^[2] Typical linewidths are of order 300 Hz (6.8×10^9), yielding a hyperfine line Q of $\cong 2 \times 10^7$. The very nature of the way the buffer gas acts causes a fundamental problem so that even excellent engineering is hard pressed to achieve frequency stabilities of better than $\cong 10^{-13}$ at several hours and provide a frequency reproducibility or retrace following several turn off/turn on cycles of 10^{-11} . For example, 0.4dB change in microwave power caused a frequency change of order 10^{-11} for one Rb unit tested at NBS.^[3]

Recent work initiated by Al Risley and Helmut Hellwig at NBS and carried out in collaboration with Jacques Vanier (University of Laval) and Hugh Robinson (Duke University),^[4] demonstrates that parafin coated cells may provide a new way to make a rubidium gas cell standard with greatly improved characteristics. The parafin wall coating provides a means to contain the atoms with very small hyperfine relaxation and, very importantly, provides a means for the atoms to average all parameters over the entire bulb. Initial experiments yield a frequency shift of $\cong 10^{-8}$ for the wall coated cell and linewidth of less than 250 Hz. Linewidths of approximately 70 Hz are ultimately expected. Signal-to-noise is comparable to that of the buffer gas cell. Tests show, for example, that the coated cell has a factor of 100 less sensitivity to changes in microwave power than the buffer gas cell. Reductions in the sensitivity to magnetic field gradients and light intensity are also expected. As for cell lifetimes, Hugh Robinson has used one closed cell for 10 years with no measureable degradation in signal or signal-to-noise.^[5]

The temperature coefficient of the wall shift is of order 1 - 2 Hz/K, [6] so that fractional instabilities due to this effect could be as low as 10^{-14} at a few hours and less than 10^{-13} per day. Aging of the wall shift has not yet been measured. I would also expect that the retrace of the coated cell could be made better than a buffer gas cell due to the factor of 10 smaller confinement frequency shift and spatial averaging. In the case of the buffer gas cell, many hours are required to reestablish the equilibrium between the gas phase and the absorbed gas on the surface of the cell after a change in temperature.

There is yet another large bias in rubidium gas cell standards due to the presence of pumping light interacting with the same energy level being probed by the microwave radiation. Absolute light shifts are of order 10^{-9} . [2] The idealized pumping lamp profile of Rb^{87} , shown in Fig. 2, has a component which tends to depopulate the desired F_2 level. This unwanted light is filtered out by using Rb^{85} as an absorber, but the filtering is not totally successful and it shifts the center of the optical spectrum, causing an output frequency shift of order 10^{-9} . Also, the hyperfine signal is typically 0.5% of the total signal, instead of $\cong 10\%$ as would be expected from an ideal source.

Recent work by Tom English, et al. (Efratom, Inc.), has shown that the frequency shift from varying the light intensity by 30% can be reduced from 10^{-9} to $\leq 1 \times 10^{-11}$ by alternately applying pumping light and microwave radiation. [7] This technique was first suggested by M. Arditi. [8] English, et al., achieved a short-term stability of $\cong 2 \times 10^{-11} \tau^{-1/2}$ using a buffer gas cell. [7]

Many problems could well be solved by using a diode laser for pumping the Rb gas cell. The diode laser can be stabilized by

standard modulation techniques and can be tuned to pump only the F_2 levels, thereby increasing the hyperfine signal to $\cong 16\%$ of the total signal as compared to 0.5% in the standard design. This would:

- 1) improve S/N by $\cong 5$
- 2) reduce light shift to $< 10^{-12}$
- 3) increase line Q by $\cong 2$
- 4) improve short-term stability to $\sim 10^{-12} \tau^{-1/2}$.

Summary of projected performance for several variations of small rubidium standards is shown in Fig. 3. Performance could be improved considerably by increasing volume.

CESIUM FREQUENCY STANDARDS

Fig. 4 shows a schematic of a cesium atomic resonator.^[1] It has become increasingly apparent that present day cesium standards are fundamentally limited beyond $\cong 1$ day by the combination of phase variations of the microwave signal across the cavity end, the finite velocity of the atoms, and the spatial variation of velocity across the beam profile due to the dispersive nature of the A and B magnet state selectors.

The frequency offset due to the average phase shift is:

$$\Delta\nu = \frac{\langle\phi\rangle\langle v\rangle}{L}$$

In my opinion, the major uncertainty and instability in the frequency is due to the fact that $\langle\phi^2\rangle^{1/2}$ may be $100 \langle\phi\rangle$.

The present state selection technique utilizing inhomogenic magnetic fields to spatially separate selected hyperfine states

causes a correlation between velocity and position within the microwave cavity window. This applies to dipole and quadrupole-hexapole systems. As a consequence of this coupling between spatial position and velocity, any effect which can cause a variation in average velocity, state composition or spatial distribution will cause a frequency shift even if $\langle\phi\rangle = 0$.^[9] Effects which can cause frequency shifts initially are variations in microwave power, C field, Majorana transitions occurring in the beam between the state selector and the microwave cavity, and even variations in the voltage on the mass analyzer before the ion collector. All of the above change the distribution of velocities contributing to the detected signal and shift the average frequency via the distributed cavity phase.

At present, there are no attractive ways to significantly lower beam velocity. Brute force attempts suffer from the low number of slow atoms due the Boltzmann Distribution, and significant laser cooling of neutral beams as proposed by Askin and also Hänsch and Schawlow^[10,11] have yet to be demonstrated.

Reduction of the distributed cavity phase shift by reducing the diameter of the cavity window can be bought only at the price of lower beam intensity. Cooling the cavities to cryogenic temperatures could reduce this effect to near zero; however, the beam would have to be carefully masked in order to prevent Cs buildup within the cavity structure.

Recent work by Wineland, Jarvis, Hellwig and Garvey at NBS indicates that the effect of the average phase shift $\langle\phi\rangle$ can be reduced to zero by implementing a 2-frequency and 2-cavity system^[12] as illustrated in Fig. 5. In such a system, the envelope of the Ramsey Resonance is detected so that the average $\langle\phi\rangle$ between two

ends is averaged to zero (see Fig 6). Since the frequency switching from ν_2 to ν_2' is fast compared to changes in $\langle\phi\rangle$, any perturbation which would change $\langle\phi\rangle$ is greatly reduced. As a consequence, such a standard should be significantly more immune to frequency changes due to microwave power changes, fluctuations in oven temperature, position of oven/detector, shock, vibration, etc.

In order to realize the full advantage of this technique, it is important that short-term stability be maintained of order $10^{-11}\tau^{-1/2}$ or better. To do this, it is necessary to open up the cavity window in order to have a wide velocity distribution so that the Ramsey envelope is narrow and to increase beam current. Under optimum conditions, it is estimated that $\sigma_y(\tau)$ of $10^{-11}\tau^{-1/2}$ can be achieved. The current NBS test bed demonstrates $\sim 10^{-10}\tau^{-1/2}$ for 4pA beam current $\langle v \rangle \cong 130$ m/s, a 30% velocity width and a cavity length of 17 cm. Opening the cavity windows should substantially improve the performance.

Reduction of the velocity dispersion across the beam profile could also be accomplished with optical state selection. The laser diodes for pumping Cs at the proper wavelength exist and state selection has been demonstrated.^[13] Fig. 5 illustrates one possible configuration. The source is a single aperture to avoid brightness variations over the oven opening, such as can occur with multihole collimators. The straight through optics should help utilize the maximum number of slow atoms. By using an optical pumping scheme completely analogous to that used with Rb, the Cs beam can be predominately pumped into the $^2S_{1/2}$ $F = 3$ manifold. Len Cutler^[14] has suggested a dual frequency optical pumping scheme by which all of the atoms could be pumped into the $F = 3$, $M_F = 0$ sublevel; thus providing approximately a factor of 4 increase in signal-to-noise over standard design. With the absence

of the A Magnet, magnetic shielding of the resonance area is easier and Majorana transitions between the various sublevels could be completely eliminated. Beam detection could be obtained by conventional magnetic state selector/hot wire ionizer or by 2 step optical ionization. Both would offer near 100% efficiency and the ability to velocity select.

The net effect of the optical pumping scheme for state selection is to totally eliminate any correlation between spatial position within the beam and thereby within the cavity opening and velocity. Variations in microwave power, for example, will now cause a change in average velocity, but not average phase shift.

So the variation of frequency with average velocity, such as by changes in microwave power, should be reduced by a factor of 10 to 100 over present designs. In addition, the straight through geometry and the efficient state selection should permit a factor of 2 reduction in average velocity resulting in:

- 1) A factor of 4 reduction of second-order Doppler shifts $\cong \frac{1}{2} \frac{v^2}{c^2} \sim 1.5 \times 10^{-14}$.
- 2) $\sigma_y(\tau)$ improved by factor of 4 to 8 $1s < \tau < 10^4s$.
- 3) $\langle \phi \rangle$ reduced by a factor of (2).
- 4) $\Delta \langle \phi \rangle$ vs microwave power reduced by $\cong 20$ to 200.
- 5) $\Delta v = \frac{\langle \phi \rangle \langle v \rangle}{L}$ reduced a factor of approximately 2 over a magnetic state selection and should be extremely stable and measureable. The offset is not measurable with high accuracy with present magnetic state selection.

If the optical pumping scheme were coupled with the 2 frequency, 2 cavity technique, then the offset would also be made zero at the expense of decreased short-term frequency stability.

Fig. 7 shows a summary of projections for various configurations of commercial sized cesium frequency standards. Additional improvements are possible with laboratory type cesium standards.

HYDROGEN FREQUENCY STANDARDS

A block design of a standard hydrogen maser oscillator or active hydrogen maser is shown in Fig. 8.^[1] This device is unique among the atomic standards being discussed now because it is an oscillator. By building up enough population in the excited hyperfine state, it can be made to oscillate. Frequency stability at a few hours is unexcelled and therefore such devices are used for the most exacting high frequency phase sensitivity receivers, such as VLBI and the JPL deep space tracking network (See for example references 15, 16 and Fig. 12). However, for long-term timekeeping application, active hydrogen devices are seldom used because the frequency drifts away due primarily to cavity pulling which causes a fractional shift of:

$$\frac{\Delta \nu}{\nu} \cong \frac{Q_C}{Q_H} \frac{(\nu_C - \nu_H)}{\nu_H}$$

Assuming a hydrogen line Q_H of 5×10^8 and a cavity Q_C of 3×10^4 results in

$$\frac{\Delta \nu}{\nu} = 0.6 \times 10^{-4} \frac{\Delta \nu_C}{\nu_H}$$

In order to achieve a stability of 10^{-15} in the output frequency the cavity frequency must be stable to 1.5×10^{-11} . Free running cavity stability of this order has never been demonstrated for

periods beyond a few hours. Long-term stability of active masers can be improved using automatic cavity tuning. One synchronously detects changes in output frequency with changes in beam flux and servos the cavity tuning to minimize output frequency changes. Stabilities of order a few times 10^{-14} have been reported. [17]

Recent work at National Bureau of Standards has produced a new concept for stabilizing the microwave cavity. [18,19,20] A simplified block diagram is shown in Fig. 9. A local probe oscillator is phase modulated at two different low frequencies f_1 and f_2 where f_2 is approximately the half-bandwidth of the hydrogen resonance and f_1 the half-bandwidth of the microwave cavity. The transmitted microwave signal is envelope detected and the resulting amplitude modulation processed in two separate synchronous detectors referenced to f_1 and f_2 respectively. The error signal recovered from the f_1 synchronous detector is used to electronically tune the cavity to the probe frequency and the error signal recovered from the f_2 synchronous detector is used to tune the probe frequency to the hydrogen hyperfine resonance frequency. This allows one to lock the cavity frequency to the hydrogen resonance with an attack time of a few seconds, thereby allowing rapid recovery from any induced cavity perturbation.

Fig. 10 shows the frequency stability realized with a conventional full-sized cavity as measured against NBS-6, one of our primary frequency standards and also the ensemble of 9 cesium standards, which generate UTC(NBS). The realized stability of 3×10^{-15} at 4 days confirms that this NBS passive hydrogen maser scheme can be effectively used to control cavity induced frequency perturbations. For a more thorough discussion of the other possible perturbations see. [18,19,20] The above data was obtained with a hydrogen hyperfine line Q of 5×10^8 . A new bulb configuration and better teflon

coating now yields a line Q of 5×10^9 with 10 times the previous signal-to-noise. Measured frequency stability at 1 s is better than 1×10^{-13} . Based on the above, one would expect a daily frequency variation of less than 1×10^{-15} for this full-sized passive hydrogen maser cavity system.

This passive system concept also makes possible the use of a small dielectrically loaded microwave cavity. The new cavity system described in [19] was designed and assembled in collaboration with David Howe and S. Jarvis, Jr. at NBS. The hyperfine line Q with a storage volume of 1.1ℓ is 1.4×10^9 at low microwave drive and 1×10^9 at operating conditions. The observed frequency stability is $1 \times 10^{-12} \tau^{-1/2}$ out to approximately 1 day. The small passive maser has been compared with UTC(NBS) for 54 days and its frequency drift was $1 \pm 1 \times 10^{-15}/\text{day}$.

Fig. 11 shows a comparison of frequency stability of hydrogen atomic standards. A line labeled H(Active) is the best reported in the literature. [21] The time-keeping ability of various atomic standards is shown in Figs. 12 and 13. [22] The data on the passive masers clearly shows that active cavity control can be used to greatly improve long-term frequency stability of hydrogen masers. Furthermore, this technique greatly simplifies the thermal vacuum design, thereby decreasing cost, weight and complexity.

STORED IONS

A new class of microwave frequency standards based on stored ions is presently under study. These devices appear to hold the possibility of achieving frequency stabilities of order 10^{-16} and absolute accuracy of order 10^{-15} . These devices are explained by

D. J. Wineland in these proceedings, and are the only systems which fundamentally reduce both first and second-order Doppler effects to sub 10^{-14} levels. For example, the cavity phase shifts encountered with Cs standards is a form of residual first-order Doppler shift.

The principles of ion storage based frequency standards are described elsewhere.^[23] Basically, the ions are contained within an electromagnetic trap with dimensions of a few cm or less. Containment times are typically hours to days which, in principle, makes possible extremely large line Q's for hyperfine transitions, even at microwave frequencies. The ions can be cooled to sub-Kelvin temperatures using lasers tuned to the lower side of an allowed electric dipole transition. Each scattered photon carries off approximately 20 mk of energy if the laser is detuned by 500 MHz. Recent work^[24] clearly shows that sub-Kelvin temperatures are easily achievable in the case where appropriate lasers exist to pump the ions.

One proposed scheme for a stored ion standard has the following half cycle:

- 1) state select ions using optical pumping,
- 2) induce hyperfine transitions with probe tuned to the high frequency side of the hyperfine resonance and the laser off,
- 3) optically pump ions to determine how many made the transition and to cool the ions.

In the next half cycle the same three steps are repeated; however, the probe frequency applied in step 2 is moved from the high frequency to the low frequency side of the hyperfine resonance.

The maximum frequency stability that can be realized for N ions having a hyperfine resonance frequency ν_0 is

$$\sigma(\tau) = \frac{2}{\tau_0 N} \frac{1}{\pi \nu_0} \tau^{-1/2}$$

where τ_0 is the total cycle time or $2(\tau_1 + \tau_2 + \tau_3) = \tau_0$. Values for $\sigma_y(1s)$ vary from 10^{-12} to 10^{-15} for some of the systems under consideration. At present, the most serious impediment to this effort is a lack of suitable lasers to overlap ions having attractive other properties for the application.

SUMMARY

In the above, I have presented what I feel to be the most serious perturbations to frequency stability of rubidium, cesium and hydrogen devices. Most of these are perturbations essentially due to the concepts on which the standards are based. I feel that there is great opportunity for substantial improvement in frequency stability in both laboratory and field settings and I have indicated how I think these improvements can be obtained.

ACKNOWLEDGEMENTS

I wish to thank many colleagues for stimulating discussions on this topic, especially H. Hellwig, S. R. Stein, A. Risley, D. A. Howe, D. J. Wineland, D. W. Allan, J. Vanier, H. Robinson and P. L. Bender.

REFERENCES

1. H. Hellwig, NBS Technical Note 616, 2nd Revision.
2. See for example, P. Davidovits and R. Novick, Proc. of IEEE, 54, 155-170, 1966.
3. A. Risley, G. Busca, Proc. 32nd Annual Symposium on Frequency control, 169-179, 1978.⁺
4. A. Risley, S. Jarvis, Jr. and J. Vanier, Proc. 33rd Annual Symposium on Frequency Control, 1979.⁺
5. H. Robinson, Private communication, 1979.
6. Jacque Vanier, Private communication, 1979.
7. T. C. English, E. Jechart, and T. M. Kwon, Proc. 10th Annual PTTI, 147-168, 1979
8. M. Arditi, U.S. Patent 3234483, Feb. 8, 1966.
9. See for example, D. J. Wineland, D. W. Allan, D. J. Glaze, H. Hellwig and S. Jarvis, Jr., IEEE Trans. on I&M, Vol. IM-25, 453-458, 1976.
10. T. W. Hänsch and A. L. Schawlow, Opf. Commun. 13, 68, 1975.
11. A. Askin, Phys. Rev. Lett. 24, 156, 1970 and 25, 1321, 1970 and 40, 729, 1978.
12. R. M. Garvey, H. Hellwig, D. J. Wineland, and S. Jarvis, Jr., Proc. 9th annual PTTI, 571, 1978.
13. J. L. Picque, IEEE Journal of Quantum Electronics, QE-10, 892, 1974. and Metrologia 13, 115, 1977.
14. L. S. Cutler, Private communication, 1979.
15. W. K. Klemper, Proc. IEEE, 60, 602-609, 1972.
16. R. Sydnor, Proc. 11th Annual PTTI, 1979.
17. C. Audoin, P. Lesage, J. Viennet and R. Barillet, Proc. 32nd Annual Syms. on Frequency Control, 531-541, 1978⁺; D. Morris and K. Vakagiri, Metrologia 12, 1-6, 1976; H. E. Peters, Proc. 5th Annual 283-316, 1973; and C. Finnie, R. Sydnor and A. Sward Proc. 25th Annual Symposium on Frequency Control, 348, 1971.⁺

18. F. L. Walls and H. Hellwig, Proc. 30th Annual Symposium on Frequency Control, 473-480, 1976.⁺
19. F. L. Walls and D. A. Howe, Proc. 32nd Annual Symposium on Frequency Control, 482-498, 1978.⁺
20. F. L. Walls and D. A. Howe, Proc. 33rd Annual Symposium on Frequency Control, 1979.⁺
21. M. W. Levine, R. F. Vessot and E. M. Mattison, Proc. 32nd Annual Symposium on Frequency Control, 477-485, 1978.⁺
22. Adapted from a paper by D. W. Allan and H. Hellwig, IEEE Position Location and Navigation Symposium, 29-36, 1978. Available from IEEE, Ref. #78CH 1414-2 AES.
23. D. J. Wineland, R. E. Drullinger and F. L. Walls, Phy. Rev. Letts. 40, 1639-1642, 1978.
24. F. L. Walls, D. J. Wineland and R. E. Drullinger, Proc. 32nd Annual Symposium on Frequency Control, 453-459, 1978.⁺

⁺Available from Electronic Industries Assoc., 2001 Eye Street N.W., Washington, D.C. 20006.

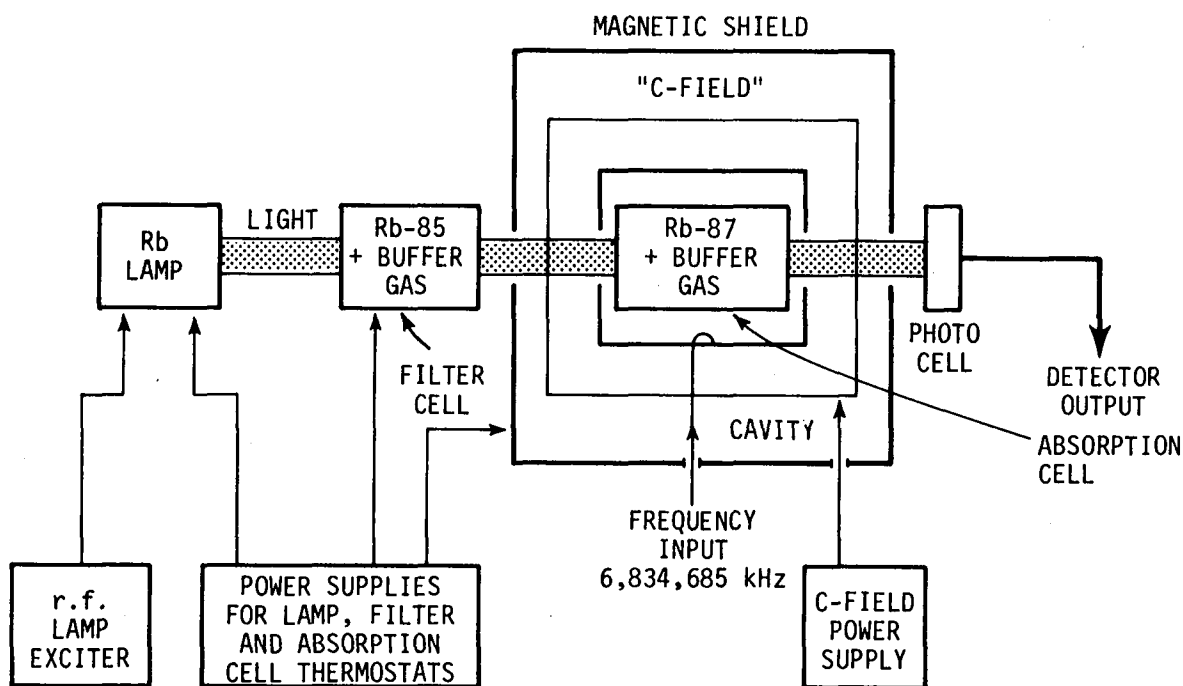


Figure 1. Simplified Diagram of a Typical Rubidium Atomic Resonator

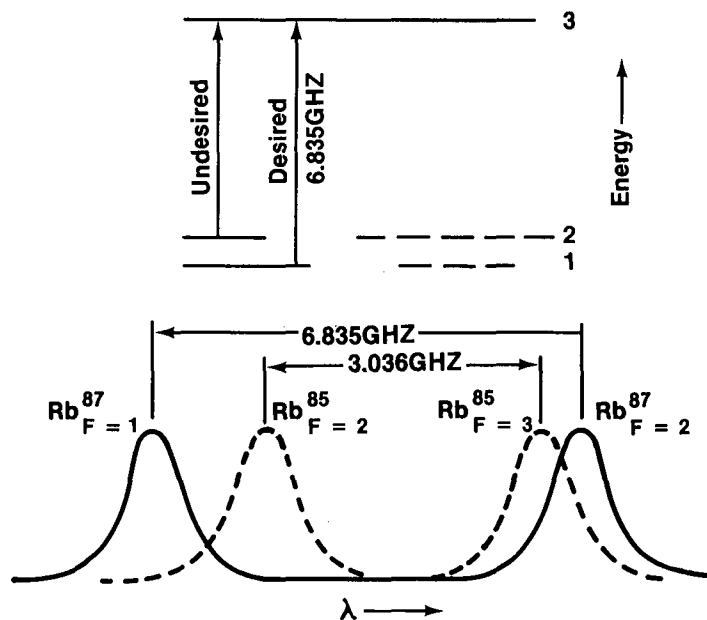


Figure 2. Levels of Interest for Optical Pumping of Rubidium

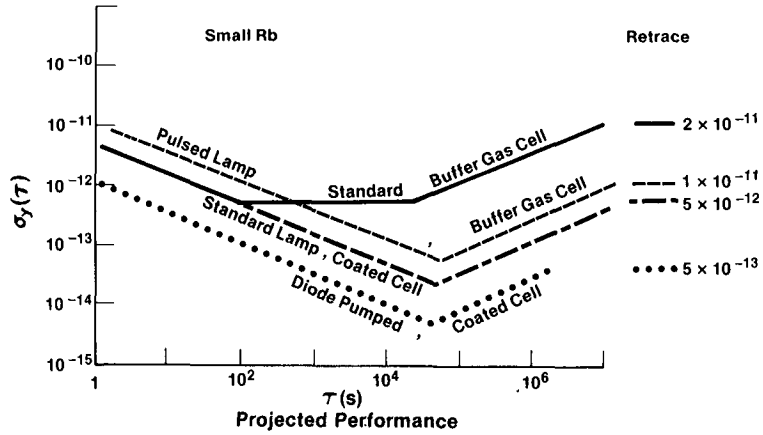


Figure 3. The Projected Performance of a Small Rubidium Standards with Various Features are Shown. The Solid Line is the Typically Achieved Performance of Small Rubidium Devices. Selected Units have Performed Better Especially Under Environmental Control^[1].

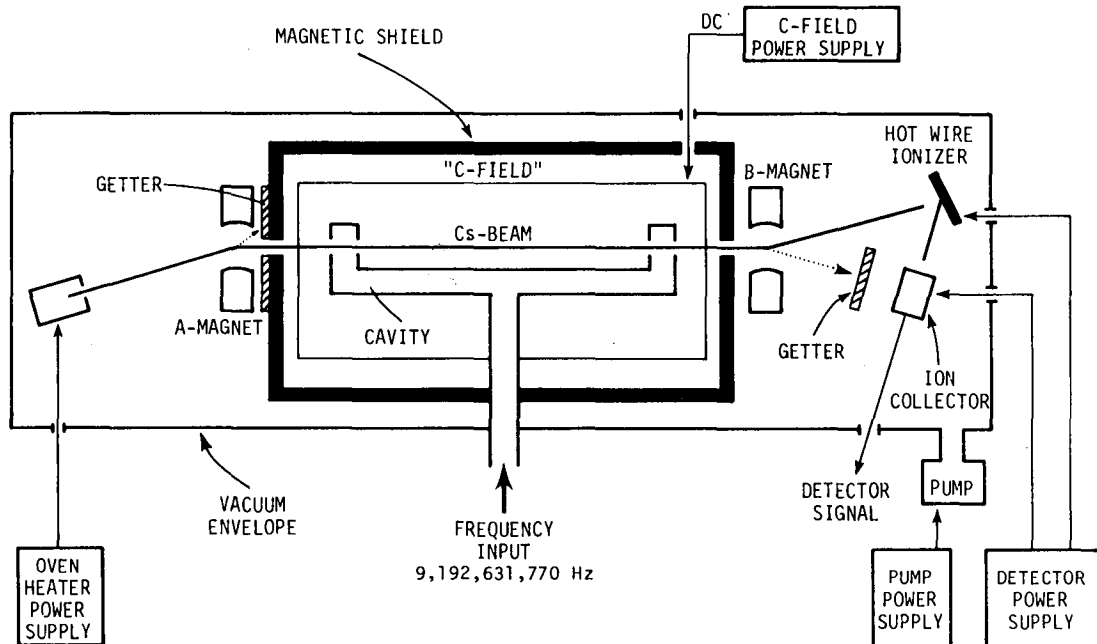


Figure 4. Simplified Diagram of a Cesium Beam Atomic Resonator

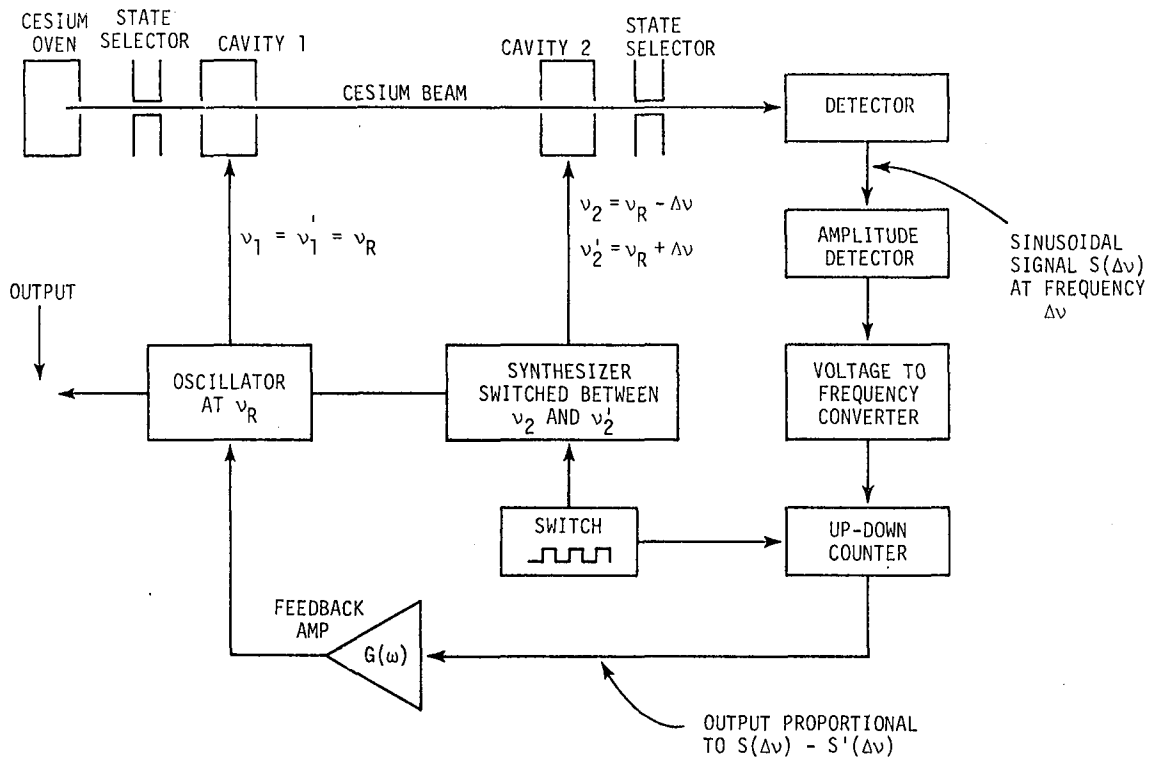


Figure 5. Simplified Diagram of One Possible 2 Cavity-2 Frequency Configuration.[11]

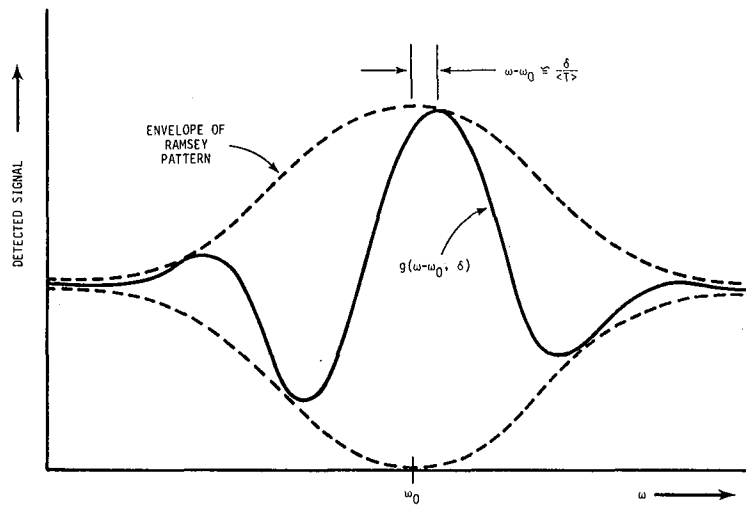


Figure 6. Ramsey Pattern for a Phase Shift Between the Two Cavity Ends. Dotted Line Shows the Ramsey Envelope

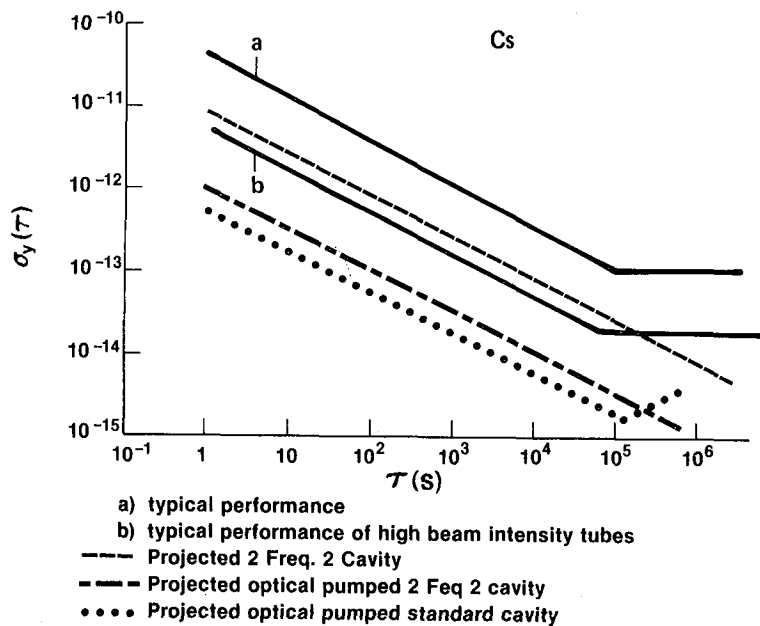


Figure 7. Projected Performance for Several Configurations of Commercial Sized Cesium Frequency Standards. The Solid Lines are Typically Realized Values for Commercial Devices. Selected Units Perform Somewhat Better at 10^6 s Especially Under Environmental Control.

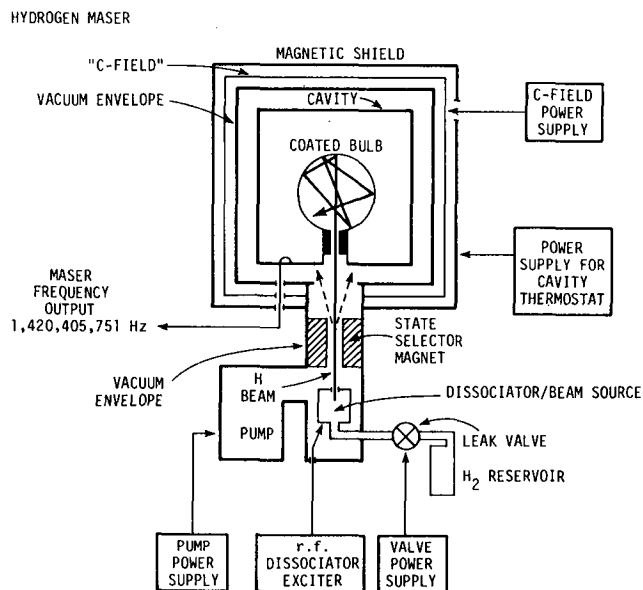


Figure 8. Simplified Diagram of an Active Hydrogen Maser Oscillator.

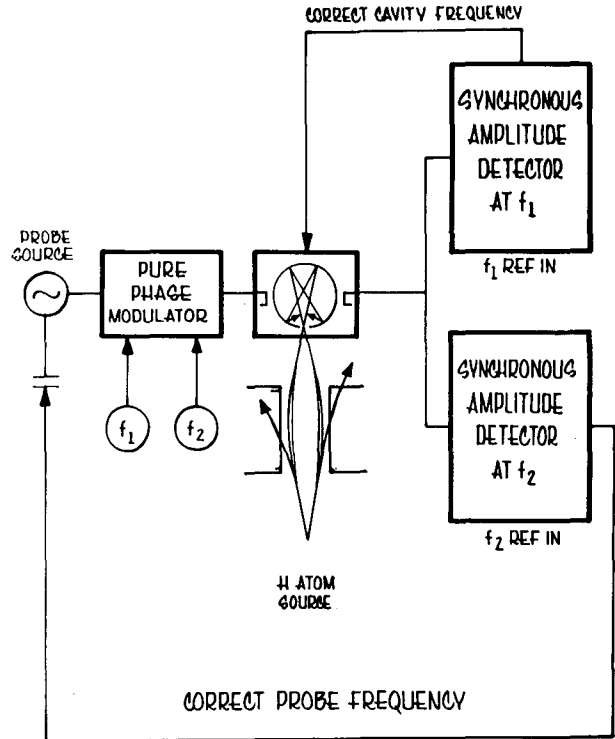


Figure 9. Simplified Diagram of One Possible Passive Hydrogen Maser Frequency Standard.

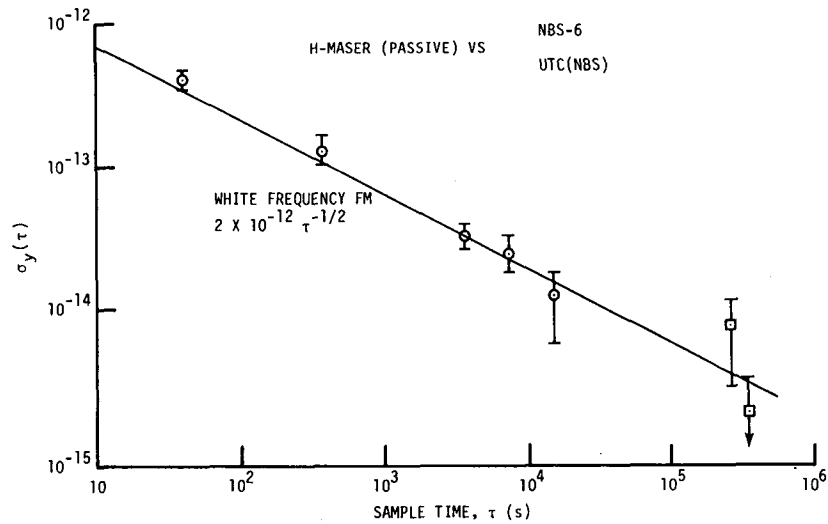


Figure 10. Joint Fractional Frequency Stability of Large Passive Hydrogen Maser vs. Cesium Standards. The Last Point is 3 Samples at 4 Days.

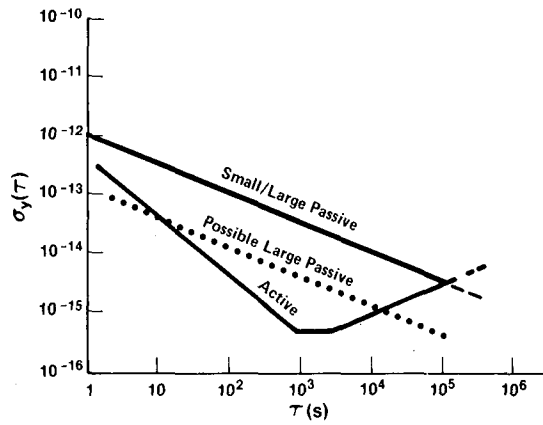


Figure 11. Fractional Frequency Stability of Hydrogen Masers. Solid Lines are Measured While the Dotted Line is Projected Performance.

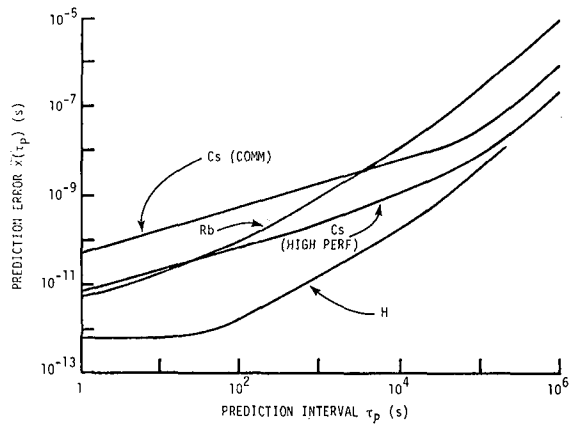


Figure 12. Minimum Time Prediction Error for Several Atomic Standards Using "Normal" Frequency Stability Performance.[21]

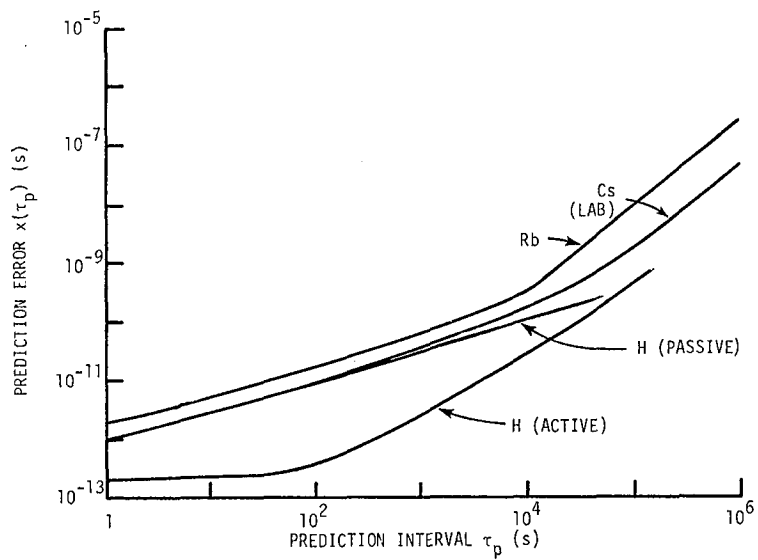


Figure 13. Minimum Time Prediction Error for Several Atomic Standards Under Near Ideal Laboratory Conditions. [21] Cs(Lab) Refers to Large Primary Cesium Standards, While H Passive Refers to the Data from the Original Large Passive Performance. [17] Projected Large Passive Performance is 5-10 Times Better.

QUESTIONS AND ANSWERS

MR. FISCHER:

I noticed on the slide of the rubidium stability there. It seemed like what I noticed to be a random walk of frequency was indicated for all the longer Taus. I wonder if you could comment on that and the fact that they all turned over at about the same Tau, close to 10 to the 5th seconds.

DR. WALLS:

Well, lots of systematic effects appear to come in at somewhere between 12 and 24 hours. It is an environmental effect. It is usually not a true drift. But it is some sensitivity to small temperature changes, to gradients that happen because of temperature changes in the room or whatever. And I think it is quite typical for standards, when they start to deteriorate that they come out as Tau to the one-half rather than Tau to the one.

Now if you are effected by something like cavity pulling, cavity drift, that too may look linear for a while, but I suspect that it slows down to Tau to the plus one-half or even flatter for a while.

MR. PLEASURE:

Dr. Cutler disclosed how he proposes to pulse a cesium atom in a laser, is there another transmission involved?

DR. WALLS:

I suggest you talk to him. It is a refinement of some things in the literature, namely, by using two optical pumping signals you can force them to tumble into the two middle ones where the transition probability is smaller for movement from the optical pumping. But I suggest you talk to him about the details.

MR. PLEASURE:

How does the hydrogen maser have an amplifier that doesn't fluctuate in phase? In other words you are Q-multiplying the cavity of the hydrogen maser, isn't there a phase fluctuation in the amplifier?

DR. WALLS:

In the passive maser there is no Q-multiplication. I will show you here. You do phase modulation on this side and on the output transmitted signal you detect amplitude modulation which tells you the

detuning between, in one case the probe oscillator in the center of the hydrogen resonance, and in the other case between the probe oscillator and the center of the cavity resonance. So you do phase modulation here. All detection on this side is amplitude sensitive and not phase sensitive.

CLOCK PERFORMANCE, RELIABILITY AND COST INTERRELATIONSHIPS

Martin W. Levine
Frequency and Time Systems, Inc.
Danvers, Massachusetts

ABSTRACT

Clock manufacturers have encountered major difficulties in attempting to supply reasonably-priced, reliable clocks for critical aerospace applications. The basic problems arise from the inherent technical difficulties of designing and fabricating equipment to provide performance at the limits of the state-of-the-art in demanding environments, but the difficulties are compounded by inconsistent and unstandardized specification practices, and by an emphasis on initial acquisition costs, rather than on life-cycle-costs. Conventional parts-stress analyses, which do not provide a useful indication of the reliability of a clock, lead to increased parts costs for high-performance aerospace clocks without commensurate benefits in improved reliability or performance. The characterization of clocks in term of the mean-time-between-resynchronizations, facilitates the estimation of life-cycle costs and provides a means to evaluate clocks in a realistic fashion for specific systems applications.

INTRODUCTION

There is concern in our industry, users as well as suppliers, over the reliability and the acquisition costs of high-performance clocks and frequency standards. Such concerns can be related to the complex interaction between cost, performance and reliability in the design and fabrication of clocks. Certainly there are similar relationships in all technologies; but there are unique aspects to the clock problem, particularly with the respect to a useful definition of clock reliability. Although our primary interest here is with instruments intended for long-term operation in spacecraft, the same considerations are applicable to a wide range of environments and applications, from standards laboratories to oil-exploration rigs, in which uncompromising performance and reliability are essential.

A pragmatic approach is to carefully examine the impact of certain categories of customer specifications and requirements on the cost, reliability and performance of clocks. The issues of parts selection and parts stress analyses, "qualification", nonstandard interfaces, and operation or "life-cycle" costs are of particular concern in any discussion of cost, reliability and performance tradeoffs. The situation is further complicated by the extreme difficulty of abstracting clock specifications from the system design. A clock which may be quite adequate in one system may be considered inadequate in the context of a second system, even in instances in which the missions of the two systems are identical.

PARTS STRESS ANALYSIS

Mean-time-between-failure (MTBF) estimates based on electronic parts stress analysis are a valuable tool in the reliability engineer's kit. Used with care and understanding, and in conjunction with failure mode and effects and worst-case analyses, MTBF calculations are an aid to a complete understanding of the operational characteristics of an item of equipment. But because the MTBF estimate is relatively simple to calculate, and provides a single unambiguous number as the result of the calculation, the MTBF tends to be given a great deal more attention than it deserves. A review of the basics of parts stress reliability predictions may help to clarify the limitations of the parts-stress MTBF estimate.

MTBF Calculations

Failure rate models have been established for the heavily-used electronic parts: integrated circuits, transistors, resistors and capacitors. The models and the corresponding experience factors are compiled in a military handbook, MIL-HDBK-217.¹ From this handbook, the failure rate model for a discrete semiconductor device in failures per 10⁶ hours is

$$\lambda_p = \lambda_b (\Pi_E \times \Pi_A \times \Pi_{S2} \times \Pi_C \times \Pi_Q) \quad (1)$$

where

- Π_E is the environmental factor
- Π_A is the application factor
- Π_{S2} is the voltage stress factor
- Π_C is the complexity factor
- Π_Q is the quality factor

The voltage-stress factor and the quality factor are cost-sensitive; that is, tradeoffs are possible between cost of the device and the failure rate.

An example is instructive. Table I lists the appropriate factors for a NPN silicon transistor used in a benign ground environment (a laboratory or similar protected environment). The transistor will be operated at a collector voltage of 40% of V_{CBO} .

TABLE I

MEAN-TIME-TO-FAILURE EXAMPLE

NPN SILICON TRANSISTOR

Π_E	= 1	Ground Benign Environment, 25°C
Π_A	= 1.5	Linear amplifier application
Π_Q	= 0.2	JANTXV quality level
Π_{S2}	= 0.48	Voltage stress level = $0.4 \times V_{CBO}$
Π_C	= 1.0	Single transistor complexity

$\lambda_p = 0.0014$ Failures per 10^6 hours

All factors from MIL-HDBK-217B

Once the failure rates of the individual parts are determined, the failure rate of the equipment, λ_{EQUIP} can be computed by summing over all parts,

$$\lambda_{EQUIP} = \sum_{i=1}^m \lambda_{pi}$$

where

m is the number of parts in the equipment

and

λ_{pi} is the failure rate of the i^{th} part.

As examples of the results of such calculations, the following results were obtained for two typical frequency standards:

- a.) Precision 5 MHz Crystal Oscillator: $\lambda_{\text{EQUIP}} = 470,000$ hours
(Ground Benign, 25°C)
- b.) Cesium Beam Frequency Standard: $\lambda_{\text{EQUIP}} = 68,000$ hours
(Ground Benign, 25°C)

It should be noted that these estimates include all electronic piece parts, but exclude the precision quartz resonator and the cesium beam tube resonators. This exclusion will be discussed in greater detail later.

Parts Cost Considerations

The voltage stress and the quality factors were earlier indicated to be cost-sensitive items. The calculated part failure rate can be reduced by selecting derated parts and by choosing high-quality parts. All other things being equal, a higher-voltage rated capacitor will be more expensive than a lower-voltage device and similar arguments apply to transistors and resistors. In most instances, the economic impact of derating is moderate and the effect on equipment reliability is substantial and cost effective. Note, however, that there are pitfalls to an undisciplined attempt to achieve low failure rates through part derating. Transistor voltage stress level is an excellent example - the selection of a device with a high V_{CBO} rating may sacrifice other desirable characteristics such as switching speed and result in an overall lower equipment reliability in practice. The cost impact of higher quality parts can be very high, however. Table II is a listing of the purchase price of typical Established-Reliability capacitors, in single unit quantities, as a function of the failure level of the device. Prices of established reliability parts have been volatile recently, so that only the relative prices should be considered.

Parts, including Established Reliability types, used in equipment intended for critical applications are generally required to be rescreened - tested by the equipment manufacturer upon receipt from the factory or distributor. Rescreening costs can be considerable, often greater than the purchase price of the parts themselves, and difficult to accurately predict. The actual costs of the electrical and mechanical screening tests and of the required destructive physical analyses (dissection and microscopic examination of samples of each lot) are only a portion of the total costs attributable to

rescreening. The loss of entire lots of parts due to excessive failure rates in either electrical, mechanical or destructive testing, may require the procurement of from three to ten times the quantity of parts normally required.

TABLE II

ESTABLISHED-RELIABILITY PARTS COST EXAMPLE

Capacitor: Solid Tantalum, 22MF, 50VDC \pm 10%
Type CSR13G226M

<u>Failure Level</u>	<u>Failure Rate Factor (Π_Q)</u>	<u>Price</u>
L	1.5	----
M	1.0	\$10.28
P	0.3	13.15
R	0.1	21.80
S	0.03	30.45

Limitations of Parts Stress Analysis

It should be reemphasized that parts stress analysis is only one of a number of sophisticated analytical techniques available to the reliability engineer. Taken by itself, a parts stress analysis does have certain value. It can illustrate the reliability improvements possible by replacement of lower quality parts by higher quality parts and the tradeoff of part costs versus increased MTBF. Perhaps the most important use of parts stress analysis is to provide a quick and simple means for estimating the relative failure rates of competitive equipment all other things being equal. A simplified technique, parts count reliability prediction, can be used for this purpose before the circuit design has even been completed, if the approximate parts count in each generic part category (resistor, capacitor, relay, etc.) can be estimated.

Parts stress analysis, however, cannot be used to compare equipment of varying complexity. In fact, **noncritical application of parts stress analyses** in these cases can be misleading. A multistage-stage transistor amplifier of marginal performance is a simple illustrative example: an additional stage of gain will improve the

reliability of the amplifier in the commonly understood sense of the word. The parts stress analysis taken alone, however, indicates a decrease in the MTBF.

The extension of this concept to clocks and frequency standards is straightforward. Stated simply, the MTBF estimates do not indicate the relative reliabilities of different clocks, or different types of clocks, when applied in real-world systems. The precision quartz crystal oscillator, discussed earlier in this section, with a MTBF of 470,000 hours, is not necessarily more reliable than a cesium beam frequency standard with a MTBF of 68,000 hours. If a system specification requirement is that a frequency shall be maintained to within 1×10^{-10} of an initial value, then the quartz oscillator will "fail" within a matter of days or weeks due to its frequency aging, whereas the cesium beam frequency standard could operate satisfactorily for about 7 years.

There is another, perhaps more fundamental, limitation of the application of parts stress analysis to state-of-the-art clocks and frequency standards: the inadequate reliability data base for the resonators; precision quartz crystals, rubidium cells and lamps, and cesium beam tubes. Parts-stress MTBF estimates are statistical data based on many millions of hours of user experience with a large number of electronic piece parts. It is not meaningful to factor into these estimates failure rates for resonators based on a limited sample of a few dozen to a few hundred parts. The examples shown above assumed that the MTBF was not limited by resonator failure; an adequate treatment of the subject, although² admittedly of utmost importance, is beyond the scope of this paper.

QUALIFICATION

Military and aerospace equipment is normally "qualified"; validated by test and analysis to survive and operate in a specified environment. Qualification is an expensive and time-consuming process, justified by the expectation that the qualified equipment can be deployed with confidence.

There is an unfortunate corollary to the concept of a qualified item of equipment; unless the specific test and analytical sequences are completed, the unit is unqualified. This fact has become a powerful inhibitor to the use of existing or previously developed clock and frequency standards in new systems. Each system or platform has its own specification and corresponding environmental and performance requirements. The resulting design changes dictate further qualification testing, adding to the cost

spiral without significantly improving either performance or reliability.

In addition, different and incompatible requirements for similar space vehicles or for different portion of the same payload are not unusual. The lack of standardization, however, may go beyond objective requirements of the actual environmental conditions; test requirements are sometimes specified in conflicting and incompatible terms, even in cases in which the actual physical conditions are similar or identical. Shock and vibration requirements are particularly subject to requirements proliferation. Shock testing for example can be specified in terms of hammer blows, pyrotechnic simulation spectra or time-domain pulse shapes and it is often difficult or impossible to analytically verify that a clock which has been qualified to one set of shock criteria will prove satisfactory under a different set of test conditions.

The major casualty of the proliferation of specifications and the non-standardization of requirements is the "off-the-shelf" high-reliability clock or frequency standard. For the reasons outlined above, clock manufacturer cannot prequalify the instrument and offer it as a standard item. It follows, therefore, that production runs are always short and that clock prices reflect the inability of the manufacturer to amortize development, documentation and project management costs over a large number of units. Furthermore, reliability inevitably suffers when only a small number of items are fabricated. The normal product maturation process (learning curve) by which design and workmanship problems encountered in the early production units are corrected in later production runs never has a chance to operate.

SPECIAL INTERFACES AND FREQUENCIES

The primary purpose of a system clock is to provide a stable, reliable and precise time or frequency reference. This challenges the clock manufacturer if the requirements of the system specification are at or near the limits of the state-of-the-art and new or unique interface requirements such as special output levels, multiple outputs, "TTL-compatibility", special ground isolation, or operation from non-standard supply voltage are an additional, and often costly, burden.

When a special or non-standard interface is specified, the clock manufacturer must incur not only the engineering costs associated with the development of new circuitry and mechanical packaging, but documentation, reliability engineering and qualification testing

expenses as well. Even if the basic frequency control circuits and resonators are proven and reliable, the qualification legacy may be lost because of the addition of the special features.

The specification by a user of a non-standard or unusual frequency for a high-performance clock presents the clock manufacturer with a difficult measurement problem, one that may be unique to our industry. If state-of-the-art performance is required, the manufacturer is usually instrumented to measure frequency stability and phase noise spectra at a few commonly used frequencies such as 5.000 or 10.23 MHz. The only feasible technique for certain measurements at non-standard frequencies may be the fabrication of additional units or of special test systems. Therefore, certain specification requirements may not be economically feasible at all for a small production order.

CLOCK COST EXAMPLES

It may be useful to examine two illustrative examples of some of the relative cost elements of high-performance clocks for spaceflight applications. The examples are composites and are not intended to represent the pricing of any specific instruments. The relative costs in both cases are for small production quantities and the parts and parts screening costs reflect the distortions caused by minimum lot-size procurements. The per-unit parts cost would be considerably less for larger production quantities.

Precision Quartz Crystal Oscillators

Table III shows a composite relative cost breakdown for a quantity of four space-qualified crystal oscillators.

All electronic parts in this example are to be ordered to JANTXV or to Established Reliability Level "S" and subjected to rescreening and a sampling DPA.

TABLE III

PRECISION CRYSTAL OSCILLATOR COST EXAMPLE

Parts		44%
Purchase	19%	
Rescreening and DPA	25%	
Manufacturing and Test		8%
Qualification Test		4%
Program Management		30%
Design and Development		14%
TOTAL		<u>100%</u>

Atomic Frequency Standards

A second example, shown in Table IV, is a quantity of four space-qualified atomic frequency standards. The parts are to be selected to the same standards as in the previous example.

TABLE IV

ATOMIC FREQUENCY STANDARD COST EXAMPLE

Parts		28%
Purchase	14%	
Rescreening and DPA	14%	
Manufacturing and Test		15%
Qualification Test		7%
Program Management		30%
Design and Development		20%
TOTAL		<u>100%</u>

A moderate amount of engineering effort, primarily reliability and parts selection oriented, has been assumed. Major changes in the basic design, such as any of the interface characteristics, would require substantial increases in the design and development costs.

It should be noted that a very significant fraction of the costs shown are unrelated to the specific technology of the clock but rather arise from the reliability, testing and management aspects of the program. Since these cost elements tend to be similar for equipments of roughly the same complexity, the cost differentials between high-reliability, high-performance clocks based on different timekeeping systems can be expected to be much smaller than for the respective commercial counterparts. Flight-qualified cesium and rubidium frequency standards, for example, are roughly equivalent with respect to initial acquisition costs.

RELIABILITY AND LIFE-CYCLE COSTS

The previous discussion has been primarily concerned with the acquisition costs of clocks. In most cases, however, the operational costs of the system far exceed the procurement costs and the total life-cycle costs must be considered in the selection of a clock or frequency standard for a particular system application.

It is difficult to treat adequately the subject of life-cycle costing without a more careful consideration of the performance and reliability of the system clock. In general, the mission of any system can be accomplished over a wide range of system clock performance capabilities. With less stable or less precise clocks, the system must be resynchronized more often than with more stable and precise clocks but, in principle at least, mean-time-between-resynchronizations (MTBR) can be traded off directly for system clock performance. Neglecting systematic errors, a precision quartz crystal oscillator requires resynchronization at 1-day (approximately) intervals to maintain one-microsecond time accuracy. A rubidium frequency standard requires resynchronization about every 10 days for the same accuracy, and cesium frequency standard about every 100 days. The resynchronization process may require frequent travelling clock trips or additional radio-frequency channels and may be difficult or expensive because of security or operational considerations, but the principle is still valid. It is interesting that the MTBR, which is derived from the performance of the clock and the requirements of the system is also a useful measure of the reliability of the clock in the specific application. The probability of outright failure of the clock cannot be neglected, but in those cases in which the MTBR is much less than the MBTF, the MBTR number must be considered to be a primary indicator of clock reliability.

The lifetime cost of resynchronization; the total life of the system divided by the MTBR and multiplied by the cost per resynchronization, can be computed readily for a large variety of systems. For example, at the Deep Space Network, operated by the Jet Propulsion Laboratories, preliminary estimates have been made of the tradeoff of operational costs for network time synchronization by simultaneous radio telescope observations of quasars versus the cost of acquiring and operating improved atomic frequency standards.³ The improved clocks extend the MTBR by approximately a factor of ten and for network operational costs of \$500 to \$1000 per hour per tracking station, the life-cycle costing exercise favors the use of the improved standards, even at very high acquisition cost levels.

Although it is not possible to generalize broadly from this example, it appears that for multi-user, continuous-duty applications such as spread-spectrum communications systems and navigation satellite systems, operational costs dominate the life-cycle-costing estimates. In these instances the acquisition costs of the system clock is a secondary consideration and the primary concern of the system designer should be the MTBR.

CONCLUSION

The ability of the clock manufacturer to supply reasonably priced clocks and frequency standards for high-reliability applications would be greatly enhanced by the standardization of clock frequencies, interfaces and environmental requirements. Conversely, the cost of clocks for aerospace applications is inflated by the very small production quantities required for most systems and the consequent small base over which development and management costs can be amortized.

Stable, high-performance clocks improve the reliability of systems as measured by the mean-time-between-resynchronizations. Therefore, there does not exist a one-to-one relationship between clock complexity and reliability, in contrast to the conventional parts-stress analysis of failure rates. It also follows that the total operational costs of a system are inversely proportional to the MBTR and that the system designer must include resynchronization costs as well as procurement costs in the life-cycle-cost estimates.

Finally, the focus on the electronic circuit performance clocks without an equivalent effort of obtain data on the resonators may be misleading to the designer as well as the user.

REFERENCES

- (1) "Reliability Prediction of Electronic Equipment" Military Standardization Handbook MIL-HDBK-217B. US Government Printing Office, 1976,
- (2) D.B. Percival, G.M.R. Winkler, "Timekeeping and the Reliability Problem", Proceedings 29th Annual Symposium on Frequency Control, VS Army Electronics Command, Fort Monmouth, N.J. pp 412-416 (1975). Copies available from Electronic Industries Association, 2001 Eye St, NW, Washington, D.C. 20006
- (3) E. Thom, private communication, 1979

QUESTIONS AND ANSWERS

QUESTION:

I liked it very much, but I wish you could have included some idea of how often these costs are not typical of contract by delivery price. You never once mentioned the fact that so many manufacturers count on delivery and then you have people sitting around with nothing to do because some other supplier has not given them or has a good excuse for not delivering.

DR. LEVINE:

My experience has been that everybody working on a system is hoping and praying that somebody else will come in late.

THE FREQUENCY AND TIME STANDARD AND ACTIVITIES AT THE BEIJING INSTITUTE OF RADIO METROLOGY AND MEASUREMENTS

H. T. Wang

Abstract

The Beijing Institute of Radio Metrology and Measurements (BIRMM), as a calibration center and a research division of radio metrology and measurements and frequency control devices for the system of space technology in China, has made some progress in PTTI research work in recent years. This paper will review some of PTTI activities briefly.

Frequency measurement is one of the routine jobs of BIRMM. Now there have been three kinds of frequency measuring systems: a system of frequency comparison, a system of phase comparison and a system of time comparison.

In cooperation with other organizations from 1978 to the second quarter of 1979, two experiments on time synchronization were carried out. With the help of the portable cesium clock in determining the time delay between two stations, one experiment of time synchronization, chiefly sponsored by the Central Bureau of Metrology, of China, between Nanjing (China) and Raisting (West Germany) by using the "Symphony" satellite, has achieved a result with an accuracy of 30 ns and an uncertainty of about 10 ns. The other experiment, applying the television pulse technique for time synchronization, has yielded a result with an error of about 0.5 μ s in 24 hours.

In order to measure the short-term frequency stability of crystal oscillators or other frequency sources, BIRMM, in cooperation with the Wuhan Institute of Physics, developed a rubidium maser atomic frequency standard about two years ago. BIRMM has developed a short-term stability measuring system with a time-domain stability resolution $\sigma_y(2, \tau) < 1 \times 10^{-12}/\tau$ (sec) and a frequency-domain stability resolution $s_\phi(f) \approx 10^{-12}/f + 10^{-15}$.

Additional new PTTI items under consideration will be mentioned briefly, too.

1. Frequency measurement

BIRMM began its PTTI activities not long ago. The basic frequency standard founded in BIRMM is a commercial cesium beam atomic frequency standard (2 sets, type 3200, imported from Switzerland). Its frequency accuracy has been checked with the Loran-C receiver and has proved to be 1×10^{-11} . A crystal oscillator of type XSD with a time aging rate less than 1×10^{-10} /day is used as a working standard for frequency calibration. There have been set up the systems of frequency comparison, phase comparison and time comparison. The operation of these systems will be described below.

A. System of frequency comparison

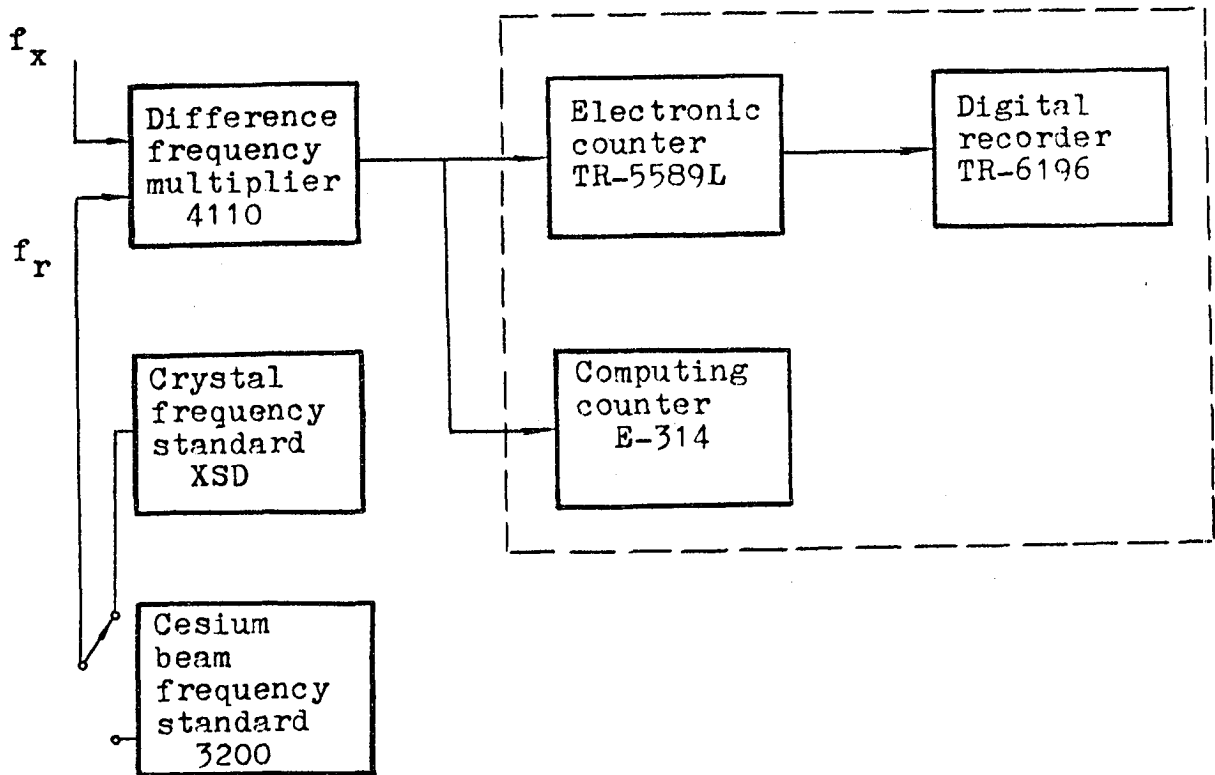


Figure 1. Functional block diagram of the system of frequency comparison

The limit sensitivity of the system is not only dependent on the uncertainty caused by the noise of the difference frequency multiplier 4110 itself, but on the resolution of the system. There exist experimental data for the former. The latter may be calculated as follows:

Frequency resolution $R_f = 1/Mf_0\tau$ where M is an effective multiplying factor, f_0 is the nominal value of the frequency measured and τ is the sample time.

Sample time	Uncertainty caused by 4110 itself	resolution of the system	The limit sensitivity of the system
1 sec	$<4 \times 10^{-12}$	1×10^{-11}	$\approx 1 \times 10^{-11}$
10 sec	$<3 \times 10^{-12}$	1×10^{-12}	$\approx 3 \times 10^{-12}$
100 sec	$<5 \times 10^{-13}$	1×10^{-13}	$\approx 5 \times 10^{-13}$

Uncertainties caused by reference sources are given below.

Type of reference source	Drift-rate/day of the reference source	Error introduced by short-term stability of the reference source		
		1 sec	10 sec	100 sec
Crystal oscillator XSD	5×10^{-11}	3×10^{-12}	3×10^{-12}	2×10^{-12}
Cesium frequency standard 3200	10^{-14} 10^{-15}	3×10^{-11}	1×10^{-11}	3×10^{-12}

It can be seen from the above table that when XSD is used as a reference source in measuring long-term stability or aging rate/day, a 10 sec sample time can be applied to calibrate the frequency standard below 5×10^{-10} /day. But when 3200 is used as a reference source in measuring long-term stability or aging rate/day, in order to calibrate the frequency sources below 3×10^{-11} /day, 100 sec sample time must be applied due to the limit of the short-term stability of 3200 cesium frequency standard, so that the calibration error will be one order of magnitude lower than the error of the calibrated equipment.

B. System of phase comparison

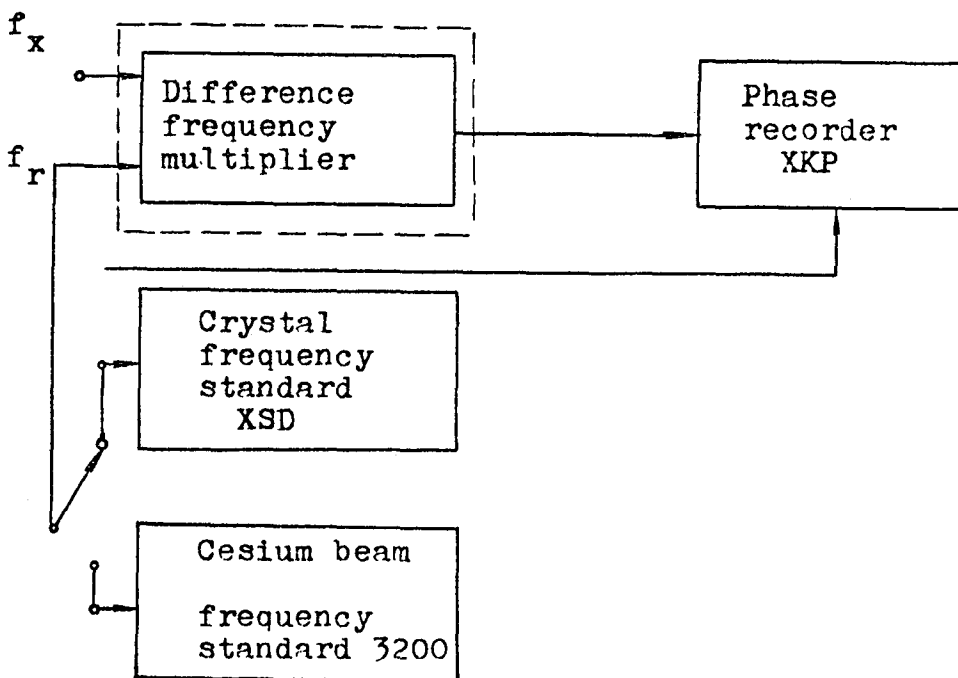


Figure 2. Functional block diagram of the system of phase comparison

The dashed line in the block diagram indicates that a measuring equipment can be added to increase the resolution of the system, if necessary.

The resolution of the system of phase comparison can be calculated by:

$$R\phi = \frac{1}{M f_0 \tau N}$$

where M is the multiplying factor of the difference frequency multiplier, f_0 is the nominal value of the frequency measured (in Hz), τ is the sample time (in sec) and N is the number of division in the width of the recording paper.

According to the above equation, the resolution of the system (when $M = 1$, i.e. without use of a difference frequency multiplier) is the function of the sample time and the input frequency as shown in the following table.

Resolution of the system Sample time	Input frequency	100 KHz	1MHz	5MHz
	10^3 sec		2×10^{-10}	2×10^{-11}
10^4 sec		2×10^{-11}	2×10^{-12}	4×10^{-13}
10^5 sec		2×10^{-12}	2×10^{-13}	4×10^{-14}

Calibration error of the system of phase comparison: the calibration errors for various sample times are given below, assuming the input of the phase comparator to be 1 MHz.

Sample time τ	Resolution of XKP	Measurement error due to accumulated difference time of XKP	error Introduced by XKP in measuring sample time	error of XKP
10^3 sec	2×10^{-11}	5×10^{-11}	1×10^{-9}	1×10^{-9}
10^4 sec	2×10^{-12}	5×10^{-12}	1×10^{-10}	1×10^{-10}
10^5 sec	2×10^{-13}	5×10^{-13}	1×10^{-11}	1×10^{-11}

It can be seen from the above table that in order to reduce the error of the system an external standard clock should be used in measuring sample time.

3. System of time comparison

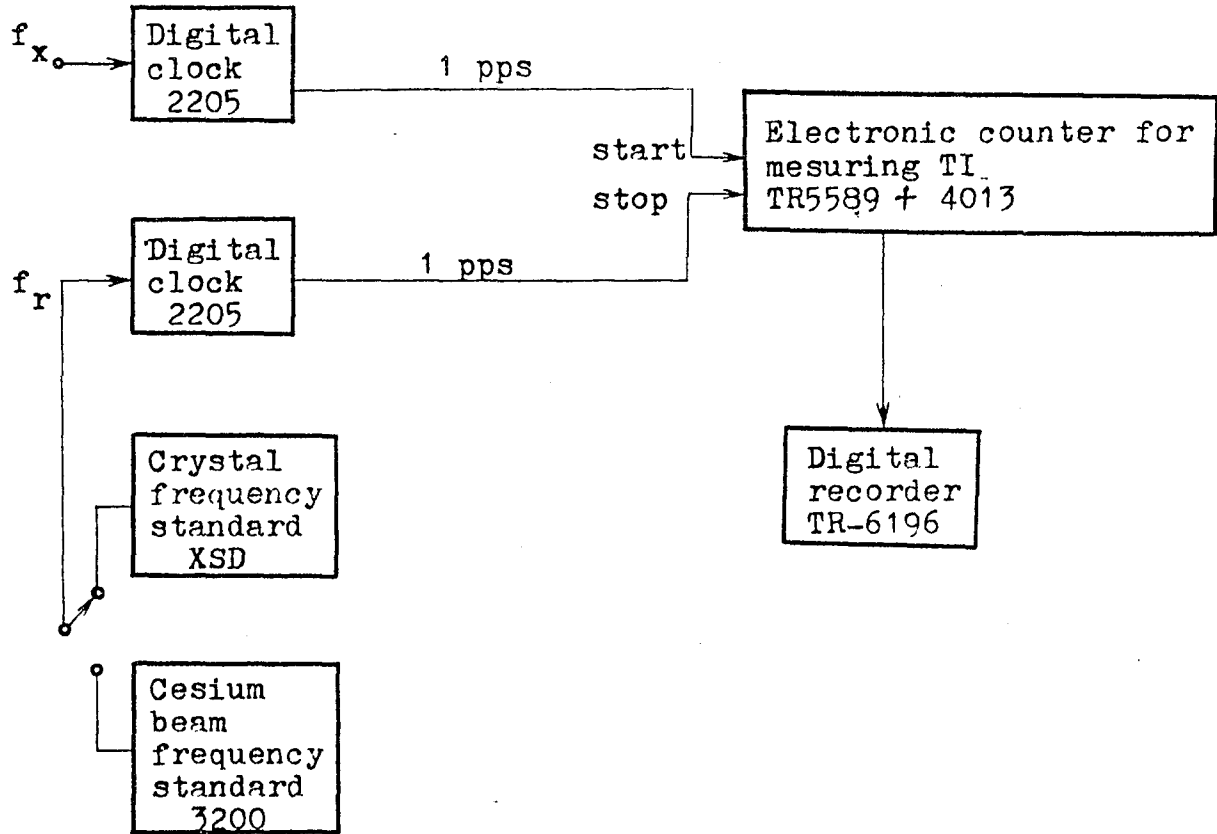


Figure 3. Functional block diagram of the system of time comparison

The resolution of the system of time comparison can be calculated by:

$$R_t = \frac{\tau_0}{\tau}$$

where τ_0 is the time base for time measurement and τ is the sample time. The resolution of the system is given below.

Time base \ Sample time	$1\mu s$ ($10^{-6} s$)	$0.1\mu s$ ($10^{-7} s$)	$10ns$ ($10^{-8} s$)
$10^3 sec$	$1 \cdot 10^{-9}$	$1 \cdot 10^{-10}$	$1 \cdot 10^{-11}$
$10^4 sec$	$1 \cdot 10^{-10}$	$1 \cdot 10^{-11}$	$1 \cdot 10^{-12}$
$10^5 sec$	$1 \cdot 10^{-11}$	$1 \cdot 10^{-12}$	$1 \cdot 10^{-13}$

The calibration error of the system of time comparison depends on the phase jitter and phase jump caused by the frequency divider of digital clock 2205 and on the resolution of the system. Generally speaking, the phase jump of the phase divider is recognizable and the phase jitter is very small. Thus the calibration error of the system is chiefly dependent upon the resolution of the system.

The items for calibration and comparison BIRMM can deal with and the accuracy BIRMM can obtain are given in the following table.

Type of the frequency standard being calibrated or compared	Items for calibration and comparison and their accuracy				
	Stability (1 sec)	Stability (10 sec)	Stability (day)	Drift rate/day	Accuracy
Crystal frequency standard	2×10^{-12}	5×10^{-12}	$1 \times 10^{-9} \sim 3 \times 10^{-11}$	$1 \times 10^{-9} \sim 3 \times 10^{-11}$	1×10^{-10}
Rubidium gase cell frequency standard	2×10^{-12}	5×10^{-12}	3×10^{-13} (intercomparison)	1×10^{-12} (phase comparison method)	1×10^{-10}
Commercial cesium beam frequency standard	2×10^{-12}	5×10^{-12}	3×10^{-13} (intercomparison)		1×10^{-11} Receive Loran-C

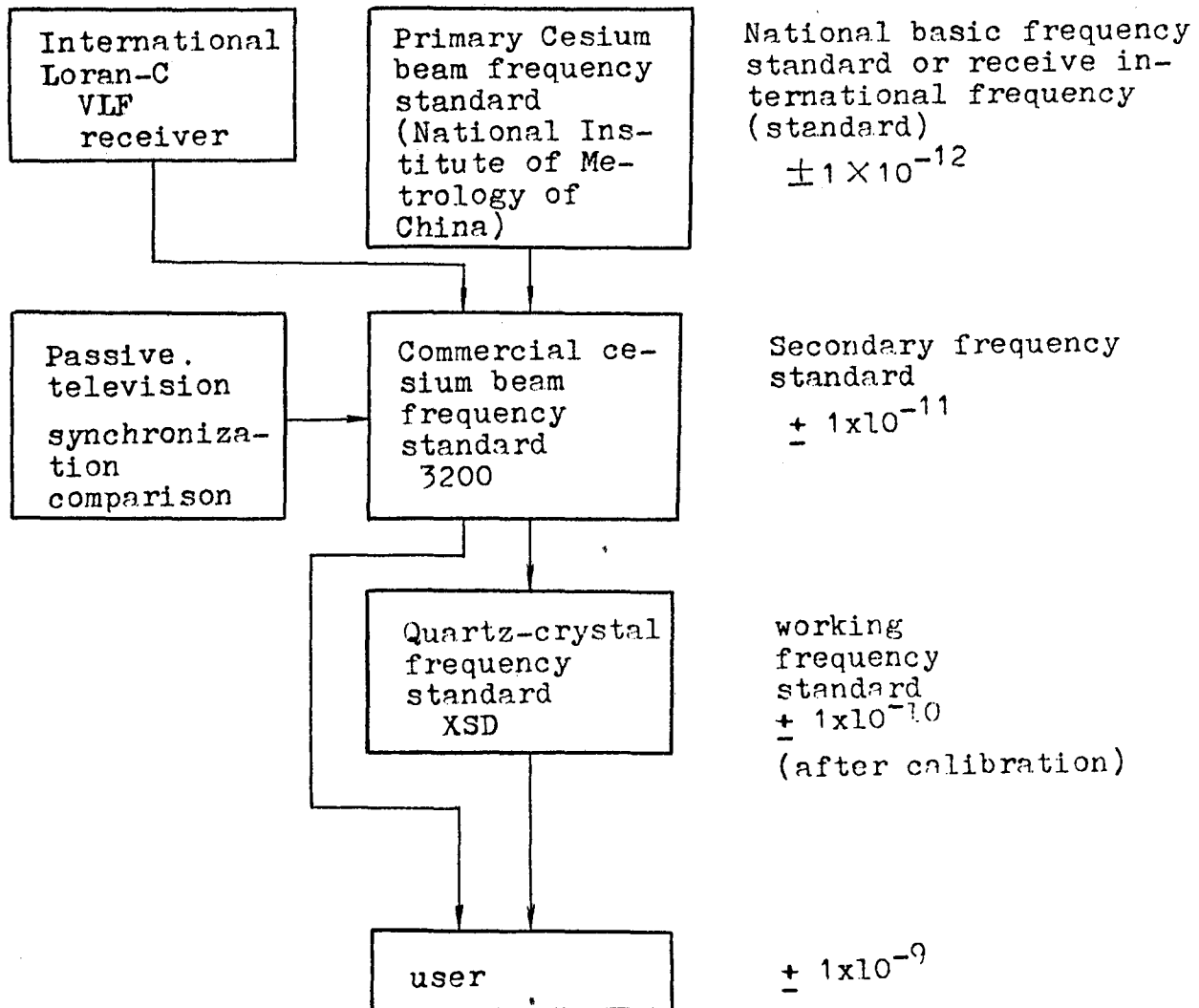


Figure 4. Schematic diagram of the hierarchy of frequency accuracy

II. Measurement of short-term frequency stability and a survey of the research work

Short-term frequency stability of precision frequency sources is a problem to solve urgently, which the system of space technology has been dealing with recently. BIRMM has undertaken some research work in this area with the following achievements:

A. Principal technical characteristics

- (1) Frequency measurement range
 1 MHz, 2.5 MHz, 5 MHz, 10MHz, 100 MHz,
 $M \times 100\text{MHz}$ ($M=45$ to 70)
- (2) Form of input signals
 Continuous sinusoidal wave

(3) Resolution of the measuring system

- a. Resolution of time-domain stability
Allan variance $\sigma_y(2, \tau) < 1 \times 10^{-12}/\tau$
 τ is in sec. f_h (bandwidth) is 10KHz
- b. Resolution of frequency-domain stability
phase noise power spectral density
 $S\phi(f) < 10^{-12}/f + 10^{-15}$
 f is Fourier frequency in Hz.

B. Standard reference sources

- (1) Rubidium maser atomic frequency standard (active rubidium frequency standard)

To increase the measurement accuracy of short-term frequency stability, BIRMM in cooperation with the Wuhan Institute of Physics under the Academy of sciences of China has developed a rubidium maser atomic frequency standard as a reference source for the test of short-term frequency stability. The maser was developed by the Wuhan Institute of Physics, while the electronic circuits (including a phase-lock receiver, a 100MHz quartz-crystal oscillator and a 311KHz frequency synthesizer) were developed by BIRMM.

The schematic diagram of the maser, the functional block diagrams of the phase-lock receiver and 311KHz frequency synthesizer are given below.

Two models were successfully developed in 1977, with the maser having a copper cavity. The short-term frequency stability of these two models of the maser proved to be $5 \times 10^{-13}/\tau$. (τ is in sec.)

For further improving the characteristics three new models have been developed recently. Some modification has been made in the maser and the electronic circuits.

The maser has a microcrystalline glass cavity instead of the copper cavity. The low-noise elements and components being used, the noise of the electronic circuits has been reduced and the operation reliability has increased.

The following technical characteristics are obtained after the preliminary test.

- a. Output frequency stability of the maser is indicated in the following table and the curves.
 - b. Output power of the maser $(1.5-2) \times 10^{-10}W$
- (2) Besides the rubidium maser atomic frequency standard, 100MHz and 5MHz quartz-crystal oscillators have been developed as reference sources for the test of short-term frequency stability.

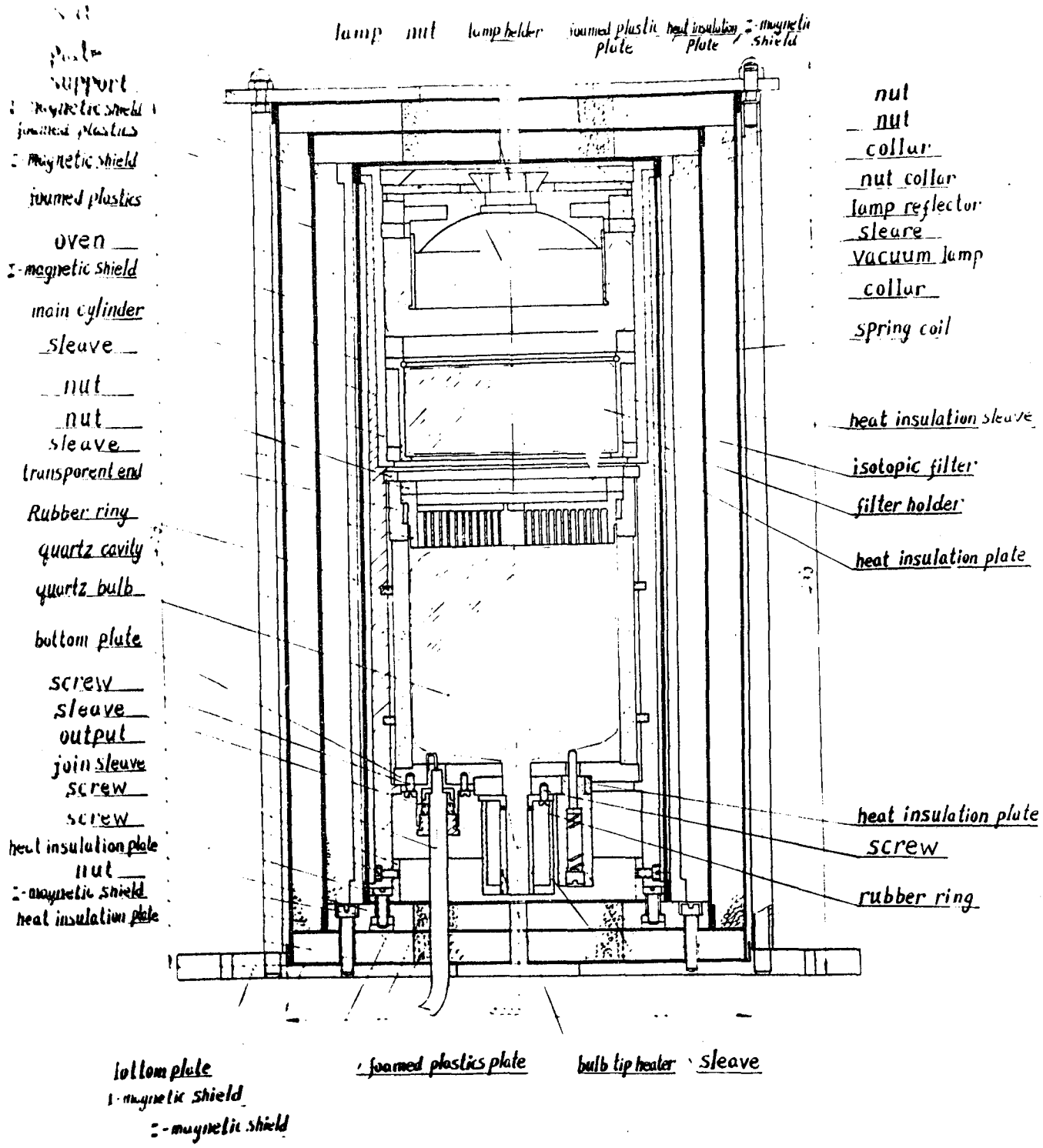


Diagram of Rb^{87} maser ($Rb^{87} M_2$)

Figure 5. The structural scheme of the rubidium maser

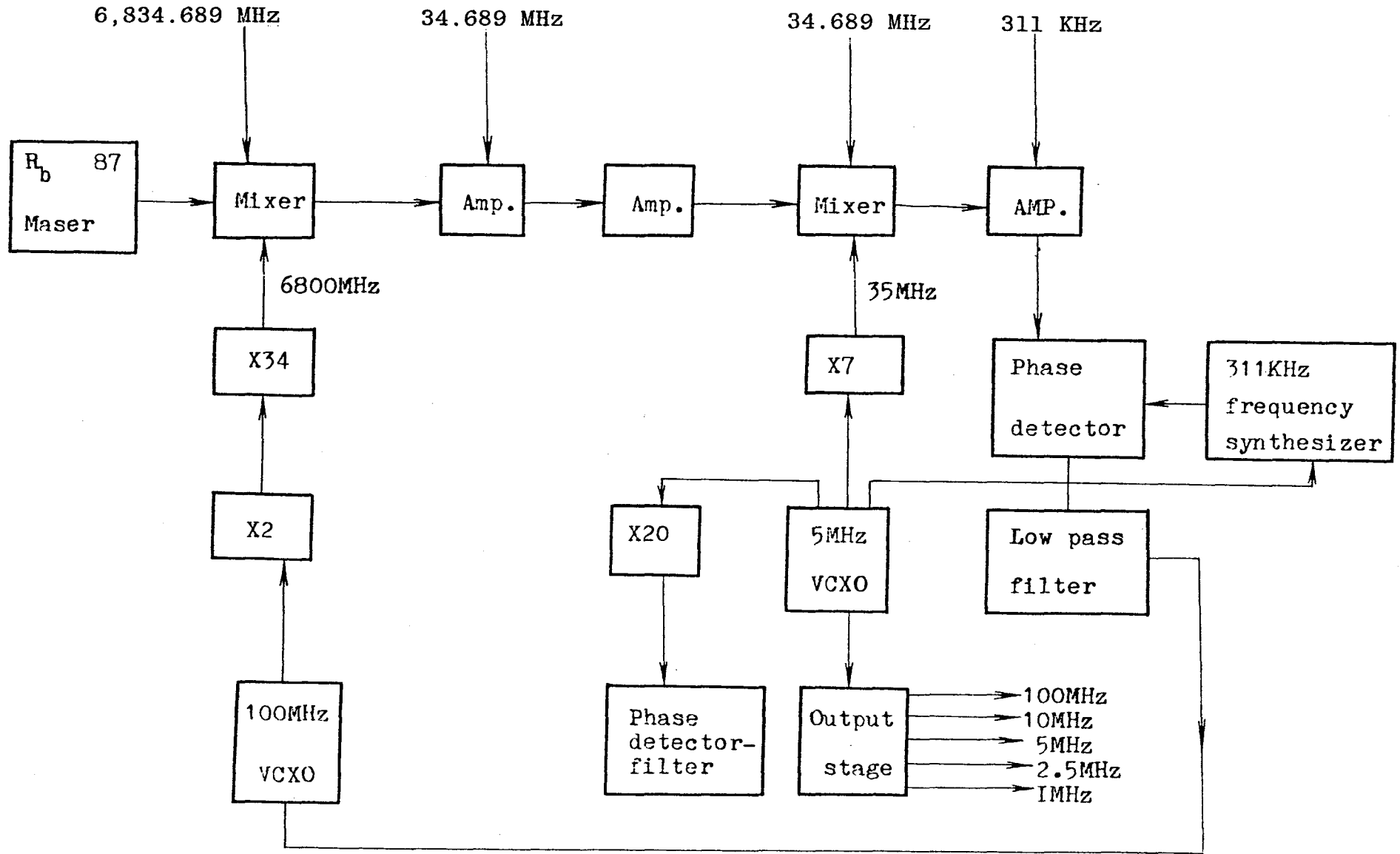


Figure 6. Functional block diagram

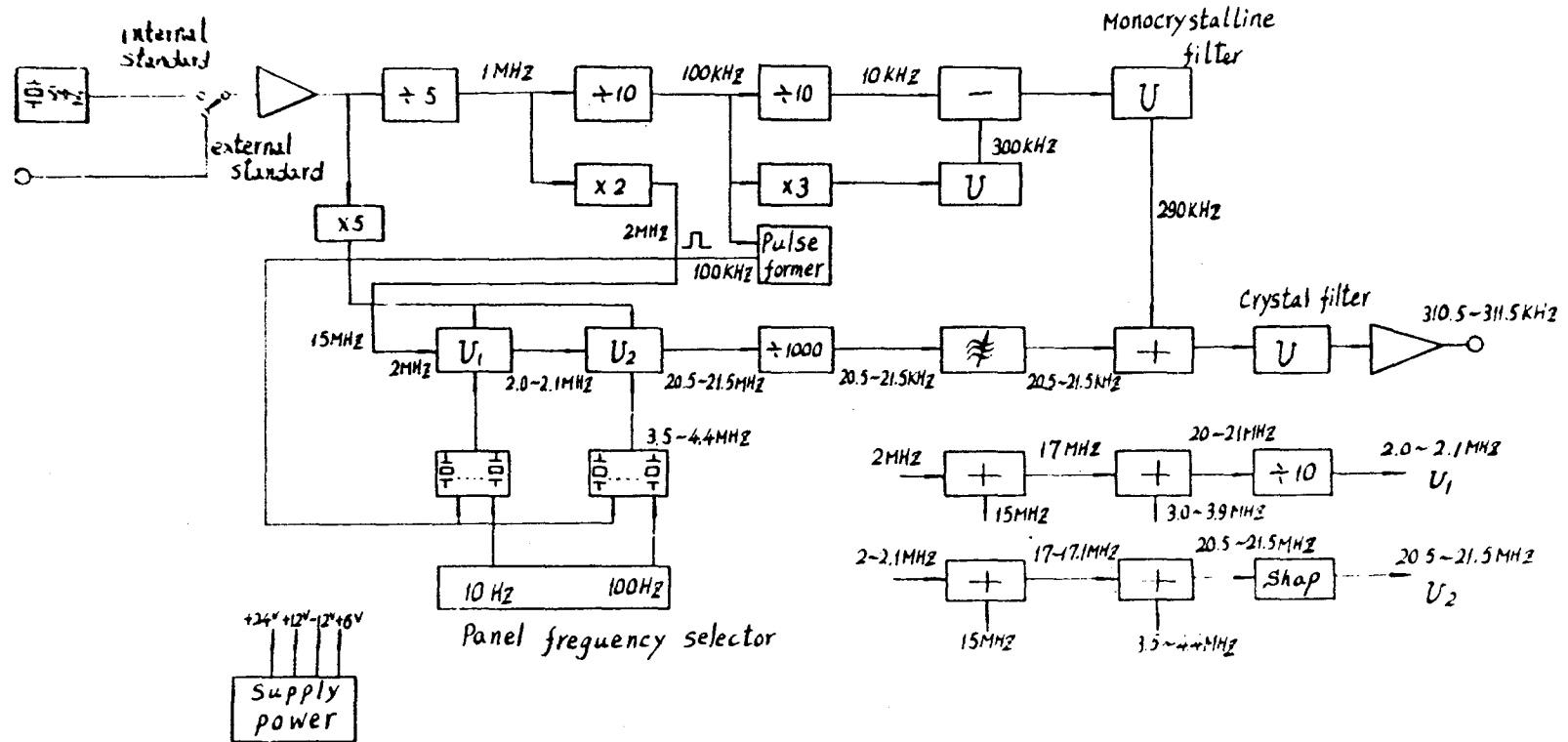


Figure 7. Functional block diagram of frequency synthesizer

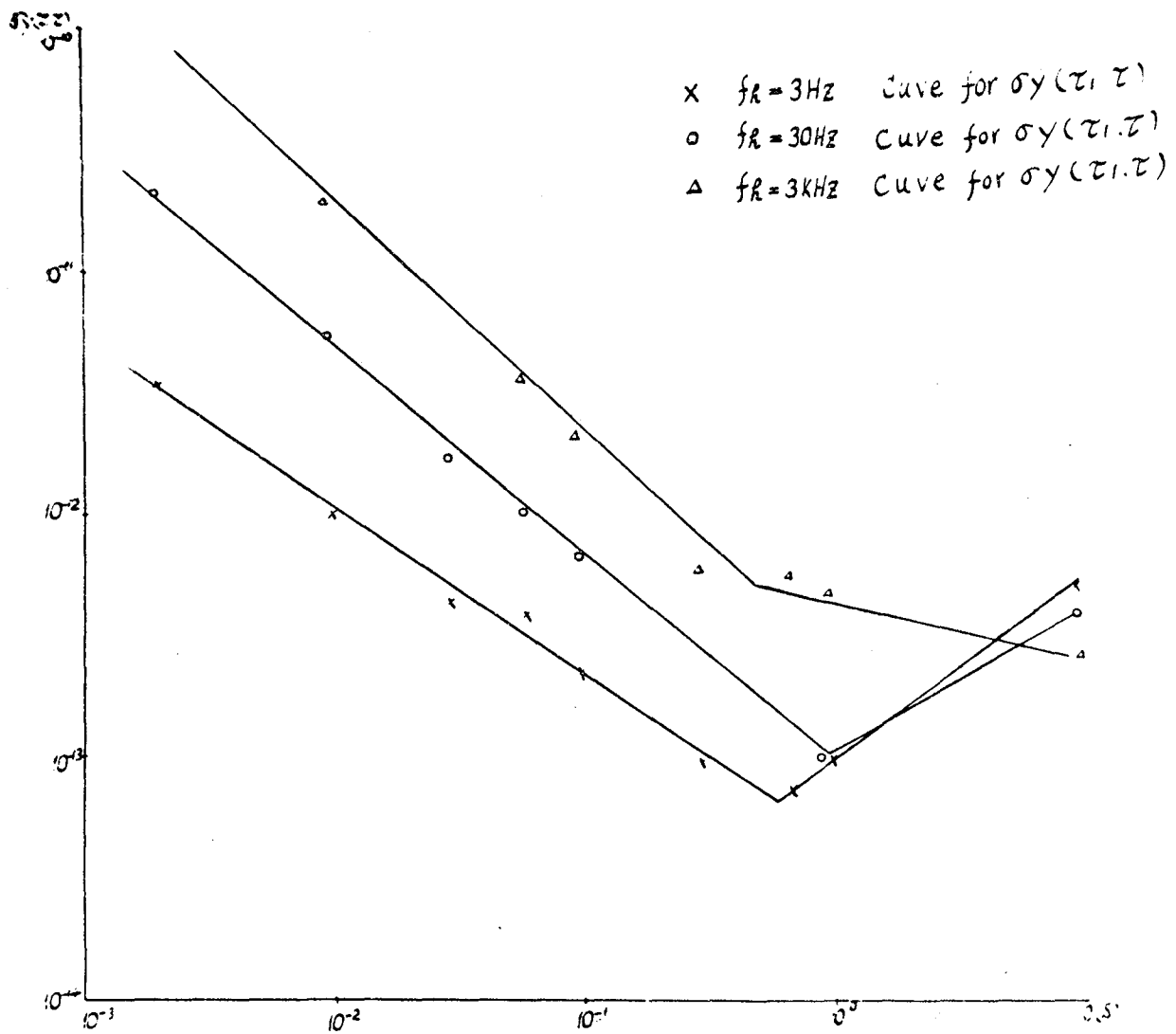


Figure 8. Characteristic curves obtained in test of the short-term frequency stability of PBR-MII maser

3. Comparators

A. Time-domain comparator

A multi-period measuring system was used to meet the requirements of measurement of short-term frequency stability with 1 ms—1 sec sample time.

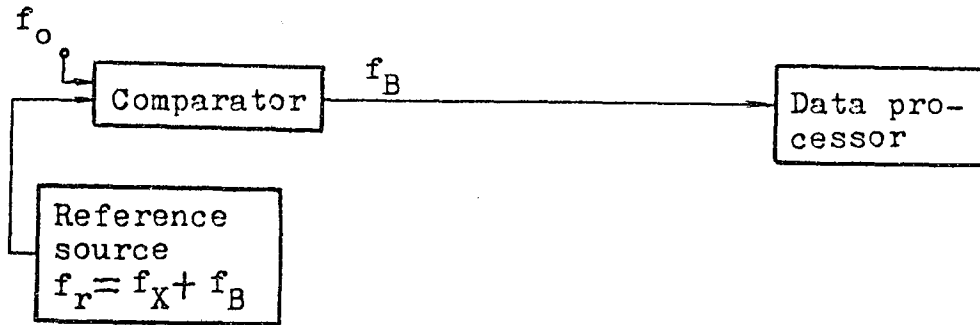


Figure 9. Functional block diagram of the multi-period measuring system

The limit sensitivity of the measuring system depends on the uncertainty caused by the noise in the comparator and on the resolution of the system. The former is determined by experiments. The latter is calculated by

$$R_T = \frac{f_B}{Mf_o} = \frac{\tau_o}{\tau}$$

where f_B is the beat frequency, τ_o is the time base of the counter, τ is the sample time, M is the error multiplying factor and f_o is the frequency measured.

(100MHz + 1KHz) crystal oscillator serves as the reference source of the comparator. With the help of a low noise frequency multiplier the frequencies of various sources being measured can be multiplied up to 100 MHz, then the beat frequency period (or multi-period) of mixed frequency can be measured and processed with the computing counter.

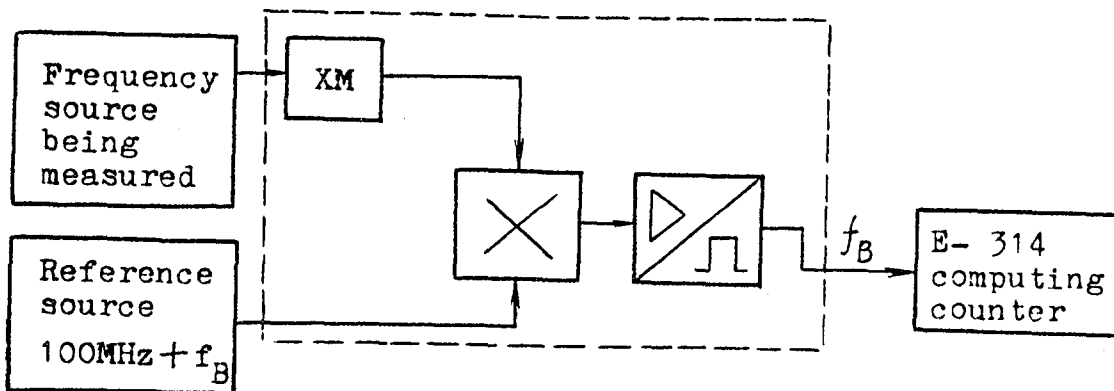


Figure 10. Functional block diagram of the time-domain stability comparator

The possible measuring accuracy for various frequency sources being measured is given in the following table.

Frequency being measured f_0	1 MHz	2.5 MHz	5 MHz	100MHz
Frequency multiplying factor M	5×20	2×20	20	1
Measuring Accuracy (τ in sec.)	$5 \times 10^{-12} / \tau$	$1 \times 10^{-12} / \tau$	$5 \times 10^{-13} / \tau$	$5 \times 10^{-13} / \tau$
Test bandwidth (f_b)	10KHz	10KHz	10KHz	10KHz

B. Frequency-domain comparator

The frequency-domain comparator developed by BIRMM uses a correlative zero beat method, in other words, two-channel zero beat method, based upon the single-channel beat zero method. With the help of two identical single-channels it measures the correlative components, thus improving its resolution and reducing residual noise of the phase-detecting amplifier. The block diagram is given below.

5MHz or 100MHz quarts crystal oscillator is used as reference source. The time constant of the phase lock loop is changeable. The phase noise levels of various Fourier frequencies are analyzed by the narrowband analog spectrum analyzer. The results are post-processed later on.

The narrowband analog spectrum analyzer has the following characteristics:

frequency range	from 5 Hz to 50 KHz
bandwidth	1 Hz, 3 Hz, 10 Hz, 30 Hz, 100 Hz, 300 Hz
sensitivity	30nv
dynamic range	80db

The residual phase noise $S_{\phi R}(f)$ of the measuring equipment is shown in the table.

Fourier frequency f (Hz)	10	100	1,000	10,000
Residual phase noise $S_{\phi R}(f)$ (db)	-135	-145	-155	-155

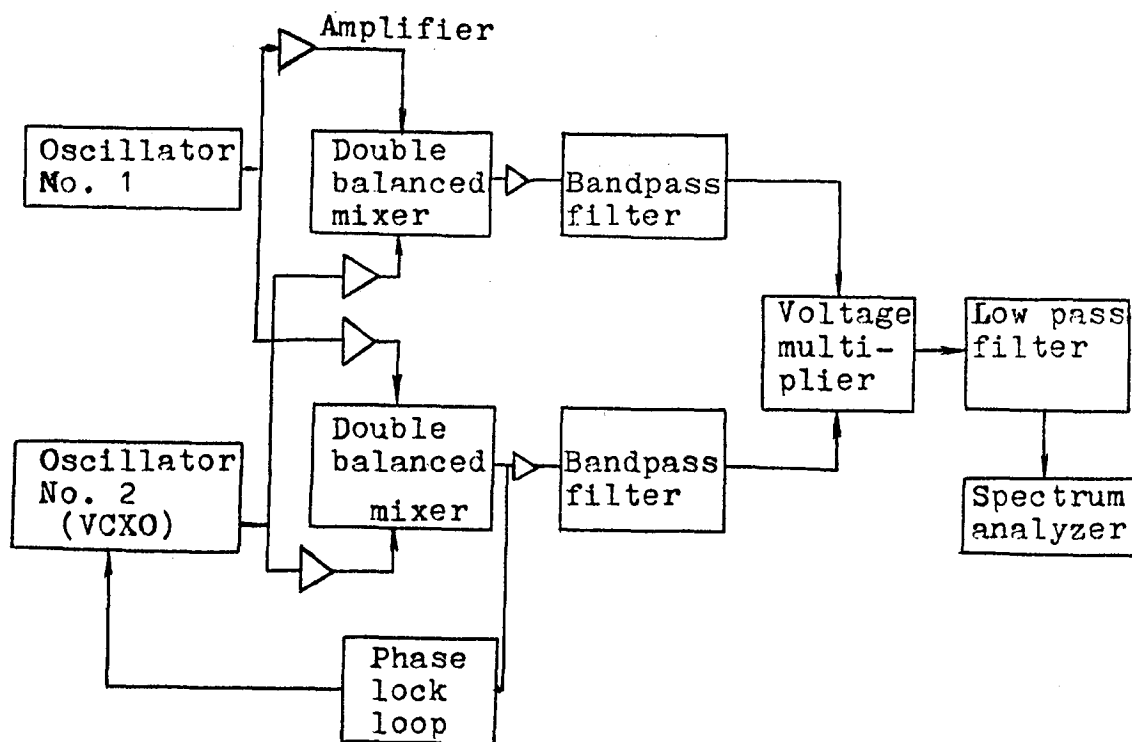


Figure 11. Functional block diagram of the frequency-domain comparator with a correlative zero beat method

The use of television signals for precision time and frequency comparisons

A. BIRMM has undertaken the work of precision time and frequency comparisons using the passive television method in order to compare its atomic frequency standard with atomic frequency standards of other institutes of our country at a remote distance.

B. The principle of operation and the functional block diagram of the TV line-6 synchronizing system:

The television system of our country is a system with 25 frames per second and 625 lines per frame and with interlaced scanning. Its vertical scanning frequency is 50 Hz, whereas the horizontal scanning frequency is 15625 Hz. Passive television synchronization is based on the measurement of the time difference between the arrival of a certain television synchronizing reference pulse and a local clock second pulse. The clock difference between two locations and the frequency accuracy are determined by means of the post-exchange of the data. The first horizontal synchronizing pulse after the vertical and equalizing pulses of the odd field (the first field) is chosen as a reference pulse, i.e. line-6 of the odd field. Since the television frame frequency is 25 Hz, the clocks at two locations must be synchronized so that there would be no multivalence. This can be easily done by comparison with the BPV time signals (short-wave time signals transmitted by the Shanghai Observatory of China). The functional block diagram of the measuring system is shown below.

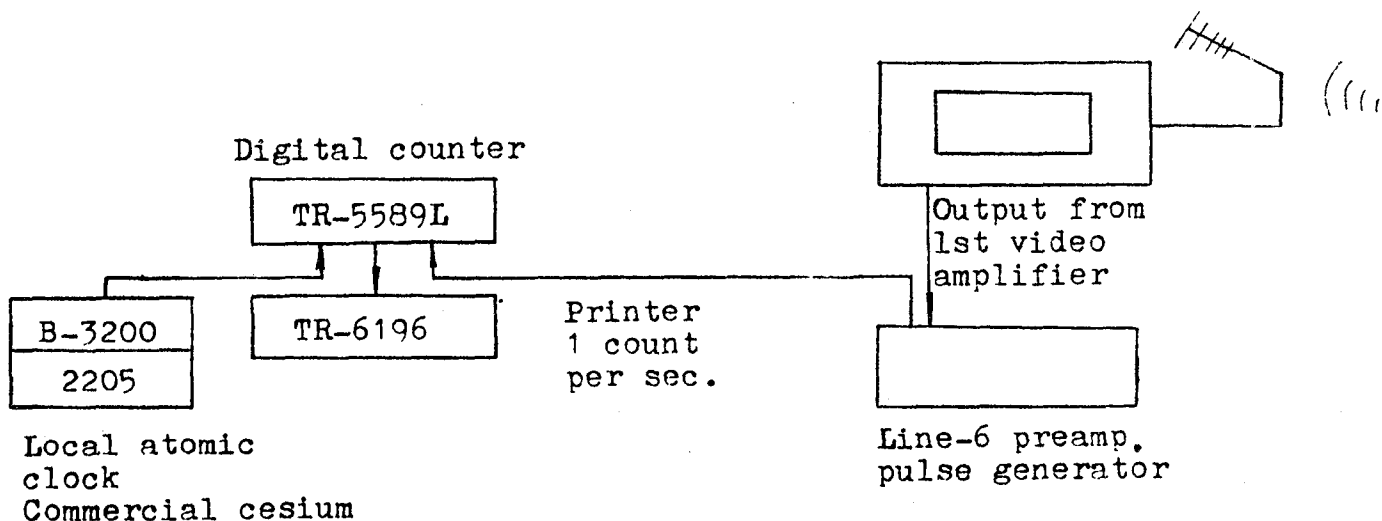


Figure 12. Functional block diagram of the TV line-6 synchronizing system

We have made it a rule to make two comparisons every day from 19 o'clock 15 minutes 0 second to 19 o'clock 15 minutes 45 seconds and from 20 o'clock 15 minutes 0 second to 20 o'clock 15 minutes 45 seconds (Beijing time). Each comparison lasts 45 seconds, and one value is taken in every second. Two average values are calculated every day, i.e. one at 19 o'clock, the other at 20 o'clock.

C. The result of the test:

(1) Stability of the relative time difference between the Beijing Institute of Radio Metrology and Measurements and the Beijing Observatory

$$\text{Standard deviation } \sigma = \sqrt{\frac{\sum (\Delta\tau_i - \Delta\tau)^2}{N-1}}$$

ΔT_i denotes the relative time difference

N denotes the number of measurements

at 19 o'clock $\sigma = 0.32 \mu s$

at 20 o'clock $\sigma = 0.3 \mu s$

Allan variance

at 19 o'clock $\sigma = 0.23 \mu s$

at 20 o'clock $\sigma = 0.24 \mu s$

(2) Accuracy of the frequency calibration

The relative frequency deviation of the BIRMM commercial cesium clock during two months in comparison with the portable rubidium clock of the Beijing Observatory is shown below.

$$\frac{\Delta f}{f} = \frac{\sigma}{\tau} \quad \tau = 86400 \text{ sec.}$$

Standard variance at 19 o'clock $\frac{\Delta f}{f} = 3.7 \cdot 10^{-12}$

at 20 o'clock $\frac{\Delta f}{f} = 3.4 \cdot 10^{-12}$

Allan variance at 19 o'clock $\frac{\Delta f}{f} = 2.4 \cdot 10^{-12}$

at 20 o'clock $\frac{\Delta f}{f} = 2.6 \cdot 10^{-12}$

(3) Determination of the time-delay difference between the Beijing Observatory and BIRMM by using a portable clock:

The portable clock is a commercial cesium one imported from Switzerland. It took sedan four hours to transport the clock (to go and to come back).

The result of the comparison is as follows.

The serial number of the transportation	1	2	3	4	5
Time-delay difference (μs)	44.7	44.4	44.6	44.8	45.2

Uncertainty $0.3 \mu s$ (standard deviation)

(4) Conclusion

The following conclusion can be drawn from the two-month continuous comparison.

a. The different readings of the counter after the two continuous measurements which have been made every twenty four hours will approximately give the relative clock difference between two stations. The stability is $\sigma < 0.5\mu\text{s}$, in other words, the two measurements separated by twenty four hours have achieved the 5×10^{-12} accuracy of frequency calibration.

b. Time-delay difference between two stations can be measured with an accuracy within $0.3\mu\text{s}$ using a portable clock. Therefore the BIRMM clock can be precisely synchronized with the clocks of the Beijing Observatory or other remote places within $0.3\mu\text{s}$ (UTC).

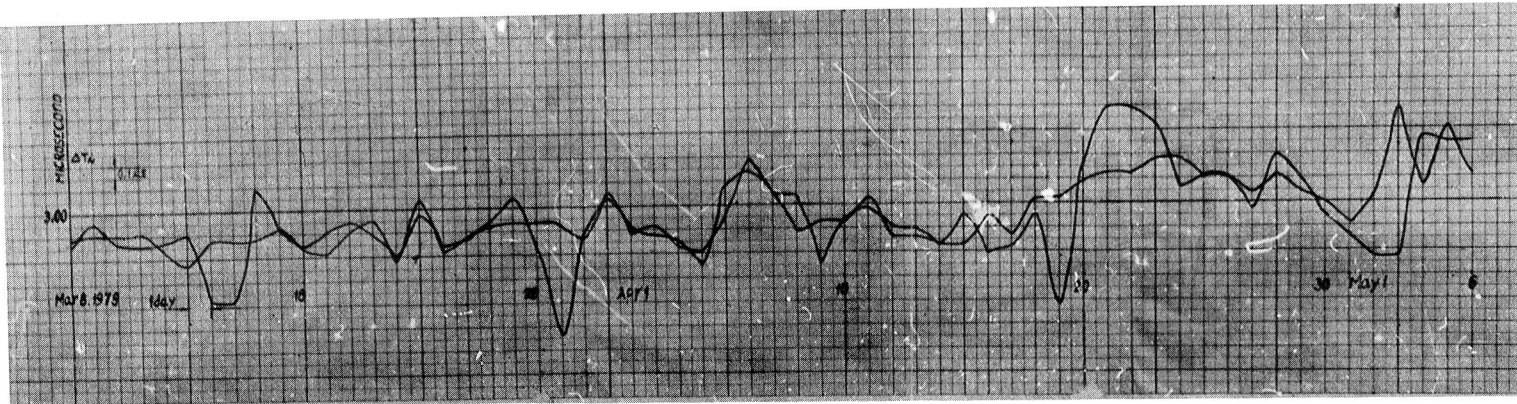


Figure 13. Curves obtained in the test of stability of the relative time difference

4. Time synchronization test by using satellites

Time synchronization via satellites is an advanced technique under development generally recognized in the world. The technique provides high accuracy, large coverage, long transmission distance and short comparison time and requires low cost for building the station. BIRMM took part in the experiment of time synchronization by using the "Symphony" satellite organized by the Central Bureau of Metrology of China.

Three experiments were carried out. Two of them were conducted in China from March 1, 1979 to March 10 and from March 21 to March 31. The other experiment was conducted with a foreign country from June 18 to June 27. The comparison test with the portable clock was made in the period of all the experiments.

From March 1 to March 10 the experiment was conducted between Beijing and Shanghai.

From March 21 to March 31 the experiment was conducted between Shanghai and Nanjing.

From June 18 to June 27 the experiment was conducted between Nanjing (China) and Raisting (West Germany).

The experiment version by using the noncoherent two-way method (or simultaneous two-way method) and the results obtained are presented.

A. Principle of noncoherent two-way method (simultaneous two-way method) for time synchronization test.

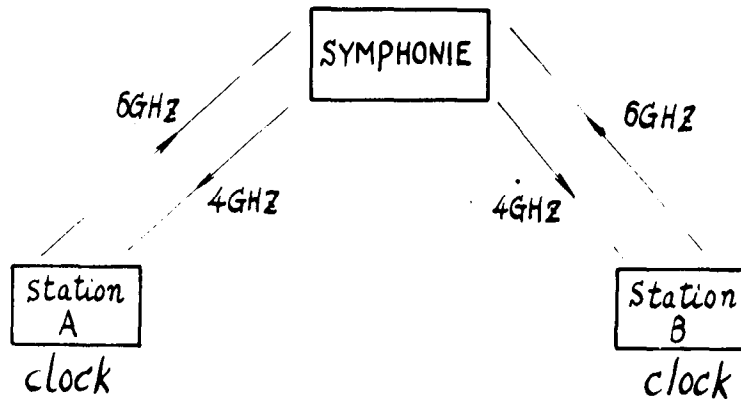


Fig 14

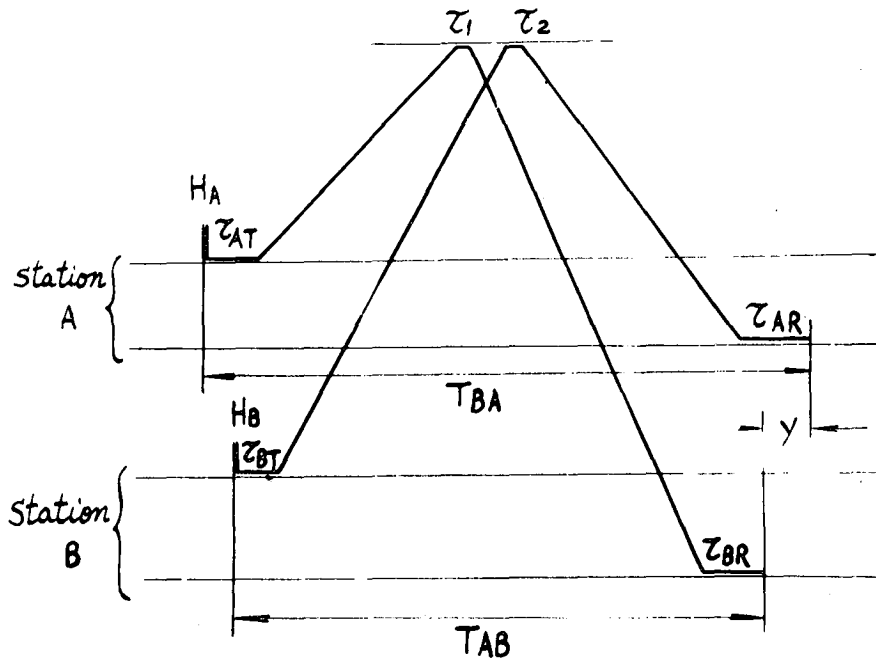


Fig 15

Simultaneous two-way method can be expressed as follows: two ground stations transmit standard time signals to each other at the same moment and receive the standard time signal transmitted by each other. To test the method is one of the important purposes of the experiment. The functional block diagram and the principle of operation are given above in Figures 14 and 15. With the help of the above-mentioned method it is quite easy to obtain T_{BA} and T_{AB} . T_{AB} is the time difference between the standard time signal transmitted by station A and the clock time of station B which is measured by the time interval counter of station B. T_{BA} is the time difference between the standard time signal transmitted by station B and the clock time of station A which is measured by the time interval counter of station A.

If we express the clock difference between station A and station B by Δt

$$\Delta t = H_1 - H_2 = \frac{T_{AB} - T_{BA}}{2} - \left[\frac{t_{AT} - t_{AR}}{2} + \frac{t_{BR} - t_{BT}}{2} + \frac{t_1 - t_2}{2} \right]^2 \quad (1)$$

$$\text{Let } M = \frac{t_{AT} - t_{AR}}{2} + \frac{t_{BR} - t_{BT}}{2} + \frac{t_1 - t_2}{2}$$

then

$$\Delta t = \frac{T_{AB} - T_{BA}}{2} - M \quad (2)$$

B. Parameters used in the experiments in China

$$\Delta t = H_1 - H_2 = \frac{T_{AB} - T_{BA}}{2} \left[\frac{T_{AT} - T_{AR}}{2} + \frac{T_{BR} - T_{BT}}{2} + \frac{T_1 - T_2}{2} \right]^2 \quad (1)$$

$$\text{Let } M = \frac{T_{AT} - T_{AR}}{2} + \frac{T_{BR} - T_{BT}}{2} + \frac{T_1 - T_2}{2},$$

then

$$\Delta t = \frac{T_{AB} - T_{BA}}{2} - M \quad (2)$$

A transponder was employed in the experiment to carry out the test of two-way method. The transmission power of the ground station was restricted in order that the satellite transponder could work in the allowable range.

C. Parameters used in the experiment with West Germany

	Uplink	Downlink	EIRP
Shanghai ground station	6096 MHz	3905 MHz	78dbw
Nanjing ground station	6130 MHz	3865 MHz	79dbw
Beijing ground station	6130 MHz	3865 MHz	79dbw

Two satellite transponders were used in this experiment, thus the transmission power of the ground station increased and the synchronization accuracy improved.

D. Results of the experiments

Places for the experiment	Antenna elevation and carrier-noise ratio	Test method	Stability (ns)	Accuracy (ns)
Shanghai Beijing	6.4°/8.6° 9~11db	two-way	70	71
Shanghai Nanjing	6.4°/8° 9~12db	two-way	70	75

Nanjing Raisting	8°/23° 16~18 db	two-way	9	29
---------------------	--------------------	---------	---	----

E. Determination of the clock difference by the clock transport

The accuracy of the portable clock (stability and accuracy) depends on the quality of the clock and the time interval between trips. The shorter the time interval, the higher the accuracy. In general, the accuracy lies within 10~200 ns. The portable clock we used for the experiment is a 3200 commercial cesium clock. It was transported by air. The transport test was carried out on purpose to determine the value M and the accuracy of satellite time synchronization by using the two-way method.

The result of the transport test is as follows.

From . . . to	Number of the trips	Time interval	Stability (ns)
Shanghai- Beijing	10	Once a day (24 hours)	14
Shanghai- Nanjing	7	Every two days (48 hours)	28
Nanjing- Raisting	4	Different for each case. In the first case to go and to return took 12 days. In the second case to go and to return took 13 days.	30

It can be seen from the equation (2) that the value M must be measured accurately, besides the calculation after post-exchanging T_{AB} and T_{BA} , when the clock difference Δt is found by using the two-way method. There are two approaches to determine M. One approach is to measure precisely $T_{AT} - T_{AR}$, $T_{BR} - T_{BT}$, $T_1 - T_2$, then to calculate M. It is a quite complicated and difficult job. And it still remains one of the problems to solve in satellite time synchronization research. The more precise the value M, the higher the accuracy of time synchronization. Thus there should be a very precise measurement for time delay of the ground station. The other is to determine the value M by using the portable clock.

5. New PTTI items under consideration

A. To set up a hydrogen maser atomic frequency standard

In order to improve the accuracy and stability of frequency standard of this institute, BIRMM has completed installation of the hydrogen maser atomic standard developed by the Shanghai Institute of Metrology and Measurements. BIRMM expects the frequency accuracy to be improved to $(1\sim 5)\times 10^{-12}$ in 1980. (by using the hydrogen maser atomic standard).

B. To set up the BIRMM local atomic time scale as a part of the atomic time scale of our country.

A clock group made up of two hydrogen maser atomic standards and two cesium clocks (and more clocks will be added in 1980) is used for time keeping to set up at (BIRMM).

C. To further improve the characteristics of the rubidium maser atomic frequency standard and to increase its reliability. The performance of the short-term frequency measuring system will be further improved too.

D. To deal with the research work of transfer from frequency domain to time domain in the area of short-term frequency stability measurement and to undertake the development of automatic measuring equipment.

E. To study frequency calibration technique by using the colour television subcarrier frequency method.

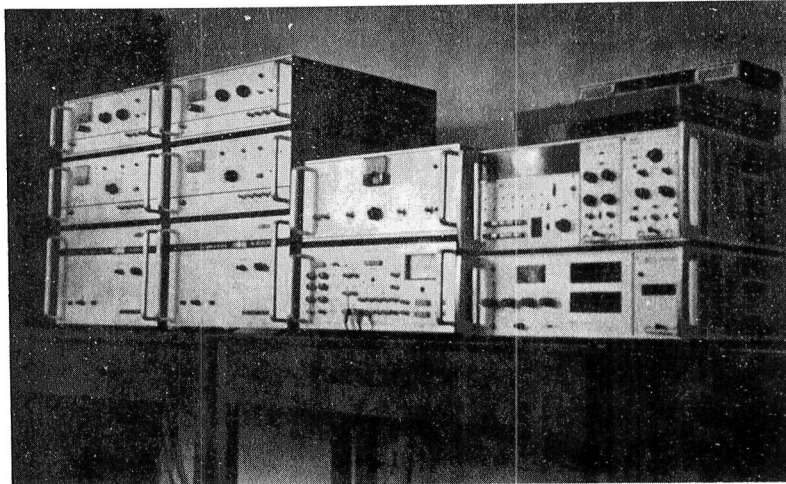


Figure 16. Short-term frequency stability measuring system
Two rubidium atomic frequency standards
(far left and the second from the left)
Reference frequency source
(the second upper one from the right)
Comparator
(the second lower one from the right)
Computing counter (far right)

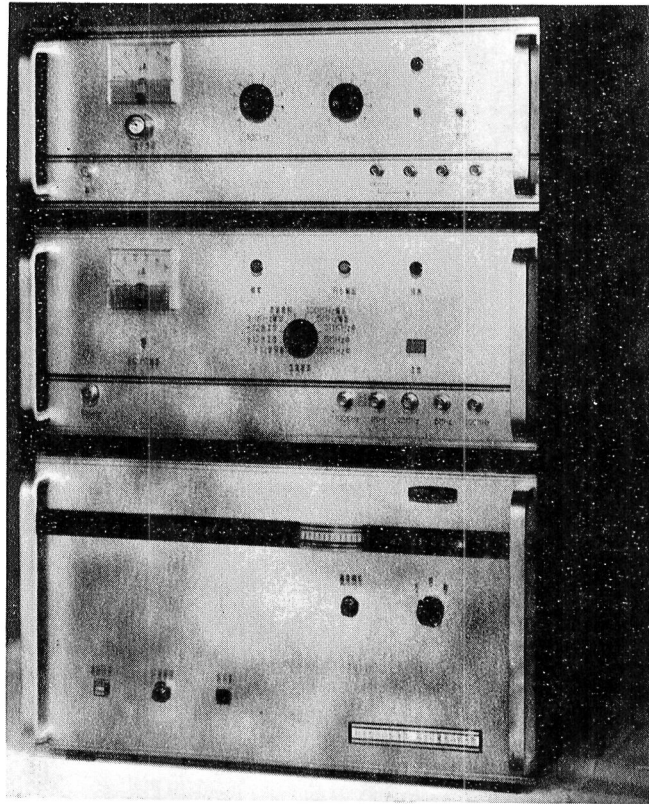


Figure 17. Rubidium maser atomic frequency standard 311 KHz frequency synthesizer (above). Phase-lock receiver (center). Rubidium maser (below).

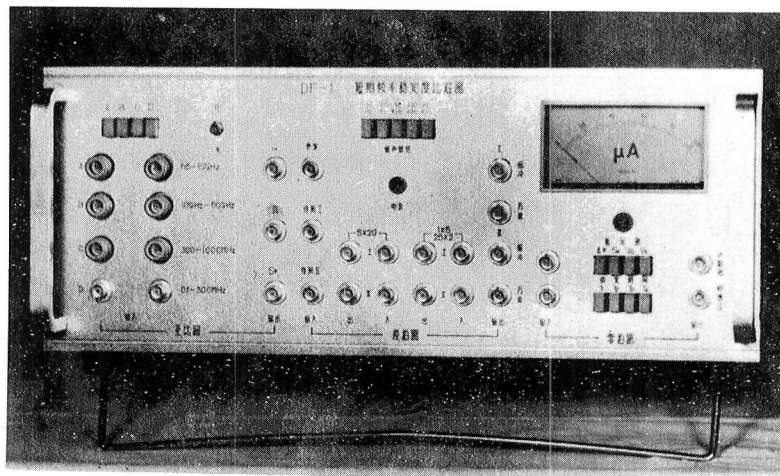


Figure 18. Short-term frequency stability comparator, the time-domain comparator and the frequency-domain comparator are mounted in one unit.

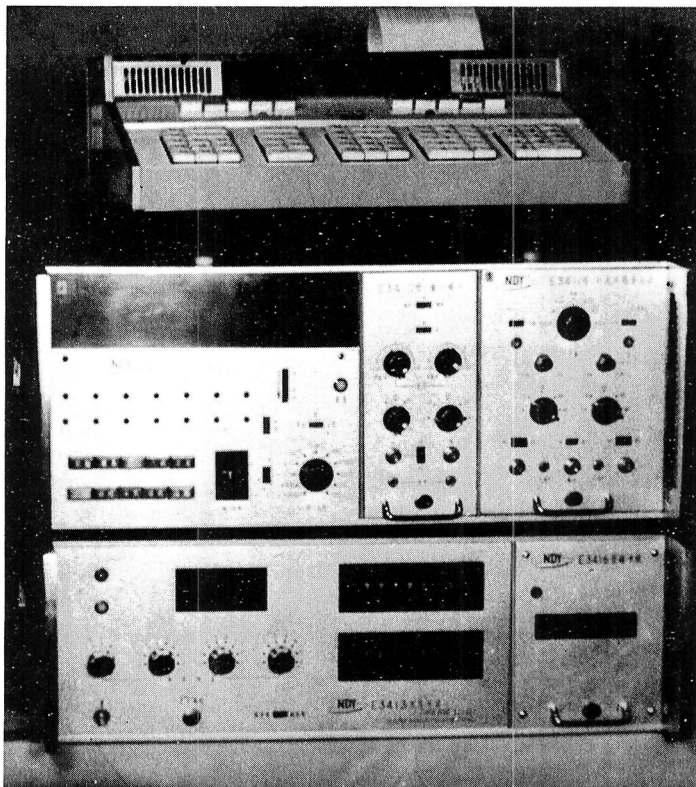


Figure 19. Data processor. (E-314 computing counter produced by the Nanjing Communication Instruments Factory)

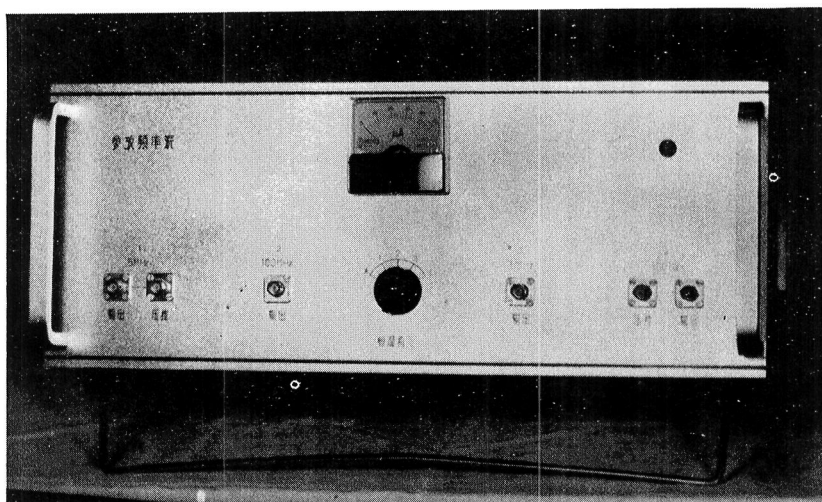


Figure 20. Short-term stability reference frequency source

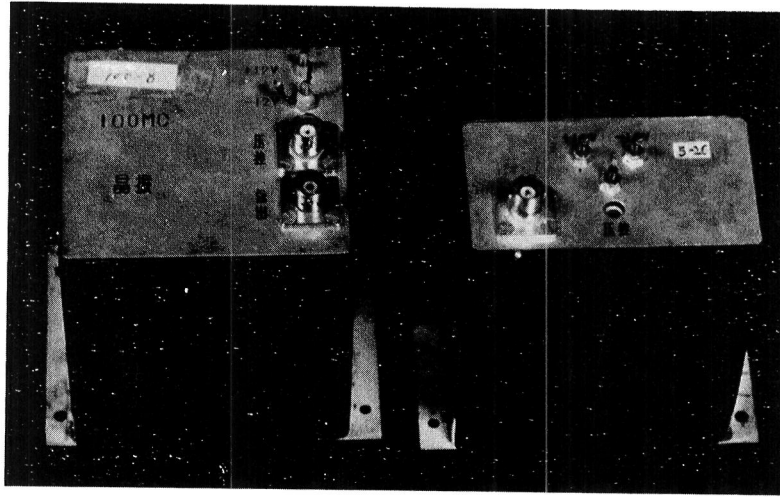


Figure 21. 100 MHz crystal oscillator
5 MHz crystal oscillator

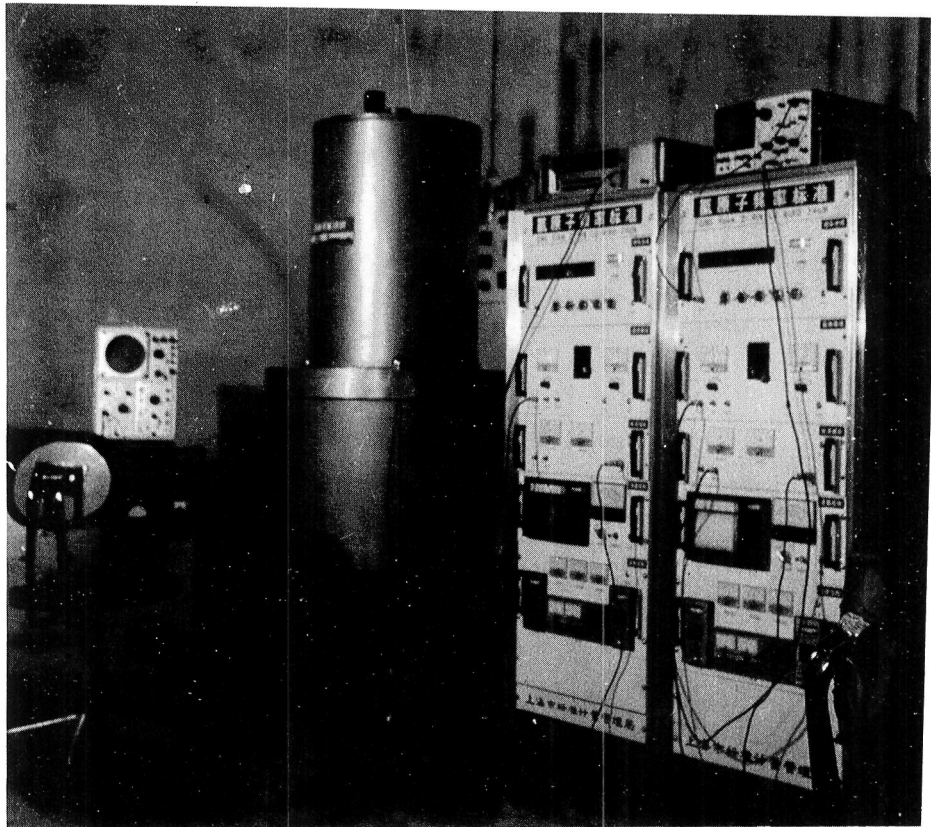


Figure 22. Hydrogen maser atomic frequency standard developed for BIRMM by the Shanghai Institute of Metrology and Measurements

RECENT PROGRESS OF THE RESEARCH WORKS
ON FREQUENCY AND TIME AT THE NIM

Huang Bingying

National Institute of Metrology
Of China, Beijing

1. INTRODUCTION

Research works on frequency and time have been engaged for many years at the NIM. We do the research and development on the primary cesium beam standard and the high-precision crystal oscillator, keep the atomic time and calibrate frequency standards. We also study how to transfer the standard frequency and time at the highest precision. Now, our primary cesium beam installation has been operated to give an accuracy of $1.2 \cdot 10^{-12}$ (1σ). Basing on it, some improvements are being made to attain an uncertainty goal of the order of 10^{-13} . Furthermore, two important experiments have been done in the last two years. One of them was the standard frequency transfer via TV color subcarrier. The frequency stability of σ_y (30 min.) = $4 \cdot 10^{-12}$ has been obtained. Another test was the time synchronization via the Germany-French "Symphonie" satellite. The best results are as follows: the random fluctuation of direct measurement data is $1\sigma_R$ (RMS) < 10 ns, and the absolute error of clock synchronization is $1\sigma_A$ (RMS) < 30 ns.

2. PRIMARY CESIUM STANDARD

In our cesium beam tube, the interaction region is 3.68 m in length. The Ramsey linewidth is about 46 Hz and the arrangement of the beam optics is a typical dipole system. Square wave phase modulation at 43 Hz is used. An accuracy of $1.2 \cdot 10^{-12}$ (1σ) and a stability (σ_y , 1 hour) of $5 \cdot 10^{-13}$ have been obtained last year. After that, we started to make some improvements on the beam optics, the cavity, the C-field, the vacuum system and the environment. Now, a narrower Ramsey linewidth of 28 Hz has been observed. It is expected that the uncertainty of the order of 10^{-13} will be attained after finishing all these improvements.

3. STANDARD FREQUENCY TRANSFER VIA TV COLOR SUBCARRIER

Firstly, we have developed some equipments for this experiment. The major one is the frequency synthesizer at 4.43 ... MHz which is used for color subcarrier frequency in our TV system. We have measured the errors of these equipments and compared the simultaneously obtained data of standard frequency measurements made in Beijing and other cities such as Wuxan, Shanghai and Kuangchow. The results of these measurements show that the stability of the standard frequency transfer via TV color

subcarrier is about $4 \cdot 10^{-12}/30$ min. within our TV network. We plan to realize the standard frequency and time dissemination via the TV signal in the near future.

4. TIME SYNCHRONIZATION VIA THE "SYMPHONIE" SATELLITE

A series of tests about the two-way delayed noncoherent time synchronization via the Germany-French "Symphonie" satellite have been done in this year. The results obtained are listed in the following table:

<u>Ground Stations</u>	<u>Type of the Errors (ns)</u>	
	σ_R (RMS)	σ_A (RMS)
Shanghai-Beijing March, 1979	70	71
Shanghai-Nanjing March, 1979	70	75
Nanjing (China)- Raisting (Germany) June, 1979	9	29

In this table, the σ_R and σ_A have the same meaning mentioned above.

Many other units, especially the PTB of FRG, have taken part in the experiments. Here, we would like to thank them for their valuable cooperation. We just attempted to march out the first step, and we shall continue to do more research works in order to build up the time synchronization system via the satellite in our country.

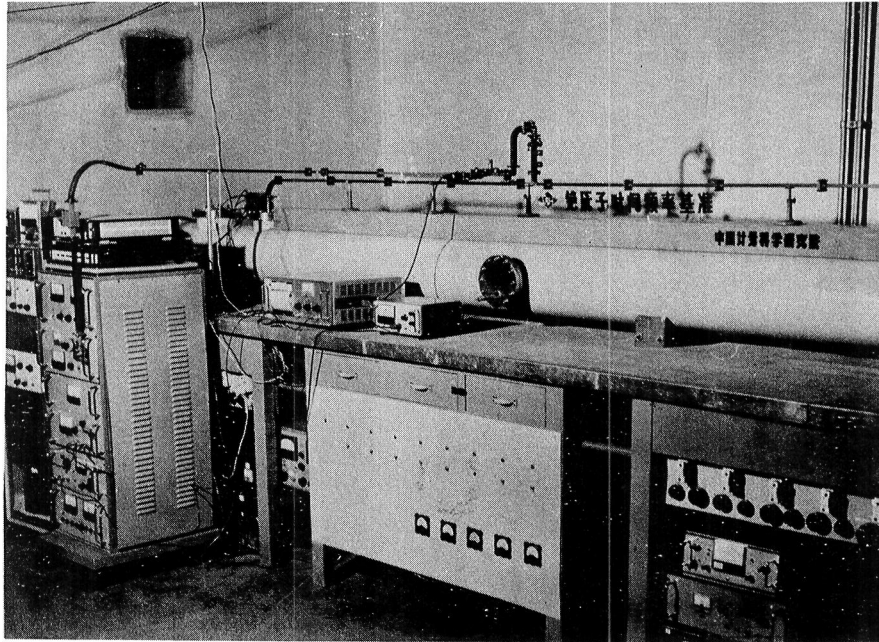


Fig. 1. Primary Cesium Standard

QUESTIONS AND ANSWERS

DR. COSTAIN:

Yes. Just very quickly, as I mentioned privately I think you will have very great difficulty in establishing the excellence of a primary standard when you only have a commercial standard as reference. I would suggest that the quickest and the best to do is to build another primary standard because you need something just as good or better to compare it with.

MR. Bing-ying Huang, National Institute of Metrology of China, Beijing

Thank you.

11TH ANNUAL PRECISE TIME AND TIME INTERVAL

REGISTRATION

Irvin Agree
NASA/GSFC
Code 813.3
Greenbelt, MD 20771

David W. Allan
National Bureau of Standards
325 Broadway
Boulder, CO 80303

Ralph T. Allen
NAVELEX
Code 51023A
Washington, DC 20360

Carroll O. Alley
University of Maryland
Department of Physics
College Park, MD 20742

C. R. Anderson
Hughes Aircraft Co.
625 Norfolk Way
Aurora, CO 80011

Michael Arnoldt
Fernmeldetechnisches Zentralamt
C-17-3
Postfach 5000
6100 Darmstadt
GERMANY

Heinz Badura
Efratom Calif. Inc.
18851 Bardeen Ave.
Irvine, CA 92715

Arthur Ballato
U. S. Army Electronics Command
Ft. Monmouth, NJ 07703

O. J. Baltzer
TRACOR, Inc.
6500 Tracor Ln.
Austin, TX 78721

John A. Bangert
Defense Mapping Agency
6500 Brookes Ln.
Bethesda, MD 20014

James A. Barnes
National Bureau of Standards
325 Broadway
Boulder, CO 80302

C. A. Bartholomew
Naval Research Laboratory
Code 7962
4555 Overlook Ave., SW
Washington, DC 20375

Alvin Bates
Johns Hopkins University
Johns Hopkins Rd.
Laurel, MD 20810

Jacques Beavssier
ONERA
11 Rve Louis Boussa
RD 91320 Wisso
FRANCE

Gerhard Becker
PTB
Bundesallee 100
D33-Braunschweig
WEST GERMANY

Roger E. Beehler
National Bureau of Standards
325 Broadway
Boulder, CO 80303

Raymond Besson
ENSMM
La Bouloie Rte. Gray
Besancon
FRANCE 25030

Ken Beutler
Jet Propulsion Laboratory
3500 Oak Grove Dr.
Pasadena, CA 91103

Albert B. Bierman
The Aerospace Corp.
2350 East El Segundo
El Segundo, CA 90245

Martin B. Bloch
F.E.I.
3 Delaware Dr.
New Hyde Park, NY 11042

Eric Blomberg
SAO
60 Garden St., P151
Cambridge, MA 02138

J. S. Boulanger
National Research Council of Canada
Ottawa, Ontario
CANADA K1A0R6

J. C. Bowerman
NAVELEX
Code 46014
Washington, DC 20360

Mary A. K. Braunstein
ANA-LOG Inc.
7655 Old Spring House Rd.
McLean, VA 22102

Ed Bregstone
U.S. Coast Guard
2607 Central Ave.
Alexandria, VA 22302

James Buisson
Naval Research Laboratory
Code 7966
4555 Overlook Ave, SW
Washington, DC 20375

Stanley A. Butman
Jet Propulsion Laboratory
M5. 238-420
4800 Oak Grove Dr.
Pasadena, CA 91103

Jin-Tao Cai
Chinese Society of Astronautics
Beijing
CHINA

Roy Cashion
Satellite Navigation
621 Lofstrand Ln.
Rockville, MD 20850

Laura G. Charron
U. S. Naval Observatory
34th & Mass. Ave., NW
Washington, DC 22180

Craig M. Cheetham
Jet Propulsion Laboratory
4800 Oak Grove Dr.
Pasadena, CA 91103

Arthur G. Chenoweth
Lockheed MSD
535 Starboard Dr.
San Mateo, CA 94404

A. R. Chi
NASA/GSFC
Code 810
Greenbelt, MD 20771

Lehner Christoph
DFVLR/GSOC-ZDBS
Postfach 156
8120 Weilheim
WEST GERMANY

Robert J. Coates
NASA/GSFC
Code 900
Greenbelt, MD 20771

Richard C. Coffin
Jet Propulsion Laboratory
4800 Oak Grove Dr.
Pasadena, CA 91103

Jimmie B. Collie
NESEC
6341 Route 29
Portsmouth, NH 23703

Glenn A. Conover
Labarge Inc.
1101 17th St., NW
Washington, DC 20036

Dr. C. C. Costain
National Research Council of Canada
Div. of Physics
Ottawa, Ontario
CANADA K1A0R6

Stephen A. Cresswell
Federal Electric
Vandenberg AFB, CA 93437

David Curkendall
Jet Propulsion Laboratory
4800 Oak Grove Dr.
Pasadena, CA 91103

Leonard S. Cutler
Hewlett Packard Co.
3500 Deer Cr. Rd.
Palo Alto, CA 94034

Fredrick Danzy
Naval Research Laboratory
4555 Overlook Ave.
Washington, DC 20375

Carolyn Brandt Davis
ANA-LOG Inc.
7655 Old Springhouse Rd.
McLean, VA 22102

Walter N. Dean
Verdes Engineering
26619 Shorewood Rd.
Rancho Palos Verdes, CA 90274

Rudolf Decher
NASA/Marshall Space Flight Center
Huntsville, AL 35812

B. Louis Decker
DMA Aerospace Ctr.
402 Devon Court
Ballwin, MO 63011

Walter Derengowski
T. E. Corp.
3702 Perry Ave.
Kensington, MD 20795

E. Detoma
NASA/GSFC
Code 814.2
Greenbelt, MD 20771

Ralph E. Dickerson
Naval Surface Weapons Center
Code F-14
Dahlgren, VA 22448

Lawrence Doepke
DMAAC
9418 Oakwood Manor
St. Louis, MO 63126

Thomas P. Donaher
Spectracom
30 Elmcroft Rd.
Rochester, NY 14609

R. W. Donaldson
Westinghouse
P. O. Box 1897 MS 935
Baltimore, MD 21203

Ernest S. Drake
Hewlett Packard Co.
5301 Stevens Creek
Santa Clara, CA 95050

Hugues Duchaussoy
IRET
4 Rue Du Dome
Paris
FRANCE 75116

Richard L. Ealum
DMAAC
7014 Christopher Dr.
St. Louis, MO 63129

Roger L. Easton
Naval Research Laboratory
Code 7960
4555 Overlook Ave., SW
Washington, DC 20375

Warren E. Edwall
RCA Corp.
1901 N. Moore St.
Arlington, VA 22209

Robert Edwards
Defense Mapping Agency
6500 Brooks Ln.
Bethesda, MD 20014

Richard Eichinger
Bendix Field Engr.
9250 Route 108
Columbia, MD 21045

Bryant Ellis
Weather Chron
5144 Peachtree Road
Atlanta, GA 30341

R. F. Ellis
Austron Inc.
1915 Kramer Ln.
Austin, TX 78758

Donald A. Emmons
FTS
182 Conant St.
Danvers, MA 01923

Glen E. Eubanks
CNO OPNAV 952
Naval Oceanography
Washington, DC 20350

Dean C. Ewalt
IBM
18100 Frederick Pike
Gaithersburg, MD 20760

William A. Feess
The Aerospace Corp.
2350 E. El Segundo Blvd.
El Segundo, CA 90245

Mike Fischer
Hewlett Packard Co.
5301 Stevens Creek Blvd.
Santa Clara, CA 95050

R. F. Fleming
S. N. Inc.
621 Lofstrand Ln.
Rockville, MD 20850

Melinda M. Force
Hewlett Packard Co.
5301 Stevens Creek
Santa Clara, CA 95050

Hugh S. Fosque
NASA Hdq.
600 Independence Ave., SW
Washington, DC

Steve Friedman
ILC Data Device Co.
105 Wilbur Pl.
Bohemia, NY 11716

George Fruhling
Pacific Missile T. C.
Code 4133
Point Mugu, CA 93041

Jose A. M. Fuentes
OLA89 FMS PMEL
Bolling AFB
Washington, DC 20332

Richard Fulper, Jr.
Naval Research Laboratory
4555 Overlook Ave., SW
Washington, DC 20375

Larry M. Galloway
AGMC
Newark AFS
Newark, OH 43055

Charles E. Gambill
AGMC
Newark AFS, OH 43055

Peter C. Garriga
Hughes Aircraft
849 Penn St.
El Segundo, CA 90245

R. J. Gerharz
Dept. of Defense
USANVL Bldg. 357
Ft. Belvoir, VA 22060

Joseph N. Goeser
Bendix FEC
9250 Rt. 108
Columbia, MD 21045

Seymour Goldberg
BG&G Inc.
35 Congress St.
Salem, MA 01970

M. Granveaud
Bureau International
De L'Heure
6 Observatoi
Paris
FRANCE

Richard L. Greenspan
C. S. Draper Lab., Inc.
550 Technology Square
Cambridge, MA 02139

Lloyd F. Griffith
ITT/FEC DT250
P. O. 1886
Vandenberg AFB, CA 93111

R. Glenn Hall
U. S. Naval Observatory
Washington, DC 20390

Donald L. Hammond
Hewlett Packard Co.
1501 Page Mill Rd.
Palo Alto, CA 94304

Samuel N. Harmatuk
Consultant
1575 Odell St.
Bronx, NY 10462

Jeannie Haynie
Naval Surface Weapons Center
Dahlgren, VA 22448

Bruce R. Hermann
Naval Surface Weapons Center
K13
Dahlgren, VA 22448

Walter A. Hickman
1 Munnings Dr.
Sudbury, MA 01776

Wolfgang Hietzke
Jet Propulsion Laboratory
Ms 179/123
4800 Oak Grove Dr.
Pasadena, CA 91103

Patrick Hill
FTS
182 Conant St.
Danvers, MA 01923

John C. Hoen
Dept. of Defense
9800 Savage Road
Fort Meade, MD 20755

Juan Horat
Observatorio Naval
Av. Espana No. 2099
Buenos Aires
ARGENTINA

Norman Houlding
Mitre Corp.
P. O. Box 208
Bedford, MA 01730

David A. Howe
National Bureau of Standards
325 Broadway
Boulder, CO 80303

Carl Hruska
York University
269 Banbury Rd.
Don Mills, Ontario
CANADA M3B3C7

Quyen Hua
Stanford Telecomm
1195 Bordeaux
Sunnyvale, CA 94086

Bing-Ying Huang
National Institute of Metrology
Beijing
CHINA

Edward A. Imbier
Smithsonian Institute
60 Garden St.
Cambridge, MA 02138

Herbert S. Ingraham
COMSAT Laboratories
22300 Comsat Dr.
Clarksburg, MD 20734

Norman J. Jansen
U. S. Air Force
Hq. AGMC
Newark, AFS, OH 43055

J. Jespersen
National Bureau of Standards
325 Broadway
Boulder, CO 80302

Andrew C. Johnson
Naval Observatory
Washington, DC 20390

Robert Kaarls
Natl. Serv. Metrology
P. O. Box 654 Delft
NETHERLANDS

Alfred Kahan
USAF/RADC
Hanscom AFB, MA 01731

Peter Kartaschoff
Generaldirektionptt
ABT Forschung U ENTW
Bern
SWITZERLAND 3030

William W. Kellogg
Lockheed Missiles
Bldg. 154, P. O. Box 504
Sonnyvale, CA 94088

Robert Kern
Kernco Inc.
28 Harbor St.
Danvers, MA 01923

Dieter Kirchner
Technical University Graz
Inffeldgasse 12
Graz
AUSTRIA A-8010

W. J. Klepczynski
U. S. Naval Observatory
Washington, DC 20390

Stephen H. Knowles
Naval Research Laboratory
4555 Overlook Ave., SW
Washington, DC 20375

Robert M. Kovacs
Kentron Int, Inc.
Box 1207
APO, San Francisco, CA 96555

Paul F. Kuhnle
Jet Propulsion Laboratory
4800 Oak Grove Dr.
Pasadena, CA 91103

Jack Kusters
Hewlett Packard Co.
5301 Stevens Creek
Santa Clara, CA 95050

Donald Lander
Austron Inc.
1800 Old Meadow Rd.
McLean, VA 22102

Leonard R. Lathrem
Bendix Corp.
9250 Rt. 108
Columbia, MD

Kai C. Lau
Datametrics
340 Fordham Rd.
Wilmington, MA 01887

Edward W. Lauffer
Efratom
18851 Bardeen Ave.
Irvine, CA 92715

J. D. Lavanceau
Lt International
4907 Asbury Ln.
Bethesda, MD 20014

Dr. Robertt E. Lawrence
Vitro Laboratories
14000 Georgia Ave.
Silver Spring, MD 20910

Felix Lazarus
Hewlett Packard Agency
19 Ch. Chateau-Bloc
1219 Le Lignon
Geneva
SWITZERLAND

Warren Lefrancois
MUCTC
920 St. Aubin
Montreal, Quebec
CANADA H4M2K1

David Lerner
Current Designs Corp.
210 E. 86 St.
New York, NY 10028

S. Leschiutta
Istituto Elettrotecnico Nazionale
Str. Delle Cacce, 91
Torino,
ITALY 10135

Vestal R. Lester
Hughes Aircraft Co.
19631 Strathern St.
Reseda, CA 91335

Martin W. Levine
FTS
182 Conant St.
Danvers, MA 01923

Ronald Lindsay SD/YEE
GPS Program Office
P. O. Box 92960 Worldway PS
Los Angeles, CA 90009

Lionel Lipschultz
Johns Hopkins University
Applied Physics Laboratory
Johns Hopkins Rd.
Laurel, MD 20810

David Loomis
USAF Elmendorf AFB
7130 Chester Ct.
Anchorage, AK 99504

Donald W. Lynch
Naval Research Laboratory
4555 Overlook Ave., SW
Washington, DC 20375

George A. Madrid
Jet Propulsion Laboratory
4800 Oak Grove Dr.
Pasadena, CA 91103

Harold G. Majeran
Dept. of Defense
9800 Savage Rd.
Ft. Meade, MD 20755

Matthew Maloof
Naval Research Laboratory
4555 Overlook Ave., SW
Washington, DC 20375

Edward Mattison
Smithsonian Observatory
60 Garden St.
Cambridge, MA 02138

Charles May
Johns Hopkins University
Applied Physics Laboratory
Johns Hopkins Rd.
Laurel, MD 20810

Robert M. McCannon
Weatherchron
5144 Peachtree Rd.
Atlanta, GA 30341

Thomas McCasvill
Naval Research Laboratory
Code 7966
4555 Overlook Ave., SW
Washington, DC 20375

Paullo J. McConahy
Applied Physics Laboratory
Johns Hopkins University
Johns Hopkins Rd.
Laurel, MD 20810

A. O. McCoubrey
National Bureau of Standards
Gaithersburg, MD 20760

Richard McDarmont
Metric Systems
73G No. Beal St.
Ft. Walton Beach, FL 32548

Michael D. McGuire
Hewlett Packard Laboratory
3500 Deer Creek Rd.
Palo Alto, CA 94304

David McKerrow
Embassy of Canada
1746 Mass. Ave.
Washington, DC 20036

Thrygve R. Meeker
Bell Laboratories
555 Union Blvd.
Allentown, PA 18103

Marvin Meirs
Freq. Elect, Inc.
3 Delaware Dr.
New Hyde Park, NY 11040

Mendez Quinones
National Bureau of Standards
325 Broadway
Boulder, CO 80302

Edwin E. Mengel
Johns Hopkins University
Applied Physics Laboratory
Johns Hopkins Rd.
Laurel, MD 20810

Tom Mingle
Hewlett Packard Co.
5301 Stevens Creek
Santa Clara, CA 95050

G. Missout
Hydro Quebec
1800 Montee Ste Julie
Varenes, Quebec
CANADA

D. H. Mitchell
Kentron International, Inc.
P. O. Box 4819
Yuma, AZ 85364

Ivan I. Mueller
Ohio State University
Dept. of Geodetic Science
1958 Neil Ave.
Columbus, OH 43210

James A. Murray Jr.
Naval Research Laboratory
Code 7562
4555 Overlook Ave., SW
Washington, DC 20375

Ronnie W. Myers
Austron Inc.
1915 Kramer Ln.
Austin, TX 78758

Lawrene W. Nelson
General Electric Co.
P. O. Drawer QQ
Santa Barbara, CA 93101

Stephen Nichols
Naval Research Laboratory
Code 7586
4555 Overlook Ave., SW
Washington, DC 20375

Jerry R. Norton
Johns Hopkins University
Applied Physics Laboratory
Johns Hopkins Rd.
Laurel, MD 20810

Klemens Nottarp
Inst f Angew Geodesy
Sat Obs Station Wettzell
Kuetzting
WEST GERMANY D-8493

O. Jay Oaks
Naval Research Laboratory
4555 Overlook Ave., SW
Washington, DC 20795

Jack O'Hara
Marktron Inc.
57 W. Timonium Rd.
Timonium, MD 21093

George Oja
U.S. Navy Met. Eng. Ctr.
P. O. Box 2436
Pomona, CA 91766

William S. Orr
CBSI
221 S. 85th E. Ave.
Tulsa, OK 74112

Terry N. Osterdock
Hewlett Packard Co.
5301 Stevens Creek
Santa Clara, CA 95030

Eugene J. O'Sullivan
Mitre Corp.
P. O. Box 208
Bedford, MA 01730

Thomas J. Parello
Frequency & Time System
182 Conant St.
Danvers, MA 01923

John H. Pels
Austron Inc.
1915 Kramer Ln.
Austin, TX 75758

H. E. Peters
Sigma Tau Standards Corp.
Box 1877; 1014 Hackberry Ln.
Tuscaloosa, AL 35403

Edward A. Pettit
USAF ESMC/RSM
Patrick AFB, FL 32925

David H. Phillips
Naval Research Laboratory
4555 Overlook Ave., SW
Washington, DC 20375

Gail K. Phillips MZ 8227-I
General Dynamics/Electronics
P. O. 81127
San Diego, CA 92138

William R. Philipsen
Houper, Assoc.
2300 9th St. South
Arlington, VA 22204

John D. H. Pickington
Royal Greenwich Obs.
Herstmonceux Castle
Hailsham, E. Sussex
UNITED KINGDOM

Wm. G. Pixton
Ford Aerospace
3939 Fabian Way
Palo Alto, CA 94303

Myron Pleasure
Chronotechnology Assoc.
37-13 74th St.
Jackson Heights, NY 11372

George E. Price
Austron
1915 Kramer Ln.
Austin, TX 78785

Kenneth Putkovich
U.S. Naval Observatory
Washington, DC 20390

Eduardo J. Ramon
Observatorio Naval
Av. Espana
Buenos Aires
ARGENTINA

Prof. Norman Ramsey
Harvard University
Cambridge, MA 02138

James R. Ransom
Westinghouse Elec.
107 East Susquehanna Ave.
Towson, MD 21204

Elza K. Redman
Dept. of Defense
9800 Savage Rd.
Fort Meade, MD 20755

Dr. Victor Reinhardt
NASA/GSFC
Code 814.2
Greenbelt, MD 20760

Dale E. Ringer
Rockwell Intrl. Corp.
12214 Lakewood Blvd.
Downey, CA 90241

Ron Roloff
Bendix
9850 Rt. 108
Columbia, MD

David E. Ross
System Development Corp.
2500 Colorado Ave.
Drop 31-05
Santa Monica, CA 90406

Ben D. Roth
DMAHTC-GST (SD/YEUP)
6500 Brookes Ln.
Washington, DC 20315

Lauren J. Rueger
Johns Hopkins University
Applied Physics Laboratory
Johns Hopkins Rd.
Laurel, MD 20810

James W. Ryan
NASA/GSFC
Code 922
Greenbelt, MD 20771

Ted Saffos
Naval Surface Weapons Center
Code F14
Dahlgren, VA 22448

Walter Saldarini
EG&G Inc.
35 Congress St.
Salem, MA 01970

J. Y. Savard
Laval University
Quebec City
CANADA

Wolfgang Schlueter
JFAG; GF Weinbergstr
Frankfurt, 80
WEST GERMANY D6230

John G. Schmid
USAF WSMC RSDE
Bldg. 8500
Vandenberg AFB, CA 93437

William H. Schneider
AFSC RADC DCCW
Griffiss AFB, NY 13441

Stephen Schramm
General Electric Co.
803 Worthington Dr.
Exton, PA 19341

David C. Scull
U.S. Coast Guard
2112 Wittington Blvd.
Alexandria, VA 22308

Dr. B. E. H. Serene
European Space Agency
78 Rue E. Belin
31055 Toulouse Cedex
FRANCE

Leonard F. Shepard
ILC Data Device Corp.
105 Wilbur Place
Bohemia, NY 11716

Steven L. Silverman
Naval Surface Weapons Center
72 Philip Dr.
Princeton, NJ 08540

Dr. V. R. Singh
National Physical Laboratory
Hillside Rd.
New Delhi
INDIA 110012

Alexander Skopetz
NASA/GSFC
Code 7304
Greenbelt, MD 20771

Arthur E. Smith
Data Collection Div.
Rang. Inst. 545. Dept.
P.M.T.C. Point Mugu, CA 93042

Joseph T. Sonsini
U.S. Air Force
PSC Box 305
Hanscom AFB, MA 01731

Dr. S. Starker/DFVLR
Hochfrequenztechnik Institut Fuer
D-8031 Oberpfaffenhofen
Post Wessling
WEST GERMANY

Samuel R. Stein
National Bureau of Standards
325 Broadway
Boulder, CO 80303

C. S. Stone
Tracor Inc.
6500 Tracor Ln.
Austin, TX 78721

Harris A. Stover
DCA
1860 Wiehle Ave.
Reston, VA 22090

John Strain
Frequency Elec.
13975 Conn. Ave. No. 210
Silver Spring, MD 20906

Herbert Stratemeyer
EG&G Inc.
35 Congress St.
Salem, MA 01970

Herb Stringer/50330
E-Systems/Garland
P. O. Box 226118
Dallas, TX 75266

Edmund Sullivan
EG&G Inc.
35 Congress St.
Salem, MA 01970

Richard L. Sydnor
Jet Propulsion Laboratory
4800 Oak Grove Dr.
Pasadena, CA 91103

J. B. Thomas
Jet Propulsion Laboratory
4740 Hampton Rd.
La Canada, CA 91011

J. W. Tomlin
Hughes Aircraft Co.
12457 E. Cedar Cir.
Aurora, CO 80012

Kenneth M. Uglow
Research Consultant
P. O. Box 2260
Sarasota, FL 33578

Jacques Vanier
Universite Laval
Quebec
CANADA G1K7P4

Lester B. Veenstra
Comsat Laboratory
22300 Comsat Dr.
Clarksburg, MD 20734

Pierre Venne
Canadian Broadcasting
1400 Dorchester East
Montreal, Quebec
CANADA H2H-2C1

R. F. C. Vessot
SAO
60 Garden St.
Cambridge, MA 02138

J. R. Vetter
Johns Hopkins University
Applied Physics Laboratory
Johns Hopkins Rd.
Laurel, MD 20810

John R. Vig
U.S. Army ERADCOM
Attn: Delet, MQ
Ft. Monmouth, NJ 07703

Raymond Vohden
U.S. Naval Observatory
Washington, DC 20390

Alan J. Waiss
Electrospace Sys. Inc.
Box 2668
Arlington, VA 22202

E. S. Walker
Hughes Aircraft Co.
P. O. Box N
Aurora, CO 80041

W. C. Walker
Pan Am AF ESMC
Bldg. 989 MU 840
Patrick AFB, FL 32925

Fred L. Walls
National Bureau of Standards
325 Brodway
Boulder, CO 80303

Harry T. M. Wang
Hughes Research Laboratory
3011 Malibu Canyon
Malibu, CA 90265

Hong-Tang Wang
Institute of Radio
Metrology & Meas.
Beijing
CHINA

Clark Wardrip
NASA/GSFC
Code 814
Greenbelt, MD 20771

Andre Wavre
Oscilloquartz SA
Brevards IG
Neuchatel
NETHERLANDS 2000

Gart Westerhout
U.S. Naval Observatory
34th & Mass. Ave., NW
Washington, DC 20390

Joe White
Naval Research Laboratory
Code 7962
4555 Overlook Ave., SW
Washington, DC 20375

Gary Whitworth
Johns Hopkins University
Applied Physics Laboratory
Johns Hopkins Rd.
Laurel, MD 20810

P. C. Wildhagen
The Aerospace Corp.
P. O. Box 92957
Los Angeles, CA 90009

J. D. Williams
NGS
P. O. Box 1
Corbin, VA 22446

Ralph E. Willison
Applied Physics Laboratory
9204 Crosby Rd.
Silver Spring, MD 20910

Warren L. Wilson
Fairchild Test Systems
707 Spindrift Dr.
San Jose, CA 95134

David J. Wineland
National Bureau of Standards
325 Broadway
Boulder, CO 80303

Gernot M. R. Winkler
U.S. Naval Observatory
Washington, DC 20390

C. R. Wright
FAA
AAF360
Atlantic City, NJ 08405

Yoshiyuki Yasuda
Radio Research Laboratories
2-1, 4-chome, Nukui-Kitamachi Koganei
Tokyo
JAPAN 184

Larry E. Young
Jet Propulsion Laboratory
630 Groveview Ln.
La Canada, CA 91011

Thomas Yunck
Jet Propulsion Laboratory
4800 Oak Grove Dr.
Pasadena, CA 91103

Ji-Sheng Zhang
Xian Cneter Satellite
Tracking & Tele.
Xian
CHINA

Miles M. Zich
NAVALEX
Code 51023Z
Washington, DC 20360

Plato Zorzy
Deltek
Shetland Ind. Park
P. O. Box 2074
Salem, MA 01970

BIBLIOGRAPHIC DATA SHEET

1. Report No. NASA CP 2129	2. Government Accession No.	3. Recipient's Catalog No.	
4. Title and Subtitle Proceedings of the Eleventh Annual Precise Time and Time Interval (PTTI) Applications and Planning Meeting		5. Report Date April 1980	
		6. Performing Organization Code Code 814	
7. Author(s) Schuyler C. Wardrip, Editor		8. Performing Organization Report No.	
9. Performing Organization Name and Address Goddard Space Flight Center Greenbelt, MD 20770		10. Work Unit No.	
		11. Contract or Grant No.	
		13. Type of Report and Period Covered	
12. Sponsoring Agency Name and Address National Aeronautics and Space Administration Naval Electronic Systems Command Naval Research Laboratory U.S. Naval Observatory Defense Communications Agency		14. Sponsoring Agency Code	
		15. Supplementary Notes	
16. Abstract These proceedings contain the papers presented at the Eleventh Annual Precise Time and Time Interval (PTTI) Applications and Planning Meeting, including questions and answers following presentations. The purpose of the meeting was to give PTTI managers, systems engineers, and program planners a transparent view of the state-of-the-art, an opportunity to express needs, a view of important future trends, and a review of relevant past accomplishments; to provide PTTI users with new and useful applications, procedures, and techniques; to allow the PTTI researcher to better assess fruitful directions for research efforts.			
17. Key Words (Selected by Author(s)) Time, Time transfer, Time dissemination, time measurement		18. Distribution Statement STAR category 70	
19. Security Classif. (of this report) Unclassified	20. Security Classif. (of this page) Unclassified	21. No. of Pages 702	22. Price*

National Aeronautics and
Space Administration

SPECIAL FOURTH CLASS MAIL
BOOK

Postage and Fees Paid
National Aeronautics and
Space Administration
NASA-451



Washington, D.C.
20546

Official Business
Penalty for Private Use, \$300

NASA

POSTMASTER: If Undeliverable (Section 158
Postal Manual) Do Not Return
